

LOCKHEED MARTIN ENERGY RESEARCH LIBRARIES



3 4456 0515612 1

CENTRAL RESEARCH LIBRARY

ORNL-4937

Cy1

PHYSICS Division • Annual PROGRESS REPORT

Period Ending December 31, 1973

OAK RIDGE NATIONAL LABORATORY
CENTRAL RESEARCH LIBRARY
DOCUMENT COLLECTION

LIBRARY LOAN COPY

DO NOT TRANSFER TO ANOTHER PERSON

If you wish someone else to see this
document, send in name with document
and the library will arrange a loan.

UCN-7969
(3-3-67)



OAK RIDGE NATIONAL LABORATORY

OPERATED BY UNION CARBIDE CORPORATION • FOR THE U.S. ATOMIC ENERGY COMMISSION

Printed in the United States of America. Available from
National Technical Information Service
U.S. Department of Commerce
5285 Port Royal Road, Springfield, Virginia 22151
Price: Printed Copy \$7.60; Microfiche \$1.45

This report was prepared as an account of work sponsored by the United States Government. Neither the United States nor the United States Atomic Energy Commission, nor any of their employees, nor any of their contractors, subcontractors, or their employees, makes any warranty, express or implied, or assumes any legal liability or responsibility for the accuracy, completeness or usefulness of any information, apparatus, product or process disclosed, or represents that its use would not infringe privately owned rights.

ORNL-4937
UC-34—Physics

Contract No. W-7405-eng-26

PHYSICS DIVISION
ANNUAL PROGRESS REPORT
For Period Ending December 31, 1973

P. H. Stelson, Director
G. R. Satchler, Associate Director

MAY 1974

OAK RIDGE NATIONAL LABORATORY
Oak Ridge, Tennessee 37830
operated by
UNION CARBIDE CORPORATION
for the
U.S. ATOMIC ENERGY COMMISSION

LOCKHEED MARTIN ENERGY RESEARCH LIBRARIES



3 4456 0515612 1

Reports previously issued in this section are as follows:

ORNL-2718	Period Ending March 10, 1959
ORNL-2910	Period Ending February 10, 1960
ORNL-3085	Period Ending February 10, 1961
ORNL-3268	Period Ending February 10, 1962
ORNL-3425	Period Ending January 31, 1963
ORNL-3582	Period Ending December 31, 1964
ORNL-3778	Period Ending December 31, 1964
ORNL-3924	Period Ending December 31, 1965
ORNL-4082	Period Ending December 31, 1966
ORNL-4230	Period Ending December 31, 1967
ORNL-4395	Period Ending December 31, 1968
ORNL-4513	Period Ending December 31, 1969
ORNL-4659	Period Ending December 31, 1970
ORNL-4743	Period Ending December 31, 1971
ORNL-4844	Period Ending December 31, 1972



Contents

1. CYCLOTRON LABORATORY RESEARCH PROGRAM	1
Introduction – E. E. Gross	1
Experimental Studies of the Giant Resonance Region of the Nuclear Continuum – F. E. Bertrand, E. E. Gross, D. J. Horen, D. C. Kocher, M. B. Lewis, and E. Newman	2
Heavy-Ion Elastic and Inelastic Scattering	11
Excitation Functions for Scattering of Identical Bosons – M. L. Halbert, C. B. Fulmer, S. Raman, M. J. Saltmarsh, A. H. Snell, and P. H. Stelson	11
Interference between Coulomb and Nuclear Excitation in the Inelastic Scattering of ^{11}B Ions from ^{208}Pb – J. L. C. Ford, Jr., K. S. Toth, D. C. Hensley, R. M. Gaedke, P. J. Riley, and S. T. Thornton	13
Coulomb-Nuclear Interference in $^{22}\text{Ne} + ^{88}\text{Sr}$ Inelastic Scattering – E. E. Gross, H. G. Bingham, M. L. Halbert, D. C. Hensley, and M. J. Saltmarsh	15
Heavy-Ion Transfer Reactions	17
Single-Nucleon Transfer Reactions Induced by ^{11}B Ions on ^{208}Pb – J. L. C. Ford, Jr., K. S. Toth, G. R. Satchler, D. C. Hensley, L. W. Owen, D. M. DeVries, R. M. Gaedke, P. J. Riley, and S. T. Thornton	17
Heavy-Ion-Induced Two-Nucleon Transfer – M. J. Saltmarsh, E. E. Gross, M. L. Halbert, R. K. Cole, G. Hagemann, L. Riedinger	21
($^6\text{Li},t$) and ($^6\text{Li},^3\text{He}$) Reactions on ^{12}C at 60 MeV – H. G. Bingham, M. L. Halbert, D. C. Hensley, E. Newman, K. W. Kemper, and L. A. Charlton	23
Transfer and Compound-Nuclear Reactions in the Interactions of ^{12}C with ^{239}Pu and ^{238}U – R. L. Hahn, P. F. Dittner, K. S. Toth, and O. L. Keller	25
Heavy-Ion Fission and Fusion	26
Spontaneous Fission Isomer Excitation in the ^{20}Ne Ion Coulomb Excitation of ^{239}Pu ? – C. E. Bemis, Jr., Franz Plasil, Robert L. Ferguson, E. E. Gross, and A. Zucker	26
Heavy-Ion-Induced Fission – Franz Plasil, Robert L. Ferguson, and Frances Pleasonton	28
Heavy-Ion Fusion Reactions – H. G. Bingham, C. R. Bingham, E. E. Gross, M. J. Saltmarsh, and A. Zucker	31
Rotational Bands in Deformed Nuclei	33
Backbending Rotational Bands in Even- A Nuclei – L. L. Riedinger, P. H. Stelson, G. B. Hagemann, E. Eichler, D. C. Hensley, N. R. Johnson, R. L. Robinson, R. O. Sayer, and G. J. Smith	33
Decoupled Rotational Bands in $^{163,165}\text{Yb}$ – L. L. Riedinger, P. H. Stelson, G. B. Hagemann, E. Eichler, D. C. Hensley, N. R. Johnson, R. L. Robinson, R. O. Sayer, and G. J. Smith	35

Coulomb Excitation of Ground Bands in $^{160,162,164}\text{Dy}$ with ^{20}Ne and ^{35}Cl Ions – R. O. Sayer, E. Eichler, N. R. Johnson, D. C. Hensley, and L. L. Riedinger	38
Lifetimes of Rotational States in ^{154}Sm – R. J. Sturm, N. R. Johnson, M. W. Guidry, R. O. Sayer, E. Eichler, N. C. Singhal, and D. C. Hensley,	41
Lifetimes of Rotational States in ^{232}Th by the Doppler-Shift–Recoil-Distance Technique – N. R. Johnson, R. J. Sturm, E. Eichler, M. W. Guidry, R. O. Sayer, N. C. Singhal, G. D. O’Kelley, and D. C. Hensley	42
Multiple Coulomb Excitation of ^{236}U – M. W. Guidry, R. J. Sturm, N. R. Johnson, E. Eichler, G. D. O’Kelley, R. O. Sayer, G. B. Hagemann, D. C. Hensley, and L. L. Riedinger	44
Lifetimes of Rotational States in ^{236}U by the Doppler-Shift–Recoil-Distance Technique – M. W. Guidry, R. J. Sturm, G. D. O’Kelley, N. R. Johnson, E. Eichler, R. O. Sayer, and N. C. Singhal.	46
New Isotopes and Spectroscopy	47
X-Ray Identification of Transfermium Elements – C. E. Bemis, Jr., R. J. Silva, D. C. Hensley, O. L. Keller, Jr., J. R. Tarrant, L. C. Hunt, P. F. Dittner, R. L. Hahn, and C. D. Goodman	47
Decay Scheme Studies in the 82-Neutron Region; New Isotopes, ^{146}Tb and ^{148}Dy – K. S. Toth, E. Newman, D. C. Hensley, C. R. Bingham, and W.-D. Schmidt-Ott	49
Measurement of Alpha-Decay Branching Ratios for Rare-Earth Isotopes – K. S. Toth, E. Newman, R. L. Hahn, C. R. Bingham, and W.-D. Schmidt-Ott	53
UNISOR Project – E. H. Spejewski, H. K. Carter, R. L. Mlekodaj, W. D. Schmidt-Ott, and and E. F. Zganjar	57
Properties of Levels in ^{116}Sn – L. L. Riedinger, L. H. Harwood, R. W. Lide, and C. R. Bingham	62
Chemistry of Nobelium, Element 102 – O. L. Keller, R. J. Silva, W. J. McDowell, and J. R. Tarrant	64
Light-Ion and Meson Research	65
Back-Angle Alpha-Particle Scattering – W. W. Eidson, C. C. Foster, C. B. Fulmer, S. A. Gronemeyer, D. C. Hensley, M. B. Lewis, N. M. O’Fallon, and R. G. Rasmussen	65
53.4-MeV ^3He Scattering from Samarium Isotopes – N. M. Clarke, R. Eagle, C. B. Fulmer, R. J. Griffiths, and D. C. Hensley	70
Differential Cross Sections for $^{10}\text{B}(p,n)^{10}\text{C}$ and $^{11}\text{B}(p,n)^{11}\text{C}$ and Some Macroscopic Reaction Relationships – C. D. Goodman, H. W. Fielding, and D. A. Lind.	72
A Search for Delayed Gamma Rays from ^{88}Y – C. D. Goodman, R. L. Bunting, and R. J. Peterson	73
(p,t) Reaction Studies of Nickel Isotopes – M. Greenfield, G. Vourvopoulos, D. McShan, and S. Raman	73
Core Polarization in Inelastic Proton Scattering from ^{209}Bi at 61 MeV – Alan Scott, M. Owais, and F. Petrovich	76
Inelastic Scattering of 61-MeV Protons from ^{92}Mo – Alan Scott and M. L. Whiten	76
Meson Physics – E. E. Gross, C. A. Ludemann, and M. J. Saltmarsh	76
Cyclotron Laboratory Accelerator Development Program	77
Summary – J. A. Martin	77
Heavy-Ion Beam Development – E. D. Hudson, M. L. Mallory, R. S. Lord, J. E. Mann, J. A. Martin, R. K. Goosie, and F. Irwin	77

ORIC Cryopumps – J. E. Mann, R. S. Lord, W. R. Smith, and A. W. Alexander	82
Computer Control of the ORIC – C. A. Ludemann, J. M. Domaschko, S. W. Mosko, K. Hagemann, E. Madden, and E. McDaniel	85
ORIC Data Acquisition Computer System – D. C. Hensley and C. A. Ludemann	88
ORIC RF System – S. W. Mosko	90
ORIC Magnet Power Supply Improvement Program – W. E. Lingard, S. W. Mosko, and J. A. Martin . . .	94
Vertical Focusing for the Broad-Range Spectrograph – E. E. Gross, J. B. Ball, M. T. Collins, V. Odilivak, and D. L. Hillis	94
Heavy-Ion Proposal Studies – J. A. Martin, P. H. Stelson, J. K. Bair, L. N. Howell, E. D. Hudson, J. W. Johnson, R. S. Lord, C. A. Ludemann, J. E. Mann, M. L. Mallory, M. B. Marshall, G. S. McNeilly, S. W. Mosko, and A. Zucker	95
Shielding Measurements – H. M. Butler, C. B. Fulmer, and K. M. Wallace	102
Oak Ridge Isochronous Cyclotron Operations – H. L. Dickerson, H. D. Hackler, J. W. Hale, C. L. Haley, R. S. Lord, M. B. Marshall, S. W. Mosko, E. Newman, G. A. Palmer, E. G. Richardson, A. W. Riikola, L. A. Slover, C. L. Viar, A. D. Higgins, E. W. Sparks, and K. M. Wallace	103
Accelerator Information Center – 1973 – F. T. Howard	106
2. VAN DE GRAAFF LABORATORY	108
Introduction – C. D. Moak and R. L. Robinson	108
Heavy-Ion Reactions	110
Evidence for Coexistence of Spherical and Deformed Shapes in ^{72}Se – J. H. Hamilton, A. V. Ramayya, W. T. Pinkston, R. L. Robinson, H. J. Kim, R. O. Sayer, R. M. Ronningen, G. Garcia-Bermudez, and H. K. Carter	110
High-Spin States in ^{42}Ca – R. L. Robinson, H. J. Kim, W. T. Milner, R. O. Sayer, G. J. Smith, J. C. Wells, Jr., and J. Lin	112
In-Beam Gamma Rays from the $^{28}\text{Si}(^{16}\text{O},\alpha p\gamma)^{39}\text{K}$ Reaction – H. J. Kim, R. L. Robinson, and W. T. Milner	114
In-Beam Gamma-Ray Spectroscopy of Magic and Nearly Magic Nuclei ($Z = 28$) – G. J. Smith, R. L. Robinson, R. O. Sayer, and W. T. Milner	115
In-Beam Gamma-Ray Spectroscopy of ^{64}Zn via the $^{51}\text{V}(^{16}\text{O},p2n)$ Reaction – R. O. Sayer, R. L. Robinson, W. T. Milner, G. J. Smith, J. C. Wells, Jr., and J. Lin	116
Recoil-Distance Lifetime Measurements – R. O. Sayer, N. C. Singhal, W. T. Milner, R. L. Robinson, J. H. Hamilton, A. V. Ramayya, and G. J. Smith	117
Rotational and Quasi-Rotational Bands in Even-Even Nuclei – R. O. Sayer, J. S. Smith III, and W. T. Milner	119
Excitation of Rotational Bands in ^{20}Ne by the $^{10}\text{B}(^{16}\text{O},^6\text{Li})$ Reaction – J. L. C. Ford, Jr., J. Gomez del Campo, S. T. Thornton, R. L. Robinson, and P. H. Stelson	121
Population of High-Spin States in ^{22}Na by Means of the $^{10}\text{B}(^{16}\text{O},\alpha)$ Reaction – J. Gomez del Campo, J. L. C. Ford, Jr., S. T. Thornton, R. L. Robinson, P. H. Stelson, and J. B. McGroory	122
Absolute Cross Sections for the $^{61}\text{Ni}(^{16}\text{O},X)$ Reactions – J. C. Wells, R. L. Robinson, H. J. Kim, and J. L. C. Ford, Jr.	123
Heavy-Ion Neutron Yields – J. K. Bair, P. D. Miller, and P. H. Stelson	126
Comparison of Cross Sections for the Ni, Cu, Zn ($^{16}\text{O},xn$) Reactions with Theory – R. L. Robinson and J. K. Bair	126

Coulomb Excitation	129
Coulomb Excitation of Vibrational-Like States in the Even- <i>A</i> Actinide Nuclei – F. K. McGowan, C. E. Bemis, Jr., W. T. Milner, J. L. C. Ford, Jr., R. L. Robinson, and P. H. Stelson	129
Oxygen-16 Coulomb Excitation in the Actinide Region with the Enge Magnetic Spectrometer – C. E. Bemis, Jr., F. K. McGowan, W. T. Milner, R. L. Robinson, P. H. Stelson, and J. L. C. Ford, Jr.	131
Coulomb-Nuclear Interference for Alpha Particles on Deformed Nuclei – C. E. Bemis, Jr., F. K. McGowan, P. H. Stelson, W. T. Milner, R. L. Robinson, J. L. C. Ford, Jr., and W. Tuttle	132
Beta, Gamma, and Octupole Vibrational States and Hexadecapole Deformations in ^{156,158} Gd – J. H. Hamilton, R. M. Ronningen, L. L. Riedinger, A. V. Ramayya, G. Garcia-Bermudez, R. L. Robinson, and P. H. Stelson	134
Coulomb Excitation of ^{176,178,180} Hf – J. H. Hamilton, L. Varnell, R. M. Ronningen, A. V. Ramayya, J. Lange, L. L. Riedinger, R. L. Robinson, and P. H. Stelson	135
Neutron Physics	136
Search for an Electric Dipole Moment of the Neutron, and Other Cold-Neutron Experiments at the Institute Laue-Langevin, Grenoble, France – P. D. Miller and W. B. Dress	136
Search for an Electric Dipole Moment of the Neutron – W. B. Dress, P. D. Miller, P. Perrin, and N. F. Ramsey	137
Proposal to Redetermine the Magnetic Moment of the Neutron – W. B. Dress, P. D. Miller, N. F. Ramsey, P. Perrin, and C. Guet.	140
Search for Doubly Radiative <i>np</i> Capture – P. Perrin, C. Guet, W. B. Dress, and P. D. Miller	140
Light-Ion Reactions and Internal Conversion Coefficients	141
Low-Lying States in ¹¹¹ In and ¹¹³ In – H. J. Kim and R. L. Robinson	141
Proton Size Resonances in Tin Isotopes – C. H. Johnson, J. K. Bair, and C. M. Jones	143
<i>M4</i> Conversion Coefficients and <i>E5</i> Transitions – S. Raman, R. L. Auble, W. T. Milner, T. A. Walkiewicz, R. Gunnink, and B. Martin	144
Atomic and Solid-State Physics	147
Atomic Structure and Collisions Experiments – I. A. Sellin, H. H. Haselton, R. Laubert, J. Richard Mowat, D. J. Pegg, R. S. Peterson, R. S. Thoe, P. M. Griffin, M. D. Brown, Sheldon Datz, Bailey Donnally, R. Kauffman, J. R. Macdonald, P. Richard, and W. W. Smith	147
Influence of Ionic Charge State on the Stopping Power of 27.8- and 40-MeV Oxygen Ions in the [011] Channel of Silver – C. D. Moak, B. R. Appleton, J. A. Biggerstaff, M. D. Brown, S. Datz, H. F. Krause, and T. S. Noggle	152
Velocity Dependence of the Stopping Power of Channeled Iodine Ions – C. D. Moak, B. R. Appleton, J. A. Biggerstaff, S. Datz, and T. S. Noggle	153
Hyperchanneling: I. Investigations for High-Energy Heavy Ions in Silver – B. R. Appleton, J. H. Barrett, J. A. Biggerstaff, C. D. Moak, S. Datz, and T. S. Noggle	155
<i>K</i> and <i>L</i> X-Ray Production Cross Sections from Heavy-Ion Bombardment – Jerome L. Duggan and P. D. Miller	157
Accelerator Operation, Development, and Applications	159
Status Report on the Tandem Van de Graaff Accelerator – G. F. Wells, R. L. Robinson, F. A. DiCarlo, J. W. Johnson, N. F. Ziegler, G. K. Werner, D. M. Galbraith, and R. P. Cumby	159
Tandem Data-Logging System – J. A. Biggerstaff, W. T. Milner, and N. F. Ziegler	161
Tandem Control System – N. F. Ziegler	161

Developments in Computer and Data Acquisition Systems – J. A. Biggerstaff, W. T. Milner, J. W. McConnell, and N. F. Ziegler	162
Proton Microanalysis Using a Lithium Ion Beam – J. A. Biggerstaff	164
The Heavy-Ion Source Program	164
Multiply Charged Heavy-Ion Source System Studies – G. D. Alton, E. D. Hudson, C. M. Jones, and M. L. Mallory	164
Absolute Yields of High Charge States for 20-MeV Iodine Ions Small-Angle-Scattered from Xenon and Argon – P. D. Miller, C. M. Jones, B. Wehring, J. A. Biggerstaff, G. D. Alton, C. D. Moak, Q. C. Kessel, and L. B. Bridwell	165
Ion Optics Capabilities – G. D. Alton and H. Tamagawa	167
Measurements on INTEREM – H. Tamagawa, C. M. Jones, N. H. Lazar, and W. M. Good	167
Penning Ion Source Test Facility – M. L. Mallory, E. D. Hudson, C. M. Jones, and S. W. Mosko	168
Charge-Changing Cross Sections for Multiply Charged Heavy Ions at Low Velocity – E. W. Thomas	169
Elastic Scattering of Positrons by Hydrogen – G. D. Alton, M. Reeves, and W. R. Garrett	170
Theoretical Shunt Impedance Model for Spirally Loaded RF Resonant Cavities – P. Z. Peebles, Jr. and C. M. Jones	170
Superconducting Resonant Cavities – J. P. Judish, C. M. Jones, P. Z. Peebles, Jr., and W. T. Milner	171
3. ELECTRON LINEAR ACCELERATOR (ORELA)	174
Introduction – J. A. Harvey	174
Subthreshold and Threshold Neutron Fission of ^{234}U – J. W. T. Dabbs, G. D. James, and N. W. Hill	176
Neutron Total Cross Section of ^{234}U from 3 to 3000 eV – J. A. Harvey, G. D. James, N. W. Hill, and R. H. Schindler	177
Polarized-Neutron, Polarized-Target Fission of ^{235}U and ^{237}Np at ORELA – G. A. Keyworth, J. W. T. Dabbs, F. T. Seibel, and N. W. Hill	178
Neutron Total Cross Sections of Transuranium Nuclides – J. A. Harvey, N. W. Hill, R. W. Benjamin, C. E. Ahlfeld, F. B. Simpson, and O. D. Simpson	179
Neutron-Induced Fission of ^{249}Cf – J. W. T. Dabbs, C. E. Bemis, Jr., G. D. James, N. W. Hill, M. S. Moore, and A. N. Ellis	181
Optimized Detection of Fission Neutrons with Large Liquid Scintillators – N. W. Hill, J. W. T. Dabbs, and H. Weaver	182
Gold Neutron Capture Cross Section from 3 to 550 keV – R. L. Macklin and J. Halperin	183
Neutron Capture in Sulfur to 1100 keV – J. Halperin, R. L. Macklin, and R. R. Winters	185
Neutron Total Cross Section of ^6Li from 100 eV to 1 MeV – J. A. Harvey and N. W. Hill	187
The $^{57}\text{Fe}(n,\gamma)^{58}\text{Fe}$ Reaction and Shell-Model Calculations of ^{58}Fe Levels – S. Raman, G. G. Slaughter, W. M. Good, J. A. Harvey, J. B. McGrory, and D. Larson	188
Search for a Neutron Resonance in ^{207}Pb at 16.8 MeV – J. A. Harvey, W. M. Good, N. W. Hill, and R. H. Schindler	193
Nonexistence of a Giant $M1$ Resonance in ^{208}Pb – J. A. Harvey, W. M. Good, N. W. Hill, and R. H. Schindler	194

The $^{16}\text{O} + n$ Total Cross Section: Diagnostics and Refinements – C. H. Johnson, J. L. Fowler, L. A. Galloway, and N. W. Hill	195
Potential Scattering of Neutrons by Calcium – J. L. Fowler and C. H. Johnson	196
Neutron Total Cross Sections in the keV Energy Range – W. M. Good, J. A. Harvey, and N. W. Hill	198
Status Report on the Oak Ridge Electron Linear Accelerator (ORELA) – J. A. Harvey, F. C. Maienschein, T. A. Lewis, H. A. Todd, and J. G. Craven	202
4. THEORETICAL PHYSICS	204
Introduction – G. R. Satchler	204
Developments in Many-Body Theory of Nuclei – Richard L. Becker, R. W. Jones, N. M. Larson, Franz Mohling, L. W. Owen, M. R. Patterson, and R. J. Philpott	205
Large Uncertainties in Nuclear Proton Densities Permitted by Elastic Scattering Data – Richard L. Becker and James A. Smith	210
Shock Waves in Heavy-Ion Collisions – T. A. Welton and C. Y. Wong	212
Adaptation of Direct Reaction Computer Codes for Use with Heavy Ions – L. W. Owen and G. R. Satchler	213
Viscosity and Fusion Reactions – H. H. K. Tang and C. Y. Wong	213
Calculation of Single-Nucleon Transfer Reactions with Heavy Ions on ^{208}Pb – L. W. Owen and G. R. Satchler	214
Studies with “Realistic” Interactions for Inelastic Nucleon Scattering – K. T. R. Davies, W. G. Love, and G. R. Satchler	216
Gaussian Potentials Equivalent to the “Sussex” Matrix Elements – R. H. Tookey and G. R. Satchler	216
Target-Spin Effects on Elastic Scattering Cross Sections – W. G. Love, G. R. Satchler, and C. B. Fulmer	217
Asymmetric Fission of ^{236}U in a Self-Consistent <i>K</i> -Matrix Model – D. Kolb, R. Y. Cusson, and H. W. Schmitt	219
A Strong-Coupling Approach to the Truncation of Large Shell-Model Calculations – L. B. Hubbard and J. B. McGroary	221
Extension of the Capabilities of the Shell-Model Computer Programs – E. C. Halbert and J. B. McGroary	223
Supercharged Nuclei and Exotic Shapes – R. Y. Cusson, K. T. R. Daves, D. Kolb, S. J. Krieger, and C. Y. Wong	224
Nuclei with Discrete Symmetries – H. H. K. Tang and C. Y. Wong	226
Astrophysics: Toroidal Galaxies and Toroidal Stars – S. D. Blazier and C. Y. Wong	226
An Improved Method for Constructing a Filter Function for Processing High-Coherence Electron Micrographs – T. A. Welton	227
5. STATUS REPORT OF THE NUCLEAR DATA PROJECT – R. L. Auble, J. B. Ball, F. E. Bertrand, Y. A. Ellis, W. B. Ewbank, B. Harmatz, D. J. Horen, H. J. Kim, D. C. Kocher, M. B. Lewis, M. J. Martin, F. K. McGowan, W. T. Milner, S. Raman, and M. R. Schmorak	233
6. HIGH ENERGY ACTIVITIES – H. O. Cohn, R. D. McCulloch, W. M. Bugg, G. T. Condo, and E. L. Hart	236

7. ELECTRON SPECTROSCOPY PROGRAM	239
Introduction – T. A. Carlson	239
Quantitative Model for ESCA – W. J. Carter III, T. A. Carlson, and G. K. Schweitzer	240
Satellite Structure in X-Ray Photoelectron Spectroscopy of Transition-Metal Compounds – T. A. Carlson, J. C. Carver, L. J. Saethre, F. Garcíá Santibáñez, and G. A. Vernon	243
8. HYPERFINE INTERACTIONS IN SOLIDS – Felix E. Obenshain, J. O. Thomson, P. G. Huray, J. Thompson, J. C. Love, J. C. Williams, R. Graetzer, and P. Scholl	248
Introduction	248
⁵⁷ Fe Mössbauer Measurements of Iron-Cobalt Alloys	249
Magnetic Behavior of Iron and Cobalt Impurities in Silver	250
⁶¹ Ni Mössbauer Studies of Substituted Nickel Spinels	251
⁶¹ Ni Mössbauer Effect in Nickel Compounds	253
Magnetic Susceptibility Measurements	254
9. MOLECULAR SPECTROSCOPY	256
Millimeter and Submillimeter Spectra of Tritium-Substituted Water and Ammonia – H. W. Morgan, P. A. Staats, F. DeLucia, P. Helminger, and W. Gordy	256
10. HIGH RESOLUTION ELECTRON MICROSCOPY PROGRAM – R. E. Worsham, W. W. Harris, J. E. Mann, E. G. Richardson, and N. F. Ziegler	258
11. PUBLICATIONS	263
Book, Journal, and Proceedings Articles	263
Theses	276
Annual Report	276
Topical Reports	276
12. PAPERS PRESENTED AT SCIENTIFIC AND TECHNICAL MEETINGS	277
13. OMNIANA	285
Announcements	285
Personnel Assignments	285
Miscellaneous Professional Activities of Divisional and Associated Personnel	287
Colloquia and Seminars Presented by the Physics Division Staff and Associates	290
Physics Division Seminars	291
Ph.D. Thesis Research	293
M.S. Thesis Research	294
Undergraduate Student Guests	294
Cooperative Education Program	294
Guest Assignees – Students Not Engaged in Thesis Research at ORNL	294

Consultants under Subcontract with Union Carbide Corporation Nuclear Division – ORNL	295
Consultants under Contract Arrangement with Oak Ridge Associated Universities	295
Annual Information Meeting	297
Radiation Control and Safety	297

1. Cyclotron Laboratory Research Program

INTRODUCTION

E. E. Gross

The research program at the Oak Ridge Isochronous Cyclotron (ORIC) Laboratory is becoming increasingly dominated by heavy-ion research. This trend is brought about by scientific interest in a new field of research and by advances in cyclotron technology which have made available a large variety of heavy-ion beams. Nevertheless, the cyclotron continues to be used for its light-ion capabilities. The most notable example is the use of a unique capability for producing 60-MeV polarized proton beams to study the collective nature of recently discovered giant resonances at high excitation. The analyzing power of the giant resonance at 16.5 MeV excitation in ^{58}Ni was measured with this beam.

Research with heavy-ion beams during the past year covered the gamut from atomic x-ray yields to nuclear physics and nuclear chemistry, and a number of these experiments are of great interest. In one experiment, element 104 was uniquely identified by an ingenious x-ray–alpha-particle coincidence measurement. The result confirms the Berkeley discovery claim, and a similar experiment to check the Russian discovery claim is in progress. Other isotope discovery experiments have discovered a total of seven new isotopes during the past year. Three of these were discovered using the recently activated UNISOR isotope separator, which is the only isotope separator on line with a heavy-ion cyclotron in the West.

Several significant contributions were made to the field of high spin states within rotational bands. Using the $^{156}\text{Gd}(^{20}\text{Ne}, 6n)$ reaction, a new “backbending” rotational band in ^{170}W was discovered. The discovery of two decoupled bands in ^{165}Yb , one which backbends and one which does not, is also reported, as is the possible coexistence of a spherical and a deformed band in ^{188}Hg . The “backbending” effect in some rotational bands is not a completely understood phenomenon and certainly contains information on the internal nature of the nucleus. Using a specially designed plunger, another group has succeeded in measuring the lifetimes of states up to the 10^+ member of the rotational band in ^{232}Th and up to the 10^+ member in ^{154}Sm . Finally, excitation functions were measured for the 4^+ members of rotational bands excited by two-proton transfer or two-neutron pickup by a ^{20}Ne beam incident on targets of ^{160}Gd , ^{162}Dy , and ^{154}Sm .

Heavy-ion experiments in the related fields of fission and fusion were also actively pursued. An upper limit of about $3 \times 10^{-34} \text{ cm}^2$ for the Coulomb excitation cross section of the ^{239}Pu fission isomer by ^{20}Ne ions was established. The fission products resulting from the compound system formed by ^{20}Ne bombardment of ^{107}Ag were measured. From the measurements, it was inferred that the compound system, $^{127}\text{La}^*$, could not be formed with an angular momentum of more than about $52\hbar$. The inhibiting effect of angular momentum on the fusion process was also observed for the fusion of ^{40}Ar and ^{58}Ni . Using quartz track detectors, the fusion cross section for this system was

obtained at several energies, and the angular momentum cutoff effect was clearly observed.

Progress in our understanding of the ion-ion optical potential was made in the past year. The interference between Coulomb and nuclear excitation of collective nuclear states was used to sensitively probe the nuclear potential near the nuclear surface for the systems $^{11}\text{B} + ^{208}\text{Pb}$ and $^{22}\text{Ne} + ^{88}\text{Sr}$. In the case of ^{22}Ne , the Coulomb-nuclear interference pattern could not be explained by the usual direct-reaction theory, and two-step processes may be playing a role in this case. Elastic scattering excitation functions for $^{16}\text{O} + ^{16}\text{O}$ and for $^{12}\text{C} + ^{12}\text{C}$ were extended from the tandem energy range up to the full capabilities of the ORIC cyclotron. The resonance-like structure observed in the lower-energy excitation function for $^{16}\text{O} + ^{16}\text{O}$ was found to continue throughout the higher energy range. A program to investigate heavy-ion reaction mechanisms and spectroscopy was also active, especially for single-nucleon transfer reactions in $^{11}\text{B} + ^{208}\text{Pb}$ and in $^{12}\text{C} + ^{90}\text{Zr}$.

The success of the heavy-ion research program is indebted to a vigorous development program. During the past year, many new heavy-ion beams, and especially metallic ion beams, have been added to ORIC's arsenal. A new ion source containing a rotating cathode has been designed, fabricated, and successfully tested in a specially designed ion-source test stand. The new source should result in longer source life and in more convenient operation. Recently, cryopumping panels have been installed near the center of the cyclotron, and an increase of $^{40}\text{Ar}^{4+}$ beam intensity by up to a factor of 18 was observed. Steady progress has also been made toward computer control and monitoring of the cyclotron.

This summary is only a partial listing of the research accomplishments of approximately 80 scientists who have participated in experiments at the Cyclotron Laboratory during the past year. The following pages contain a more comprehensive account of this research program.

EXPERIMENTAL STUDIES OF THE GIANT RESONANCE REGION OF THE NUCLEAR CONTINUUM

F. E. Bertrand	D. C. Kocher ¹
E. E. Gross	M. B. Lewis
D. J. Horen	E. Newman

Studies of the giant resonance region of the nuclear continuum via inelastic scattering of medium-energy projectiles have received considerable attention over the last three years following the discovery (e.g., the work of M. B. Lewis and F. E. Bertrand²) of a giant resonance in nuclei other than the well-known isovector ($T = 1$) giant dipole ($E1$) resonance. This new resonance was presumed to be an isoscalar ($T = 0$) giant quadrupole ($E2$) resonance. The experimental work and theoretical interpretations for the new resonance phenomena have been reviewed by G. R. Satchler.³

During the past year a variety of measurements on giant resonances have been made at ORIC, mainly via inelastic scattering of 60- to 67-MeV protons. The inelastically scattered protons were detected by photographic emulsion plates placed in the focal plane of the

broad-range magnetic spectrograph. This technique yields proton spectra over a wide range of excitation energies without having to apply corrections required in a counter experiment.

The recent measurements at ORIC were made for a variety of purposes. (1) Proton spectra were obtained for many nuclei and over a wide range of excitation energy in order to study the systematic behavior of the new giant resonance observed by Lewis and Bertrand² and to search for additional resonances. (2) For the new resonance, detailed measurements of the cross section angular distribution and of the angular distribution of the analyzing power for incident polarized protons were made in order to resolve an ambiguity in the resonance spin. (3) Measurements have been made to study the effect of a permanent deformation for the ground state of the target nucleus on the excitation of giant resonances. (4) Preliminary measurements have been made with deuteron beams, since deuterons may selectively excite isoscalar giant resonances.

1. Mass systematics and energy spectra. Proton spectra for four nuclei obtained by Lewis, Bertrand, and Horen⁴ are shown in Fig. 1. For each nucleus, the

region of the nuclear continuum above the neutron separation energy shows the pronounced resonance structure observed by Lewis and Bertrand.² The peak in

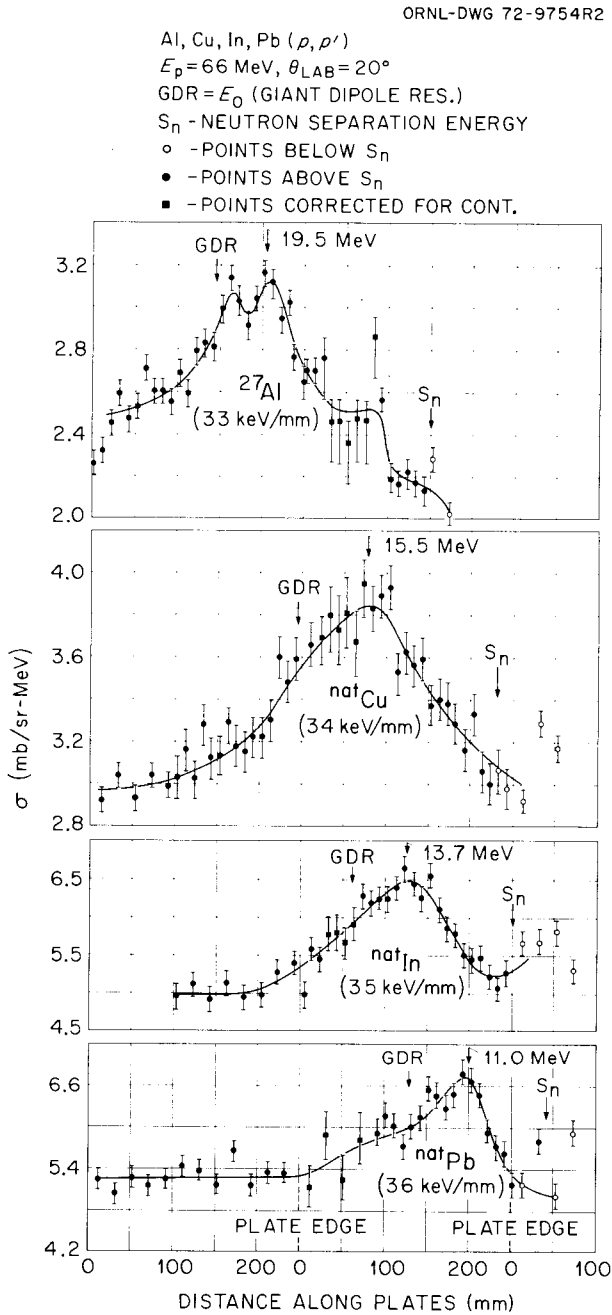


Fig. 1. Proton inelastic scattering spectra in the giant resonance region for Al, Cu, In, and Pb at $E_p = 66$ MeV, $\theta_L = 20^\circ$. The known energy of the giant dipole resonance (GDR), the neutron separation energy S_n , and the energy calibration are given for each target. Open circles indicate data below S_n , solid circles indicate data above S_n , and solid squares are data corrected for contaminants.

the resonance is consistently located 2 to 3 MeV below the energy of the well-known giant dipole resonance.

Proton spectra covering a range of excitation energies up to about 40 MeV for the nuclei ^{40}Ca , ^{46}Ti , ^{58}Ni , ^{90}Zr , ^{144}Sm , ^{154}Sm , and ^{208}Pb were obtained by F. E. Bertrand, E. E. Gross, D. C. Kocher, and E. Newman. Sample spectra for ^{40}Ca and ^{90}Zr are shown in Figs. 2 and 3. As in Fig. 1, the pronounced peak centered below the $E1$ resonance is evident. The spectra above the $E1$ resonance show no evidence for additional resonances. The expected energy of an isovector $E2$

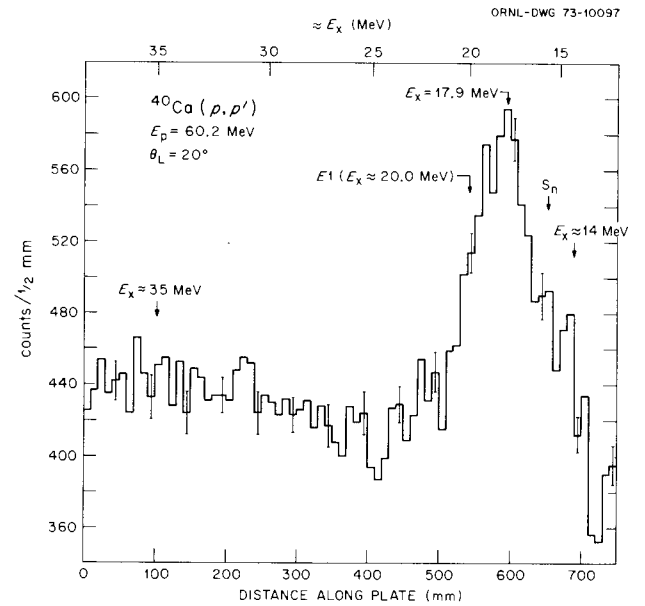


Fig. 2. Spectrum for $^{40}\text{Ca}(p, p')$. S_n is the neutron separation energy, and $E1$ is the known energy of the giant dipole resonance.

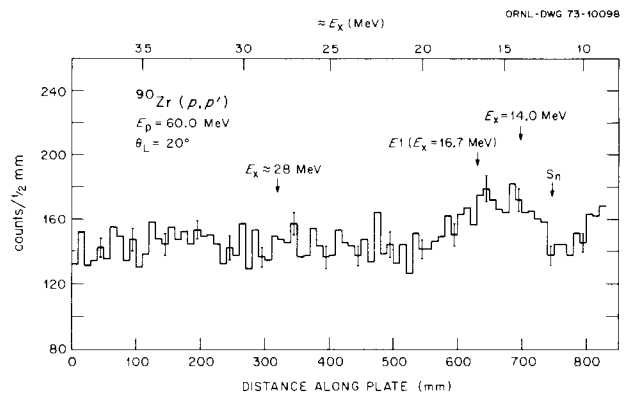


Fig. 3. Spectrum for $^{90}\text{Zr}(p, p')$. S_n and $E1$ have the same meaning as in Fig. 2.

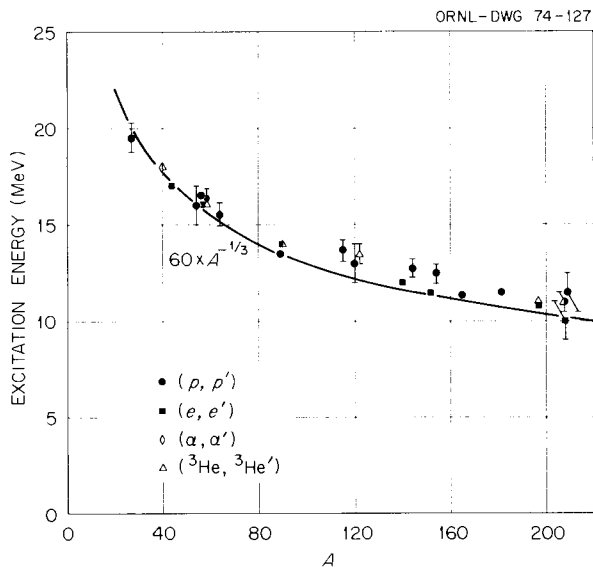


Fig. 4. Summary of the excitation energies for the new giant resonance plotted against mass number A . The curve is the excitation energy predicted by Mottelson for an isoscalar giant quadrupole resonance.

resonance (see ref. 3) is shown. This resonance should have a cross section of about one-eighth of the cross section for the isoscalar $E2$ resonance located below the $E1$ resonance. The isovector resonance is thus very difficult to observe in (p, p') , since the cross section for the unstructured continuum is large. The ^{40}Ca spectrum shows evidence for a weaker resonance near $E_x = 14$ MeV. Measurements at several angles are being analyzed in an attempt to characterize this structure.

The excitation energies of the pronounced resonance below the $E1$ resonance, as seen by a variety of incident projectiles, are summarized in Fig. 4. The observed excitation energy of $E_x \approx 63A^{-1/3}$ MeV is in good agreement with the prediction of Mottelson (see ref. 3) for the energy of an isoscalar giant quadrupole resonance.

2. Studies of the giant resonance at $E_x \approx 63A^{-1/3}$ MeV in spherical nuclei. The pronounced resonance at $E_x \approx 63A^{-1/3}$ MeV was initially interpreted by Lewis and Bertrand² as the isoscalar quadrupole excitation predicted by Mottelson. Satchler⁵ showed, however, that due to the relatively large uncertainties in the measured resonance cross sections in (p, p') , the interpretation of the resonance as a giant monopole ($E0$) excitation could not be ruled out.

The first attempt to resolve this ambiguity was made by Lewis, Bertrand, and Horen⁴ in a study of the $^{208}\text{Pb}(p, p')$ reaction. The spectra in the resonance

region at $\theta_L = 20^\circ$ and 28° are shown in Fig. 5. The resonance shows some fine structure similar to that seen in electron inelastic scattering (see ref. 3). The shaded portions of the spectra give the region of excitation energy for which the relative cross section was obtained by subtracting the assumed contribution from the underlying continuum shown. This region minimizes unwanted contributions from the $E1$ resonance. The result for the cross section at 28° relative to the cross section at 20° is shown in Fig. 6. Comparison with the distorted-wave Born approximation (DWBA) predictions shows that the measurement is consistent only with the $E2$ interpretation.

More extensive measurements to resolve the ambiguity in spin assignments for the giant resonance were made by Kocher, Bertrand, Gross, Lord, and Newman.⁶ Since calculations by Satchler⁵ predicted that a measurement of the analyzing power of the resonance for incident polarized protons could distinguish between the $E2$ and $E0$ interpretations, the $^{58}\text{Ni}(\vec{p}, p')$ reaction was studied using the polarized proton beam from the atomic beam source at ORIC. Beam currents of about 3 nA on target with polarization $p_y \approx 50\%$ were obtained.

The polarized-beam spectra at $\theta_L = 20^\circ$ are shown in Fig. 7. At all angles, the spectra in the unstructured continuum above $E_x = 24$ MeV show a very small asymmetry $\epsilon \equiv (\sigma_{\text{up}} - \sigma_{\text{down}})/(\sigma_{\text{up}} + \sigma_{\text{down}})$. On the other hand, the resonance structure centered at $E_x = 16.5 \pm 0.5$ MeV exhibits a pronounced asymmetry. A weaker resonance near $E_x = 13.5$ MeV is also observed.

Figure 8 shows the cross sections in the continuum region at different angles. The shape of the $E1$ resonance, as obtained from total photonuclear cross section measurements, is shown at the top of the figure. One sees that the resonance structure can be observed only at the forwardmost angles. At 40° (not shown) the spectrum is characterized by an essentially constant cross section between $E_x \approx 14$ and 30 MeV.

Figure 9 illustrates that the spectra can reasonably be decomposed into contributions from the underlying continuum, the $E1$ resonance, and the resonances centered at $E_x = 16.5$ and 13.5 MeV. The assumed cross section for the underlying continuum in the resonance region is based on spectra for ^{58}Ni and neighboring nuclei⁷ at angles where the resonance cross sections are unobservably small. The shape of the $E1$ contribution was assumed to be given by the total photonuclear cross section shown in Fig. 8. Symmetric shapes were assumed for the other two resonances. While the decomposition shown in Fig. 9 is reasonable, it may not be unique. Therefore, the resonance cross sections are

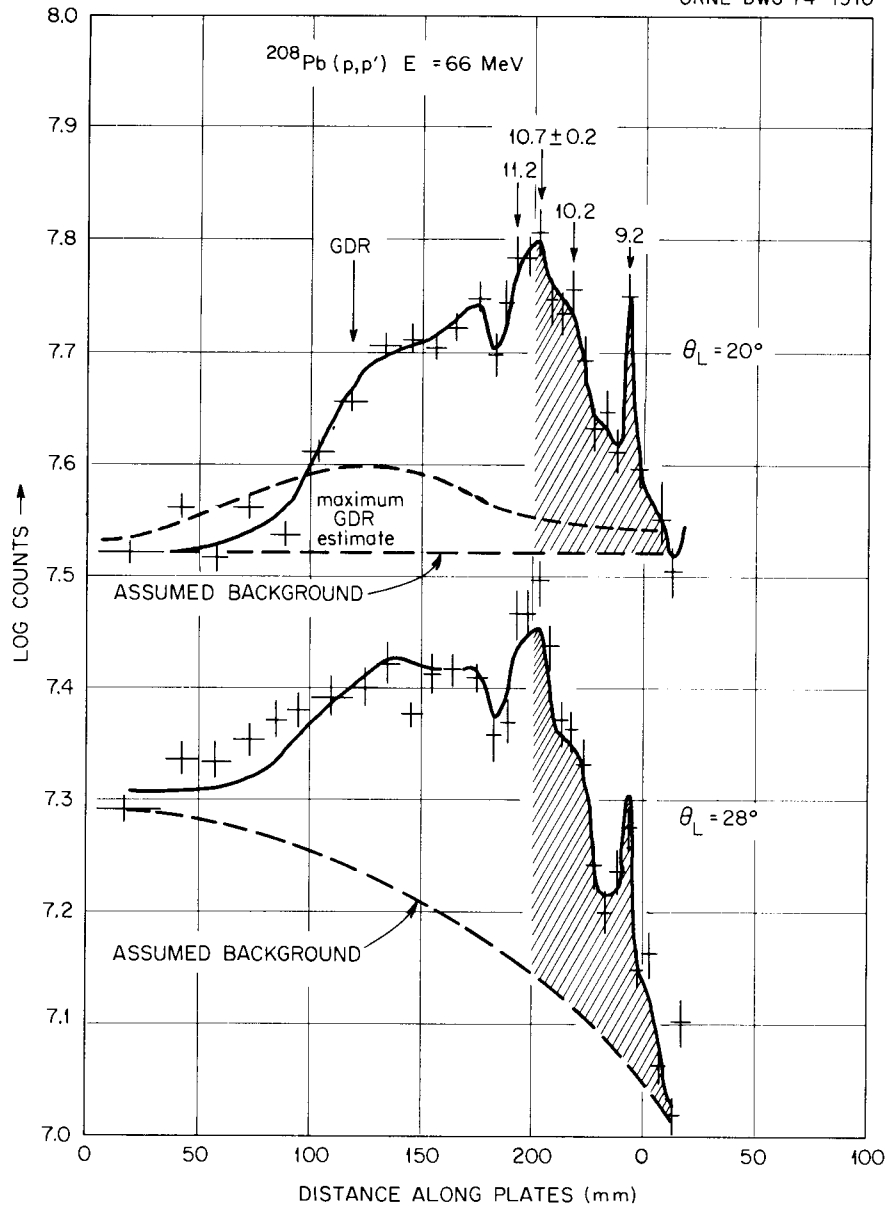


Fig. 5. Spectra for $^{208}\text{Pb}(p,p')$ at $\theta_L = 20^\circ$ and 28° . Note that the plot is semilogarithmic. GDR is the known energy of the giant dipole resonance.

usually obtained by analyzing a region of the spectrum large enough to include most of the new resonance and the $E1$ resonance.

The cross sections for the resonance structure in ^{58}Ni between $E_x \approx 12.7$ and 23.7 MeV, excluding estimated contributions from the 13.5-MeV resonance, are shown in Fig. 10. The curves are based on DWBA predictions for $E0$, $E1$, and $E2$ excitations normalized to the strengths predicted by energy-weighted sum rules. The

measured angular distribution shows a clear preference for the $E1 + E2$ curve.

The analyzing power for the 16.5-MeV resonance was obtained from the polarized-beam spectra in the region $E_x \approx 14.6$ to 16.7 MeV. As shown in Fig. 9, the chosen region minimizes the unwanted contribution from the $E1$ resonance. The contributions from the underlying continuum and the $E1$ resonance were subtracted from the spectrum as illustrated in Fig. 9. The analyzing

power for the underlying continuum in the resonance region was assumed to be the same as the observed analyzing power above $E_x \approx 24$ MeV. The analyzing power for the $E1$ resonance was extracted from the spectra in the region $E_x \approx 20.6$ to 23.0 MeV, where the contribution from the 16.5-MeV resonance is negligible.

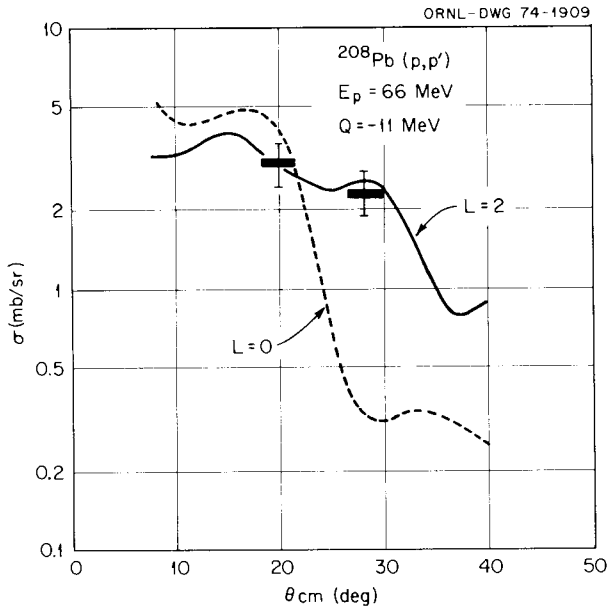


Fig. 6. Cross sections in the $^{208}\text{Pb}(p,p')$ reaction for the shaded portion of the spectra in Fig. 5. The curves are DWBA predictions for $E2$ and $E0$ excitations normalized to the measured cross section at 20° . The uncertainties in the measurements are relative only.

The analyzing powers extracted for the 16.5-MeV resonance are shown in Fig. 11. The solid curve is the DWBA prediction for an $E2$ excitation employing a spin-orbit deformation of the Oak Ridge type. The other curves are predictions of Satchler⁵ for two different models for an $E0$ excitation. For an $E0$ excitation the Oak Ridge spin-orbit deformation is equivalent to the exact full Thomas form. The measured analyzing powers are better described by the $E0$ predictions than by the $E2$ prediction.

The results for $^{58}\text{Ni}(\vec{p},p')$ thus appear to be ambiguous in that the analyzing power for a narrow region of the spectrum suggests an $E0$ excitation, but the cross section for the entire resonance region shows a preference for the $E2$ interpretation. It is possible that there is considerable $E0$ strength in the region $E_x \approx 14.6$ to 16.7 MeV, but if that be the case, the cross sections in Fig. 10 show that the total $E0$ strength would have to be small compared with the $E2$ strength in the entire resonance region. Shown in Fig. 12 are the relative cross sections for the resonance in the region $E_x \approx 14.6$ to 16.7 MeV (open circles) compared with DWBA predictions. The data are best described by the $E2$ curve, but the increase in cross section forward of 20° suggests that some $E0$ strength may be present. However, no definitive conclusion can be made from the measurements. It appears that data at more forward angles are required to determine the presence of an $E0$ resonance.

A more likely explanation for the ambiguity between the cross section and the analyzing power in $^{58}\text{Ni}(\vec{p},p')$ is that the DWBA predictions for the analyzing power shown in Fig. 11 do not provide a quantitative

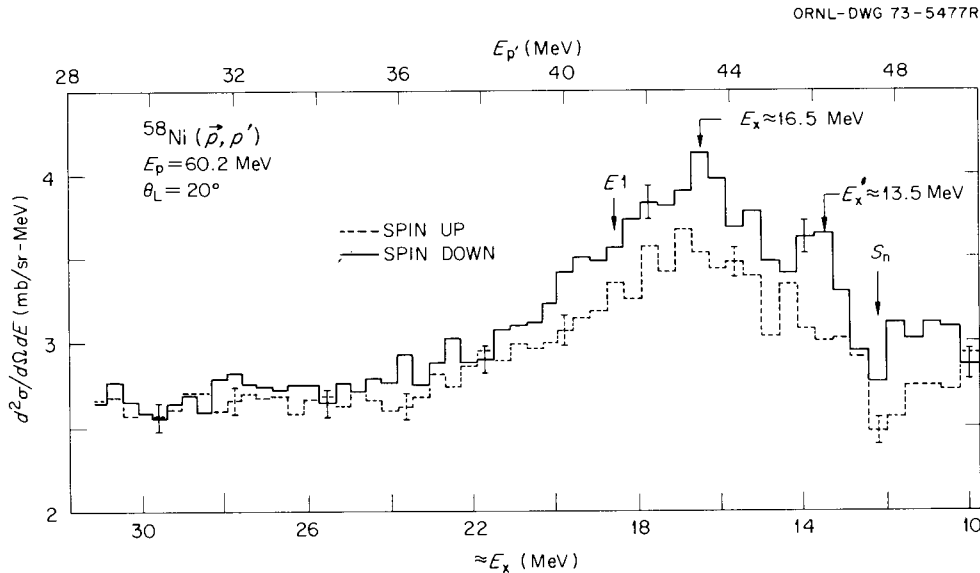


Fig. 7. Polarized-beam spectra for $^{58}\text{Ni}(\vec{p},p')$ at $\theta_L = 20^\circ$. $E1$ and S_n have the same meaning as in Fig. 2.

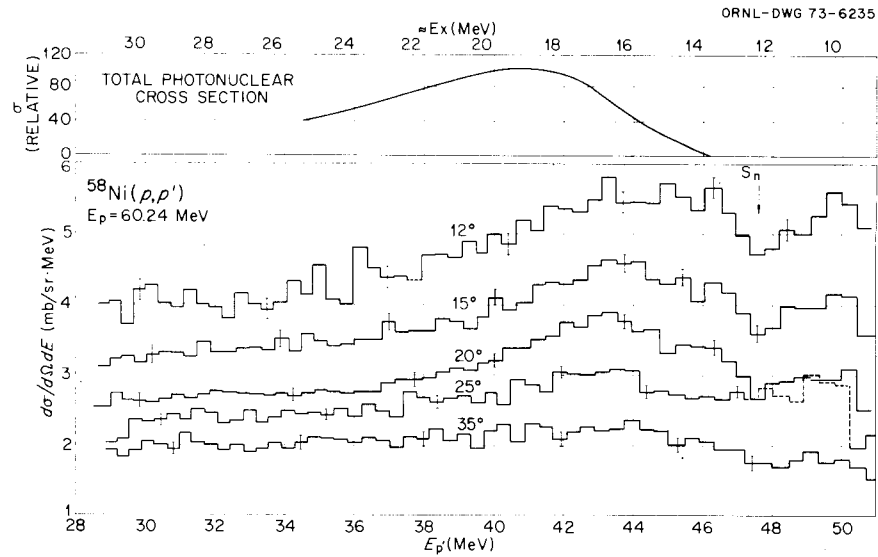


Fig. 8. Unpolarized-beam spectra for $^{58}\text{Ni}(p,p')$ as a function of scattering angle. The curve at the top of the figure is assumed to describe the shape of the $E1$ resonance.

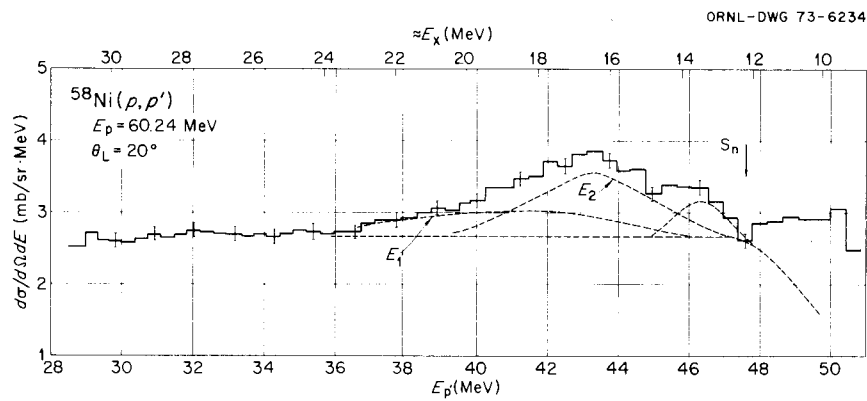


Fig. 9. Unpolarized-beam spectrum for $^{58}\text{Ni}(p,p')$ at $\theta_L = 20^\circ$. S_n has the same meaning as in Fig. 2. The dashed curves indicate a decomposition of the spectrum in the resonance region into contributions from the underlying continuum, the $E1$ resonance, and the resonances at $E_x \approx 16.5$ and 13.5 MeV.

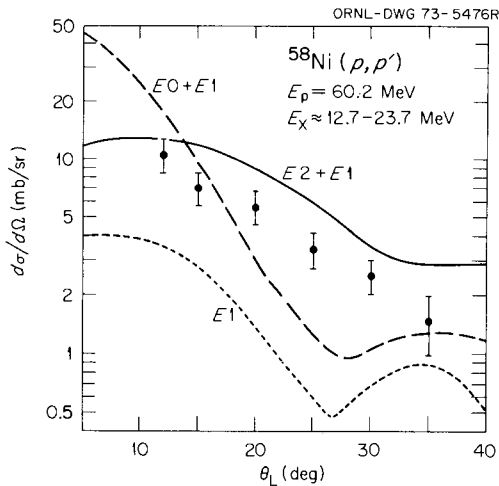


Fig. 10. Cross sections for $^{58}\text{Ni}(p,p')$ in the giant resonance region ($E_x \approx 12.7$ to 23.7 MeV) compared with DWBA predictions.

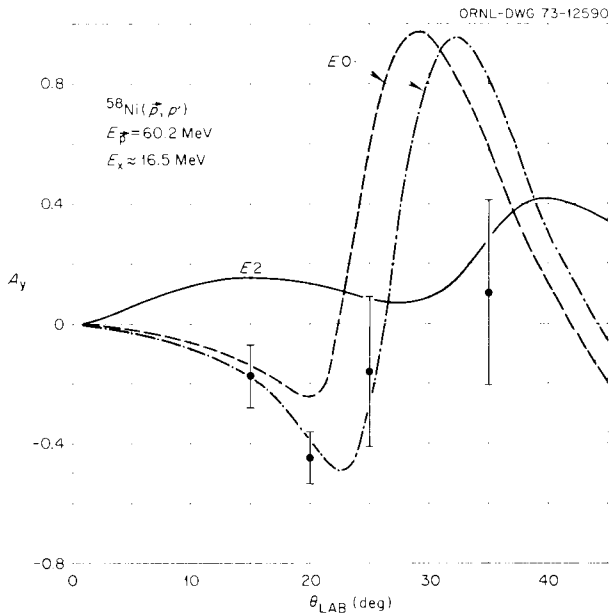


Fig. 11. Analyzing powers for $^{58}\text{Ni}(p,p')$ in the region $E_x \approx 14.6$ to 16.7 MeV compared with DWBA predictions.

description of the measurements. The use of spin-orbit distortions of the full Thomas form does yield predicted analyzing powers which are more negative than those shown in Fig. 11 ($A_y = 0.06, 0.00,$ and -0.08 at $\theta_L = 10^\circ, 20^\circ,$ and 30° , respectively), but the relatively large negative values measured at 15° and 20° are not reproduced. The adequacy of the DWBA is being investigated by Kocher, Bertrand, Gross, and Newman by extracting the analyzing powers for low-lying bound states in ^{58}Ni for which the spin and parity are known. Preliminary results show that for 2^+ and 4^+ states, the measured analyzing powers near 20° are always considerably more negative than the DWBA predictions employing spin-orbit distortions of the full Thomas form and the same optical-model parameters used in the calculations for Fig. 11. The problem of the DWBA predictions for the analyzing power of the 16.5-MeV resonance is currently being investigated by performing calculations with different optical-model parameters and by obtaining additional data for the resonance and for strongly excited 2^+ and 3^- collective levels. DWBA calculations aside, it was observed in the preliminary results that the measured analyzing powers for known 2^+ bound states are similar to the measurements for the 16.5-MeV resonance shown in Fig. 11. Unfortunately, no collective 0^+ levels are known, so that Satchler's calculations for a monopole excitation cannot be tested.

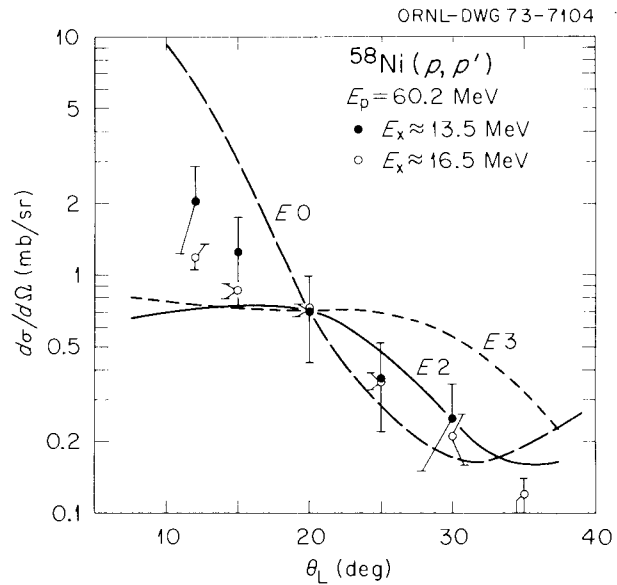


Fig. 12. Cross sections for $^{58}\text{Ni}(p,p')$ for the resonance at $E_x \approx 13.5$ MeV and cross sections in the region $E_x \approx 14.6$ to 16.7 MeV compared with DWBA predictions. The last two quantities are normalized to the cross section for the 13.5-MeV resonance at $\theta_L = 20^\circ$. The uncertainty in the relative cross sections for the 16.5-MeV resonance is statistical only.

The weaker resonance at $E_x \approx 13.5$ MeV shown in Fig. 7 is of interest, because a similar resonance observed in $^{56}\text{Fe}(e,e')$ (see ref. 3) was tentatively given an $E3$ assignment. The resonance cross sections shown in Fig. 12 appear to rule out the $E3$ assignment, but a definite assignment from (p,p') measurements requires further analysis.

3. Measurements on deformed nuclei. One difficulty in interpreting (p,p') spectra in the giant resonance region results from the incomplete separation between the $E1$ resonance and the stronger resonance 2 to 3 MeV lower in energy. It is usually assumed that the shape of the $E1$ resonance in (p,p') is the same as the shape of the resonance observed in photonuclear reactions. This assumption can be examined by comparing (p,p') spectra for a spherical nucleus with spectra for a deformed nucleus, since it is well known that the $E1$ resonance is split in deformed nuclei.

Such a comparison has been made for ^{144}Sm and ^{154}Sm by Horen, Bertrand, and Lewis.⁸ The spectra at 20° for both nuclei are shown in Fig. 13. The spectrum for the spherical nucleus ^{144}Sm shows evidence for two peaks -- one at $E_x \approx 15.4$ MeV, in excellent agreement with the known $E1$ resonance energy, and the other at

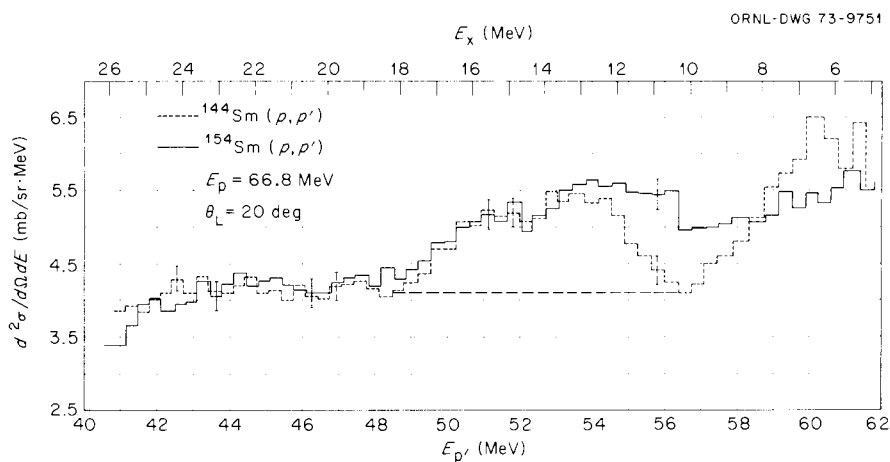


Fig. 13. Spectra for ^{144}Sm , $^{154}\text{Sm}(p,p')$ at $\theta_L = 20^\circ$. The long dashed line shows the assumed underlying continuum in the resonance region for ^{144}Sm .

$E_x \approx 12.9$ MeV, in good agreement with the prediction for the presumed $E2$ resonance. The surprising result is that the spectrum for the deformed nucleus ^{154}Sm is identical to the ^{144}Sm spectrum above $E_x \approx 13$ MeV. From photonuclear measurements, the $E1$ resonance in ^{154}Sm should be split into two peaks of roughly equal strength at $E_x \approx 12.4$ and 16.1 MeV, but there is no evidence for this in the spectrum.

There are two possible interpretations for the similarity between the ^{144}Sm and ^{154}Sm spectra. First, it is possible that the quadrupole resonance is also split in ^{154}Sm in such a way as to compensate for the splitting of the dipole resonance and produce a spectrum similar to that for ^{144}Sm . However, no significant splitting of quadrupole strength has been observed in bound states in deformed samarium nuclei. Second, the observed cross section in the region of the $E1$ resonance in ^{144}Sm at $E_x \approx 15.4$ MeV is about a factor of 2 larger than the cross section predicted by the DWBA from the assumed $E1$ sum-rule strength. Therefore, resonances other than the $E1$ may be contributing to the cross section near this energy, and the splitting of the $E1$ resonance in ^{154}Sm thus cannot be observed.

An unambiguous interpretation of the resonances observed in ^{144}Sm and ^{154}Sm is not yet possible. These measurements cast doubt on previous assumptions for the excitation of the $E1$ resonance in (p,p') , so that further work is clearly in order.

Another interesting feature of the samarium spectra in Fig. 13 is the pronounced difference in cross sections below $E_x \approx 12$ MeV. One possible explanation is that the density of collective levels is much greater in the deformed nucleus than in the spherical nucleus. In any

event, while the assumed cross section contribution for the underlying continuum seems reasonable for ^{144}Sm , the assumed contribution may be inappropriate for ^{154}Sm .

The spectrum in the resonance region for a deformed nucleus has been further investigated by Lewis and Horen in a study of the $^{238}\text{U}(p,p')$ reaction. A spectrum at 20° is shown in Fig. 14. One notes that the resonance at $E_x \approx 10.5$ MeV appears to be superposed on a continuum which increases smoothly from the region above the resonance into the bound-state region below the neutron separation energy S_n . This effect differs markedly from the constant cross section for the underlying continuum usually assumed for spherical nuclei. A second important feature of this spectrum is the apparent absence of the $E1$ resonance. About two-thirds of the $E1$ strength in ^{238}U is centered near $E_x = 14$ MeV, which occurs at about 100 mm on the second plate. At this excitation energy there is no evidence for a significant cross section above the underlying continuum.

The cross sections obtained for the 10.5-MeV resonance are shown in Fig. 15. If one assumes that no $E1$ strength is present, the measurements are seen to be in good agreement with an $E2$ DWBA prediction which exhausts most of the expected sum-rule strength.

4. Measurements of (d,d') spectra. One possibility for unraveling the separate contributions for the isovector $E1$ resonance and the isoscalar $E2$ resonance is to compare spectra taken with incident particles with different isospin. For example, deuterons, with $T = 0$, should excite only isoscalar resonances in a self-conjugate nucleus like ^{40}Ca . Preliminary measurements

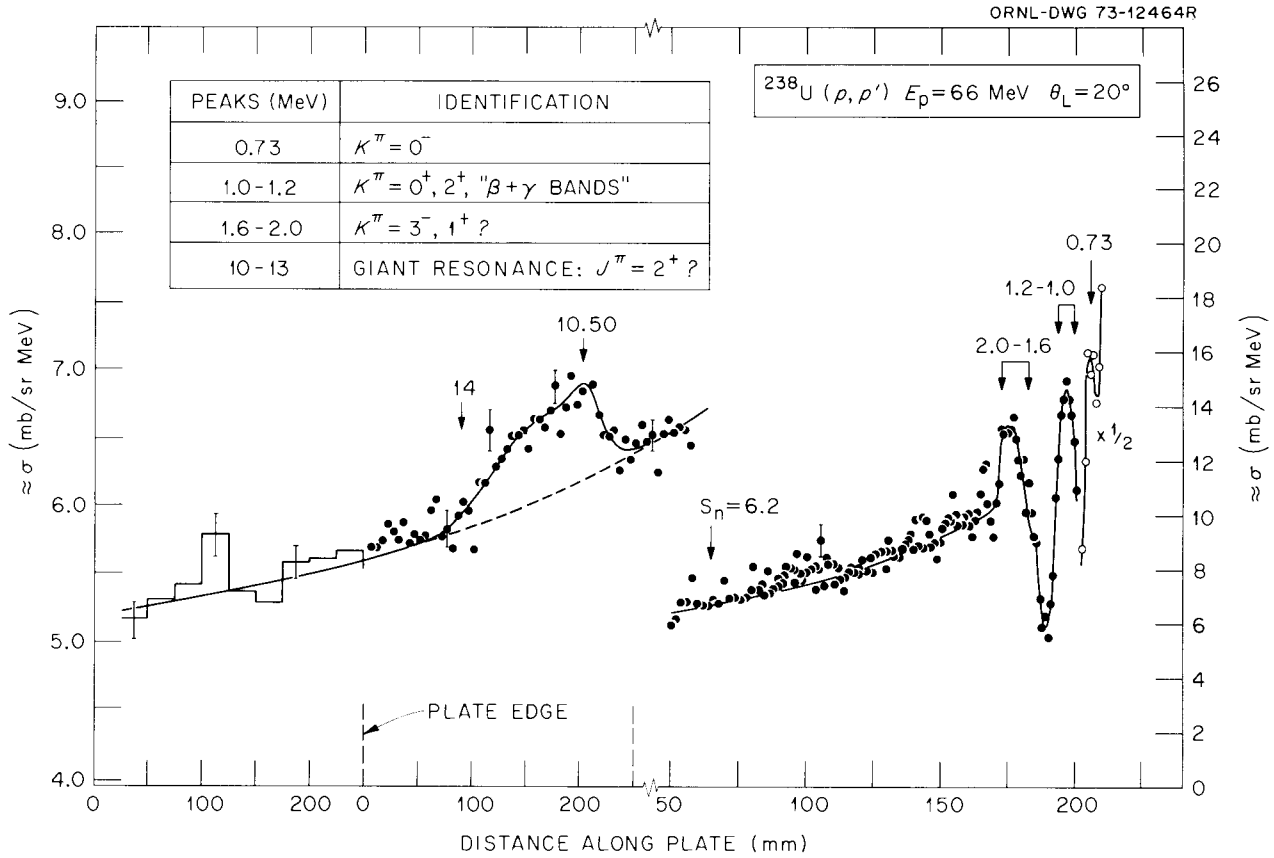


Fig. 14. Spectrum for $^{238}\text{U}(p, p')$. S_n has the same meaning as in Fig. 2. The dashed line shows the assumed underlying continuum in the resonance region.

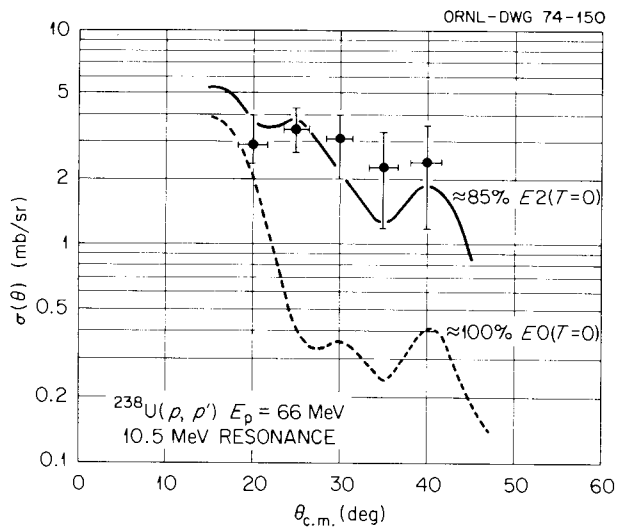


Fig. 15. Cross sections for $^{238}\text{U}(p, p')$ in the resonance region near $E_x = 10.5$ MeV compared with DWBA predictions.

at $E_d = 46$ MeV have been made by Bertrand, Gross, Kocher, and Newman for the nuclei ^{40}Ca , ^{58}Ni , ^{144}Sm , and ^{154}Sm . The deuteron spectra appear to be similar to proton spectra for the same nuclei, but a detailed comparison awaits further analysis.

In summary, an extensive series of measurements on the inelastic excitation of giant resonances has been made at ORIC during the past year. The purpose of most of this work has been to study the giant resonance at $E_x \approx 63A^{-1/3}$ MeV. Measurements of the differential cross section for proton inelastic scattering from ^{58}Ni , ^{208}Pb , and ^{238}U indicate that this resonance is the isoscalar giant quadrupole resonance predicted by Mottelson. However, several problems have arisen during the course of this work which tend to cloud the simple picture that the observed resonance structure consists of the isovector giant quadrupole resonance and the isoscalar giant quadrupole resonance. First, a satisfactory explanation of the measured analyzing power in $^{58}\text{Ni}(\vec{p}, p')$ has not yet been obtained. Second, the spectra for ^{238}U and the comparison between the

spectra for ^{144}Sm and ^{154}Sm indicate that our understanding of the $E1$ resonance as excited in (p,p') is incomplete. Finally the comparison between spectra for spherical and deformed nuclei points out once again our lack of understanding of the structure of the continuum underlying the resonances. This is a particularly serious problem because the continuum cross section is large compared with the resonance cross sections even in the most favorable cases. Further experiments are planned at ORIC to investigate these problems.

1. Nuclear Information Research Associate. Work supported by the National Science Foundation through the National Academy of Sciences-National Research Council, Committee on Nuclear Science.

2. M. B. Lewis and F. E. Bertrand, *Nucl. Phys. A* **196**, 337 (1972).

3. G. R. Satchler, *Rev. Mod. Phys.*, to be published.

4. M. B. Lewis, F. E. Bertrand, and D. J. Horen, *Phys. Rev. C*, **8**, 398 (1973).

5. G. R. Satchler, *Particles Nucl.* **5**, 105 (1973).

6. D. C. Kocher, F. E. Bertrand, E. E. Gross, R. S. Lord, and E. Newman, *Phys. Rev. Lett.* **31**, 1070 (1973); erratum, *Phys. Rev. Lett.* **32**, 264 (1974).

7. F. E. Bertrand and R. W. Peelle, *Phys. Rev. C*, **8**, 1045 (1973).

8. D. J. Horen, F. E. Bertrand, and M. B. Lewis, *Phys. Rev.*, to be published.

HEAVY-ION ELASTIC AND INELASTIC SCATTERING

EXCITATION FUNCTIONS FOR SCATTERING OF IDENTICAL BOSONS

M. L. Halbert	M. J. Saltmarsh
C. B. Fulmer	A. H. Snell ¹
S. Raman	P. H. Stelson

Elastic scattering of ^{16}O by ^{16}O at 90° (c.m.) was measured at Chalk River² up to 17.5 MeV (c.m.) and at Yale^{3,4} up to about 40 MeV. The excitation function produced by the Chalk River group is smooth, very different from the one measured for $^{12}\text{C} + ^{12}\text{C}$ in the same energy region.² However, the Yale results^{3,4} on $^{16}\text{O} + ^{16}\text{O}$ display unusually pronounced and regular structure from 20 to 30 MeV, more so than $^{12}\text{C} + ^{12}\text{C}$ at similar energies.^{5,6} With ORIC we have a valuable tool to search for such structure at higher energies and provide new tests of the many models that have been invoked to explain these results.

Thus far we have measured the excitation function at 90° for $^{16}\text{O} + ^{16}\text{O}$ from 35 to 88 MeV (c.m.) and for $^{12}\text{C} + ^{12}\text{C}$ from about 37 to 60 MeV (c.m.). The ^{16}O data are ready for publication.⁷ An abbreviated account

of the results is given below. The $^{12}\text{C} + ^{12}\text{C}$ results shown below were obtained in our first cyclotron run on this system and will be extended to higher energies.

We intend to study $^{40}\text{Ca} + ^{40}\text{Ca}$. This experiment awaits the development of a long-lived source of intense $^{40}\text{Ca}^{9+,10+}$ beams. The cyclotron improvements at the end of 1973 and those scheduled for 1974 may make such studies possible.

Experimental Method

The products of a 90° c.m. elastic event appear at 45° (lab) on opposite sides of the beam. They are detected in coincidence by a pair of 10×50 mm silicon surface-barrier counters. The counter collimators are curved in order to accept a large solid angle (0.008 sr) while maintaining good polar-angle resolution in the defining slit ($\pm 0.57^\circ$ wide). The conjugate-counter aperture is 3.25 times wider and 6% taller to allow for multiple scattering and possible misalignment. The coincidence efficiency was measured for 20.2-MeV (lab) ^{16}O on 60- to $100\text{-}\mu\text{g}/\text{cm}^2$ quartz targets.⁸ It was found to be 0.95 ± 0.05 , in good agreement with an estimate of 0.94 obtained from consideration of multiple-scattering effects. Some of the early data were obtained with different slits, and an empirical correction for lost coincidences (about 20%) was applied to the data.

$^{16}\text{O} + ^{16}\text{O}$ Scattering

Our results are shown by the full circles in Fig. 1 and by the heavy line in Fig. 2. The absolute cross sections require knowledge of the oxygen content of the quartz targets. This was measured in two ways, by $^{16}\text{O} + ^{16}\text{O}$ scattering below the Coulomb barrier (Mott scattering) and by scattering of 36.8-MeV protons, for which the cross section is precisely known.⁹ The results of the two methods agree satisfactorily and give us confidence that the $^{16}\text{O} + ^{16}\text{O}$ cross sections are known to $\pm 15\%$.

The most remarkable result from this experiment is the persistence of strong structure into the higher-energy region. The light curves in Figs. 1 and 2 are predictions from various optical models as calculated with the program HIGENOA.¹⁰ Curve Y is from the four-parameter Yale potential^{3,4} with energy-dependent imaginary well. Curve Y6 was predicted by the six-parameter Yale potential,¹¹ while curve A is from a strongly absorbing potential¹² often used for ^{16}O reactions on medium-weight nuclei. An extension of parameters was required above $E = 36$ MeV c.m. for curve F, the one with the l -dependent imaginary

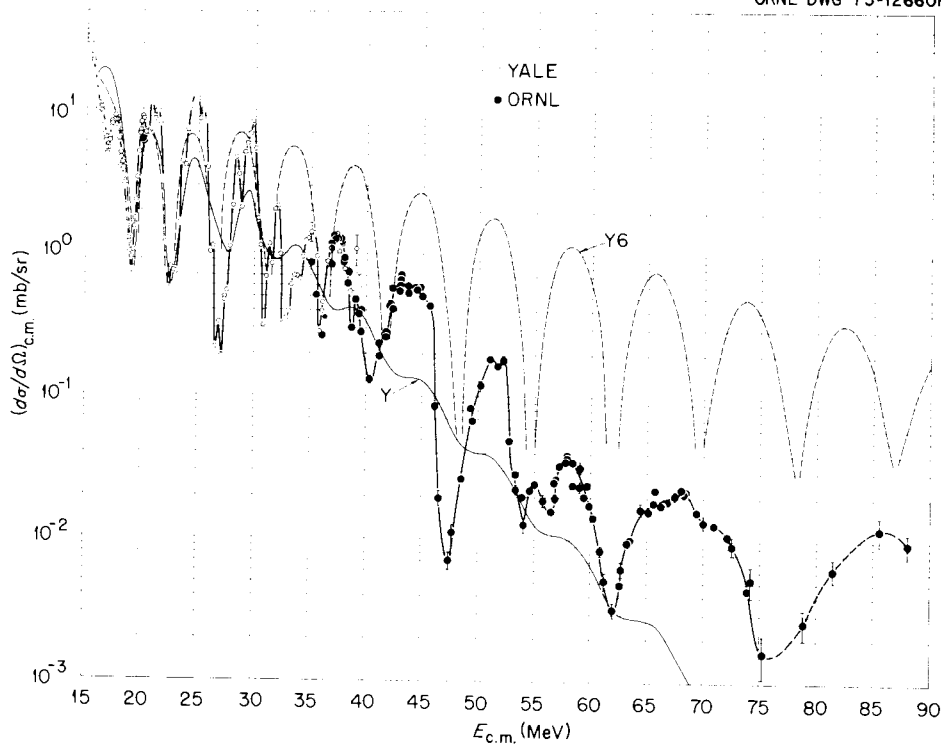


Fig. 1. Excitation function for $^{16}\text{O} + ^{16}\text{O}$ elastic scattering at 90° c.m. Experimental data are represented by the points connected by the heavy line. \bullet — Oak Ridge data, \circ — Yale data [R. H. Siemssen et al., *Phys. Rev. Lett.* **19**, 369 (1967); **20**, 175 (1968); J. V. Maher et al., *Phys. Rev.* **188**, 1665 (1969)]. An upper limit of 0.002 mb/sr was obtained for 102.5 MeV; this point is not shown. The light curves are optical-model predictions: Y is from the four-parameter Yale potential (R. H. Siemssen et al., loc. cit.; J. V. Maher et al., loc. cit.), and Y6 is from their six-parameter potential [A. Gobbi et al., *Phys. Rev. C* **7**, 30 (1973)].

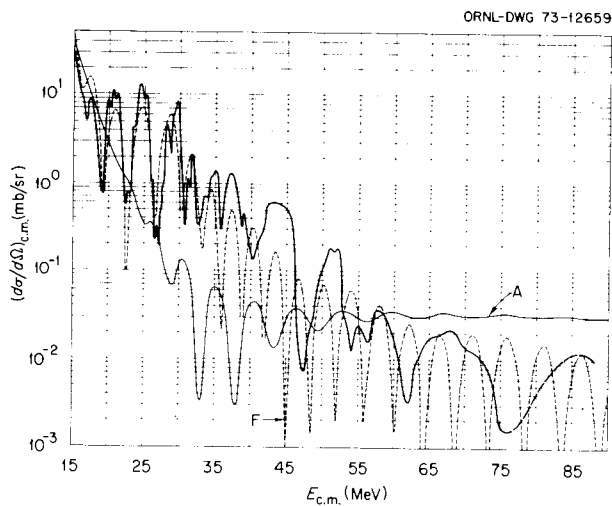


Fig. 2. Excitation function for $^{16}\text{O} + ^{16}\text{O}$ elastic scattering at 90° c.m. The experimental data shown in Fig. 1 are represented by the heavy line. Curve A is predicted by a typical strongly absorbing optical potential [G. C. Morrison et al., *Phys. Rev. Lett.* **28**, 1662 (1972)]. Up to 36 MeV, curve F is identical with the prediction given by Chatwin et al. [*Phys. Rev. C* **1**, 795 (1970)]; above 36 MeV we used $\bar{R} = 9.8$ and $\bar{Q} = -20$ in their formulas.

potential. We took $\bar{R} = 9.8$, $\bar{Q} = -20$ following a suggestion by D. Robson. Except for the width of the oscillations, it is the most successful of the four potentials shown.

$^{12}\text{C} + ^{12}\text{C}$ Scattering

The results in Fig. 3 are preliminary and await verification by repeated measurements. Moreover, the target was natural carbon; at a deep minimum such as we found at 51 MeV (c.m.), the ^{13}C content of the target may make a significant contribution to the observed yield, since the coincidence requirement does not prevent some of the $^{12}\text{C} + ^{13}\text{C}$ coincidences from being detected. We will repeat measurements in this energy region with a target depleted of ^{13}C .

The contrast between the carbon and the oxygen results is quite striking. The carbon results show little structure except for the broad dip at 51 MeV.

1. Consultant.
2. D. A. Bromley, J. A. Kuehner, and E. Almquist, *Phys. Rev.* **123**, 878 (1961).

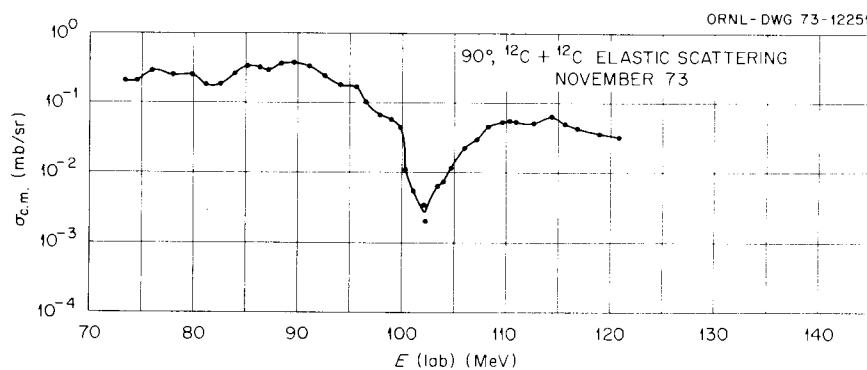


Fig. 3. Preliminary results for excitation function for ^{12}C on ^{12}C at 90° c.m.

3. R. H. Siemssen, J. V. Maher, A. Weidinger, and D. A. Bromley, *Phys. Rev. Lett.* **19**, 369 (1967); **20**, 175 (1968).
4. J. V. Maher, M. W. Sachs, R. H. Siemssen, A. Weidinger, and D. A. Bromley, *Phys. Rev.* **188**, 1665 (1969).
5. W. Reilly, R. Wieland, A. Gobbi, M. W. Sachs, and D. A. Bromley, *Proceedings of the International Conference on Reactions Induced by Heavy Ions, Heidelberg, 1969*, ed. R. Bock and W. R. Hering (North-Holland, 1969), p. 95.
6. R. Wieland, A. Gobbi, L. Chua, M. W. Sachs, D. Shapira, R. Stokstad, and D. A. Bromley, *Phys. Rev. C* **8**, 37 (1973).
7. M. L. Halbert, C. B. Fulmer, S. Raman, M. J. Saltmarsh, A. H. Snell, and P. H. Stelson, to be published.
8. D. N. Braski of the Isotopes Division prepared these targets by ion bombardment of quartz.
9. W. T. H. van Oers and J. M. Cameron, *Phys. Rev.* **184**, 1061 (1969).
10. F. G. J. Perey, C. Y. Wong, and L. W. Owen, private communication.
11. A. Gobbi, R. Wieland, L. Chua, D. Shapira, and D. A. Bromley, *Phys. Rev. C* **7**, 30 (1973), Fig. 3c.
12. G. C. Morrison, H. J. Körner, L. Greenwood, and R. H. Siemssen, *Phys. Rev. Lett.* **28**, 1662 (1972).

INTERFERENCE BETWEEN COULOMB AND NUCLEAR EXCITATION IN THE INELASTIC SCATTERING OF ^{11}B IONS FROM ^{208}Pb

J. L. C. Ford, Jr. R. M. Gaedke¹
 K. S. Toth P. J. Riley²
 D. C. Hensley S. T. Thornton³

Inelastic scattering of heavy ions often results from collisions in which the probabilities for both nuclear and Coulomb excitation are significant. The analysis of such processes may furnish additional information concerning the optical-model parameters for heavy-ion scattering, as well as the phase of the nuclear interaction.⁴ The interference between nuclear and Coulomb excitation may result in minima in the angular distributions or excitation functions indicating when the nuclear absorption begins to become appreciable.

Such effects have been observed in the inelastic scattering of both light and heavy ions to the first excited states of nuclei (see, e.g., refs. 5–8), and inelastic scattering⁵ of 43.7-MeV ^3He ions from ^{208}Pb shows interference minima for higher excited states as well. We report here the observation of marked interference patterns in the angular distributions for four states of ^{208}Pb excited in the inelastic scattering of 72.2-MeV ^{11}B ions.

Results and Discussion

Angular distributions were measured between 35° and 75° in the laboratory system for the 3^- , 5^- , 2^+ , and 4^+ states at 2.61, 3.20, 4.10, and 4.31 MeV in ^{208}Pb , respectively. The differential cross section for elastic scattering was measured down to a laboratory angle of 20° . Figure 1 displays these measurements. At a center-of-mass angle near 51° , where the effect of nuclear absorption begins to depress the elastic cross section severely below the Rutherford value, all four excited-state angular distributions show a marked interference effect. This angle corresponds to a distance of closest approach of about 14 fm between the centers of the interacting nuclei.

Optical-model fits to the elastic data were made using a version of the program GENOA extended to many partial waves.⁹ The theoretical curves shown in Fig. 1 for the inelastic scattering were calculated using the distorted-wave code DWUCK,¹⁰ modified to permit calculations over a greater number of partial waves and out to larger radii. The distorted-wave Born-approximation (DWBA) form factor for inelastic scattering was then given by the collective model of Bassel et al.¹¹ Included in the form factor are the parameters β_L^C and β_L^N , the respective deformations of the charge distribution and optical model. In addition, the optical-

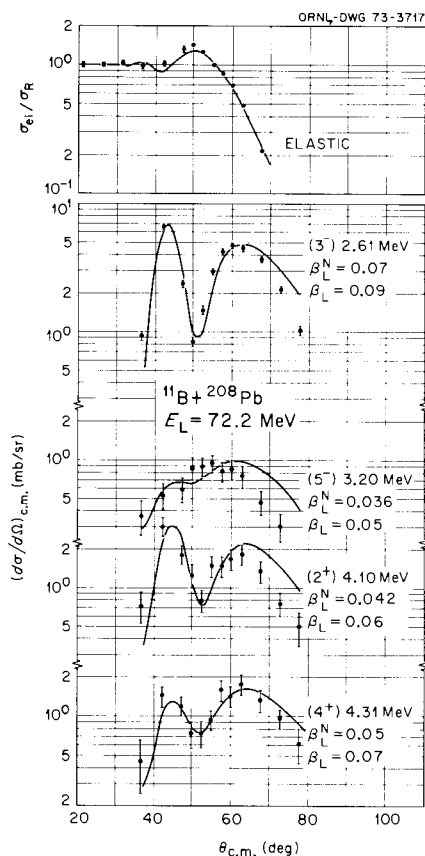


Fig. 1. Angular distributions for the $^{208}\text{Pb}(^{11}\text{B}, ^{11}\text{B})$ reaction at an incident energy of 72.2 MeV. The curves are optical-model and DWBA calculations using parameters discussed in the text.

model form factor contains the phase α , determined by the values of V and W (the real and imaginary wells) as follows:

$$Ue^{i\alpha} = V + iW, \quad (1)$$

where U is the optical-model potential.

Acceptable fits to the elastic scattering data were obtained for a variety of potentials. The theoretical prediction for the elastic scattering data shown in Fig. 1 was calculated with the following parameters: $V = 21.6$ MeV, $W = 5.7$ MeV, $r_0 = 1.34$ fm, and $\alpha = 0.42$ fm. The Coulomb radius parameter was 1.34 fm. The peak near 50° in the elastic cross section was better described if a shallower imaginary potential was used, but the corresponding fits to the inelastic data were then less satisfactory.

The predictions shown in Fig. 1 for the inelastic groups were calculated using these same parameters for both the entrance and exit channels of the reaction and using similar parameters in the form factor, except that W was increased to 8.1 MeV. If the elastic scattering value of 5.7 MeV for W had been used for the form factor, the calculated angular distribution for the 3^- state would have been shifted about 2° to the right of the experimental data. An increase in the value of W in the form factor to 8.1 MeV (an increase in phase angle from 15° to about 20°) leads to the satisfactory fits shown in Fig. 1. The change of phase is also required to fit the other inelastic angular distributions shown in Fig. 1. Acceptable fits to the inelastic data were also obtained using other potentials that gave satisfactory fits to the elastic scattering, but each potential still required this shift in phase.

Table 1. Deformation parameters for states in ^{208}Pb

E_x (MeV)	J^π	This work ^a		$(^{16}\text{O}, ^{16}\text{O}')^b$		β_L				
		β_L^N	β_L	β_L^N	β_L	$(p,p')^c$	$(p,p')^d$	$(p,p')^e$	$(^3\text{He}, ^3\text{He}')^f$	$(\alpha,\alpha')^g$
2.61	3^-	0.065	0.089	0.060	0.085	0.12	0.11	0.098	0.12	0.12
3.20	5^-	0.036	0.05	0.036	0.051	0.072	0.059	0.043	0.03	0.067
4.10	2^+	0.042	0.06	0.030	0.043	0.058	0.050	0.053	0.06	0.055
4.31	4^+	0.05	0.07			0.066		0.062	0.054	0.071

^aCalculated with $V = 21.6$, $W = 5.7$ MeV for the entrance and exit channels, $V = 21.6$, $W = 8.1$ MeV for the form factor, $r_c = r_0 = 1.34$ fm, and $a = 0.42$ fm.

^b $E_{^{16}\text{O}} = 104$ MeV. F. D. Becchetti et al., *Phys. Rev. C* 6, 2215 (1972).

^c $E_p = 24.5$ MeV. J. Saudinos et al., *Nucl. Sci. Appl.* 3(2), 22 (1967).

^d $E_p = 40$ MeV. A. Scott and M. P. Fricke, *Phys. Lett.* 20, 654 (1966).

^e $E_p = 61$ MeV. N. P. Mather, cited by M. B. Lewis, *Nucl. Data Sheets* B5, 260 (1971).

^f $E_{^3\text{He}} = 43.7$ MeV. F. T. Baker and R. Tickle, *Phys. Rev. C* 5, 544 (1972).

^g $E_\alpha = 42$ MeV. J. Alster, *Phys. Rev.* 141, 1138 (1966).

The Coulomb radius parameter and deformation parameter, β_L^C , for the form factor of the 3^- state were taken to be 1.2 fm and 0.10, respectively, as quoted by Barnett and Phillips¹² from Coulomb excitation of ^{208}Pb . The nuclear deformation parameter for the 3^- state was adjusted until the best agreement with the data was achieved, giving a value of 0.065 for β_L^N . Since Coulomb excitation values for β_L^C are not available for the other inelastic states observed, the ratio β_L^C/β_L^N for all levels was fixed at the value determined for the 3^- state, and the value of β_L^N was then adjusted to obtain agreement between theory and experiment.

The deformation parameters corresponding to the fits shown in Fig. 1 are listed in Table I and are compared with values obtained from other inelastic scattering experiments.^{5,8,12-16} The parameter β_L^N is the $^{11}\text{B} + ^{208}\text{Pb}$ optical-model deformation, and from this a target deformation, β_L , may be defined by the following relation,¹⁷ assuming that the deformation length βR is the physically significant quantity:

$$\beta_L R = \beta_L^N R_{\text{om}}. \quad (2)$$

The target mass radius is defined by $R = r_0 A_2^{1/3}$, whereas the optical-model radius is given by $R_{\text{om}} = r_0(A_1^{1/3} + A_2^{1/3})$. It can be seen in the table that the deformation parameters obtained with different projectiles are in good agreement.

In conclusion, we would say that heavy-ion inelastic scattering at energies above the Coulomb barrier appears to be well described by DWBA theory and that the corresponding deformation parameters agree with those obtained by light-ion measurements. It is difficult to understand the phase shift required to fit the elastic and inelastic data simultaneously unless the collective form factor is only approximately correct in heavy-ion scattering or unless the optical model in the exit channel, corresponding to elastic scattering from excited states, requires modification.

1. Trinity University, San Antonio, Tex.
2. University of Texas, Austin, Tex.
3. University of Virginia, Charlottesville, Va.
4. G. R. Satchler, *Phys. Lett.* **33B**, 385 (1970); *Particles Nucl.* **2**, 265 (1971).
5. F. T. Baker and R. Tickle, *Phys. Lett.* **32B**, 47 (1970); *Phys. Rev.* **C5**, 544 (1972).
6. W. Brückner, J. G. Merdinger, D. Pelte, U. Smilansky, and K. Traxel, *Phys. Rev. Lett.* **30**, 57 (1973).
7. F. Videbaek, I. Chernov, P. R. Christensen, and E. E. Gross, *Phys. Rev. Lett.* **28**, 1072 (1972).
8. F. D. Becchetti, D. G. Kovar, B. G. Harvey, J. Mahoney, B. Mayer, and F. G. Pühlhofer, *Phys. Rev.* **C6**, 2215 (1972).

9. F. G. Perey, unpublished; C. Y. Wong and L. W. Owen, private communication.

10. P. D. Kunz, unpublished; L. W. Owen, private communication.

11. R. H. Bassel, G. R. Satchler, R. M. Drisko, and E. Rost, *Phys. Rev.* **128**, 2693 (1962).

12. A. R. Barnett and W. R. Phillips, *Phys. Rev.* **186**, 1205 (1969).

13. G. R. Satchler, H. W. Broek, and J. L. Yntema, *Phys. Lett.* **16**, 52 (1965); J. Saudinos, G. Vallois, and O. Beer, *Nucl. Sci. Appl.* **3**, No. 2, 22 (1967).

14. A. Scott and M. P. Fricke, *Phys. Lett.* **20**, 654 (1966).

15. N. P. Mather, Ph.D. thesis, University of Delhi, 1969 (unpublished); M. B. Lewis, *Nucl. Data* **B5**, 260 (1971).

16. J. Alster, *Phys. Rev.* **141**, 1138 (1966); *Phys. Lett.* **25B**, 459 (1967).

17. A. M. Bernstein, *Advan. Phys.* **3**, 325 (1969); *Phys. Lett.* **29B**, 332 (1969).

COULOMB-NUCLEAR INTERFERENCE IN $^{22}\text{Ne} + ^{88}\text{Sr}$ INELASTIC SCATTERING

E. E. Gross M. L. Halbert
H. G. Bingham D. C. Hensley
M. J. Saltmarsh

The most accurate information we have about the nucleus has generally come from the use of the electromagnetic force as a probe (e.g., electric multipole moments, charge radii). The interest, then, in observing interference phenomena between Coulomb and nuclear effects is the hope that our understanding of the Coulomb force will lead to a better understanding of the nuclear force. Such an interference phenomenon has been well known in light-ion inelastic excitation of collective nuclear states,^{1,2} but the effect has recently taken on a new interest with the advent and ready availability of heavy-ion beams. The reason for the new interest is simply that the interference effect is much more pronounced and well defined with heavy-ion beams than with light-ion beams because the de Broglie wavelength is smaller for heavy ions and thus represents a more sensitive probe of the nuclear surface.

As revealed by inelastic excitation of the first 2^+ states in ^{58}Ni , ^{88}Sr , and ^{142}Nd by ^{16}O beams,³ the interference pattern appeared to be located about 2.5 fm out from the nuclear touching distance [$1.25(A_1^{1/3} + A_2^{1/3})$ fm] and to have a width of only about 1 fm. It is therefore of interest to explore this structure with an even smaller de Broglie wavelength. We therefore looked at inelastic excitation of the 2^+ state in ^{88}Sr with a ^{22}Ne beam and at the same time observed the interference effect on the beam particle itself. The data consist of inelastic excitation functions at 175° lab for $^{88}\text{Sr}^*$ (1.835 MeV) and $^{22}\text{Ne}^*$ (1.275 MeV) shown in

Fig. 1. To facilitate analysis of these data with the DWBA collective model,⁴ we have also measured the elastic excitation function (Fig. 2) and an elastic angular distribution at 65.4 MeV (Fig. 3).

Concerning the inelastic excitation functions of Fig. 1, the following observations can be made regarding the data. At low beam energies and large distances of closest approach (scale at the top of Fig. 1), the inelastic cross section increases, in agreement with what would be expected from Coulomb excitation. Near 55 MeV lab energy ($D \approx 12.5$ fm) the nuclear force begins to play a role in the excitation process, and the interference pattern begins to develop and reach a minimum near 57 MeV for the level in ^{22}Ne and near 58 MeV for the level in ^{88}Sr . The general shape of the

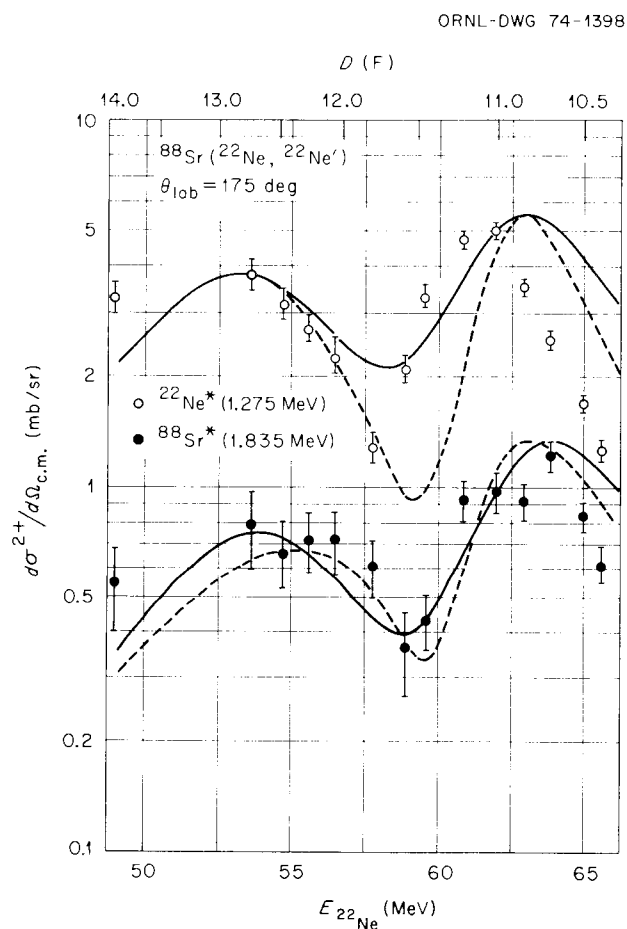


Fig. 1. Inelastic scattering excitation functions at 175° lab for the first 2^+ states in ^{88}Sr (lower figure) and ^{22}Ne (upper figure). The data are shown as points with error bars. The curves are DWBA collective-model predictions. The dashed curve is a calculation based on the potential NB5 of Table 1, whereas the solid curve is based on the potential OR1 of Table 1.

interference pattern for $^{88}\text{Sr}^*$ (1.835 MeV) obtained with inelastic scattering of ^{22}Ne beams is essentially the same as that observed with ^{16}O beams.³ The shift of the interference minimum of $^{22}\text{Ne}^*$ (1.275 MeV) relative to that for $^{88}\text{Sr}^*$ (1.835 MeV) will take on special significance when we discuss the DWBA analysis of these data. A similar shift has been noted for ^7Li and ^{18}O beams.⁵

To analyze these data with the DWBA collective model, we first determine an optical potential to represent the elastic scattering data. As we are inter-

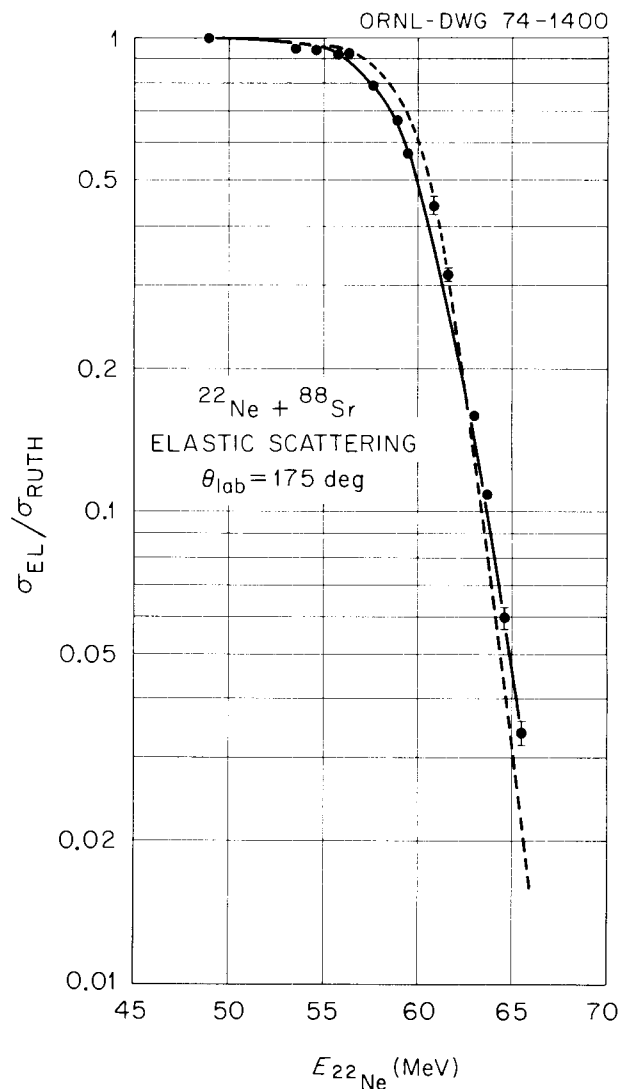


Fig. 2. Elastic scattering excitation function at 175° lab for $^{22}\text{Ne} + ^{88}\text{Sr}$. The data are represented by points with typical error bars. The dashed curve is an optical-model calculation using the parameters NB5 in Table 1. The solid curve is an optical-model calculation using the potential OR1 of Table 1.

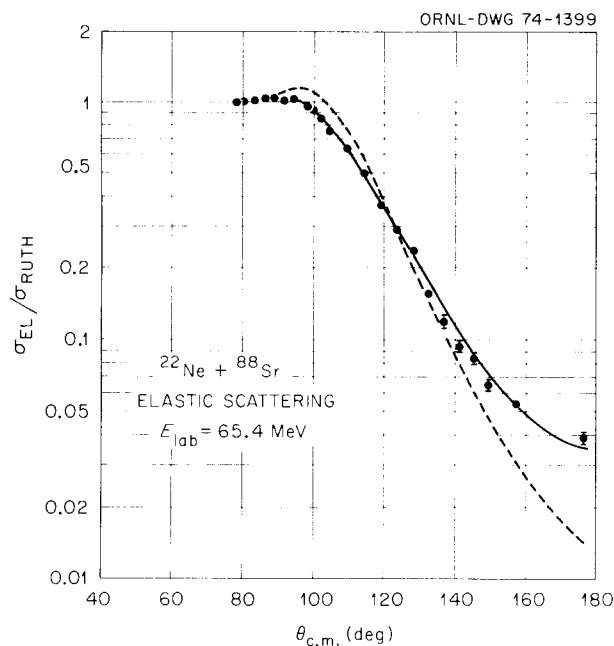


Fig. 3. Elastic angular distribution for $^{22}\text{Ne} + ^{88}\text{Sr}$ scattering. The data are shown as points with typical error bars. The dashed curve is an optical-model prediction for the potential NB5 of Table 1, and the solid curve is the prediction for potential OR1 of Table 1.

ested in comparing ^{22}Ne inelastic scattering with ^{16}O inelastic scattering from ^{88}Sr , we start with the $^{16}\text{O} + ^{88}\text{Sr}$ potential,³ which is compared with the data in Figs. 2 and 3 and shown by dotted curves. Searching on the parameters with the program GENOA⁶ yields the results shown by the solid curves. The two potentials (NB5 as the dotted curve; OR1 as the solid curve) are compared in Table 1. The collective model DWBA calculations with these potentials are shown as the dotted and solid curves in Fig. 1. Coulomb and nuclear deformation parameters have been adjusted to fit the relative magnitude of the two bumps.

Table 1. Optical-model parameters

	V (MeV)	r_0 (fm)	a (fm)	W (MeV)	r' (fm)	a' (fm)
NB5	23.73	1.3	0.568	3.30	1.4	0.323
OR1	21.54	1.3	0.56	9.54	1.4	0.36

The $^{88}\text{Sr}^*$ (1.835 MeV) inelastic excitation data are well represented by this calculation and confirm the success of the method for heavy-ion beams previously demonstrated for ^{16}O inelastic scattering from ^{58}Ni , ^{88}Sr , and ^{142}Nd targets,³ ^{16}O inelastic scattering from a ^{208}Pb target,⁷ and ^{11}B inelastic scattering from a

^{208}Pb target.⁸ The successful extension of the DWBA collective model to heavy-ion inelastic scattering would therefore seem to be well established, and therefore it is definitely a surprise that the method fails in accounting for the shift in the interference minimum and the general shape of the inelastic excitation function for the 1.275-MeV 2^+ collective state in ^{22}Ne (upper part of Fig. 1). This failure of the direct-reaction assumption suggests the importance of multistep processes for this reaction.

1. M. Samuel and U. Smilansky, *Phys. Lett.* **28B**, 318 (1968).
2. R. J. Pryor, F. Rösler, J. X. Saladin, and K. Alder, *Phys. Lett.* **32B**, 26 (1970).
3. P. P. Christensen, I. Chernov, E. E. Gross, R. Stockstad, and F. Videbaek, *Nucl. Phys.* **A207**, 433 (1973).
4. R. H. Bassel, G. R. Satchler, R. M. Drisko, and E. Rost, *Phys. Rev.* **128**, 2693 (1962).
5. K. Katori, C. L. Fink, G. C. Morrison, J. L. Yntema, and B. Zeidman, "Symposium on Heavy-Ion Transfer Reactions," Argonne Informal Report PHY-1973B, p. 557 (1973).
6. F. G. Perey, private communication.
7. F. D. Becchetti, D. G. Kovar, B. G. Harvey, J. Mahoney, B. Mayer, and F. G. Pühlhofer, *Phys. Rev.* **C6**, 2215 (1972).
8. J. L. C. Ford, K. S. Toth, D. C. Hensley, R. M. Gaedke, P. J. Riley, and S. T. Thornton, *Phys. Rev.* **C8**, 1912 (1973).

HEAVY-ION TRANSFER REACTIONS

SINGLE-NUCLEON TRANSFER REACTIONS INDUCED BY ^{11}B IONS ON ^{208}Pb

J. L. C. Ford, Jr. L. W. Owen¹
 K. S. Toth D. M. DeVries²
 G. R. Satchler R. M. Gaedke³
 D. C. Hensley P. J. Riley⁴
 S. T. Thornton⁵

Elastic and inelastic scattering and transfer reactions between heavy ions are peripheral phenomena. We need to understand these first steps in the interaction between two heavy ions before we can use them as tools to do nuclear spectroscopy and before we can fully appreciate the more complicated processes that can take place. Because of this, our initial efforts have concentrated on targets of nuclei whose spectroscopy is already quite well understood, namely, those with doubly closed shells.

Single-nucleon heavy-ion transfer reactions are dominated by kinematic effects below the Coulomb barrier (see, e.g., ref. 6). At energies well above the barrier, kinematic effects may still be important, but one expects the reaction mechanism to be direct and

interpretable in terms of a DWBA analysis. Measurements involving single-nucleon transfer with ^{12}C ions,⁷ ^{11}B ions,⁸ and ^{16}O ions⁹ on ^{208}Pb at high bombarding energies gave angular distributions which were structureless and single-peaked at the angle corresponding to the classical Rutherford orbit for grazing collisions. Despite this classical nature, systematic differences were observed⁷ between neutron pickup and proton stripping with heavy ions. For ^{12}C ions incident on ^{208}Pb , the peak angles for neutron pickup shifted to higher values with increasing excitation energy in the residual nucleus, in contrast to proton stripping, where the peak angle remained constant.⁷ This effect, as well as the possible j and L dependence of heavy-ion reactions which has been observed in (^{12}C , ^{11}B) and (^{16}O , ^{15}N) reactions,¹⁰ is not reproduced by standard distorted-wave treatments.

Recoil effects in particular appear to be important and must be taken into account to describe the reaction adequately by a DWBA treatment.¹¹ A more complete understanding of heavy-ion single-nucleon transfer reactions is thus not only necessary to reliably extract spectroscopic information from such reactions, but also in order to form the basis for understanding more complicated heavy-ion reactions. In addition, two-step and other indirect processes may be important in single-nucleon transfer with heavy ions, permitting the excitation of states not accessible with light-ion reactions.¹²

We report here an investigation of transfer reactions induced by ^{11}B incident on ^{208}Pb at an incident energy of 72.2 MeV. All four single-nucleon transfer reactions – (^{11}B , ^{10}B), (^{11}B , ^{12}B), (^{11}B , ^{10}Be), and (^{11}B , ^{12}C) – were observed, and angular distributions for final states in ^{209}Pb , ^{207}Pb , ^{209}Bi , and ^{207}Tl were measured. In some instances, particle groups corresponding to excitation of the outgoing light reaction product were also observed. A DWBA analysis including effects due to recoil¹¹ was then made, and spectroscopic factors were extracted.

Experimental Results

In the present experiment, 72.2-MeV ^{11}B ions were used to bombard a 100- $\mu\text{g}/\text{cm}^2$ -thick ^{208}Pb target. Reaction products were detected at the focal plane of an Elbek spectrograph using a 60-cm-long position-sensitive proportional counter of the Borkowski-Kopp design.¹³ In addition to determining the position of the detected particle along the focal plane, it was also possible to obtain the particle's energy loss in the counter. This ΔE signal served to identify the particle type.

The high-energy portions of the energy spectra for the neutron pickup and stripping reactions, $^{208}\text{Pb}(^{11}\text{B}, ^{12}\text{B})^{207}\text{Pb}$ and $^{208}\text{Pb}(^{11}\text{B}, ^{10}\text{B})^{209}\text{Pb}$, are shown in Fig. 1 for a laboratory angle of 55° . The proton pickup and stripping reactions, $^{208}\text{Pb}(^{11}\text{B}, ^{12}\text{C})^{207}\text{Tl}$ and $^{208}\text{Pb}(^{11}\text{B}, ^{10}\text{Be})^{209}\text{Bi}$, are shown in Figs. 2 and 3 for laboratory angles of 52.5° and 47.5° respectively. All four reactions predominantly populate single-particle or hole states.¹⁴ In Fig. 3, strong peaks are seen at energies consistent with the excitation of the emitted ^{10}Be nucleus to its first 2^+ level at 3.37 MeV, along with excitations in ^{209}Bi . Note that these peaks are

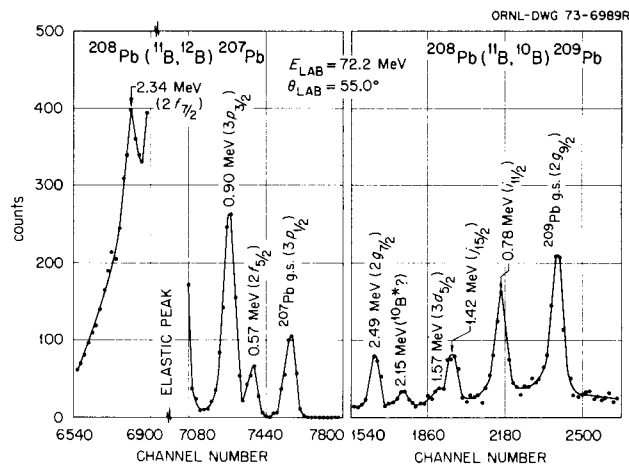


Fig. 1. Energy spectra measured at 55° (lab) and an incident energy of 72.2 MeV for the (^{11}B , ^{12}B) and (^{11}B , ^{10}B) reactions on ^{208}Pb , leading to states in ^{207}Pb and ^{209}Pb respectively.

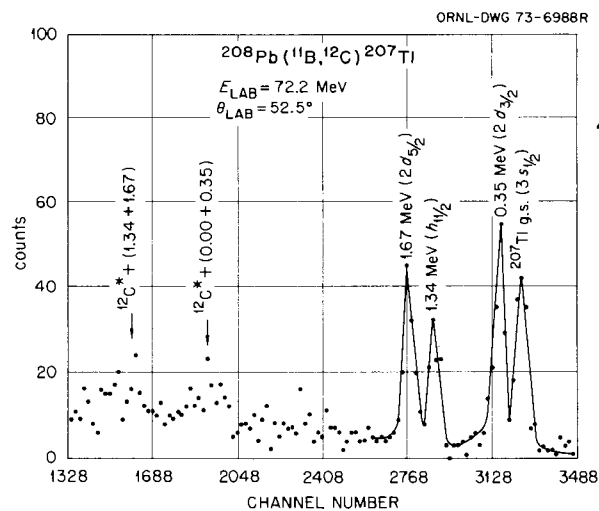


Fig. 2. An energy spectrum measured at 52.5° (lab) and an incident energy of 72.2 MeV for the (^{11}B , ^{12}C) reaction on ^{208}Pb , leading to states in ^{207}Tl .

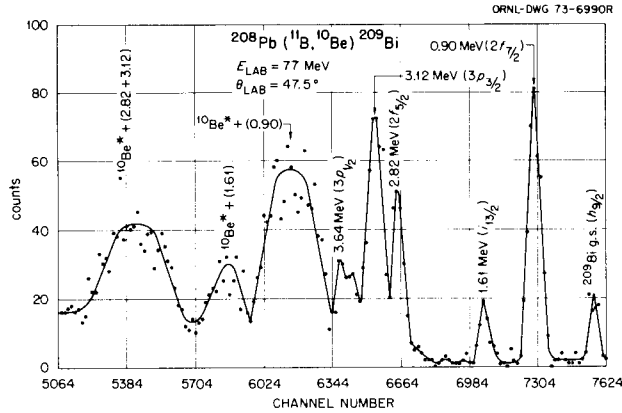


Fig. 3. A high-energy portion of the energy spectrum measured at 47.5° (lab) and an incident energy of 72.2 MeV for the $(^{11}\text{B}, ^{10}\text{Be})$ reaction on ^{208}Pb , leading to states in ^{209}Bi .

Doppler-broadened as a result of gamma-ray emission from the 3.37-MeV state in ^{10}Be . There is also evidence in Fig. 2 for weak groups corresponding to ^{12}C particles being left in their first excited state at 4.43 MeV.

Angular distributions were determined for the strongly excited states, and these are shown in Figs. 4–7. Curves shown in these figures are the results of finite-range DWBA calculations that take recoil effects into account and use optical potentials obtained by fitting elastic data for ^{11}B and ^{12}C on ^{208}Pb . The spectroscopic factors obtained for the strong transitions are consistent with their exciting largely single-particle or single-hole states. Details of the experiment and its analysis are being prepared for publication. Some aspects of the DWBA analysis are discussed elsewhere in this report.

1. Computer Sciences Division.
2. University of Washington, Seattle, Wash.
3. Trinity University, San Antonio, Tex.
4. University of Texas, Austin, Tex.
5. University of Virginia, Charlottesville, Va.
6. R. M. Gaedke, K. S. Toth, and I. R. Williams, *Phys. Rev.* **141**, 966 (1966).
7. J. S. Larsen, J. L. C. Ford, Jr., R. M. Gaedke, K. S. Toth, J. B. Ball, and R. L. Hahn, *Phys. Lett.* **92B**, 205 (1972).
8. A. Anyas-Weiss, J. Becker, T. A. Belote, J. C. Cornell, P. S. Fisher, P. H. Hudson, A. Menchaca-Rocha, A. D. Panagiotou, and D. K. Scott, *Phys. Lett.* **45B**, 231 (1973).
9. D. G. Kovar, B. G. Harvey, F. D. Becchetti, J. Mahoney, D. L. Henrie, H. Homeyer, W. von Oertzen, and M. A. Nagarajan, *Phys. Rev. Lett.* **30**, 1075 (1973).
10. D. G. Kovar, F. D. Becchetti, B. G. Harvey, F. Pülhoffer, J. Mahoney, D. W. Miller, and M. S. Zisman, *Phys. Rev. Lett.* **29**, 1023 (1972).

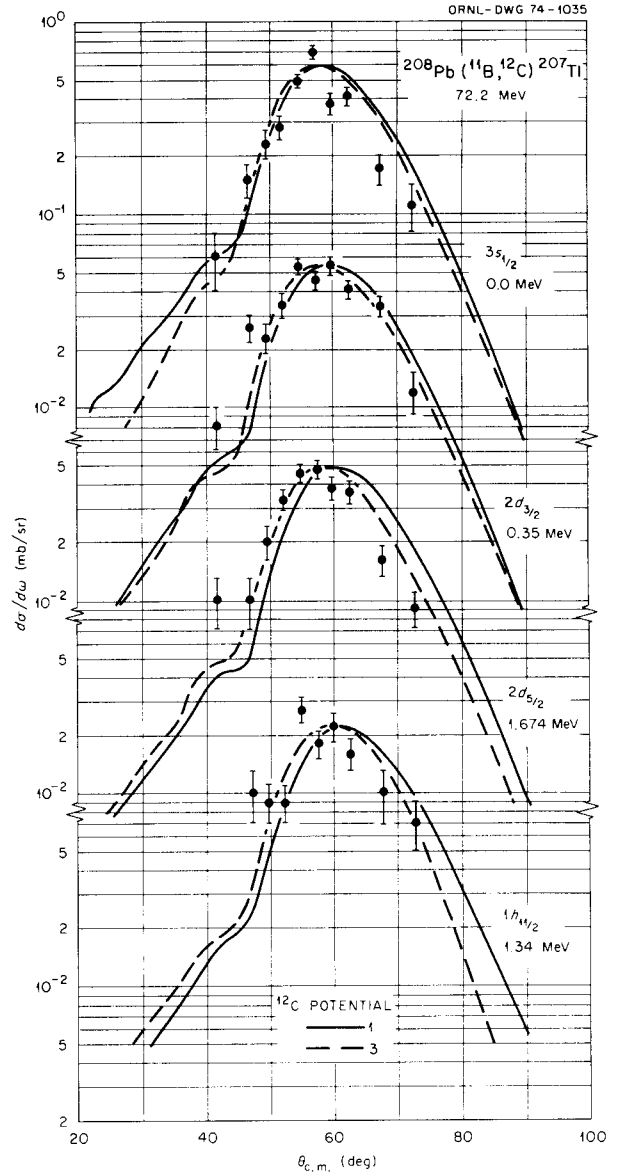


Fig. 4. Angular distributions for various final states populated in the reaction $^{208}\text{Pb}(^{11}\text{B}, ^{12}\text{C})^{207}\text{Tl}$. Curves are the results of DWBA calculations.

11. R. M. DeVries and K. I. Kubo, *Phys. Rev. Lett.* **30**, 325 (1973); R. M. DeVries, *Phys. Rev.* **C8**, 951 (1973).
12. S. Landowne, R. A. Broglio, and R. Liotta, *Phys. Lett.* **43B**, 160 (1973).
13. C. J. Borkowski and M. K. Kopp, *Rev. Sci. Instrum.* **39**, No. 10, 1515 (1968); C. J. Borkowski and M. K. Kopp, *IEEE Trans. Nucl. Sci.* **NS-17**, No. 3, 340 (1970).
14. *Nucl. Data Sheets* **5**, 205 (1971).

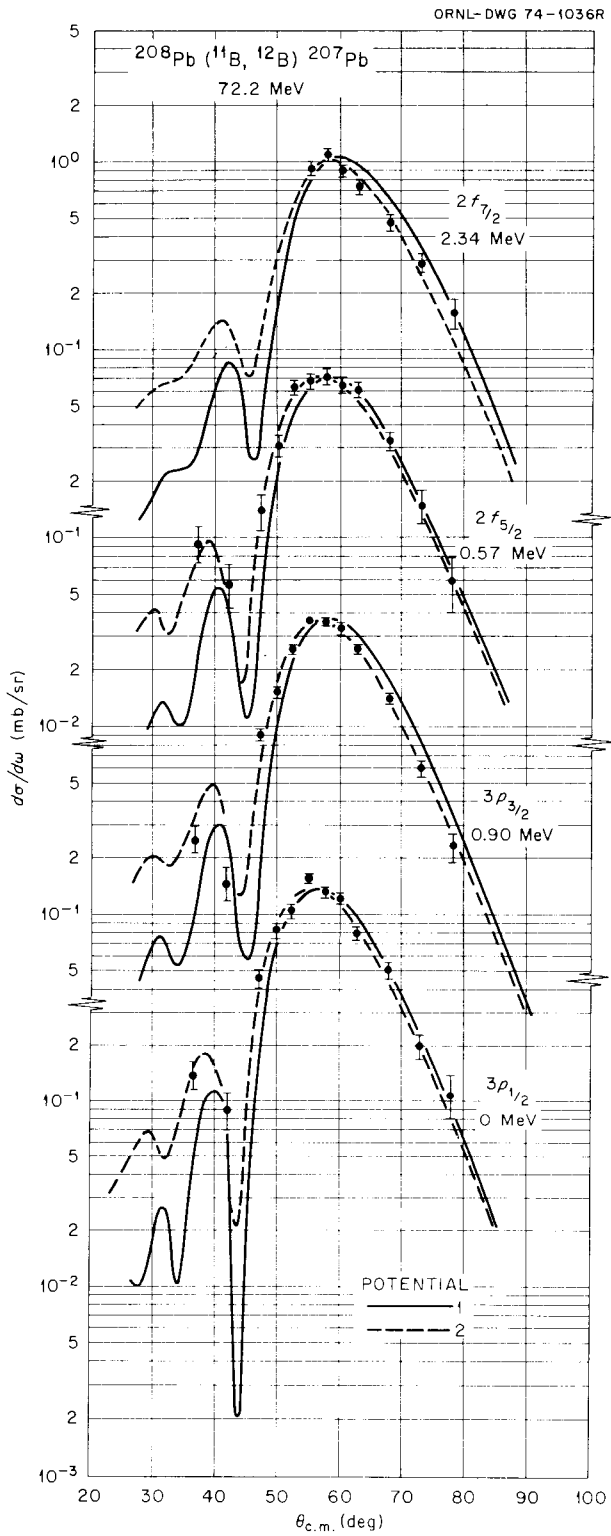


Fig. 5. Angular distributions for various final states populated in the reaction $^{208}\text{Pb}(^{11}\text{B}, ^{12}\text{B})^{207}\text{Pb}$. Curves are the results of DWBA calculations.

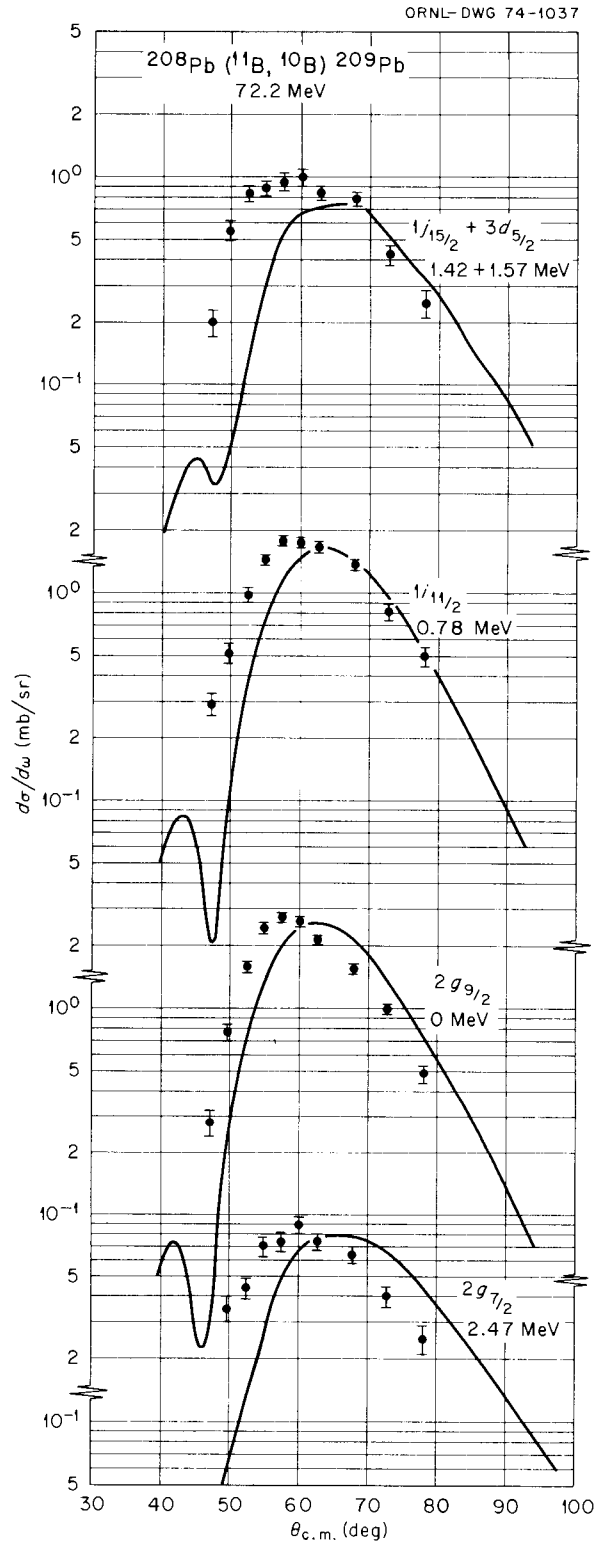


Fig. 6. Angular distributions for various final states populated in the reaction $^{208}\text{Pb}(^{11}\text{B}, ^{10}\text{B})^{209}\text{Pb}$. Curves are the results of DWBA calculations.

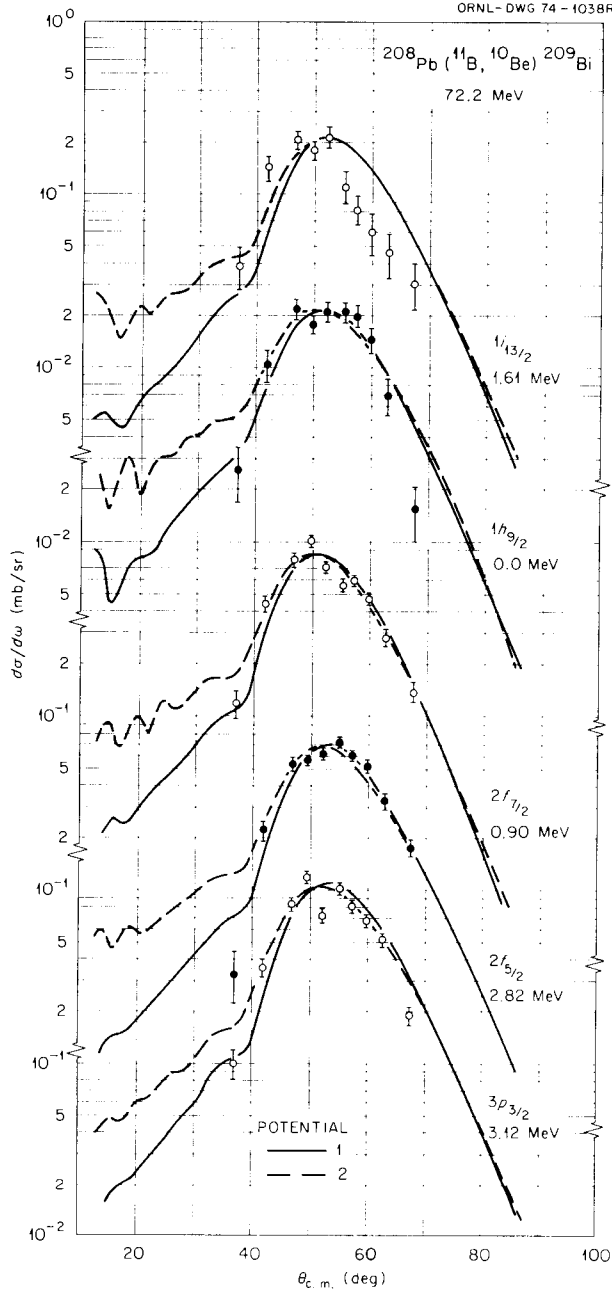


Fig. 7. Angular distributions for various final states populated in the reaction $^{208}\text{Pb}(^{11}\text{B}, ^{10}\text{Be})^{209}\text{Bi}$. Curves are the results of DWBA calculations.

some hope for the future.⁴ Most of the effort to date has been focused on the reaction mechanisms involved, for example, whether compound-nucleus formation or some few-step direct process describes a particular reaction.⁵ For reactions near the Coulomb barrier the semiclassical picture of a projectile following a well-defined trajectory⁶ is used to describe the gross features of the transfer process.⁷ The concepts of grazing incidence, Q matching, and angular momentum matching are easy to visualize and apply when the de Broglie wavelength of the projectile is small. As the projectile mass is increased, this semiclassical approach becomes more appropriate, but the difficulties of particle identification become more severe if conventional light-ion techniques are employed. We have avoided this difficulty in the present work by using prompt deexcitation gamma rays to identify the final nucleus, a technique previously used by a group at Munich⁸ to study four-nucleon transfer.

Two-nucleon transfer reactions were studied using ^{20}Ne beams from the ORIC on targets of ^{154}Sm , ^{160}Gd , and ^{162}Dy . Gammas from the known rotational bands of the final nuclei were detected in coincidence with the backscattered particle. Excitation functions were obtained over an energy range spanning the Coulomb barrier, corresponding to semiclassical grazing incidence.

There is a very high probability for Coulomb excitation of the rotational nuclei in both entrance and exit channels of the systems which were investigated. We therefore assume that most of the transfer cross section results in a cascade down the rotational band of the final nucleus. Naively one may envisage the interaction proceeding in three stages: Coulomb excitation in the entrance channel, transfer of two nucleons as the systems touch, and finally Coulomb excitation in the exit channel.

Preliminary results are shown in Figs. 1–3, where we have plotted the excitation functions for the yield of high-energy backscattered ions coincident with gamma rays from the $4^+ \rightarrow 2^+$ transition in the final nucleus. For all targets we see events corresponding to inelastic scattering, two-neutron pickup from the target ($+2n$), and two-proton stripping ($-2p$). Two-neutron stripping

HEAVY-ION-INDUCED TWO-NUCLEON TRANSFER

M. J. Saltmarsh	R. K. Cole ¹
E. E. Gross	G. Hagemann ²
M. L. Halbert	L. Riedinger ³

Heavy-ion-induced transfer reactions have not generally proved very useful as spectroscopic tools as compared with the equivalent light-ion reactions, although recent successes of DWBA calculations offer

and two-proton pickup were not seen. The excitation functions for the transfer reactions exhibit the usual bell-shaped form, except for the case of the $-2p$ reaction on ^{160}Gd (Fig. 2), where the transfer yield is obscured by the presence of a 2.6% ^{158}Gd impurity in our target.

The absence of $-2n$ or $+2p$ events may be accounted for by Q -value effects. The optimum Q values for a reaction near the Coulomb barrier may be estimated from the formula⁹

$$Q_{\text{opt}} = E_i \left(\frac{Z_f Z_f}{Z_i^2} - 1 \right),$$

where E_i is the relative energy of the initial system. Table 1 shows the values of Q_{opt} calculated for a laboratory energy of 85 MeV compared with threshold Q values from the mass tables.¹⁰ The $-2n$ and $+2p$ reactions can only occur if there is a large mismatch in Q value.

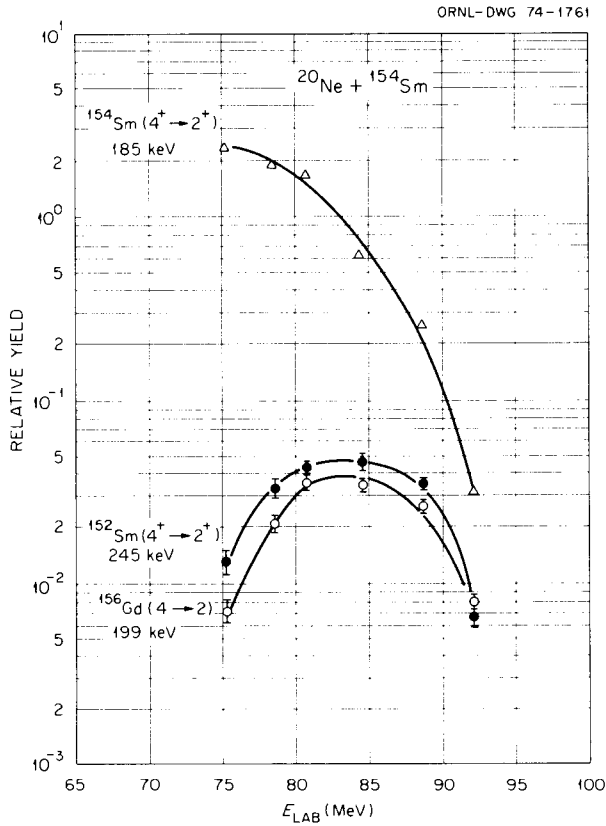


Fig. 1. Particle-gamma coincidence yields as a function of energy for the $^{20}\text{Ne} + ^{154}\text{Sm}$ system. The solid lines are drawn to guide the eye. No correction has been made for variations in gamma detection efficiency.

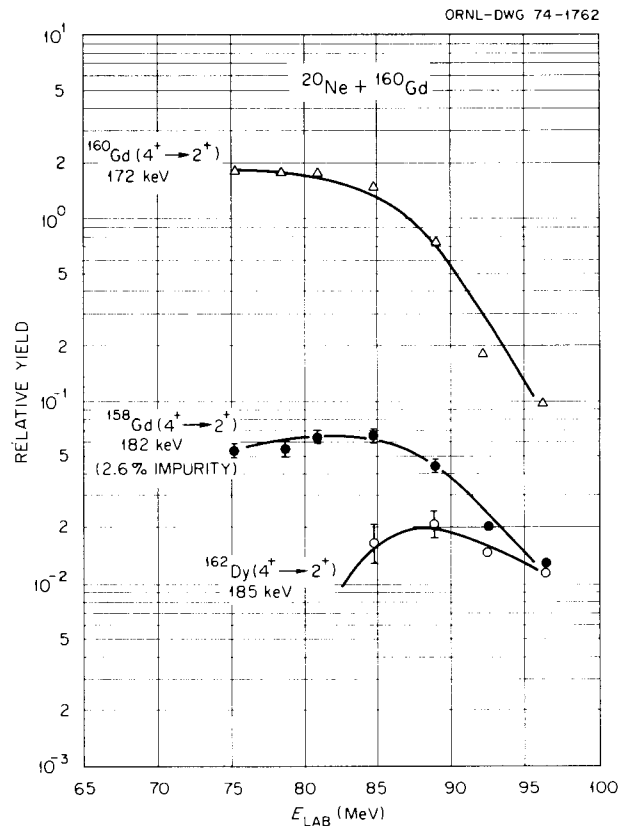


Fig. 2. Results for the $^{20}\text{Ne} + ^{160}\text{Gd}$ system. See Fig. 1 for further details. The $+2n$ yield is largely obscured by a 2.6% ^{158}Gd target impurity.

Table 1. Comparison between threshold and optimum Q values for ^{20}Ne projectiles

Target	$2n$ stripping		$2n$ pickup		$2p$ stripping		$2p$ pickup	
	Q	Q_{opt}	Q	Q_{opt}	Q	Q_{opt}	Q	Q_{opt}
^{154}Sm	-15.4	0	3.3	0	-6.2	-13.1		+12.1
^{160}Gd	-15.9	0	3.7	0	-6.0	-13.2		12.3
^{162}Dy	-16.1	0	1.0	0	-10.1	-13.3	-8.4	12.4

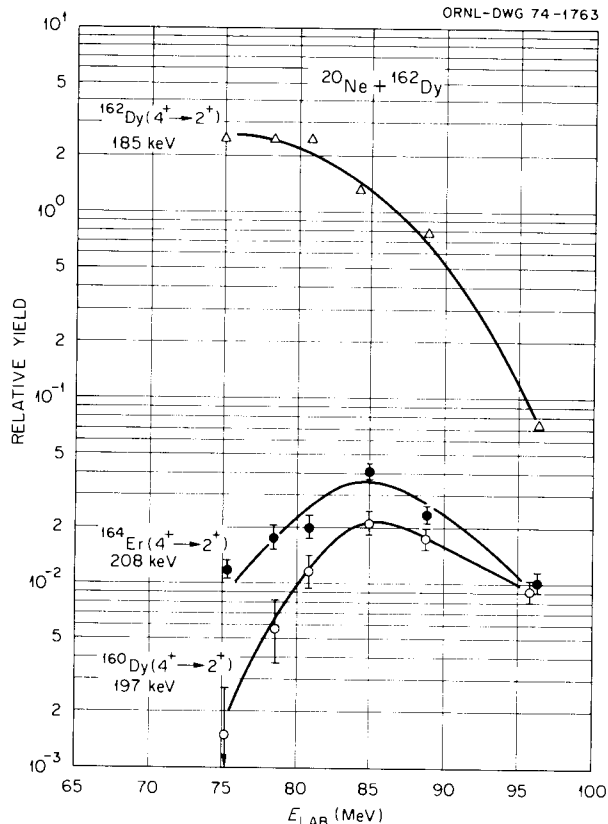


Fig. 3. Results for the $^{20}\text{Ne} + ^{162}\text{Dy}$ system. See Fig. 1 for further details.

In further analysis of the data, we hope to extract the energy dependence of Q_{opt} for the three systems.

1. University of Southern California, Los Angeles, Calif.
2. Niels Bohr Institute, Copenhagen, Denmark.
3. Consultant from the University of Tennessee, Knoxville, Tenn.
4. See, for example, R. DeVries and K. Kubo, *Phys. Rev. Lett.* **30**, 325 (1973); J. B. Ball, O. Hansen, J. S. Larsen, D. Sinclair, and F. Videbaek (to be published).
5. S. Kahana, *Proceedings of the Argonne Symposium on Heavy-Ion Transfer Reactions*, p. 385, Argonne National Laboratory (1973).
6. G. Breit, M. H. Hull, and R. L. Gluckstern, *Phys. Rev.* **87**, 74 (1952).
7. See, for example, G. Breit and M. E. Ebel, *Phys. Rev.* **103**, 679 (1956); H. J. Körner, G. C. Morrison, L. R. Greenwood, and R. H. Siemssen, *Phys. Rev. C* **7**, 107 (1973).
8. H. Bohn, G. Daniel, M. R. Maier, P. Kienle, J. G. Cramer, and D. Proetel, *Phys. Rev. Lett.* **29**, 1337 (1972).
9. P. Buttle and L. Goldfarb, *Nucl. Phys.* **78**, 409 (1966).
10. J. H. E. Mattauch, W. Thiele, and A. H. Wapstra, *Nucl. Phys.* **64**, 1 (1965).

$(^6\text{Li},t)$ AND $(^6\text{Li},^3\text{He})$ REACTIONS ON ^{12}C AT 60 MeV

H. G. Bingham E. Newman
M. L. Halbert K. W. Kemper¹
D. C. Hensley L. A. Charlton¹

Lithium-induced three-nucleon transfer reactions have been successfully used to identify analog states in mirror nuclei in low-energy (≤ 24 MeV) studies of p and sd shell nuclei.² These studies suffer from two complications. Compound-nucleus effects may be important, and barrier inhibition in the exit channel places an uncertainty in the relative population strengths of high-spin members of a particular configuration coupling. An intermediate-energy study (36 MeV) of the $^{16}\text{O}(^6\text{Li},t)$ reaction³ indicated that both these difficulties could be eased with higher-energy studies.

The studies^{2,3} of $(^6\text{Li},t)$ and $(^6\text{Li},^3\text{He})$ reactions indicated a strong selectivity for final-state configurations in which a three-nucleon cluster was transferred. Reactions with higher-energy ^6Li should preferentially excite higher-spin members of such a configuration and populate them much more strongly than states having the same spin coupling but different configuration. Consequently, we have made a study of the $^{12}\text{C}(^6\text{Li},t)$ and $^{12}\text{C}(^6\text{Li},^3\text{He})$ reactions at 60 MeV.

The beam of 60-MeV $^6\text{Li}^{2+}$ ions was produced by the Oak Ridge Isochronous Cyclotron. The maximum beam current on target was about 200 nA (station 18). A conventional two-counter telescope was used for particle detection, and a two-dimensional array of ΔE vs $E + \Delta E$ served for particle identification. The targets used were $250\text{-}\mu\text{g}/\text{cm}^2$ natural carbon. The energy resolution was about 200 keV. The uncertainty in excitation energy of the states observed with this system is estimated to be about 200 keV. The elastic scattering was measured in a separate experiment.

Energy spectra for the $(^6\text{Li},^3\text{He})$ and $(^6\text{Li},t)$ reactions at 10° are shown in comparison in Fig. 1. The correspondence of mirror states in the two reactions is striking. Strongly populated states extend to over 15 MeV in excitation and agree very well in relative strength with states at similar excitation energies from the analogous $(^10\text{B},^7\text{Li})$ and $(^10\text{B},^7\text{Be})$ reactions.⁴ The cross sections for the ^6Li -induced reactions are about five times larger than for the ^{10}B reactions.

The $(^6\text{Li},^3\text{He})$ and $(^6\text{Li},t)$ reactions on ^{12}C at this energy should strongly populate high-spin members of three-particle, four-hole ($3p\text{-}4h$) states, particularly those with $(d_{5/2})^3$ configuration, and $2p\text{-}3h$ states in $^{15}\text{N}\text{-}^{15}\text{O}$. The level ordering of states with $(d_{5/2})^3$ configuration ($J_{\text{max}} \leq 1\frac{3}{2}$) should, from weak-

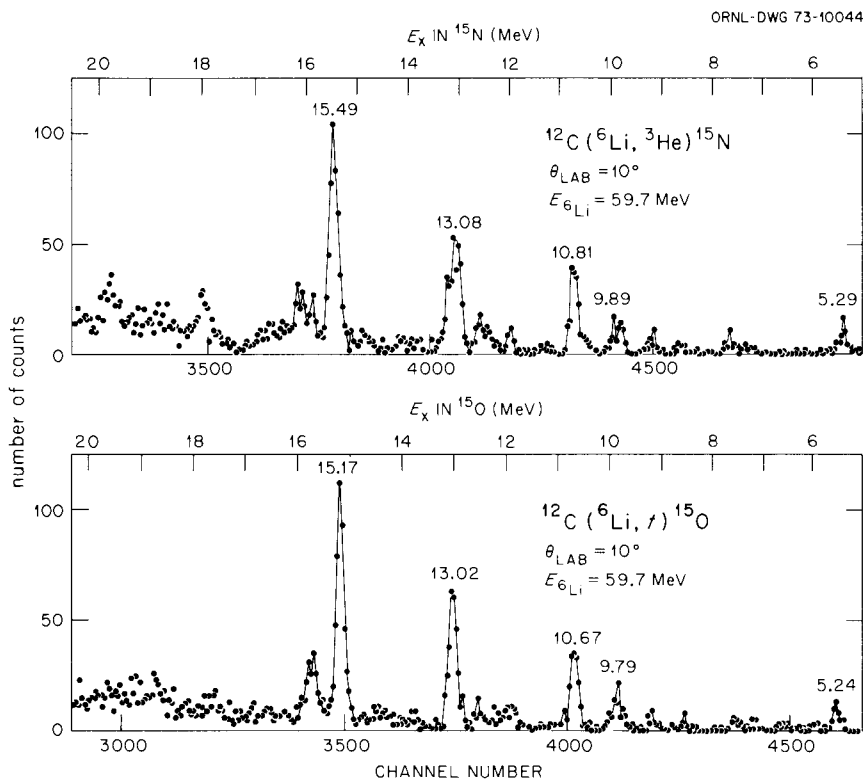


Fig. 1. Energy spectra from the $^{12}\text{C}(^6\text{Li},^3\text{He})^{15}\text{N}$ and $^{12}\text{C}(^6\text{Li},t)^{15}\text{O}$ reactions obtained at a laboratory angle of 10° . Excitation energy in the residual nucleus is plotted on the top scale for each reaction.

coupling arguments, resemble the $K = 0^+$ ground-state rotational band in $A = 19$ ($1/2^+$, $5/2^+$, $3/2^+$, $9/2^+$, $13/2^+$, $7/2^+$, $11/2^+$). The relative intensities should be proportional to $2J_f + 1$.

The states at 15.49 and 15.17 MeV in ^{15}N and ^{15}O , respectively, because of their strength relative to other observed states, would appear to be the $13/2^+$ members of the $(d_{5/2})^3$ configuration. The 13.08- and 13.02-MeV states have previously been identified^{4,5} as $[(d_{5/2})^2(p_{1/2})^{-3}]_{11/2^-}$ states. The candidates for the $9/2^+$ member of the $(d_{5/2})^3$ configuration are the 10.81- and 10.67-MeV states in ^{15}N and ^{15}O respectively. From a recent measurement of the $^{12}\text{C}(^7\text{Li},\alpha)$ reaction it has been suggested that a strongly populated state at 12.56 MeV in ^{15}N is a more likely candidate,⁶ but this state is weakly populated in our $(^6\text{Li},^3\text{He})$ measurement. A more definitive study of the gamma-decay systematics of this state is presently being carried out.⁷

A recent cluster-model calculation⁸ for ^{15}N based on an inert ^{12}C core plus a triton gives good agreement with the experimentally observed ordering of the suspected $(d_{5/2})^3_{13/2^+,9/2^+}$ and $[(d_{5/2})^2(p_{1/2})^{-3}]_{11/2^-}$ states

(see Fig. 2). The $(d_{5/2})^3_{11/2^+}$ and $[(d_{5/2})^2(p_{1/2})]_{9/2^-}$ states are predicted to occur at 25 MeV in excitation and are beyond the range of observation in the $(^6\text{Li},^3\text{He})$ reaction (however, a known $9/2^-$ state⁵ at 11.95 MeV is very weakly populated in this reaction).

The number of $A = 15$ levels known at these excitation energies is enormous. One wonders whether closely spaced states are being populated with comparable strength. Also, the excitation energies of the strong groups inferred from the ^{10}B reactions⁴ differ by several hundred keV from the energies obtained from the ^6Li data. Accordingly, we have made spectrograph measurements (40 keV resolution) of the $(^6\text{Li},t)$ reaction at 5° , 10° , and 15° . Figure 3 shows the 10° spectrum; analysis of the data is in progress.

1. Florida State University, Tallahassee, Fla.
2. H. G. Bingham, H. T. Fortune, J. D. Garrett, and R. Middleton, *Phys. Rev. Lett.* **26**, 1448 (1971); H. G. Bingham, H. T. Fortune, J. D. Garrett, and R. Middleton, *Phys. Rev. C* **7**, 57 (1973); C. H. Holbrow, H. G. Bingham, and J. D. Garrett, *Bull. Amer. Phys. Soc.* **17**, 465 (1972).
3. A. D. Panagiotou and H. E. Gove, *Nucl. Phys.* **A196**, 145 (1972).

ORNL-DWG 74-1720

19.78		20.0	7 $\frac{1}{2}$
18.00		17.25	5 $\frac{1}{2}$
16.16		15.70	13 $\frac{1}{2}$
15.49	15.82 13 $\frac{1}{2}$		
13.08	11 $\frac{1}{2}$	13.20	11 $\frac{1}{2}$
12.60		12.85	3 $\frac{1}{2}$
11.95		11.55	1 $\frac{1}{2}$
10.81	(9 $\frac{1}{2}$)	10.93	9 $\frac{1}{2}$
9.89	(7 $\frac{1}{2}$)	9.95	7 $\frac{1}{2}$
9.15		8.65 8.95 5 $\frac{1}{2}$	3 $\frac{1}{2}$
7.62		8.60	1 $\frac{1}{2}$
5.29	5 $\frac{1}{2}$		

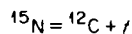
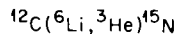


Fig. 2. Comparison of some experimentally observed states in the $^{12}\text{C}(^6\text{Li}, ^3\text{He})$ reaction with cluster-model calculations assuming $^{15}\text{N} = ^{12}\text{C} + t$. The calculated positive parity states correspond to a $(d_{5/2})^3$ configuration, and the calculated negative parity states correspond to a $(d_{5/2})^2(p_{1/2})^{-3}$ configuration.

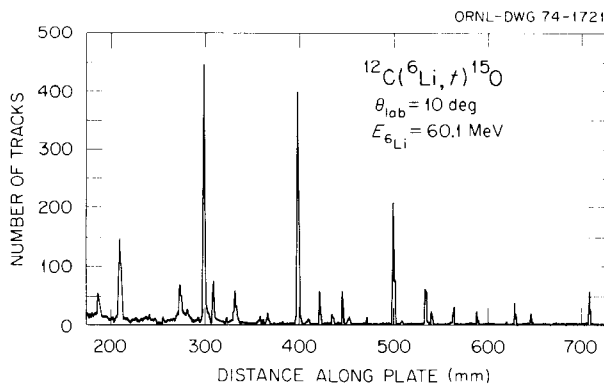


Fig. 3. Energy spectrum from the $^{12}\text{C}(^6\text{Li}, t)^{15}\text{O}$ reaction obtained at a laboratory angle of 10° using a broad-range spectrograph with kinematic compensation in the focal plane.

4. K. Nagatani, D. H. Youngblood, R. Kenefick, and J. Bronson, *Phys. Rev. Lett.* **31**, 250 (1973).

5. C. C. Lu, M. S. Zisman, and B. G. Harvey, *Phys. Rev.* **186**, 1086 (1969).

6. I. Tserruya, B. Rosner, and K. Bethge, *Nucl. Phys.* **A213**, 22 (1973).

7. L. K. Fifield, private communication (1974).

8. J. P. Vary, *Bull. Amer. Phys. Soc.* **18**, 1414 (1973), and private communication (1974).

TRANSFER AND COMPOUND-NUCLEAR REACTIONS IN THE INTERACTIONS OF ^{12}C WITH ^{239}Pu AND ^{238}U

R. L. Hahn¹ K. S. Toth
P. F. Dittner¹ O. L. Keller¹

Studies of the interactions of heavy ions (H.I.) with heavy elements, besides adding to our knowledge of the different mechanisms operative² in reactions such as $(\text{H.I.}, xn)$ and $(\text{H.I.}, \alpha yn)$ and of the ensuing competition between particle emission and fission,³ also have application in attempts to produce and identify new nuclides. For example, knowledge of the details of the angular distributions of recoil nuclei has been used as support for identification of transactinide elements.⁴

As reported previously,⁵ range and angular distributions were measured at ORIC for the reactions $^{239}\text{Pu}(^{12}\text{C}, \alpha 2n \text{ and } 3n)$ and $^{238}\text{U}(^{12}\text{C}, 5n \text{ and } 6n)$, leading to the radioactive products ^{245}Cf and ^{244}Cf . Figure 1 shows the centroids of the various range distributions plotted vs bombarding energy. The data for the $\text{U}(^{12}\text{C}, xn)$ reactions, as expected, seem indicative of compound nuclear reactions; full-momentum transfer from projectile to compound system requires a linear dependence of recoil energy (and thus of range if R is proportional to E) upon bombarding energy. The two straight lines for $\text{U} + \text{C}$ are ranges calculated with the range-energy relations of Northcliffe and Schilling⁶ and of Steward⁷ and reflect differences in their treatments of nuclear stopping.

The $^{239}\text{Pu} + ^{12}\text{C}$ data in Fig. 1 show clearly that compound processes are not involved in the $(^{12}\text{C}, \alpha xn)$ reactions. The recoil ranges are large at low energies, being about 2 times as large as that expected for full-momentum transfer at 67 MeV, and decrease rapidly to low values at high energies.

Similar differences between the reactions with ^{238}U and ^{239}Pu are seen in the recoil angular distributions shown in Fig. 2. For $^{238}\text{U} + ^{12}\text{C}$, the distributions are forward peaked and decrease rapidly with increasing angle; this behavior again is characteristic of compound-nuclear reactions. The vertical dashed lines in the figure

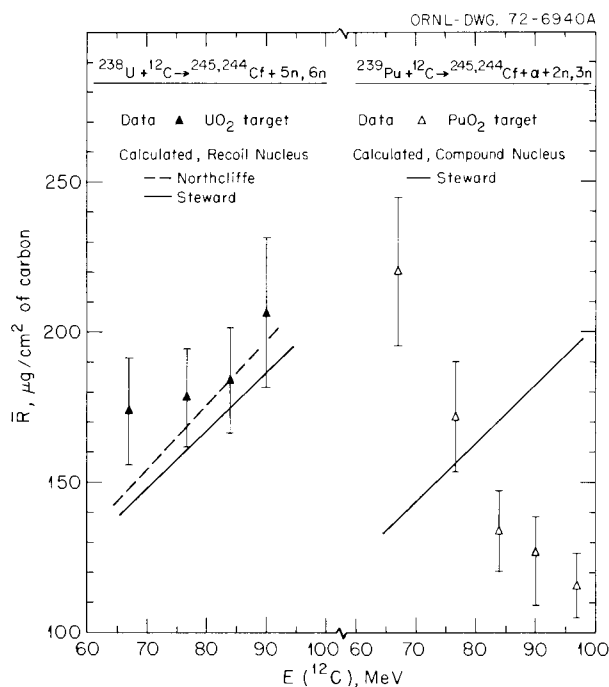


Fig. 1. Average ranges \bar{R} vs bombarding energy for ^{245}Cf and ^{244}Cf arising from the reactions $^{238}\text{U} + ^{12}\text{C}$ and $^{239}\text{Pu} + ^{12}\text{C}$. The straight lines are ranges calculated for compound-nucleus reactions.

show the maximum angles at which the californium nuclides should be observed, as calculated from reaction kinematics; the data obtained at angles larger than these limiting angles are indicative of straggling that occurs in the targets (with thicknesses less than $200 \mu\text{g}/\text{cm}^2$).

The angular distributions for $^{239}\text{Pu} + ^{12}\text{C}$ are rather broad and display a maximum at about 17° in the measurements done at 75.5 and 83 MeV. These data, together with the ranges shown in Fig. 1, are thought to be characteristic of transfer reactions and, in particular, of the transfer of a beryllium cluster from the ^{12}C projectile to the target nucleus. Model-dependent calculations are presently being carried out for such transfer processes.

1. Chemistry Division.

2. A. Zucker and K. S. Toth, "Heavy-Ion Induced Nuclear Reactions" in *Nuclear Chemistry*, vol. 1, Academic Press, New York, 1968.

3. T. Sikkeland et al., *Phys. Rev.* **169**, 1000 (1968); **172**, 1232 (1968).

4. G. N. Flerov et al., JINR (Dubna) preprint P7-5164 (1970).

5. R. L. Hahn et al., *Phys. Div. Annu. Progr. Rep. Dec. 31, 1972*, ORNL-4844, p. 89.

6. L. C. Northcliffe and R. F. Schilling, *Nucl. Data Tables A7*, 233 (1970).

7. P. G. Steward, University of California report UCRL-18127 (1968).

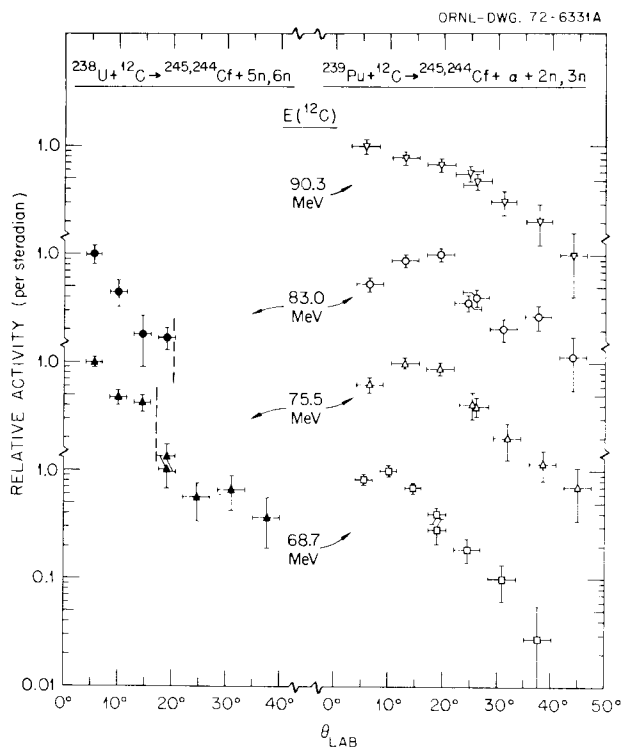


Fig. 2. Angular distributions of the recoil nuclei ^{245}Cf and ^{244}Cf arising from the reactions $^{238}\text{U} + ^{12}\text{C}$ and $^{239}\text{Pu} + ^{12}\text{C}$. The vertical dashed lines show the maximum angles at which the californium nuclides should be observed, as calculated from the reaction kinematics, and so indicate the degree of straggling in the targets.

HEAVY-ION FISSION AND FUSION

SPONTANEOUS FISSION ISOMER EXCITATION IN THE ^{20}Ne ION COULOMB EXCITATION OF ^{239}Pu ?

C. E. Bemis, Jr.¹ Robert L. Ferguson¹
 Franz Plasil E. E. Gross
 A. Zucker²

Fission induced by the time-dependent electromagnetic field of a passing ion is an intriguing possibility that has been investigated theoretically by several authors. Wilets and co-workers³ have used a classical model which is adiabatic and involves no intrinsic target excitation. Beyer et al.⁴ have used a quantum mechanical approach which considers excitation through the β -vibrational states and have evaluated cross sections for both the Coulomb-induced fission process and the related case of fission isomer excitation. Classical dynamical and quantum mechanical calculations have been reported by Riesenfeld and Thomas⁵ and extended by Holm and Greiner,⁶ the latter considering

the important influence of nuclear forces on the Coulomb excitation processes.

The above calculations show that Coulomb-induced fission is likely only with very heavy ion projectiles, for example, xenon at about 5 MeV/nucleon, and that the cross sections are quite substantial for backward scattering, although the various cross-section estimates differ by orders of magnitude.

The excitation, population, and subsequent observation of spontaneous fission isomeric states is inherently easier to experimentally perform than the pure Coulomb-induced fission process because the fission events are delayed, relative to the time of excitation, by the lifetime of the isomeric state. Thus observation of delayed fission events in pulsed-beam experiments can serve as a very sensitive indicator of the population of fission isomeric states.

We have chosen to investigate and detect the possible Coulomb excitation of fission isomeric states using ^{20}Ne ions accelerated at the Oak Ridge Isochronous Cyclotron as a prelude to the exciting possibility of observing the direct Coulomb fission process that may be possible with a new heavy-ion facility at ORNL capable of accelerating xenon and still heavier ions. The excitation of fission isomeric states in the second minimum of the nuclear potential is not unlike the process most likely involved in the direct Coulomb fission process, since both presumably require the nucleus to be transformed to much larger equilibrium quadrupolar deformations. The Coulomb excitation processes responsible for the excitation of fission isomeric states will also be involved in the induced Coulomb fission process.

The 8.5- μsec fission isomeric state in ^{239}Pu ,⁷ which has previously been produced in the $^{239}\text{Pu}(d, pn)$ and $^{238}\text{Pu}(d, p)$ reactions,⁷ the $^{236}\text{U}(\alpha, n)$ and $^{238}\text{U}(\alpha, 3n)$ reactions,⁸ the $^{239}\text{Pu}(n, n')$ and $^{240}\text{Pu}(n, 2n)$ reactions,⁹ the $^{239}\text{Pu}(\gamma, \gamma')$ reaction,¹⁰ and the $^{240}\text{Pu}(\gamma, n)$ reaction,¹¹ was chosen for our investigations because the isomeric state is sufficiently well characterized and the target material, ^{239}Pu , could be prepared in sufficiently high isotopic quality to preclude possible interferences from the ground-state spontaneous fission activity of even-even isotopic impurities. From analyses of some of the fission isomer excitation functions,¹² the excitation energy of the isomeric state was determined to be 2.20 ± 0.20 MeV.

A fast beam deflection system using 1-m-long horizontal parallel plates was developed for use in these experiments. The plates were located in the beam line just after extraction from the cyclotron, and it was found that the application of 6 kV to one of the plates was sufficient to deflect a 100- to 120-MeV $^{20}\text{Ne}^{5+}$

beam about 1.5 cm in the horizontal plane about 10 m downstream. A plate was used to intercept the deflected beam, while the undeflected beam was transmitted to the target station.

A 120- $\mu\text{g}/\text{cm}^2$ isotopically pure ^{239}Pu target on a 1.1-mg/cm² nickel foil backing was prepared in an isotope separator and used in the experiments. A recoil catcher foil, also 1.1-mg/cm² nickel foil, was placed about 3 cm downstream at an angle of 45° to the beam and was viewed by two large-area Si(Au) surface-barrier detectors located at 90° to the beam on either side of the catcher foil. The recoil ^{239}Pu atoms from elastic and inelastic scattering had to pass through the nickel target backing before stopping in the nickel catcher foil. This arrangement only allowed those ^{239}Pu recoils which resulted from elastic and inelastic scattering of 100-MeV ^{20}Ne ions at angles greater than about 90°_{lab} to reach the collector foil. The two detectors were operated in fast coincidence, and both detector pulses were processed together with the output of a time-to-amplitude converter which indicated the time of the fission event relative to the end of the 20- μsec beam burst. The three-parameter correlated data were stored and buffered onto magnetic tape.

Two experiments were conducted using 100-MeV and 117-MeV $^{20}\text{Ne}^{5+}$ ions. Only one delayed fission event was observed in these experiments, which corresponds to a production cross section of about 3.2×10^{-34} cm² integrated over ^{20}Ne scattering angles in the range 90° to 180°_{lab} as dictated by our experimental arrangement. In view of the optimistic estimates of Holm and Greiner,⁶ the meaning of this small cross section is not clear.

We have recently learned of similar Coulomb excitation experiments using 60-MeV ^{12}C ions and 740-MeV ^{136}Xe ions in attempts¹³ to excite the 200-nsec fission isomer in ^{238}U . Cross section upper limits of 10^{-33} cm² and 10^{-31} cm², respectively, were determined. Although our limits for ^{20}Ne ions and the fission isomer of ^{239}Pu are somewhat lower than the above, we conclude that further attempts to Coulomb-excite fission isomers by us will have to await a new heavy-ion accelerator capable of accelerating the heaviest ions to suitable energies.

1. Chemistry Division.

2. Director's Division.

3. E. Guth and L. Wilets, *Phys. Rev. Lett.* **16**, 30 (1966); L. Wilets, E. Guth, and J. S. Tenn, *Phys. Rev.* **156**, 1349 (1967).

4. K. Beyer and A. Winther, *Phys. Lett.* **30B**, 296 (1969); K. Beyer, A. Winther, and U. Smilansky in *Nuclear Reactions Induced by Heavy Ions*, ed. R. Bock and W. Hering, North-Holland Publ. Co., Amsterdam, 1970, p. 804.

5. P. W. Riesenfeldt and T. D. Thomas, *Phys. Rev. C* **2**, 711 (1970).
6. H. Holm and W. Greiner, *Nucl. Phys. A* **195**, 333 (1972).
7. S. M. Polikanov and G. Sletten, *Nucl. Phys. A* **151**, 656 (1970).
8. H. C. Britt, S. C. Burnett, B. H. Erkkila, J. E. Lynn, and W. E. Stein, *Phys. Rev. C* **4**, 1444 (1971).
9. A. G. Belov, Yu. P. Gangrsky, B. Dalkhsuren, A. M. Kucher, T. Nagy, and D. M. Nadkarni, Joint Institute for Nuclear Research report JINR E15-6807, Dubna, U.S.S.R. (1972).
10. Yu. P. Gangrskii, B. N. Markov, I. F. Kharisov, and Yu. M. Tsipenyuk, *JETP Lett.* **14**, 370 (1971).
11. Yu. P. Gangrskii, V. N. Markov, I. F. Kharisov, and Yu. M. Tsipenyuk, *Yad. Fiz.* **16**, 271 (1972).
12. H. C. Britt, M. Bolsterli, J. R. Nix, and J. L. Norton, *Phys. Rev. C* **7**, 801 (1973).
13. Yu. P. Gangrsky, B. N. Markov, N. Khanh, Yu. Ts. Oganessian, and P. Z. Khien, Joint Institute of Nuclear Research preprint P7-7022, Dubna, U.S.S.R. (1973).

HEAVY-ION-INDUCED FISSION

Franz Plasil Robert L. Ferguson¹
 Frances Pleasonton

I. Introduction

During 1973 we have initiated a program of heavy-ion-induced fission at ORIC. The first systems that we have studied involve relatively light fissioning nuclei, such as ^{127}La and ^{153}Tb . The motivation for our investigations has been provided by several developments. There is experimental^{2,3} as well as theoretical⁴ evidence that high angular momenta can lower the fission barrier drastically. This effect not only influences the decay properties of compound nuclei⁵ but may also play a role in determining the compound-nucleus formation probability.^{5,6} Calculations indicate⁴ that for angular momenta greater than about 100h the fission barrier vanishes for all nuclei. Thus a field of research of irresistible scope has opened up — the study of fissioning systems throughout the nuclear mass table, including relatively very light systems.

Aside from general questions regarding the nature of the fission process in nuclei as light as ^{127}La , we also had several specific objectives in mind. First, it is known⁷ that in the case of the $^{107}\text{Ag} + ^{20}\text{Ne}$ reaction at 173 MeV, only about 40% of the estimated total reaction cross section can be accounted for by evaporation residue products (compound nuclei that have deexcited by emitting neutrons, protons, and alpha particles). One of our objectives was to determine how much of the remaining 60% of the total reaction can be accounted for by fission. Second, we wished to deter-

mine fission barriers (for nonrotating nuclei) from our data. The barriers can then be compared with various predictions, such as those based on the liquid drop model, on the “droplet” model, and on recent calculations of Krappe and Nix.⁸ The mass region $100 < A < 130$ is particularly favorable for such comparisons, since here the various predictions differ by as much as 10 MeV from each other.

A third objective was to isolate angular momentum effects on fission barriers, and thus check the validity of liquid drop predictions.⁴ This we intended to accomplish by choosing two reactions in which angular momentum effects are substantially different, such as in the reactions $^{133}\text{Cs} + ^{20}\text{Ne} \rightarrow [^{153}\text{Tb}^*] \rightarrow \text{fission}$ and $^{141}\text{Pr} + ^{12}\text{C} \rightarrow [^{153}\text{Tb}^*] \rightarrow \text{fission}$. Finally, we were interested in the nature of the mass and total kinetic energy distributions. At the so-called Businaro-Gallone point (in the mass region of rhodium), liquid drop model calculations^{9,10} indicate that saddle-point shapes lose stability toward small deformations in the mass asymmetry degree of freedom. This implies that for systems heavier than about rhodium, fission mass distributions are expected to be peaked at symmetric mass divisions, while for nuclei lighter than rhodium, mass distributions are predicted to have a minimum at symmetric mass divisions. The mass distributions are predicted to broaden with decreasing compound nucleus mass,¹⁰ until they become essentially flat near rhodium. Since the lightest fissioning nucleus for which fragment mass distribution results were available was ^{186}Os ,¹¹ systems in the region of lanthanum represent a considerable step in the direction of the Businaro-Gallone point, and the widths of the mass distributions from such systems are of particular interest.

II. Neon-Induced Fission of Silver

The first reaction we studied was $^{107}\text{Ag} + ^{20}\text{Ne} \rightarrow [^{127}\text{La}^*] \rightarrow \text{fission}$.¹² The study consisted of three parts: (1) angular correlation at a bombarding energy of 165.6 MeV, (2) excitation function from 110.4 MeV to 165.6 MeV, (3) mass and total kinetic energy measurements at 165.6 MeV.

The angular correlation study was done by observing coincident fragment pairs with one collimated detector and one position-sensitive detector. The measurement indicated that observed fragments result from the fission of a system that involved all of the momentum of the incoming projectile (consistent with compound-nucleus formation prior to fission).

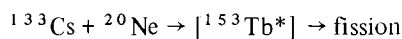
We have attempted to extract the fission barrier from the fission excitation function by means of the compound-nucleus deexcitation program ALICE,^{5,13}

which allows for multiple neutron, proton, and ^4He evaporation in competition with fission, and which includes angular-momentum-dependent fission barriers. The absolute magnitude of the nonrotating fission barrier, B_f , and the ratio of the level density parameter for fission, a_f , to the level density parameter for particle emission, a_p , were treated as adjustable parameters. It was not possible to obtain agreement with the measured excitation function with any B_f and a_f/a_p combination. Furthermore, the highest fission cross section (at 165.6 MeV ^{20}Ne lab energy) was found to be only 73.3 mb, thus accounting for only a small fraction of the estimated total reaction cross section of 1740 mb. There were indications^{1,2} that our data can be understood on the basis of energy-dependent limitations on compound-nucleus formation. This point can, however, only be checked by the measurement of compound-nucleus evaporation residue cross sections. Such studies are currently in progress and will, hopefully, enable us to determine B_f unambiguously.

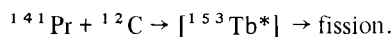
In the third section of our study of the fission of ^{127}La , we have compared the full width at half maximum (FWHM) of our measured mass distribution with the calculated FWHM.¹⁰ The measured value was found to be 36 amu, while the theoretical prediction was 38 amu. This agreement is remarkably good, in contrast with the case of the total kinetic energy distribution, where our measured FWHM of 22 MeV compared with a calculated FWHM of 14 MeV.

III. Fission of the ^{153}Tb Compound Nucleus

Our most recent results are the fission excitation functions for the reactions



and



The compound-nucleus excitation energy ranged from 70 MeV to 120 MeV in the ^{20}Ne case and from 70 MeV to about 100 MeV in the ^{12}C case. Over an identical range in excitation energy, the difference in cross section between the two fissioning systems is very probably due to the different values of angular momentum involved. Thus, at a comparable excitation energy, we would expect the fission cross section σ_f from the ^{20}Ne -induced fission of ^{133}Cs to be higher than that from the ^{12}C -induced fission of ^{141}Pr since the higher angular momentum brought in by the ^{20}Ne ion results in a greater lowering of the fission barrier. The results

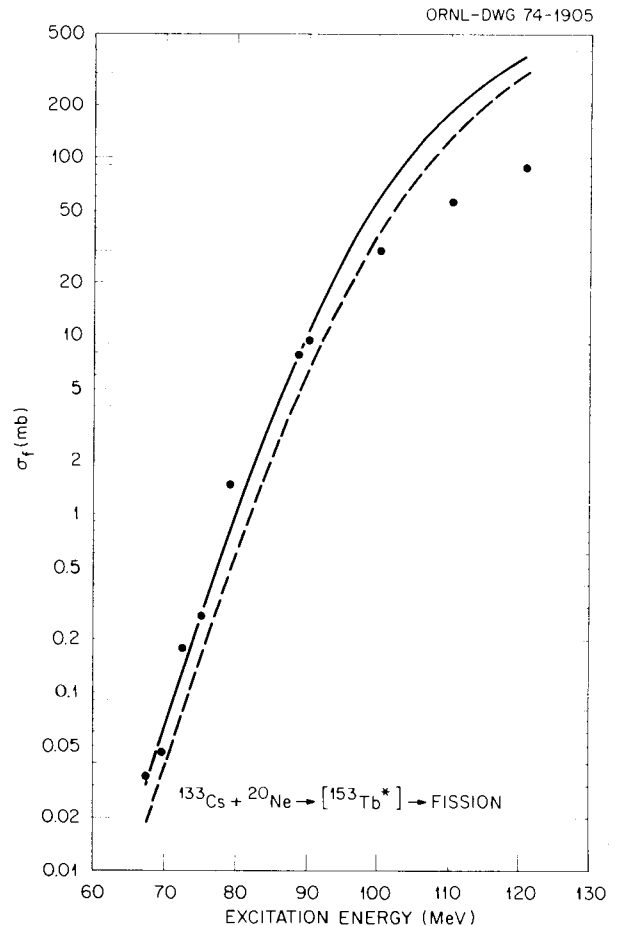


Fig. 1. Fission excitation function for the fission of the ^{153}Tb compound nucleus produced in ^{20}Ne bombardments of ^{133}Cs . Closed circles give experimental data points. Solid and dashed curves are calculated excitation functions (see text); $B_f = 0.8B_f^{\text{LD}}$ for both curves, and $a_f/a_p = 1.0$ for the solid curve and 0.98 for the dashed curve.

are shown in Figs. 1 and 2. The experimental values of the fission cross section are given by the closed circles. It can be seen that at a given excitation energy, σ_f is higher for the ^{20}Ne than for the ^{12}C case. At an excitation energy of 90 MeV, for example, $\sigma_f \cong 0.7$ mb for the ^{12}C bombardment compared with $\sigma_f \cong 10$ mb for the ^{20}Ne reaction.

The solid and dashed curves of Figs. 1 and 2 represent fits to the experimental data obtained from the compound-nucleus deexcitation program ALICE.¹³ As in the ^{127}La case, the absolute value of the fission barrier B_f and the ratio of the level density parameters a_f/a_p were treated as adjustable parameters. The angular momentum dependence of B_f , however, was taken from liquid drop model calculations,⁴ and the variation of B_f

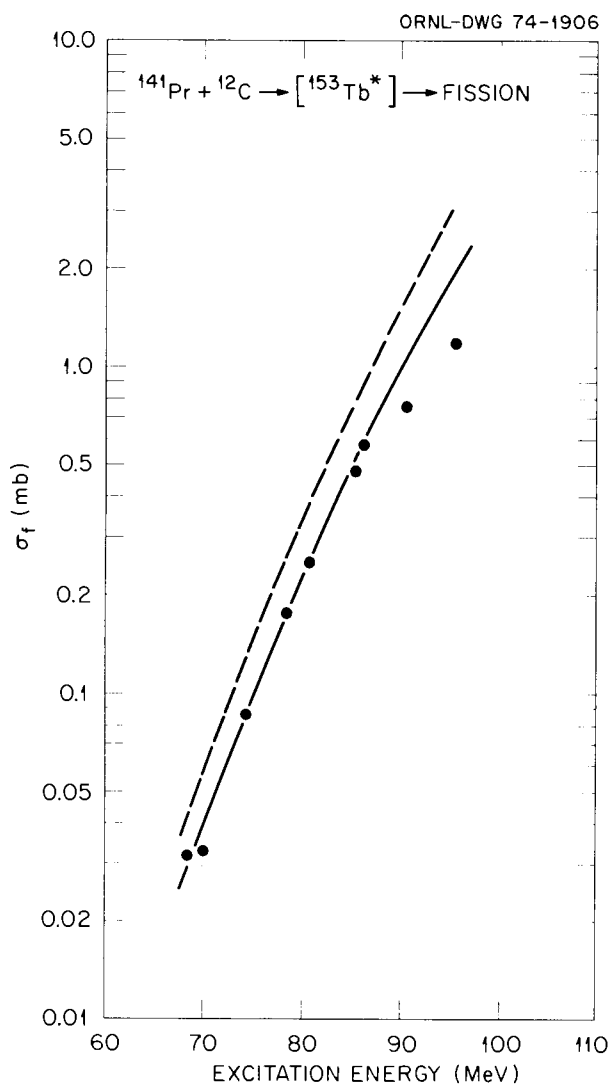


Fig. 2. Fission excitation function for the fission of the ^{153}Tb compound nucleus produced in ^{12}C bombardments of ^{141}Pr . Symbols are the same as in Fig. 1; $B_f = 0.8B_f^{\text{LD}}$ for both curves, and $a_f/a_v = 0.965$ for the solid curve and 0.98 for the dashed curve.

was made by varying k in the expression $B_f = kB_f^{\text{LD}}$, where B_f^{LD} is the liquid drop value of B_f .

The fission barriers associated with the solid curves of Figs. 1 and 2 are given by $B_f = 0.8B_f^{\text{LD}}$ in both cases, while a_f/a_v is 0.965 in the ^{12}C case and 1.0 in the ^{20}Ne case. It can be seen that the fit to the steep part of the excitation function is good in both cases up to an excitation energy of about 90 MeV. The fits given by the solid curves are "best fits" in the sense that they follow the experimental data over the greatest range of excitation energies. They are, however, based on the assumption that the compound-nucleus cross section

σ_{CN} is equal to the estimated total reaction cross section σ_{R} ; that is, $\sigma_{\text{CN}}/\sigma_{\text{R}} = 1$. This assumption almost certainly does not hold over the entire range of excitation energies studied in this work, and thus the fission barrier is not uniquely determined from our fit. The deviation of the solid curve from the data points at higher excitation energies is most apparent in the ^{20}Ne case and can, very probably, be accounted for by a decreasing $\sigma_{\text{CN}}/\sigma_{\text{R}}$ ratio with increasing excitation energy. Thus, while adequate fits to our data can be obtained, the unambiguous determination of B_f can only be made if $\sigma_{\text{CN}}/\sigma_{\text{R}}$ is known. For this purpose, measurements of evaporation residue cross sections are again required.

The dashed curves in Figs. 1 and 2 are for $B_f = 0.8B_f^{\text{LD}}$ and $a_f/a_v = 0.98$. It is reasonable to expect that both excitation functions should be adequately described with one set of parameters, since the same compound nucleus is involved. The dashed curves show the extent to which such a simultaneous fit is possible. While the fit is by no means perfect, it is probably fairly reasonable, particularly in view of the uncertainties concerning the $\sigma_{\text{CN}}/\sigma_{\text{R}}$ ratio, which may be different in the two cases.

We conclude that angular momentum effects in fission can be understood reasonably well in terms of the rotating liquid drop model⁴ and that the variation of fission barriers with angular momentum given by the model is probably adequate. We also emphasize that unambiguous extraction of fission barriers from fission excitation functions is only possible when the evaporation residue excitation functions are also known. We are presently in the process of measuring the required evaporation residue cross sections.

1. Chemistry Division.
2. J. Gilmore, S. G. Thompson, and I. Perlman, *Phys. Rev.* **128**, 2276 (1962).
3. T. Sikkeland, *Phys. Rev.* **135**, B669 (1964).
4. S. Cohen, F. Plasil, and W. J. Swiatecki, Lawrence Berkeley Laboratory report LBL-1502 (1972); to be published in *Annals of Physics*.
5. M. Blann and F. Plasil, *Phys. Rev. Lett.* **29**, 303 (1972); M. Blann and F. Plasil, to be published.
6. H. H. Gutbrod, F. Plasil, H. C. Britt, B. H. Erkkila, R. H. Stokes, and M. Blann in *Proceedings of the Third IAEA Symposium on the Physics and Chemistry of Fission* (Rochester, N.Y., August 1973), paper IAEA-SM-174/59.
7. J. B. Natowitz, *Phys. Rev.* **C1**, 623 (1970).
8. H. J. Krappe and J. R. Nix in *Proceedings of the Third IAEA Symposium on the Physics and Chemistry of Fission* (Rochester, N.Y., August 1973), paper IAEA-SM-174/12.
9. U. L. Businaro and S. Gallone, *Nuovo Cim.* **5**, 315 (1957).
10. J. R. Nix, *Nucl. Phys.* **A130**, 241 (1969).
11. F. Plasil, D. S. Burnett, H. C. Britt, and S. G. Thompson, *Phys. Rev.* **142**, 696 (1966).

12. F. Plasil, R. L. Ferguson, and F. Pleasonton in *Proceedings of the Third IAEA Symposium on the Physics and Chemistry of Fission* (Rochester, N.Y., August 1973), paper IAEA-SM-174/71.

13. M. Blann and F. Plasil, *ALICE: A Nuclear Evaporation Code*, USAEC report COO-3494-10.

HEAVY-ION FUSION REACTIONS

H. G. Bingham E. E. Gross
C. R. Bingham¹ M. J. Saltmarsh
A. Zucker²

In recent years there has been a considerable increase in the number of measurements³⁻⁶ dealing with the interaction of heavy ions and target nuclei to form compound systems (fusion). The general question of the interaction mechanism for these reactions gives rise to more pertinent and specific questions on barrier heights, interaction radii, channel effects, and limiting angular momentum effects on cross-section systematics for fusion reactions.

How does one effectively and efficiently measure integrated cross sections for heavy systems where the fusion product angular distribution is spread only a few degrees from the beam direction? Two methods of detection have been developed which have enjoyed some degree of success, gas proportional counters⁴ with thin entrance windows and track detectors.⁵ But proportional counters have one distinct disadvantage in measuring fusion products, and that is their inability because of size and count-rate limitations to go forward of 3°. That is not to say track detectors are faultless. Registration efficiency, radiation damage levels, and etch rates for optimum track exposure plague the reliability factor for most track detector measurements. However, glass or quartz track detectors appear to have complete registration efficiency under normal conditions and optimum damage sensitivity for intermediate and heavy masses.⁷

Using quartz track detectors, we have measured cross sections for argon-induced fusion on targets of titanium, nickel, copper, and silver at incident energies from 115 MeV to 189 MeV. Targets were of the order 70 $\mu\text{g}/\text{cm}^2$ thick and were prepared by vacuum evaporation of the metal onto 40- $\mu\text{g}/\text{cm}^2$ carbon backings, except for the nickel target, which was self-supporting. Beam intensities were monitored by silicon surface-barrier detectors placed at $\pm 15^\circ$ with respect to the beam, assuming that the yields from each target were given by the Rutherford law. Beam intensities for the track detector in-beam measurements were obtained by comparison of $K\alpha$ yields from a Si(Li) detector at 135°

to $K\alpha$ yields associated with the Rutherford yields of the $\pm 15^\circ$ surface-barrier detectors.

The quartz track detectors exposed to fusion products were etched in a 26% hydrofluoric acid bath (at about 21°C) for 5 min to reveal etch pits, the signature of a heavy charged particle. Figure 1 is a scanning electron micrograph (SEM) taken at 10,000X of a region on a quartz disk that was exposed to argon plus copper fusion products and then etched. These disks were then automatically scanned in the region of the beam spot at a magnification of 1600X using an image-analyzing computer. The scanning procedure consisted of a sizing of each etch pit encountered and the increment of a storage register representing its average size. The resultant measurement appears as the number of etch pits scanned having diameters which fall between predetermined limits as in Fig. 2. The fusion products appear as the largest etch pits encountered. The smaller pits represent fission, inelastic scattering, and few-nucleon transfer reactions. These conclusions are based on SEM calibrations of etch pit diameters using ³²S (101 MeV), ⁴⁰Ar (115, 150, 190 MeV), ⁵⁶Fe (60 MeV), ⁶⁵Cu (50 MeV), ⁸³Kr (87 MeV), and ¹²⁹Xe (101 MeV) beams. These beams correspond to average fission and fusion products of the systems studied.

To date we have measured fusion cross sections for argon ions on targets of titanium, nickel, copper, and silver at several energies, and the results of these measurements are given in Table 1. The errors associated with each measurement represent the cumulative experimental uncertainties and are typically 10%. The largest single uncertainty is that associated with distinguishing fusion tracks from those of fission, inelastic scattering, etc., but that uncertainty is generally 5% or less.

The distance of closest approach (D) for forming a compound system (fusion) is simply the touching radius, $D = r_e(A_1^{1/3} + A_2^{1/3})$, where r_e is the effective nuclear unit radius and A_1 and A_2 are the projectile and target masses respectively. The total reaction cross section may be expressed in a semiclassical formulation as $\sigma_R = \pi x^2$, where x is the impact parameter. If it is evaluated in the region just above the Coulomb barrier where fusion is the predominant process, then $\sigma_R = \pi D^2$, and the distance of closest approach is quite sensitive to the details of the fusion cross section, and r_e is easily extracted. The values of r_e extracted in such a manner from our fusion measurements are summarized in Table 2. These values are somewhat larger than what might be expected from theoretical considerations,⁸ except for the case of argon on titanium, which is much smaller than the expected value.

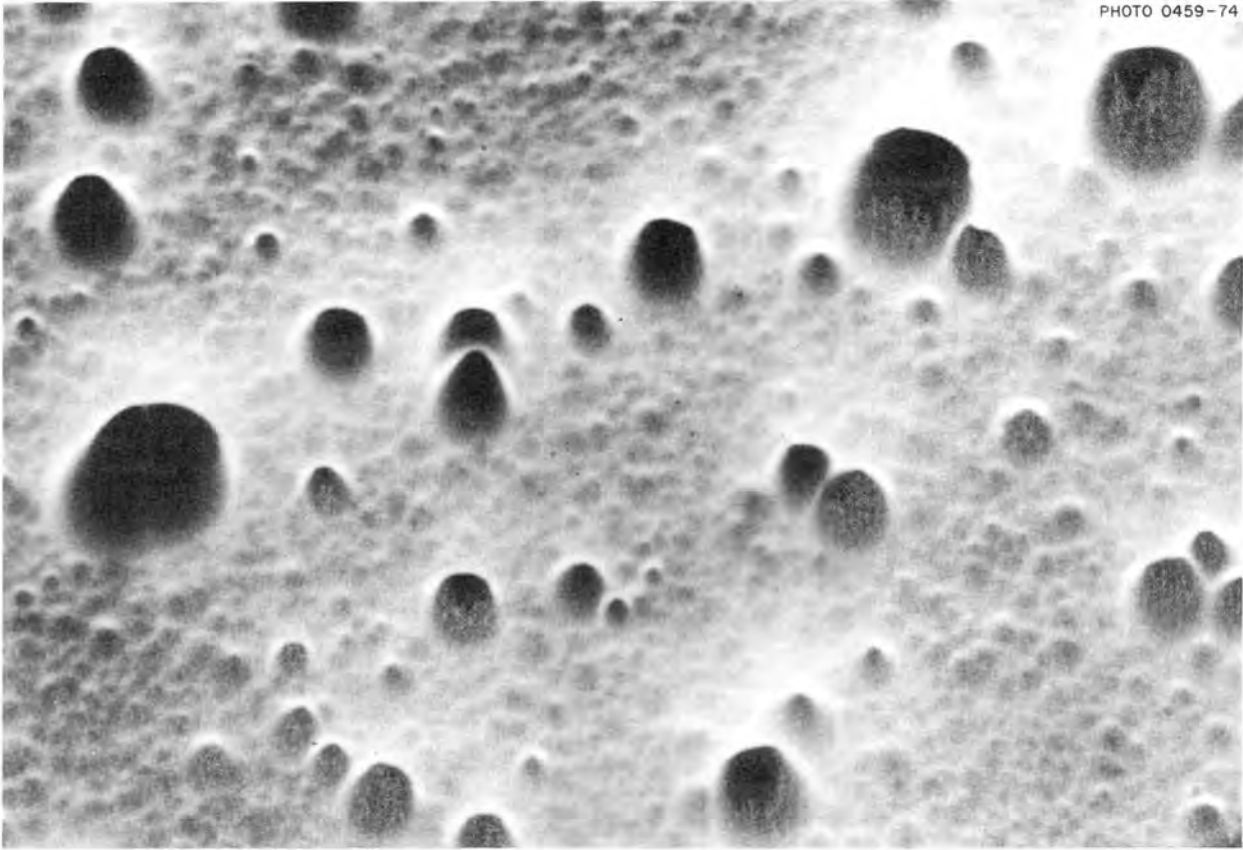


Fig. 1. Scanning electron micrograph taken at 10,000 \times of a region on a quartz track detector that has been exposed to 190-MeV argon plus copper fusion products and etched in a 26% hydrofluoric acid bath for 5 min. The large holes correspond to fusion or "heavy" products, and the smaller holes are fission, inelastic scattering, etc.

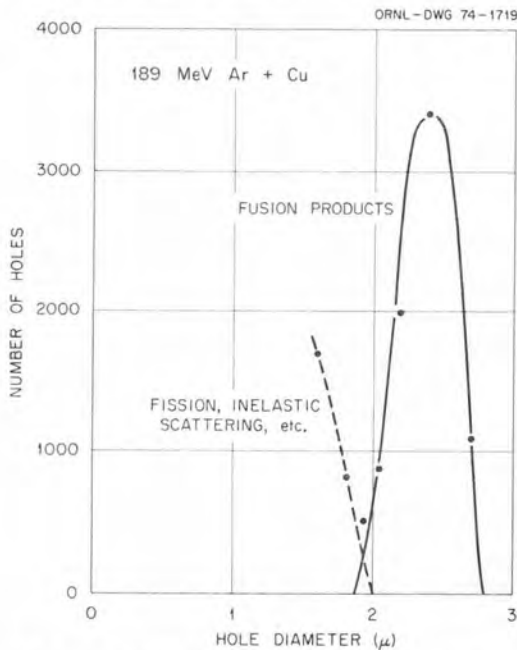


Fig. 2. Sample of raw data output from a beam spot scan by an image-analyzing computer. It shows the number of holes within a given diameter limit encountered in a complete scan.

Table 1. Fusion cross section for argon on titanium, nickel, copper, and silver

^{40}Ar energy (MeV)	Cross section (mb)			
	Ti	Ni	Cu	Ag
115	98^{+30}_{-50}	192^{+65}_{-130}		
151	804 ± 80	892 ± 90		
189	1065 ± 100	928 ± 93	1634 ± 160	(0)

Table 2. Radius and barrier height parameters extracted from fusion cross sections for argon on targets of titanium, nickel, and copper

Target	r_e (fm)	Approximate barrier height (MeV)
Ti	1.35	110
Ni	1.50	112
Cu	1.50	112

For argon on nickel, the fusion cross section increases rapidly above the barrier up to some critical energy and then levels off. Combining these results with those of Gutbrod and Plasil,⁹ it appears that the limiting angular momentum⁶ for this system increases slowly with energy. This conclusion would appear to be consistent with the argon plus titanium results, but additional data on this and other systems are necessary for a complete analysis.

1. Consultant from the University of Tennessee, Knoxville, Tenn.
2. Director's Division.
3. For example, see L. Kowalski, J. C. Jodogne, and J. Miller, *Phys. Rev.* **169**, 894 (1968).
4. H. H. Gutbrod, W. G. Winn, and M. Blann, *Nucl. Phys.* **A213**, 267 (1973).
5. J. B. Natowitz, *Phys. Rev.* **C1**, 623 (1970).
6. M. Blann and F. Plasil, *Phys. Rev. Lett.* **29**, 303 (1972).
7. M. Lecerf and J. Péter, *Nucl. Instrum. Methods* **104**, 189 (1972).
8. C. Y. Wong, *Phys. Lett.* **42B**, 186 (1972).
9. H. H. Gutbrod and F. Plasil, to be published.

ROTATIONAL BANDS IN DEFORMED NUCLEI

BACKBENDING ROTATIONAL BANDS IN EVEN-A NUCLEI

L. L. Riedinger¹ D. C. Hensley
P. H. Stelson N. R. Johnson³
G. B. Hagemann² R. L. Robinson
E. Eichler³ R. O. Sayer⁴
G. J. Smith⁵

In many studies of rotational bands in even-even deformed nuclei over the years, experimentalists had noted smooth, systematic deviations of the energy levels from the $I(I+1)$ prediction for a rigid rotor. The theorists were able to interpret these deviations as resulting, for example, from gradual breakdown in nucleon pairing or from centrifugal stretching. Then, in 1971, Johnson et al.⁶ observed large deviations beginning suddenly at the 14^+ state in ^{160}Dy . Plotted on a graph of \mathcal{J} , the moment of inertia, vs the square of ω , the rotational angular velocity, the energies of such a band follow an S-shaped (backbending) curve, characterized by rapid increases in \mathcal{J} .

Since those experiments in Stockholm, other backbending bands have been found, mostly in the neutron-deficient isotopes of gadolinium, dysprosium, and erbium. Much of this work at various laboratories has been performed with (α, xn) reactions, resulting in limitations on nuclei accessible and on angular momen-

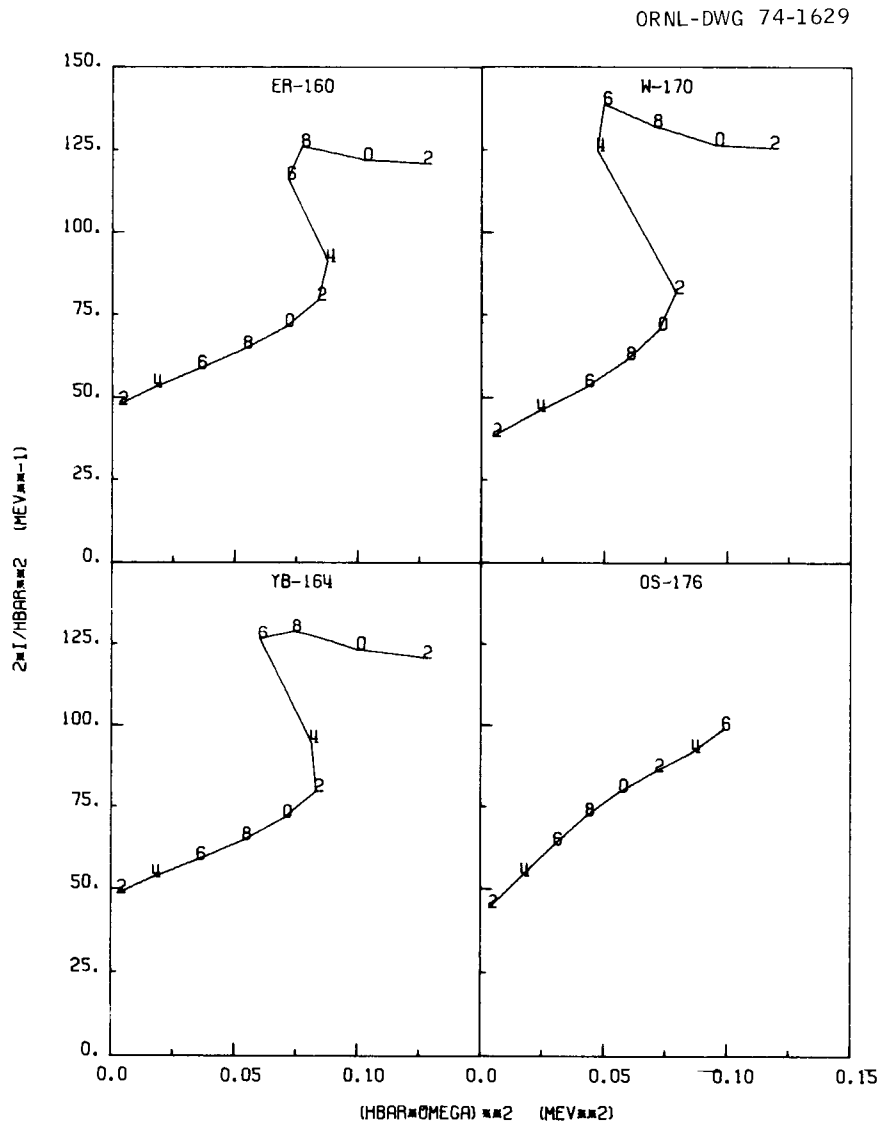
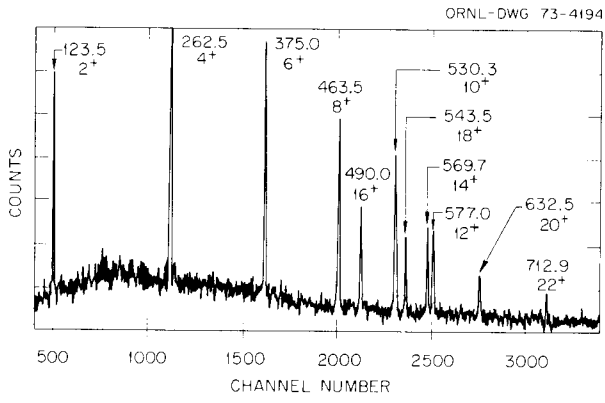
tum imparted to the residual nucleus. We thus began a program of investigating rotational bands in deformed nuclei using carbon, oxygen, neon, and argon beams from ORIC. The purpose has been not only to reach new cases of backbending in isotopes far from stability but also to study the mechanism by which the ground-state band is populated in the yrast cascade of the nucleus.

Our experiments so far have consisted primarily of excitation function measurements, to assign gamma rays to certain reaction products, and gamma-gamma coincidence measurements, which order the gamma-ray transitions into a rotational band. The latter experiments involve accumulating up to 40 million coincident events in a list on magnetic tapes while extracting pertinent gated spectra during the data taking. To check the gamma-ray multiplicities, we have recently begun a series of gamma-ray angular distribution measurements relative to the beam direction.

The four even-even nuclei studied have been ^{160}Er , ^{164}Yb , ^{170}W , and ^{176}Os . The reactions used in each are given in Table 1. The first two nuclei were investigated because previous data were available from Jülich through the $(\alpha, 8n)$ reaction.⁷ In the case of ^{160}Er , Lieder et al.⁷ established the ground-state band (GSB) up to the 18^+ member. We have evidence for two higher members of the yrast cascade to which we tentatively assign $I^\pi = 20^+$ and 22^+ . An unresolved problem is the fact that the angular distribution experiments of Lieder et al.⁷ indicate that the 640-keV gamma ray ($20 \rightarrow 18$ in our tentative scheme) does not have the usual stretched $E2$ character. We are planning experiments to test this point. In ^{164}Yb , the Jülich group detected transitions up to the $16 \rightarrow 14$, which had an intensity of about 25% of the $4 \rightarrow 2$. In our experiments, we detected the $16 \rightarrow 14$ with the same approximate intensity, but due to the greater selectivity of the $(^{12}\text{C}, 4n)$ and $(^{20}\text{Ne}, 6n)$ reactions, we were also able to establish the 18^+ , 20^+ , and 22^+ members of the GSB. Figure 1 displays a summed coincidence spectrum for the $^{156}\text{Gd}(^{12}\text{C}, 4n)^{164}\text{Yb}$ reaction. Figure 2 contains

Table 1. Reactions used in experiments

Final nucleus	Reaction	Beam energy (MeV)
^{160}Er	$^{152}\text{Sm}(^{12}\text{C}, 4n)$	70
	$^{124}\text{Sn}(^{40}\text{Ar}, 4n)$	145
^{164}Yb	$^{156}\text{Gd}(^{12}\text{C}, 4n)$	70
	$^{150}\text{Nd}(^{20}\text{Ne}, 6n)$	118
^{170}W	$^{156}\text{Gd}(^{20}\text{Ne}, 6n)$	129
^{176}Os	$^{162}\text{Dy}(^{20}\text{Ne}, 6n)$	126



the \mathcal{J} vs ω^2 plot for the nuclei of interest. In ^{160}Er , ^{164}Yb , and ^{170}W the moment of inertia approaches a constant value after the backbending, rather than before. It must be emphasized that these spin assignments are tentative in all cases until angular distribution measurements can be performed. Assuming that these assignments are correct, one notes that in three of the four cases studied the GSB is populated up to $I = 22$. This seems to be the limit for seeing discrete transitions. The Brookhaven group⁸ has reached the same spin in ^{158}Dy .

Upon proving that (H.I., xn) reactions were better than (α , xn) for populating and detecting the highest members of the GSB, we performed experiments on nuclei which had not been well studied before. In ^{170}W , we observed a coincident cascade of 11 gamma rays, which may represent transitions from levels up to $I = 22$. Once again, the characteristic backbending shape is seen (Fig. 2). This represents the third case of backbending nucleus with 96 neutrons (also ^{164}Er , ^{166}Yb , and ^{168}Hf). The $N = 98$ nuclei of these four elements do not backbend, and thus $N = 96$ appears to be an upper limit for such an effect. There are exceptions to this rule, however. For example, Warner et al.⁹ observe a backbending GSB in ^{182}Os ($N = 106$).

The case of ^{176}Os ($N = 100$) is interesting, in that the GSB, rather than bending backward, bends slightly forward after the 8^+ member. This is suggestive of a more obvious case of forward bending in the mercury isotopes, for example, ^{186}Hg . In that case, Proetel et al.¹⁰ see a vibrational-type sequence up to $I = 6$, followed by a rotational band up to $I = 14$. In addition, Hamilton et al.¹¹ recently observed a similar effect in the yrast sequence of ^{72}Se . These changes can possibly be interpreted as a shift from a spherical or oblate shape in the ground state to a prolate deformed shape at or above $I = 6$. Perhaps a similar transition from one potential minimum to another is occurring in ^{176}Os and other nuclei in this region with $N > 100$.¹² The general backbending shape, by contrast, is thought to result in some way from sudden collapse in pairing between all, or at least a few high- j , neutrons.

1. Consultant from the University of Tennessee, Knoxville, Tenn.

2. Niels Bohr Institute, Copenhagen, Denmark.

3. Chemistry Division.

4. Consultant from Furman University, Greenville, S.C. (also, sponsored by Vanderbilt Univ., Nashville, Tenn.).

5. Postdoctoral Fellow under appointment with Oak Ridge Associated Universities.

6. A. Johnson, H. Ryde, and J. Starkier, *Phys. Lett.* **34B**, 605 (1971).

7. R. M. Lieder, H. Beuscher, W. F. Davidson, P. John, H. J. Probst, and C. Mayer-Boricke, *Z. Phys.* **257**, 147 (1972).

8. P. Thieberger, A. W. Sunyar, P. C. Rogers, N. Farle, O. C. Kistner, E. der Mateosian, S. Cochavi, and E. H. Averbach, *Phys. Rev. Lett.* **28**, 972 (1972).

9. R. A. Warner, F. M. Bernthal, J. S. Boyno, T. L. Khoo, and G. Sletten, *Phys. Rev. Lett.* **31**, 835 (1973).

10. D. Proetel, R. M. Diamond, P. Kienle, J. R. Leigh, K. H. Maier, and F. S. Stephens, *Phys. Rev. Lett.* **31**, 896 (1973).

11. J. H. Hamilton, A. V. Ramayya, W. T. Pinkston, R. M. Ronningen, G. Garcia-Bermudez, H. K. Carter, R. L. Robinson, H. J. Kim, and R. O. Sayer, *Phys. Rev. Lett.* **32**, 239 (1974).

12. J. L. Wood, private communication.

DECOUPLED ROTATIONAL BANDS IN $^{163,165}\text{Yb}$

L. L. Riedinger¹ D. C. Hensley
P. H. Stelson N. R. Johnson³
G. B. Hagemann² R. L. Robinson
E. Eichler³ R. O. Sayer⁴
G. J. Smith⁵

In addition to our experiments on backbending rotational bands in even-even nuclei, we have performed (H.I., $xn\gamma$) measurements on $^{163,165}\text{Yb}$. The purpose is to hopefully isolate the cause of backbending by studying the behavior of rotational bands built on the excitation of a single neutron in different Nilsson states. We have performed excitation function and gamma-gamma coincidence measurements using beams of ^{12}C , ^{20}Ne , and ^{22}Ne from ORIC. Angular distribution measurements are planned for the near future.

It is remarkable that the experimental gamma-ray spectrum for an odd-neutron ytterbium isotope looks quite similar to that measured in even- N ^{164}Yb . A summed coincidence spectrum from the reaction $^{148}\text{Nd}(^{22}\text{Ne}, 5n)^{165}\text{Yb}$ at 109 MeV is shown in Fig. 1. The gamma-ray cascade observed is quite similar to the $I \rightarrow I - 2$ transitions seen in a $K = 0$ band in an even-even nucleus. A similar cascade is observed in ^{163}Yb . This phenomenon is best explained by the decoupling model of Stephens et al.⁶ An effect of rotation is the tendency to align, through the Coriolis force, the individual angular momentum, j , of the odd neutron with the rotational angular momentum, R . This effect would be most extreme on the neutrons excited into high- j Nilsson orbits, since the Coriolis force depends on $\mathbf{R} \times \mathbf{j}$. In the region of the light dysprosium, erbium, and ytterbium nuclei, the highest- j levels near the Fermi surface are those resulting from various projections of the $i_{13/2}$ particle on the nuclear symmetry axis. Next in importance are the $h_{9/2}$ states. If

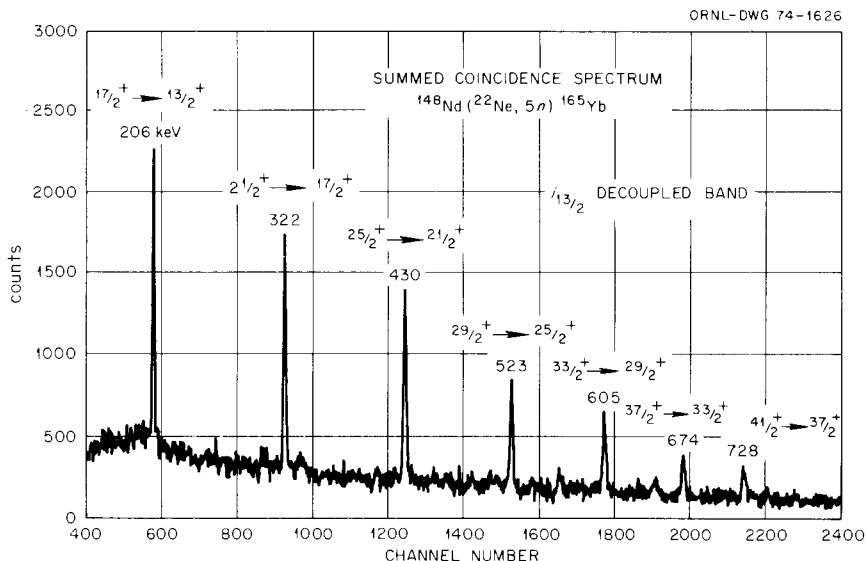


Fig. 1. Gamma-ray coincidence spectrum corresponding to the sum of individual background-subtracted spectra gated by each member of the cascade.

the rotational velocity is high enough, j and R might align fully, which means that the odd neutron no longer experiences the rotation of the core (it is decoupled). In this condition, the rotational band is merely that expected for a $K = 0$ band of the even-even core.

Decoupled bands in deformed nuclei were first seen in the light odd erbium isotopes.^{7,8} The sequences seen in $^{163,165}\text{Yb}$ are quite similar and are thus assigned spins and parities partially by analogy. The energies of the members of these cascades in each nucleus are given in Table 1. From systematics of levels of odd- N nuclei in this region, we conclude that the lowest number of the $i_{13/2}$ mixed band should be $\frac{9}{2}^+$. In ^{165}Yb , a candidate for the $^{13/2} \rightarrow \frac{9}{2}$ transition was found in singles, but not yet in coincidence, measurements. Beginning at $^{13/2}^+$, one then sees a cascade of six gamma rays in ^{163}Yb , seven in ^{165}Yb , which are assigned to be $\Delta I = 2$ transitions. Angular distribution measurements to verify the $E2$ character of these gamma rays are not yet in hand. As one goes up in the band, these spacings become very similar to the $I_i - 1^{3/2} \rightarrow I_f - 1^{3/2}$ spacings in $^{164,166}\text{Yb}$. This is demonstrated in Fig. 2, a plot of energy spacings in the odd- N band compared with those in the even- N band. Initially, the band is not completely decoupled; for example, the $^{17/2} \rightarrow ^{13/2}$ transition energy in ^{165}Yb is 83% greater than the average of the $2 \rightarrow 0$ energies in ^{164}Yb and ^{166}Yb . Gradually, however, the ratio tends toward an equilibrium value of 1.17 for ^{165}Yb and 1.13 for ^{163}Yb . In both cases this

Table 1. Transition energies (keV) between members of bands in ^{163}Yb and ^{165}Yb

I_i	I_f	^{163}Yb , $i_{13/2}$ band	^{165}Yb	
			$i_{13/2}$ band	$h_{9/2}$ band
9/2	5/2			198
13/2	9/2		~80	287
17/2	13/2	202.8	205.9	365
21/2	17/2	345.0	322.1	431
25/2	21/2	463.0	429.2	490
29/2	25/2	557.3	523.5	517
33/2	29/2	629.9	605.1	478
37/2	33/2	680.3	674.8	478
41/2	37/2		728.5	581
45/2	41/2			648
15/2	11/2		209	
19/2	15/2		339	
23/2	19/2		453	
27/2	23/2		549	
31/2	27/2		630	

ratio rises slightly for the $^{37/2}$ and $^{41/2}$ members. These are equivalent to the $I = 12$ and 14 states of the even-even core, at which point backbending begins for both ^{164}Yb and ^{166}Yb . The increase in the ratio indicates that the odd- N decoupled band does not backbend as one might expect. This was seen in the light erbium isotopes^{6,7} and is explained by Grosse et al.⁷ as a blocking effect. That is, the decoupled $i_{13/2}$

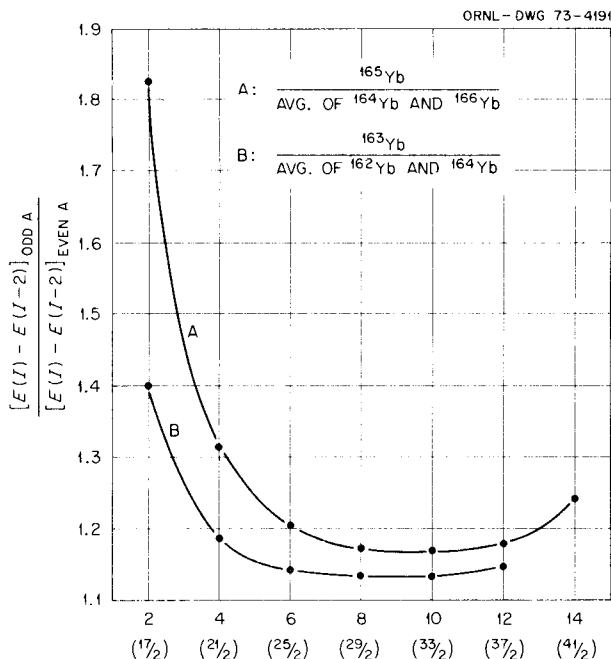


Fig. 2. The ratio of energies of $\Delta I = 2$ spacings in the $i_{13/2}$ decoupled band of ^{163}Yb and ^{165}Yb to spacings of the adjacent even- A band.

neutron, in its aligned position, blocks other $i_{13/2}$ neutrons from decoupling from the even-even core and thus retards core backbending. The plot of \mathcal{J} , the moment of inertia, vs the square of ω , the rotational velocity, for this $i_{13/2}$ band in ^{165}Yb is shown in Fig. 3. The backbending is apparent for ^{164}Yb but is not present for the $i_{13/2}$ decoupled band.

Other gamma rays of smaller intensities are seen in ^{165}Yb . For example, $\Delta I = 2$ transitions from the $^{15/2}_2$, $^{19/2}_2$, $^{23/2}_2$, $^{27/2}_2$, and $^{31/2}_2$ members of the $i_{13/2}$ band are listed in Table 1. This cascade is weaker since the levels are shifted up in energy by the Coriolis interaction. We think that the $^{11/2}_2$ and $^{15/2}_2$ levels are slightly below the $^{13/2}_2$ and $^{17/2}_2$ states, respectively; however, the $^{19/2}_2$, $^{23/2}_2$, etc., levels have higher excitation energies than those of $^{21/2}_2$, $^{25/2}_2$, etc.

Another weak cascade of nine or ten coincident gamma rays is seen in ^{165}Yb . These are listed in the last column of Table 1. These gamma rays are tentatively assigned to $\Delta I = 2$ transitions from levels of spins and parities $^{9/2}_2^-$ through $^{45/2}_2^-$. Isihara et al.⁹ reported from (p, xn) measurements the $^{5/2}_2^-$, $^{7/2}_2^-$, and $^{9/2}_2^-$ members of what they called the $^{5/2}_2^-$ (523) orbit, a level originating

from the $f_{7/2}$ shell-model state. Two of the same transitions are seen in our work, and so we are confident that we are observing the same band. However, we prefer to assign these levels to a band built on the $^{3/2}_2^-$ (521) orbit, an $h_{9/2}$ state, mainly by analogy to ^{157}Dy . There, Klamra et al.¹⁰ construct the ground-state band ($^{3/2}_2^-$ [521]) with transition energies remarkably similar to the ones seen in ^{165}Yb . The energies are so similar that we feel confident that we are seeing the same type of band. To verify this, we are planning more experiments to search for the proposed $^{5/2}_2^- \rightarrow ^{3/2}_2^-$ transition, which should be around 60 keV.

This band in ^{165}Yb seems to decouple in a way similar to the one built on the $i_{13/2}$ levels. Although the structure in ^{157}Dy was seen¹⁰ only up to $I = 2^{1/2}_2$, clear evidence for gradual decoupling was present. The importance of this band in ^{165}Yb is that it seems to backbend (Fig. 3), if our tentative assignments are correct. From the model of Stephens, this would seem quite logical, since an aligned $h_{9/2}$ neutron would not block the decoupling of $i_{13/2}$ neutrons from the core and thus would not prevent backbending. A similar deduction was made by Grosse et al.¹¹ when they found that the decoupled $h_{11/2}$ proton in the odd holmium isotopes did not prevent backbending. If our tentative conclusions are correct, the presence of two decoupled bands in ^{165}Yb , one which backbends and one which does not, would be even more striking proof that the decoupling of $i_{13/2}$ neutrons is the prime cause of backbending for these nuclei.

1. Consultant from the University of Tennessee, Knoxville, Tenn.
2. Niels Bohr Institute, Copenhagen, Denmark.
3. Chemistry Division.
4. Consultant from Furman University, Greenville, S.C.
5. Postdoctoral Fellow under appointment with Oak Ridge Associated Universities.
6. F. S. Stephens, R. M. Diamond, J. R. Leigh, T. Kammuri, and K. Nakai, *Phys. Rev. Lett.* **29**, 438 (1972).
7. E. Grosse, F. S. Stephens, and R. M. Diamond, *Phys. Rev. Lett.* **31**, 840 (1973).
8. H. Beuscher, W. F. Davidson, R. M. Lieder, and C. Mayer-Boricke, *International Conference on Nuclear Physics, Munich*, p. 189.
9. M. Isihara, H. Kawakami, N. Yoshikawa, H. Kusakari, M. Sakai, and K. Ishii, *Inst. Nucl. Study, Tokyo, Annu. Rep. 1970*, p. 45.
10. W. Klamra, S. A. Hjorth, J. Boutet, S. Andre, and D. Barneoud, *Nucl. Phys. A* **199**, 81 (1973).
11. E. Grosse, F. S. Stephens, and R. M. Diamond, *Phys. Rev. Lett.* **32**, 74 (1974).

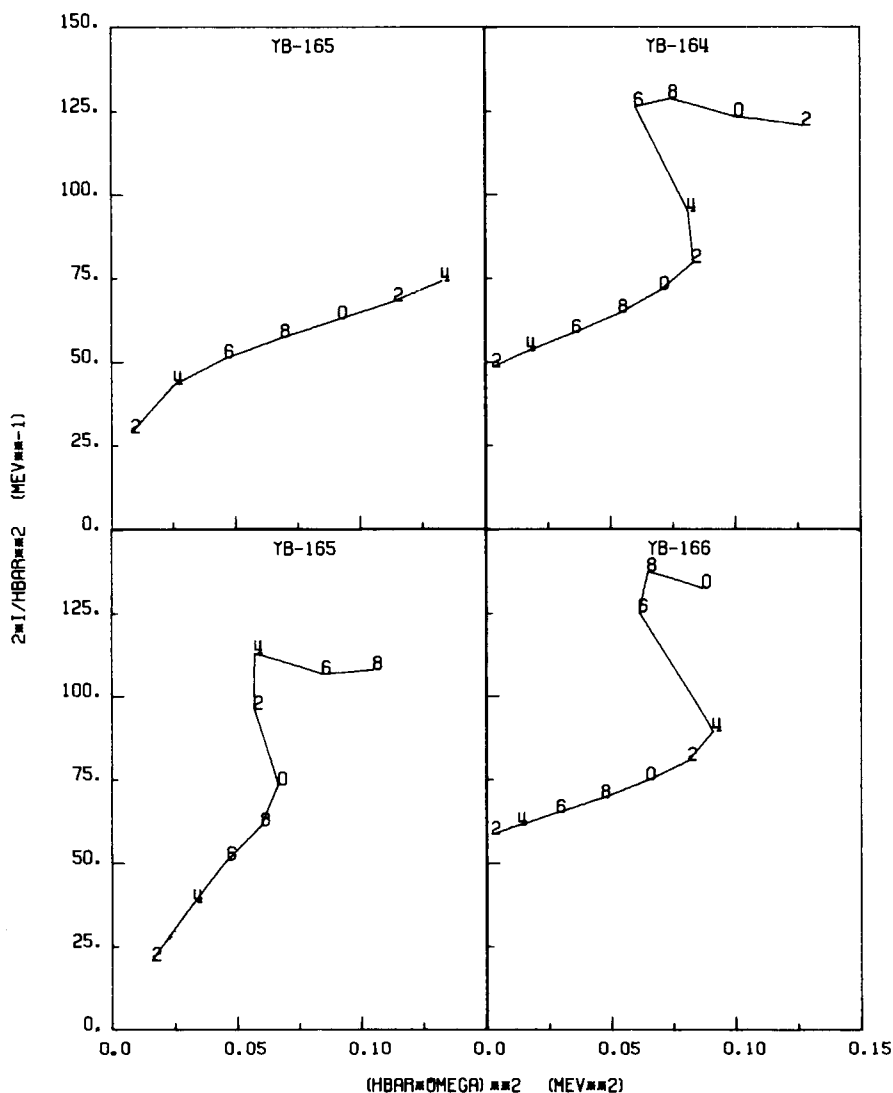


Fig. 3. A graph of $2I/\hbar\omega$ vs $(\hbar\omega)^2$ for the ground-state bands in ^{164}Yb and ^{166}Yb and two decoupled bands in ^{165}Yb . For the odd- A bands the spins on the curves correspond to $I - 13/2$ for the $i_{13/2}$ band (upper left) and $I - 9/2$ for the $h_{9/2}$ band (lower left).

COULOMB EXCITATION OF GROUND BANDS IN $^{160,162,164}\text{Dy}$ WITH ^{20}Ne AND ^{35}Cl IONS

R. O. Sayer¹ N. R. Johnson²
E. Eichler² D. C. Hensley
L. L. Riedinger³

Energy spacings of levels in the ground-state bands of even-even rare-earth nuclei have received extensive experimental investigation. Theoretical calculations based on microscopic models⁴ indicate that centrifugal stretching, Coriolis antipairing, and fourth-order crank-

ing-model corrections contribute to the observed small departures from the $I(I+1)$ rule. These factors should cause the intraband $B(E2)$ values to deviate from the rigid-rotor predictions, but the deviations are expected to be less than present experimental accuracies for $I \lesssim 8$. Prior to the beginning of this work, no $B(E2)$ values for $I > 8$ for good rotors had been reported.

Multiple Coulomb excitation of states up to $J^\pi = 12^+$ in the ground band of $^{160,162,164}\text{Dy}$ was measured to test the rigid-rotor prediction for intraband $B(E2)$ ratios. The deexcitation gamma rays were observed in

singles and in the particle-gamma coincident mode following excitation by ^{20}Ne or ^{35}Cl ions from the Oak Ridge Isochronous Cyclotron. $B(E2)$ values were extracted by comparing experimental excitation probabilities with theoretical values calculated with the Winther-de Boer computer code. Vibrational states, $E4$ Coulomb excitation, and quantal corrections were included in the calculations. To check for Coulomb-nuclear interference, we set a narrow digital window,

127.6 to 120.9 MeV, and a wide digital window, 127.6 to 108.7 MeV, on the heavy-ion energy for one of the ^{35}Cl -gamma runs. If $R_0 = 1.2A^{1/3}$ fm, the corresponding separation distances between surfaces were 5.0 to 5.8 fm for the narrow window and 5.0 to 7.7 fm for the wide window. Since the experimental probabilities extracted with the two windows were in good agreement, we doubt that Coulomb-nuclear interference is significant in the present work.

ORNL-DWG. 72-11994A

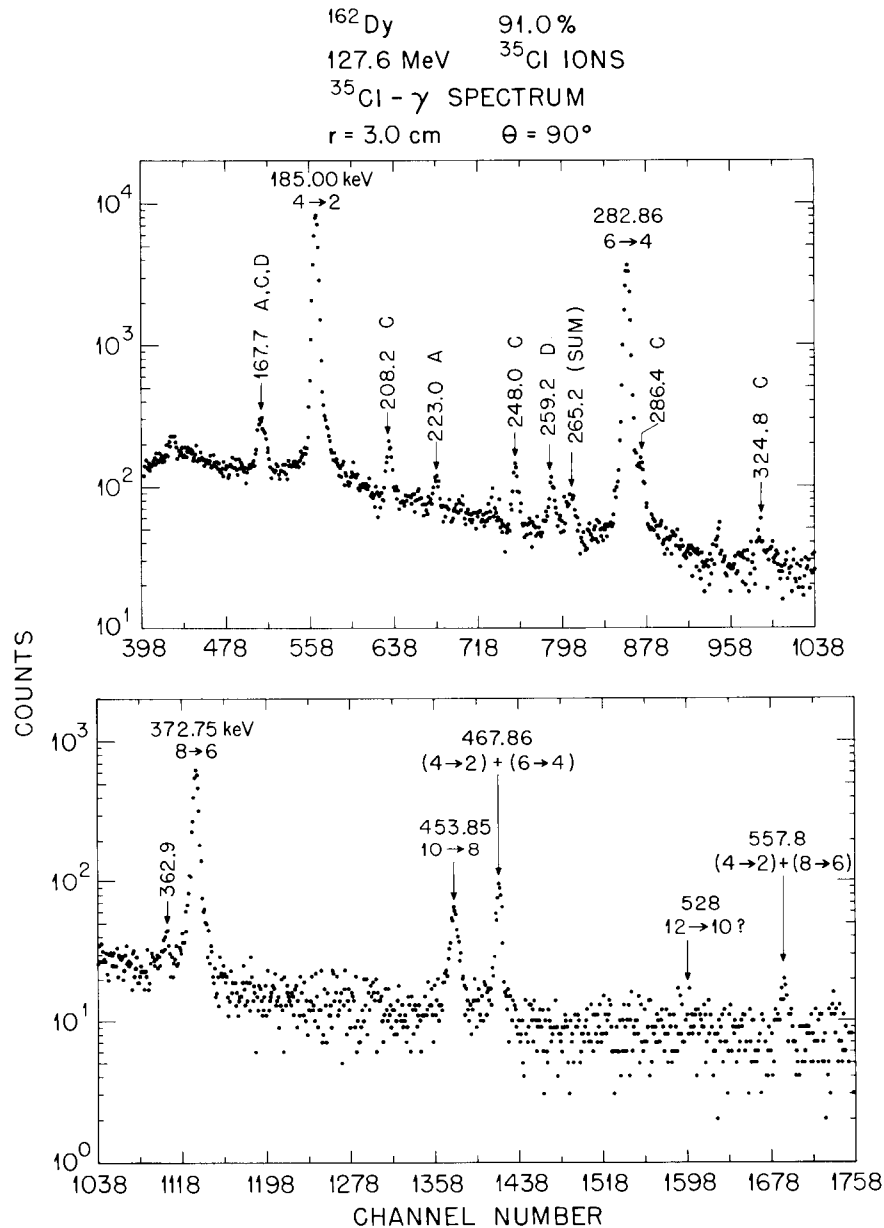


Fig. 1. Ge(Li)-detector spectrum of gamma rays in coincidence with ^{35}Cl ions backscattered from a ^{162}Dy target. Peaks labeled A, C, and D are attributed to the isotopic impurities $^{161,163,164}\text{Dy}$ respectively.

A sample spectrum of the gamma rays from ^{162}Dy in coincidence with backscattered ^{35}Cl ions is shown in Fig. 1. Our best $B(E2)$ values are given in Table 1 and compared graphically in Fig. 2 with recent Notre Dame⁵ results from Coulomb excitation with ^{16}O ions. There is excellent agreement between the two sets of data for the $2 \rightarrow 4$ and $4 \rightarrow 6$ transitions and a slight systematic discrepancy for the $6 \rightarrow 8$ transitions.

Two surprising features can be seen in Fig. 2. One is the 10 to 15% dip in $B(E2; 4 \rightarrow 6)$ below the rotational prediction, and the other is a jump in $B(E2)$ values at the 10^+ state. If other perturbing factors are ignored, centrifugal stretching is implied by the $B(E2; 8 \rightarrow 10)$ values, whereas the dip in $B(E2; 4 \rightarrow 6)$ could be explained only by a reduction in the nuclear deformation, that is, shrinking. The present data suggest that other perturbing factors must exert an important influence on the $B(E2)$ values in the ground bands of $^{160,162,164}\text{Dy}$.

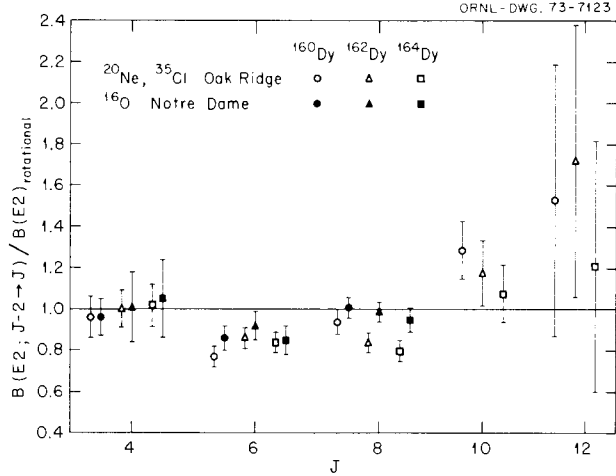


Fig. 2. Comparison of $B(E2)$ values derived from Coulomb excitation measurements with rigid-rotor predictions.

1. Consultant from Furman University, Greenville, S.C. (also, sponsored by Vanderbilt University, Nashville, Tenn.).
2. Chemistry Division.
3. Consultant from the University of Tennessee.

4. See R. M. Diamond, G. D. Symons, J. L. Quebert, K. H. Maier, J. R. Leigh, and F. S. Stephens, *Nucl. Phys. A* **184**, 481 (1972), and refs. 2-17 therein.
5. R. N. Oehlberg, L. L. Riedinger, A. E. Rainis, A. G. Schmidt, E. G. Funk, and J. W. Mihelich, *Bull. Amer. Phys. Soc.* **17**, 537 (1972); *Nucl. Phys.*, in press.

Table 1. Summary of best values for double probability ratios from particle-gamma coincident data and best $B(E2)$ values

Nucleus	$B(E2; 0 \rightarrow 2)^a$ ($e^2 \cdot 10^{-48} \text{ cm}^4$)	J/I	$\left[\frac{R(J/I)_{\text{exp}}}{R(J/I)_{\text{theory}}} \right]^b$	$B(E2; I \rightarrow J)^c$ ($e^2 \cdot 10^{-48} \text{ cm}^4$)	$\left[\frac{B(E2; I \rightarrow J)}{B(E2; I \rightarrow J)_{\text{rot}}} \right]^d$
^{160}Dy	5.057	4/2		2.50 ± 0.25	0.96 ± 0.10
		6/4	0.788 ± 0.023	1.78 ± 0.09	0.77 ± 0.05
		8/6	0.970 ± 0.042	2.05 ± 0.13	0.94 ± 0.06
		10/8	1.334 ± 0.116	2.73 ± 0.27	1.29 ± 0.14
		12/10	1.58 ± 0.68	3.17 ± 1.37	1.53 ± 0.66
^{162}Dy	5.128	4/2		2.64 ± 0.24	1.00 ± 0.09
		6/4	0.856 ± 0.036	2.00 ± 0.09	0.86 ± 0.05
		8/6	0.879 ± 0.027	1.85 ± 0.10	0.84 ± 0.05
		10/8	1.221 ± 0.159	2.53 ± 0.34	1.18 ± 0.16
		12/10	1.78 ± 0.67	3.62 ± 1.39	1.72 ± 0.66
^{164}Dy	5.403	4/2		2.83 ± 0.31	1.02 ± 0.11
		6/4	0.866 ± 0.051	2.06 ± 0.11	0.84 ± 0.05
		8/6	0.839 ± 0.032	1.86 ± 0.11	0.80 ± 0.05
		10/8	1.110 ± 0.131	2.44 ± 0.32	1.08 ± 0.14
		12/10	1.25 ± 0.62	2.68 ± 1.35	1.21 ± 0.61

^aValue used in theoretical calculations. See Lobner et al., *Nucl. Data A7*, 495 (1970).

^bTheoretical values were calculated with the Winther-de Boer computer code using rotational $E2$ matrix elements. Errors quoted do not include errors in the theoretical $R(J/I)$ values.

^cTheoretical uncertainties are included in the quoted errors. Singles data and particle-gamma data were used to determine $B(E2; 4 \rightarrow 6)$ and $B(E2; 6 \rightarrow 8)$ values for $^{162,164}\text{Dy}$.

^dQuoted errors include error in $B(E2; 0 \rightarrow 2)$.

LIFETIMES OF ROTATIONAL STATES
IN ^{154}Sm

R. J. Sturm¹ R. O. Sayer⁴
N. R. Johnson² E. Eichler²
M. W. Guidry³ N. C. Singhal⁵
D. C. Hensley

The Doppler-shift–recoil-distance method is currently considered to be the most reliable method to measure lifetimes in the range of 1 psec to 1 nsec. Direct determination of the lifetimes of nuclear states is very important, since they yield absolute transition probabilities. From these quantities it is possible to get the related electromagnetic matrix elements, which provide critical tests of nuclear models.

The method is based on the Doppler-shift principle. A thin target (typically 1 mg/cm²) is stretched and mounted parallel to a metallic lead stopper. A heavy-ion beam (e.g., $^{40}\text{Ar}^{8+}$) incident on the target produces Coulomb excitation – in our case, of the members of the ground-state band of ^{154}Sm – and causes target nuclei to recoil into vacuum.

If a recoiling ion comes to rest before the excited state decays, the gamma ray emitted has its characteristic energy. However, if the nucleus decays in flight, the gamma ray is shifted to a higher energy corresponding to the added momentum of the recoiling ion. The gamma-ray spectrum is measured with a Ge(Li) detector located behind the stopper at 0° to the beam direction

and operated in coincidence with backscattered (160° to 174°) ^{40}Ar projectiles which are intercepted by an annular silicon surface-barrier detector.

As the separation between the target and stopper is varied, the intensities of the “shifted” (S) and “unshifted” (U) gamma-ray peaks also vary in a manner depending on the lifetime of the excited nuclear state.

The natural logarithm of the ratio of the unshifted peak to the total (shifted plus unshifted peaks) plotted as a function of target-stopper separation yields a line the slope of which is inversely proportional to the mean life of the nuclear state. Such a plot for the $10^+ \rightarrow 8^+$, $8^+ \rightarrow 6^+$, and $6^+ \rightarrow 4^+$ transitions of ^{154}Sm is shown in Fig. 1.

It is important to emphasize that the uncorrected ratios extracted from the raw data usually show a nonlinear behavior. This is due to several perturbing effects, which are listed below.

1. The solid angle of the detector is increased when a recoiling nucleus moves towards the stopper.
2. The effective solid angle of the detector is a function of recoil velocity because of the forward bending of gamma rays emitted in flight (relativistic effect).
3. The detector efficiencies for unshifted and shifted gamma rays are different.
4. The feeding from higher-lying states with comparable lifetimes changes the shape of the decay curve.
5. The hyperfine interaction of the nucleus with unpaired electrons of the highly ionized atom causes a loss of nuclear alignment with increasing time. This means that the angular distribution of emitted gamma rays is changed during flight.

A computer program has been developed to correct for these effects. Since a proper correction requires the knowledge of the lifetime of the nuclear state under consideration, the final value of the lifetime is determined by an iterative process. In principle the program can handle an unlimited number of feeding states and feeding cascades.

Our first lifetime measurements were done on the deformed nucleus ^{154}Sm . States up to a spin of 10^+ were Coulomb-excited in two different runs with an $^{40}\text{Ar}^{8+}$ beam (145 MeV and 153 MeV respectively). A rolled ^{154}Sm foil of 1 mg/cm² thickness was used as a target. From the first run (145-MeV ^{40}Ar , long distance range) we were able to extract the lifetimes of the 4^+ and 6^+ rotational states. The second run (153-MeV ^{40}Ar , short distance range) yielded the lifetimes of the 6^+ , 8^+ , and 10^+ rotational states.

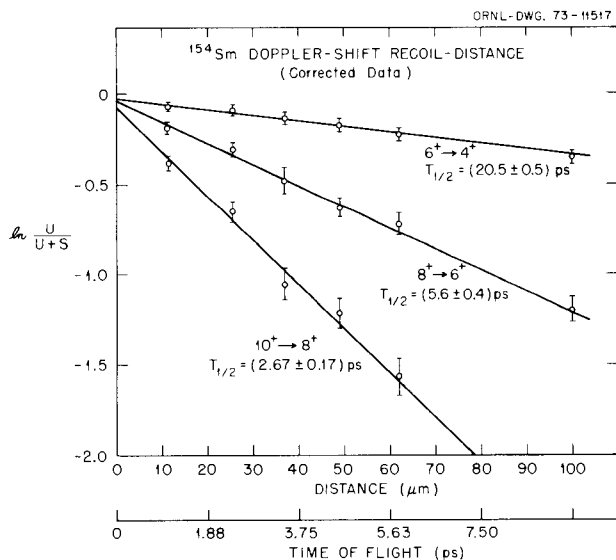


Fig. 1. Plot of $\ln [U/(U+S)]$ vs the separation distance between the target and stopper for the 6^+ , 8^+ , and 10^+ members of the ^{154}Sm ground-state rotational band.

Table 1. Summary of half-lives and $B(E2)$ values for ^{154}Sm

Transition	E (keV)	$T_{1/2}$ (psec)	Exp. $B(E2)$ (e^2b^2)	$B(E2)$, exp./rot. theory
$2 \rightarrow 0$	81.99		$(0.86 \pm 0.006)^a$	$1.00^b \pm 0.007$
$4 \rightarrow 2$	184.8	154 ± 8	1.25 ± 0.06	1.07 ± 0.06
$6 \rightarrow 4$	276.9	$\begin{pmatrix} 21.0 \pm 0.3 \\ 20.5 \pm 0.5 \end{pmatrix}$	1.55 ± 0.022	1.14 ± 0.02
$8 \rightarrow 6$	358.9	5.6 ± 0.4	1.64 ± 0.12	1.17 ± 0.09
$10 \rightarrow 8$	430.2	2.67 ± 0.17	1.42 ± 0.09	0.98 ± 0.06

^a $B(E2)$ value measured by Coulomb excitation [T. K. Saylor, J. X. Saladin, I. Y. Lee, and U. A. Erb, *Phys. Lett.* **42**, 51 (1972)].

^bNormalized to unity for the $2 \rightarrow 0$ transition.

The measured half-lives of ^{154}Sm are given in Table 1. The two values for the $6^+ \rightarrow 4^+$ transition are separate evaluations of the first and the second runs respectively. The excellent agreement demonstrates the good reproducibility of plunger data.

The lifetime of the 10^+ state requires some additional remarks. Due to the short half-life of this state (2.67 psec) the unshifted peak should show a considerable DSA (Doppler shift attenuation) structure. However, since the statistics are poor, it is not clear cut that all events above the background between unshifted and shifted peak are attributable to DSA structure. Probably there are one or more weak peaks beneath the DSA part, which can change the lifetimes significantly. Further studies of this problem are in progress.

For each half-life measured we have computed the corresponding $B(E2)$ value (see column 4 of Table 1). The ratio of measured to theoretical $B(E2)$ values is given in column 5 of Table 1. The theoretical values are based on the rotational model. The large increase of this ratio for higher-spin states indicates a large change in intrinsic structure with higher angular velocity of the rotating core.

1. Max Kade Foundation Fellow, University of Marburg, Marburg, Germany.

2. Chemistry Division.

3. Oak Ridge Graduate Fellow from the University of Tennessee under appointment with the Oak Ridge Associated Universities to ORNL Chemistry Division.

4. Consultant from Furman University, Greenville, S.C. (also, sponsored by Vanderbilt University, Nashville, Tenn.).

5. Vanderbilt University, Nashville, Tenn., Postdoctoral Fellow with ORNL Chemistry Division.

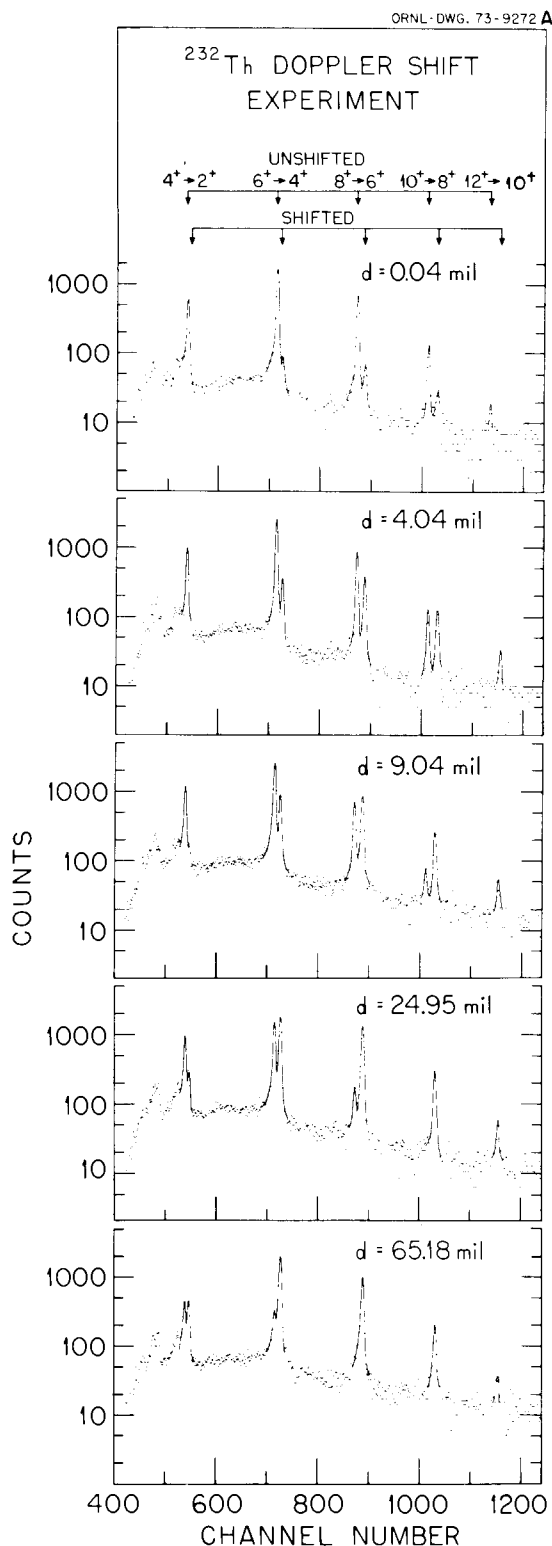
LIFETIMES OF ROTATIONAL STATES IN ^{232}Th BY THE DOPPLER-SHIFT-RECOIL-DISTANCE TECHNIQUE

N. R. Johnson¹ R. O. Sayer⁴
R. J. Sturm² N. C. Singhal⁵
E. Eichler¹ G. D. O'Kelley¹
M. W. Guidry³ D. C. Hensley

The main aspect of our Coulomb excitation program at ORIC is a continuing investigation of the behavior of deformed actinide nuclei at high spins. For example, in a study of the multiple Coulomb excitation process in ^{232}Th and ^{238}U with ^{40}Ar projectiles, we⁶ were able to establish that the shapes of the nuclei are characteristic of large positive rather than negative hexadecapole moments. Some reservation is introduced into such a conclusion, since it is necessary to rely on the rotational model for the required $E2$ and $E4$ matrix elements in the Winther de Boer computer program.

Since the emission of $E4$ radiation cannot compete with the $E2$ process in the deexcitation of these rotational states, a direct measurement of their lifetimes provides the $E2$ matrix elements in a model-free manner. Thus a major objective now is to obtain such lifetime data for the actinide nuclei.

We have used the Doppler-shift-recoil-distance technique to measure the lifetimes of members of the ground-state band in ^{232}Th up through a spin of 10^+ . A beam of 152-MeV ^{40}Ar projectiles from ORIC was used to Coulomb-excite the states in 1.5-mg/cm² metallic thorium foils. The experimental details are described in a separate report.⁷



The type of data obtained in these experiments is illustrated in Fig. 1, which shows the spectra of shifted and unshifted gamma-ray peaks at several target-stopper separations. In Fig. 2 we show for each transition a plot of the ratio of the unshifted gamma-ray peak to the sum of the shifted plus the unshifted peaks as a function of both the target-stopper separation and the equivalent time of flight of the recoiling thorium nuclei. These data have been corrected for several small perturbing effects. (For details on these corrections see ref. 7). A summary of the half-lives determined here is given in column 3 of Table 1.

For each half-life, we have computed the corresponding reduced electric quadrupole transition probability, $B(E2)$, and compared it with the prediction of the rotational model. As seen in column 5 of Table 1, there is good agreement between experiment and theory for all states. Not only does this result agree with the rotational model, but in addition it lends support to our earlier conclusion that the sign of the $E4$ moment in ^{232}Th is positive.

1. Chemistry Division.
2. Max Kade Foundation Fellow, University of Marburg, Marburg, Germany.
3. Oak Ridge Graduate Fellow from the University of Tennessee under appointment with the Oak Ridge Associated Universities to ORNL Chemistry Division.
4. Consultant from Furman University, Greenville, S.C. (also, sponsored by Vanderbilt University, Nashville, Tenn.).
5. Vanderbilt University, Nashville, Tenn., Postdoctoral Fellow assigned to ORNL Chemistry Division.
6. E. Eichler, N. R. Johnson, R. O. Sayer, D. C. Hensley, and L. L. Riedinger, *Phys. Rev. Lett.* **30**, 568 (1973).
7. R. J. Sturm, N. R. Johnson, M. W. Guidry, R. O. Sayer, E. Eichler, N. C. Singhal, and D. C. Hensley, "Lifetimes of Rotational States in ^{154}Sm ," this report.

Fig. 1. Spectra of shifted and unshifted gamma rays in ^{232}Th at several target-stopper separations.

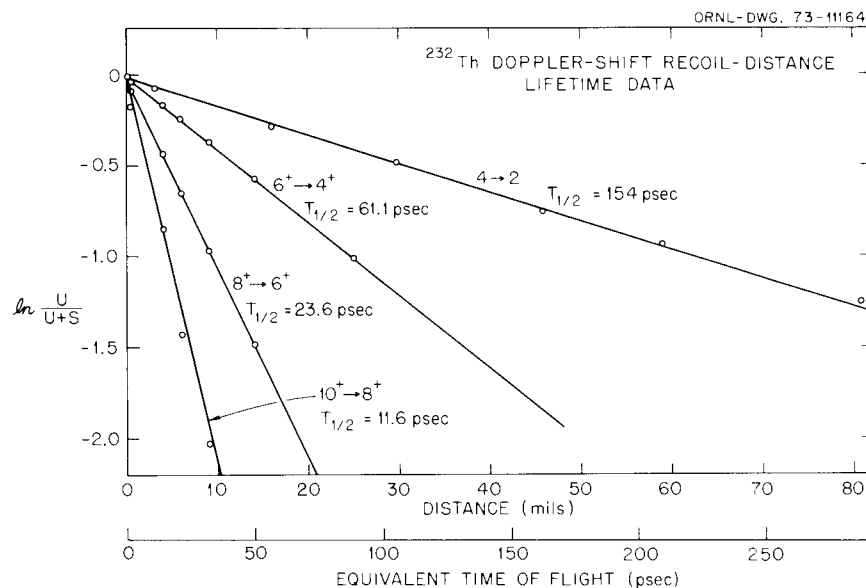


Fig. 2. Plot of ratios of unshifted to sum of unshifted plus shifted gamma-ray peak intensities as a function of target-stopper separation for ^{232}Th .

Table 1. Summary of half-life and $B(E2)$ data for ^{232}Th

Transition	E (keV)	$T_{1/2}$ (psec)	Exp. $B(E2)$ (e^2b^2)	$B(E2)$, exp./theory
$2 \rightarrow 0$	49.37		1.84 ^a	1.00 ^b
$4 \rightarrow 2$	112.75	154 ± 9	2.56	0.97 ± 0.05
$6 \rightarrow 4$	171.00	61.1 ± 3.8	2.87	0.99 ± 0.06
$8 \rightarrow 6$	223.84	23.6 ± 1.7	2.94	0.97 ± 0.07
$10 \rightarrow 8$	270.47	11.6 ± 1.9	2.72	0.88 ± 0.14

^aC. E. Bemis, Jr., F. K. McGowan, J. L. C. Ford, W. T. Milner, P. H. Stelson, and R. L. Robinson, *Phys. Rev. C* **6**, 1466 (1973).

^bNormalized to unity.

MULTIPLE COULOMB EXCITATION OF ^{236}U

M. W. Guidry¹ G. D. O'Kelley³
 R. J. Sturm² R. O. Sayer⁴
 N. R. Johnson³ G. B. Hagemann⁵
 E. Eichler³ D. C. Hensley
 L. L. Riedinger⁶

Coulomb excitation work with alpha particles⁷ has demonstrated the presence of significant hexadecapole deformation in ^{236}U . Unfortunately the sign of the hexadecapole moment cannot be established by such an experiment. It is possible to remove this sign ambiguity through heavy-ion multiple Coulomb excitation.

The multiple Coulomb excitation of ^{236}U has been performed with a 152.4-MeV $^{40}\text{Ar}^{8+}$ beam from the Oak Ridge Isochronous Cyclotron using the thick-target technique. The gamma spectrum of Fig. 1 was taken in coincidence with backscattered heavy ions and exhibits peaks corresponding to cascade $E2$ transitions from all levels in the ground-state rotational band through the 12^+ state (excluding the 2^+ state, which is almost entirely converted). Peak areas were extracted and used to compute experimental excitation probabilities. The Winther-de Boer Coulomb excitation code,⁸ modified to include a thick target⁹ and $E4$ matrix elements,¹⁰ and employing rotational matrix elements derived from the $B(E2; 0^+ \rightarrow 2^+)$ value of Bemis et al.⁷ was used to compute theoretical excitation probabilities.

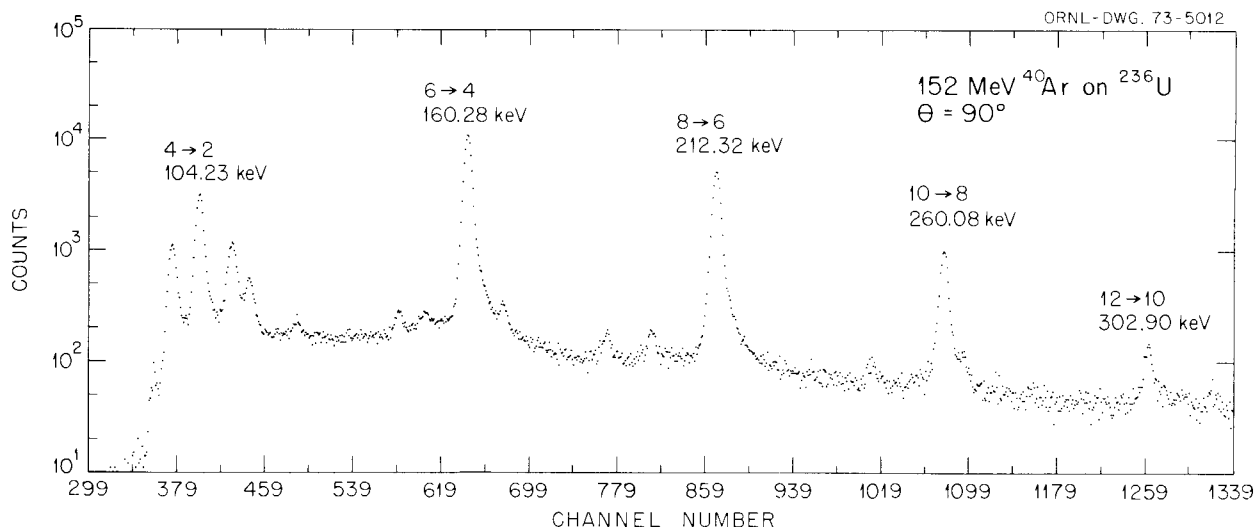


Fig. 1. ^{236}U Ground-state rotational band in coincidence with backscattered 152.4-MeV $^{40}\text{Ar}^{8+}$ ions.

Table 1. Ratios of experimental to theoretical Coulomb excitation probabilities for the ground-state rotational band in ^{236}U

	$M(E2)$ only ^a	$M(E4)$ (+) ^b	$M(E4)$ (-) ^c
Ratios, experimental/theory			
6^+ level	1.00 ± 0.05	1.00 ± 0.05	1.00 ± 0.05
8^+ level	1.16 ± 0.05	1.07 ± 0.05	1.31 ± 0.07
10^+ level	1.13 ± 0.08	0.95 ± 0.07	1.32 ± 0.12
12^+ level	1.14 ± 0.20	0.83 ± 0.13	1.29 ± 0.25
Matrix elements			
$\langle 2^+ M(E2) 0^+ \rangle$	-3.40	-3.40	-3.36
$\langle 4^+ M(E4) 0^+ \rangle$	0	1.23	1.99

^aRatios are normalized to the 6^+ level, $(P_{\text{exp}}/P_{\text{theor}})_{6^+} = 0.74$.

^bRatios are normalized to the 6^+ level, $(P_{\text{exp}}/P_{\text{theor}})_{6^+} = 0.80$.

^cRatios are normalized to the 6^+ level, $(P_{\text{exp}}/P_{\text{theor}})_{6^+} = 0.78$.

Table 1 presents a comparison of experimental probabilities with those computed using $E2$ matrix elements alone and $E2$ elements in conjunction with $E4$ elements derived from the positive and negative values, respectively, for the hexadecapole moment. The good agreement between experimental and theoretical values using the $E4$ matrix elements derived from the positive $E4$ moment (contrasted with the significant deviations for those derived from the negative $E4$ moment)

supports the assignment of a positive sign to the ^{236}U hexadecapole moment. Similar conclusions have been reported¹¹ for earlier work on ^{238}U and ^{232}Th .

At this stage the data of Table 1 have not been corrected for quantum mechanical deviations from the semiclassical Winther-de Boer treatment, inclusion of relevant vibrational matrix elements in the calculation, or the effect of $E6$ or higher-order moments. We must therefore give some consideration to these corrections and their effect on the data.

The Winther-de Boer code is based on a semiclassical approach and does not treat the projectile dynamics in a rigorous quantum mechanical fashion. The magnitude of quantal effects through spin 8^+ has been investigated,¹²⁻¹⁴ and extrapolation to higher states suggests that this correction increases with spin and may lower the semiclassical excitation probability by 10 to 15% for the 10^+ and 12^+ states.

The correction due to coupling of vibrational states to the ground band may be investigated by inclusion of the relevant matrix elements in the calculation. The ^{236}U vibrational states are similar to those of ^{238}U , where previous work¹¹ suggests that this correction will raise the theoretical excitation probabilities by less than 5 to 10%.

The effect of $E6$ moments cannot currently be included in our computer code. We expect these contributions to be small, however, and their neglect should not introduce appreciable error.

One must additionally question the validity of using the rotational model to derive the set of $E2$ and $E4$

matrix elements used in the calculation. Preliminary lifetime measurements on ^{236}U using the Doppler-shift-recoil-distance technique¹⁵ suggest that the $E2$ transition probabilities are rotational through spin 10^+ , and we assume the $E4$ matrix elements to show analogous behavior.

With these considerations the primary corrections appear to be the quantum mechanical and vibrational effects. Because these act in opposite directions, they should largely cancel for the lower-spin states. At the higher spins the quantal corrections should dominate and may be the cause of the decrease in the experimental/theoretical ratio for $M(E4)$ (+) at the 12^+ state (Table 1). This is a preliminary conclusion, however, and is predicated upon a proper treatment of vibrational states, rotational behavior of the $M(E4)$ matrix elements, and neglect of $E6$ transition moments.

1. Oak Ridge Graduate Fellow from the University of Tennessee, Knoxville, Tenn., under appointment from the Oak Ridge Associated Universities to ORNL Chemistry Division.

2. Max Kade Foundation Fellow from University of Marburg, Marburg, Germany.

3. Chemistry Division.

4. Consultant from Furman University, Greenville, S.C. (also, sponsored by Vanderbilt University, Nashville, Tenn.).

5. Visiting scientist from Niels Bohr Institute, Copenhagen, Denmark.

6. Consultant from the University of Tennessee, Knoxville, Tenn.

7. C. E. Bemis, Jr., F. K. McGowan, J. L. C. Ford, Jr., W. T. Milner, P. H. Stelson, and R. L. Robinson, *Phys. Rev.* C8, 1466 (1973).

8. A. Winther and J. de Boer in *Coulomb Excitation*, ed. by K. Alder and A. Winther (Academic, New York, 1966), p. 303.

9. R. O. Sayer, Ph.D. thesis, University of Tennessee, 1968.

10. A. Holm, private communication.

11. E. Eichler, N. R. Johnson, R. O. Sayer, D. C. Hensley, and L. L. Riedinger, *Phys. Rev. Lett.* 30, 568 (1973).

12. K. Alder, R. Morf, and F. Roesel, *Phys. Lett.* 32B, 645 (1970).

13. K. Alder, F. Roesel, and R. Morf, *Nucl. Phys.* A186, 449 (1972).

14. K. Alder, private communication.

15. M. W. Guidry, R. J. Sturm, G. D. O'Kelley, N. R. Johnson, E. Eichler, R. O. Sayer, and N. C. Singhal, "Lifetimes of Rotational States in ^{236}U by the Doppler-Shift-Recoil-Distance Technique," this report.

LIFETIMES OF ROTATIONAL STATES IN ^{236}U BY THE DOPPLER-SHIFT-RECOIL-DISTANCE TECHNIQUE

M. W. Guidry¹ N. R. Johnson³
R. J. Sturm² E. Eichler³
G. D. O'Kelley³ R. O. Sayer⁴
N. C. Singhal⁵

Half-lives for the 6^+ , 8^+ , and 10^+ members of the ^{236}U ground-state rotational band have been determined by the recoil-distance technique following Coulomb excitation produced by 152-MeV $^{40}\text{Ar}^{8+}$ projectiles at ORIC. Corrections for (1) energy dependence of detection efficiency, (2) positional and velocity dependence of solid angle, and (3) multistage cascade feeding have been applied in a manner described in a previous report.⁶ The correction for alignment attenuation has not been applied at this time, as the necessary parameters must be determined in a forthcoming experiment.

Figure 1 is a plot of $\ln R$ vs target-stopper distance D for the $6^+ \rightarrow 4^+$, $8^+ \rightarrow 6^+$, and $10^+ \rightarrow 8^+$ transitions, where R is the experimentally determined ratio of intensity in the unshifted peak to total unshifted and shifted intensity (suitably corrected for the perturbing effects mentioned above).

The half-lives extracted from these data and a comparison of corresponding $B(E2)$ values with rotational predictions are shown in Table I. The constancy of the $B(E2)$ ratios as a function of spin is indicative of rotational behavior for these states. The effect of the omitted correction for alignment attenuation is ex-

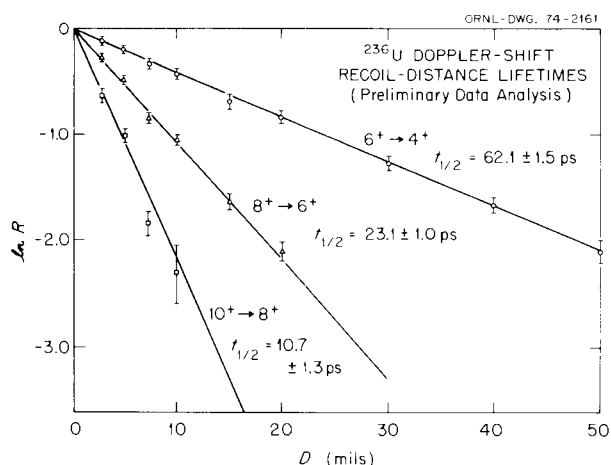


Fig. 1. $\ln R$ vs target-stopper distance for ^{236}U .

Table 1. ^{236}U half-lives and $B(E2)$ values

Transition	$T_{1/2}$ (exp.) ^a (psec)	$B(E2)/B(E2)_{\text{rot}}$ ^b
$6^+ \rightarrow 4^+$	62.1 ± 1.5	0.85 ± 0.05
$8^+ \rightarrow 6^+$	23.1 ± 1.0	0.92 ± 0.06
$10^+ \rightarrow 8^+$	10.7 ± 1.3	0.87 ± 0.14

^aAlignment attenuation not included.

^bComputed using $B(E2; 0^+ \rightarrow 2^+)$ of Bemis et al. [C. E. Bemis, Jr., F. K. McGowan, J. L. C. Ford, Jr., W. T. Milner, P. H. Stelson, and R. L. Robinson, *Phys. Rev. C* **8**, 1466 (1973)].

pected to lower these experimental/rotor ratios by 5 to 10% or less.

The extension of this work to higher-spin states, correction for alignment attenuation, and a comparison with multiple Coulomb excitation data on this nucleus⁷ should provide valuable insight into the validity of the rotational model in the actinide region and the reliability of multiple Coulomb excitation work on high-spin states.

1. Oak Ridge Graduate Fellow from the University of Tennessee, Knoxville, Tenn., under appointment from Oak Ridge Associated Universities.

2. Max Kade Foundation Fellow from University of Marburg, Marburg, Germany.

3. Chemistry Division.

4. Consultant from Furman University, Greenville, S.C. (also, sponsored by Vanderbilt University, Nashville, Tenn.).

5. Vanderbilt University Postdoctoral Fellow assigned to ORNL Chemistry Division.

6. R. J. Sturm, N. R. Johnson, M. W. Guidry, R. O. Sayer, E. Eichler, N. C. Singhal, and D. C. Hensley, "Lifetimes of Rotational States in ^{154}Sm ," this report.

7. M. W. Guidry, R. J. Sturm, N. R. Johnson, E. Eichler, G. D. O'Kelley, R. O. Sayer, G. B. Hagemann, D. C. Hensley, and L. L. Riedinger, "Multiple Coulomb Excitation of ^{236}U ," this report.

NEW ISOTOPES AND SPECTROSCOPY

X-RAY IDENTIFICATION OF TRANSFERMIUM ELEMENTS

C. E. Bemis, Jr.¹ J. R. Tarrant¹
 R. J. Silva¹ L. C. Hunt¹
 D. C. Hensley P. F. Dittner¹
 O. L. Keller, Jr.¹ R. L. Hahn¹
 C. D. Goodman

We have reported² the conclusive determination of the atomic number of element 104 by an extended

x-ray identification technique. This technique relies on the observation of x rays from the daughter element in coincidence with alpha particles from the decay of the parent element. The x rays can arise from atomic rearrangements following internal conversion processes in the deexcitation of the daughter element, if the alpha decay should proceed to excited nuclear states.

We studied the 4.5-sec alpha-emitting isotope $^{257}\text{104}$, first produced in 1969 by Ghiorso and coworkers.³ The isotope was produced at the ORIC in the $^{249}\text{Cf}(^{12}\text{C},4n)^{257}\text{104}$ reaction at 73 MeV. The reaction products, recoiling out of the ^{249}Cf target, were thermalized in a small helium-filled chamber, continually pumped through a 0.013-in. orifice, and collected on a small disk of aluminum (1.43 cm in diameter and 0.053 cm thick). After a bombardment and collection time of about 10 sec, the catcher disk was pneumatically transferred a distance of 10 m in 1.7 sec to a heavily shielded counting room, where it was automatically positioned between an alpha-particle detector and a high-resolution photon detector. The following information was stored for each detected alpha particle: (1) alpha-particle pulse height, (2) pulse height of any coincident photon, (3) time relationship (0 to 100 μsec) between the alpha particle and the photon, (4) time of detection of the alpha particle in milliseconds relative to the arrival of the catcher disk.

Some 30,000 10-sec counting cycles were performed, during which about 3000 atoms of $^{257}\text{104}$ were produced and some 1000 alpha particles from the decay of these atoms were observed. An alpha-particle energy spectrum representing a portion of our data is shown in Fig. 1. Alpha particles associated with the decay of $^{257}\text{104}$ are expected to lie in the energy range between 8.5 and 9.1 MeV.

In Fig. 2, we show our experimental photon energy spectrum in histogram form for those photons correlated in time ($0 < t < 100 \mu\text{sec}$) with all alpha particles in the energy range 8.5 to 9.1 MeV. The K -series x-ray spectra predicted for elements with $Z = 100$ through 103 are shown in Fig. 2 and were constructed using the energies calculated by Carlson et al.⁴ and the intensities calculated by Lu, Malik, and Carlson.⁵ The effect of our instrumental energy resolution has been included also. Our measured energies for the $K\alpha_2$ and $K\alpha_1$ lines are 120.9 ± 0.3 and 127.2 ± 0.3 keV, respectively, and compare favorably with those predicted by Carlson et al. for $Z = 102$: 121.020 and 127.42 keV respectively.

It is quite clear from an examination of Fig. 2 that our experimental coincident photon spectrum can match in energy and intensity the theoretical K x-ray spectrum for $Z = 102$ only. Therefore, since we have

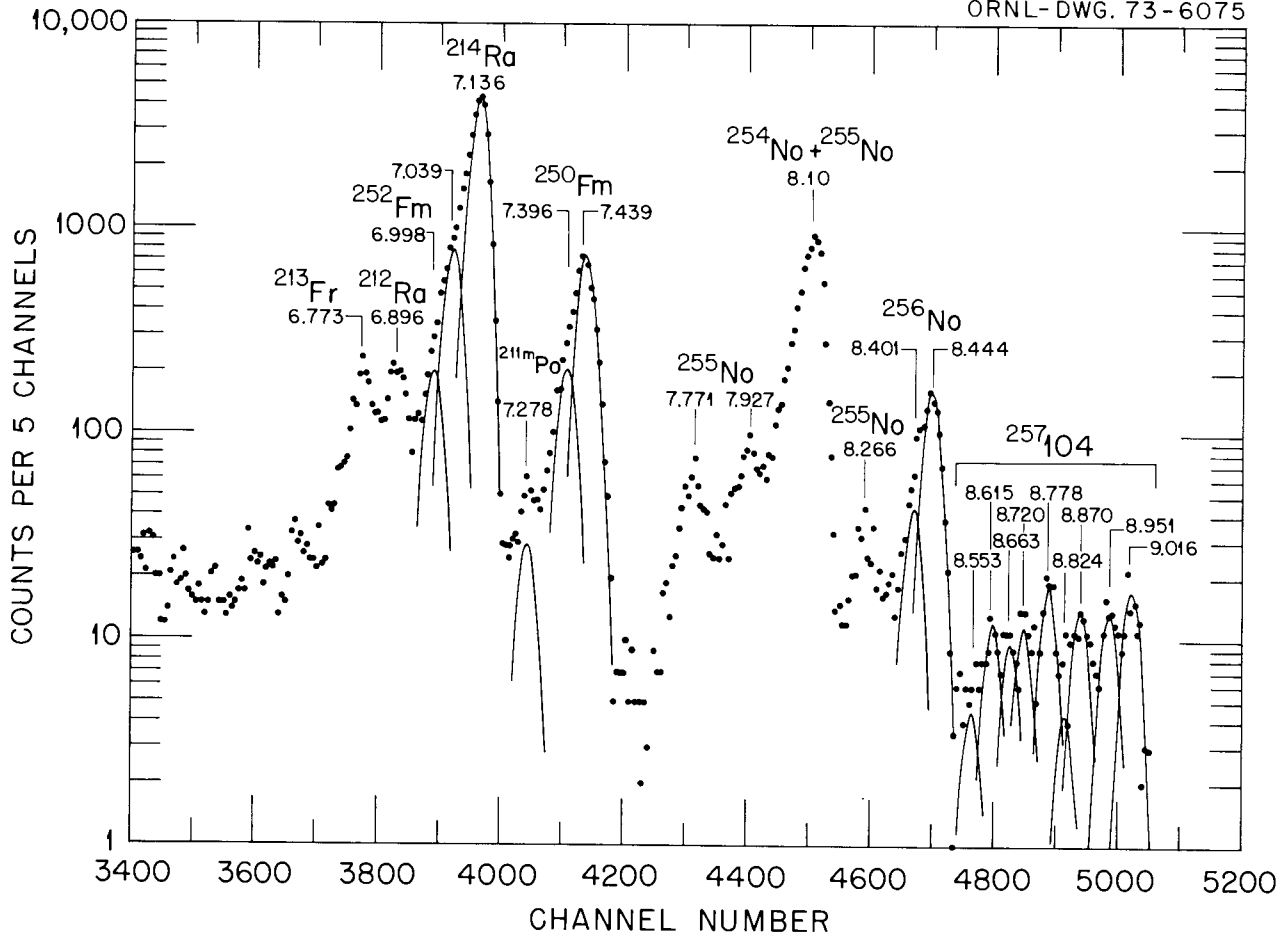


Fig. 1. Alpha-particle energy spectrum for activities produced in the bombardment of ^{249}Cf with 73.0-MeV ^{12}C ions for a total of 31.3 μAhr . Counting time is 11 sec, and the energy range expected for alpha events from the decay of $^{257}\text{104}$ is indicated.

observed *K*-series x rays characteristic of atomic number $Z = 102$ in coincidence with alpha particles (with $Z = 2$), we have established that the atomic number of the alpha-decaying parent is $Z = 104$. In addition, this demonstrates that a conclusive atomic-number determination may be made with the production of only a few thousand atoms.

We plan next to study the decay properties of $^{259}\text{104}$ in an effort to determine its fission decay branch.

The following changes to our experimental system are being studied and implemented, to prepare for a study of very short lived transfermium elements.

1. Changeover from a pneumatic-rabbit transfer system to a fast tape transfer system. The tape system will move collected activity some 10 ft through the shield

wall to our detectors in under 300 msec, and this should permit the study of quite short-lived activities. In addition, the tape system is more reliable and requires much less attention and maintenance, a must for long-duration experiments.

2. A possible increase in photon detection efficiency from about 15% to about 18% (absolute full-energy detection).

3. The use of logarithmic amplifiers to permit analysis of alpha particles and fission particles with a single amplifier system.

4. The development of a fast "read-on-the-fly" scaler for the analysis of x rays occurring prior to the appearance of a fission event.

5. Further optimization of the target assembly so that more beam current can be tolerated.

Upon completion of these changes, a long study of $^{260}_{105}$ is intended, with particular emphasis on any decay branch through $^{260}_{104}$. The search for element 106 should begin immediately thereafter.

1. Chemistry Division.
2. C. E. Bemis, Jr., R. J. Silva, D. C. Hensley, O. L. Keller, Jr., J. R. Tarrant, L. D. Hunt, P. F. Dittner, R. L. Hahn, and C. D. Goodman, *Phys. Rev. Lett.* **31**, 647 (1973).
3. A. Ghiorso, M. Nurmi, J. Harris, K. Eskola, and P. Eskola, *Phys. Rev. Lett.* **22**, 1317 (1969); A. Ghiorso, M. Nurmi, J. Harris, K. Eskola, and P. Eskola, *Nature* **229**, 603 (1971).
4. T. A. Carlson, C. W. Nestor, Jr., F. B. Malik, and T. C. Tucker, *Nucl. Phys.* **A135**, 57 (1969).
5. C. C. Lu, F. B. Malik, and T. A. Carlson, *Nucl. Phys.* **A175**, 289 (1971).

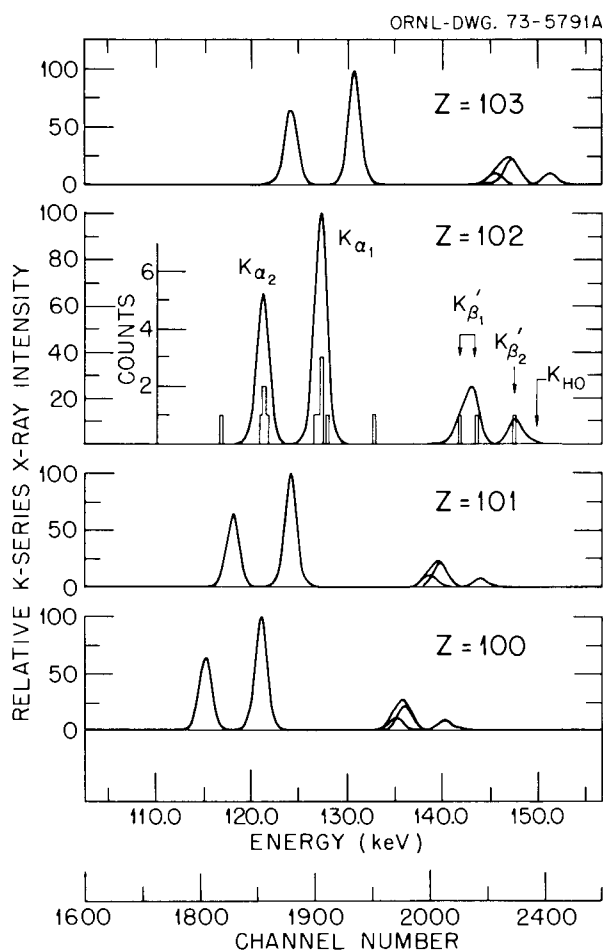


Fig. 2. Characteristic K-series x-ray spectra expected for elements with $Z = 100$ through 103. The experimental photon spectrum coincident with alpha particles in the energy range 8.5 to 9.1 MeV is shown in histogram fashion under the curve labeled 102 and forms the basis for a conclusive identification of element 104.

DECAY SCHEME STUDIES IN THE 82-NEUTRON REGION; NEW ISOTOPES, ^{146}Tb AND ^{148}Dy

K. S. Toth D. C. Hensley
E. Newman C. R. Bingham¹
W.-D. Schmidt-Ott²

The study of isotopes with 81, 82, and 83 neutrons is a prerequisite for extending shell-model calculations to this region of the periodic table. In particular, the assumption of a doubly magic $N = 82$, $Z = 50$ core for 82-neutron odd-mass nuclei allows detailed microscopic calculations³ of the properties of their levels. Previously we investigated levels in ^{145}Eu (ref. 4) and in ^{145}Sm (ref. 5) by combining data from decay scheme and transfer reaction studies. The unavailability of stable targets with $N = 82$ beyond ^{144}Sm essentially rules out the investigation of nuclei with $Z > 63$ by means of direct reactions, and, instead, one must rely on decay scheme and in-beam gamma-ray studies. During the past year, we utilized the ORIC heavy-ion beams and a helium gas-jet-capillary transport system to produce and investigate the decay properties of terbium and dysprosium isotopes in the 82-neutron region. In the course of these studies, two new isotopes were discovered, namely, 23-sec ^{146}Tb and 3.1-min ^{148}Dy .

Levels in ^{147}Gd

The investigation of levels in ^{147}Gd is an outgrowth of our earlier study⁵ of levels in its isotone, ^{145}Sm . There, by examining data for even- Z , $N = 83$ isotopes, we predicted the approximate excitation energies for several as yet unreported single-neutron states in ^{147}Gd (see Fig. 1). In-beam data are available⁶ for that particular nucleus together with information obtained in ^{147}Tb decay studies.^{7,8} Chu, Franz, and Friedlander⁷ were the first to report the existence of two isomers in ^{147}Tb , one with a 1.6-hr half-life and the other, apparently a high-spin isomer, with a half-life of 2.5 min. A decay scheme for the 1.6-hr species was later published by Afanasiev et al.⁸ Nevertheless it was apparent that a more detailed investigation of the decay properties of the two ^{147}Tb isomers was necessary to supplement the in-beam gamma-ray measurements. Shortly after the study was begun, it became obvious that the gamma rays reported⁷ for the 2.5-min species were in fact associated with a high-spin isomer in ^{148}Tb . We therefore undertook a search for a high-spin isomer in ^{147}Tb and found it to have a 1.9 ± 0.1 min half-life. (A recent paper⁹ also reports the existence of

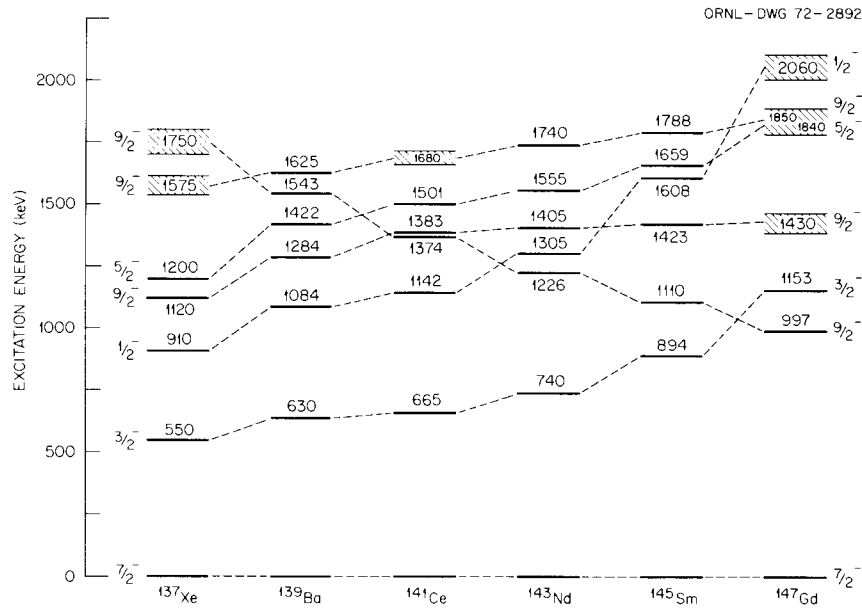


Fig. 1. Excitation energies of negative-parity levels for $N = 83$ isotones. Dashed lines connect levels which are assumed to have basically the same neutron configuration. Cross-hatched areas indicate predicted excitation energies of several so far unreported levels.

ORNL-DWG 73-7098

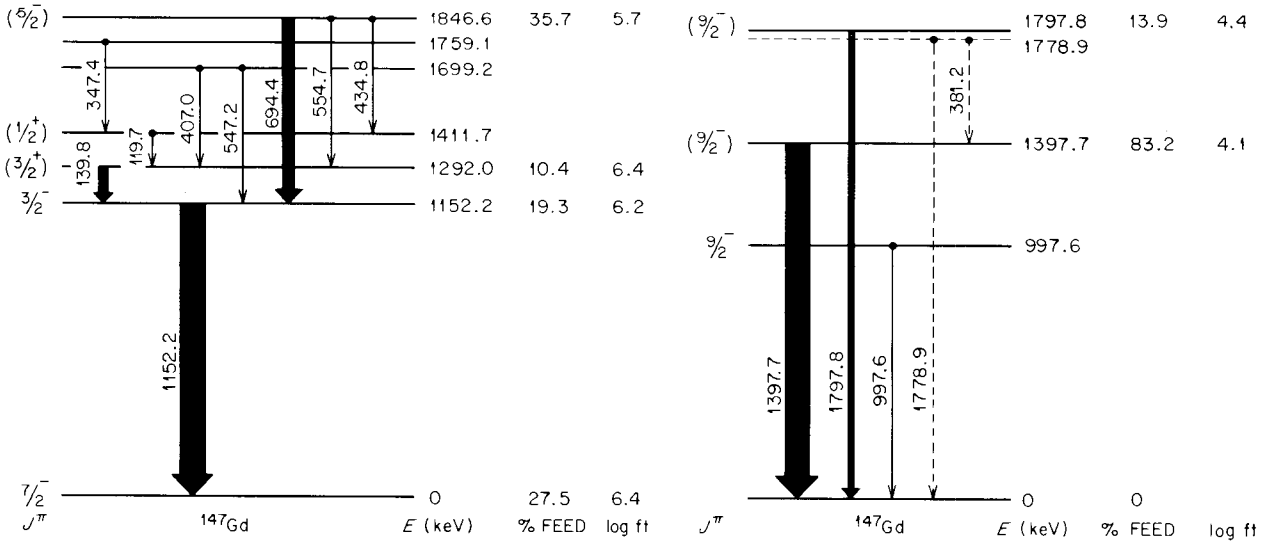
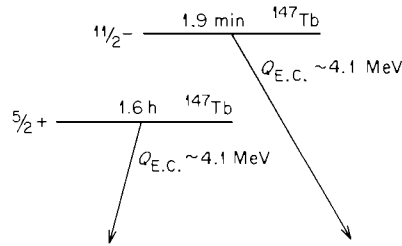


Fig. 2. Decay schemes for 1.6-hr and 1.9-min ^{147}Tb .

a short-lived ^{147}Tb isomer, with a half-life of 1.83 ± 0.06 min.)

The two isomeric states in ^{147}Tb almost certainly are due to the odd 65th proton being in either the $d_{5/2}$ or $h_{11/2}$ orbital. In the study⁴ of levels in ^{145}Eu , the systematics of single-proton centroids in odd-mass $N=82$ isotones were examined. For ^{145}Eu the first three states are as follows: 0 keV ($d_{5/2}$), 330 keV ($g_{7/2}$), and 716 keV ($h_{11/2}$). The indication, however, was that with increasing Z the $h_{11/2}$ orbital was dropping rapidly in excitation energy while the $g_{7/2}$ orbital was rising. The possibility that in ^{147}Tb these orbitals would cross, giving rise to an $E3$ isomer, is now confirmed by the fact that a high-spin isomer has been found.

The decay schemes for the two isomers are shown in Fig. 2. The spin assignments of the ^{147}Gd ground state and its two lowest excited levels at 997.6 and 1152.2 keV appear to be well described^{5,6} by the neutron orbitals $f_{7/2}$, $h_{9/2}$, and $p_{3/2}$. The parities of the levels at 1292.0 and 1411.5 keV must be positive, because internal-conversion-electron measurements⁸ indicate that the 119.7- and 139.8-keV transitions are $M1 + E2$ and $E1$ respectively. In the decay of ^{145}Eu to levels in ^{145}Sm , two positive-parity states, $3/2^+$ and $1/2^+$, are observed⁵ lying above the $3/2^-$ single-neutron state. On the basis of a similar pattern of direct feeding and subsequent deexcitation, spins of $3/2^+$ and $1/2^+$ are also assigned to the 1292.0- and 1411.5-keV ^{147}Gd levels respectively. A $5/2^-$ assignment is proposed for the level at 1846.6 keV for two reasons: (1) once again, analogously, there is a single-neutron $5/2^-$ state in ^{145}Sm at 1658.6 keV with a large amount of direct feeding from ^{145}Eu decay, and (2) this $5/2^-$ level is predicted from systematics (see Fig. 1) to lie at 1840 ± 50 keV in ^{147}Gd . The two strong gamma rays, 1397.7 and 1797.8 keV, seen in the 1.9-min ^{147}Tb decay were found to be coincident only with annihilation radiation. Because of this fact and because there are no other intense 1.9-min gamma rays, the two transitions most probably proceed directly to ground and establish levels at 1397.7 and 1797.8 keV. These states are both proposed to be $1/2^-$ on the basis of the strong direct feeding from the $h_{11/2}$ ^{147}Tb isomer and because two $1/2^-$ levels were predicted (see Fig. 1) to be located in ^{147}Gd at 1430 ± 40 and 1850 ± 50 keV.

The interested reader is referred to the work reported in ref. 6, where evidence is presented to account for the large number of ^{147}Gd levels above about 1200 keV as being due to the coupling of single-neutron states to phonon excitations in the ^{146}Gd core.

Levels in ^{146}Gd

The assignment of the new 23-sec activity to ^{146}Tb is based primarily on the fact that five of its gamma rays have been observed by Kownacki et al.¹⁰ in a $^{144}\text{Sm}(\alpha, 2n\gamma)$ study. Its decay scheme, shown in Fig. 3, is based on our coincidence data and on information from the in-beam study. The levels at 1579.5 (2^+), 2658.4 (4^+), and 2982.4 (6^+) keV were reported in ref. 10. Our coincidence data confirm the existence of these states and also establish levels at 2996.9, 3099.4, 3139.6, and 3313.4 keV. The almost equal direct feeds to the 2^+ and 4^+ states suggest that the most probable spin of ^{146}Tb is 3.

Kownacki et al.¹⁰ have made an extensive examination of states in ^{144}Sm and ^{146}Gd ; qualitatively, at least, the majority of these states can be explained on the basis of two-quasi-particle configurations. We would like to concentrate on one apparent inconsistency, which has to do with the lowest-lying 3^- state in the $N=82$ isotones. This state starts out at 3279 keV in ^{136}Xe and drops precipitously as Z increases. In ^{144}Sm it is located at 1810 keV and is strongly fed by a transition from the 4^+ state at 2191 keV. In turn it deexcites primarily to the 2^+ state at 1660 keV and very weakly to ground. The

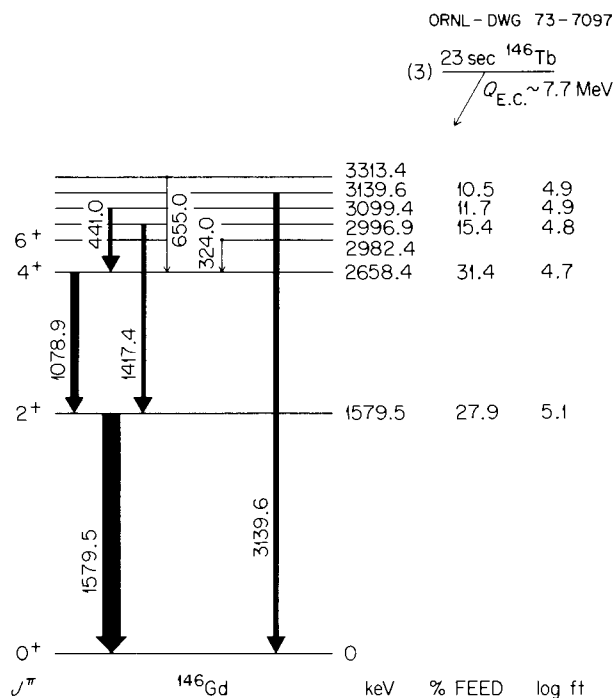


Fig. 3. Decay scheme for the new isotope ^{146}Tb .

situation in ^{146}Gd seems to be quite different — a strongly populated 3^- state has not been found.^{10,11} Instead, Kownacki et al.¹⁰ tentatively propose a state only 5 keV above the 2^+ level as being the “missing” 3^- state. They point out that this location fits reasonably well with systematics for the $N=82$ isotones. However, the $E1$, 1073.6-keV transition from the 4^+ state has an intensity which is 27.6 times less than the intensity of the $E2$, 1078.5-keV transition to the 2^+ level. In ^{144}Sm the comparable $E1$, 380.5-keV transition is 1.7 times more intense than the $E2$, 530.6-keV transition.

We were able to observe neither the 1073.6-keV transition nor the 1584.5-keV transition to ground reported in ref. 10. A search was made for two gamma rays whose energies would sum to 1078.9 keV in case the 3^- level, although still located between the 2^+ and 4^+ states, were in reality at a higher energy than 1584.5 keV. None were found. It is puzzling that the ^{146}Tb decay, which directly populates 2^+ and 4^+ states, should for some reason miss a 3^- state. The possibility that the 1078.9- and 1579.5-keV gamma rays are in reality $E2$ and $E1$ doublets is ruled out by angular correlation and conversion coefficient¹¹ measurements. Both experiments show that the transitions are $E2$ in character. An alternative explanation may be that the systematic drop in excitation energy of the 3^- state is reversed at ^{146}Gd . As noted in ref. 10, three other trends are disrupted at $Z = 64$ for the $N=82$ isotones: (1) the first 2^+ state, which increases in energy from ^{136}Xe to ^{144}Sm , suddenly drops from 1660 keV (^{144}Sm) to 1580 keV energy (^{146}Gd); (2) the lowest 4^+ and 6^+ states both increase sharply in excitation energy at ^{146}Gd ; and (3) the energy spacing between the 4^+ and 6^+ states (and, of course, between the 2^+ and 4^+ levels as well) is much greater in ^{146}Gd than in the other isotones. These differences are attributed¹⁰ to the fact that the $d_{5/2}$ proton subshell is filled at $Z=64$. If the 3^- state in ^{146}Gd does indeed lie above the 4^+ and 6^+ states (as it does in ^{136}Xe , ^{138}Ba , and ^{140}Ce), then a likely candidate would be the strongly populated level at 2996.9 keV, which deexcites by means of the 1417.4-keV transition to the 2^+ first excited state.

Decay Properties of $^{148,149}\text{Dy}$

The extension of the study of 82-neutron odd-mass nuclei to ^{147}Tb necessitates the investigation of the so far unreported nuclide ^{147}Dy . Up to now, however, the light dysprosium isotopes, with $A <$

153, have not been extensively studied with respect to their electron-capture and β^+ decay modes. In particular, before the present investigation was begun, ^{148}Dy had not been observed, and the only information available¹² for ^{149}Dy was its half-life, 4.6 ± 0.4 min, deduced from x-ray decay-curve analyses. It was therefore felt that before launching into a search for ^{147}Dy it was imperative to obtain gamma-ray data for $^{148,149}\text{Dy}$.

These two isotopes were produced in bombardments of ^{142}Nd and ^{141}Pr with ^{12}C and ^{14}N ions respectively. They were found to have the following half-lives: 3.1 ± 0.1 min for the new isotope ^{148}Dy and 4.1 ± 0.2 min for ^{149}Dy , a value that agrees with the half-life reported in ref. 12. The gamma-ray spectrum of ^{149}Dy is complex, and the gamma-gamma data are now being analyzed to deduce a decay scheme. For ^{148}Dy , only one strong transition, 620.5 keV, was observed. Because only annihilation radiation was observed in its coincidence spectrum, the transition probably proceeds directly to one of the two isomers in ^{148}Tb . No initial growth period was observed for the gamma rays of the high-spin isomer, so that the 620.5-keV transition must populate the low-spin isomer. Because the latter's spin is either 2 or 3 (see ref. 13) and because the ^{148}Dy ground state must be 0^+ , the spin of the intermediate state in ^{148}Tb is either 0 or 1.

1. Consultant from the University of Tennessee, Knoxville, Tenn.

2. UNISOR.

3. B. H. Wildenthal, E. Newman, and R. L. Auble, *Phys. Rev. C3*, 1199 (1971).

4. E. Newman, K. S. Toth, R. L. Auble, R. M. Gaedke, M. F. Roche, and B. H. Wildenthal, *Phys. Rev. C1*, 1118 (1970).

5. E. Newman, K. S. Toth, and I. R. Williams, *Phys. Rev. C7*, 290 (1973).

6. J. Kownacki, H. Ryde, V. O. Sergejev, and Z. Sujkowski, *Phys. Scr.* 5, 66 (1972).

7. Y. Y. Chu, E. M. Franz, and G. Friedlander, *Phys. Rev.* 187, 1529 (1969).

8. V. P. Afanasiev, I. I. Gromova, G. I. Iskhakov, V. V. Kuznetsov, M. Ya. Kuznetsova, and N. A. Lebedev, *Izv. Akad. Nauk SSSR, Ser. Fiz.* 35, 719 (1971) [transl.: *Bull. Acad. Sci. USSR, Phys. Ser.* 35, 659 (1971)].

9. W. W. Bowman, D. R. Haenni, and T. T. Sugihara, *Phys. Rev. C7*, 1686 (1973).

10. J. Kownacki, H. Ryde, V. O. Sergejev, and Z. Sujkowski, *Nucl. Phys. A196*, 498 (1972).

11. B. Spoelstra, *Nucl. Phys. A174*, 63 (1971).

12. C. R. Bingham, D. U. O'Kain, K. S. Toth, and R. L. Hahn, *Phys. Rev. C7*, 2575 (1973).

13. Ts. Vylov, K. Ya. Gromov, I. I. Gromova, G. I. Iskhakov, V. V. Kuznetsov, M. Ya. Kuznetsova, A. V. Potempa, and M. I. Fominykh, Dubna report No. P6-6512.

MEASUREMENT OF ALPHA-DECAY BRANCHING RATIOS FOR RARE-EARTH ISOTOPES

K. S. Toth R. L. Hahn¹
 E. Newman C. R. Bingham²
 W.-D. Schmidt-Ott³

Experimental values of alpha-decay branching ratios are useful not only for comparison with alpha-decay theories but also because they can often be used to deduce cross sections for complicated reactions in which products are identified by their alpha decay. Indeed, since the advent of high-energy heavy-ion accelerators, the observation of characteristic alpha-particle groups has been widely used in the identification of new neutron-deficient isotopes. For many of them, however, the alpha-decay branching ratios are either lacking or inaccurately determined, primarily because of their short half-lives. If these ratios were known, then in many instances relative yields could be converted to reaction cross sections.

In the present work, we report on measurements of alpha-decay branching ratios by combining the gas-jet technique with the use of high-resolution Ge(Li) x-ray detectors. This combination does away with the necessity of chemical separations for the preparation of thin sources suitable for an alpha-particle counting and for the elimination of elemental fractions other than the one of interest. The technique is useful for isotopes with half-lives down to a few seconds, because a capillary can be used to transport the gas jet to a shielded position so that alpha-particle, x-ray, and gamma-ray counting can be made simultaneously.

The technique was first tested by measuring branching ratios for ^{149m}Tb, ¹⁵⁰Dy, and ¹⁵¹Dy, nuclides for which previous determinations were available.⁴ Then the system was used for measurements on the alpha-emitting high- and low-spin isomers of ¹⁵¹⁻¹⁵⁴Ho, whose half-lives range from about 36 sec to about 12 min. In only two instances, namely, 35.6-sec ¹⁵¹Ho (ref. 5) and 9.3-min ¹⁵³Ho (ref. 6), had experimental alpha-decay branches been previously measured for these holmium alpha emitters. In addition, this study represents the first systematic investigation of alpha-decay rates for a series of isotopes of an odd-*Z* element in the rare-earth region.

Branching ratios were deduced in the main by determining the number of $K\alpha_1$ x rays emitted and then applying appropriate correction factors to obtain the total number of electron-capture and positron decays. For ^{152,154}Ho, where the gamma-ray spectral measurements could be used to extract information concerning their decay to ^{152,154}Dy, it was possible to

Table 1. Experimental alpha-decay branching ratios

Nucleus	Present data	Ref. 1
¹⁵⁰ Dy	0.32 ± 0.05	0.18 ± 0.02
¹⁵¹ Dy	0.055 ± 0.008	0.059 ± 0.006
^{149m} Tb	(2.0 ± 0.4) × 10 ⁻⁴	(2.5 ± 0.5) × 10 ⁻⁴

1. R. D. Macfarlane and D. W. Seegmiller, *Nucl. Phys.* **53**, 449 (1964).

deduce alternate, and thus independent, alpha-decay branching ratios.

The alpha-decay branching ratios deduced for ¹⁵⁰Dy, ¹⁵¹Dy, and ^{149m}Tb are shown in Table 1 and compared with published results.⁴ It is seen that our ratios for ^{149m}Tb and ¹⁵¹Dy are in agreement with the previously determined values. In the case of ¹⁵⁰Dy, our value of 0.32 is substantially greater than that reported in ref. 4. The disagreement remains even if the error limits in both investigations are taken into account.

Some support for the higher branching ratio comes from reported⁷ cross sections for the formation of ¹⁵⁰Dy and ¹⁵¹Dy in (heavy ion, *xn*) reactions; those for ¹⁵⁰Dy are consistently larger than the ones for ¹⁵¹Dy. The cross sections had been obtained by detecting the alpha decay of ¹⁵⁰Dy and ¹⁵¹Dy and then correcting the alpha-disintegration rate by applying the branching ratios of ref. 4. Figure 1 shows the maximum cross sections obtained for the two isotopes, produced in the interaction of various combinations of even-even targets and projectiles, plotted as a function of the number of neutrons emitted from the compound system. Part *a* shows the peak cross sections as reported in ref. 7, while part *b* shows the same results if the present branching ratios are used. It is clear that in Fig. 1*b*, not only are the two sets of cross sections similar in value, but they now show a more systematic variation with the number of emitted neutrons. Consider also the excitation functions reported by Alexander and Simonoff⁷ for the reactions ¹⁴¹Pr(¹⁴N,4*n*)¹⁵¹Dy and ¹⁴¹Pr(¹⁴N,5*n*)¹⁵⁰Dy. Here again the cross section for the formation of ¹⁵⁰Dy is about a factor of 2 greater than the one for ¹⁵¹Dy, whereas if the present alpha-decay branching ratios are utilized, the two sets of cross sections become essentially equal. This is shown in Fig. 2, where in addition to the data points we include the same two excitation functions as recently calculated by Zganjar⁸ using the computer code developed by Blann and collaborators (see, e.g., ref. 9). The calculation (1) predicts correctly the bombarding energies at which the two cross sections peak, although

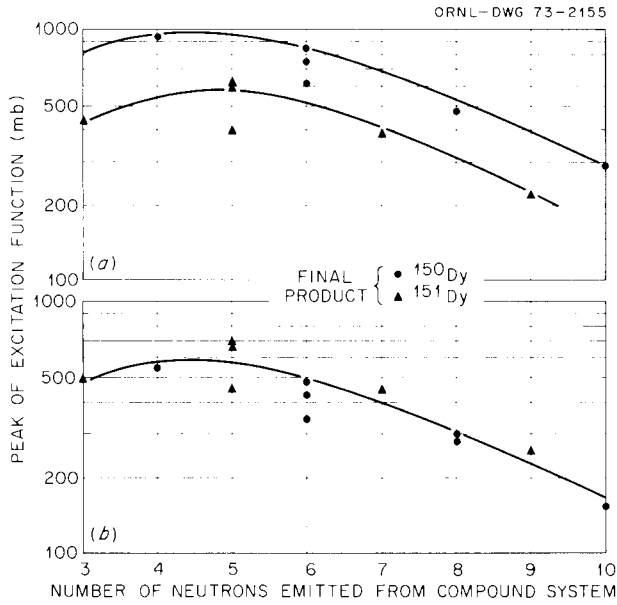


Fig. 1. Maximum cross sections for the formation of ^{150}Dy and ^{151}Dy in various (heavy ion, xn) reactions induced by even-even projectiles on even-even targets. Part *a* shows the data as reported by J.M. Alexander and G. N. Simonoff [*Phys. Rev.* 133, B93 (1964)]; part *b* shows cross sections deduced when the presently determined branching ratios are used to obtain total disintegration rates.

the widths of both calculated excitation functions are much less than those indicated by the data points, and (2) is in better agreement with the data when these are corrected with the presently determined branching ratios.

Our alpha-decay branching ratios for the holmium isomers are summarized in Table 2 and compared with previously reported values. As mentioned earlier, in only two cases, namely, the high-spin ^{151}Ho isomer and the low-spin ^{153}Ho isomer, had experimental values been previously measured; our data agree with the earlier results. The remaining branches (taken from refs. 5 and 10) are estimates based on assumed reaction cross sections. Even so, discrepancies outside error limits appear only for the ^{152}Ho isomers. There the estimated values are much larger than ours. Because the main features of the decay of the ^{152}Ho isomers to ^{152}Dy now seem to be fairly well established,¹¹ we feel that, within the quoted error limits, our data are correct.

From the branching ratios, alpha-decay half-lives can be determined and then considered within the framework of some alpha-decay-rate theory. In this manner, relative decay probabilities can be obtained after the energy dependence is removed. One convenient alpha-

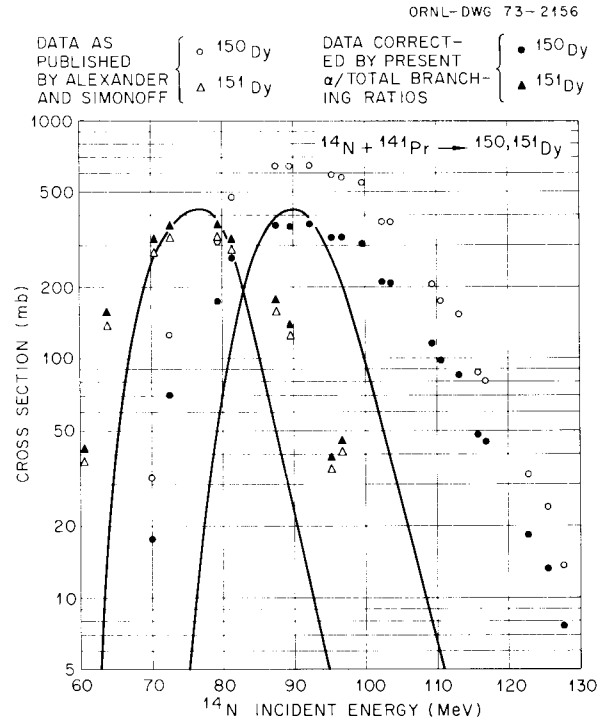


Fig. 2. Excitation functions for the reactions $^{141}\text{Pr}(^{14}\text{N},4n)^{151}\text{Dy}$ and $^{141}\text{Pr}(^{14}\text{N},5n)^{150}\text{Dy}$. Open points indicate data as reported by J. M. Alexander and G. N. Simonoff [*Phys. Rev.* 133, B93 (1964)]; closed points show the same data when these are corrected by the alpha-decay branching ratios determined in the present investigation. Curves represent excitation functions calculated by using a computer code based on the theory of W. G. Winn et al. [*Nucl. Phys.* A188, 423 (1972)].

decay formalism has been developed by Rasmussen.¹² In it an alpha-decay reduced width, δ^2 , is defined by the equation

$$\lambda = \delta^2 P/h, \quad (1)$$

where λ is the decay constant, h is Planck's constant, and P is the penetrability factor calculated for a barrier that includes an optical-model potential derived from the analysis of alpha-particle scattering data. A centrifugal barrier is also included so that an l dependence can be taken into account.

Table 3 summarizes the reduced widths calculated for the holmium isomers by using alpha half-lives derived from our values of branching ratios given in Table 2. The calculations were for $l = 0$ alpha waves, so that hindrances could be noted. In Fig. 3 we have plotted these reduced widths and have indicated a band of values which, because they encompass δ^2 's for even-

Table 2. Alpha-decay branching ratios

Isomer	Present work from --			Previous work
	X rays	Decay scheme	Parent-daughter relationship	
^{151}Ho low spin	0.09 ± 0.04 0.13 ± 0.04		<0.11	0.24 ± 0.14^a
^{151}Ho high spin	0.13 ± 0.05 0.18 ± 0.05			0.20 ± 0.05^a
^{152}Ho low spin	0.017 ± 0.003	0.03 ± 0.01	<0.07	0.30 ± 0.15^a
^{152}Ho high spin	0.064 ± 0.013	0.04 ± 0.01		0.19 ± 0.05^a
^{153}Ho low spin	$(1.2 \pm 0.5) \times 10^{-3}$ $(1.8 \pm 0.8) \times 10^{-3}$			$(3 \pm 2) \times 10^{-3a}$ $(1.2 \pm 0.7) \times 10^{-3b}$ $(0.8 \pm 0.5) \times 10^{-3c}$
^{153}Ho high spin	$(3.4 \pm 1.7) \times 10^{-4}$ $(5.1 \pm 2.5) \times 10^{-4}$			
^{154}Ho low spin	$(1.7 \pm 0.4) \times 10^{-4}$	$(2.8 \pm 0.9) \times 10^{-4}$		$(4.2 \pm 2.4) \times 10^{-4c}$
^{154}Ho high spin	$<2 \times 10^{-5}$	$<10^{-5}$		

^aR. D. Macfarlane and R. D. Griffioen, *Phys. Rev.* **130**, 1491 (1963).

^bR. L. Hahn, K. S. Toth, and T. H. Handley, *Phys. Rev.* **163**, 1291 (1967).

^cN. A. Golovkov, S. K. Khvan, and V. G. Chumin in *Proceedings of the International Symposium on Nuclear Structure, Dubna, 1968* (IAEA, Vienna, 1969), p. 27.

Table 3. Alpha-decay reduced widths, δ^2

Isomer	E_α (MeV)	Partial alpha half-life (sec)	Reduced width (MeV)
^{151}Ho low spin	4.607 ± 0.003	$(5.22 \times 10^2)^a$ $(3.62 \times 10^2)^b$ $(>4.3 \times 10^2)^c$	0.0066 ± 0.0039 0.0096 ± 0.0053 <0.0081
^{151}Ho high spin	4.517 ± 0.003	$(2.74 \times 10^2)^a$ $(1.98 \times 10^2)^b$	0.038 ± 0.016 0.052 ± 0.019
^{152}Ho low spin	4.387 ± 0.003	$(0.83 \times 10^4)^b$ $(0.47 \times 10^4)^d$ $(>0.2 \times 10^4)^c$	0.0062 ± 0.0015 0.011 ± 0.004 <0.029
^{152}Ho high spin	4.453 ± 0.003	$(0.82 \times 10^3)^b$ $(1.31 \times 10^3)^d$	0.030 ± 0.008 0.0174 ± 0.0053
^{153}Ho low spin	4.011 ± 0.005	$(4.65 \times 10^5)^a$ $(3.10 \times 10^5)^b$	0.021 ± 0.010 0.031 ± 0.017
^{153}Ho high spin	3.910 ± 0.005	$(3.53 \times 10^5)^a$ $(2.36 \times 10^5)^b$	0.125 ± 0.065 0.18 ± 0.09
^{154}Ho low spin	3.937 ± 0.005	$(4.17 \times 10^6)^b$ $(2.53 \times 10^6)^d$	0.0067 ± 0.0020 0.0110 ± 0.0044
^{154}Ho high spin	3.721 ± 0.005	$(>9.7 \times 10^6)^b$ $(>1.95 \times 10^7)^d$	<0.08 <0.04

^aFrom x rays, decay energy from 1971 Mass Tables.

^bFrom x rays, corrected decay energy.

^cFrom parent-daughter relationship.

^dFrom decay scheme.

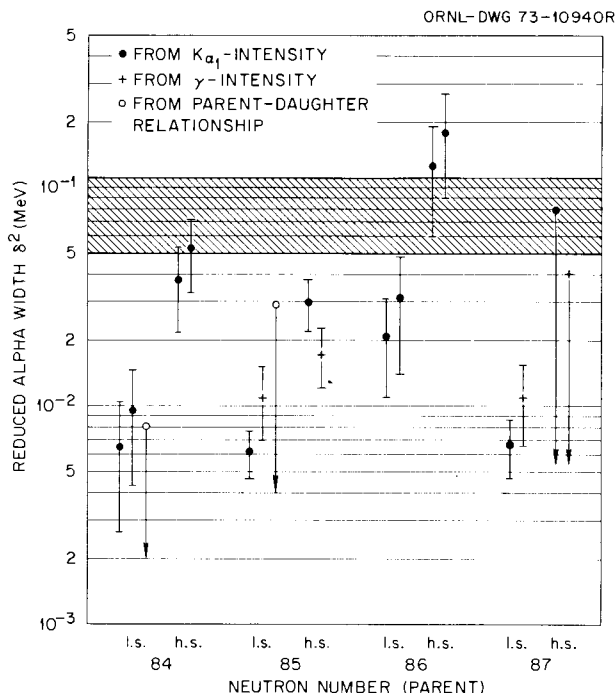


Fig. 3. Alpha-decay reduced widths for the holmium isomers. These isomers are identified by neutron number – e.g., ^{151}Ho has 84 neutrons – and by the letters l.s. (low spin) and h.s. (high spin). The cross-hatched band encompasses reduced widths for doubly even rare-earth nuclei, values that can be considered to represent unhindered alpha decay. Closed and open points and crosses identify the method by which a given alpha-decay branching ratio was deduced.

even rare-earth alpha emitters,¹³ can be taken to represent unhindered alpha decay. The figure shows, as has been known from studies in the heavy elements, that for odd- A nuclei, reduced widths range from those of even-even nuclei down to much smaller values. The introduction of an alpha wave other than zero does raise the reduced width value, but for the emission of alpha particles, the centrifugal barrier plays only a subordinate role. It has been pointed out¹⁴ that instead of changes in multipolarities, it may be the necessity of forming an alpha particle from unpaired nucleons that slows down the alpha-decay rate of an odd- A nucleus; for cases where the odd-nucleon wave function remains unchanged, alpha decay may proceed at an unhindered rate.

The $^{152,154}\text{Ho}$ isomers, each with two unpaired nucleons, as might be expected, appear to have hindered alpha decays. Aside from the fact that the two terbium daughters have high- and low-spin isomers as well, nothing is known about their level structures. Thus one can say little about the states involved in the alpha decays of the $^{152,154}\text{Ho}$ isomers.

The ^{153}Ho isomers, presumably due to the 67th proton being in the $h_{11/2}$ and $d_{5/2}$ orbitals, have reduced widths in the unhindered range. This suggests that their alpha decays proceed to states in ^{149}Tb represented by the same proton orbitals. Macfarlane¹⁵ indeed proposed that the alpha-decaying ^{149}Tb isomers were due to $h_{11/2}$ and $d_{5/2}$ proton orbitals. He also had evidence to indicate that the $h_{11/2}$ state was the

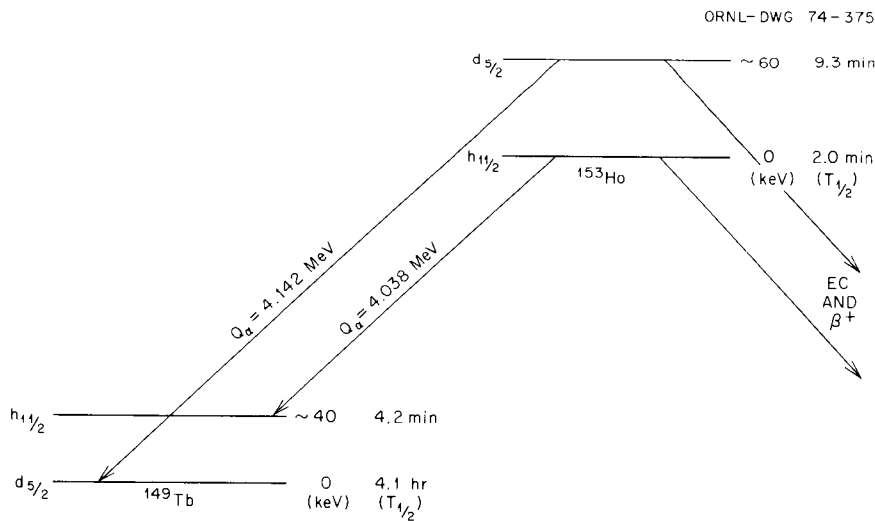


Fig. 4. Proposed alpha-decay schemes for the ^{153}Ho isomers. If the $h_{11/2}$ state in ^{149}Tb is about 40 keV above the $d_{5/2}$ ground state [see R. D. Macfarlane, *Phys. Rev.* **126**, 274 (1962)], then the indication is that in ^{153}Ho the situation is reversed, with the $d_{5/2}$ state lying about 60 keV above the $h_{11/2}$ state.

isomer and was located about 40 keV above the $d_{5/2}$ ground state. In Fig. 4 we show alpha-decay schemes for the ^{153}Ho isomers that are consistent with unhindered alpha-decay rates.

When the ^{151}Ho isomers were discovered,⁵ the proposal was that their alpha-decay schemes were as shown in Fig. 4 for the ^{153}Ho pair. As in the case of ^{153}Ho , the reduced width for the high-spin ^{151}Ho isomer is in the unhindered range, and the indication here again is that the alpha decay involves states represented by the $h_{11/2}$ proton orbital. The alpha decay of the low-spin ^{151}Ho isomer, however, seems to be hindered, and thus raises the question as to whether the $d_{5/2}$ orbital is involved in both the initial and final states. In fact, if an $l = 3$ alpha wave (assuming that the decay proceeds to the $h_{11/2}$ state) is used, then the calculated reduced width is in the unhindered range. From a recent study (see elsewhere in this annual report), it appears that, as in the case of ^{149}Tb , the ground state of ^{147}Tb (1.6 hr) is represented by the $d_{5/2}$ orbital, while the $h_{11/2}$ state (1.9 min) is located at some unknown higher excitation energy. Thus the suggestion that the $d_{5/2}$ ^{151}Ho state decays to the $h_{11/2}$ ^{147}Tb level despite an unfavorable spin change is made even more unlikely by the greater decay energy available for the transition to the $d_{5/2}$ ground state. It is therefore not clear why, in contrast to the case in ^{153}Ho , the ^{151}Ho low-spin isomer alpha decay should exhibit hindrance. Interestingly, however, the ratio of δ^2 for the high-spin to that of the low-spin isomer is about 5 for both ^{151}Ho and ^{153}Ho .

Our study of the holmium isomers shows that, as in the heavy elements, alpha decay for odd- A nuclei in the rare earths can proceed at widely varying rates, with reduced widths differing by factors of up to about 25. This particular point is being looked into further. We have now made similar measurements for the neighboring even- Z nuclides, $^{152,153}\text{Dy}$ and $^{152-155}\text{Er}$; these data, in the process of being analyzed, are intended to complement the information obtained so far.

1. Chemistry Division.

2. Consultant from the University of Tennessee, Knoxville, Tenn.

3. UNISOR.

4. R. D. Macfarlane and D. W. Seegmiller, *Nucl. Phys.* **53**, 449 (1964).

5. R. D. Macfarlane and R. D. Griffioen, *Phys. Rev.* **130**, 1491 (1963).

6. R. L. Hahn, K. S. Toth, and T. H. Handley, *Phys. Rev.* **163**, 1291 (1967).

7. J. M. Alexander and G. N. Simonoff, *Phys. Rev.* **133**, B93 (1964).

8. E. F. Zganjar, Louisiana State University at Baton Rouge, private communication.

9. W. G. Winn, H. H. Gutbrod, and M. Blann, *Nucl. Phys.* **A188**, 423 (1972).

10. N. A. Golovkov, S. K. Khvan, and V. G. Chumin in *Proceedings of the International Symposium on Nuclear Structure, Dubna, 1968* (International Atomic Energy Agency, Vienna, Austria, 1969), p. 27.

11. W. W. Bowman, D. R. Haenni, and T. T. Sugihara, *Progress in Research, Cyclotron Institute, Texas A&M University*, 1972 (unpublished), p. 43; 1973 (unpublished), p. 30.

12. J. O. Rasmussen, *Phys. Rev.* **113**, 1593 (1959).

13. R. D. Macfarlane, J. O. Rasmussen, and M. Rho, *Phys. Rev.* **134**, B1196 (1964).

14. J. O. Rasmussen in *Alpha-, Beta- and Gamma-Ray Spectroscopy*, ed. K. Siegbahn (North-Holland, Amsterdam, 1965), p. 701.

15. R. D. Macfarlane, *Phys. Rev.* **126**, 274 (1962).

UNISOR PROJECT

E. H. Spejewski R. L. Mlekodaj
H. K. Carter W. D. Schmidt-Ott
E. F. Zganjar

The UNISOR project was initiated for the study of nuclei lying far from the line of beta stability by means of an isotope separator connected on-line to the ORIC. This effort is a cooperative venture of 12 universities,¹ ORNL, and ORAU. It is supported by these institutions and by the U.S. Atomic Energy Commission.

The major components of the system were installed and tested in late 1972. There remained, however, the successful development of a target-ion-source combination before the facility could be used for experiments. This component is the crucial part of an on-line system, its function being to separate the reaction products from the target material and to introduce them into the ion source of the isotope separator. Two such target-ion-source combinations have been under development: the so-called Pingis type and one employing a helium-jet transport system. Both types take advantage of the high linear-momentum transfer which takes place in heavy-ion reactions.

The initial version of the Pingis-type ion source is shown in Fig. 1. In this version, the target foil forms part of the anode cylinder wall, and the reaction products enter the ion source simply by recoiling out of the target. Although it was demonstrated in late 1972 that this approach works in principle, a number of problems remained before it could be used for experiments with the desired degree of reliability. The major difficulties were breakage of target foils of some elements under moderate-intensity cyclotron beams,

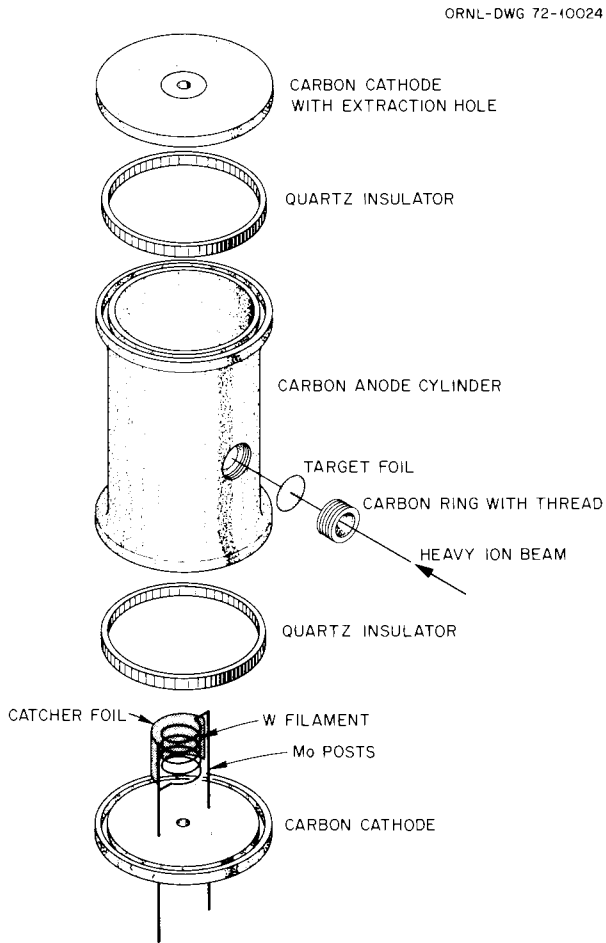


Fig. 1. Initial configuration of the Pingis target-ion source.

and a system efficiency lower than required for on-line experiments. A number of modifications were tried in the effort to solve these problems, some of which were successful. Major improvements resulted from design changes having the effect of cooling the target and from operating the ion source under rather severe temperature conditions. The latter increased diffusion of the products from the catcher foil and probably increased the ionization probability. For a rhodium or palladium target in the initial ion-source configuration, the target would break after an average of about 2 hr of irradiation by a 0.1-particle- μA beam of ^{16}O ions, and the system efficiency was estimated to be less than 0.1%. With the changes made by the summer, a rhodium or palladium target would remain intact for roughly 8 hr or longer under ^{16}O beams as high as 0.6 particle- μA . In addition, the estimated system efficiency had risen to about 3%, a figure approaching the maximum to be expected for an oscillating-electron ion source.

The second target-ion source under development employs a helium-jet system² to transport the products to the ion source of the isotope separator. In order to maintain the pressure in the ion source within an operable range, a system of "skimmers" is used to reduce the amount of helium entering the ion source. The initial configuration of this "skimmer" system is shown in Fig. 2, in which a simple collection chamber is shown at the position now occupied by the ion source. This system is considerably more complex in practice than the Pingis; however, it offers the possibility of using almost every element as a target and also permits

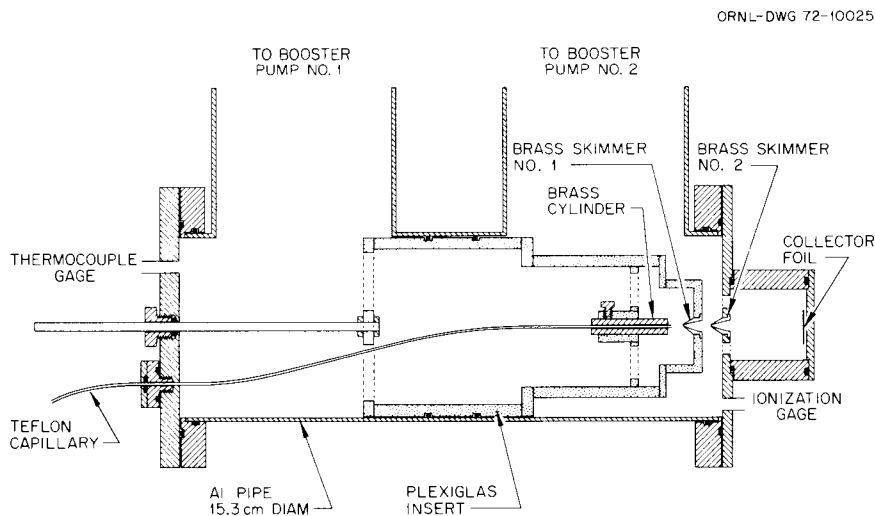


Fig. 2. "Skimmers" for the helium-jet system.

easier cyclotron operations. In the initial test of this helium-jet system performed in 1972, the total system efficiency was so low as to be effectively indeterminate. Since that time, a number of modifications have been made and tested. These include changes in geometry of various parts of the system, revised operating conditions for the ion source, introduction of other support or stabilization material directly into the ion source, direct cooling of the skimmers, and introduction of other materials into the reaction chamber. Steady improvements have been attained in this system, and, by the late summer of 1973, reliable operations could take place with total system efficiencies of approximately 0.7% for elements like iodine and indium and about 0.1% for rare earths. With these efficiencies, the system is usable in selected portions of the nuclear chart. In particular, it offers the only possibility developed at any laboratory for the study of rare earths in an on-line configuration.

Studies have also been begun in order to use the helium-jet transport system directly onto a collection foil or tape which can be quickly transferred to a detector station, for example, the UNISOR tape trans-

port system. This system will increase the data-gathering efficiency by permitting difficult measurements, for example, coincidence experiments, to be performed in a relatively short time period, once the nuclear species and its major decay transitions have been identified by means of the isotope separator.

With the successful improvements in the target-ion-source combinations, particularly the Pingis type, the emphasis of the UNISOR program changed during the summer from primarily developmental work to an emphasis on the experimental program. Although some data had been obtained and a few discoveries made during the developmental tests, these data were, in general, not of the desired spectroscopic quality. Initial investigations began with a study of the neutron-deficient xenon and iodine isotopes, a region familiar from the target-ion-source test experiments. Studies of the level structure of the light mercury isotopes were also begun because of the great interest in the possibility of nuclear deformation in this region. A summary of the results from the experiments performed in 1973 is shown in Table 1. This table contains, of course, the barest of information and does not represent the

Table 1. Summary of initial UNISOR results

Isotope	Half-life	Decay mode and major transitions
^{117}Xe	61 ± 2 sec	β^+ , EC: $Q = 5.0 \pm 0.3$ MeV γ : 221, 295, 519, 639, 661 keV, others
^{117}I	2.20 ± 0.05 min	β^+ , EC γ : 274, 295, 303, 326, 684 keV
^{116}Xe	60 ± 2 sec	β^+ , EC: $Q = 4.4 \pm 0.3$ MeV γ : 105, 192, 226, 248, 300, 311, 413, 923 keV
^{116}I	2.9 ± 0.2 sec	β^+ , EC: $Q = 7.3 \pm 0.2$ MeV γ : 540, 679, 1219 keV
^{115}Xe	12 ± 2 sec	β^+ , EC; no gamma
^{115}I	23.5 ± 1.0 sec	β^+ , EC: ($Q = 5.5 \pm 0.2$ MeV) γ : 276, 285, 459, 710 keV
$^{115\text{m}}\text{Te}$	28 ± 3 sec	β^+ , EC γ : 476, 587, 787, 1390 keV
^{190}Tl	~ 3.2 min	β^+ , EC γ : 306, 417, 487, 620, 732, 841 keV, others
^{189}Tl	1.4 ± 0.1 min	β^+ , EC γ : 216, 228, 318, 445 keV
	2.3 ± 0.2 min	β^+ , EC γ : 334, 451, 522, 942 keV
^{188}Tl	71 ± 3 sec	β^+ , EC γ : 412, 460, 504, 592, 772, 795 keV, others
^{186}Tl	48 ± 3 sec	β^+ , EC γ : 357, 402, 405, 424 keV

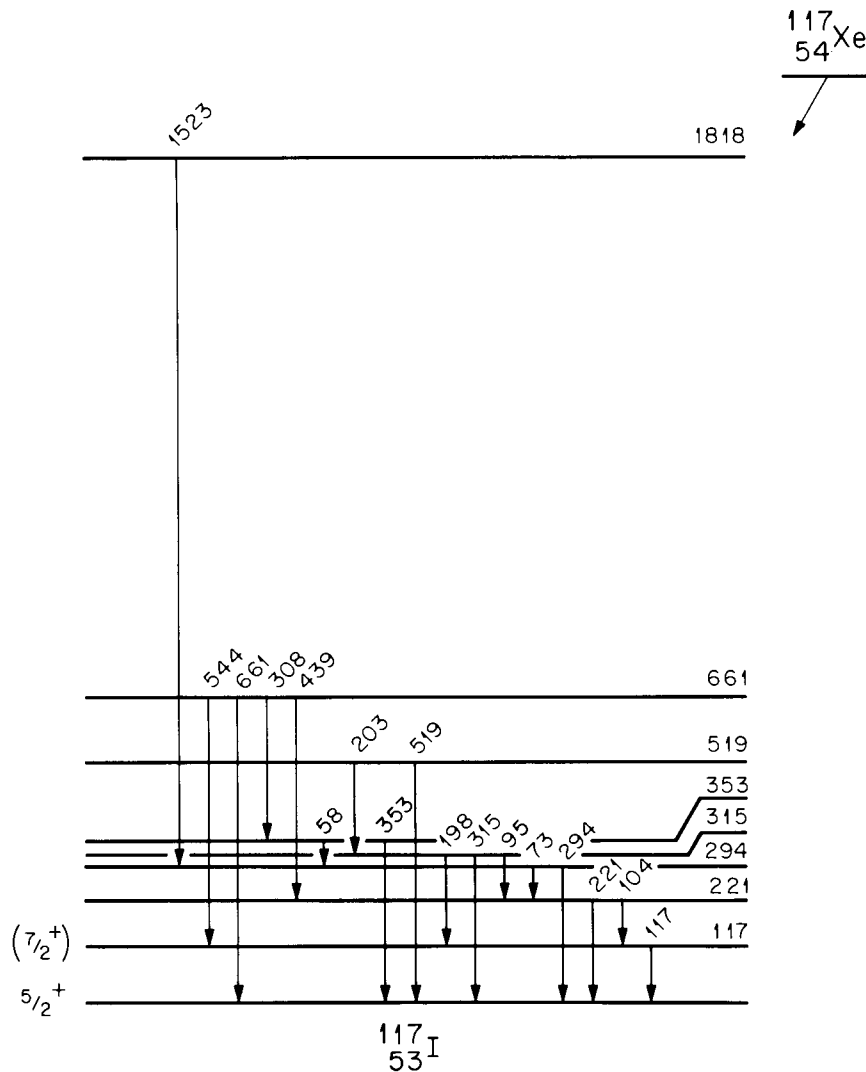


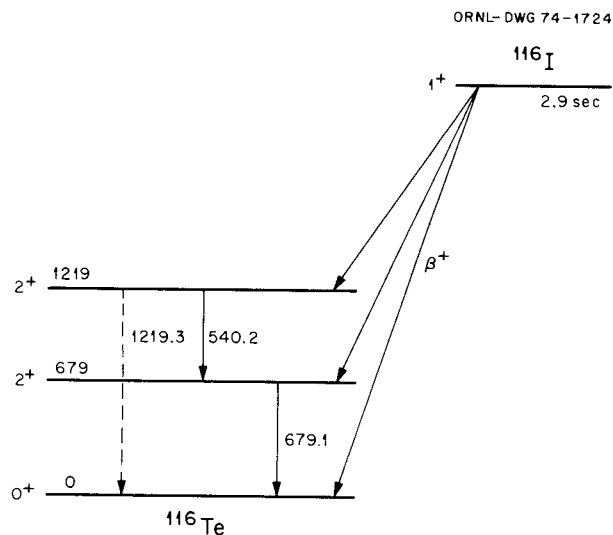
Fig. 3. The decay scheme of ^{117}Xe .

totality of the results obtained. As examples of these, in Figs. 3–6 are shown the level schemes obtained for ^{117}I , ^{116}Te , ^{190}Hg , and ^{188}Hg , as determined from the measurements made at UNISOR.

Of particular interest is the apparent coexistence of spherical and deformed shapes in ^{188}Hg . A change from spherical to deformed shapes has been postulated³ going up in the yrast band beginning with the 6^+ , 1508-keV state. It is interesting to note that the newly found level at 1207 keV (4^+) is at approximately the correct position to be the lower member of a rotational sequence of which the yrast band states with spins of 6^+ and larger are the upper members. In addition, the

1776-keV (6^+) level corresponds closely to states, presumably spherical, known in the heavier even-even mercury isotopes.

The thallium experiments also point out the advantage of having a heavy-ion beam for production of neutron-deficient nuclei. The large angular momentum transferred by the heavy-ion beams has permitted the formation of high-spin isomers in the thallium isotopes. This, in turn, has permitted the investigation of high-spin states in the mercury daughters. In similar experiments,⁴ these states were not observed, presumably because the high-spin states are not produced in the proton-spallation process.

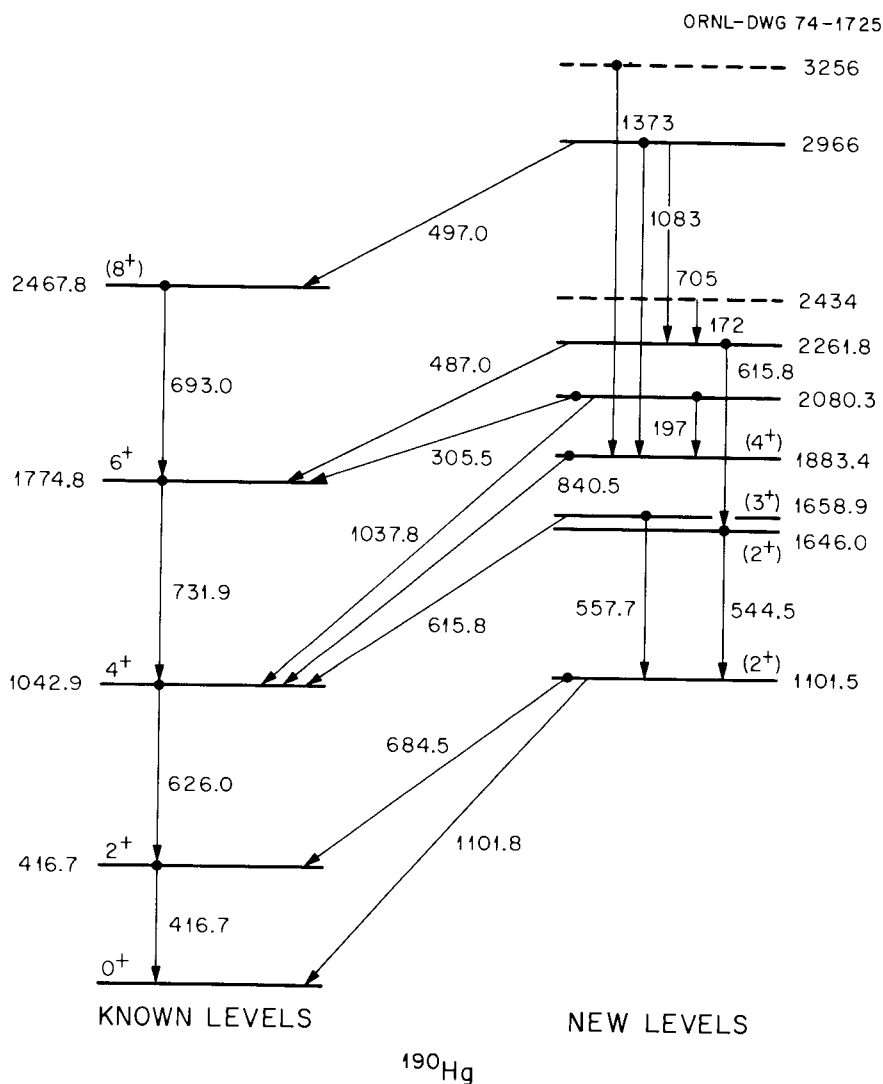
Fig. 4. The decay scheme of ^{116}I .

1. University of Alabama in Birmingham, Georgia Institute of Technology, Emory University, Furman University, University of Kentucky, Louisiana State University, University of Massachusetts, University of South Carolina, University of Tennessee, Tennessee Technological University, Vanderbilt University, and Virginia Polytechnic Institute and State University.

2. W.-D. Schmidt-Ott, R. L. Mlekodaj, and C. R. Bingham, *Nucl. Instrum. Methods* **108**, 13 (1973).

3. D. Proetel et al., *Phys. Rev. Lett.* **31**, 896 (1973); R. M. Diamond, private communication.

4. J. Vandlik et al., *Izv. Akad. Nauk SSSR, Ser. Fiz.* **34**, 1656 (1970); *Bull. Acad. Sci. USSR, Phys. Ser.* **34**, 1472 (1971).

Fig. 5. Levels in ^{190}Hg populated in the decay of ^{190}Tl .

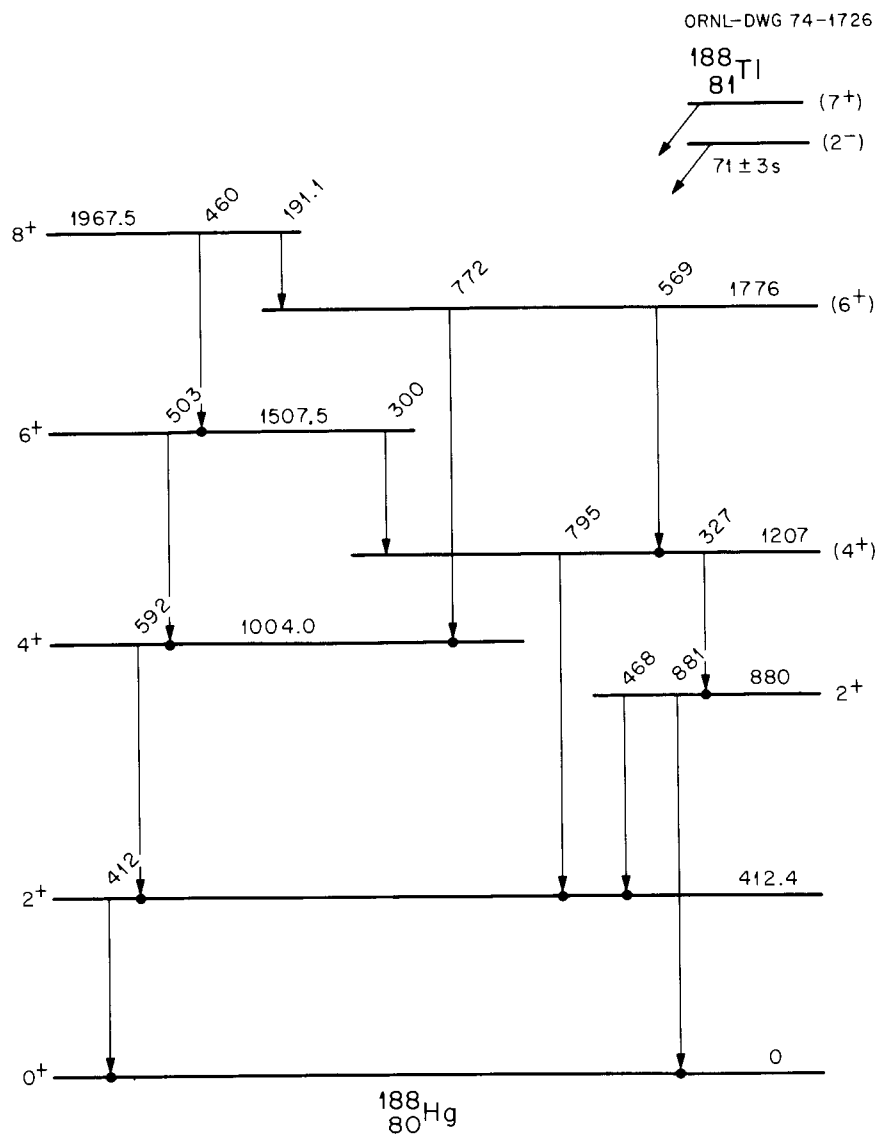


Fig. 6. Decay scheme of $^{188g+m}\text{Tl}$.

PROPERTIES OF LEVELS IN ^{116}Sn

L. L. Riedinger¹ R. W. Lide¹
L. H. Harwood¹ C. R. Bingham¹

For some time it has been known² that two closely lying 2^+ states in ^{116}Sn at 2112 and 2226 keV are somewhat different in behavior. Inspired by a recent study of these levels populated from the ^{116}In decay,³ we have performed measurements on the decay of ^{116}Sb in order to complement the ^{116}In data.

Sources of 2.5-hr ^{116}Te were made at ORIC by bombardment of 30 mg of ^{116}Sn in oxide form with

27-MeV ^3He , utilizing the $(^3\text{He},3n)$ reaction. These tellurium sources decay through 15-min ^{116}Sb to levels in ^{116}Sn . Gamma-ray measurements were performed in the singles and coincidence modes. Half-life analysis led to definite assignments of 16 gamma rays to the decay chain, while the evidence is more tentative for 32 additional peaks. Of these, at least 10 can be associated with known levels⁴ in ^{116}Sb , while 18 are assigned to transitions between 12 levels in ^{116}Sn (see Fig. 1).

Some of the properties of the two 2^+ states at 2112 and 2226 keV are summarized in Table 1. The difference in population from ^{116}In and ^{116}Sb is striking. The level at 2226 keV is heavily populated in

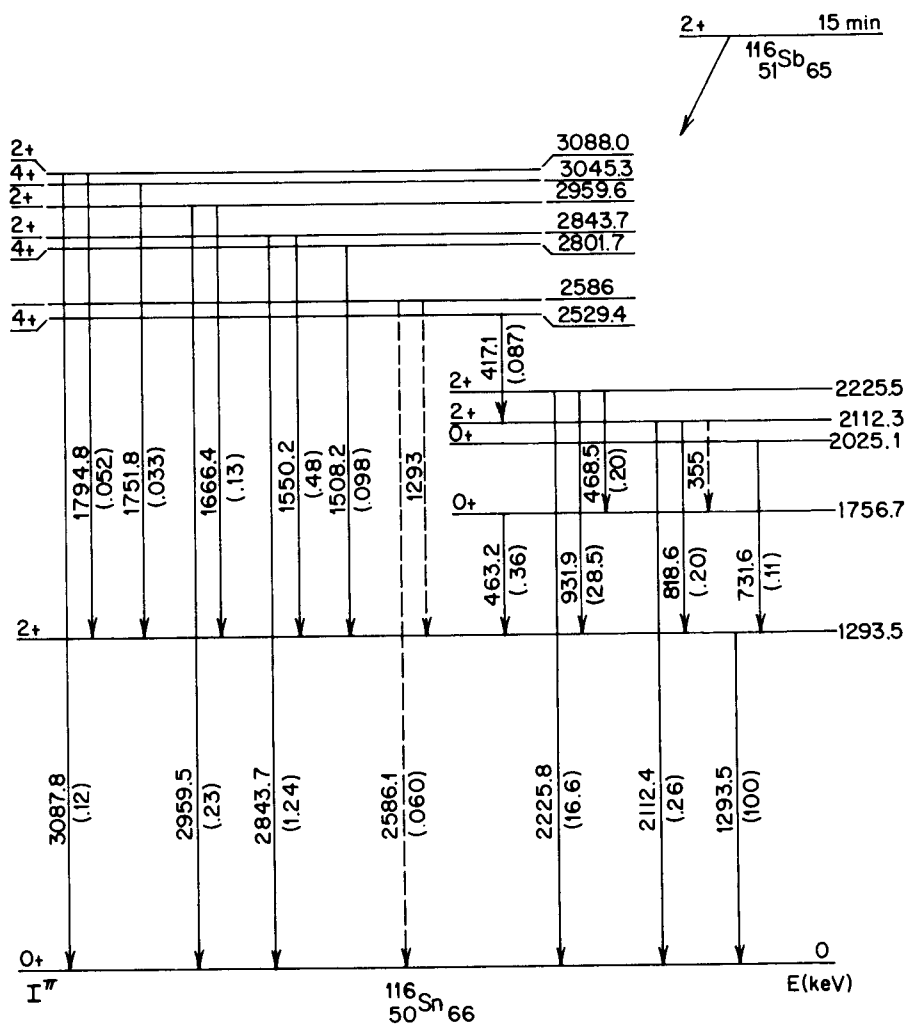


Fig. 1. Levels populated in the decay of $^{116}\text{Te} \rightarrow ^{116}\text{Sb} \rightarrow ^{116}\text{Sn}$. Relative intensities of gamma rays are given in parentheses.

Table 1. Comparison of properties of 2^+ levels

Level energy (keV)	$\frac{B(E2; 2^{+'} \rightarrow 2^+)}{B(E2; 2^{+'} \rightarrow 0^+)}$	$\frac{B(E2; 2^{+'} \rightarrow 2^+)}{B(E2; 2^{+'} \rightarrow 0^+)}$	Multipolarity, $2^{+'} \rightarrow 2^+$	Log ft , ^{116}Sb
2111.9	68 ± 4^a	1.78 ± 0.10^a	$76\% E2^a$	7.0
2225.6	133 ± 8	4.4 ± 0.7		4.6

^aS. L. Gupta et al., to be published.

the antimony decay ($\log ft = 4.6$), while the state at 2112 keV has a much larger $\log ft$ of 7.0. By contrast, the lower of the two is fed strongly from a 4^+ state at 2528 keV in the indium decay, while transitions from the 2226-keV state are not seen.³ The branching ratios

from the two states are also somewhat different. In both cases, transitions to the ground, first 2^+ , and first 0^+ states are seen. In the vibrational model, one would try to view one of these 2^+ states around 2 MeV and one of the 0^+ states (either at 1757 or 2025 keV) as

members of a two-phonon triplet of levels. Then the transition changing one vibrational phonon would be greatly favored over the $\Delta n = 0$ or 2 transitions. The $2^{+'} \rightarrow 2^{+}$ $\Delta n = 1$ transition from the 2226-keV level seems to be more enhanced than the corresponding transition from the 2112-keV state. The $2^{+'} \rightarrow 0^{+}$ gamma ray from each 2^{+} level seems too large, indicating that in this vibrational picture the 2025-keV 0^{+} state may be a better candidate for the two-phonon member. Another important comparison to be made is in the $E2/M1$ admixture in the $2^{+'} \rightarrow 2^{+}$ transition. In the case of the 2112-keV state, Gupta et al.³ measured a 76% $E2$ component in this transition, while the admixture for the 932-keV transition from the 2226-keV state is not yet known. We are planning angular correlation experiments to measure this.

Most recent theoretical treatments of the even- A tin nuclei have viewed the states below 2.5 MeV not as vibrational in nature, but rather as combinations of two quasi-particle excitations. Clement and Baranger⁵ explain in their pairing plus quadrupole calculations the existence of a 0^{+} and a 4^{+} state around 2 MeV and a higher 2^{+} around 2.7 MeV. The origin of second 0^{+} and 2^{+} states around 2 MeV, and the reasons for the difference in branching of the two 2^{+} states appear to be theoretically unexplained.

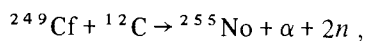
1. University of Tennessee, Knoxville, Tenn.
2. See, for example, R. W. Fink, G. Anderson, and J. Kantele, *Ark. Fys.* **19**, 323 (1961).
3. S. L. Gupta, G. Garcia-Bermudez, N. C. Singhal, A. V. Ramayya, J. Lange, and J. H. Hamilton, to be published.
4. C. B. Morgan, J. Guile, R. A. Warner, W. B. Chaffee, W. C. McHarris, W. H. Kelly, E. M. Bernstein, and R. Shamu, Michigan State Annual Report, 1971-72, p. 29.
5. D. M. Clement and E. U. Baranger, *Nucl. Phys.* **A120**, 25 (1968).

CHEMISTRY OF NOBELIUM, ELEMENT 102

O. L. Keller¹ W. J. McDowell²
R. J. Silva¹ J. R. Tarrant¹

The relation between atomic number and chemical properties is the most basic problem in chemistry, and one of the reasons for making transuranium elements is to provide more information on that subject. Some results on nobelium (element 102) have recently been obtained by R. J. Silva, W. J. McDowell, O. L. Keller, J. R. Tarrant, and G. N. Case of the Chemistry and Chemical Technology Divisions.

These experiments employed the isotope ^{255}No ($T_{1/2} = 223$ sec) produced by the reaction



using the same ^{249}Cf target that was used for the recent identification³ of element 104. Some 500 to 1000 atoms of ^{255}No were obtained for experimentation in each 10-min bombardment. The nobelium was caught on an anodized aluminum disk, transported pneumatically to the laboratory over the chemistry beam line, dissolved, and carried through solvent extraction and ion exchange experiments. For each kind of experiment, appropriate samples of comparison elements (with radiotracers) were put through the same chemical procedure.

A few years ago, nobelium was expected to have chemical properties dictated by its presence in the predominantly trivalent rare-earth-like upper actinide series. The recent ORNL work confirmed the surprising discovery by Silva and co-workers⁴ a few years ago that nobelium is stable as the divalent rather than trivalent ion and then went on to compare No^{2+} chemistry with other characteristic divalent ions such as Cd^{2+} , Co^{2+} , and the alkaline earths. Figure 1 illustrates one such experiment which involved extraction of No^{2+} into di-2-ethylhexylphosphoric acid, HDEHP. The No^{2+}

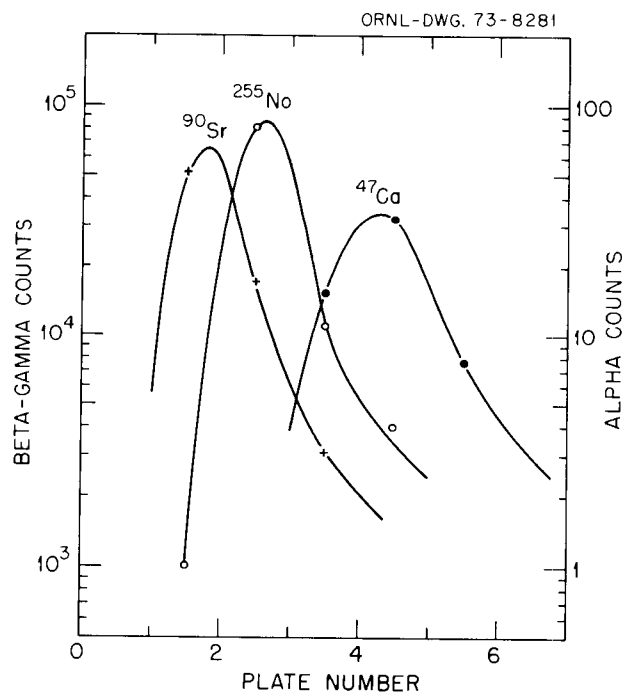


Fig. 1. Elution with 0.025 M HCl of No^{2+} relative to Ca^{2+} and Sr^{2+} from a column using di(2-ethylhexyl)phosphoric acid on an inert support.

comes out between Ca^{2+} and Sr^{2+} , the elements it resembles most. The finding that element 102 has decided to go all the way back to elements 20 and 38 in the alkaline-earth series to find its chemical brothers appears at first sight to be surprising. The periodicity of elemental properties enshrined on every laboratory wall in the form of the periodic table appears to be disregarded. Fortunately a fragmentary understanding of nobelium's behavior can already be glimpsed through relativistic quantum mechanical theories and calculations of L. J. Nugent, K. L. Vander Sluis, C. W. Nestor, T. A. Carlson, and their co-workers at ORNL and elsewhere.

1. Chemistry Division.
2. Chemical Technology Division.
3. C. E. Bemis, Jr., R. J. Silva, D. C. Hensley, O. L. Keller, Jr., J. R. Tarrant, E. D. Hunt, P. F. Dittner, R. L. Hahn, and C. D. Goodman, *Phys. Rev. Lett.* 31, 647 (1973).
4. R. J. Silva, T. Sikkeland, M. Nurmia, A. Ghiorso, and E. K. Hulet, *J. Inorg. Nucl. Chem.* A31, 3405 (1969).

LIGHT-ION AND MESON RESEARCH

BACK-ANGLE ALPHA-PARTICLE SCATTERING

W. W. Eidson ¹	D. C. Hensley
C. C. Foster ²	M. B. Lewis
C. B. Fulmer	N. M. O'Fallon ²
S. A. Gronemeyer ²	R. G. Rasmussen ¹

Back-angle scattering measurements offer a sensitive probe for investigating some nuclear reaction models and mechanisms. This can be seen by presenting the differential cross section in the usual partial wave expansion

$$\sigma(\theta) \sim \left| \sum_l (2l+1) \exp(i\delta_l) \sin \delta_l P_l(\cos \theta) \right|^2,$$

where each partial wave l contributes coherently to the total cross section. For forward angles, $\cos \theta \sim 1$ and $P_l \sim 1$ for all l , whereas for angles near 180° , $\cos \theta \sim -1$ and $P_l \sim (-1)^l$. The latter condition may result in a severe cancellation of amplitudes depending on the precise value of the phase shift δ_l . Even small defects or omissions in the theoretical description of the reaction may give rise to large discrepancies when compared with back-angle data. In addition, since the absorptive terms in the potentials are rather large for composite ion scattering, alpha-particle scattering should provide a good test case.

The back-angle scattering facility consists of a magnet and scattering chamber arranged so that the incoming beam is deflected by the magnetic field onto the target foils and backscattered particles are then deflected by the magnetic field in the opposite direction, away from the beam and toward a detector, permitting angles from about 150° through and past 180° to be measured.

During the past year, extensive elastic and inelastic alpha-particle scattering data were taken at 28.3 MeV and 40.1 MeV on a variety of targets near $A = 28, 60,$ and 90 . Figure 1 shows the major part of the 40-MeV elastic data. For ^{28}Si and ^{27}Al (not included in Fig. 1) the ratio to Rutherford of the 180° cross section is

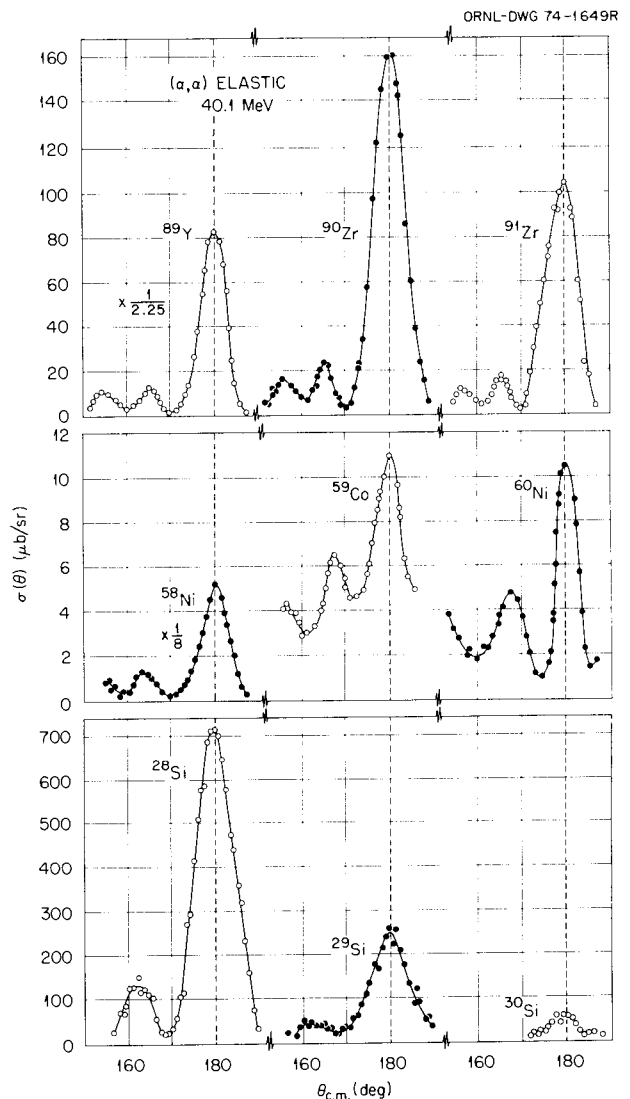


Fig. 1. Large-angle 40.1-MeV alpha elastic scattering angular distributions for several targets. Data from ^{27}Al are very similar to those for ^{28}Si at this energy.

approximately 1. The 180° elastic cross section for 40-MeV alpha particles on ^{116}Sn is about a factor of 100 lower than that for ^{90}Zr . There is considerable and, apparently, significant variation in the 180° cross sections for neighboring targets at both energies.

In going from 28.3 MeV to 40.1 MeV, the 180° elastic cross sections increase by 50% for ^{27}Al , decrease by a factor of 3 for ^{28}Si , decrease by a factor of 7.5 for ^{58}Ni , and increase by 25% for ^{90}Zr . Excitation functions for back-angle data below 30 MeV for targets from aluminum to copper³⁻⁵ show pronounced structure, and the structure varies significantly for neighboring targets. Significant structure in the excitation functions evidently persists at least to 40 MeV, and some excitation function data at 40 MeV will probably be necessary for an adequate analysis of some of the more interesting features of our data. Much of the analysis and interpretation of our data is under way, and we present some of the detailed analysis below.

Back-Angle Scattering of Alpha Particles to the 3^+ Unnatural Parity State of ^{24}Mg

Inelastic scattering of alpha particles to unnatural parity states cannot proceed at any angle by a simple direct mechanism. In fact, as was pointed out by Eidson and Cramer,⁶ a higher-order process such as multiple scattering, exchange, knockout, or compound-nucleus formation must be responsible. And such a reaction is forbidden rigorously by spin and parity arguments to occur at 0° and 180° by any reaction mechanism.

More recently, Eberhard and Trombik⁷ measured the (α, α') reaction to the 5.22-MeV 3^+ state of ^{24}Mg over the energy range of 14 to 19 MeV. They found that they could fit the energy-averaged angular distribution with a modified Hauser-Feshbach calculation. The implication here is that energy averaging over the 5-MeV range of bombarding energies should eliminate any direct components in the reaction, so that the result will be essentially pure compound nucleus. Their average angular distribution and the Hauser-Feshbach prediction are symmetric around 90° , gradually rising on both sides to pronounced maxima near 15° and 165° ; the predictions vanished at 0° and 180° . Their data do not extend beyond 165° .

The observed differential cross sections in the present experiment for scattering to the same 3^+ state in ^{24}Mg are shown in Fig. 2. Both the 28-MeV and the 40-MeV data are shown. The shapes of the distributions are essentially identical with no significant l dependence as might be expected in a direct process. The only significant difference is that the 40-MeV differential

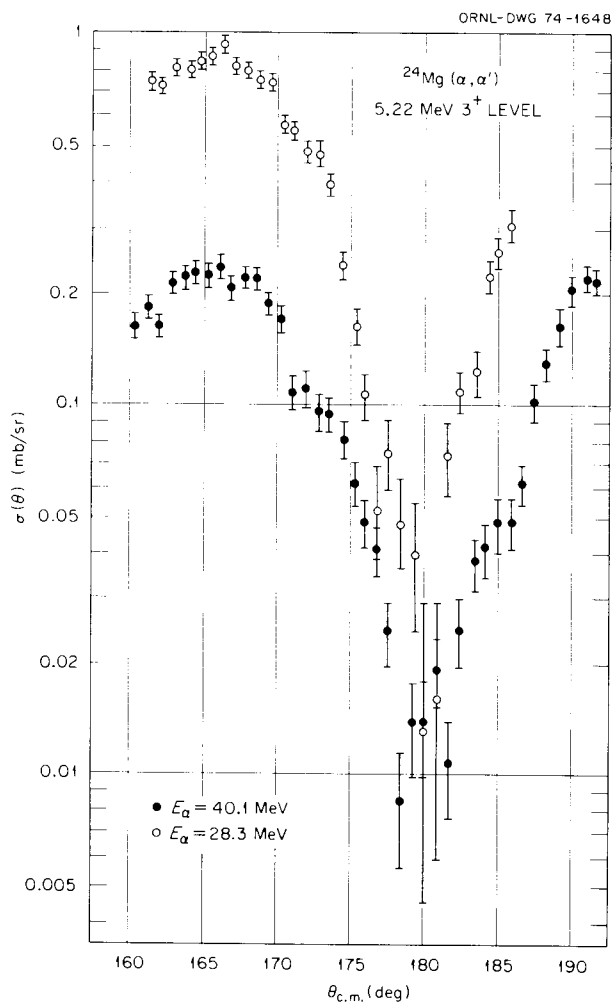


Fig. 2. Large-angle alpha inelastic scattering to the 3^+ unnatural parity state of ^{24}Mg at 5.22 MeV.

cross section is a factor of 5 smaller in overall magnitude. The shape of the back-angle peak near 165° is the same at both energies and appears to be quantitatively similar to the 165° peak predicted by Eberhard and Trombik.

Kokame et al.⁸ measured $\sigma(\theta)$ for 28.5-MeV alpha-particle inelastic scattering to this 3^+ level in ^{24}Mg over the angular range 20° to 90° . Their data when combined with ours indicate that the angular distribution is symmetric around 90° and consequently support the Eberhard and Trombik compound-nucleus description.

Angular distribution measurements, at back angles, of alpha-particle scattering to unnatural parity states in even-even nuclei may provide a quantitative measure of the compound-nucleus component in a given reaction.

If the structure and magnitude of the large-angle (165°) peak do indeed turn out to be due to a pure compound-nucleus mechanism, then this information can be fed back into the interpretation of the elastic and other inelastic channels of the reaction.

More data are needed on additional targets (such as ^{28}Si) over a wider range of energies so that careful fitting with a Hauser-Feshbach calculation can really test the validity of the above conclusion. Work is proceeding on the Hauser-Feshbach fitting of the data.

Coupled Channels and Back-Angle Scattering

As was shown by Tamura,⁹ the first two levels in ^{60}Ni can be reasonably well characterized as one- and two-phonon vibration levels. A two-phonon level cannot be treated by the usual distorted-wave Born approximation but can be handled with a coupled-channel treatment. The forward-angle cross section of the two-phonon levels (near 2.2 MeV) is known to be small compared with that for the one-phonon level (at 1.33 MeV),¹⁰ whereas the opposite trend is observed at large angles, as shown in Fig. 3. Figure 4 compares the same back-angle distributions with that for elastic scattering. In the initial experiment the 2^+ and 0^+ doublet near 2.2 MeV was not resolved, but a subsequent higher-resolution measurement shows that the yield for the 0^+ is only some 20% of that for the 2^+ level and varies rather slowly with angle.

Coupled-channel calculations were performed with the code JUPITOR (Karlsruhe version).¹¹ The optical-model parameters were obtained from a fit to 49.7-MeV alpha-particle elastic scattering ($\theta = 20^\circ$ to 110°)¹² on ^{60}Ni . These initial parameters are $V_R = 97$, $r_R = 1.48$, $a_R = 0.59$, $W_D = 45.0$, $r_I = 1.39$, $a_I = 0.40$, and $r_C = 1.3$.

Distorted-wave calculations indicated that the forward-angle predictions depend most on the real part of the optical-model potential while the back-angle predictions are much more sensitive to the absorption part. Thus the search routine in the code JUPITOR was utilized to determine the preferred shape and magnitude of the imaginary part of the optical-model potential, which could be used in the coupled-channel calculations.

A number of searches for optimum fits to the back-angle data were performed with and without the forward-angle scattering data included. Starting with the parameters given above, the searches consistently resulted in *smaller magnitude* and *extent* for the imaginary well. Typical results are listed in Table 1. When we generalized the potential to include both

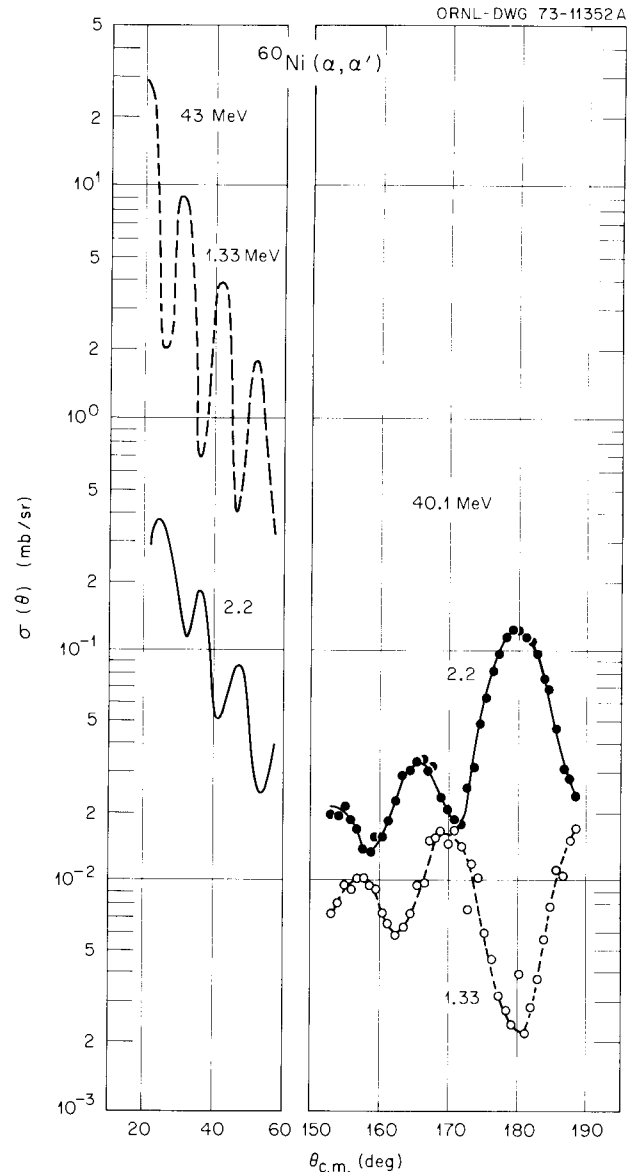


Fig. 3. Forward-angle and large-angle alpha inelastic scattering angular distributions in ^{60}Ni . The angular distributions labeled "2.2" are for the 2^+ level at 2.158 MeV and the (0^+) level at 2.286 MeV. The forward-angle data are from H. W. Brock et al., *Phys. Rev.* **126**, 1514 (1962).

volume and surface potential shapes, the preferred combination was an "interfering" potential, that is, *opposite* signs between terms as shown in Table 2. Both the trends in Table 1 and Table 2 are consistent in that they show the need for reducing the "surface" reaction contribution to the imaginary potential.

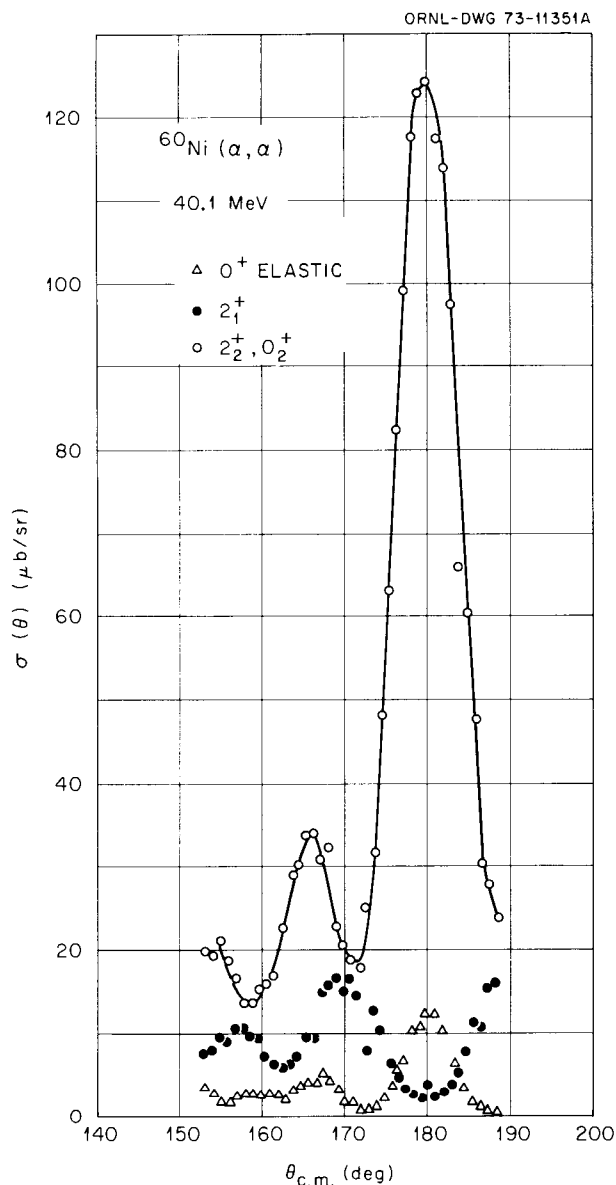


Fig. 4. Large-angle 40.1-MeV alpha elastic and inelastic scattering angular distributions for ^{60}Ni .

The interfering potential is interesting not only because it fits the data better than conventional potentials without further changing r_I and a_I but also because it shows more directly the physical origin of the imaginary potentials. Since the one-phonon 2_1^+ excitation takes place at the nuclear surface, it contributes to the surface optical-model potential. When the $0^+ - 2_1^+$ coupling is included in a coupled-channel calculation, this surface potential must, consequently, be *decreased* relative to the remainder of the imaginary potential.

Table 1. Parameters for absorptive part of the potential without volume absorption used in the coupled-channel calculations for ^{60}Ni

Parameters for the real well are given in the text			
	W_D	r_I	a_I
Initial value	45	1.39	0.40
Final value	36	1.35	0.39

Table 2. Volume and surface well depths of potential used in coupled-channel calculations for ^{60}Ni

Final values of geometry terms in Table 1 were used

	W	W_D
Initial value	20	20
Final value	40	-10

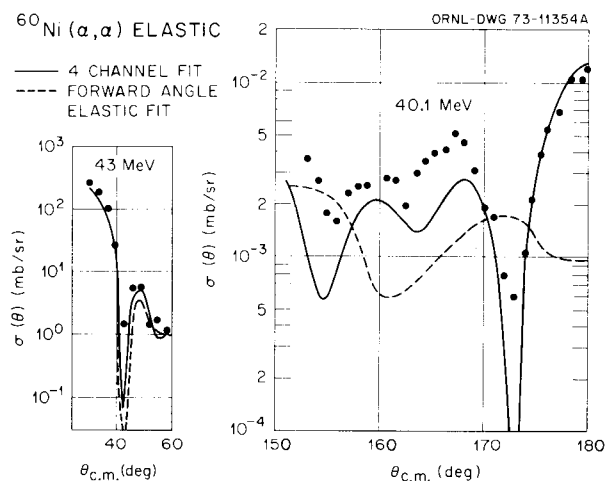


Fig. 5. Forward-angle and back-angle fits to elastic scattering data from ^{60}Ni . The forward-angle data are from H. W. Brock et al., *Phys. Rev.* 126, 1514 (1962).

In addition to improving the fits to the inelastic angular distributions, the parameters from the coupled-channel searches resulted in considerably better fits to the elastic scattering angular distribution in the region near 180° , as illustrated in Fig. 5.

We find that back-angle elastic and inelastic scattering are particularly dependent upon reaction-channel coupling. Once the channel coupling problem is understood, it may be possible to study the microscopic form factor prescriptions of the excited states in ^{60}Ni with back-angle cross-section measurements.

Silicon Target Data

In order to study possible isotope dependence of elastic and inelastic scattering of alpha particles, back-angle angular distributions were measured at 40.1 MeV for several low-lying excited states for $^{28,29,30}\text{Si}$. Figure 1 presents the measured elastic angular distributions. All of the angular distributions have a maximum at 180° except for the one for the 4^+ state of ^{28}Si at 4.61 MeV. The cross section for the first 2^+ state is higher than the elastic $\sigma(180^\circ)$ for ^{28}Si and is 5 times larger in ^{30}Si than the elastic $\sigma(180^\circ)$. Similar behavior of the cross sections of the ground and second 2^+ states for ^{60}Ni at 40 MeV was discussed above, and it is likely that coupled-channel analysis of $^{28,30}\text{Si}$ would be helpful in determining the absorptive part of the optical-model potentials as in the ^{60}Ni case.

A six-parameter optical-model fit to forward-angle $^{28}\text{Si}(\alpha,\alpha)$ data at 40 MeV taken by Gonchar et al.¹³ has been performed using the code SNOOPY 4.¹⁴ The solid line in Fig. 6 is the corresponding elastic scattering angular distribution calculated using the parameters

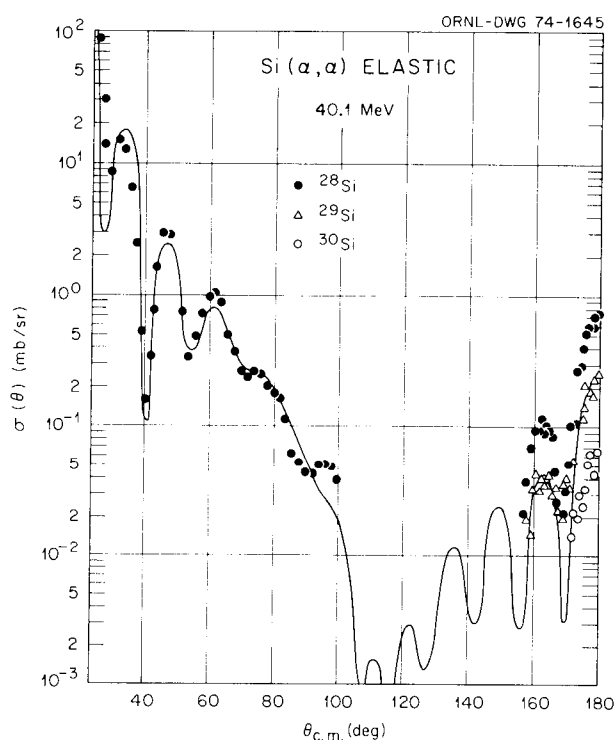


Fig. 6. 40-MeV alpha elastic scattering from silicon isotopes. The forward-angle data for ^{28}Si are from V. Y. Gonchar et al., *Sov. J. Nucl. Phys.* 5, 843 (1967). The solid line is the optical-model prediction for a fit to the forward-angle data. Parameters are: $V_R = 115$, $r_R = 1.24$, $a_R = 0.696$, $W_D = 50.5$, $r_I = 0.727$, $a_I = 0.60$, and $r_C = 1.3$.

listed in the caption. At back angles the predicted cross sections are lower by about a factor of 3 than our measurements for ^{28}Si . Our distributions for $^{28,30}\text{Si}(\alpha,\alpha)$ are also shown in this figure. By comparing these distributions with some for $^{32,34}\text{S}$ which are considered enhanced by Oeschler et al.,¹⁵ we conclude that the back-angle cross sections for each of $^{28,29,30}\text{Si}$ at 40.1 MeV are enhanced.

The larger than usual back-angle cross sections obtained in the calculation are related to the narrow, diffuse absorptive part of the optical potential used. Such a potential reduces the absorption near the nuclear surface, thereby emphasizing contributions to the elastic channel of particles scattered with angular momentum approximately equal to Kr . At a single energy and for a given target isotope, it is possible, by using such a distorted imaginary potential, to get reasonable agreement between calculated and measured

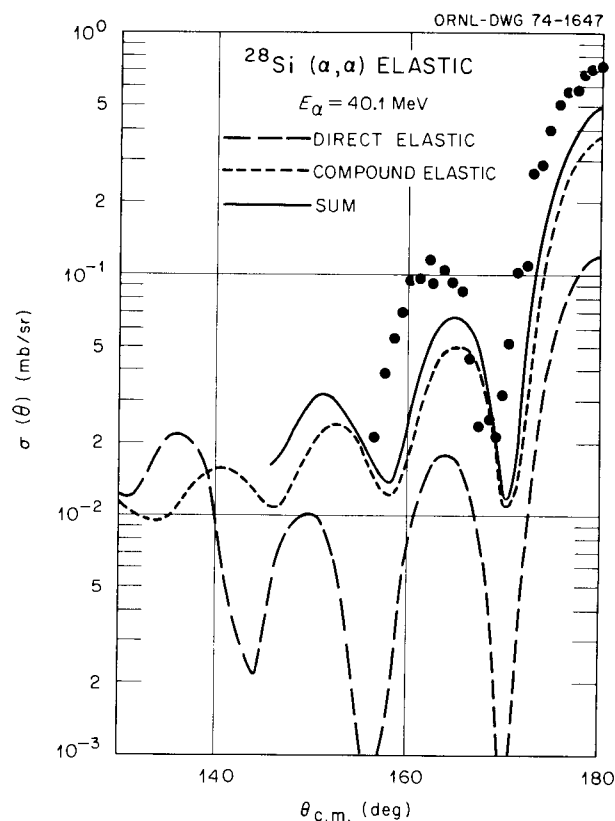


Fig. 7. Comparison of calculated compound elastic and direct elastic cross sections and the incoherent sum with 40-MeV elastic scattering data for ^{28}Si . The optical-model parameters are: $V_R = 90$, $r_R = 1.55$, $a_R = 0.60$, $W_D = 20.0$, $r_I = 1.55$, $a_I = 0.60$, $r_C = 1.50$. Compound-nucleus parameters [defined by K. A. Eberhard and W. Trombik, *Nucl. Phys.* A193, 489 (1972)] are: $W_{CC} = 1.5$, $\sigma^2 = 16.6$, $\rho_0 = 6 \times 10^4$.

angular distributions even when there is back-angle enhancement. But an optical model with smooth dependence on energy and A can be expected to reproduce neither the broad fluctuations which are seen in the 180° alpha elastic scattering excitation functions for ^{28}Si at lower energies¹⁶ nor the apparent strong isotope dependence of the back-angle cross sections seen in Fig. 1.

Compound elastic scattering has been shown⁷ to make an important contribution at lower energies to the elastic alpha scattering cross section. Figure 7 shows the results of a calculation using a modified version of SNOOPY 4¹⁴ and an optical-model potential with standard imaginary parameters and reasonable compound-nuclear parameters. It is apparent that compound elastic contributions may be very important at back angles for alpha scattering from ^{28}Si . Other calculations indicate that the isotope dependence of the compound elastic cross section at 180° is such as to fall off approximately as do the measured 180° cross sections for $^{28,29,30}\text{Si}$. Further and more complete calculations are in process.

53.4-MeV ^3He SCATTERING FROM SAMARIUM ISOTOPES

N. M. Clarke¹ C. B. Fulmer
R. Eagle¹ R. J. Griffiths²
D. C. Hensley

The stable even isotopes of samarium provide an interesting target group for studying the effects of collective motion on elastic and inelastic scattering. They span the transition from a closed neutron shell (^{144}Sm) through vibrational isotopes into the rare-earth region of permanent deformation. Previous measurements and analyses have been reported for proton^{3,4} and alpha-particle^{5,6} scattering at 50 MeV.

In the present work, ^3He scattering measurements were performed at 53.4 MeV on targets of ^{148}Sm , ^{150}Sm , ^{152}Sm , and ^{154}Sm . These and the previously reported⁷ measurements for ^{144}Sm at the same energy extend the data on both the samarium isotopes and the ^3He -nucleus interaction to a region of target mass not previously studied as extensively.⁸

For the present measurements, which were done as a collaboration between ORNL and King's College of the University of London, a bombarding energy of 53.4 MeV was selected so the data and those of ref. 7 would be for the same energy for all of the even samarium isotopes.

The measurements on ^{148}Sm and ^{150}Sm were performed at the Variable Energy Cyclotron at AERE, Harwell, where the high beam intensity (up to 1400 nA on target) permitted the data to be extended to 150° , where the cross sections have become extremely small. Better energy resolution was needed for the measurements on ^{152}Sm and ^{154}Sm , and, consequently, the broad-range magnetic spectrograph at ORIC was used for these measurements. Angular distributions of elastic scattering and inelastic scattering to the first 2^+ level were measured for each target.

The elastic scattering cross sections (including those reported in ref. 7 for ^{144}Sm) are plotted as ratio to Rutherford in Fig. 1. For ^{148}Sm and ^{150}Sm the cross sections decrease with angle more than ten orders of magnitude, down to about 20 nb/sr at 150° . The lower beam current and smaller solid angle at ORIC made measurements much beyond 90° infeasible.

The decrease of the ratio-to-Rutherford plots shown in Fig. 1 for 53.4-MeV ^3He is very similar to that reported for 50-MeV alpha particles in ref. 6. The alpha-particle data, however, show more structure in the angular distributions than we observe in the ^3He data. The structure is more pronounced in the alpha-particle angular distributions for the vibrational iso-

1. Drexel University, Philadelphia, Pa.
2. University of Missouri, St. Louis, Mo.
3. P. T. Sewell, J. C. Hafele, C. C. Foster, N. M. O'Fallon, and C. B. Fulmer, *Phys. Rev. C* **7**, 690 (1973).
4. W. W. Eidson, C. C. Foster, C. B. Fulmer, J. C. Hafele, D. C. Hensley, and N. M. O'Fallon, *Phys. Div. Annu. Progr. Rep. Dec. 31, 1972*, ORNL-4844, p. 61.
5. A. Budzanowski, K. Chyla, R. Czabański, K. Grotowski, L. Jarczyk, B. Kamys, A. Kapuściak, S. Micek, J. Ploskonka, A. Strzalkowski, J. Szmidler, Z. Wróbel, L. Zastawniak, and R. Zybert, *Nucl. Phys. A* **211**, 463 (1973).
6. W. W. Eidson and J. G. Cramer, *Phys. Rev. Lett.* **9**, 497 (1962).
7. K. A. Eberhard and W. Trombik, *Nucl. Phys. A* **193**, 489 (1972).
8. J. Kokame, K. Fukunaga, N. Inoue, and H. Nakamura, *Phys. Lett.* **8**, 342 (1964).
9. T. Tamura, *Rev. Mod. Phys.* **37**, 679 (1965).
10. H. W. Broek, T. H. Braid, J. L. Yntema, and B. Zeidman, *Phys. Rev.* **126**, 1514 (1962).
11. T. Tamura, ORNL-4152; a revision of the code by H. Rebel and G. W. Schweimer (at Kernforschungszentrum Karlsruhe) was used.
12. C. B. Fulmer and J. C. Hafele, *Electronuclear Div. Annu. Progr. Rep. Dec. 31, 1970*, ORNL-4649.
13. V. Y. Gonchar, K. S. Zheltonog, G. N. Ivanov, V. I. Kanashevich, S. V. Laptev, and A. V. Yushkov, *Sov. J. Nucl. Phys.* **5**, 843 (1967).
14. P. Schwandt, unpublished.
15. H. Oeschler, H. Schroder, H. Fuchs, L. Baum, G. Gaul, H. Ludecke, R. Santo, and R. Stock, *Phys. Rev. Lett.* **28**, 694 (1972).
16. C. C. Foster, N. M. O'Fallon, J. C. Hafele, and C. B. Fulmer, *Bull. Amer. Phys. Soc.* **18**, 118 (1973).

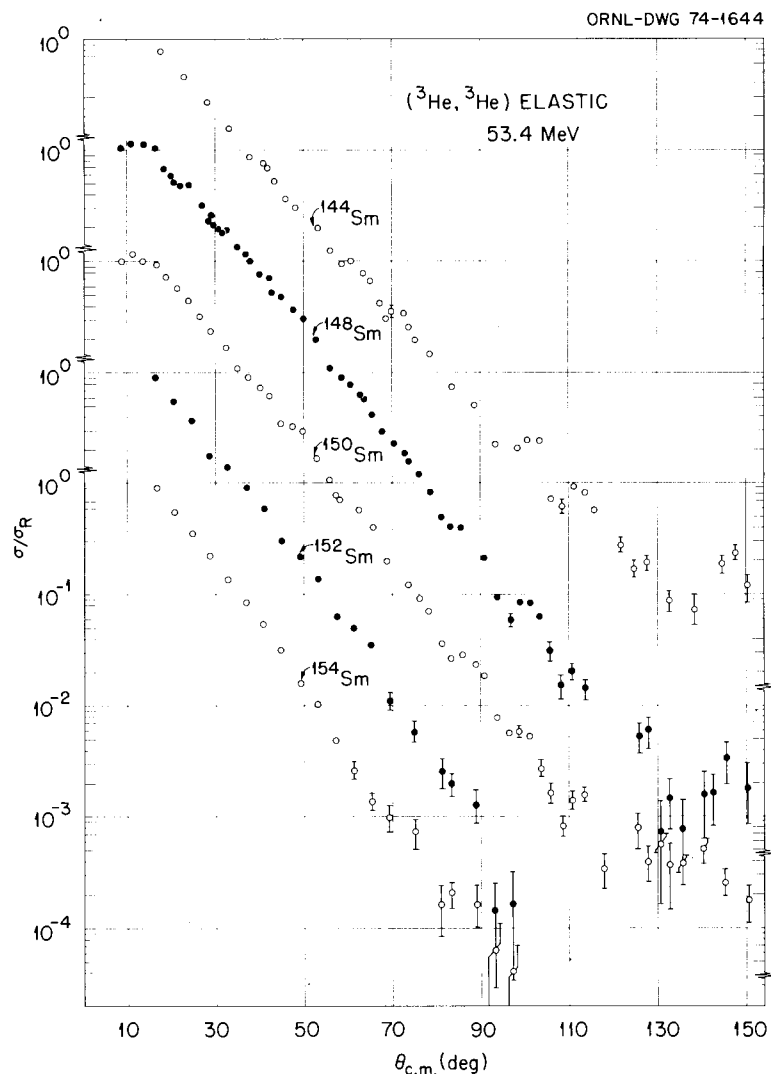


Fig. 1. Ratio-to-Rutherford elastic scattering angular distributions for 53.4-MeV ${}^3\text{He}$ particles on samarium isotopes. Relative uncertainties less than 10% are not shown. The data for ${}^{144}\text{Sm}$ are from P. B. Woollam et al., *Nucl. Phys. A*189, 321 (1972).

topes than for the rotational isotopes, but, otherwise, the distributions are virtually undistinguishable. The ${}^3\text{He}$ angular distributions are distinctive principally in the falloff of cross section with angle, and it is puzzling that the largest difference is between ${}^{144}\text{Sm}$ and ${}^{148}\text{Sm}$. For the proton data of ref. 3, the angular distributions for ${}^{144}\text{Sm}$ and ${}^{148}\text{Sm}$ were very similar, and a larger falloff was observed for the heavier isotopes.

A number of optical-model analyses were performed with the code GENOA.⁹ The five data sets were fitted simultaneously with the geometry parameters common to all data sets but with the real and imaginary well depths data-set dependent. For all of the searches a

spin-orbit well depth of 2.8 MeV (from an earlier study¹⁰) was used. Starting values of parameters from the work of Woollam et al.⁷ which resulted in a potential with a volume integral, J_R , of about 330 MeV fm³ per nucleon for the real part of the potential were used. Typical results are listed in Table 1.

The potentials listed in Table 1 are consistent with the preferred potential obtained from an analysis of ${}^3\text{He}$ scattering data from ${}^{60}\text{Ni}$ at a wide range of energy.¹¹ A consistent result in all of the simultaneous optical-model fits was the behavior of J_R . For ${}^{148}\text{Sm}$ there was a small increase over the value obtained for ${}^{144}\text{Sm}$, and for the heavier isotopes it was smaller by 10 to 20 MeV fm³. Similar variations in J_R were also

Table I. Optical-model potentials obtained from a simultaneous fit to the five data sets shown in Fig. 1

The geometry parameters, suggested by the work of P. B. Woollam et al. [*Nucl. Phys.* **A189**, 321 (1972)], were fixed at values of $r_R = 1.13$ fm, $a_R = 0.802$ fm, $r_I = 1.185$ fm, and $a_I = 0.832$ fm. V_S was also fixed at 2.8 MeV

Target	V (MeV)	W_D (MeV)	$J_R/A_i A_T$ (MeV fm ³)	Rms radius of real well (fm)	σ_R (mb)
¹⁴⁴ Sm	140.2	27.6	334	5.471	2141
¹⁴⁸ Sm	145.2	26.5	344	5.506	2162
¹⁵⁰ Sm	137.9	25.2	327	5.523	2156
¹⁵² Sm	134.9	23.0	319	5.541	2137
¹⁵⁴ Sm	136.8	22.9	323	5.558	2153

observed in the earlier analysis⁴ of 50-MeV proton scattering data from the samarium isotopes.

Further analyses of the elastic and inelastic scattering data are under way.

1. King's College, University of London, London, England.
2. Visiting scientist from King's College, University of London, London, England.
3. C. B. Fulmer, F. G. Kingston, A. Scott, and J. C. Hafele, *Phys. Lett.* **32B**, 454 (1970).
4. P. B. Woollam, R. J. Griffiths, F. G. Kingston, C. B. Fulmer, J. C. Hafele, and A. Scott, *Nucl. Phys.* **A179**, 657 (1972).
5. D. L. Hendrie, N. K. Glendenning, B. G. Harvey, O. N. Jarvis, H. H. Dahm, J. Sardimos, and J. Mahoney, *Phys. Lett.* **26B**, 127 (1968).
6. N. K. Glendenning, D. L. Hendrie, and O. N. Jarvis, *Phys. Lett.* **26B**, 131 (1968).
7. P. B. Woollam, R. J. Griffiths, and N. M. Clarke, *Nucl. Phys.* **A189**, 321 (1972).
8. ³He elastic scattering has been measured at 59.8 MeV for ¹⁴⁴Sm; C. B. Fulmer and J. C. Hafele, *Phys. Div. Annu. Progr. Rep. Dec. 31, 1971*, ORNL-4743, p. 48.
9. F. G. Perey, unpublished. The integration parameters were: $R_{\max} \sim 15$ fm; $L_{\max} = 40$; $H = 0.1$ fm.
10. C. B. Fulmer and J. C. Hafele, *Phys. Rev. C* **7**, 632 (1973).
11. C. B. Fulmer and J. C. Hafele, *Phys. Rev. C* **8**, 172 (1973).

DIFFERENTIAL CROSS SECTIONS FOR ¹⁰B(p,n)¹⁰C AND ¹¹B(p,n)¹¹C AND SOME MACROSCOPIC REACTION RELATIONSHIPS

C. D. Goodman H. W. Fielding¹ D. A. Lind¹

The reactions ¹⁰B(p,n)¹⁰C and ¹¹B(p,n)¹¹C are examples of cases for which simple macroscopic relationships impose restrictions on the reaction

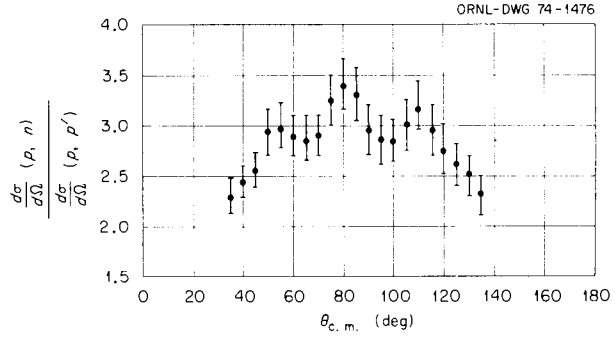


Fig. 1. Ratio of ¹⁰B(p,n)¹⁰C to ¹⁰B(p,p')¹⁰B*.

cross sections. Furthermore, calculated microscopic wave functions already exist in the literature.² Thus, these reactions provide interesting testing ground for nuclear reaction theory.

We have been able to take advantage of the ease of operation and good energy resolution of the University of Colorado time-of-flight system to obtain energy spectra with more than adequate energy resolution at 18 laboratory angles between 6° and 143°. So far we have made measurements using 16-MeV and 23-MeV protons. The targets were self-supporting evaporated films of enriched ¹⁰B and ¹¹B.

Simple arguments of isospin symmetry can be used to relate the differential cross sections for ¹⁰B(p,n)¹⁰C and ¹⁰B(p,p')¹⁰B* (where ¹⁰B* signifies the state that is the analog of ¹⁰C). The (p,n) cross section should be a factor of 2 larger but should match the (p,p') cross section in angular shape and in its energy fluctuations until the Coulomb effects spoil the simple symmetry. Our measured ratios are plotted in Fig. 1 and appear to show a departure from the simple predictions.

For ¹¹B(p,n)¹¹C the macroscopic Lane model provides a description of the transition to the $3/2^-$ ground state of ¹¹C as the result of a ($\tau \cdot T$) interaction potential. One can use a simple orthogonality argument to show that the matrix element for that interaction leading to any other state, in particular to the $3/2^-$ state at 4.79 MeV, must be equal to zero. Thus we can compare a transition in which the Lane potential is operative to a transition in which it is inoperative even though the other macroscopic quantum numbers are the same.

Previous measurements of ¹¹B(p,n)¹¹C did not resolve the 4.79-MeV $3/2^-$ state,^{3,4} and the angular distributions for both ¹⁰B(p,n)¹⁰C and ¹¹B(p,n)¹¹C have very few data points, due to the general difficulty of performing time-of-flight measurements.

We have been able to obtain clean energy spectra with energy resolution much better than needed to resolve the levels and have found significant differences in the angular distributions for the two $3/2^-$ states that should be attributable to the structure differences. Analysis of the data is being carried out at the University of Colorado.

1. Physics Department, University of Colorado, Boulder, Colo.
2. S. Cohen and D. Kurath, *Nucl. Phys.* **73**, 1 (1965).
3. J. D. Anderson, C. Wong, J. W. McClure, and B. D. Walker, *Phys. Rev.* **136**, B118 (1964).
4. A. S. Clough, C. J. Batty, B. E. Bonner, and L. E. Williams, *Nucl. Phys.* **A143**, 385 (1970).

A SEARCH FOR DELAYED GAMMA RAYS FROM ^{88}Y

C. D. Goodman R. L. Bunting¹
R. J. Peterson¹

In the energy level scheme of ^{88}Y some confusion exists in the 10- to 20-keV interval just above 700 keV excitation energy. Gabbard et al.² have proposed that a 2^- level lies in that interval, and other authors^{3,4} have proposed that 1^+ or 2^- and 6^+ and 7^+ levels lie in the region. No single experiment has seen the several levels resolved, and the question remains whether the levels seen in different reactions at approximately 700 keV are the same or different.

We are attempting to test whether the reactions $^{91}\text{Zr}(p,\alpha)^{88}\text{Y}$ and $^{90}\text{Zr}(d,\alpha)^{88}\text{Y}$ excite the same or different levels in the interval of interest. The (p,α) reaction should excite the 2^- level by a first-order process, and the (d,α) reaction should not. We are, therefore, looking for gamma rays associated with the 2^- decay in coincidence with alpha particles of the appropriate energy.

With the beam on, the gamma-ray intensity is too high to make the experiment feasible. The 2^- level, however, should deexcite to the 1^+ level at 393 keV, which has a half-life of 0.3 msec. Thus we can look for delayed gamma rays.

We make use of the beam pulsing system at the University of Colorado cyclotron. Each time an alpha particle of appropriate energy is detected, a logic pulse is generated that triggers the multichannel analyzer to begin to record a series of 16 gamma-ray spectra taken at 0.1-msec intervals. The "acquire" signal from the analyzer is used to turn off the cyclotron rf voltage so that there is no beam while the gamma spectra are taken.

We have found that the beam dies in less than 20 μsec , and the background gamma intensity is tolerably low. In our preliminary runs, however, we did not record enough alpha events to draw any definite conclusions about the energy levels.

1. Physics Department, University of Colorado, Boulder, Colo.
2. F. Gabbard, G. Chenevert, and K. K. Sekharan, *Phys. Rev.* **C6**, 2167 (1972).
3. Y. S. Park, H. D. Jones, and D. E. Bainum, *Phys. Rev.* **C4**, 778 (1971).
4. J. R. Comfort and J. P. Schiffer, *Phys. Rev.* **C4**, 803 (1971).

(p,t) REACTION STUDIES OF NICKEL ISOTOPES

M. Greenfield¹ D. McShan²
G. Vourvopoulos¹ S. Raman

Angular distributions have been measured for final states up to 8-MeV excitation observed in the $^{64,62,60,58}\text{Ni}(p,t)^{62,60,58,56}\text{Ni}$ reactions at 40-MeV proton bombarding energies. This study was initiated with the following objectives: (1) investigation of the reaction mechanism, especially with regard to coupled-channel and two-step reaction processes; (2) investigation of the structure of the nickel isotopes by testing the assumption of a ^{56}Ni closed core (is it necessary, for instance, to invoke large core excitation to explain the observed cross sections), and (3) investigation of the importance of two-particle correlations and pairing vibrations.

The data-taking portion of the experiment was completed in three runs of 40-hr duration each. Photographic plates were exposed in the broad-range spectrograph at ten angles between 7° and 45° lab for total integrated proton bombardments of 500 to 2000 μC . Target thicknesses ranged from 0.5 to 1.5 mg/cm^2 . Under these conditions, cross sections of the order of a microbarn could be measured reliably.

The photographic plates for the $^{58,60}\text{Ni}(p,t)^{56,58}$ reactions have already been scanned and analyzed. Plates for the $^{62}\text{Ni}(p,t)^{60}$ reaction have been scanned and are presently being analyzed and spot checked. Scanning of the plates for the $^{64}\text{Ni}(p,t)^{62}$ reaction is in progress and should be completed shortly.

Tables 1 and 2 show the levels observed in the $^{58,60}\text{Ni}(p,t)^{56,58}$ reactions, preliminary spin determinations, and approximate relative strengths. Spin-parity determinations are based on the results of fits to the angular distributions. Figure 1 shows angular distributions for the $J = 0, 2, 4$ members of the first band in

Table 1. Energy levels in ^{56}Ni
from $^{58}\text{Ni}(p,t)$ studies

Present work		Bruge and Leonard ^a		Davies et al. ^b	
Energy (MeV)	J^π	Energy (MeV)	J^π	Energy (MeV)	J^π
0.00	0^+	0.00	0^+	0.00	0^+
2.697 ± 0.015	2^+	2.697 ± 0.015	2^+	2.64	2^+
3.909 ± 0.018	4^+	3.956 ± 0.015	4^+	3.90	4^+
4.987 ± 0.022	0^+	5.000 ± 0.020	0^+	4.95	0^+
5.088 ± 0.040					
5.335 ± 0.029	3^-	5.339 ± 0.020	6^+	5.33	(2^+)
5.398 ± 0.017	0^+				
5.470 ± 0.020	2^+	5.483 ± 0.025	3^-		
5.968 ± 0.025	4^+	5.989 ± 0.020	(4^+)	5.90	(4^+)
6.023 ± 0.020	1^-				

^aG. Bruge and R. F. Leonard, *Phys. Rev.* **C2**, 2200 (1970).

^bW. G. Davies et al., *Phys. Lett.* **27B**, 363 (1968).

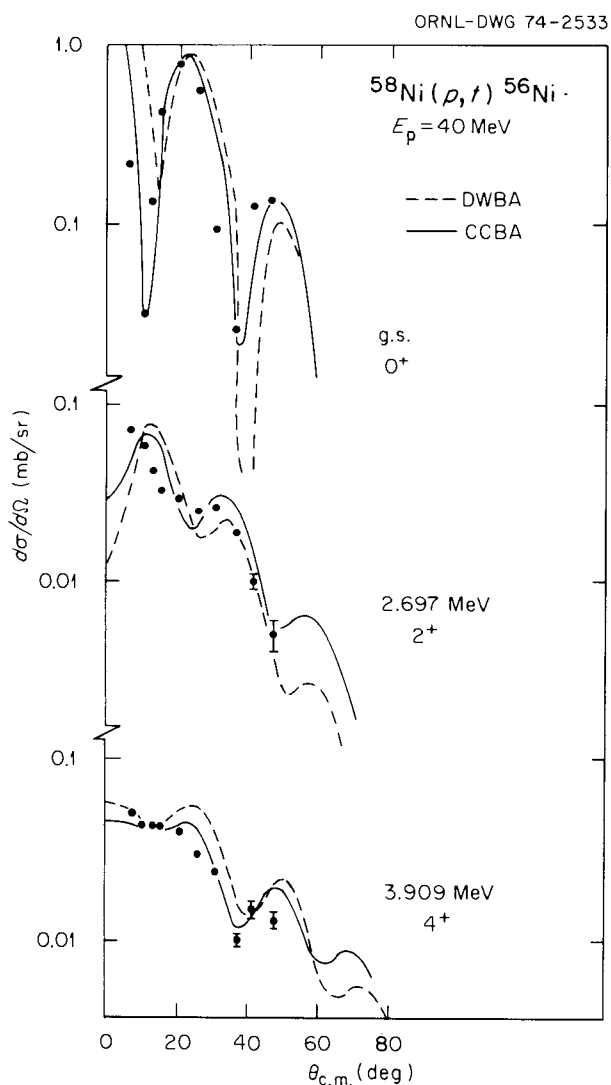


Table 2. Energy levels in ^{58}Ni

Present work			Nuclear Data Sheets ^a	
Energy (MeV)	$(d\sigma/d\Omega)_{\text{max}}$ ($\mu\text{b/sr}$)	J^π	Energy (MeV)	J^π
G.S.	806	0^+	G.S.	0^+
1.459 ± 0.006	123	2^+	1.4540	2^+
2.461 ± 0.007	27	4^+	2.4591	4^+
2.774 ± 0.009	5	(2^+)	2.7753	2^+
			2.9017	(1^+)
2.939 ± 0.020	15	0^+	2.9424	(0^+)
3.037 ± 0.009	37	$(1), (2)$	3.0378	2^+
3.266 ± 0.009	23	$(1), (2)$	3.2635	2^+
3.421 ± 0.020	1		3.4203	(3^+)
			3.526	(4^+)
			3.5309	
			3.5934	(1^+)
3.618 ± 0.006	8	4^+	3.6204	4^+
3.773 ± 0.007	<1		3.7746	(3^+)
3.889 ± 0.010	3	(2^+)	3.8985	2^+
4.103 ± 0.010	3	(2^+)	4.1079	(2)
4.298 ± 0.020	1		4.295	
4.337 ± 0.020	2		4.343	
			4.347	
			4.380	
4.397 ± 0.008	22	4^+	4.405	4^+
			4.443	
4.471 ± 0.020	12	$(4), (3)$	4.475	3^-
4.515 ± 0.020	3		4.517	
			4.536	
			4.578	
4.750 ± 0.007	33	4^+	4.754	4^+
			4.920	
			4.965	
			5.063	
			5.089	
			5.128	
5.156 ± 0.011	44	2^+	5.165	
			5.171	
			5.383	
5.488 ± 0.011		4^+	5.434	
			5.460	
			5.475	
			5.506	
5.585 ± 0.013		(3)	5.589	

^aS. Raman, *Nucl. Data Sheets* **B3(3, 4)**, 145 (1970).

Fig. 1. Angular distributions for the first three states in ^{56}Ni observed in the $^{58}\text{Ni}(p,t)$ reaction at $E_p = 40$ MeV.

ORNL-DWG 74-2534

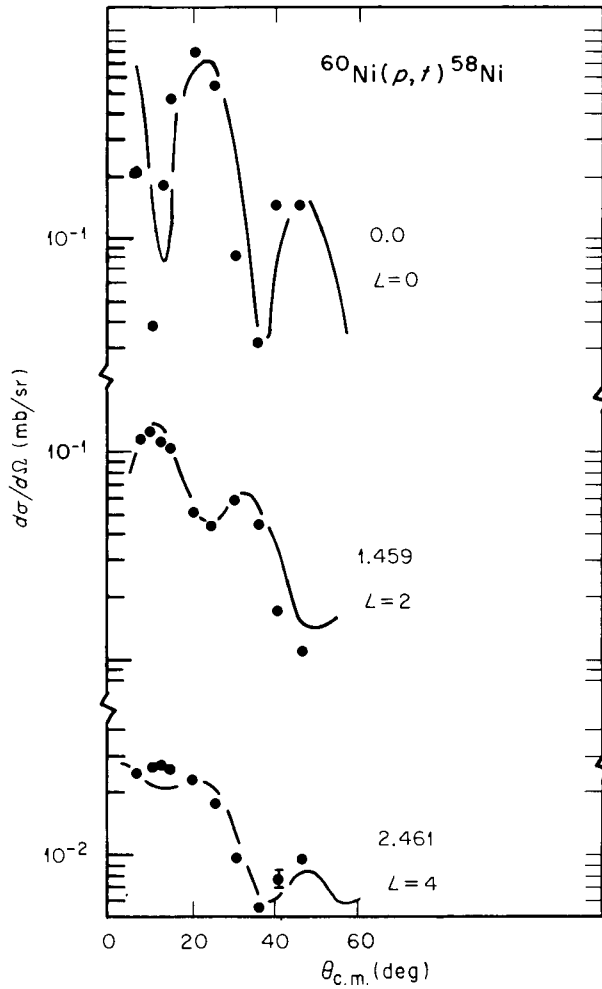


Fig. 2. Angular distributions for the first three states in ^{58}Ni observed in the $^{60}\text{Ni}(p,t)$ reaction at $E_p = 40$ MeV.

^{56}Ni . Calculations shown are DWBA zero-range with the code DWUCK and effective coupled-channel calculations. Figure 2 shows angular distributions for the first $J = 0, 2, 4$ levels in ^{58}Ni .

The shapes of angular distributions appear to unambiguously define the transferred angular momentum. However, the relative magnitudes of the zero-range calculations using several sets of wave functions do not satisfactorily reproduce the observed experimental magnitudes.

Preliminary indications are that the nickel wave functions must include large core excitation. Failure of any simple two-particle model to predict either the ordering or spacing of levels populated in the $^{58}\text{Ni}(p,t)^{56}\text{Ni}$ reaction strongly suggests large core

ORNL-DWG 74-2535

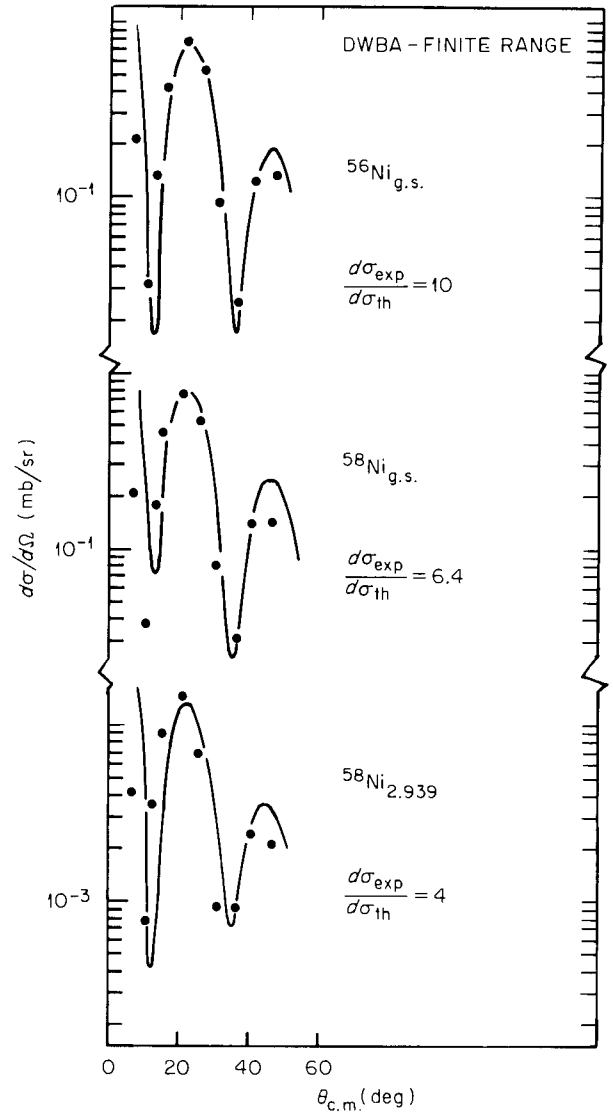


Fig. 3. Comparison of experimental and theoretical angular distributions for 0^+ states in ^{56}Ni and ^{58}Ni .

excitation as predicted by Wong and Davies.³ Their model includes large $4p-4h$ core excitations and accurately predicts both the spacing and ordering of observed levels (one of which at 5.398 was observed for the first time in this work; see Table 1).

Figure 3 shows the calculations of the DWBA finite-range code Mercury.⁴ The ^{56}Ni and ^{58}Ni wave functions used are those of Auerbach,⁵ which are based on the assumption that ^{56}Ni is an inert core and ^{58}Ni consists of two particles in the $p_{3/2}, f_{5/2},$ or $p_{1/2}$ shell.

The finite-range calculations fall below the observed magnitudes by a factor of 4 to 10 – neither absolute magnitude nor relative strengths are predicted accurately.

The excitation (albeit weakly) of the suspected nonnormal parity states at 3.42 and 3.77 MeV in ^{58}Ni (see Table 2) suggests that two-step processes may have to be included for the correct description of the $\text{Ni}(p,t)$ cross sections.

-
1. Florida A & M University, Tallahassee, Fla.
 2. Brown University, Providence, R. I.
 3. S. S. M. Wong and W. G. Davies, *Phys. Lett.* **28B**, 77 (1968).
 4. L. A. Charlton, *Phys. Rev.* **C8**, 146 (1973).
 5. N. Auerbach, *Phys. Rev.* **163**, 1203 (1967).

CORE POLARIZATION IN INELASTIC PROTON SCATTERING FROM ^{209}Bi AT 61 MeV

Alan Scott¹ M. Owais² F. Petrovich³

The differential cross sections for the excitation of the 0.90-MeV ($2f_{7/2}$) and 1.61-MeV ($1i_{13/2}$) single-proton levels and the weak-coupling multiplet at 2.62 MeV in ^{209}Bi have been measured with 61.2-MeV protons from the ORIC. The experimental shape for this 1.61-MeV level very clearly has the character of an angular momentum transfer $L = 3$. The results of collective-model calculations and microscopic-model calculations with core polarization are compared with the data. It is found that $L = 4, 6,$ and 8 core admixtures are important in the 0.90-MeV transition and that an 8% admixture of the 1^3_2 member of the 2.62-MeV multiplet in the $1i_{13/2}$ single-proton state is needed to explain the 1.61-MeV transition. The cross section for the 2.62-MeV multiplet is consistent with the weak-coupling interpretation.

-
1. ORAU Consultant from the Department of Physics, University of Georgia. Support in part by the Work-Study Program at the University.
 2. Graduate Assistant at the University of Georgia. Part of this work in M.S. thesis.
 3. Work performed at the Lawrence Berkeley Laboratory under the auspices of the U.S. Atomic Energy Commission. Present address: Department of Physics, Florida State University, Tallahassee.

INELASTIC SCATTERING OF 61-MeV PROTONS FROM ^{92}Mo

Alan Scott¹ M. L. Whiten²

The counting of proton tracks in plates exposed this fall is in progress at the University of Georgia. The aim

of this experiment is to compare the cross sections for excitation of proton states in ^{92}Mo with earlier measurements in ^{90}Zr .

MESON PHYSICS

E. E. Gross C. A. Ludemann
M. J. Saltmarsh

We are collaborating in two experimental programs at LAMPF with investigators from the University of South Carolina, Virginia Polytechnic Institute, LASL, and SIN. Both programs are scheduled for early beam time on the Low Energy Pion Line.

Our two proposals (No. 29/54 and No. 131) are directed at the understanding of the low-energy (<60 MeV) pion-nucleus interaction. Experiment No. 29/54 involves measurements of π -nucleus elastic scattering on a number of targets at energies in the range 20 MeV to 60 MeV. In experiment No. 131 we shall be looking at the reaction $\pi^+ + d \rightarrow p + p$ in the same energy range. This reaction is the simplest example of the ($\pi^+, 2p$) reaction, which dominates the imaginary term in the low-energy π^+ -nucleus optical potential. We have chosen to work in the low-energy region because it is there, where the pion-nucleon interaction is relatively weak, that one can hope to derive π -nucleus interactions from the more fundamental π -nucleon processes.

During 1973, our activities at LAMPF increased markedly as the experimental areas neared completion. We have been actively involved in setting up the Low Energy Pion Line, from the initial tests with alpha sources, through the first detection of pions at LAMPF, to the study of the secondary beam characteristics.¹ Most of the equipment for our two experiments is now at LAMPF, and we have started to check out our detectors and monitoring system in the pion beam itself. Our first data runs are scheduled for March and July (experiment No. 131) and some time in the summer or early fall for experiment No. 29/54.

-
1. R. Redwine, J. Alster, G. Bureson, R. Burman, J. Frank, K. Klare, R. Mischke, D. Moir, D. Nagle, J. P. Perroud, M. Blecher, M. Jakobson, K. Johnson, B. Freedom, and M. Saltmarsh, *Bull. Amer. Phys. Soc.* **19**, 30 (1974).

CYCLOTRON LABORATORY ACCELERATOR DEVELOPMENT PROGRAM

SUMMARY

J. A. Martin

During 1973, nearly 50 new heavy-ion beams ranging from lithium to xenon were developed. Approximately half of these were metal ions obtained from a sputtering process using xenon to bombard a metal insert in the ion source. Two 20°K cryopumps were installed in the magnet gap, giving substantial gains in heavy-ion beam intensity in initial testing. The principle of all-magnetic extraction was demonstrated in a brief test using the existing ORIC system. Magnetic extraction is an important ingredient of the "recycle" concept. The new rf power amplifier installed in 1972 was modified to give improved performance and reliability. Tube life appears to be comparable with that obtained with the 6949. As a part of the accelerator improvement program, the double-stemmed, rotating-cathode ion source tube was fabricated and bench tested. Also, most of the design of the cyclotron computer control system was completed, and installation was begun. Other improvements to ORIC include the addition of a quadrupole singlet to increase the solid angle of the broad-range spectrograph, expanded capabilities of the data acquisition system, and the commencement of a program to upgrade stability and reliability of all the power supplies for the trim coils, harmonic coils, main field, and extraction channels. A number of variants of the proposal for a National Heavy-Ion Laboratory were studied. The one of most interest at this time is for a tandem injecting into ORIC. Although this proposal does not include the large separated-sector cyclotron, it could be added at a later date.

HEAVY-ION BEAM DEVELOPMENT

E. D. Hudson	J. E. Mann
M. L. Mallory	J. A. Martin
R. S. Lord	R. K. Goosie ¹
F. Irwin	

Metal Ions

The discovery of a high-intensity copper beam while accelerating $^{130}\text{Xe}^{12+}$ is the highlight of heavy-ion beam development on the Oak Ridge Isochronous Cyclotron (ORIC) during the year 1973. The origin of the copper beam is a section of the ion source. It had been previously noted that this section of the ion source, the plasma chamber wall opposite the ion

extraction slit, was eroding. Replacement of this section with different metals, as illustrated in Fig. 1, resulted in production and acceleration of ions of these metals.

In order to understand the process, a computer code was written which traced the orbits of the particles starting from the ion source. The calculation showed that large mass-to-charge (m/q) ions, for example, $^{132}\text{Xe}^{1+}$, could not cross the accelerating gap before reversal of the rf voltage. These ions were accelerated back into the ion source and impinged upon the observed eroded area. Figure 2 shows the energy per unit charge of different m/q particles that are accelerated back into the ion source aperture as a function of initial starting phase (0° phase is the peak acceleration voltage). The calculations indicate that large m/q particles are accelerated back to the ion source with energy of over 30 keV when starting at 0° phase and 80 kV accelerating voltage. From Child's space-charge law, one expects the peak ion source extracted current to occur at 0° phase. Small m/q particles (e.g., $^{20}\text{Ne}^{2+}$) return to the source with low energy and reduced intensities compared with large m/q particles. One would expect xenon to be better than neon for production of sputtered ions, and this agrees with measurements.

Another interesting result was obtained from the acceleration of niobium. With the niobium beam, it became possible to turn off the xenon gas, and the arc

ORNL-DWG 73-10636A

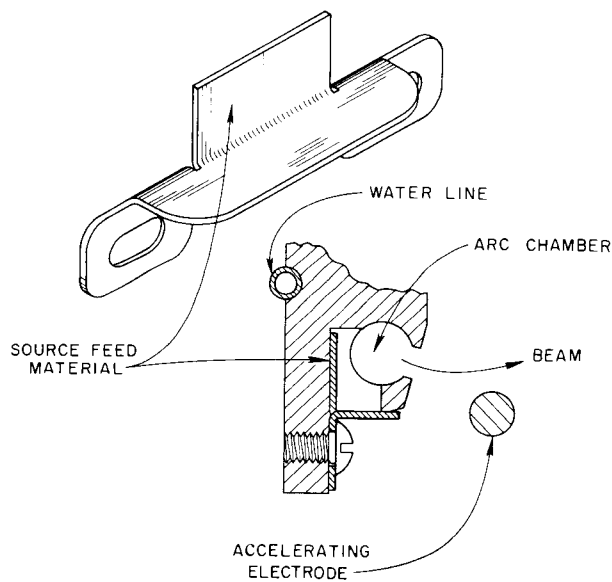


Fig. 1. Cross section of the ORIC Penning ion source in the median plane of the cyclotron. A typical metal insert and its position in the copper ion source, opposite the ion source slit, are indicated by "source feed material." Xenon ions that are unable to cross the accelerating gap return to the ion source with enough energy to sputter material from the metal insert.

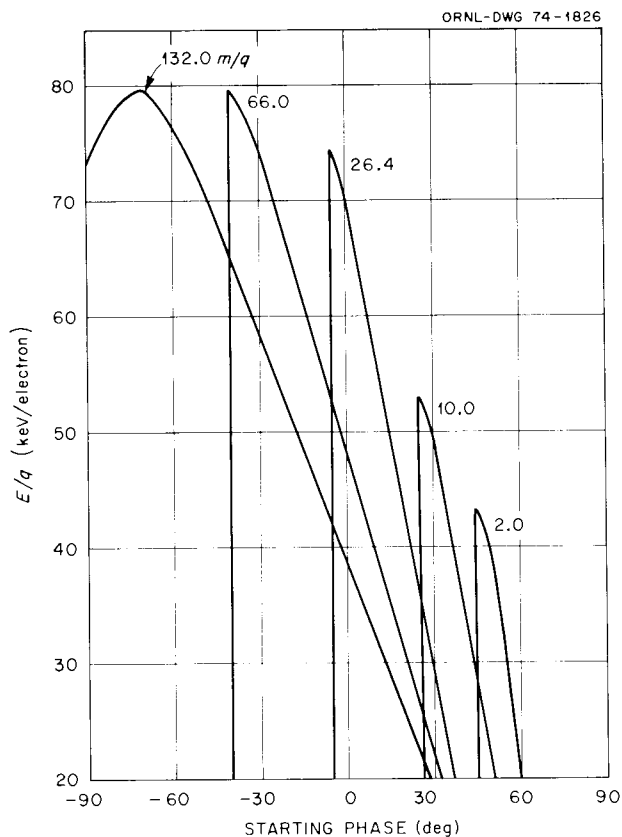


Fig. 2. The energy per unit charge for different mass-to-charge ratios for ions that return to the ion source and cause sputtering is shown for various rf starting phases. The cyclotron resonance frequency was for third harmonic $^{56}\text{Fe}^{5+}$. The rf gap was assumed to be 1 cm and the magnetic field 18 kG.

became self-sustaining with material being sputtered by the niobium ions returning to the source. Turning off the rf voltage eliminated the returning niobium ions and caused the arc to drop out.

The arc self-bombardment offers a possible explanation for two other source phenomena. After many hours of source operation, the bombarding ions returning to the source completely erode a hole through the source plasma chamber, resulting in a substantial increase in beam intensity. We assign this increase in beam to the decrease in contaminating ions in the plasma. The second phenomenon occurs immediately after applying accelerating voltage to the dec. The intensity of the extracted beam gradually decreases over a short time. This may be the time required for equilibrium conditions to occur for mixing of the contaminant ions with the desired ions in the arc plasma. Table 1 is a complete listing of ORIC heavy-ion beams. Metal ions obtained by source bombardment using xenon gas are indicated.

Table 1. ORIC extracted heavy-ion beams

ORIC maximum energy = $90q^2/A$

Particle	External beam current	Particle	External beam current
$^6\text{Li}^{1+a}$	$1\ \mu\text{A}^b$	$^{35}\text{Cl}^{3+}$	10 enA
$^6\text{Li}^{2+a}$	$8\ \mu\text{A}^b$	$^{35}\text{Cl}^{5+}$	>1 enA
$^6\text{Li}^{3+a}$	$40\ \text{enA}^b$	$^{35}\text{Cl}^{7+}$	900 enA
$^7\text{Li}^{1+a}$	650 enA	$^{36}\text{Ar}^{9+}$	$\sim 5 \times 10^5$ part./sec
$^7\text{Li}^{2+}$	$8\ \mu\text{A}$	$^{40}\text{Ar}^{2+}$	300 enA ^c
$^{10}\text{B}^{2+}$	15 enA	$^{40}\text{Ar}^{3+}$	$3\ \mu\text{A}^c$
$^{10}\text{B}^{3+}$	$8\ \mu\text{A}$	$^{40}\text{Ar}^{4+}$	15 μA
$^{10}\text{B}^{4+}$	>10 enA	$^{40}\text{Ar}^{5+}$	$1\ \mu\text{A}$
$^{11}\text{B}^{3+}$	$30\ \mu\text{A}$	$^{40}\text{Ar}^{6+}$	300 enA
$^{12}\text{C}^{1+}$	12 enA	$^{40}\text{Ar}^{7+}$	120 enA
$^{12}\text{C}^{2+a}$	1 enA	$^{40}\text{Ar}^{8+}$	$1.2\ \mu\text{A}$
$^{12}\text{C}^{3+}$	>10 μA	$^{40}\text{Ar}^{9+}$	11 enA
$^{12}\text{C}^{4+}$	>12 μA	$^{40}\text{Ar}^{10+}$	$\sim 5 \times 10^4$ part./sec
$^{12}\text{C}^{5+}$	40 enA	$^{40}\text{Ar}^{11+}$	250 part./sec
$^{12}\text{C}^{6+}$	$\sim 1\ \text{epA}$	$^{40}\text{Ca}^{6+d}$	300 enA
$^{13}\text{C}^{4+}$	6 enA	$^{40}\text{Ca}^{7+a}$	700 enA
$^{14}\text{N}^{2+}$	>20 μA	$^{40}\text{Ca}^{8+a}$	12 enA
$^{14}\text{N}^{4+}$	>20 μA	$^{48}\text{Ti}^{5+d}$	$1.2\ \mu\text{A}$
$^{14}\text{N}^{5+}$	$2\ \mu\text{A}$	$^{48}\text{Ti}^{6+d}$	360 enA
$^{15}\text{N}^{3+}$	1 enA	$^{48}\text{Ti}^{7+d}$	100 enA
$^{15}\text{N}^{4+}$	$8\ \mu\text{A}^b$	$^{48}\text{Ti}^{9+d}$	0.3 enA
$^{16}\text{O}^{1+}$	$1.3\ \mu\text{A}$	$^{52}\text{Cr}^{2+}$	1 enA ^e
$^{16}\text{O}^{2+}$	$5\ \mu\text{A}$	$^{55}\text{Mn}^{5+a}$	30 enA ^e
$^{16}\text{O}^{3+}$	300 enA	$^{54}\text{Fe}^{7+d}$	21 enA
$^{16}\text{O}^{4+}$	>4 μA	$^{54}\text{Fe}^{8+d}$	9 enA
$^{16}\text{O}^{5+}$	$20\ \mu\text{A}$	$^{56}\text{Fe}^{5+d}$	$1.2\ \mu\text{A}$
$^{16}\text{O}^{6+a}$	$1.1\ \mu\text{A}$	$^{56}\text{Fe}^{6+d}$	400 enA
$^{17}\text{O}^{1+}$	2.2 enA	$^{56}\text{Fe}^{9+}$	4 enA
$^{18}\text{O}^{2+}$	10 enA	$^{56}\text{Fe}^{10+}$	0.02 enA
$^{18}\text{O}^{5+}$	$20\ \mu\text{A}^b$	$^{56}\text{Fe}^{11+}$	500 part./sec
$^{19}\text{F}^{2+}$	$1.5\ \mu\text{A}$	$^{58}\text{Ni}^{5+d}$	$1.5\ \mu\text{A}$
$^{19}\text{F}^{6+}$	$1\ \mu\text{A}$	$^{58}\text{Ni}^{6+d}$	$3.5\ \mu\text{A}$
$^{20}\text{Ne}^{1+}$	$19\ \mu\text{A}^c$	$^{58}\text{Ni}^{7+d}$	$3\ \mu\text{A}$
$^{20}\text{Ne}^{3+}$	$5\ \mu\text{A}$	$^{58}\text{Ni}^{8+d}$	30 enA
$^{20}\text{Ne}^{4+}$	>1 μA	$^{63}\text{Cu}^{3+}$	15 enA
$^{20}\text{Ne}^{5+}$	>1 μA	$^{63}\text{Cu}^{6+d}$	$1.2\ \mu\text{A}$
$^{20}\text{Ne}^{6+}$	$3\ \mu\text{A}$	$^{63}\text{Cu}^{7+d}$	275 enA
$^{20}\text{Ne}^{7+a}$	0.04 enA	$^{63}\text{Cu}^{9+}$	$1\ \text{enA}^e$
$^{21}\text{Ne}^{1+}$	0.7 enA	$^{65}\text{Cu}^{6+d}$	450 enA
$^{22}\text{Ne}^{2+}$	800 enA	$^{64}\text{Zn}^{6+d}$	$1.5\ \mu\text{A}$
$^{22}\text{Ne}^{4+a}$	600 enA	$^{64}\text{Zn}^{7+d}$	100 enA
$^{22}\text{Ne}^{5+}$	300 enA	$^{66}\text{Zn}^{6+}$	$0.1\ \text{enA}^e$
$^{24}\text{Mg}^{5+d}$	57 enA	$^{78}\text{Kr}^{3+}$	10 enA
$^{24}\text{Mg}^{6+d}$	0.3 enA	$^{83}\text{Kr}^{9+a}$	2 enA
$^{28}\text{Si}^{3+}$	$0.1\ \text{enA}^e$	$^{84}\text{Kr}^{3+}$	32 enA
$^{28}\text{Si}^{5+a}$	300 enA	$^{84}\text{Kr}^{4+a}$	$1\ \mu\text{A}$
$^{28}\text{Si}^{6+a}$	10 enA	$^{84}\text{Kr}^{5+a}$	$2.2\ \mu\text{A}$
$^{29}\text{Si}^{3+}$	100 part./sec ^e	$^{84}\text{Kr}^{6+a}$	150 enA ^c
$^{30}\text{Si}^{6+}$	1 epA	$^{84}\text{Kr}^{9+}$	20 enA
$^{32}\text{S}^{4+}$	$9\ \text{enA}^e$	$^{86}\text{Kr}^{6+}$	>1 enA ^c
$^{32}\text{S}^{6+}$	100 enA	$^{93}\text{Nb}^{5+d}$	70 enA
$^{34}\text{S}^{2+}$	300 enA		

Table 1 (continued)

Particle	External beam current	Particle	External beam current
$^{93}\text{Nb}^{6+d}$	70 enA	$^{130}\text{Xe}^{7+a}$	4.5 enA
$^{93}\text{Nb}^{7+d}$	35 enA	$^{131}\text{Xe}^{7+a}$	15 enA
$^{93}\text{Nb}^{8+d}$	1.8 eμA	$^{132}\text{Xe}^{7+a}$	20 enA
$^{128}\text{Xe}^{7+a}$	1 enA	$^{132}\text{Xe}^{12+}$	0.1 enA
$^{129}\text{Xe}^{5+}$	3 enA ^c	$^{134}\text{Xe}^{7+a}$	8 enA
$^{129}\text{Xe}^{7+}$	90 enA ^c	$^{181}\text{Ta}^{6+}$	1 enA
$^{129}\text{Xe}^{8+}$	13 enA ^c	$^{181}\text{Ta}^{8+}$	0.2 epA
$^{129}\text{Xe}^{9+}$	0.4 enA ^c	$^{181}\text{Ta}^{9+}$	0.5 epA
$^{129}\text{Xe}^{12+a}$	1.3 enA		

^aOther beams new in 1973.

^bEnriched isotopic-abundance source feed.

^cIon source with dc extraction.

^dMetal ions from back-bombardment with xenon gas.

^eFrom ion source material of construction.

Other Beams

Other beams developed in 1973 are also indicated in Table 1. The intensity of $^{16}\text{O}^{6+}$ was larger than expected. The beam attenuation of $^{16}\text{O}^{6+}$ as a function of radius in ORIC is very small, indicating that tank pressure has little effect on this beam. The amount of $^{16}\text{O}^{7+}$ stripped in our beam transport system was down by two magnitudes compared with lower charge state beams. This can be explained by the shell effect between $^{16}\text{O}^{6+}$ and $^{16}\text{O}^{7+}$. The differential ionization potential between $^{16}\text{O}^{6+}$ (the last electron in the *L* shell) and $^{16}\text{O}^{7+}$ (the first electron in the *K* shell) is 698 eV. The differential ionization potential between $^{16}\text{O}^{5+}$ and $^{16}\text{O}^{6+}$ is only 146 eV, where no shell boundary crossing is involved. In like manner, the relative beam intensities of $\text{N}^{5+}/\text{N}^{6+}$ and of $\text{Ne}^{6+}/\text{Ne}^{7+}$ can be explained as a shell effect.

Magnetic Extraction

During 1972, we developed an acceleration concept that utilizes the simultaneous harmonic acceleration capabilities of isochronous cyclotrons (recycle). One of the needed innovations for recycle was a complete magnetic extraction system. We have now magnetically extracted various beams from ORIC. Table 2 lists these beams and their energies. Magnetic extraction was accomplished by a simple modification to our existing extraction system. The existing extraction system is composed of three elements: an electrostatic deflector, a coaxial magnetic channel with a $1/8$ -in.-thick insert (septum) positioned between the circulating and extracted beams, and a coil-compensated iron magnetic

Table 2. Magnetically extracted beams

Particle	Energy (MeV)
$^4\text{He}^{2+}$	24
$^6\text{Li}^{1+}$	4
$^6\text{Li}^{3+}$	36
$^{12}\text{C}^{2+}$	8
$^{16}\text{O}^{2+}$	10
$^{16}\text{O}^{3+}$	23

channel. The exit of the electrostatic channel is normally coupled to the entrance of the coaxial magnetic channel and is adjustable radially. In 1972, a small adjustment (deflection exit mechanism) was added to the exit of the electrostatic deflector and the entrance of the coaxial magnetic channel to allow better operational alignment between the two extraction elements. By simply extending the range of the deflector exit mechanism to $3/4$ in. and positioning the electrostatic deflector at maximum radius, the entrance of the coaxial magnetic channel was exposed to the circulating beam. Beam separation calculations indicated that a group of particles have enough turn separation to clear the $1/8$ -in. coaxial insert. The deflection normally imparted by the electrostatic deflector was achieved by operating the coaxial magnetic channel at a higher current than required for normal extraction. The electrostatic deflector can be replaced with a thin-septum magnet that can extract all beams from ORIC at percentages comparable with those presently achieved.

Simultaneous Harmonic Beam Acceleration and Magnetic Extraction

An experimental verification of some of the computer calculation for recycle has been achieved by utilizing the transit time difference at the first gap for harmonic beams. Calculations of the transit time of particles for crossing the first acceleration gap as a function of *rf* harmonics indicated the desirable phase shift between harmonic beams needed to simulate the recycle phase history. Figure 3 is the transit angle for various *m/q* particles at an initial starting phase of -60° . (Negative phase means the ions are ahead of the *rf* peak voltage.) A beam of $^{16}\text{O}^{2+}$ on the third harmonic requires a transit angle of 65° . Its phase at the next gap crossing would be $+5^\circ$. A beam of $^{16}\text{O}^{6+}$ on the first harmonic requires a transit angle of 30° , and its phase at the second gap crossing is -30° . Similar transit angle differences are obtained for other initial starting phases.

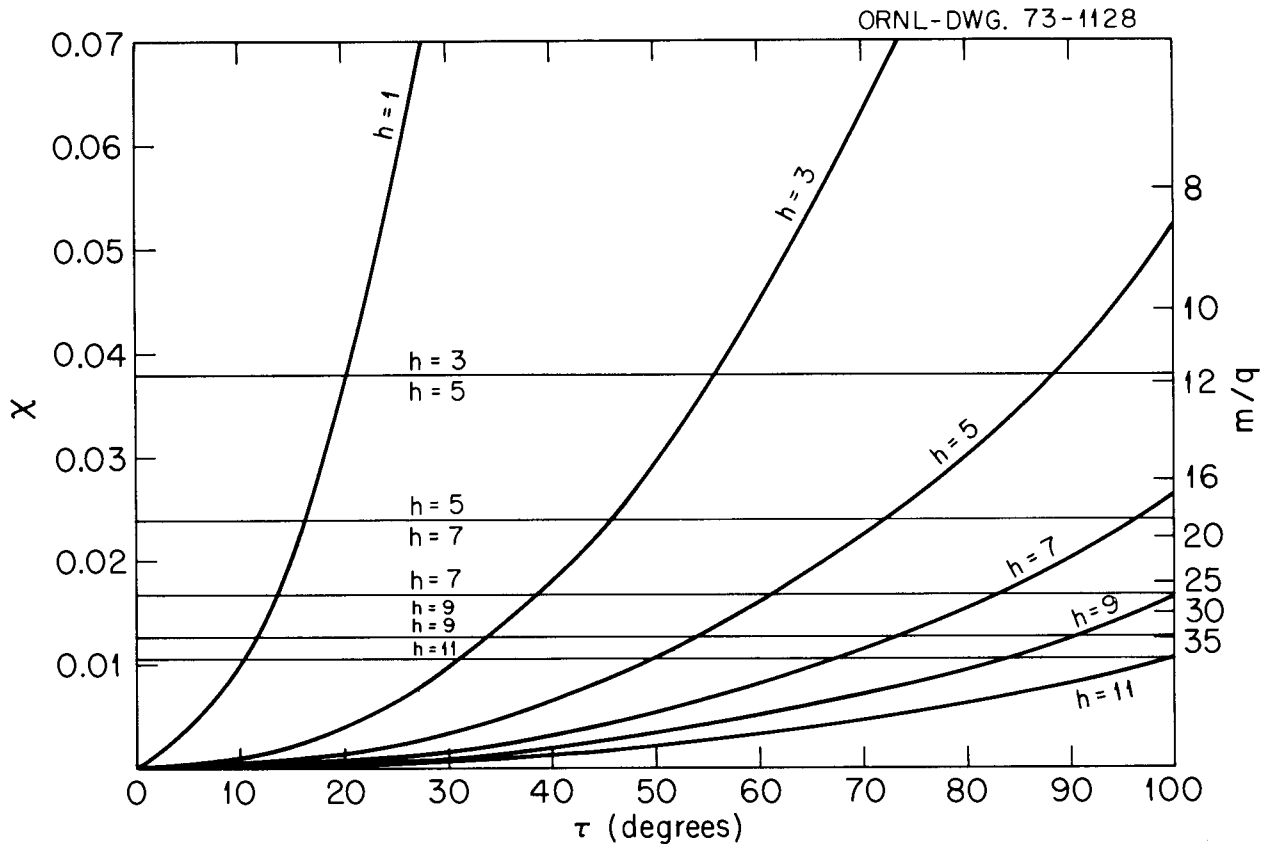


Fig. 3. The transit angle in rf degrees as a function of χ (a geometry parameter) for an initial starting phase of -60° . For a given geometry, χ is related to a particular value of m/q . The transit angle for a given m/q value is larger for the higher harmonics.

The phase difference of 35° after the first gap crossing between the first and third harmonic beams is similar to the phase history desired for simultaneous harmonic acceleration of two beams. The first two-beam experiments were acceleration of $^{16}\text{O}^{6+}$ and $^{16}\text{O}^{2+}$ to full extraction radius. The two beams were alternately extracted with the normal extraction system of ORIC by varying only the deflector voltage by the theoretical amount.

The next step was the development of simultaneous magnetic extraction of two beams. Calculations indicated that $^6\text{Li}^{1+}$ on the third harmonic and $^6\text{Li}^{3+}$ on the first harmonic at an $E_0 = 24$ MeV would have the turn separation to match the coaxial insert width. The betatron oscillation amplitude gives additional turn separation. A high-intensity beam of $^6\text{Li}^{1+}$ was magnetically extracted and positively identified by standard energy and stripping measurements. Identification of the $^6\text{Li}^{3+}$ companion beam was difficult because of the high intensity of $^6\text{Li}^{1+}$. It was necessary to defocus the extracted beams with a quadrupole until an acceptable count rate was maintained, giving a small count rate for

the $^6\text{Li}^{3+}$. An example of the spectrum obtained is shown in Fig. 4. A second identification technique was also developed. Placing a 0.003-in. foil of aluminum in front of the detector completely stopped the $^6\text{Li}^{1+}$ and allowed tuning of the $^6\text{Li}^{3+}$ beam. A $60\text{-}\mu$ silicon detector only partially stopped the energetic $^6\text{Li}^{3+}$ beam and necessitated the use of a $300\text{-}\mu$ detector. This experiment verifies the simultaneous acceleration and magnetic extraction that are required for recycle.

Internal Ion Source with Rotating Cathodes

The lifetime of the cathodes used in the Penning ion source in ORIC depends upon the gas and amount of arc power. For argon the cathode lifetime is 2 to 4 hr. Approximately 30 min is required to change the source, followed by additional startup time. Development of an ion source that extends the lifetime of the cathode would lead to significant increase in research time. A rotating-cathode ion source has been designed, and preliminary tests of the cathode rotation feature have

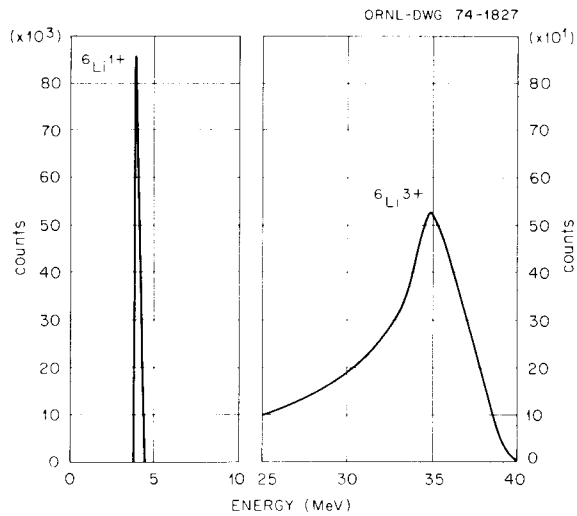


Fig. 4. The energy spectrum of ${}^6\text{Li}^{1+}$ and ${}^6\text{Li}^{3+}$ obtained from a magnetically extracted beam that is scattered at an angle of 15° from a gold foil. The intensity of ${}^6\text{Li}^{1+}$ is about 50 times greater than the ${}^6\text{Li}^{3+}$ and required the beam to be defocused before the gold foil to reduce the count rate to an acceptable value.

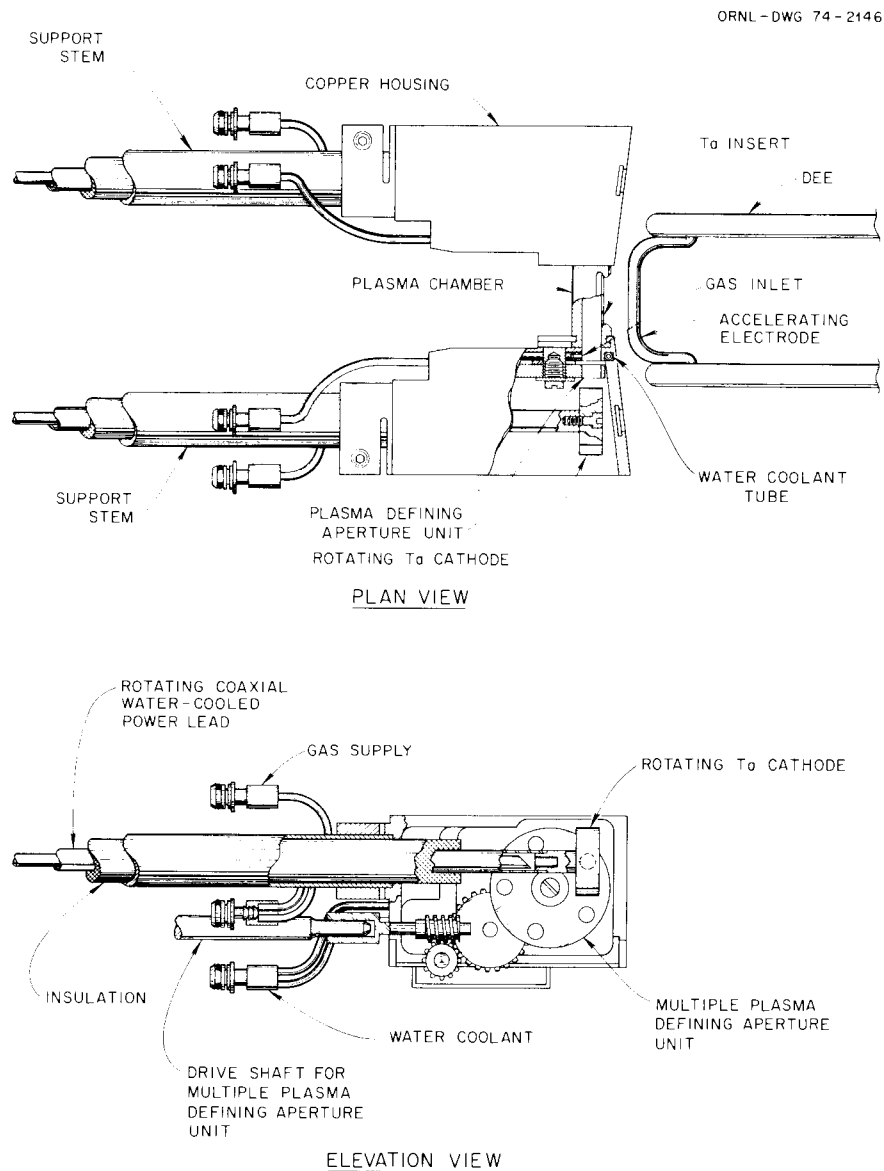


Fig. 5. A schematic drawing of the source end of the rotating-cathode ion source is shown. The cathode defining slit has multiple aperture and can be changed remotely.

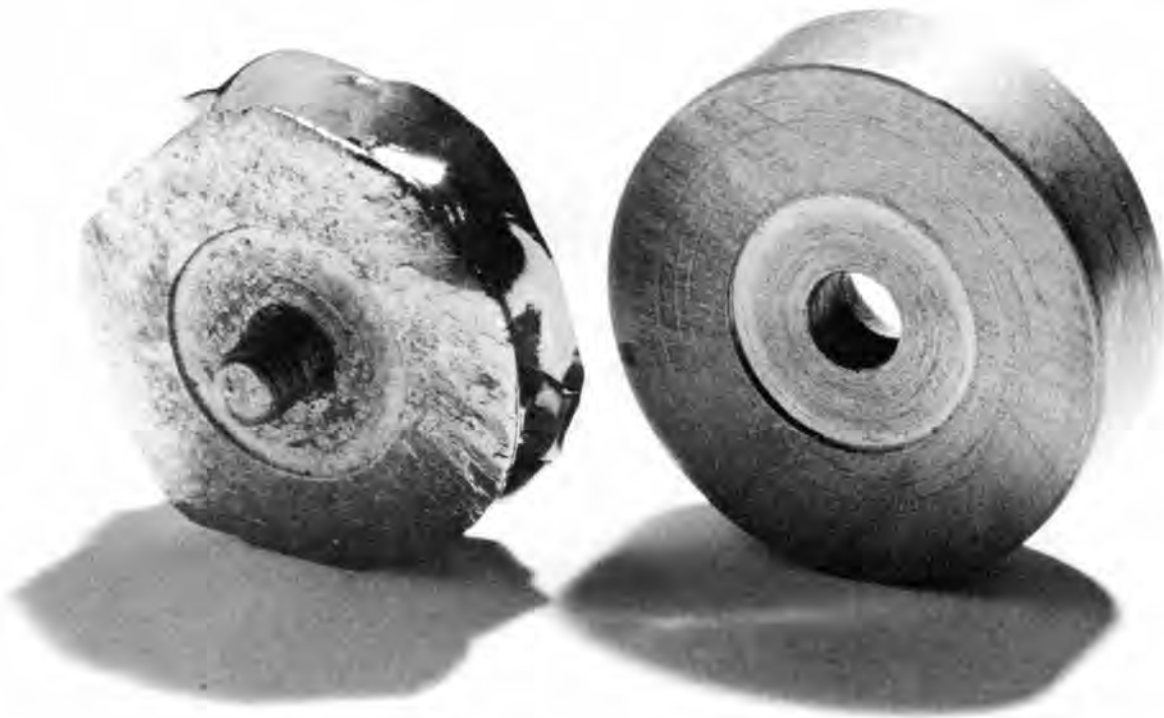


Fig. 6. A photograph of new and used cathodes for the rotating-cathode ion source. The cathode is a disk of tantalum $1\frac{1}{8}$ in. in diameter and $\frac{3}{8}$ in. thick. The used cathode has operated for 27 hr.

been made under typical arc conditions. Figure 5 is a drawing of the source. The cathodes are tantalum disks, $1\frac{1}{8}$ in. in diameter and $\frac{3}{8}$ in. thick, and are mounted on a rotating shaft. A multiple cathode defining aperture is provided.

A set of cathodes using argon gas operated for 27 hr in the test facility. The cathode rotational speed is $\frac{1}{2}$ rpm. After approximately 5 hr the cathode defining slit, which collects the sputtered tantalum from the cathodes, must be changed. This is accomplished by indexing the multiple cathode defining aperture. The arc current and voltages are the same as the present source. Figure 6 is a photograph of a new cathode and one after a 27-hr run.

The additional components necessary to adapt the cyclotron to the new source are being fabricated, and installation is scheduled to begin in May 1974. In preparation for the new source installation, we have already relocated the extraction system components and tested them with various beams and a wide range of magnetic fields. This was necessary because of the larger size of the new source, which would have caused an interference with the extraction system. The new

source also required redesign of the ion source positioner, which is mounted on the dummy dee. This has been fabricated and is awaiting installation.

1. Engineering Division.

ORIC CRYOPUMPS

J. E. Mann W. R. Smith¹
R. S. Lord A. W. Alexander²

Studies of beam attenuation vs pressure reported in 1972³ showed that for most heavy-ion beams a substantial increase in beam intensity could be made if the pressure in the circulating beam region could be significantly reduced. However, since the conductance between the circulating beam and the conventional pumping system is quite low, there was no practical way to add pumping speed in the circulating beam region except to install a pump in this region. Cryopumping appeared to be the best solution.

Two panels of 2870 cm² each, cooled to 20°K, have been installed on either side of the median plane in one quadrant of the acceleration region (Fig. 1). Preliminary

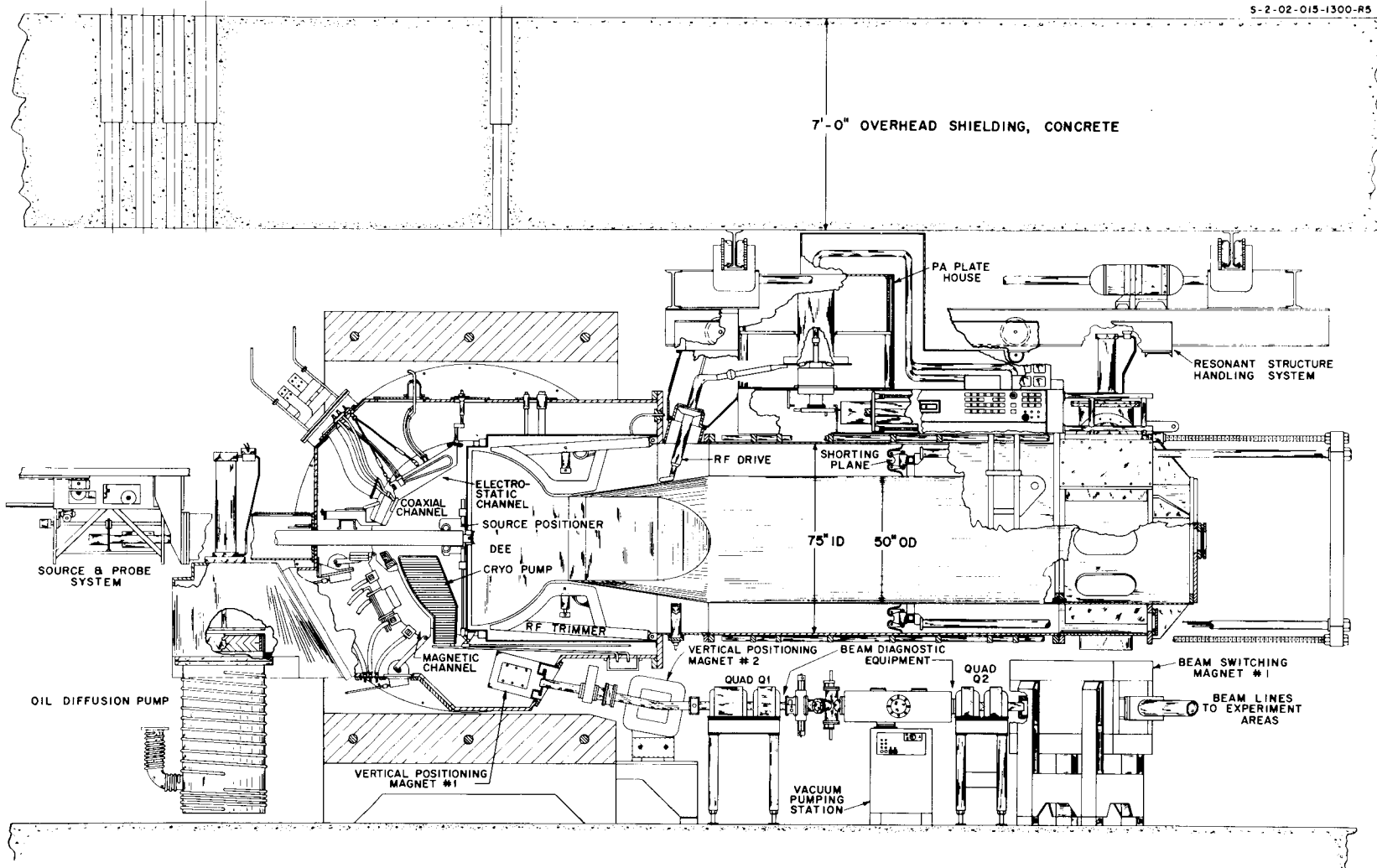


Fig. 1. Location of ORIC cryopanels in the magnet gap between the dee and the magnetic channel.

measurements have been made on pumping speed and beam improvement. The pumping speed of the diffusion pumps at the center of the tank is only about 3500 liters/sec, and the speed above the pumps is about 20,000 liters/sec. The measurements with the cryopumps operating indicate that the pumping speed at the center has been increased by about a factor of 3 to a total of 10,000 liters/sec.

Using the extracted beam intensities before and after the cool-down of the cryopanel as a measure of improvement, gains ranging from about 3 to 18 (for $^{40}\text{Ar}^{4+}$) have been seen. The improvement that is achieved depends strongly on the pressure before the cryopanel is cooled. If the initial pressure is poor, a large increase can be made (depending also on the ion species and charge state). If the initial pressure is low, only a moderate increase will be seen. In some cases the beam has increased more than the amount predicted by considering only the beam loss due to charge-changing by interaction with residual gas. The additional increase occurs close to the center, in a region that is not covered by the measuring probe, and is at present not satisfactorily explained.

The pumps (Figs. 2 and 3) are $1\frac{1}{2}$ in. thick and are spaced $\frac{1}{8}$ in. from the trim coil platter by six G-10 epoxy-glass spacers. This space is filled with super insulation to reduce the radiant heat load to the pumps and to prevent freezing the trim coil water circuits.

ORNL-DWG 74-1576

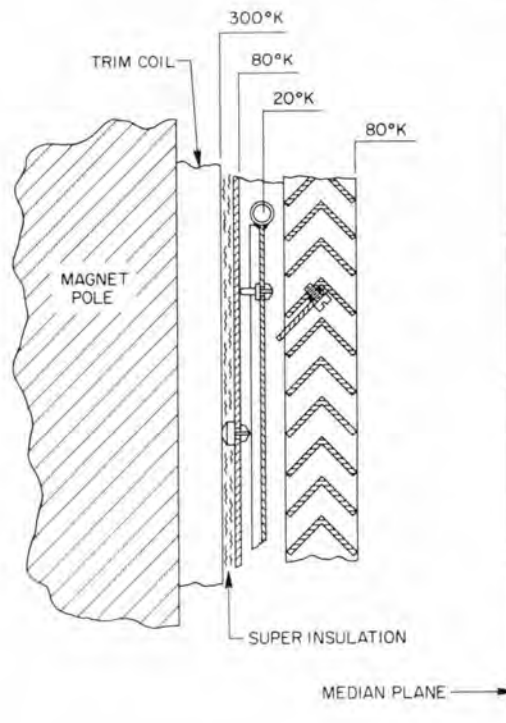


Fig. 2. Cross section of ORIC cryopanel. A mirror-image panel is located on the opposite trim coil.

PHOTO 2764-73

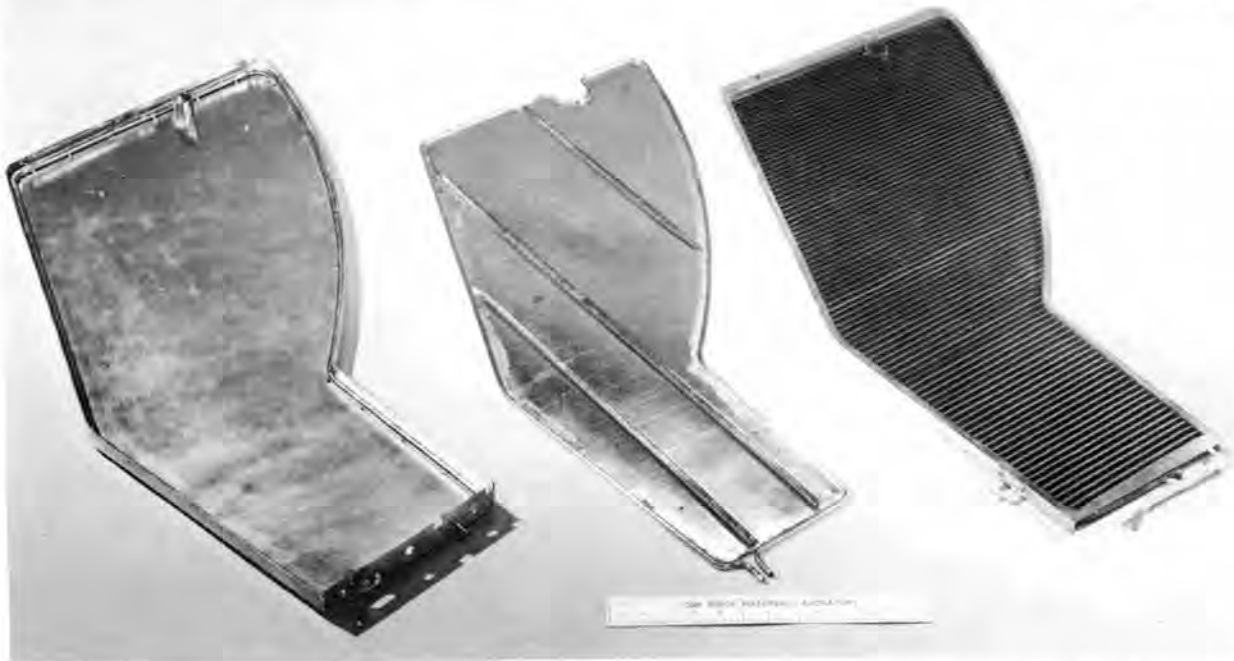


Fig. 3. Cryopanel before assembly. The 20°K panel (center) is sandwiched between the two 80°K shields. The chevron baffle (right) minimizes the radiant heat reaching the 20°K panel while allowing the entry of gas molecules from the circulating beam region.

Each 20°K panel is shielded completely from ambient temperature by an 80°K solid shield between it and the trim coil platter and by an 80°K chevron baffle facing the median plane. This baffle was chemically treated to produce a flat black surface to reduce the transmission of radiant energy to the 20°K panels. In addition, the helium transfer tubes are protected by 80°K shields.

A total of 2 W of refrigeration is required to maintain the pumps at 20°K and approximately 350 W of refrigeration for the 80°K shields. The resulting helium usage is about 2 liters/hr, and for liquid nitrogen, 6 to 10 liters/hr. With this rate of consumption, an operational cost of about \$40,000 per year for helium and \$4000 per year for liquid nitrogen would be incurred. The purchase of a helium gas refrigerator to close the cooling loop of the cryopanel and reduce the operating cost is presently being investigated.

1. Present address: ORGDP.
2. Engineering Division.
3. E. D. Hudson et al., *Phys. Div. Annu. Progr. Rep. Dec. 31, 1972, ORNL-4844*, p. 139.

COMPUTER CONTROL OF THE ORIC

C. A. Ludemann	K. Hagemann ²
J. M. Domaschko ¹	E. Madden ³
S. W. Mosko	E. McDaniel ³

The installation of a computer control system for the ORIC began in 1973. The initial implementation of the system is designed to reduce the time for setting up the cyclotron between experiments and to closely monitor the operation of the accelerator's magnet power supplies. The system will be expanded to include the monitoring and control of the rf, beam-line, and vacuum systems. Later, diagnostic devices will be interfaced so that beam quality and intensity may be optimized.

The computer is a Modular Computer Systems MCS III/5 with 24K 16-bit words of memory. The peripheral devices pertinent to control are a high-speed serial printer that provides hard copy of operation parameters, a 1.2-million-word disk storage unit that provides ready access to programs and set-point data for tuning the cyclotron, and a magnetic tape drive for recording permanent files of operation data.

The operator and computer communicate via an interactive alphanumeric/graphic CRT display and keyboard, a panel of 16 function keys, and a panel of 12 pairs of reassignable push buttons labeled by LED displays. The computer and cyclotron will communicate via a digital I/O subsystem and an 80-channel multiplexed ADC.

In order to set up the accelerator for an experiment, the cyclotron operator will choose the appropriate operation parameters from the disk library of previous run data via a menu on the CRT screen. The power supplies will be switched automatically to the appropriate loads and run up to the listed settings. The operator then assigns the pairs of push buttons to various power supplies as needed for manual control of the fine tuning of the cyclotron. He will do this rapidly by means of function keys that will automatically make "standard" assignments for most frequently used power supply combinations. He will be able also to make "special" assignments via CRT menu picking or keyboard entry. In all cases the LED displays will label the push-button pairs in order that the operator will know that he is raising/lowering the reference of a particular power supply (e.g., T6 label for the power supply feeding trim coil No. 6) or opening/closing a valve in the beam line (e.g., BLV8 label for valve No. 8 in the vacuum system). The CRT will update the status of all parameters being adjusted by the push buttons.

The computer monitors response of the power supplies and keeps track of their settings. If it detects abnormal power supply operation, the computer will alert the operator by CRT messages and audible signals. At the operator's option, the computer will store new run information in the disk library for future reference.

The multiplexed ADC system will not be connected to the various low-resolution data channels (e.g., panel meters) until the spring of 1974. However, the DVM-crossbar scanner data acquisition system, used for years to record the ORIC high-precision operating parameters, has been interfaced to the computer. The routine recording of data began in June, and set-point libraries have been generated. Two hundred data channels are available with a maximum resolution of 3 parts in 10⁶. A schematic diagram of the bidirectional interface is shown in Fig. 1. It is designed in a modular fashion to accommodate different data conversion codes as well as logic levels in the event the present DYMEC system is replaced in the future.

A large engineering effort has been expended in developing control modules for the majority of the magnet power supplies. These units do more than supply voltage references to the power supply regulators — they are surveillance modules as well. Operation of the cyclotron is severely hampered by errors in power supply regulation of a few tenths of one percent, excessive ripple at frequencies up to 360 Hz, or oscillations at frequencies up to a few kHz. The integrating DVM system described above is not able to alert the operator of such malfunctions, making diagnosis and repair a difficult process. While faster DVM

ORIC DATA ACQUISITION COMPUTER SYSTEM

D. C. Hensley C. A. Ludemann

The computer software for data acquisition, handling, and processing at the ORIC continues to develop in capability, flexibility, and ease of use. Associative memory programs to generate large two-parameter arrays (usually about 100K channels), list mode programs for two or more parameters, and in-core singles (and multisingles) programs for data acquisition are now used routinely. Spectrum multiscaling programs have been developed and are in the process of being improved. Acquisition programs are written in assembly language, and most processing routines are written in FORTRAN.

To give an idea of the capabilities and the limitations of the ORIC system, we will discuss a few of the software packages. A more elaborate discussion of the ORIC system has been published.¹

1. Gamma-gamma coincidences in the list mode. This is a program which collapses one event of either two parameters (γ_1 and γ_2) or three parameters (γ_1 , γ_2 , and "time") into one 24-bit word for data storage. Each gamma parameter is allocated 12 bits (4096 channels) of the 24, and a digital offset for both parameters is provided. Throughput rates greater than 1 kHz can be handled readily; typical rates are 200 to 500 Hz. With an input rate of 200 Hz, a magnetic tape of data is written in a little over 4 hr (about 3.5 M words). To date, many more than 40 tapes have been filled by this program, and experience shows that 10 tapes typically are needed to study relatively weak transitions.

Background processing programs allow one to select an arbitrary region of interest of one parameter and to project out the corresponding correlated spectrum for the other parameter. When gates on all peaks of interest (for both parameters) and appropriate background regions are chosen, 70 to 100 gates have been desired for some experiments. Under optimum conditions (i.e., utilizing all of core and all of the CPU time), it takes about 5 hr to scan 100 gates from one tape. Consequently a "ten-tape experiment" will easily require up to 50 hr of tape scanning time. During the experiment, however, the ADC program uses about $\frac{3}{8}$ of core, and CPU time is needed to store the data on tapes. Consequently, final data analysis must be postponed until after the experiment is over.

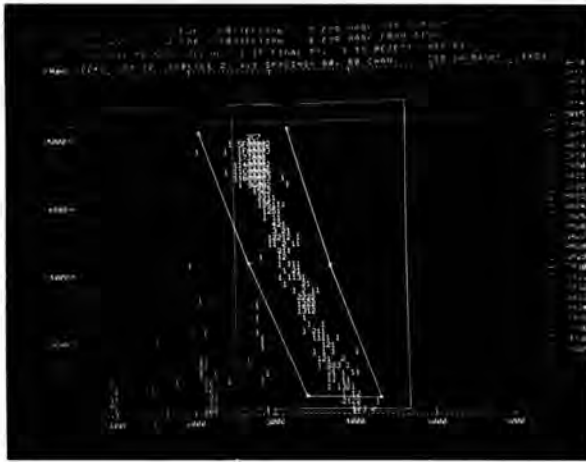
2. Spectrum multiscaling. This is a program to generate separate spectra during each of a given number of equal time intervals or bins. The various programs have the following common properties: up to six

uncorrelated parameters can be simultaneously multiscaled, an arbitrary number of bins may be used, and the amount of dead time within a given time bin is recorded in each spectrum in that bin. The "in-core" program is limited to about 10K (or 14K if more of core is allocated to the ADC program) channels. The disk "flip-flop" program has a limit of 5K (7K) channels per bin and about 350K total channels. The disk program has the special limitation that the time bins must be at least 0.5 sec wide. Both programs automatically recycle to permit accumulating on a refreshed source.

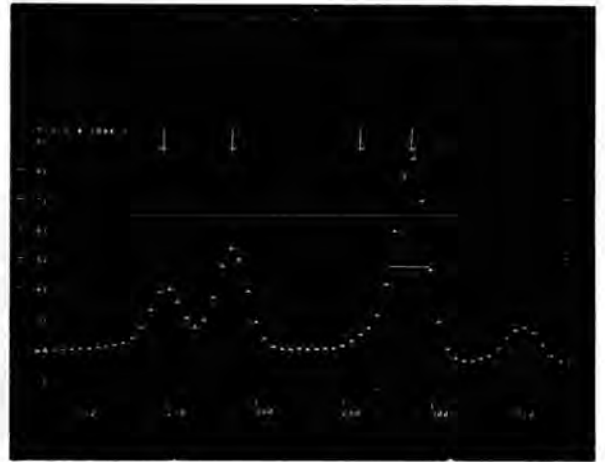
3. DSNP. This processing program handles two-parameter arrays through the graphic display terminal, particularly the generally large arrays generated by the associative-memory data acquisition programs. The program allows one to define an arbitrary region in the two-parameter map and to project this selected region onto either axis — the corresponding one-parameter spectra can be filed onto disk to be examined with other program, or simple summations can be performed directly. Provisions have been made to allow the filing onto disk of the mask which defines a region of interest, and this mask may be recalled later for use on other data files. Hard copies of the CRT image of any selected two-parameter map or its projection may be made at any time.

As with most display programs, DSNP presents a menu of options on the CRT. The user indicates the number of the option he is interested in. The joy-stick-controlled cursor is used primarily to define the regions of interest in either the two-parameter map or the one-parameter projection. Figure 1a is a photograph of the CRT screen showing the cross hairs about to indicate the closure of a mask within a particle spectrum generated by an $E-\Delta E$ counter telescope. The next operation could be the selection of option No. 4, projection of the masked area onto the energy axis. Most of the work of developing and debugging this program for the display has been carried out by M. L. Halbert.

4. PKFT. "Peak-fit" is a processing program to fit singles spectra, in a least-squares sense, with Gaussian shapes and a background. The program can fit up to five peaks simultaneously with a three-parameter polynomial or exponential background. The fitting parameters that may be varied in addition to the background parameters are peak positions, the areas of the peaks, and the FWHM of the peaks. Any or all of the quantities may be held fixed or allowed to vary, and it is possible to fix peak locations either absolutely or relative to another peak. Communication is via the



(a)



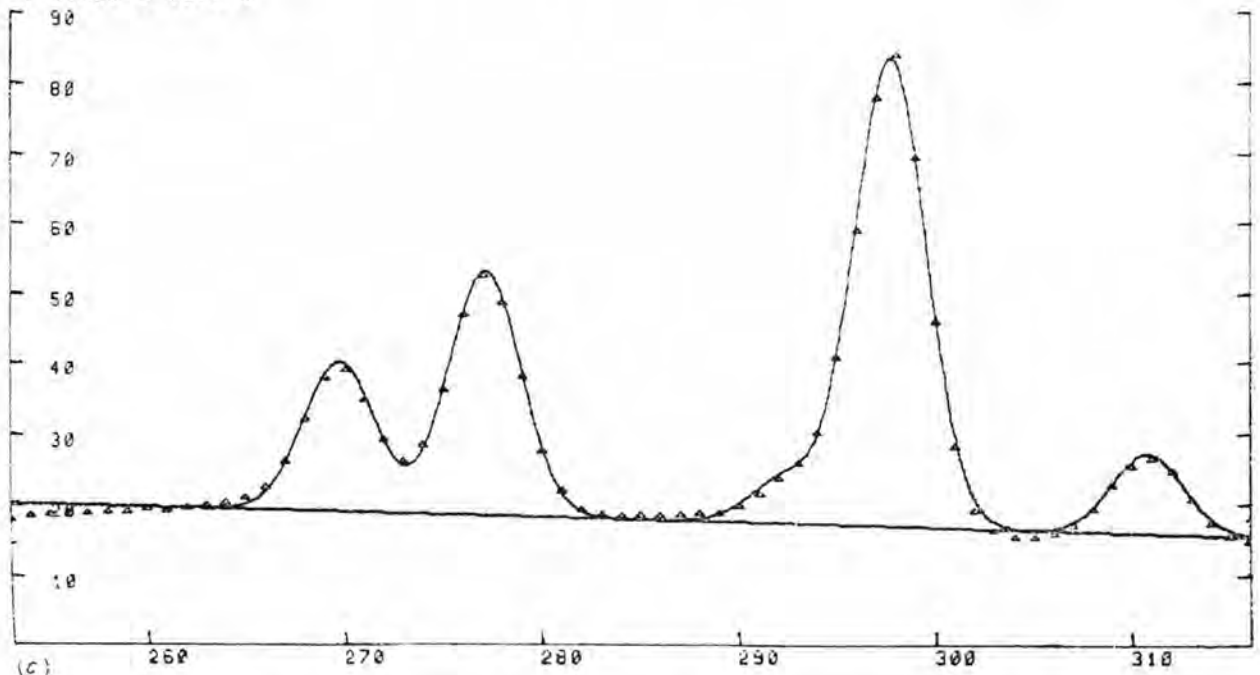
(b)

HADC NC26 FROM LDN 13 DUMPED 01/17/74 16:22.2 CHANS. 253 TO 316 COMP 1

PICK FROM MENU	PEAK	POSITION	AREA	WIDTH
CONTINUE	1	269.72 ± .07	95497. ± 2849.	4.28 ± .03
RE-START THIS CASE	2	277.10 ± .04	158274. ± 3236.	4.28 ± .03
START NEW CASE	3	292.42 ± .24	30143. ± 2546.	4.28 ± .03
PLOT FIT ON DISPLAY	4	297.71 ± .03	302975. ± 4492.	4.28 ± .03
RESULTS ON DISPLAY	5	310.79 ± .10	51269. ± 2836.	4.28 ± .03

BACKGROUND OPTION WAS POLYNOMIAL OF ORDER 1
 SORT(CHISQ/NDF) = 5.358

Y-SCALE # 10** 3



(c)

Fig. 1. Photographs of display output using the programs DSNP and PKFT.

graphic terminal, and either the joy stick or the scratch pad can be used to direct the program. Final calculations can be output on the line printer or may be copied directly from the storage tube by the hard copy unit. Data presentation options include expanding the region of interest ("zooming"), choosing linear or semilogarithmic plots, and defining the y scale. An addition to the graphic terminal is a set of seven switches whose status may be interrogated at any time by programs. These allow the user to define a set of standard options or to intercept the program in its calculations. Figure 1b is a photograph showing the cursor being used to indicate the approximate location of a fifth peak in a small region of interest of a pulse-height spectrum. The horizontal bar through peak No. 4 is the user's rough estimate of the FWHM to be used at the start of the fitting procedure. Figure 1c is a photograph of a hard-copy print of the results generated by PKFT. Peak positions, areas, and widths (constrained to be equal for all peaks in this example) are shown, in addition to the data points and the corresponding calculated fit to the spectrum. M. J. Saltmarsh was responsible for developing and debugging most of PKFT.

The ORIC data acquisition system has met the data gathering needs of the cyclotron research program for the past six years. The system software and hardware have evolved to meet the complex demands of present-day experiments. However, in the past year and a half, signs have appeared indicating that one of the major objectives of the system was beginning to be sacrificed. It was becoming more difficult to process data during the course of an experiment. Efficient use of accelerator beam time requires that data be evaluated during or shortly after acquisition.

Our system shares CPU time between a foreground data accumulation program and a single task in background. Repeatedly we were finding ourselves in a situation where the experimental counting rates "locked" the CPU in the foreground (e.g., in 100K-channel associative memory acquisition), leaving no time available for processing. In gamma-gamma list-mode operation, background time was used primarily for generating data tapes and not for data processing. When processing time was available, most of it was spent in using PKFT and DSNP, programs that require continual human interaction and which are, consequently, relatively slow. This left very little CPU time available for experimenters preparing for the next experiment or for previous users wanting to process their data tapes.

Three alternatives for meeting most of these problems were considered: (1) rewrite the system so that it would handle multiple tasks in the background, (2) make greater use of the Central Computer Facility, or (3) purchase a second computer system. When a used SEL 840A, essentially identical to the present system, became available from the manufacturer at approximately one-quarter of the original price (but with a new-product warranty), a cost study showed that alternative 3 presented the best solution to most of our problems.

This second system will be installed in early 1974. The systems software for both computers will be nearly identical, and the new computer should be able to shoulder most of the load of data processing and handling immediately. In case of temporary failure of our first computer, the second computer can be switched in to handle the data acquisition with a minimum of downtime for the experimenter. Furthermore, systems development, either hardware or software, will be possible on a regular basis. Development of microprocessor and the CAMAC front-end equipment will receive major attention in the coming year.

I. D. C. Hensley, *IEEE Trans. Nucl. Sci.* **NS-20**(1), 334 (1973).

ORIC RF SYSTEM

S. W. Mosko

Late in 1972, the ORIC rf system was converted from an RCA 6949 power amplifier to an RCA 4648 power amplifier. All major mechanical modifications were completed during 1972; however, during the early part of 1973, several minor modifications were required to achieve acceptable system performance. Since March 1973, rf system performance and especially reliability have been the best on record for ORIC.

The primary incentives for replacing the 6949 were cost (price quotation in January 1972 was \$29,000) and installation time required for the 6949 (three days minimum shutdown). It was necessary to withdraw the entire rf system from the cyclotron magnet and to lower the resonator assembly from the support crane in order to be able to insert or withdraw a PA tube through the only access hole in the top of the PA enclosure. The 4648 costs about one-fourth as much as a 6949, its power rating is equal to the 6949, and it is relatively compact. It is possible to change 4648 tubes through an access hole under the PA enclosure in a period of a few hours without disturbing the cyclotron vacuum system or electrical wiring.

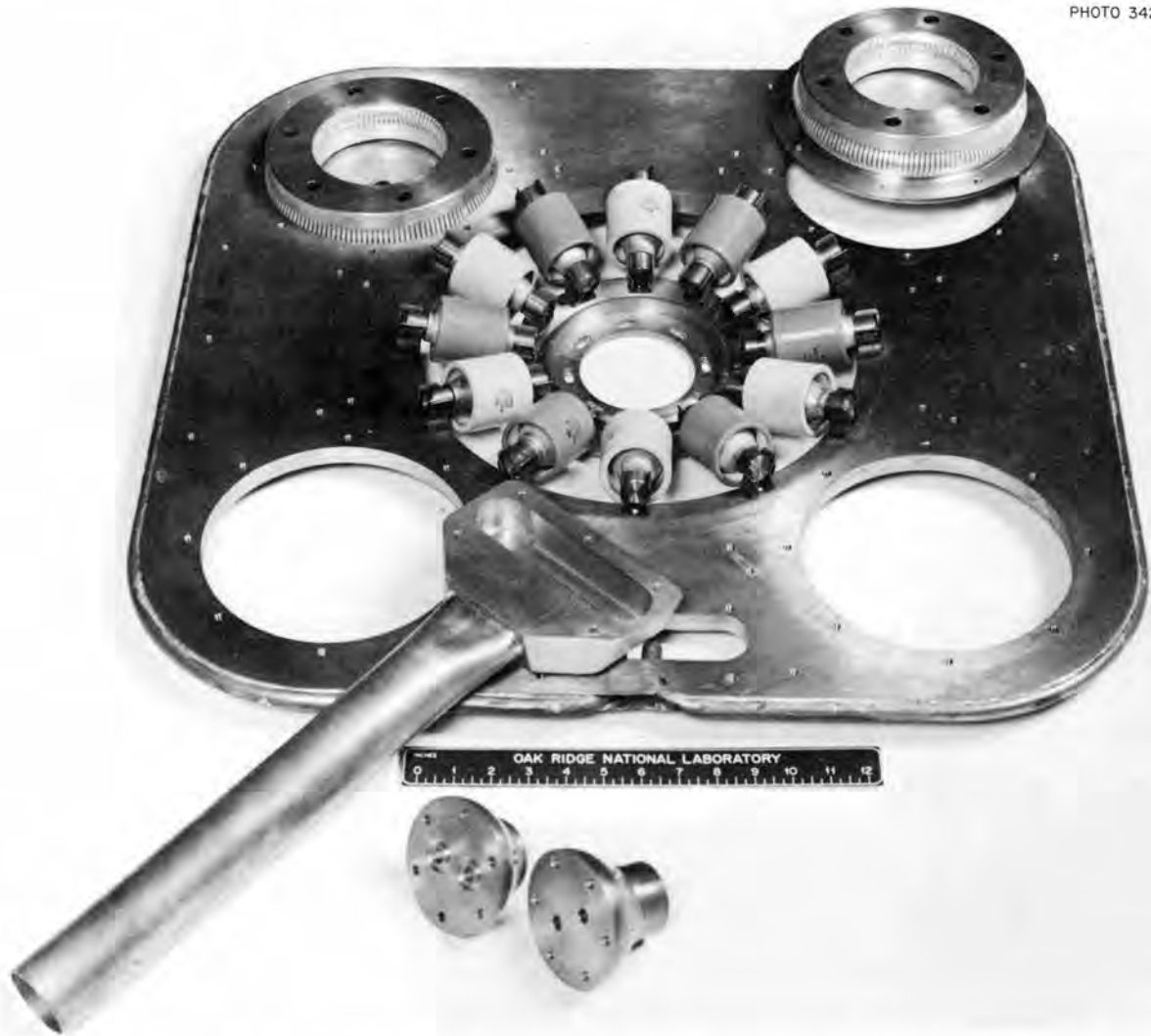


Fig. 1. The "PA plate blocking capacitor." The center ring mates with the 4648 plate. The large holes in corners and associated fittings mate with variable vacuum tuning capacitors. The rf power output connector is shown at lower left.

The high gain characteristics of the 4648 are especially attractive, since it is hoped that some form of broad-band solid-state amplifier will eventually replace the remaining tuned rf circuitry between the synthesizer and the PA. Superior rf characteristics lead to improved PA performance and eliminate neutralization problems formerly experienced with the 6949, which required reneutralization each time that the cyclotron frequency was changed.

Alterations to the PA enclosure included cutting holes to accommodate the new tube socket and to provide a route for inserting tubes from an easily accessible area below the PA. A ringed array of four each 1000-pF vacuum capacitors which formerly served as the plate

blocker was replaced by a ring of 12 each ceramic capacitors (Fig. 1), whose values are alternately 100 pF and 250 pF. Capacitance values were selected so as to avoid parallel resonances within the 7.3-to-22.5-MHz tuning range of the PA. A new PA grid contact adapter (Fig. 2) was necessary to complete connections from the existing grid tank to the 4648 grid. Relatively minor power supply changes included adding a filter choke to the dc filament power supply; the former 6949 bias power supply now serves as the 4648 screen power supply, and a new grid bias power supply was added.

Two components vital for PA stability are the low-impedance "screen bypass" capacitor and the low-impedance "grid swamping" resistance. The screen



Fig. 2. The "PA grid contact adapter." The circular contact areas mate with the 4648 input flanges. The flat inner conductor or grid lead mates with the grid pi network via the adapter at lower left.

bypass is shown in the first of three stages of development in Fig. 3. A sandwich structure is formed by separating the screen contact disk from the flat upper surface of the tube socket by a 3-mil Kapton film. The 100-in.² electrode surface area yields a capacitance of about 25,000 pF. PA stability with this configuration was marginal. Consequently, a second ground electrode with another 3-mil Kapton film was added on top of the screen contact disk, thereby increasing the capacitance to about 40,000 pF and reducing inductance slightly. The next time that removal of the screen bypass becomes necessary, it will be replaced by a new model which permits assembly of the Kapton sandwich prior to installation in the PA enclosure. PA stability is further enhanced by four each

50- Ω , 1-kW water-cooled swamping resistors which shunt the PA grid circuit. The Q of the grid pi network is now so low that automatic tuning is unnecessary.

In Fig. 4, it may be noted that we still have a neutralization network, but C_n is very small (less than 1 pF), its adjustment is not critical, and retuning is unnecessary as the resonator frequency is changed.

A 50- Ω , 50-kW water-cooled "swamping" resistor has been coupled to the PA plate resonator via a 15-pF capacitor. It loads the PA plate whenever the main cyclotron resonator is detuned, thereby preventing an rf voltage buildup in the PA plate circuit. Without damping, such a voltage buildup leads to self-oscillation of the PA. Under normal conditions the power dissipation in the swamping resistor is only a few kilowatts.



Fig. 3. The "PA tube socket." The 4648 is inserted from below. The plate and screen terminals protrude from the hole in top center. The partially assembled screen bypass capacitor is on top. Socket was fabricated from a double layer of steel for magnetic shielding with copper-clad surfaces for rf current conduction. The bottom cover on left completes the magnetic shield after tube installation.

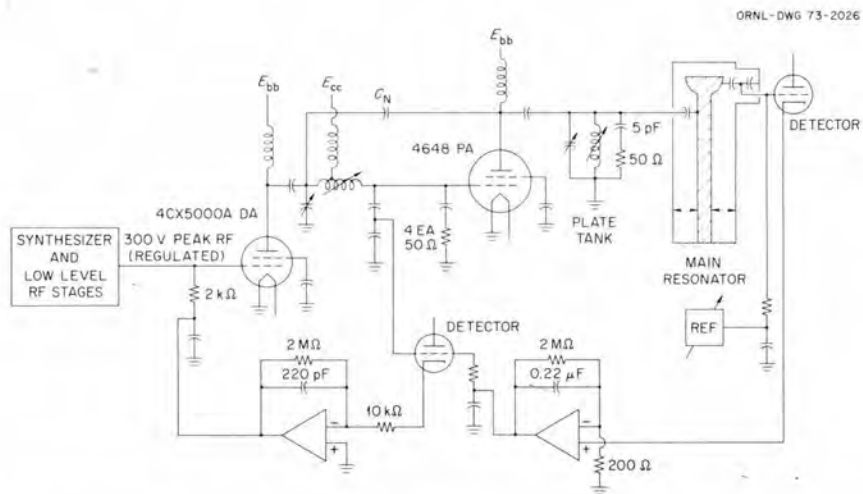


Fig. 4. A simplified schematic of the PA circuit including the driver amplifier stages, the main rf resonator, and the dee rf voltage regulator loop.

Excessive rf voltage in the PA plate resonator was a chronic problem with the former 6949 PA and was probably responsible for frequent destructive sparking in the plate tuner vacuum capacitors and in the main resonator drive capacitor. Since installation of the swamping resistor in early 1973, there have been no incidents of plate capacitor or drive capacitor damage.

As of the end of 1973, the 4648 tube has logged nearly 7000 hr of operation. The only other known user of the 4648, Lawrence Berkeley Laboratory (LBL), reports similar experience. Thus far it appears that the 4648 should have a useful lifetime at least comparable with the 6949. We are having occasional problems with clogging of the 4648 plate water course, but not nearly as frequently as reported by LBL. RCA is aware of the problem and will correct the situation in future tubes.

The rf system is using the same dee voltage regulator loop that was used with the former 6949 PA with a few minor changes. A new regulator loop is planned which will improve performance and reliability. Changes in the low-level rf amplifier stages are also under consideration.

ORIC MAGNET POWER SUPPLY IMPROVEMENT PROGRAM

W. E. Lingar¹ S. W. Mosko
J. A. Martin

An improvement program has been initiated for all of the cyclotron dc power supplies. Our objective is to obtain about an order of magnitude improvement in stability and a substantial improvement in reliability. The actual level of stability to be realized is:

Main field	1 part in 10^5
Trim coils	1 part in 10^4
Harmonic coils	1 part in 10^4
Lower channel outside coil	1 part in 10^5

Other power supplies not mentioned here will be considered at a later date, since their present status does not cause first-order contribution to beam stability.

The main field power supply, MG-1, is receiving the greatest attention. Several new components have been fabricated or purchased and will be installed early in 1974. A transducer will replace the main field 100-mV shunt and provide a more stable feedback signal at a level of 0 to 10 V. A regulated 35-A, 300-V power supply will replace the existing rotating exciter. New solid-state integrated circuits will replace existing vacuum tube amplifiers in low-level portions of the

regulator loop. Greater bandwidth and stability are expected with the new components.

Preliminary circuit design is complete for the trim coil and harmonic coil power supplies, and final design will get under way during 1974. Most effort will focus on the feedback amplifier circuitry and the reference signals which control these power supplies.

1. Instrumentation and Controls Division.

VERTICAL FOCUSING FOR THE BROAD-RANGE SPECTROGRAPH

E. E. Gross M. T. Collins¹
J. B. Ball V. Oddivak²
D. L. Hillis³

A broad-range spectrograph (BRS)⁴ of the Elbek type⁵ continues to be a very productive experimental device at the Cyclotron Laboratory. To enhance the capabilities of this instrument for low-count-rate experiments, a vertical focusing element has been added to the system. The new element consists of a vertically focusing, horizontally defocusing quadrupole singlet lens located midway between the source position (target position) and the entrance to the horizontal spectrograph magnet (Fig. 1). The quadrupole has a 3-in. aperture, is 6 in. in length, and has chamfered edges⁶ to reduce higher-order aberrations.

The magnet design was arrived at by using first-order optics⁷ calculations to locate the position of the focal plane, determine the solid angle increase due to the quadrupole, and estimate vertical and horizontal magnifications. To check the design calculations, measurements were made using a ^{244}Cm alpha-particle source⁸ (5.80- and 5.76-MeV alphas) placed at the target position. Using a solid-state position-sensitive detector placed at the calculated focal plane position, the

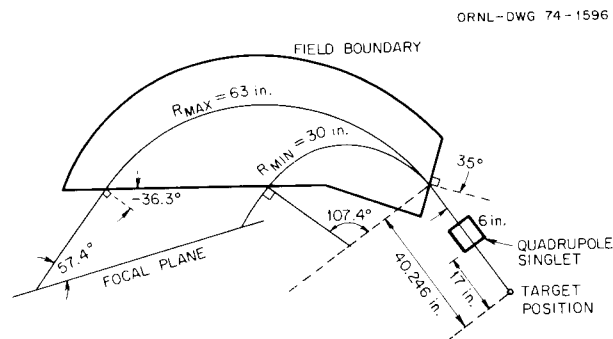


Fig. 1. Layout of the ORIC broad-range spectrograph.

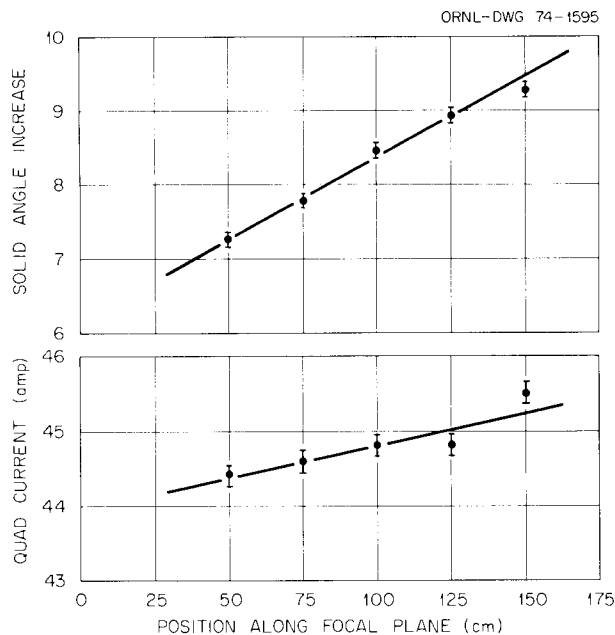


Fig. 2. The lower part of the figure shows the quadrupole current to produce a double focus image for a 5.80-MeV alpha source as a function of position along the focal plane. The upper curve shows the increase in solid angle afforded by quadrupole operation. The increase is for a 1-cm-high detector.

quadrupole current needed to maximize the count rate was determined. This quadrupole magnet calibration is shown in the lower part of Fig. 2 for 5.80-MeV alpha particles as a function of position along the focal plane. By comparing count rates with the quadrupole on to count rates with the quadrupole off, the solid angle factor increases shown in the upper part of Fig. 2 were obtained. These factors apply to a detector whose vertical height is less than the image size at the focal plane. Particles with momenta off the central momentum suffer a loss in solid angle at the detector given by Fig. 3. The off-focus condition (Fig. 3) is a slow function of $\Delta P/P$ and is independent of position along the focal plane, both desirable properties. To precisely determine the focal plane as well as vertical magnifications, a series of nuclear emulsion exposures were made with the alpha source. These measurements confirm the first-order calculations, the measured focal plane position agreeing with the calculated one to within 0.1 in. Within the resolution of the alpha source (13 keV for 5.80-MeV alphas), no deterioration in resolution was observed with the quadrupole on. Accelerator-produced beams will have to be employed to find the ultimate resolution of this system.

The main disadvantage of this system appears to be the large vertical magnification. The solid angle at the

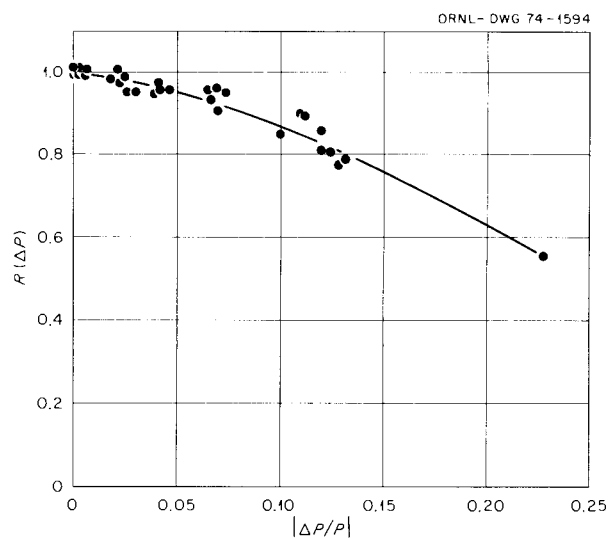


Fig. 3. The ratio of the solid angle for particles off the central momentum by an amount ΔP to the solid angle for particles with the central momentum.

detector can then depend on the source size and the detector size. However, this can be handled in at least three ways: (1) limit the beam spot so that the image is smaller than the detector, (2) have a set of calibrated alpha sources whose dimensions correspond to various beam spot sizes and use the appropriate source to calibrate the detector system before a run, or (3) calibrate with a known cross section, for example, Rutherford scattering.

1. Johns Hopkins University, Baltimore, Md.
2. Earlham College, Richmond, Ind.
3. University of Tennessee, Knoxville, Tenn.
4. J. B. Ball, *IEEE Trans. Nucl. Sci.* NS13, 1340 (1966).
5. J. Borggreen, B. Elbek, and L. P. Nielsen, *Nucl. Instrum. Methods* **24**, 1 (1963).
6. W. V. Hassenzahl, *Proc. Fourth Int. Conf. on Magnet Tech., Brookhaven, 1972*, ed. by Y. Winterbottom, p. 469.
7. T. J. Devlin, UCRL 133 (1961) (unpublished).
8. C. E. Bemis kindly provided the calibrated alpha source.

HEAVY-ION PROPOSAL STUDIES

J. A. Martin	C. A. Ludemann
P. H. Stelson	J. E. Mann
J. K. Bair	M. L. Mallory
L. N. Howell ¹	M. B. Marshall
E. D. Hudson	G. S. McNeilly ³
J. W. Johnson ²	S. W. Mosko
R. S. Lord	A. Zucker ⁴

Since publishing the proposal for a National Heavy-Ion Laboratory⁵ in the fall of 1972, a number of

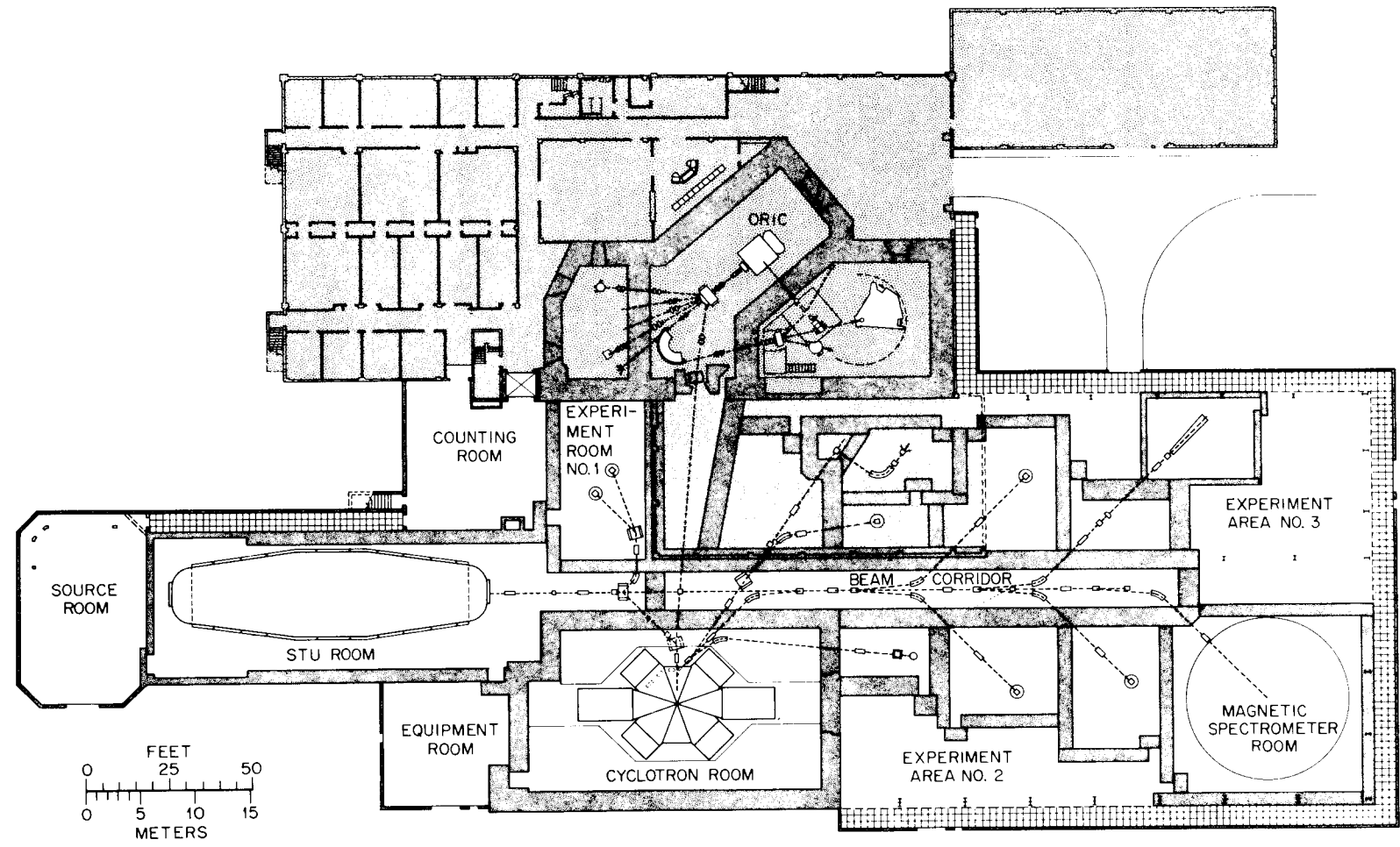


Fig. 1. The plan of the 1972 NHL proposal.

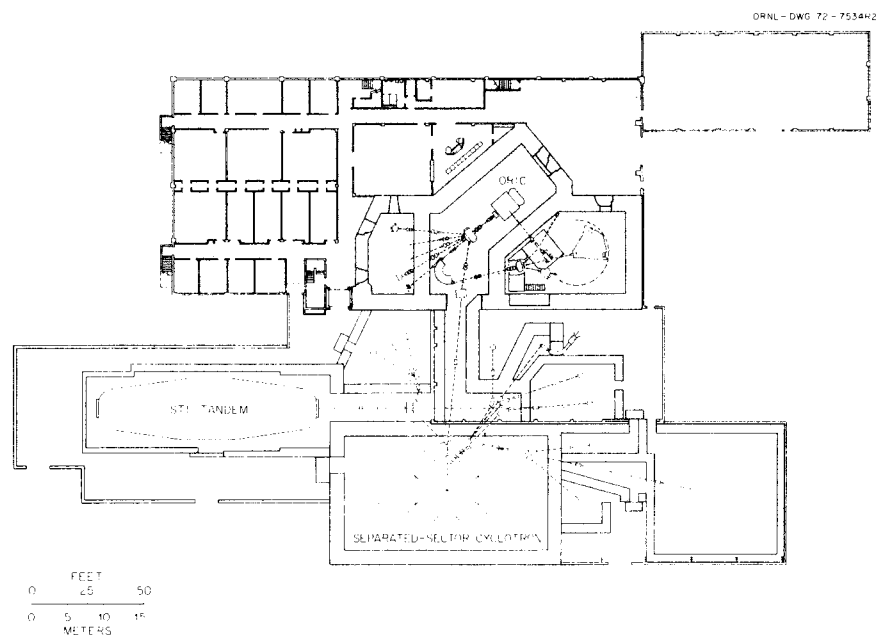


Fig. 2. The modified plan with abbreviated research area.

variants of the proposal have been developed and cost-estimated. The 1972 proposal was for a 20-MV tandem injecting into a large cyclotron of energy capability of $440q^2/A$. The facility was arranged so that the tandem could also inject beam into the ORIC for further acceleration (energy constant $90q^2/A$), or it could be used as a stand-alone accelerator. The estimated cost was approximately \$25,000,000.

A variant of considerable interest was to reduce the initial size of the new experiment areas with provision that it could be expanded later as the use of the facility expanded. Figures 1 and 2 show the original and the reduced facility. The area of the original facility was approximately 20,000 ft²; for the new design the added experiment areas totaled about 8000 ft². The reductions in building size and beam transport equipment and other economies brought the estimated cost down to approximately \$19,900,000.

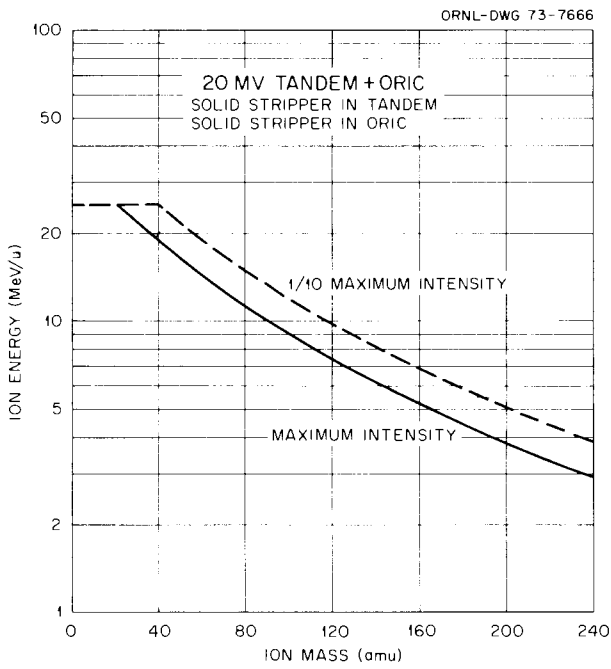
Another variant investigated was that of eliminating the tandem Van de Graaff from the plan temporarily, thus requiring full-time use of the ORIC as the injector for the large cyclotron. It would have provided beams with energy greater than 5 MeV/amu up to the region of mass 200, at intensities generally greater than 0.1 particle microampere. The layout of the plan was similar to that of Fig. 2 without the tandem. The cost of the plan was attractive, about \$13,000,000, but it suffered from the disadvantage that there could never

be more than a single beam, since the separated-sector cyclotron will not operate without an injector.

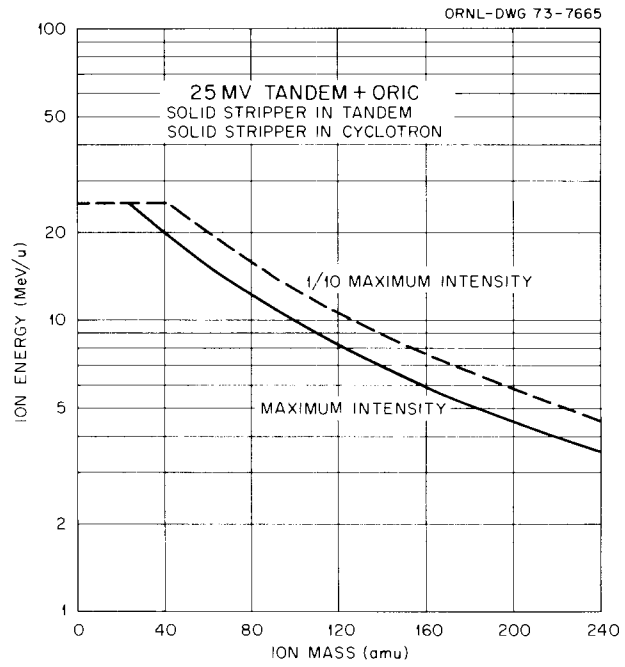
The adaptations of the 1972 plan that received the most attention were those employing a 20-MV or 25-MV tandem arranged for beam injection into the ORIC with a small added experimental area. These variants give good energies for nuclear physics to the iodine-mercury region and have an advantage of allowing independent use of both the ORIC and the tandem. The maximum ion energy vs ion mass capabilities for the 20-MV tandem with the ORIC are shown in Fig. 3. The characteristics with a 25-MV tandem are found in Fig. 4. The plans developed (Figs. 5 and 6) provide an arrangement compatible with adding a cyclotron or other new small-stage accelerator at a later date. The estimated costs of the 20-MV and 25-MV installations are roughly \$13,500,000 and \$17,000,000.⁶ These later plans are now the favored ones, and we will be developing the technical aspects of the proposals in great detail in coming months.

Injection of Tandem Beams into the ORIC

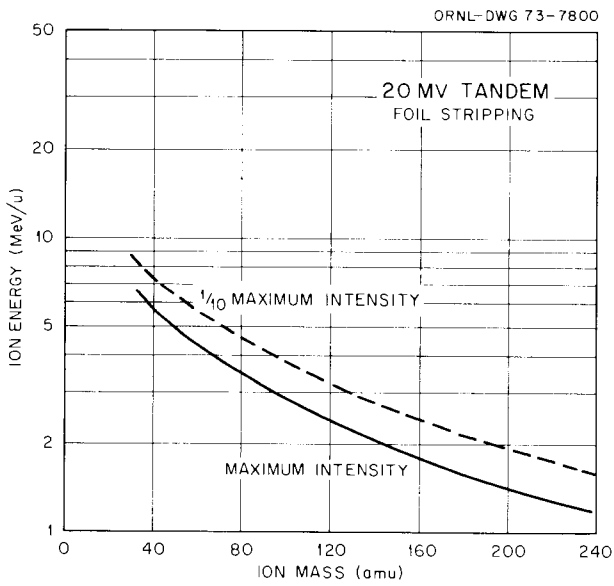
Injection of the beam from the tandem into the ORIC requires that it be brought into the magnetic field of the cyclotron at the appropriate angle so that it is bent into tangency with the orbit at just the correct radius.



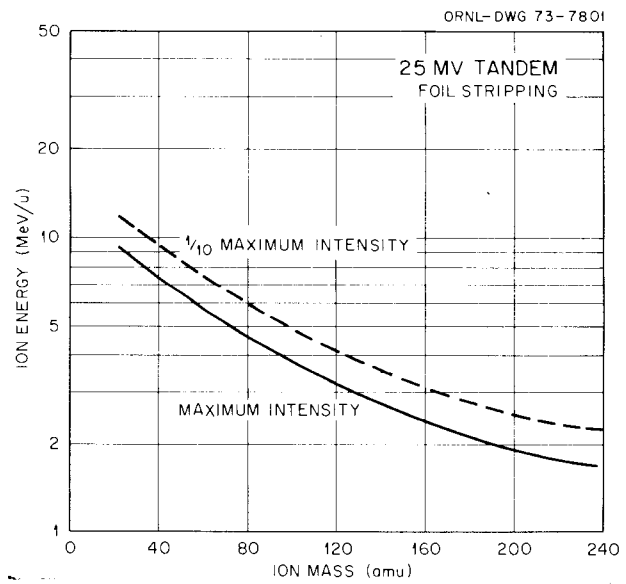
(a)



(a)



(b)



(b)

Fig. 3. Ion energy vs ion mass characteristics for 20-MV tandem. (a) Injecting into the ORIC, (b) 20-MV tandem alone. Both cases are with foil stripping in the tandem terminal.

Fig. 4. Ion energy vs ion mass characteristics for 25-MV tandem. (a) Injecting into the ORIC, (b) 25-MV tandem alone.

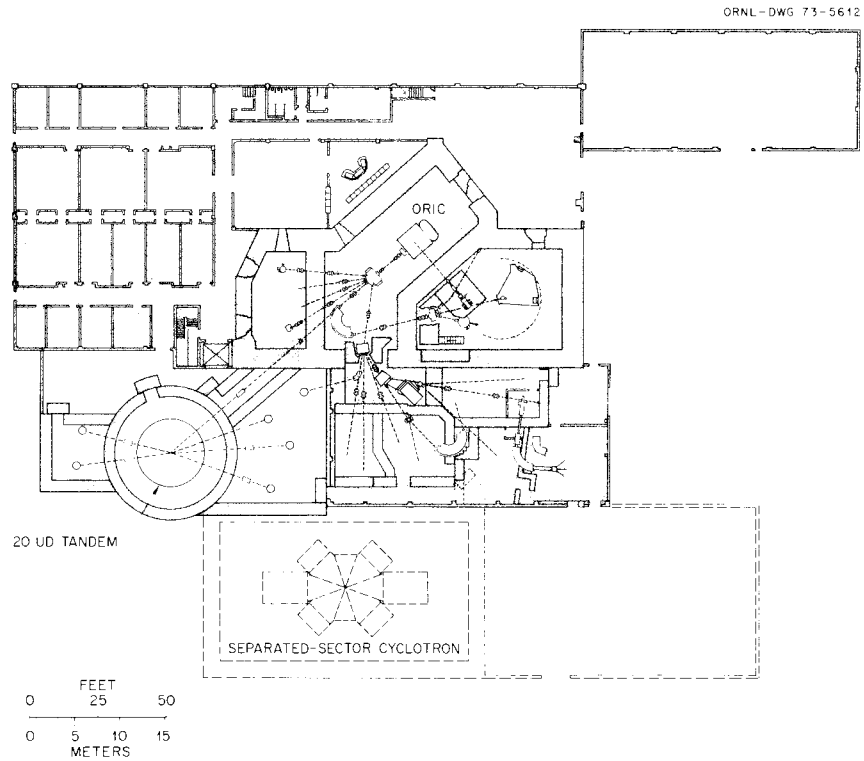


Fig. 5. The integration of a vertical tandem installation into the existing ORIC facilities. A 20-MV tandem is shown. A 25-MV tandem has a slightly larger diameter.

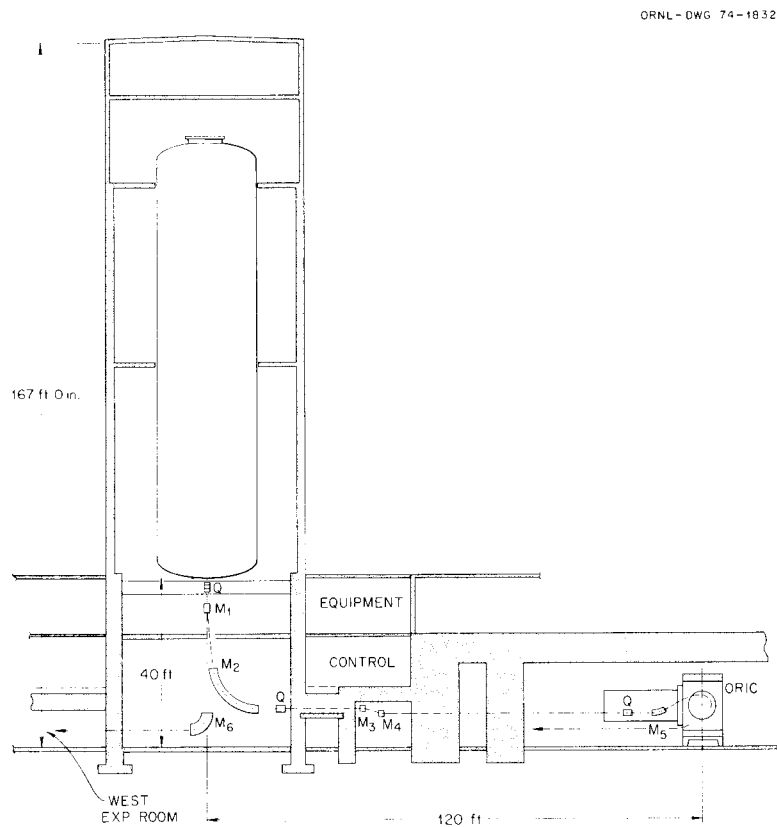


Fig. 6. Section drawing for a version of National Electrostatics Corporation 20 UD Tandem installation.

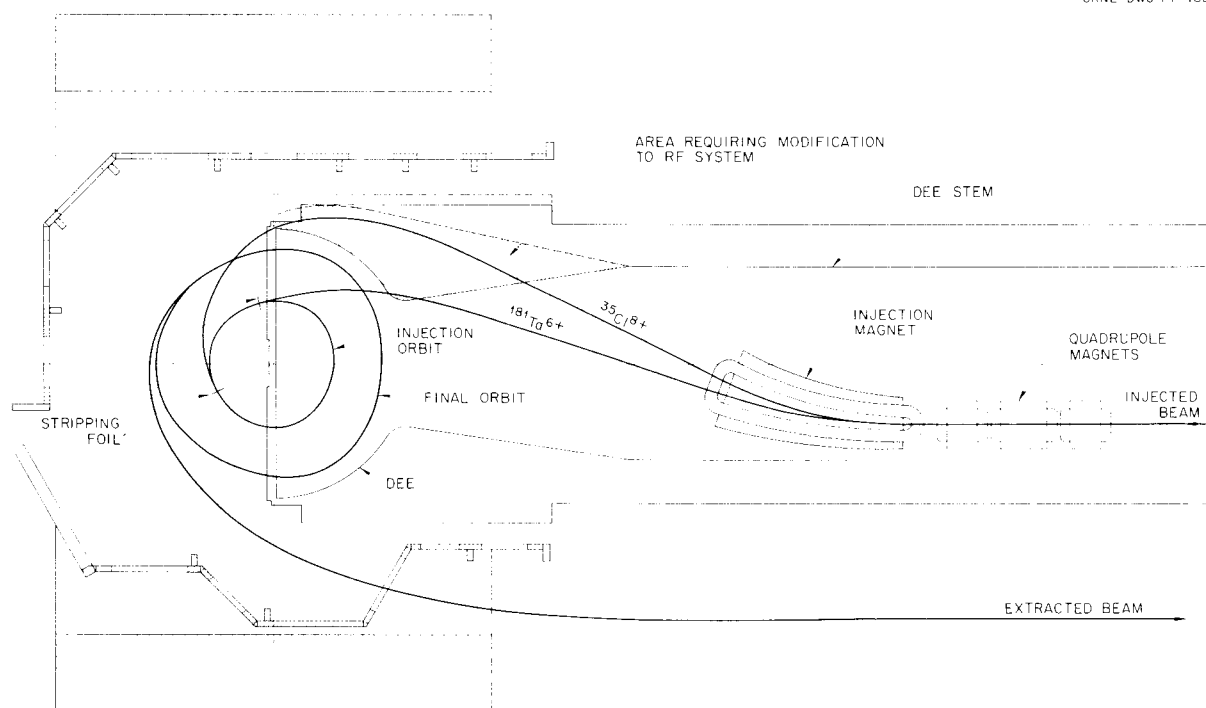


Fig. 7. Typical beam paths representing the approximate acceptance limits for the beam from a tandem entering the ORIC. The beam enters within the dee stem, is bent upward by a magnet, and is then "captured" by the cyclotron's fringe field and bent toward the center to intercept the stripping foil.

Then the ions are "captured" into the correct orbit by "stripping," that is, by passing them through a thin foil where a large number of electrons are stripped away. Two typical injection paths representing the approximate acceptance limits for the beam from the tandem are illustrated in Fig. 7. As an example of a beam within these limits, consider the acceleration of ^{127}I . In a 20-MV tandem the beam of I^- ions reaches the terminal with an energy of 20 MeV. When passed through a thin stripping foil, the most probable charge in the emergent beam is $13+$. That beam will emerge from the tandem at an energy of 280 MeV. When that beam is stripped in the cyclotron, the most probable charge state will be $36+$, and the final energy from the ORIC, according to its rating, $E = 90q^2/A$, will be 920 MeV. The final orbit radius in ORIC is 30 in.; the injection orbit for this case will be 16.5 in. Studies are being made using the General Orbit code to trace the injection path over the full range of ion masses and energies to determine the optimum computation of beam injection path and stripper locations.

Beam Bunching

The efficient injection of the beam from a dc accelerator such as a tandem into a cyclic machine such as a cyclotron requires that the beam be time-bunched into pockets that suit the acceptance characteristics of the particle accelerator. For the large NHL cyclotron the required pulse repetition rate is in the range 6 to 14 MHz with a phase acceptance of 10° for moderate energy resolution ($\Delta E/E = 10^{-3}$), and for the ORIC the frequency range will be 7 to 21 MHz with a comparable phase acceptance of $\pm 3^\circ$.

We have investigated the double-gap bunching system of the type suggested by S. Ohnuma⁷ and analyzed by R. Emigh.⁸ In this velocity modulation system a main buncher gap operated at the cyclotron frequency would be located 1.5 to 3 m from the entrance to the tandem. A second buncher gap operated at twice that frequency is located approximately one-quarter of the distance from the first cavity. To date, we have made calculations with a program that does not take into account

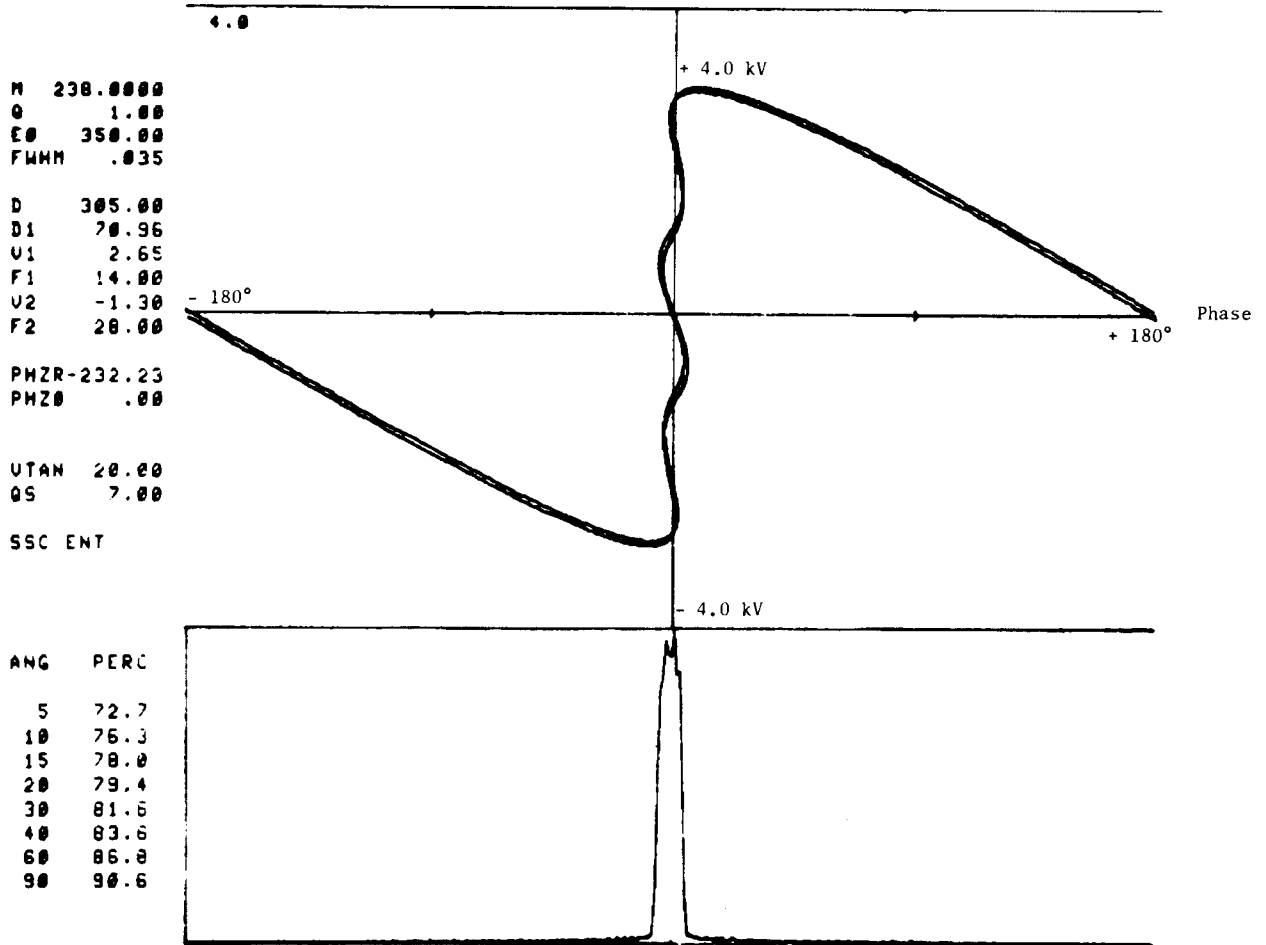


Fig. 8. Energy-phase and beam distribution for double-gap buncher system. The table gives the percentage of beam within the listed angle (\pm). Parameters are: injection voltage: 350 kV; ion: ^{238}U ; 1st buncher tandem distance: 305 cm; 1st-buncher-2nd-buncher distance: 71 cm; buncher voltages: 2.65 kV peak and 1.30 kV at frequencies of 14 and 28 MHz and relative phases of 0° and -232.2° respectively. The beam stripped to $+7$ charge state in the tandem terminal; the distance from the tandem to the cyclotron was 80 ft.

space-charge effects. Figure 8 shows the results of a calculation for uranium ions. The phase distribution is at the point of beam injection into the cyclotron. Approximately 76% of the particles are found within $\pm 10^\circ$. There is a good possibility that a buncher located in the tandem terminal will enable an additional factor of 2 reduction in bunch width. Thus it seems reasonable to predict at least 50% bunching efficiency for the requirements of either the ORIC or the large cyclotron.

Cyclotron Magnet Model

The ability to accurately design and predict magnetic fields, including such detailed phenomena as differential

hysteresis, is essential for optimizing the performance and costs of circular accelerators. We now have available for study a 0.15-scale model of the four-sector magnet previously designed and proposed for a heavy-ion accelerator to be used as a booster following injection by ORIC or by a tandem Van de Graaff. The model is fabricated from 1005 steel plate. Hill angles are 52° . The pole tip edges are rounded with a radius of 0.84 gap width, and the width of the pole has two outward steps to approximate the Rogowski profile as specified by Braams.⁹ The maximum design field is 16 kG. A punched-tape-controlled precision milling machine has been modified to position a Hall-effect probe in the field to be measured. To determine ion focusing and

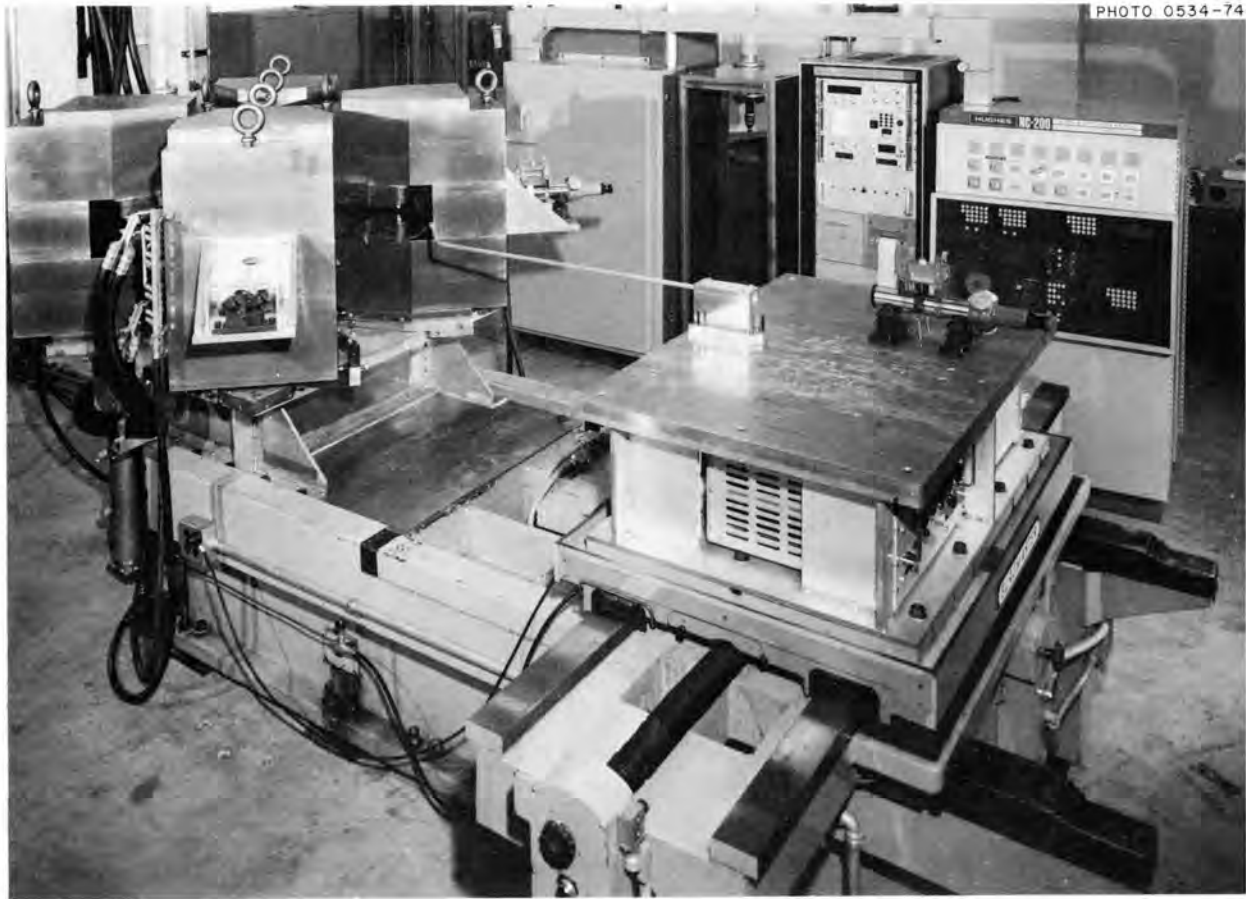


Fig. 9. The 0.15-scale four-sector magnet model for a heavy-ion cyclotron. On the right and in the foreground are the numerically controlled probe positioner and associated electronics.

orbit time characteristics, the magnetic field will be measured over a uniformly spaced mesh of several thousand points for several magnetic field levels.

Figure 9 shows the model magnet, tape-controlled milling machine, Hall-effect probe holder, and some of the associated electronics.

1. Engineering Division.

2. Instrumentation and Controls Division.

3. Computer Sciences Division.

4. Director's Division.

5. *National Heavy Ion Laboratory (NHL), a Proposal*, Oak Ridge National Laboratory, October 1972.

6. The costs given here are for illustrative and comparative purposes and are not necessarily the "official" cost, which may be based on slightly different schedules for escalation and contingency.

7. S. Ohnuma, "Minutes of the Conference on Proton Linear Accelerators," Yale University, October 1963, p. 279.

8. R. Emigh, *Proceedings of 1966 Linear Accelerator Conference, October 3-5, 1966, Los Alamos, N.M., LA-3609* (December 1966), pp. 338-45.

9. C. M. Braams, *Nucl. Instrum. Methods* **26**, 83 (1964).

SHIELDING MEASUREMENTS

H. M. Butler¹ C. B. Fulmer
K. M. Wallace¹

Earlier measurements of radiation leakage through cyclotron shield walls² demonstrated that the principal leakage is that of fast neutrons. Thus, half-value thicknesses for the overall neutron spectra from cyclotron targets are important for determination of minimum adequate shields. Half-value thicknesses for neutrons from a variety of beam-target combinations were measured earlier for concrete block shield walls at approximately right angles from the incident beam direction.³ These measurements yielded half-value thicknesses which range from 9.3 to 10.5 cm for beams of protons, deuterons, alpha particles, and carbon ions on targets of carbon, aluminum, copper, and tantalum.

It is well known that the highest-energy neutrons from reactions in the target are peaked in the forward

direction. The target station in Room C-114 in the south research addition of Building 6000 is located 12 ft from a 40-in.-thick stacked concrete block wall, making it suitable for such measurements. It was thus decided to obtain measurements in the forward direction to supplement those reported in ref. 3.

Beams of protons, deuterons, alpha particles, and carbon ions were again used to bombard thick targets of carbon, aluminum, copper, and tantalum. For each particle type, two or more incident beam energies were used. Portable fast-neutron survey meters were placed on the target side of the wall in both the forward and a lateral direction and observed by television cameras. With a steady beam current, fast-neutron, thermal-neutron, beta, and gamma radiation levels were measured outside the wall in both the forward and lateral directions. Then a stacked concrete block shield 8 in. thick and 16 in. square was placed about 4 in. downstream from the target, and the forward-angle measurements were repeated for the same beam current on the target.

A brief summary of the results is as follows:

1. The half-value thicknesses in the forward direction ranged from slightly less than 8 cm to approximately 13 cm. As was observed in the earlier measurements³ the more penetrating neutrons resulted from light-ion-induced reactions in the targets of lower atomic number. Deuterons incident on targets of carbon and aluminum resulted in neutrons requiring the most concrete for attenuation to half dose intensity.

2. The half-value thicknesses were consistently larger (by 15 to 20%) in the forward direction except for 10-MeV protons, where the half-value thicknesses were only 5% higher in the forward direction.

3. With local shielding near the target, the radiation level in the forward direction through the shield wall was reduced by a factor of 2 to 3 for most of the beam-target combinations; for 40-MeV deuterons on carbon, the reduction was by a factor of 4. The measurements demonstrate that local shielding near the target can be effectively used to reduce the shield wall thickness requirement for many situations.

1. Health Physics Division.

2. C. B. Fulmer, H. M. Butler, and K. M. Wallace, "Radiation Leakage through Thin Cyclotron Shield Walls," *Particle Accel.* **4**, 63-68 (1972).

3. H. M. Butler, K. M. Wallace, and C. B. Fulmer, "Half-Value Thicknesses of Ordinary Concrete for Neutrons from Cyclotron Targets," *Health Phys.* **24**, 438-39 (1973).

OAK RIDGE ISOCHRONOUS CYCLOTRON OPERATIONS

H. L. Dickerson	G. A. Palmer
H. D. Hackler	E. G. Richardson
J. W. Hale	A. W. Riikola
C. L. Haley	L. A. Slover
R. S. Lord	C. L. Viar
M. B. Marshall	A. D. Higgins ¹
S. W. Mosko	E. W. Sparks ²
E. Newman	K. M. Wallace ³

Introduction

The Oak Ridge Isochronous Cyclotron (ORIC) continued to be operated on a 16-shift/week schedule in 1973 except as noted below. Nuclear research programs used about 58% of the total hours available, which was 1% less than in 1972. Heavy-particle experiments used about 79% of the total nuclear research time.

Research Bombardments in 1973

A total of 6640 hr was the scheduled available time for ORIC operations in 1973 (see Table 1). Research bombardments were assigned a total of about 3820 hr,

Table 1. ORIC operations - operation analysis

	Hours	Percent
Beam on target	3317.3	50.0
Beam adjustment	394.2	5.93
Target setup	95.7	1.44
Startup and machine shutdown	641.6	9.66
Machine research	532.4	8.01
Total machine operable time	4981.2	~75.04
Source change	536.7	8.08
Vacuum outage	117.8	1.77
Rf outage	109.1	1.64
Power supply outage	101.7	1.53
Electrical component outage	154.1	2.32
Mechanical component outage	95.8	1.44
Water leak outage	56.7	0.85
Radiation outage	2.0	0.03
Total unscheduled outage	1171.9	~17.66
Scheduled maintenance	372.9	5.61
Scheduled engineering	112.0	1.68
Total	484.9	~7.29
Total time available	6640	100
Total nuclear research experiments	3820 ^a	

^a58% of total time available.

Table 2. ORIC research bombardments in 1973

Research activity	Investigators	Cyclotron time (8-hr shifts)
UNISOR ¹	Spejewski, Mlekodaj, Carter, Schmidt-Ott	88
Accelerator research and development	Mallory, Hudson, Lord, Newman	69
Scattering of identical heavy ions	Halbert, Saltmarsh, Stelson, Snell, Fulmer, Raman	61
Heavy-ion-induced fission	Plasil, Ferguson, Pleasonton	54
Doppler-shift lifetime measurements	Johnson, Sturm, ² Guidry, ³ Eichler, Sayer, ⁴ Hensley, O'Kelley, Singhal ⁵	48
Heavy-ion transfer reactions	Ford, Toth, Hensley, Riley, ⁶ Gustafson, ⁷ Snell, Gaedke, ⁸ Thornton ⁷	40
Backbending rotation bands	Riedinger, ³ Stelson, Hensley, Robinson, Sayer, ⁴ Hagemann ⁹	27
X-ray identification of element 104	Bemis, Silva, Hensley, Keller	27
Excitation of giant resonances	Bertrand, Gross, Kocher, Newman	26
Two-nucleon transfer to rotational bands	Saltmarsh, Gross, Halbert, Riedinger, ³ Hagemann, ⁹ Cole ¹⁰	25
Atomic spectroscopy	Sellin, ³ Mowatt, ³ Pegg, ³ Griffin, Haselton, ³ Peterson, ³ Lambert ³	23
Back-angle scattering	Fulmer, Hensley, Foster, ¹¹ O'Fallon, ¹¹ Eidson, ¹² Gronemeyer, ¹¹ Rasmussen ¹²	21
Search for new alpha emitters	Toth, C. Bingham, ³ Schmidt-Ott, ¹ Ijaz ¹³	20
Transplutonium chemistry	Silva, Keller, McDowell, Case, Tarrant, Peterson, ³ Zvara ¹⁴	20
Coulomb nuclear interference	H. Bingham, Gross, Halbert, Hensley, Saltmarsh	17
Coulomb-induced fission	Bemis, Gross, Ferguson, Plasil, Zucker	15
Heavy-ion elastic scattering survey	Ball, Halbert, Gross, Fulmer, Saltmarsh, Hensley, Ludemann	15
Investigation of nuclei near $N = 82$	Newman, Toth, Hensley, C. Bingham, ³ Schmidt-Ott, ¹ Ijaz ¹³	13
Complete fusion reactions	H. Bingham, Saltmarsh, C. Bingham, ³ Gross, Zucker	12
Mirror states at high excitation	H. Bingham, Halbert, Newman, Hensley	10
(p, t) reactions	Greenfield, ¹⁵ Fox ¹⁵	9
³ He scattering from Sm isotopes	Fulmer, Griffiths, ¹⁶ Hensley	8
Spectroscopy of ⁹² Mo	Scott, ¹⁷ Whiten ¹⁸	5
Shielding studies	Fulmer, Butler, Wallace	4
Spectroscopy of ³⁶ Ar	Newman, H. Bingham, Halbert, Hensley	3
Laser development	Miller, ¹⁹ Polk, ¹⁹ Fulmer	2
Neutron-deficient isotopes	Ketelle, Brosi	1
Radioactivity calibrations	O'Kelley, Eldridge, Trombka, ²⁰ Metzgar ²¹	1
Excitation functions	Fulmer	1
Spectroscopy of ¹⁷¹ Hf	Horen, Harmatz, Handley	1

1. UNISOR is a consortium of 12 universities, Oak Ridge National Laboratory, and Oak Ridge Associated Universities.

2. University of Marburg.

3. University of Tennessee.

4. Furman University.

5. Vanderbilt University.

6. University of Texas.

7. University of Virginia.

8. Trinity University.

9. Niels Bohr Institute.

10. University of Southern California.

11. University of Missouri at St. Louis.

12. Drexel University.

13. Virginia Polytechnic University.

14. Joint Institute for Nuclear Research, Dubna.

15. Florida State University.

16. King's College, University of London.

17. University of Georgia.

18. Armstrong College.

19. Redstone Arsenal.

20. Goddard Space Flight Center.

21. Jet Propulsion Laboratory.

Table 3. Analysis of beam usage by types

Particle	Energy (MeV)	Total hours assigned	Percent (approx)
Nuclear research			
Carbon	59-176	792	15.8
Sulfur	101	16	1.0
Argon	9-182	404	8.0
Copper	50	4	0
Neon	5-162	998	20.0
Lithium		128	2.5
Nitrogen	100-164	250	5.0
Nickel		40	1.0
Oxygen	22-148	1244	25.0
Boron	72-137	96	1.0
Chlorine	64-129	0	0
Xenon	34-101	0	0
Fluorine	170	48	1.0
Total, heavy-ion experiments		4020	79.0
Deuterons	18-40	120	3.0
Protons	11-67	456	10.0
Alphas	28-80	212	4.2
³ He	25-107	184	4.0
Total, light-ion experiments		972	48.3
Total, nuclear research experiments		4992	
Outage		1172	
Adjusted nuclear research experiments		3820	100.0
Machine research			
Heavy ions		352.4	66.2
Light ions		150.0	28.2
Miscellaneous		30.0	5.6
Total		532.4	100.0

or 58% of the total time available. A usable beam was on target about 3317 hr, or 50% of the total time available. Distribution of the research experiments for 1973 is shown in Table 2. A total of 458 bombardments were made with the various particle types and energies noted in Table 3.

Operations Summary

Operation has been on a 16-shift/week, 128-hr/week schedule, except for the period May 21, 1973, to July 30, 1973, when it was on a 21-shift (168-hr) week.

Initial operation of two new beam stations in the south research addition was achieved. These are the fission studies and the second transuranic research station (Fig. 1). Unscheduled outage increased from 15% to about 17% of the total available time. However, rf outage decreased from 5.5% to 1.6%. Scheduled engineering was substantially lower than last year, decreasing from about 9% to about 1.6%. The increased outage can be traced to the need for more source changes due to running heavy ions.

At the end of the year, we were in the process of relocating the extraction elements to make room for a larger source tube. At the same time a set of cryopanel was installed in the magnet gap. Preliminary tests indicate considerably improved pressure in the orbiting region.

The RCA 4648 tube installed in place of the 6949 in the rf power amplifier in the latter part of 1972 has performed satisfactorily for almost 7000 hr.

In line with power conservation, the air conditioner was shut down for the winter. Water pumps and some vacuum pumps are shut down except when actually needed, and lights in unfrequented areas are kept off. The first week under this policy indicates a power saving of approximately 20%.

Radiation Safety

Radiation safety at ORIC continued to be good in 1973. All personnel exposures and contaminations were contained within permissible limits. The maximum integrated dose received by any one individual associated with the cyclotron operations was 0.55 rem. The cyclotron operators, who continue to receive the highest exposures, received doses averaging 330 millirems, with the highest single exposure being the one mentioned above.

Continuously operating beta-gamma and alpha air monitors in and around the facility indicated effective containment of particulate radioactive materials. No responses significantly above background variance were observed.

1. Plant and Equipment Division.
2. Instrumentation and Controls Division.
3. Health Physics Division.

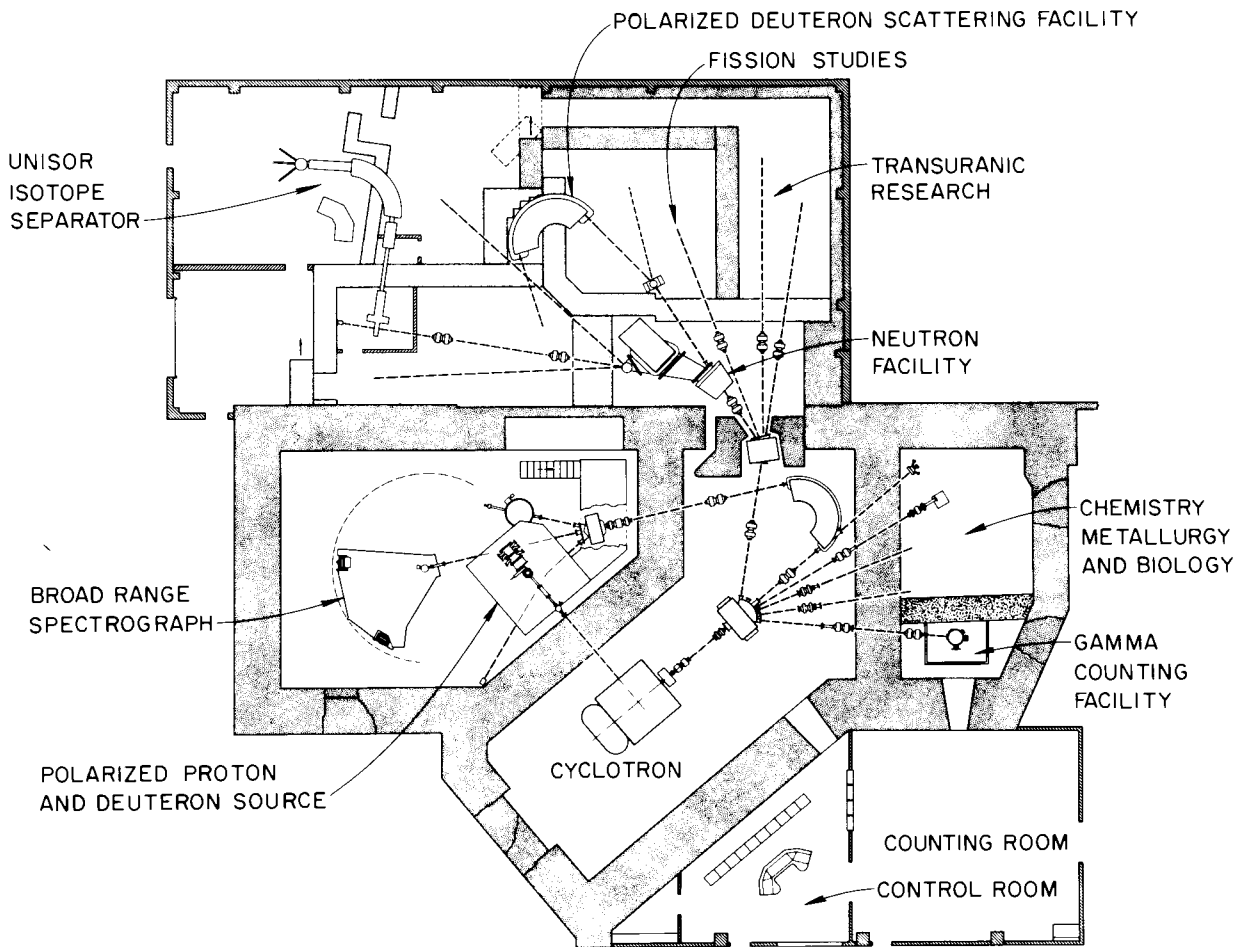


Fig. 1. Plan of ORIC experiment rooms.

ACCELERATOR INFORMATION CENTER – 1973

F. T. Howard

Two specific accelerator information center projects were initiated during the year. Both are now essentially ready for preparation of the final reports.

Early in the year a world census of tandem particle accelerators was undertaken. A preliminary list of tandem installations was compiled, with probable addresses. A brief one-page questionnaire was prepared to identify the configuration, performance, and the scheduled uses of each machine. The May mailing was to over 70 installations, about half in the United States and a somewhat greater total in 20 other countries.

Data are now in for all U.S. tandems; the preliminary tabulation lists 34 machines at 31 laboratories; there are

three double-tandems. Responses are now in for 33 machines abroad. We are still awaiting confirmation of two in France, a pair in Germany, one in East Germany, possibly another in Italy, and at least three in the U.S.S.R.

In September, before the world tandems project could be completed, a 1973 census of all types of particle accelerators in the U.S. was undertaken. This new census built upon and extended the 1969 census that we compiled in 1970 in cooperation with the Nuclear Physics Panel of the NAS Physics Survey Committee, and which was published by the National Academy of Sciences in 1972. The 1969 census had been limited to accelerators used in nuclear physics.

In preparing the preliminary list for the 1973 census we attempted to include all accelerators of any type used in any field of research. For this, a suitable brief

one-page data form was developed and widely circulated; the cover letter asked for suggestions of any additional accelerators. The first mailing in mid-September was followed by later mailings to newly suggested installations. Follow-up mailings and telephone calls were made as required. The survey is now essentially complete (Table 1).

All 144 accelerators listed in 1969 have been accounted for: 13 have been dismantled, 12 are in lay-by, and 119 are still active. We have now in our preliminary

tabulation forms 55 additional machines; these confirmed new entries include machines of several types, but mostly in the smaller, under 5 MV, category.

Analyses and tabulations of data for the "World Tandems - 1973" and for the "U.S. Accelerators - 1973" can now be prepared for publication as laboratory TM memos, and for submission to such journals as *Nuclear Instruments and Methods*, *Particle Accelerators*, or *IEEE Transactions*.

Table 1. Summary: results of 1973 census survey of particle accelerators in the United States

	Census 1969 ^a	Since 1969		Still active	New entry ^b	Census 1973 ^c
		Dismantled	To lay by			
HV tandem accelerators	30 ^d	0	0	30 ^e	2	32
HV single, ≥5 MV	15	0	3	12	0	15
HV single, <5 MV ^f	42	2	4	36 ^g	37 ^h	77
FM cyclotrons	5	2	0	3	1	4
AVF cyclotrons	18	2	0	16	6	22
Fixed frequency cyclotrons	8	3	2	3	3	8
Positive ion linacs	3	0	0	3	0	3
Electron linacs, >150 MeV	3	0	0	3	0	3
Electron linacs, <150 MeV	15	2	2	11	4	17
Betatrions	2	0	1	1	2	4
Electron synchrotrons, <1 GeV	3	2	0	1	0	1
Totals	144	13	12	119 ⁱ	55	186

^aListing only accelerators used in basic nuclear physics in 1969.

^bIncluding accelerators used in other research, as well as newly built machines.

^cIncluding new entries and machines still in lay-by.

^dSix of these can be paired to provide double-tandem performance.

^eIncludes one tandem being transferred.

^fIncludes small HV machines down to 0.1 MV.

^gThree small HV machines were transferred.

^hMany quite small HV machines; listing of some is questionable.

ⁱSome of those "still active" are currently down for repairs or remodeling.

2. Van de Graaff Laboratory

INTRODUCTION

C. D. Moak R. L. Robinson

It is interesting that during 1973, protons were used in the tandem accelerator less than 2% of the available operating hours. Two isotopes of oxygen were used for approximately 60% of the operating hours, and helium, carbon, aluminum, chlorine, and iodine made up the rest. Atomic collisions physics and nuclear physics were in the ratio 35:65 for research time. A large amount of accelerator time was occupied with installation of the new ion source system, which is now complete and operational. The 5.5-MV Van de Graaff was used principally for radiation damage simulation studies, with particular attention to the case of aluminum ions in aluminum. A visiting group made use of this machine to perform hydrogen searches on lunar specimens and on metal fracture specimens, using the lithium microprobe technique.

A total of 44 visiting scientists participated in experiments in the Van de Graaff Laboratory during the year, and, as in past years, they have contributed in many ways to the overall program.

Included in the report for the Van de Graaff Laboratory are reports of the Atomic Physics group from the University of Tennessee under I. A. Sellin and on the Ion Source Program under C. M. Jones. The University of Tennessee group has concerned itself largely with few-electron ions, because only these are amenable to detailed theoretical analysis. Jones's report contains the first, not yet comprehensive, set of absolute measurements of the charge states produced in small-angle scattering of heavy ions in gases at an energy of 20 MeV, and these lead to some interesting design possibilities for gas strippers.

A question concerning the role of conduction electrons in shielding a fast oxygen ion by a process called dynamic screening and thus affecting the ion's stopping power appears to have been resolved. An experiment has been performed in which ions of different initial charge state passed through crystal channels without electron capture or loss. The stopping powers were not equalized by screening, but differed according to the relation $S = kq^2$; some of the details follow later in this report. The channeling group has found additional evidence that the behavior of ionic stopping powers in the so-called "velocity-proportional" region does not follow theoretical predictions; some of the results appear later in this report. Continued experiments on the phenomenon called hyperchanneling are covered in this report as well.

Heavy-ion-induced reactions have been an important means for producing new neutron-deficient nuclei. Although it is anticipated that with increased projectile energy, production of nuclei still farther from the valley of stability will be achievable, the extent to which this can be done is unknown. There are theoretical calculations, but there are limited experimental data to test these calculations and, implicitly, the assumptions made in these calculations: the nature of the reaction mechanism; the spin distribution of the states formed in the compound nuclear system; the competition between particle

emission, gamma-ray emission, and fission; the dependence of the level density on spin and of yrast level on energy. We have been obtaining relevant experimental data by two techniques. In the first, absolute cross sections for the various residual products resulting in heavy-ion-induced reactions are determined through gamma-ray spectroscopy. In bombardment of ^{61}Ni with 38- to 51-MeV ^{16}O ions, 13 reaction products were identified; those with the stronger cross sections were generally found to be adequately predicted by theory. On the other hand, the theory often does poorly when the reaction cross sections are small. This suggests that present calculations need to be viewed skeptically in their predictions of exceedingly small cross sections for production of nuclei far from the valley of stability.

There is also some evidence of this in our second type of measurement. Neutrons emitted in $^{16,18}\text{O}$ -induced reactions of stable nickel, copper, and zinc targets are detected with a large graphite sphere impregnated with boron trifluoride detectors. Experimental results as a whole are in reasonable agreement with theory for projectile energies above the Coulomb barrier and substantiate the theoretical prediction that the average number of neutrons emitted per reaction is strongly dependent on the neutron richness of the target and projectile; for example, 52-MeV ^{16}O bombardments of ^{58}Ni and ^{64}Ni yield, respectively, average neutrons per reaction of 0.2 and 2.0. The poorest agreement is for the $^{16}\text{O} + ^{58}\text{Ni}$ system, which is, of the cases studied, the one farthest from the valley of stability and which, consequently, emits the fewest neutrons per reaction.

The graphite sphere has also been applied to the determination of cross sections with astrophysical interest, namely, low-energy interactions between ^{12}C and ^{13}C . The additional neutron in ^{13}C results in the cross section of the $^{13}\text{C}(^{12}\text{C},xn)$ reaction at low energies (about 4 MeV c.m.) being 50 to 100 times larger than the approximately 0.02 mb cross section obtained for the $^{12}\text{C}(^{12}\text{C},xn)$ reaction.

Because heavy-ion projectiles carry large amounts of angular momentum into nuclear reactions, high-spin states inaccessible in light-ion reactions become selectively populated. This is beautifully demonstrated in our study of ^{42}Ca , where more than a hundred low-spin states have been previously reported up to 12 MeV excitation energy. But through the $^{28}\text{Si}(^{16}\text{O},2p)$ studies, new states have been observed. From gamma-ray angular distributions and gamma-gamma angular correlations, their spins have been established as 5 to 9. In contrast to most in-beam gamma-ray studies of heavy-ion-induced reactions, where a single prominent cascade from a rotational or a quasi-rotational band is observed, there are several gamma rays of comparable intensity terminating at the 3190-keV, 6^+ state. Because these high-spin states are well separated and therefore probably unmixed, it is possible they can be explained in terms of simple few-particle configurations. That possibility is being explored.

In ^{72}Se we reported earlier a low-lying 0^+ state just 75 keV above the first 2^+ state, for which there was no explanation. We have continued to study this nucleus via the $^{58}\text{Ni}(^{16}\text{O},2p)$ reaction and now suggest that there is a coexistence of spherical and deformed shapes with the 0^{+} state as the head of the rotational band and with the two bands crossing near the 2^+ state. This explanation accounts for the lifetime obtained for the 0^{+} state and for the energies of the first and second 2^+ states assuming equal mixing of the rotational and vibrational wave functions, and it predicts the energies of a sequence of levels observed experimentally with proposed spin-parities of 4^+ , 6^+ , 8^+ , 10^+ , and 12^+ .

In-beam gamma rays from ^{64}Zn produced by the $^{51}\text{V}(^{16}\text{O},p2n)$ reaction show still another level pattern: two cascades of comparable intensity which have only weak transitions between the two and yet which are both fed via decay of a state at 4636 keV. We have no explanation for this curious structure. However, additional information is now being deduced from gamma-ray angular distributions and lifetime measurements.

Investigation of high-spin states preferentially populated through heavy-ion reactions is also being explored through charged-particle studies utilizing the Enge magnet and

position-sensitive proportional counter. Studies of the $^{10}\text{B}(^{16}\text{O},^6\text{Li})$ reaction demonstrate that the average cross sections for populating high-spin states have been well reproduced by Hauser-Feshbach calculations. This indicates that comparison of cross sections for compound-nuclear processes with Hauser-Feshbach calculations is a significant technique for assigning spins. It has been applied to the $^{10}\text{B}(^{16}\text{O},\alpha)^{22}\text{Na}$ reaction; strongly excited states are found to have energies and spins based on their average cross section that are consistent with levels predicted by the shell model to be high-spin members of the $K = 3^+$, $T = 0$; $K = 0^+$, $T = 0$; and $K = 1^-$, $T = 0$ bands.

For more than two decades, Coulomb excitation has been an important program in the Van de Graaff Laboratory for extracting nuclear properties of low-lying states in stable nuclei. It has provided valuable insight into the phonon, the rotational-vibrational, and core-single-particle coupling models. This program has continued vigorously in 1973 in three areas:

1. Studies of the even-mass $^{176,178,180}\text{Hf}$ and $^{156,158}\text{Gd}$ nuclei, which are at opposite ends of the rare-earth rotational nuclei, reveal a peculiar behavior for the 2^+ member of the β band. While the ground and γ -band 2^+ energies and $B(E2)$'s are quite similar, the β bands for both sets of nuclei have energies and $B(E2)_{\text{exc}}$ that decrease rapidly with increasing neutron number. This is surprising, since gadolinium nuclei become more deformed with increasing neutron number, while the hafnium nuclei become less deformed. Another puzzle is that no amount of mixing between the β and γ bands will explain the observed gamma-ray branches from the β 2^+ states in the gadolinium nuclei, but in $^{174,176,178}\text{Hf}$ they are explained with appropriate perturbational corrections for band mixing.

2. Coulomb excitation has been used to systematically determine transition probabilities for exciting 3^- states in actinide nuclei. Comparison of these results with the microscopic calculations of Neegard and Vogel shows that these states can be interpreted as members of the one-phonon octupole vibrational spectrum.

3. For projectile energies near the Coulomb barrier, Coulomb and nuclear interactions are comparable in magnitude, and an observable destructive interference takes place. A study of this interference is important in that it can provide information on the magnitude and shape of the potential at the nuclear surface. Thus far, this type of study has concentrated on the 2^+ states. However, we have now observed this interference from inelastic scattering of alpha particles from the 4^+ states of ^{154}Sm , ^{166}Er , ^{182}W , and ^{234}U , and actually find the onset of the interference occurs at a slightly lower projectile energy than that for the 2^+ state. The destructive interference is particularly strong (nearly a factor of 10) for ^{182}W . Possibly this is related to the sign of the hexadecapole transition moment, which for ^{182}W is negative, in contrast to the other three nuclei under investigation.

HEAVY-ION REACTIONS

EVIDENCE FOR COEXISTENCE OF SPHERICAL AND DEFORMED SHAPES IN ^{72}Se

J. H. Hamilton ¹	H. J. Kim
A. V. Ramayya ¹	R. O. Sayer ²
W. T. Pinkston ¹	R. M. Ronningen ¹
R. L. Robinson	G. Garcia-Bermudez ¹
H. K. Carter ¹	

The lowest few energy levels in even-even nuclei with $A = 70$ to 80 usually follow the pattern expected for a simple phonon vibrational model characteristic of

spherical nuclei. However, notable exceptions to this model are observed^{3,4} in $^{70,72}\text{Ge}$, where the first excited 0^{+} state energies are just above and just below the first 2^+ states. Various suggestions have been made to explain these two very low energy 0^{+} states.^{5,6}

The data on the germanium isotopes are limited to only a few low-spin states, and thus the interpretation of these levels is still open to question. Recently the 0^{+} state in ^{72}Se was observed⁷ only 75 keV above the first 2^+ 862-keV state.

Here we report measurements of absolute and relative transition rates of the low-spin states and of a proposed yrast band of even spin levels to spin 12 in ^{72}Se . We

suggest that the 0^{+} state and higher-spin states strongly excited through nuclear-induced reactions are members of a $K^{\pi} = 0^{+}$ rotational band associated with a deformed shape which coexists with the vibrational states associated with a spherical ground state. Our ^{72}Se data show a striking similarity to the very recent evidence⁸ that the yrast states in ^{186}Hg go from a near-spherical to a deformed shape at about spin 6.

First the lifetime of the 937-keV 0^{+} state in ^{72}Se was measured by a delayed coincidence technique. The ^{72}Se levels were populated by ^{72}Br ($T_{1/2} = 1.31$ min)⁷ produced by the $^{58}\text{Ni}(^{16}\text{O},pn)$ reaction with 46-MeV ^{16}O ions from the tandem Van de Graaff accelerator. The exponential decay part of the time spectra of the 1062-862-keV cascade was analyzed to yield a mean life of 22.8 ± 1.4 nsec for the 0^{+} state. The ratio of the $E0$ to $E2$ decays of the 937-keV level was measured to be 0.37 ± 0.23 . We find $B(E; 0' \rightarrow 2) = 0.32 \pm 0.06 e^2 b^2$ or 36 ± 7 spu and find $\rho(E0) = 0.176^{+0.048}_{-0.070}$.

From an in-beam gamma-gamma coincidence experiment in ^{72}Se produced by the $^{58}\text{Ni}(^{16}\text{O},2p)$ reaction and carried out with two Ge(Li) detectors, the following levels were established above the 2^{+} 1320-keV level: 1637, 4^{+} ; 2467, 6^{+} ; 3425, 8^{+} ; 4502, (10^{+}); and 5702, (12^{+}). The 10^{+} , 12^{+} assignments are tentative and are based on the strong cascade character of the transitions out of these levels.

The striking features of the ^{72}Se levels and their decays are: (1) the low energy of the 0^{+} state and its strong $B(E2)$ to the 2^{+} state, (2) the strong $2^{+} \rightarrow 0^{+}$ transition with a $B(E2)$ comparable to that of the $2^{+} \rightarrow 2^{+}$ transition, and (3) the low energy of the $4 \rightarrow 2$ transition compared to all the other transitions in the yrast band and then a regular increase in transition energy with increase in spin above $I = 4$. The first two of the above are in strong disagreement with the pure vibrational model.

The unusual character of the yrast band in ^{72}Se is seen in a plot of $2\mathcal{I}/\hbar^2$ vs $(\hbar\omega)^2$ (Fig. 1), where \mathcal{I} is the moment of inertia and $\hbar\omega$ is essentially one-half the transition energy. Sudden changes in \mathcal{I} with increase in nuclear spin indicate sudden changes in the structure of the nucleus. The curve in Fig. 1 is based on the ground and first 2^{+} states in ^{72}Se as the lowest members of the band and is markedly different from that of any other reported yrast bands (e.g., refs. 9–11), except ^{186}Hg (ref. 8). The 2^{+} and 4^{+} states have energy spacings that are reasonably characteristic of a pure spherical vibrator, as indicated by the nearly vertical rise in \mathcal{I} with increasing spin. The 6 to 12 spin states follow reasonably well the simple rotational energy formula $E_I = AI(I+1) + BI^2(I+1)^2$.

All the above data in ^{72}Se can be understood in terms of the coexistence of deformed and spherical states. Such could occur with a near-spherical ground state if there is a second minimum in the potential relatively low in energy with large deformation. We assume that the 0^{+} state is a deformed state which is the lowest member of a $K^{\pi} = 0^{+}$ rotational band. Further assume that in lowest order the 2^{+} member of this band and the 2^{+} one-phonon level are close together so there is strong mixing of the rotational and vibrational wave functions and large shifts of only these 2^{+} levels.

The 0^{+} , 4^{+} , 6^{+} , 8^{+} , 10^{+} , and 12^{+} members of the rotational band were assumed to be the levels at 937, 1637, 2467, 3425, 4502, and 5702 keV (Table 1). A least-squares fit of the rotational energy formula to the 0^{+} , 4^{+} , 6^{+} , and 8^{+} energies (relative to 0^{+}) yielded $A = 38.1$ and $B = -0.047$, from which the 2^{+} , 10^{+} , and 12^{+} energies in Table 1 were predicted. The fit is strikingly good all the way to spin 12. It is surprising that these data fit so well this relatively simple rotational formula which in general yields poor fits at high spin.

Relative $B(E2)$'s and branching ratios were calculated. The $0^{+} \rightarrow 2^{+}$ rotational transition has the strongest $B(E2)$ predicted ($1/2$ the square of the intrinsic quadrupole moment), which is supported by our large $B(E2)$. We find $B(E2; 2' \rightarrow 2)/B(E2; 2' \rightarrow 0') = 1.5 \pm 0.3$ from $B(M1) = 0$, whereas the predicted value is 0.7. If the $2' \rightarrow 2$ transition contains some $M1$ admixture the experimental ratio could be significantly lower.

Thus with a simple approach of nuclear coexistence, we can explain semiquantitatively the decay properties of the low-spin states and fit the energies of the rotational band to spin 12 remarkably well. The very

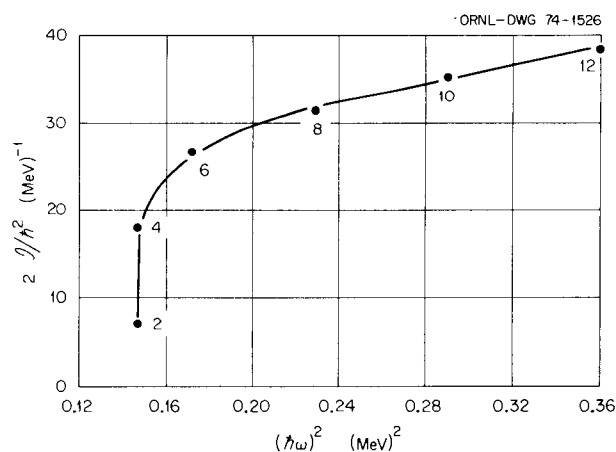


Fig. 1. A plot of $2\mathcal{I}/\hbar^2$ vs $(\hbar\omega)^2$ for ^{72}Se . The lowest point is for the $2 \rightarrow 0$ transition. For definition of $\hbar\omega$, see R. A. Sorensen, *Rev. Mod. Phys.* **45**, 353 (1973), Eq. 14d.

Table 1. Experimental energy levels in ^{72}Se and calculated levels for a rotational band built on the 937-keV 0^+ state

A fit of the 0^+ , 4^+ , 6^+ , and 8^+ experimental energies to the rotational energy equation yielded $A = 38.1$ and $B = -0.047$. From these values the 2^+ , 10^+ , and 12^+ energies were predicted as given

I^π	E exp (keV)	E calc (keV)
0^+	937	928
2^+		1155
4^+	1637	1671
6^+	2467	2444
8^+	3425	3426
10^+	4502	4549
12^+	5702	5727

low crossing of the rotational band with the "phonon states" near spin 2 and the wide energy spacings of the vibrational states is most fortunate in that one can see the effects of this crossing relatively easily.

There is a striking similarity in the behavior of the yrast level energy spacings in ^{72}Se and ^{186}Hg (ref. 8), where the $4 \rightarrow 2$ and $6 \rightarrow 4$ spacing, respectively, drop below the lower ones and then the higher ones increase with spin. It was just such a sharp bend in \mathcal{J} as in Fig. 1 followed by a linearity of the plot of \mathcal{J} vs $(\hbar\omega)^2$ for the spins above 6 in ^{186}Hg that was interpreted⁸ as evidence for a change in nuclear shape from near spherical to deformed. In each case the data indicate that the lowest-spin members are associated with near-spherical states and the high-spin states with deformed shapes, with the shift occurring at lower spin in ^{72}Se . Our data clearly show that in ^{72}Se this change is consistent with a crossing of a deformed band with the 2^+ spherical state, where we see the lower members of the deformed band. It would be most interesting to search for the lower members of the deformed band in ^{186}Hg to show the complete similarity of these cases.

1. Vanderbilt University, Nashville, Tenn.

2. Jointly supported by Vanderbilt and ORNL; on leave from Furman University.

3. D. E. Alburger, *Phys. Rev.* **109**, 122 (1958).

4. E. Eichler, P. H. Stelson, and J. K. Dickens, *Nucl. Phys.* **A120**, 622 (1968).

5. E. Ya. Lure, L. K. Peker, and P. T. Prokofev, *Izv. Akad. Nauk SSSR, Fiz. Ser.* **32**, 74 (1968).

6. K. W. C. Stewart and B. Castel, *Nuovo Cim. Lett.* **4**, 489 (1970).

7. R. L. Robinson, H. J. Kim, J. L. C. Ford, W. E. Collins, and J. H. Hamilton, *Bull. Amer. Phys. Soc.* **16**, 626 (1971); W. E. Collins et al., submitted to the *Physical Review*.

8. D. Proetel, R. M. Diamond, P. Kienle, J. R. Leigh, K. H. Maier, and F. S. Stephens, *Phys. Rev. Lett.* **31**, 896 (1973).

9. R. A. Sorensen, *Rev. Mod. Phys.* **45**, 353 (1973).

10. T. L. Khoo, F. M. Bernthal, J. S. Boyno, and R. A. Warner, *Phys. Rev. Lett.* **31**, 1146 (1973).

11. G. Scharff-Goldhaber, G. M. McKeown, A. H. Lumpkin, and W. G. Piel, Jr., *Phys. Lett.* **44B**, 416 (1973).

HIGH-SPIN STATES IN ^{42}Ca

R. L. Robinson R. O. Sayer¹
H. J. Kim G. J. Smith²
W. T. Milner J. C. Wells, Jr.³
 J. Lin³

Many studies of ^{42}Ca via light-ion reactions have revealed a myriad of states up to excitation energies of 12 MeV.⁴ Of those with assigned spins, only three have values greater than 4: a 6^+ state at 3.190 MeV and two 5^- states at 4.104 and 4.90 MeV.^{4,5} By means of the $^{28}\text{Si}(^{16}\text{O},2p)^{42}\text{Ca}$ reaction, states were produced which were suggested to have high spins because of (1) the large amount of angular momentum brought in by heavy-ion projectiles and (2) branching ratios of gamma rays from these states.⁶ In contrast to the strong single cascade of gamma rays from a rotational or quasi-rotational band that has been observed for many in-beam gamma-ray studies following heavy-ion-induced reactions, population of the 6^+ , 3190-keV state in ^{42}Ca is fragmented between several gamma rays of comparable intensity. Because ^{42}Ca has the simple structure of two neutrons plus a ^{40}Ca doubly magic core, it will be interesting to see if these high-spin states can be explained in terms of few-particle configurations. For example, the two 5^- states reported at 4.10 and 4.90 MeV have been suggested as containing $1d_{3/2}^{-1}(f_{7/2}^3)_{7/2}$ neutron configurations.

An effort has been made to extract the spins of the more strongly excited states in the $^{28}\text{Si}(^{16}\text{O},2p)^{42}\text{Ca}$ reaction from measurements of gamma-ray angular distributions and gamma-gamma angular correlations relative to the incident projectile beam. The states are given in Fig. 1; the relative intensities of the gamma rays are for bombardment of a 0.7-mg/cm² natural silicon target evaporated on a thick tantalum backing with 40-MeV ^{16}O ions. Gamma-gamma angular correlations were taken since angular distributions alone will often be consistent with more than one spin assignment and/or gamma-ray admixture. In part, this experiment was to explore the potential of gamma-gamma correlation studies for complementing angular distribution results. For our particular choice of angles, we found that the gamma-gamma correlations resolved ambiguities in spin-admixture determinations in some cases but in other cases gave the same ambiguities as the

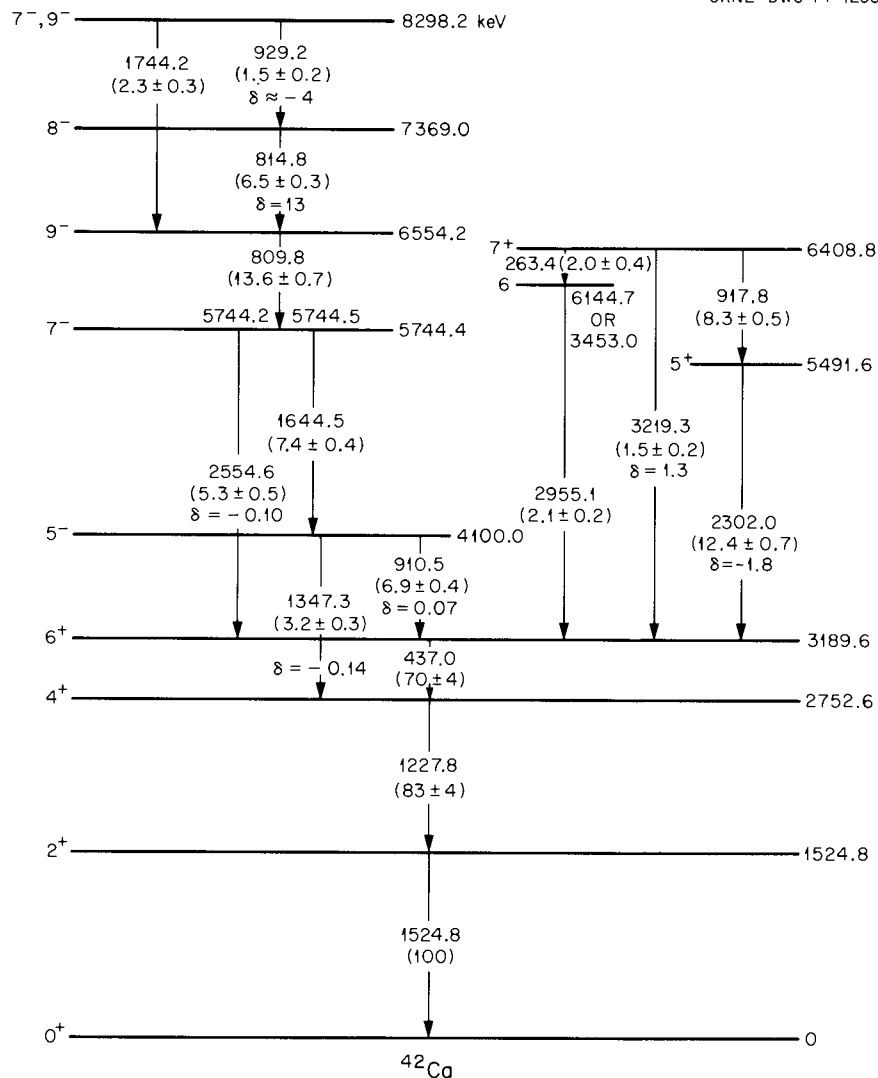


Fig. 1. Levels excited in ^{42}Ca via the $^{28}\text{Si}(^{16}\text{O}, 2p)$ reaction. The numbers associated with each transition give its energy, relative intensity, and radiative admixture.

angular distribution studies. It is possible that other angles for gamma-gamma angular correlations would be more suitable, and this needs to be investigated.

The angular distributions were measured at angles of 0° , 55° , and 90° relative to the incident beam. For the gamma-gamma angular correlations, one detector was fixed at 90° , and the second detector was placed at 0° or 270° . The beam and two detectors were in the same plane. The experimental ratios, R_{ex} , of gamma-ray intensities for different angles, normalized to the same beam current, were compared with theoretical values for different spins, admixtures, and alignments of the initial state. Results were given in terms of χ^2 plots, where

$$\chi^2 = \sum_{i=1}^n \left(\frac{R_{\text{ex}i} - R_{\text{th}i}}{\epsilon_i} \right)^2$$

The quantity ϵ_i is the experimental uncertainty in $R_{\text{ex}i}$. Depending on the particular transition, n had values of 2 to 10. Only dipole and quadrupole transitions were considered. One example is given in Fig. 2; in this case $n = 4$. $R_1 = W(0^\circ)/W(90^\circ)$ and $R_2 = W(0^\circ)/W(55^\circ)$ are ratios from the angular distribution of the 2302-keV gamma ray.

$$R_3 = W(0^\circ, 90^\circ)/W(270^\circ, 90^\circ)$$

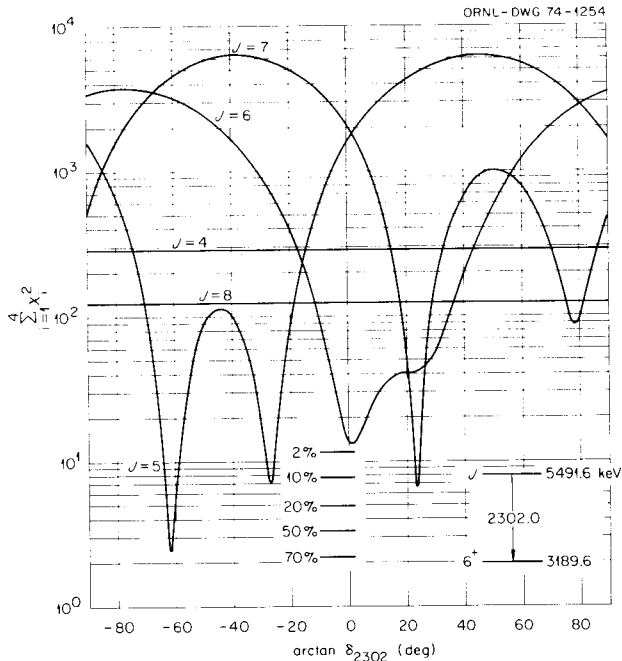


Fig. 2. Plot of χ^2 representing a comparison between the experimental and calculated values for angular distribution and gamma-gamma angular correlation results of the 2302-keV gamma ray.

and

$$R_4 = W(90^\circ, 0^\circ)/W(90^\circ, 270^\circ),$$

where for $W(\theta_1, \theta_2)$, θ_1 is the angle of the detector observing the 2302-keV gamma ray and θ_2 is for the detector observing the 437-, 1228-, and 1525-keV gamma rays. Because of the 6-4-2-0 spin sequence, the 2302-437, 2302-1228, and 2302-1525 keV gamma-gamma angular correlations all give the same results and were summed to improve statistics.

The spin assignments and admixtures, $\delta = (Q/D)^{1/2}$, most favored by the present results are illustrated in Fig. 1. Interpretation of these states is being investigated.

1. Supported jointly by Vanderbilt University and ORNL; on leave from Furman University.
2. Postdoctoral Fellow under appointment with Oak Ridge Associated Universities.
3. Tennessee Technological University, Cookeville, Tenn.
4. P. M. Endt and C. Van der Leun, *Nucl. Phys.* A214, 1 (1973).
5. Y. Dupont, P. Martin, and M. Chabre, *Phys. Rev.* 7, 637 (1973).
6. H. J. Kim, R. L. Robinson, and W. T. Milner, *Proc. International Conference on Nuclear Physics, Munich, Germany*, p. 172 (1973).

IN-BEAM GAMMA RAYS FROM THE $^{28}\text{Si}(^{16}\text{O}, \alpha p \gamma)^{39}\text{K}$ REACTION

H. J. Kim R. L. Robinson W. T. Milner

In producing ^{42}Ca discussed in the previous paper, we also observed strong peaks attributed to ^{39}K as obtained from the $^{28}\text{Si}(^{16}\text{O}, \alpha p \gamma)$ reaction. The ^{16}O projectiles extracted from the ORNL tandem accelerator had energies of 26 to 42 MeV. Two noteworthy aspects of the levels established through gamma-ray yields and gamma-gamma coincidences are: (1) none of the numerous established levels above 4 MeV were observed and (2) gamma rays from many levels above the alpha and proton separation energies were observed. Both observations are consistent with the level spins being rather high.

The levels and gamma rays identified in this study are illustrated in Fig. 1. Angular distributions have been measured for the stronger gamma rays. If we make the

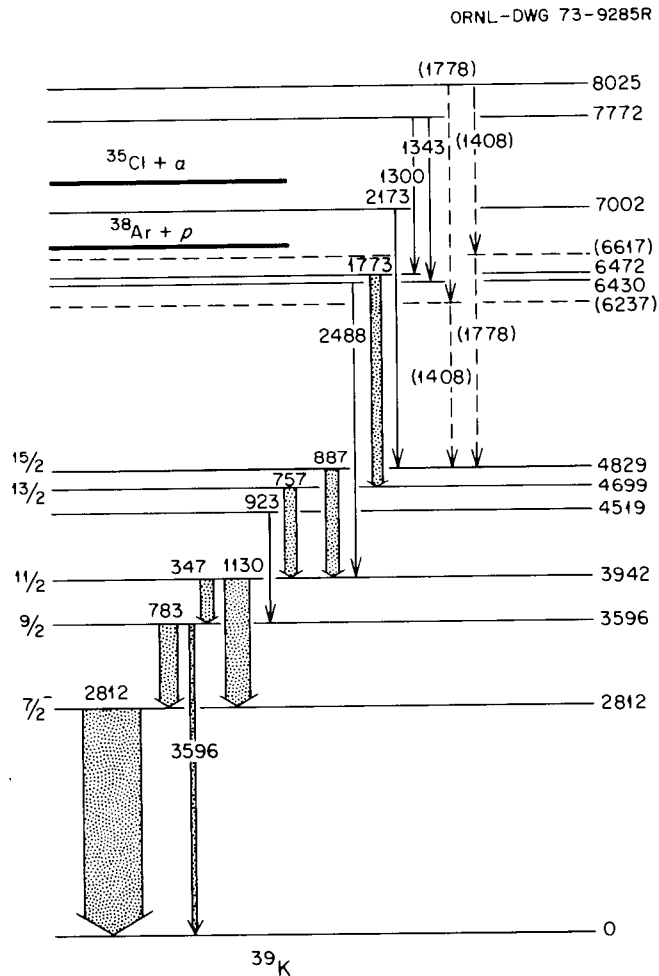


Fig. 1. Levels of ^{39}K excited in the $^{28}\text{Si}(^{16}\text{O}, \alpha p)$ reaction.

usual stretched spin assumption, the angular distribution results suggest the spins given in the figure.

IN-BEAM GAMMA-RAY SPECTROSCOPY OF MAGIC AND NEARLY MAGIC NUCLEI ($Z = 28$)

G. J. Smith¹ R. O. Sayer²
R. L. Robinson W. T. Milner

Within the last two years the use of heavy ions ($A > 4$) to initiate compound-nucleus reactions has become very popular. The result of such (H.I.,X) reactions (X = some combination of emitted protons, neutrons, and/or alpha particles) is the population of high angular momentum states in neutron-deficient nuclei. To date, most work of this type has been performed in mass regions of known or suspected nuclear deformations. Population of high angular momentum states in nuclei near closed shells should provide valuable information and tests for the shell model.

As a first step in such a study, we have used the reactions $^{45}\text{Sc}(^{16}\text{O},\text{X})$ to populate nuclei near or at the

closed proton shell $Z = 28$. (The neutron numbers in the residual nuclei are also close to the closed neutron shell $N = 28$, so that these nuclei are nearly doubly magic.) We have performed excitation functions ($36 \leq E_{^{16}\text{O}} \leq 46$ MeV) and gamma-gamma coincidence measurements at $E_{^{16}\text{O}} = 46$ MeV with a ^{45}Sc target of 1 mg/cm^2 thickness. The two major reactions observed are $^{45}\text{Sc}(^{16}\text{O},p2n)^{58}\text{Ni}$ and $^{45}\text{Sc}(^{16}\text{O},2p2n)^{57}\text{Co}$. Initial analysis of the data gives the decay schemes of ^{57}Co and ^{58}Ni shown in Figs. 1 and 2 respectively.

The spin assignments shown in Fig. 1 are taken from the adopted level scheme of ^{57}Co ,³ which is based upon several stripping and pickup reactions. The uncertainties in the higher-lying energy levels deduced from such experiments are typically 10 to 30 keV, so that of

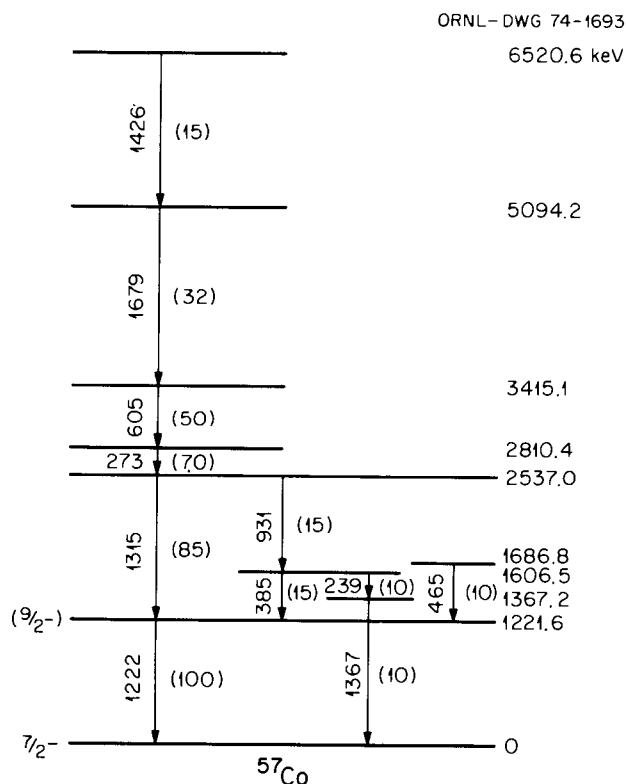


Fig. 1. Levels populated in ^{57}Co via the reaction $^{45}\text{C}(^{16}\text{O},2p2n)^{57}\text{Co}$ for 46-MeV ^{16}O ions. Intensities of gamma rays are given in parentheses. Spin assignments are from *Nucl. Data Sheets B3(3-4)*, 106 (1970).

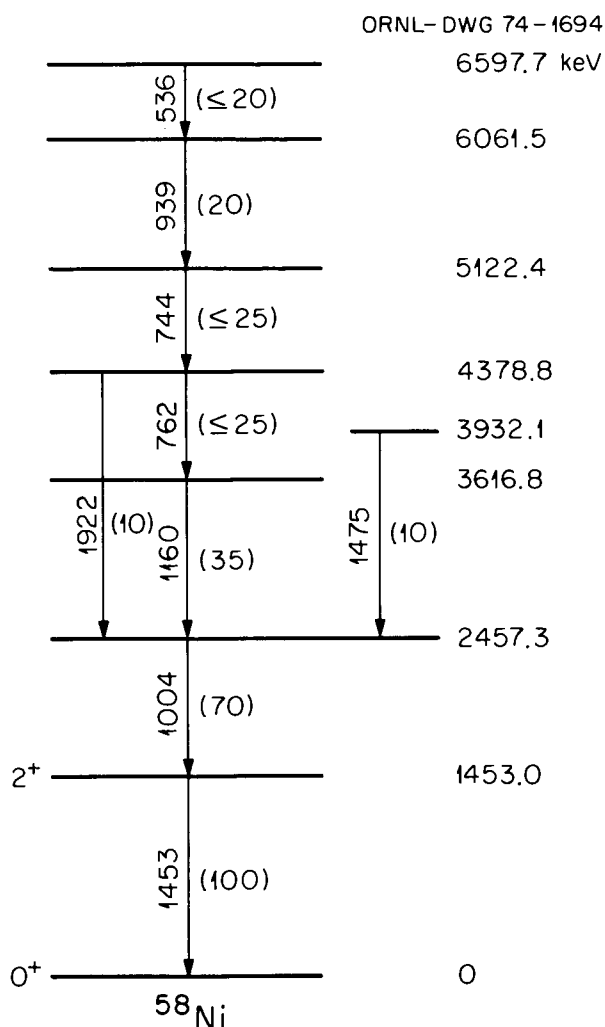


Fig. 2. Levels populated in ^{58}Ni via the reaction $^{45}\text{Sc}(^{16}\text{O},p2n)^{58}\text{Ni}$ for 46-MeV ^{16}O ions. Intensities of gamma rays are given in parentheses. Spin assignments are from *Nucl. Data Sheets B3(3-4)*, 178 (1970).

the states we observe, only the 1221.6-keV level can be said to have been populated in the stripping and pickup reactions.

In ^{58}Ni , the first three levels and the 4378.8-keV level have been previously observed via $(p,p'\gamma)$ work,⁴ and the 2^+ spin assignment of the first level is from this work. The intensities (and perhaps the order) of the 762-, 744-, and 536-keV gamma rays are uncertain at this time, because there is evidence of more than one gamma ray at each of these energies. These duplicate gamma rays may or may not be in ^{58}Ni . Further analysis should resolve this problem.

Future work will entail an angular distribution measurement for these two nuclei and population of states in other nuclei around the $N, Z = 28$ shells.

1. Postdoctoral Fellow under appointment with Oak Ridge Associated Universities.

2. Jointly supported by Vanderbilt University and ORNL; on leave from Furman University.

3. *Nucl. Data Sheets* B3(3-4), 106 (1970).

4. *Nucl. Data Sheets* B3(3-4), 178 (1970).

IN-BEAM GAMMA-RAY SPECTROSCOPY OF ^{64}Zn VIA THE $^{51}\text{V}(^{16}\text{O},p2n)$ REACTION

R. O. Sayer¹ G. J. Smith²
R. L. Robinson J. C. Wells, Jr.³
W. T. Milner J. Lin³

In-beam gamma-ray studies following heavy-ion reactions have yielded a wealth of valuable new information on high-spin states and collective structure in rare-earth and medium-mass nuclei. To date, in-beam techniques have been applied rather sparingly in the nickel-strontium region. Although quasi-rotational bands up to spin 8 or higher have been observed⁴⁻⁷ in $^{72-78}\text{Se}$, only in one case, ^{66}Zn ,⁸ has a 6^+ quasi-rotational state been identified in the nickel, zinc, and germanium nuclides.

We have measured excitation functions and angular distributions for gamma rays produced by bombardment of thick and thin (1 mg/cm^2) ^{51}V targets with 36- to 46-MeV ^{16}O ions. As predicted by theory⁹ the dominant reaction is $(^{16}\text{O},p2n)$, which leads to states in ^{64}Zn .

The excitation function and angular distribution results for gamma rays assigned to ^{64}Zn are summarized in Fig. 1 and Table 1 respectively. These data and the results of two-dimensional gamma-gamma coincident measurements were used to construct the level diagram shown in Fig. 2. The steep excitation curves for the 1687- and 642-keV gamma rays suggest high spin values for the 3994- and 4636-keV levels,

whereas the yield curves and A_2 values for the 808- and 1315-keV lines are consistent with the known J^π values of 2^+ and 4^+ for the 1799- and 2307-keV states respectively.

A tentative assignment of $J^\pi = 6^+$ for the 3994-keV state is based on the A_2 and A_4 values and on the strength of the 1687-keV transition. The negative A_2 value for the strong 642-keV transition is inconsistent with pure $E2$ radiation; therefore, the 4636-keV level cannot be the 8^+ member of a possible quasi band built on the ground state. Alpert et al.¹⁰ assign J^π values of 4^+ to a (2780 ± 30) -keV level and 5^- to a (4190 ± 30) -keV level seen in their (α,α') work. Our data for the 2737- and 4237-keV states are consistent with $J^\pi = 4^+$ and 5^- respectively. For example, the A_2 value for the 1500-keV line gives $\delta = (M2/E1)^{1/2} =$

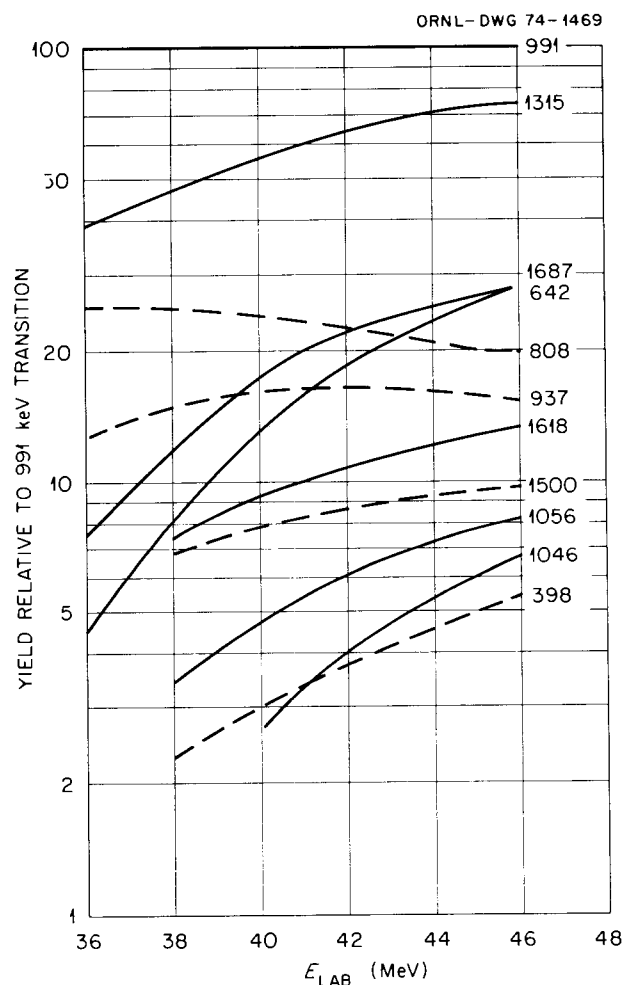


Fig. 1. Yield of gamma rays from the $^{51}\text{V}(^{16}\text{O},p2n)^{64}\text{Zn}$ reaction relative to the yield of the 991.6-keV $2 \rightarrow 0$ gamma ray as a function of projectile energy. A target of thickness 1 mg/cm^2 was used.

Table 1. Gamma-ray angular distribution results for 46-MeV ^{16}O ions on a thick ^{51}V target

$$W(\theta) = 1 + g_2 A_2 P_2(\cos \theta) + g_4 A_4 P_4(\cos \theta)$$

g_2 and g_4 are finite solid angle correction factors

E_γ (keV)	A_2	A_4	Transition
991.6	0.298 ± 0.021	-0.03 ± 0.02	$2 \rightarrow 0$
1315.2	0.350 ± 0.023	-0.06 ± 0.02	$4 \rightarrow 2$
1687.0	0.334 ± 0.016	-0.01 ± 0.01	$6 \rightarrow 4$
641.8	-0.104 ± 0.013	-0.02 ± 0.01	$4636 \rightarrow 3994$
1618.4	-0.101 ± 0.028	0.06 ± 0.02	$3925 \rightarrow 2307$
1056.6	0.418 ± 0.035	-0.05 ± 0.03	$4982 \rightarrow 3925$
1046.6	0.305 ± 0.050	0.01 ± 0.04	$5682 \rightarrow 4982$
1799.5	0.287 ± 0.030	0.06 ± 0.02	$2' \rightarrow 0$
807.9	-0.017 ± 0.013	-0.03 ± 0.01	$2' \rightarrow 2$
937.1	0.312 ± 0.033	-0.02 ± 0.03	$2737 \rightarrow 1799$
430.0	0.09 ± 0.05	-0.05 ± 0.04	$2737 \rightarrow 2307$
1500.5	0.112 ± 0.029	0.01 ± 0.02	$4237 \rightarrow 2737$
398.6	-0.174 ± 0.028	0.00 ± 0.02	$4636 \rightarrow 4237$
744.4	0.02 ± 0.08	0.12 ± 0.06	$4982 \rightarrow 4237$

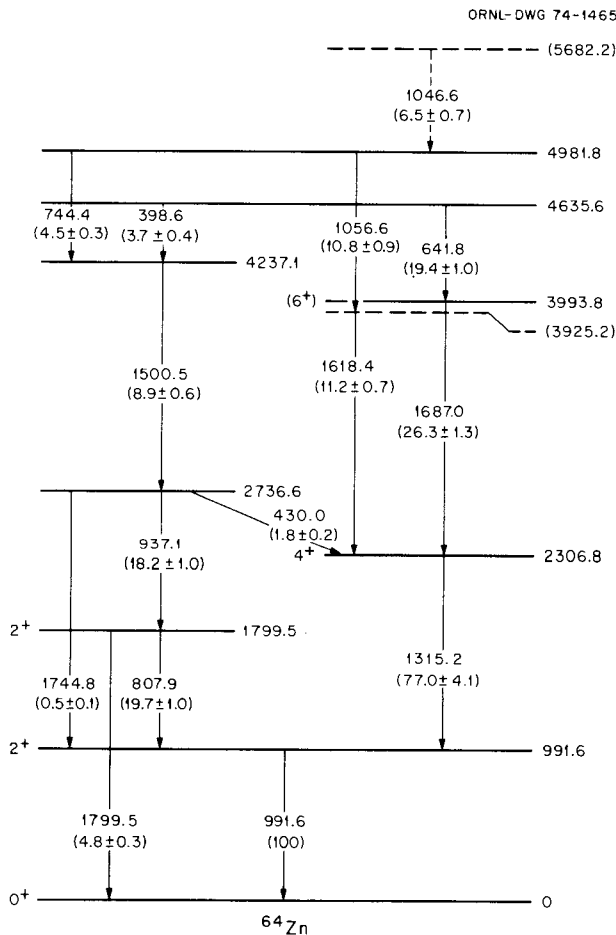


Fig. 2. Levels in ^{64}Zn observed via the $^{51}\text{V}(^{16}\text{O},p2n)$ reaction. The intensities, normalized to 100 for the 991.6-keV line, are those measured for 46-MeV ^{16}O ions incident on a thick ^{51}V target.

0.24 ± 0.02 , or a 5.8% $M2$ admixture, if $5^-(E1+M2)$ 4^+ is assumed. However, the weakness of the 1745-keV $4' \rightarrow 2$ transition is disturbing; we find $B(E2; 4' \rightarrow 2')/B(E2; 4' \rightarrow 2) = 810 \pm 160$.

A striking feature of the levels populated in the ($^{16}\text{O},p2n$) reaction is the absence of significant cross-feeding between the 2307-3994 keV yrast sequence and the 2737-4237 keV sequence. The side-feeding from unobserved transitions to both 4^+ states is about 50%. Both sequences are fed by transitions from the 4636-keV state that have large negative A_2 values.

Calculations to determine possible J^π values for high-lying states will be performed. Analysis of recoil-distance lifetime measurements and a more detailed search of the gamma-gamma coincident data for weak transitions are in progress.

1. Jointly supported by Vanderbilt University and ORNL; on leave from Furman University.

2. Postdoctoral Fellow under appointment with Oak Ridge Associated Universities.

3. Tennessee Technological University.

4. R. M. Lieder and J. E. Draper, *Phys. Rev. C* **2**, 531 (1970).

5. E. Nolte, W. Kutschera, Y. Shida, and H. Morinaga, *Phys. Lett.* **33B**, 294 (1970).

6. H. J. Kim, R. L. Robinson, W. T. Milner, and W. T. Bass, ORNL-4743 (1972).

7. W. G. Wyckoff and J. E. Draper, *Phys. Rev. C* **8**, 796 (1973).

8. O. E. Kraft et al., Program, XXI National Conference on Nuclear Spectroscopy and Structure, Acad. Nauk SSSR, p. 48 (1971).

9. M. Blann, *Phys. Rev.* **157**, 869 (1967), and private communication.

10. N. Alpert, J. Alster, and E. J. Martens, *Phys. Rev. C* **2**, 974 (1970).

RECOIL-DISTANCE LIFETIME MEASUREMENTS

R. O. Sayer¹ R. L. Robinson
N. C. Singhal² J. H. Hamilton²
W. T. Milner A. V. Ramayya²
G. J. Smith³

Many interesting new collective states in the nickel-krypton nuclei have been observed via in-beam gamma-ray experiments, but lifetimes have seldom been determined because conventional electronic and Coulomb excitation techniques cannot usually be applied. Since the lifetimes can be vital clues to the character of these collective motions, we have initiated a program of recoil-distance-Doppler-shift measurements at the ORNL tandem accelerator.

A particularly interesting case for study is the unstable nucleus ^{72}Se . The spectroscopic data suggest⁴ the coexistence of a spherical ground state with a deformed sequence built on the 937-keV 0^+ level.

There may also be such a coexistence in ^{186}Hg , where the first 2^+ and 4^+ states have vibrational-like spacings and the yrast levels with spins 6 to 14 have rotational spacings.⁵ One might expect larger $B(E2)$ values between the rotational levels than between the vibrational-like levels. Since the 4^+ "spherical" state and the 6^+ "deformed" state presumably are rather dissimilar, the $B(E2; 4 \rightarrow 6)$ may be small. On the other hand, strong mixing between "spherical" and "deformed" states near the crossing point is likely to wash out a possible reduction in $B(E2)$. Nonetheless, we felt that experimental lifetimes of the quasi-rotational states in ^{72}Se might provide a test of the coexistence model and possibly shed light on the extent of admixtures between states.

High-spin states in ^{72}Se were populated by the $^{58}\text{Ni}(^{16}\text{O}, 2p)$ reaction with 44 to 46-MeV ^{16}O ions from the tandem Van de Graaff. A precision plunger apparatus⁶ was employed in conjunction with a 24% Ge(Li) gamma-ray detector. Targets of thickness 0.5 to 1.0 mg/cm² were stretched over a conical annulus to a high degree of flatness and parallelism with a lead-covered stopper that could be positioned relative to the target to a precision of 2.5 μm . Gamma-ray spectra were acquired for several target-stopper distances, and results for four of the closer distances are presented in Fig. 1. The $2 \rightarrow 0$ and $4 \rightarrow 2$ unshifted peaks stand out clearly, but the 834-keV impurity line almost masks the $6 \rightarrow 4$ unshifted peak.

Figure 2 contains plots of R , the ratio of unshifted intensity to total intensity, vs the target-stopper distance, D . The constant background, which arises from the $T_{1/2} = 1.3$ min ^{72}Br decay following the $(^{16}\text{O}, pn)$ reaction, appreciably worsens the accuracy with which lifetimes can be extracted. However, a more serious problem for the $2 \rightarrow 0$ and $4 \rightarrow 2$ transitions is the effect of the 50 to 60% feeding from higher states. For example, inclusion of feeding reduced the extracted $2 \rightarrow 0$ lifetime by 35%.

A computer code was written to perform least-squares fits to the $\ln R$ vs D data corrected for (1) long-lived radioactivity, (2) two-stage cascade feeding from higher-lying states, (3) side-feeding from two higher states, (4) geometric and relativistic solid angle effects, and (5) smearing of the velocity distribution due to the finite size of the gamma-ray detector.⁷ Illustrations of the corrected data and best fits for the $2 \rightarrow 0$ and $4 \rightarrow 2$ transitions are given in Fig. 3. Note that the two fits have $R = 1$ intercepts that differ by only 1 μm .

Our preferred values of τ and $B(E2)$, given in Table 1, must be considered preliminary until the side-feeding and possible attenuation of gamma-ray angular distri-

butions by hyperfine interactions are taken into account. However, the former effect tends to increase τ , whereas the latter tends to decrease τ , so that some cancellation occurs. Interestingly, the $B(E2; 0 \rightarrow 2)$ value for ^{72}Se corresponds to $\beta_2 = 0.19 \pm 0.02$, which is significantly smaller than the β_2 value of 0.34 for the ^{74}Se nucleus. The ratio $B(E2; 4 \rightarrow 2)/B(E2; 2 \rightarrow 0) = 2.2_{-0.7}^{+1.4}$ is in good agreement with the vibrational prediction, although the uncertainties are large. Our

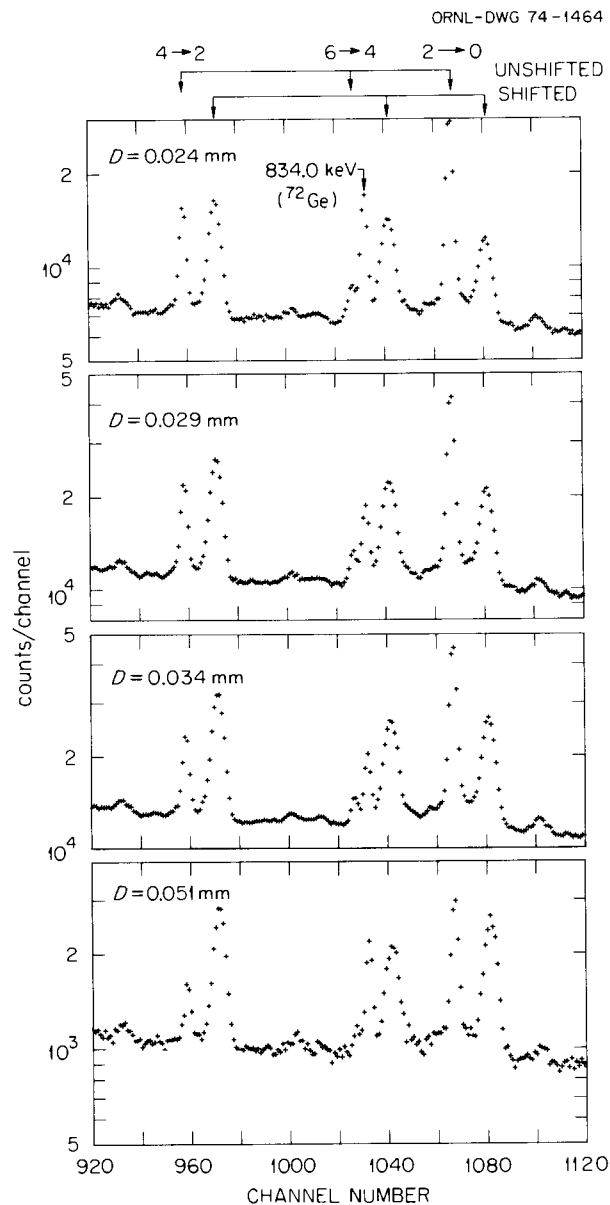


Fig. 1. Gamma-ray spectra for 44-MeV ^{16}O ions on a 0.5-mg/cm² ^{58}Ni target. D is the distance between target and stopper, and the $I \rightarrow I - 2$ values denote transitions in ^{72}Se .

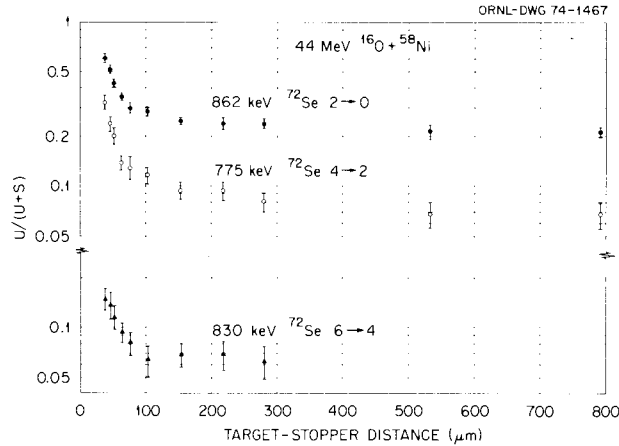


Fig. 2. Plot of R as a function of target-stopper distance for transitions in ^{72}Se .

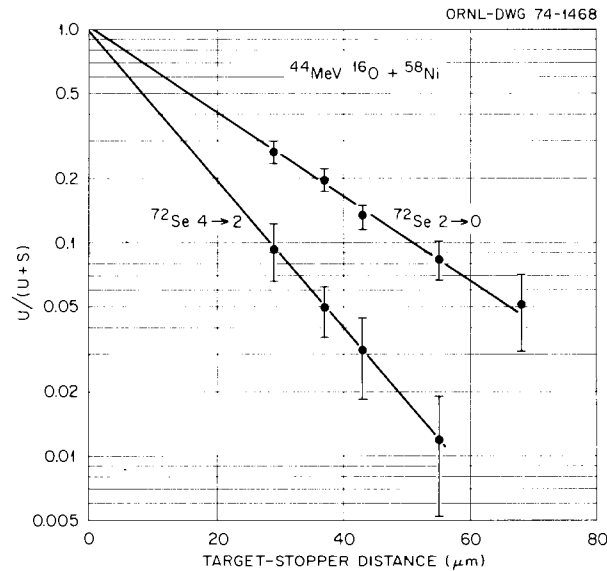


Fig. 3. Plot of R vs D using corrected data for the $2 \rightarrow 0$ and $4 \rightarrow 2$ transitions.

Table 1. Preliminary $B(E2)$ values for ^{72}Se

Transition, $f \rightarrow i$	E_γ (keV)	τ (psec)	$B(E2; f \rightarrow i)$ ($e^2 10^{-50} \text{ cm}^4$)	$B(E2)_{\text{ex}}$ B_{sp}
$2 \rightarrow 0$	862	5.7 ± 1.2	$3.0^{+0.8}_{-0.5}$	17^{+5}_{-3}
$4 \rightarrow 2$	775	4.5 ± 1.7	$6.5^{+3.9}_{-1.8}$	13^{+7}_{-4}
$6 \rightarrow 4$	830	6.5 ± 3.6	$3.2^{+4.0}_{-1.2}$	5^{+6}_{-2}

present $6 \rightarrow 4$ lifetime value has a rather large uncertainty, and we are analyzing the $8 \rightarrow 6$ transition to improve our estimate of the feeding correction for the 6^+ level.

These experiments will be done at higher projectile energy to enhance population of high-spin states, and gamma-gamma coincident measurements to minimize contamination of gamma rays from competing reactions are being considered. Analysis of recoil-distance measurements utilizing the $^{60}\text{Ni}(^{16}\text{O}, 2p)^{74}\text{Se}$ and $^{51}\text{V}(^{16}\text{O}, p2n)^{64}\text{Zn}$ reactions is in progress.

1. Jointly supported by Vanderbilt University and ORNL; on leave from Furman University.

2. Vanderbilt University, Nashville, Tenn.

3. Postdoctoral Fellow under appointment with Oak Ridge Associated Universities.

4. J. H. Hamilton, A. V. Ramayya, W. T. Pinkston, R. M. Ronnigen, G. Garcia-Bermudez, H. K. Carter, R. L. Robinson, H. J. Kim, and R. O. Sayer, *Phys. Rev. Lett.* **32**, 239 (1974).

5. D. Proetel, R. M. Diamond, P. Kienle, J. R. Leigh, K. H. Maier, and F. S. Stephens, *Phys. Rev. Lett.* **31**, 896 (1973).

6. Designed and constructed by E. Chandler, Plant and Equipment Division, and E. Eichler, N. R. Johnson, and R. Sturm, Chemistry Division. We are indebted to Drs. Eichler, Johnson, and Sturm for valuable suggestions for the data analysis procedures and helpful discussion of the physical processes involved.

7. M. W. Guidry and R. Sturm have developed a more elaborate code which includes multistage cascade feeding corrections and the attenuation of gamma-ray angular distributions by the hyperfine interaction.

ROTATIONAL AND QUASI-ROTATIONAL BANDS IN EVEN-EVEN NUCLEI

R. O. Sayer¹ J. S. Smith III²
W. T. Milner

Experimental and theoretical interest in rotational states was spurred by the recent discovery³ that the nuclear moment of inertia of ^{160}Dy increases sharply at spin 12. Soon afterward, Johnson et al.⁴ found that the rotational frequency of ^{162}Er increases as expected up to spin 14, then decreases from spin 14 to spin 16, and once again increases above spin 16. This "back-bending" behavior is best illustrated by the now-familiar S-shaped plot of the moment of inertia, \mathcal{J} , as a function of the square of the rotational frequency, $\hbar\omega$.

Numerous heavy-ion in-beam experiments performed in the past two years have led to the construction of rotational sequences of states up to very high spins. In three cases,⁵⁻⁷ states with spin 22 have been observed. The accuracy and extent of these new data indicate a need for a more up-to-date compilation of rotational levels than those of Mariscotti et al.⁸ and Sakai.⁹

Recently Saethre et al.¹⁰ fitted a phenomenological expansion in terms of the angular velocity to experimental energies of rotational states in 63 doubly even nuclei from ^{128}Ce to ^{194}Pt . However, these authors did not include nuclei outside the cerium-platinum region, and they considered only the ground-state bands. Moreover, approximately 75 new high-spin members of the ground bands in the cerium-platinum region have been found since the work of Saethre et al.

We have undertaken a compilation of transition energies between states in rotational and quasi-rotational ground bands in all even-even nuclei. To date, 185 ground bands with states of spin 6 or higher have been found. Selected cases of bands built on excited 0^+ states will be included. Previous compilations⁸⁻¹¹ have been especially helpful, but original papers were scanned whenever possible. A search of the literature through August 31, 1973, has been completed, and review of more recent papers is in progress.

Since a plot of $2\mathcal{J}/\hbar^2$ vs $(\hbar\omega)^2$ is quite sensitive to deviations from rotational behavior, a computer code was written to generate the desired plots from the experimental energies. Sample plots are given in Fig. 1, where the number I denotes the point that corresponds

to the transition $I \rightarrow I - 2$. Straight lines are drawn between points as a visual guide and do not necessarily indicate any functional form for the variation of \mathcal{J} with ω^2 .

1. Jointly supported by Vanderbilt University and ORNL; on leave from Furman University.
2. Furman University.
3. A. Johnson, H. Ryde, and J. Sztarkier, *Phys. Lett.* **34B**, 605 (1971).
4. A. Johnson, H. Ryde, and S. A. Hjorth, *Nucl. Phys.* **A179**, 753 (1972).
5. P. Thieberger, A. W. Sunyar, P. C. Rogers, N. Lark, O. C. Kistner, E. der Mateosian, S. Cochavi, and E. H. Auerbach, *Phys. Rev. Lett.* **28**, 972 (1972).
6. P. H. Stelson, G. B. Hagemann, D. C. Hensley, R. L. Robinson, L. L. Riedinger, and R. O. Sayer, *Bull. Amer. Phys. Soc.* **18**, 581 (1973).
7. L. L. Riedinger, private communication.
8. M. A. J. Mariscotti, G. Scharff-Goldhaber, and B. Buck, *Phys. Rev.* **178**, 1864 (1969).
9. M. Sakai, *Nucl. Data* **A8**, 323 (1970); *Nucl. Data* **A10**, 511 (1972).
10. O. Saethre, S. A. Hjorth, A. Johnson, S. Jagare, H. Ryde, and Z. Szymanski, *Nucl. Phys.* **A207**, 486 (1973).
11. J. L. Wood, Institut für Angewandte Kernphysik, KFK Enterner Bericht 1/72-1, September 1972.

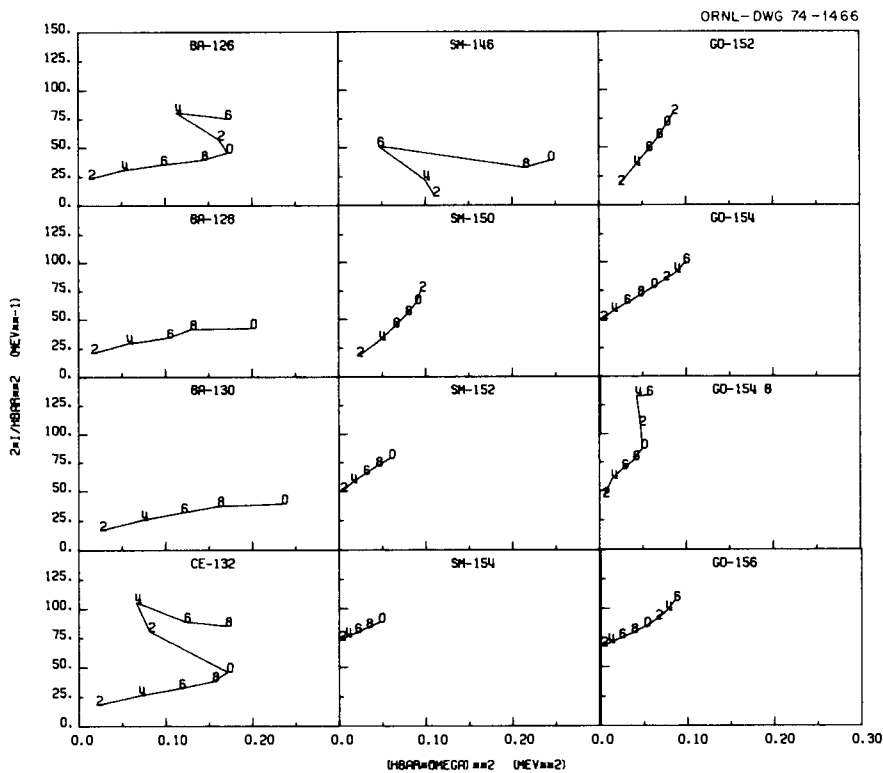


Fig. 1. Sample plots of $2\mathcal{J}/\hbar^2$ vs $(\hbar\omega)^2$.

EXCITATION OF ROTATIONAL BANDS
IN ^{20}Ne BY THE $^{10}\text{B}(^{16}\text{O}, ^6\text{Li})$ REACTION

J. L. C. Ford, Jr. S. T. Thornton²
J. Gomez del Campo¹ R. L. Robinson
P. H. Stelson

Measured cross sections for light ions emitted in such processes as the $^{10}\text{B}(^{16}\text{O}, d)$, $^{10}\text{B}(^{16}\text{O}, \alpha)$, $^{12}\text{C}(^{12}\text{C}, \alpha)$, and $^{12}\text{C}(^{16}\text{O}, \alpha)$ reactions have been well reproduced by Hauser-Feshbach calculations (see, e.g., refs. 3-7). Since heavy-ion reactions preferentially populate high-spin states, comparison of such data with statistical reaction models potentially provides a significant technique for assigning spin values to high-spin states. The reliability of this approach for reactions involving the emission of more complex nuclei has been explored in the present work. Cross sections for states of known

spins in ^{20}Ne excited through the $^{10}\text{B}(^{16}\text{O}, ^6\text{Li})$ reaction were compared with Hauser-Feshbach calculations. The good agreement between these calculations and the data indicates that such a comparison is useful for suggesting spin values at high excitation energies, and this method has been used to delineate the rotational bands in ^{20}Ne .

Thin ^{10}B targets were bombarded by ^{16}O ions from the Oak Ridge tandem accelerator. The ^{10}B targets were typically 10 to 30 $\mu\text{g}/\text{cm}^2$ thick and enriched to about 95% in ^{10}B . The reaction products were detected by a 60-cm-long position-sensitive proportional counter⁸⁻¹⁰ located at the focal plane of an Enge split-pole magnetic spectrograph.

In addition to the position information obtained from the timing signals, the energy lost in the detector served as a ΔE signal for particle identification. Excitation

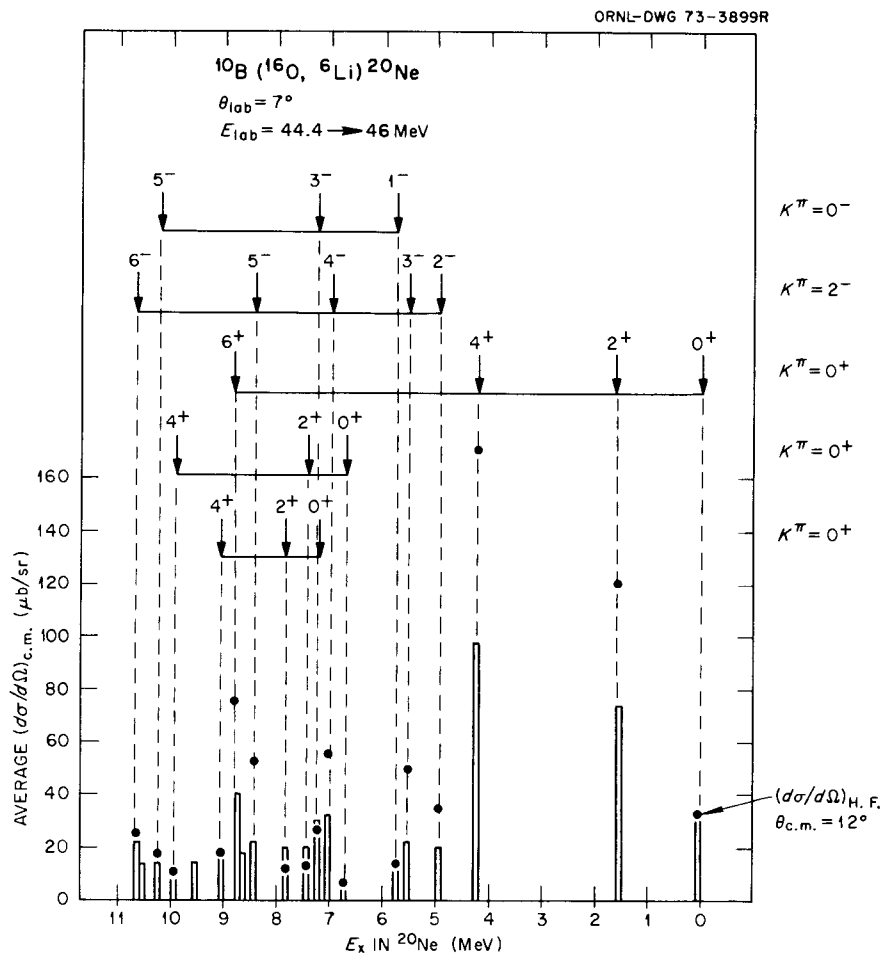


Fig. 1. A histogram of the measured $^{10}\text{B}(^{16}\text{O}, ^6\text{Li})^{20}\text{Ne}$ cross sections averaged over the energy interval 44.4 to 46.0 MeV. The points indicate the cross sections calculated for these states in ^{20}Ne using Hauser-Feshbach theory and the spins shown on the figure. The level diagram of ^{20}Ne has been separated into the different rotational bands.

functions at 7° (lab) have been measured for the $^{10}\text{B}(^{16}\text{O},^6\text{Li})$ reaction in 400-keV intervals from 44.4 to 46.0 MeV, in the laboratory system.

Experimental cross sections may be compared with the average cross sections computed from Hauser-Feshbach theory provided that the reaction is due to a compound-nuclear statistical process and that the data have been averaged over an energy interval sufficiently broad to damp out the strong statistical fluctuations which occur in heavy-ion reactions. Since data in the present experiment were measured over a 1.6-MeV (0.61 MeV c.m.) interval in bombarding energy, the average of the experimental cross sections over this interval should damp out the fluctuations, which have widths of 100 to 150 keV. Figure 1 shows histograms for the average cross sections observed for the $^{10}\text{B}(^{16}\text{O},^6\text{Li})$ reaction.

The $^{10}\text{B} + ^{16}\text{O}$ reactions appear to be due to compound-nucleus formation. The extensive excitation functions and angular distributions measured for the $^{10}\text{B}(^{16}\text{O},\alpha)$ reaction, which supplement the results reported in this paper, have been compared with fluctuation and Hauser-Feshbach calculations.³ The results are generally compatible with the compound process. The Hauser-Feshbach calculations were made with the computer code HELGA expanded to allow calculations with many partial waves and large radii.¹¹ A total of ten reactions leading to different final nuclei were contained in the calculation, which included both total and differential cross sections for the states of interest. The calculated cross sections are shown as dots in Fig. 1 for comparison with the average experimental cross sections. In view of the uncertainties in the optical-model parameters, particularly for exit channels corresponding to highly excited states, and in the energy and spin dependence of the level density parameters for high-lying states, the agreement is surprisingly good.

1. University of Mexico, Mexico City.

2. University of Virginia, Charlottesville, Va.

3. J. Gomez del Campo, J. L. C. Ford, Jr., S. T. Thornton, R. L. Robinson, and P. H. Stelson, to be published.

4. J. L. C. Ford, Jr., J. Gomez del Campo, S. T. Thornton, R. L. Robinson, and P. H. Stelson, to be published.

5. L. R. Greenwood, K. Katori, R. E. Malmin, T. H. Braid, J. C. Stoltzfus, and R. H. Siemssen, *Phys. Rev. C* **6**, 2112 (1972).

6. E. W. Vogt, D. McPherson, J. Kuehner, and E. Almquist, *Phys. Rev.* **136**, B99 (1964).

7. R. Stokstad, cited by R. Middleton, *Proceedings of Heavy-Ion Summer Study*, CONF-720669, ed. by S. T. Thornton, Oak Ridge National Laboratory, June 1972 (National Technical Information Services, U.S. Dept. of Commerce, Springfield, Va.), p. 315, and private communication.

8. C. J. Borkowski and M. K. Kopp, *Rev. Sci. Instrum.* **39**(10), 1515 (1968).

9. C. J. Borkowski and M. K. Kopp, *IEEE Trans. Nucl. Sci. NS-17*(3), 340 (1970).

10. J. L. C. Ford, Jr., P. H. Stelson, and R. L. Robinson, *Nucl. Instrum. Methods* **98**, 199 (1972).

11. S. K. Penny, private communication.

POPULATION OF HIGH-SPIN STATES IN ^{22}Na BY MEANS OF THE $^{10}\text{B}(^{16}\text{O},\alpha)$ REACTION

J. Gomez del Campo ¹	R. L. Robinson
J. L. C. Ford, Jr.	P. H. Stelson
S. T. Thornton ²	J. B. McGroory

Recently, there has been a great deal of interest in high-spin states in light nuclei, particularly the higher members of the rotational bands of *s-d* shell nuclei (see, e.g., refs. 3–5). Heavy-ion reactions may selectively populate states that have high excitation energies³ and usually have high spins.⁴ Here we report a study of the level structure of ^{22}Na up to excitation energies of about 14 MeV by means of the $^{10}\text{B}(^{16}\text{O},\alpha)$ reaction. The observed symmetry of the alpha-particle angular distributions around 90° (c.m.), together with the analyses of the extensive excitation function measurements in terms of correlation functions and probability distributions, strongly suggests a compound-nucleus mechanism for the reaction. A comparison of the measured heavy-ion cross sections with the results of Hauser-Feshbach calculations indicates this is a significant technique for suggesting spin values. Excellent agreement for the higher-spin members of the rotational bands of ^{22}Na was found between shell-model predictions and the results of the Hauser-Feshbach calculations.

Enriched ^{10}B targets with thicknesses of about 20 $\mu\text{g}/\text{cm}^2$ were bombarded with ^{16}O ions extracted from the Oak Ridge tandem accelerator. The emitted alpha particles were detected with a 60-cm-long position-sensitive detector⁶ placed in the focal plane of an Enge split-pole magnetic spectrograph. Angular distributions were measured at a bombarding energy of 46 MeV between 10° and 135° (c.m.) for excited states below 8 MeV in ^{22}Na and at forward angles for states between 8 and 14 MeV in excitation energy.

Candidates for the high-spin members of the various bands were suggested by comparing the experimental spectra with the Hauser-Feshbach predictions, as calculated with the computer program HELGA,⁷ for the intensity of different spin states as a function of excitation energy and with the results of extensive shell-model calculations. These calculations are similar

to other shell-model calculations in this region reported previously.⁸ The effective residual interaction used was one developed for this mass region by Preedom and Wildenthal.⁹ The first three levels of the ground-state band and the first two levels of the $K = 0^+$, $T = 0$ band were used to determine the residual interaction. The interaction was essentially forced to reproduce these five levels. The shell-model calculations are purely predictive for all the remaining higher-spin states.

Figure 1 summarizes our assignments for the members of the $K = 3^+$, $T = 0$ and $K = 0^+$, $T = 0$ bands of ^{22}Na . The dots are the experimentally observed states, and the crosses are those predicted by the shell model. The extrapolated candidates for the members of the $K = 1^-$, $T = 0$ band are shown as well, although the selection of these states is more ambiguous than for the positive-parity bands.

1. University of Mexico, Mexico City.
2. University of Virginia, Charlottesville, Va.
3. R. Middleton, J. D. Garrett, and H. T. Fortune, *Phys. Rev. Lett.* **28**, 1436 (1970).
4. A. Gobbi, P. R. Maurenz, L. Chua, R. Hadsell, P. D. Parker, M. W. Sachs, D. Shapira, R. Stokstad, R. Wichand, and D. A. Bromley, *Phys. Rev. Lett.* **26**, 396 (1971).

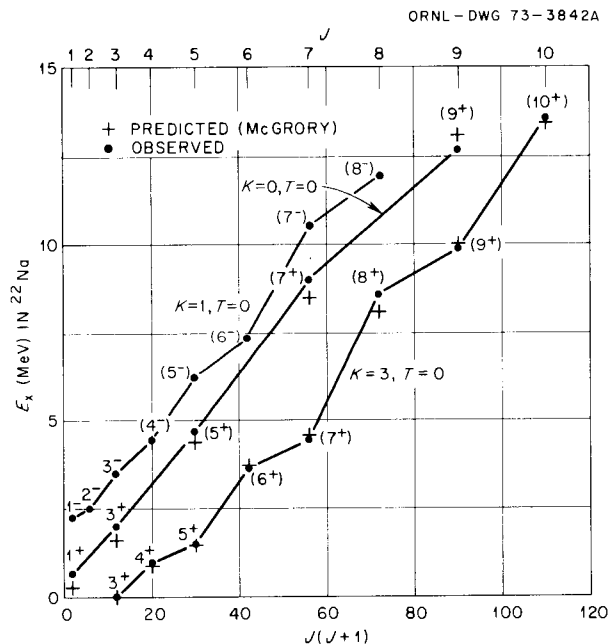


Fig. 1. A plot of the $K = 3^+$, $T = 0$; $K = 0^+$, $T = 0$; and $K = 1^-$, $T = 0$ rotational bands in ^{22}Na . The dots represent the experimentally observed states, and the crosses are the result of extensive shell-model calculations.

5. H. T. Fortune, *Proceedings of the Heavy-Ion Summer Study*, CONF-720669, ed. by S. T. Thornton, Oak Ridge National Laboratory, June 1972 (National Technical Information Services, U.S. Dept. of Commerce, Springfield, Va.), p. 353.

6. J. L. C. Ford, Jr., P. H. Stelson, and R. L. Robinson, *Nucl. Instrum. Methods* **98**, 199 (1972).

7. S. K. Penny, Oak Ridge National Laboratory, private communication.

8. E. C. Halbert, J. B. McGrory, B. H. Wildenthal, and S. P. Pandya in *Advances in Nuclear Physics*, vol. 4, ed. by M. Baranger and E. Vogt (Plenum Press, New York, 1971), p. 315.

9. B. M. Freedom and B. H. Wildenthal, *Phys. Rev. C* **7**, 1633 (1972).

ABSOLUTE CROSS SECTIONS FOR THE $^{61}\text{Ni}(^{16}\text{O}, X)$ REACTIONS

J. C. Wells¹ H. J. Kim
R. L. Robinson J. L. C. Ford, Jr.

We have continued a program of measuring the cross sections of as many exit channels as possible for reactions induced with heavy-ion projectiles. The principal motivation was to investigate quantitatively heavy-ion reactions as a tool for producing neutron-deficient nuclei by providing data that can be used to test existing models which predict the cross sections for such reactions. These studies are being conducted in a mass region and projectile energy range where most of the reaction products can be readily identified by gamma rays from the resulting radioactivities and in-beam gamma rays.

Here we report results for bombardment of a 1-mg/cm² target enriched to 99% in ^{61}Ni with 38.5- to 51.0-MeV ^{16}O ions from the Oak Ridge tandem accelerator. Gamma-ray spectroscopy was used to identify the reaction products as discussed in ref. 2.

The experimental results are illustrated in Figs. 1-5. Two sets of theoretical predictions are also illustrated. The first, denoted as "calculated without spin" in the figures, was calculated with the program BLANNTL written by Blann³ and modified to include a transmission coefficient subroutine written by Smith.⁴ The second calculations, "calculated with spin," were performed with the program ALICE.⁵ Both versions assume statistical decay of neutrons, protons, and alpha particles from a compound nucleus. In BLANNTL, the same level density is taken for all spins. The program ALICE improves on the program BLANNTL by including a spin-dependent level density and assuming each type of particle removes a constant angular momentum; these were: $l_{\text{neutron}} = 2$, $l_{\text{proton}} = 3$, and $l_{\text{alpha}} = 10$.

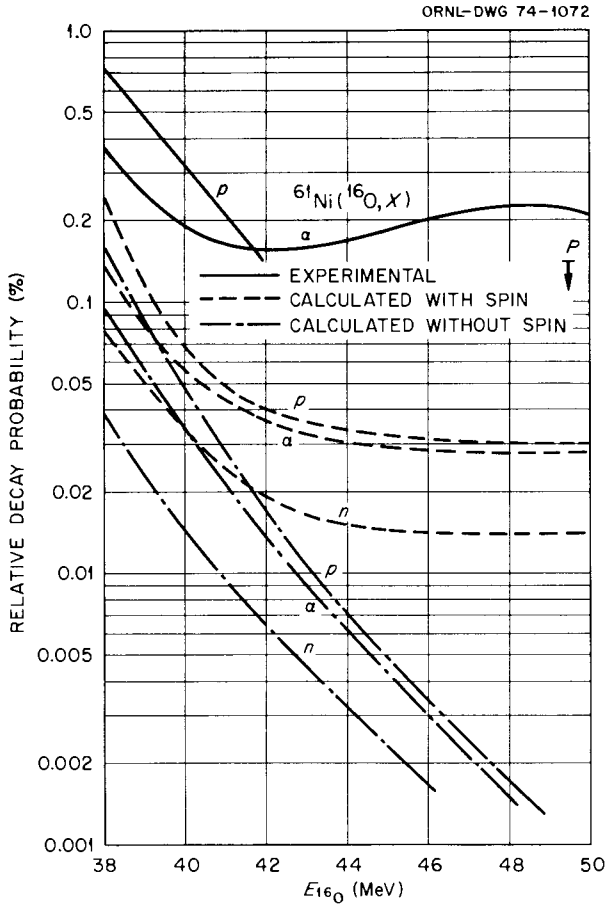
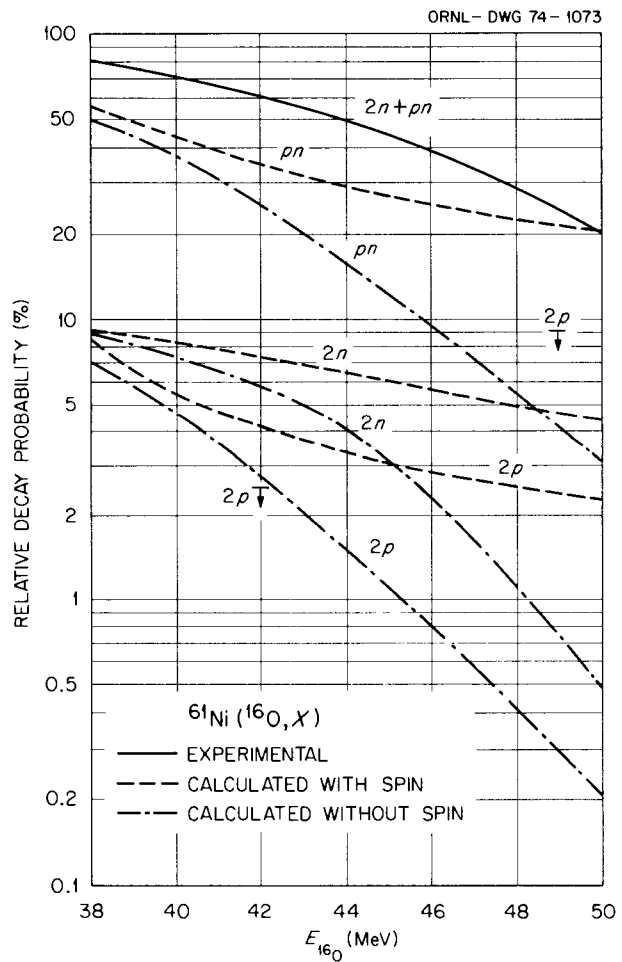


Fig. 2. Comparison of relative experimental cross sections for $^{61}\text{Ni}(^{16}\text{O}, X)$ reactions with predictions for statistical decay from a compound nucleus where X is 2n, 2p, or pn. Cross sections are given in percent of the total reaction cross section.

Fig. 1. Comparison of relative experimental cross sections for $^{61}\text{Ni}(^{16}\text{O}, X)$ reactions with predictions in which neutrons, protons, and alpha particles are assumed to statistically decay from a compound nucleus. Cross sections are given in percent of the total reaction cross section.



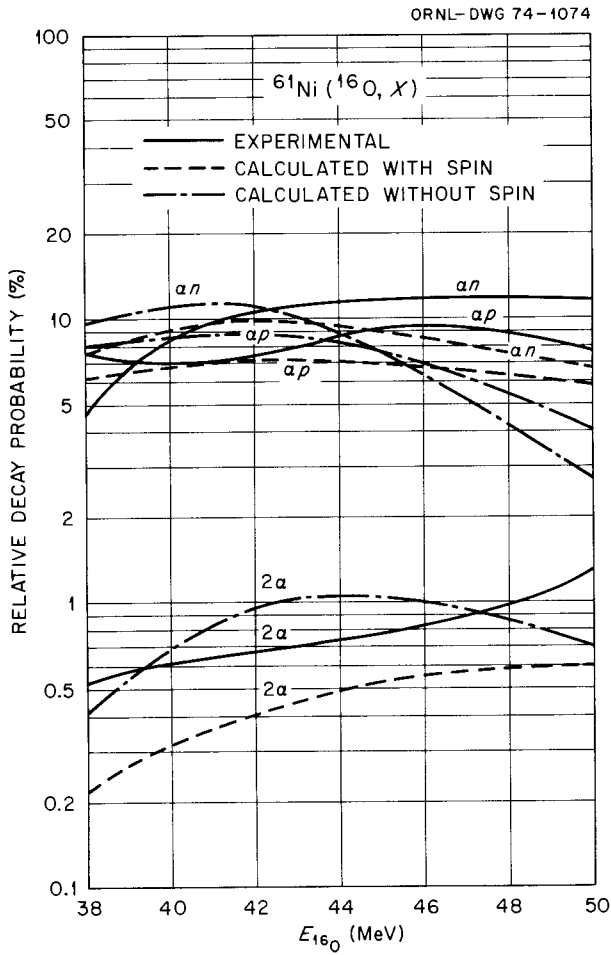
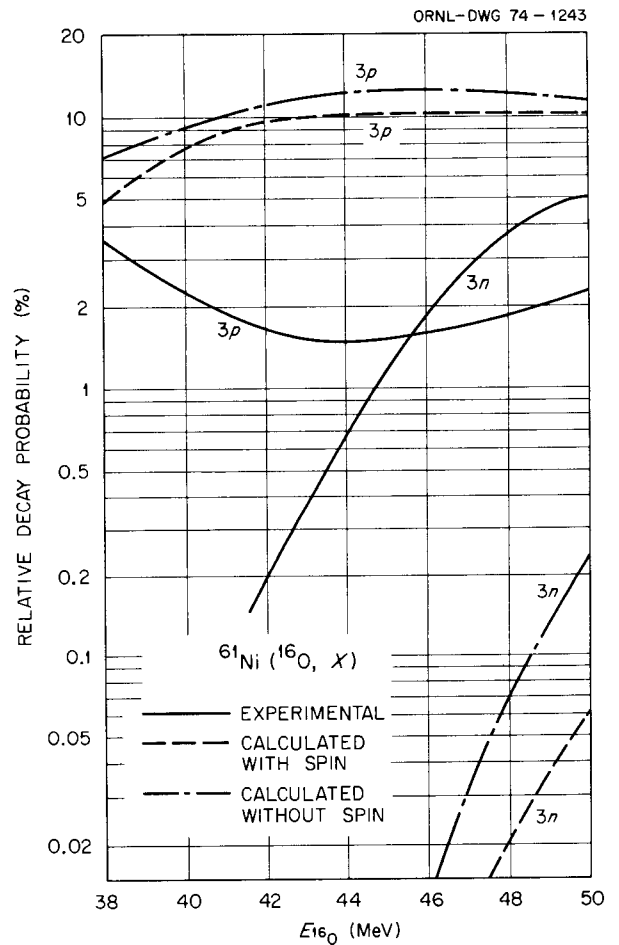


Fig. 4. Comparison of relative experimental cross sections for $^{61}\text{Ni}(^{16}\text{O}, X)$ reactions with predictions for statistical decay from a compound nucleus where X is $3n$ or $3p$. Cross sections are given in percent of the total reaction cross section.

Fig. 3. Comparison of relative experimental cross sections for $^{61}\text{Ni}(^{16}\text{O}, X)$ reactions with predictions for statistical decay from a compound nucleus where X is 2α , an , or ap . Cross sections are given in percent of the total reaction cross section.



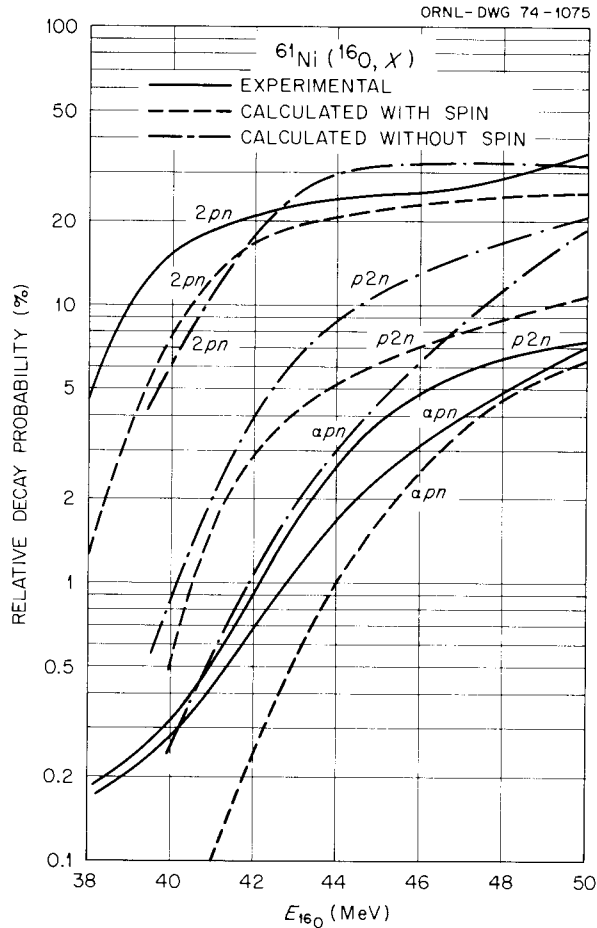


Fig. 5. Comparison of relative experimental cross sections for $^{61}\text{Ni}(^{16}\text{O},\text{X})$ reactions with predictions for statistical decay from a compound nucleus where X is $2pn$, $p2n$, or apn . Cross sections are given in percent of the total reaction cross section.

Except for the ($^{16}\text{O},3p$) channel, the agreement between experiment and theory is best for reactions in which theory predicts a large cross section (more than 5% of the total cross section). Generally the "with-spin" calculations are more similar to experiment. There are several very large differences which occur for the weaker reactions. (This may be significant in terms of calculating production of nuclei well away from stability, since these are very weak reactions.) For example, experimental cross sections for reactions in which one nucleon is emitted are at the higher projectile energies a decade larger than theory (see Fig. 1). In particular, note in Fig. 4 that the experimental cross section for the ($^{16}\text{O},3n$) reaction, the one that takes us farthest from the valley of stability at this projectile energy, is much larger than calculated.

1. Tennessee Technological University, Cookeville, Tenn.
2. R. L. Robinson, H. J. Kim, and J. L. C. Ford, Jr., *Phys. Rev.*, to be published.
3. M. Blann, *Phys. Rev.* **157**, 860 (1967); *Proc. Heavy Ion Summer Study*, ORNL, CONF-720669, ed. by S. T. Thornton, p. 269 (1972).
4. W. R. Smith, *Comput. Phys. Commun.* **1**, 106 (1969).
5. M. Blann and F. Plasil, private communication.

HEAVY-ION NEUTRON YIELDS

J. K. Bair P. D. Miller
P. H. Stelson

Nuclear cross sections for the low-energy interactions between various combinations of carbon and oxygen beams and targets have, in addition to their usual nuclear physics value, considerable astrophysical interest. We are, therefore, in the progress of extending our previously reported¹ work on the neutron yield resulting from the bombardment of thin targets by ^{16}O and ^{18}O beams to include bombardments by carbon beams.

We now have obtained preliminary neutron yield curves from well above the Coulomb barrier down to center-of-mass energies of 3.9 MeV for $^{12}\text{C}(^{12}\text{C},xn)$ and to 3.5 MeV for $^{13}\text{C}(^{12}\text{C},xn)$. Target thicknesses were approximately $50\ \mu\text{g}/\text{cm}^2$. The ^{12}C on ^{12}C data show considerable structure, in agreement with the measurements of Patterson et al.;² this is in marked contrast to the ^{12}C on ^{13}C case, where no structure is observed. The $^{12}\text{C}(^{13}\text{C},xn)$ cross section at the very low energies is 50 to 100 times that of the $^{12}\text{C}(^{12}\text{C},xn)$ reaction, thus necessitating a rather large correction for the small amount of ^{13}C in our normal isotopic mixture " ^{12}C " targets. When we make this correction, we obtain a preliminary cross section of 0.017 mb at a center-of-mass energy of 4.21 MeV; this compares with Patterson's value of $(0.014 \pm 30\%)$ at their lowest bombarding energy of 4.23 MeV. No previous $^{13}\text{C}(^{12}\text{C},xn)$ measurements are available for comparison.

1. W. B. Dress, J. K. Bair, C. H. Johnson, and P. H. Stelson, *Bull. Amer. Phys. Soc.* **17**, 530 (1972).
2. J. R. Patterson, H. Winkler, and C. S. Zaidins, *Astrophys. J.* **157**, 367 (1969).

COMPARISON OF CROSS SECTIONS FOR THE Ni, Cu, Zn ($^{16}\text{O},xn$) REACTIONS WITH THEORY

R. L. Robinson J. K. Bair

An important application of heavy-ion projectiles is in the production of new and scantily studied neutron-

deficient nuclei. However, it is not known how far from stability nuclei can be made by this technique in detectable quantity. Predictions have been made using a model in which light particles are statistically emitted from a compound nucleus formed with the heavy-ion projectile and target nucleus. But there are many unknowns in these complex calculations: What are the spin distributions of the states in the compound-nuclear system? What is the dependence of the level density on spin and of yrast level on energy? What is the competition between particle emission, gamma-ray emission, and fission? How important is preequilibrium decay? And there is still limited quantitative information about these cross sections.

In order to produce nuclei far from the valley of beta stability, predominantly neutrons must be evaporated. Bair, Dress, Johnson, and Stelson¹ have recently determined the absolute cross sections for neutrons emitted in reactions between $^{16,18}\text{O}$ and $^{58,60,61,62,64}\text{Ni}$, $^{63,65}\text{Cu}$, and $^{64,66,67,68,70}\text{Zn}$, for projectile energies between 36 and 55 MeV. We have compared these results with calculated values obtained from the product of (1) the reaction cross section predicted by an optical model and (2) the number of neutrons emitted per reaction resulting from evaporation from a compound nucleus. For the optical-model calculations, the program GENOA was used;² the parameters, taken from the work of Christensen et al.,³ were: $V = 29.4$ MeV, $r_0 = r'_0 = 1.30$ fm, $a = a' = 0.491$ fm, $W = 2.43$ MeV, and $r_0(\text{coul}) = 1.25$ fm. The evaporation calculations were made with a computer program developed by Blann.⁴ This version assumed the same level density for all spins. As has been observed experimentally, these calculations do predict a strong dependence of neutron emission on the neutron richness of the target nucleus and projectile. Figure 1 gives one example of this.

Figures 2 and 3 show comparisons between the experimental and calculated results for the nickel isotopes. Similar plots exist for the copper and zinc targets. In most cases the experimental values fall

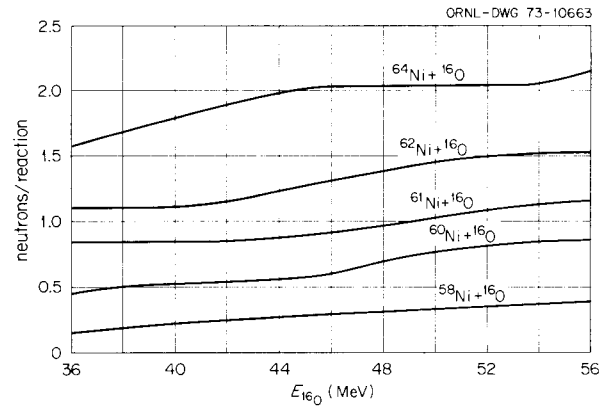


Fig. 1. Predicted number of neutrons emitted per reaction for bombardment of nickel isotopes with ^{16}O ions.

somewhat above the calculated values for the low projectile energies (below the classical Coulomb barrier). In this region the predicted reaction cross section is highly sensitive to the choice of optical-model parameters and could be brought into agreement with appropriate parameters. The worst agreement at the higher projectile energies is for the $^{16}\text{O} + ^{58}\text{Ni}$ reaction. This is the reaction which leads to the compound nucleus farthest from the valley of stability and in which the fewest number of neutrons per reaction are emitted. Thus, for the reaction of most importance in terms of making nuclei far from stability, the predictions are the worst.

1. J. K. Bair, W. B. Dress, C. H. Johnson, and P. H. Stelson, private communication and *Bull. Amer. Phys. Soc.* 17, 530 (1972).

2. F. G. Perey, private communication.

3. P. R. Christensen, I. Chernov, E. E. Gross, R. Stokstad, and F. Videbaek, *Nucl. Phys.* A207, 433 (1973).

4. M. Blann, *Phys. Rev.* 157, 860 (1967); *Proc. Heavy Ion Summer Study*, ORNL, CONF-720669 (ed. by S. T. Thornton, p. 269 (1972).

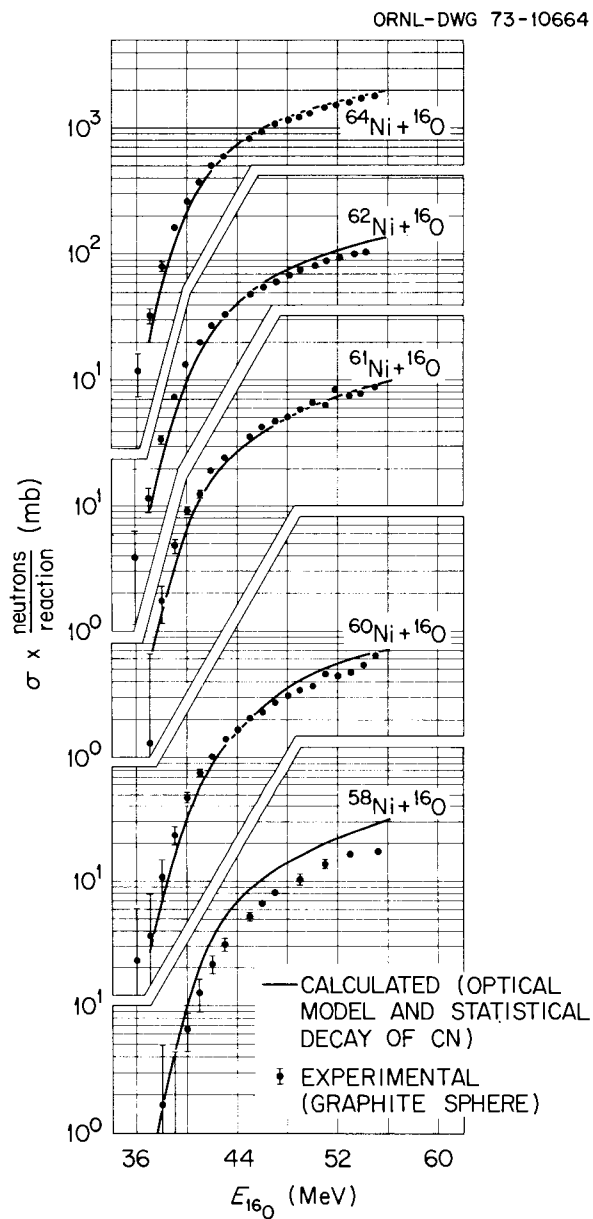


Fig. 2. Comparison of the experimental cross sections for neutron emission obtained by Bair et al. with calculated values for $^{16}\text{O} + \text{Ni}$ reactions. Experimental values from J. K. Bair et al., private communication and *Bull. Amer. Phys. Soc.* 17, 530 (1972).

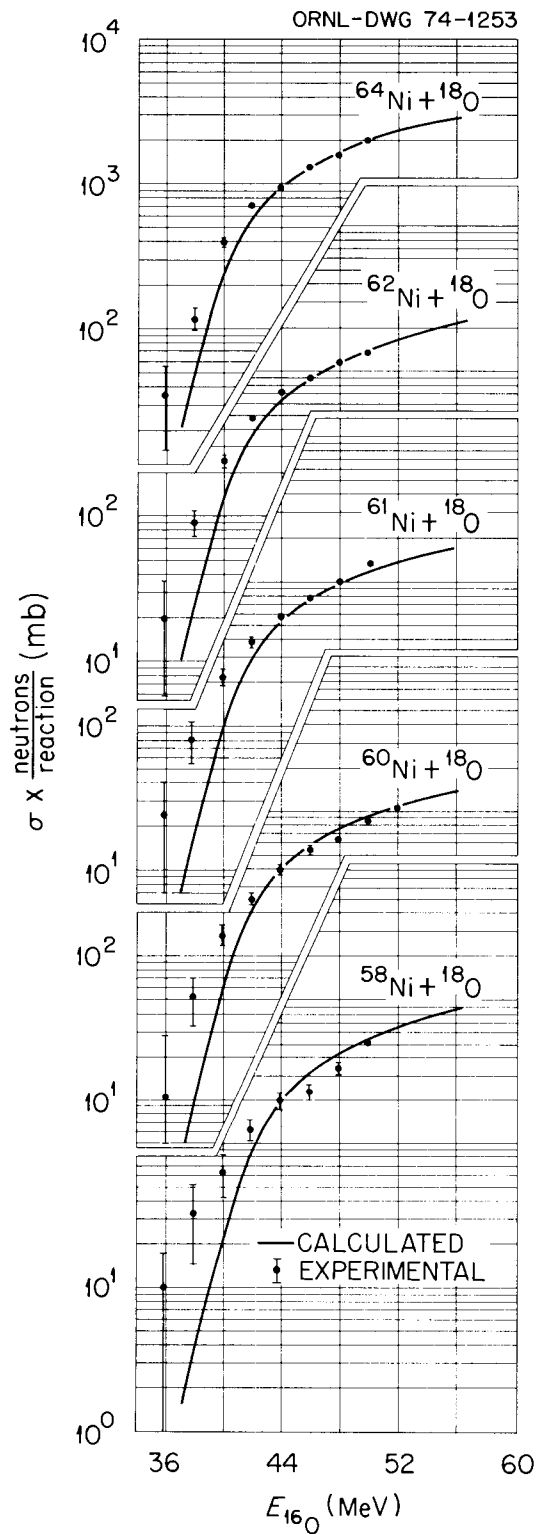


Fig. 3. Comparison of the experimental cross sections for neutron emission obtained by Bair et al. with calculated values for $^{18}\text{O} + \text{Ni}$ reactions. Experimental values from J. K. Bair et al., private communication and *Bull. Amer. Phys. Soc.* 17, 530 (1972).

COULOMB EXCITATION

COULOMB EXCITATION OF VIBRATIONAL-LIKE STATES IN THE EVEN-*A* ACTINIDE NUCLEI

F. K. McGowan J. L. C. Ford, Jr.
 C. E. Bemis, Jr.¹ R. L. Robinson
 W. T. Milner P. H. Stelson

The low-lying negative-parity states in radium and lighter thorium isotopes have very low energies. These states could possibly be interpreted as rotational states of a static octupole deformation. However, theoretical calculations which minimize the total potential energy with respect to deformations by Vogel² indicate a stable equilibrium shape with $\beta_{30} = 0$. An alternative interpretation is that these states are members of the one-phonon octupole vibrational spectrum which contains four states $K = 0, 1, 2,$ and 3 with associated rotational spectra. This vibrational interpretation provides an interesting theoretical framework with which to compare the experimental information. The microscopic calculations of $B(E3, 0 \rightarrow 3)$ for the 3^- members of the one-phonon octupole quadruplet by Neegard and Vogel,³ which included the influence of the Coriolis coupling between states with K and $K \pm 1$, are in good agreement with the experimental data for nuclei in the rare-earth region. The inclusion of the Coriolis interaction in the microscopic calculations is required to

explain satisfactorily the distribution of the $B(E3)$ strength⁴ among the one-phonon octupole vibrational states. On the other hand, for nuclei in the actinide region, there are very few experimental $B(E3, 0 \rightarrow 3)$ to compare with the microscopic calculations.⁵

This communication summarizes the $B(E\lambda, 0 \rightarrow J = \lambda)$ deduced from measured Coulomb excitation probabilities in the actinide nuclei. The experiments were performed using ^4He ions accelerated in the EN tandem. The scattered ^4He ions from $25\text{-}\mu\text{g}/\text{cm}^2$ actinide targets were detected at the focal plane of an Enge split-pole spectrometer by a position-sensitive gas proportional detector. The experimental results for $B(E\lambda, 0 \rightarrow J = \lambda)$ are given in Table 1. A comparison between the microscopic calculations of the $B(E3, 0 \rightarrow 3)$ for the 3^- members of the one-phonon octupole quadruplet and the experimental results is presented in Table 2. For those cases where the K, J^π assignments are known, the general features of the experimental data are reproduced by the Coriolis-coupled wave functions and confirms the basic assumption about the structure of octupole states in the deformed actinide nuclei.

-
1. Chemistry Division.
 2. P. Vogel, *Nucl. Phys.* **A112**, 583 (1968).
 3. K. Neegard and P. Vogel, *Nucl. Phys.* **A145**, 33 (1970).
 4. K. Neegard and P. Vogel, *Phys. Lett.* **30B**, 75 (1969).
 5. K. Neegard and P. Vogel, *Nucl. Phys.* **A149**, 217 (1970).

Table 1. Experimental results for $B(E\lambda, 0 \rightarrow J = \lambda)$

For those cases where the K, J^π assignments of the states are not known from other nuclear spectroscopy studies, the $B(E\lambda, 0 \rightarrow J = \lambda)$ are given for both assignments $J = 2^+$ and $J = 3^-$

Nucleus	Level (keV)	K, J^π	$E\lambda$	$B(E\lambda, 0 \rightarrow J)$ ($e^2 b^\lambda$)	$B(E\lambda)/B(E\lambda)_{sp}^a$
^{230}Th	572	$0, 3^-$	$E3$	0.64 ± 0.06	29 ± 3
	677	$0, 2^+$	$E2$	0.046 ± 0.006	1.10 ± 0.14
	781	$2, 2^+$	$E2$	0.123 ± 0.013	2.9 ± 0.3
	1009 or 1012	$?, 2^+$	$E2$	0.084 ± 0.013	2.0 ± 0.3
^{232}Th	774	$0, 2^+$	$E2$	0.50 ± 0.07	23 ± 3
	774	$0, 3^-$	$E3$	0.45 ± 0.05	20 ± 2
	785	$2, 2^+$	$E2$	0.122 ± 0.008	2.9 ± 0.2
	1106	$1, 3^-$	$E3$	0.26 ± 0.05	11.5 ± 2.3
^{234}U	849.6 or 851.6	$0, 3^-$	$E3$	0.59 ± 0.07	26 ± 3
	926.9	$0, 2^+$	$E2$	0.098 ± 0.013	2.3 ± 0.3
	1023	$2, 2^+$	$E2$	0.123 ± 0.013	2.9 ± 0.3
	1023	$2, 3^-$	$E3$	0.22 ± 0.05	9.5 ± 2.3
^{236}U	1312	$?, 3^-$	$E3$	0.22 ± 0.07	9.7 ± 2.9
	745	$0, 3^-$	$E3$	0.53 ± 0.07	23 ± 3
	959	$2, 2^+$	$E2$	0.18 ± 0.02	4.2 ± 0.4
	1040	$?, 3^-$	$E3$	0.31 ± 0.08	13.5 ± 3.4
^{238}U	1150	$?, 3^-$	$E3$	0.16 ± 0.06	7 ± 2.5
	732	$0, 3^-$	$E3$	0.64 ± 0.06	27 ± 2.5
	966	$0?, 2^+$	$E2$	0.017 ± 0.007	0.4 ± 0.2
	998	$?, 3^-$	$E3$	0.24 ± 0.05	10 ± 2
	1037	$0, 2^+$	$E2$	0.063 ± 0.009	1.4 ± 0.2
	1060	$2, 2^+$	$E2$	0.127 ± 0.009	2.9 ± 0.2
^{238}Pu	1169	$?, 3^-$	$E3$	0.28 ± 0.07	12 ± 3
	1224	$?, 2^+$	$E2$	0.022 ± 0.013	0.5 ± 0.3
	661	$0, 3^-$	$E3$	0.71 ± 0.12	30 ± 5
	983	$0, 2^+$	$E2$	0.166 ± 0.022	3.8 ± 0.5
^{240}Pu	649	$0, 3^-$	$E3$	0.41 ± 0.06	17 ± 2.5
	938	$2, 2^+$	$E2$	0.079 ± 0.018	1.8 ± 0.24
^{242}Pu	833	$0, 3^-$	$E3$	0.42 ± 0.07	17 ± 3
	1020	$?, 3^-$	$E3$	0.45 ± 0.07	19 ± 3
	1102	$?, 2^+$	$E2$	0.157 ± 0.018	3.5 ± 0.4
^{244}Pu	708	$?, 3^-$ or $?, 2^+$	$E3$	0.30 ± 0.10	12 ± 4
	960	$?, 3^-$ or $?, 2^+$	$E3$	0.045 ± 0.013	1.0 ± 0.3
	960	$?, 3^-$ or $?, 2^+$	$E3$	0.37 ± 0.07	15 ± 3
	1020	$?, 2^+$	$E2$	0.059 ± 0.013	1.3 ± 0.3
	1020	$?, 3^-$ or $?, 2^+$	$E3$	1.16 ± 0.12	47 ± 5
	1111	$?, 3^-$ or $?, 2^+$	$E3$	0.195 ± 0.018	4.3 ± 0.4
^{244}Cm	970	$?, 3^-$ or $?, 2^+$	$E3$	0.59 ± 0.10	24 ± 4
	970	$?, 3^-$ or $?, 2^+$	$E3$	0.104 ± 0.018	2.3 ± 0.4
	1038	$?, 3^-$ or $?, 2^+$	$E3$	0.52 ± 0.07	21 ± 3
	1038	$?, 2^+$	$E2$	0.082 ± 0.014	1.8 ± 0.3
^{246}Cm	1187	$?, 3^-$ or $?, 2^+$	$E3$	0.32 ± 0.07	13 ± 3
	1187	$?, 2^+$	$E2$	0.054 ± 0.014	1.2 ± 0.3
	1187	$?, 3^-$ or $?, 2^+$	$E3$	0.96 ± 0.12	39 ± 5
	1187	$?, 2^+$	$E2$	0.168 ± 0.023	3.7 ± 0.5
^{248}Cm	1124 or 1128	$2, 2^+$	$E2$	0.224 ± 0.046	4.9 ± 1.0
	1128	$1, 3^-$	$E3$	1.31 ± 0.03	52 ± 11
^{248}Cm	1050	$?, 3^-$ or $?, 2^+$	$E3$	1.07 ± 0.13	42 ± 5
	1050	$?, 2^+$	$E2$	0.180 ± 0.023	3.9 ± 0.5
	1100	$?, 3^-$ or $?, 2^+$	$E3$	0.41 ± 0.10	16 ± 4
1100	$?, 2^+$	$E2$	0.069 ± 0.019	1.5 ± 0.4	

$${}^a B(E\lambda)_{sp} = \left(\frac{2\lambda + 1}{4\pi} \right) \left(\frac{3}{\lambda + 3} \right)^2 (0.12A^{1/3})^{2\lambda} e^2 b^\lambda \text{ for } J_i = 0, J_f = \lambda.$$

Table 2. Comparison of experimental and microscopic calculations of $B(E3, 0 \rightarrow 3)$ for the 3^- members of the one-phonon octupole quadruplet

Nucleus	Experiment			Theory		
	K, J^π	$E(3^-)$ (keV)	$B(E3, 0 \rightarrow 3)$ ($10^{-2}e^2b^3$)	α, J^π	$E(3^-)$ (keV)	$B(E3, 0 \rightarrow 3)$ ($10^{-2}e^2b^3$)
^{230}Th	$0, 3^-$	572	64 ± 6	$0, 3^-$	430	73
	$1, 3^-$	1012	$\leq(50 \pm 7)$	$1, 3^-$	940	28
				$2, 3^-$	1120	4
^{232}Th				$3, 3^-$	1324	10
	$0, 3^-$	774	45 ± 5	$0, 3^-$	546	59
	$1, 3^-$	1106	26 ± 5	$1, 3^-$	945	26
				$2, 3^-$	1100	1.3
^{234}U				$3, 3^-$	1323	9
	$0, 3^-$	850	$\leq(59 \pm 7)$	$0, 3^-$	801	36
	$2, 3^-$	1023	22 ± 5	$1, 3^-$	1298	1.4
	$?, 3^-$	1312	22 ± 7	$2, 3^-$	1041	19
^{236}U				$3, 3^-$	1507	5
	$0, 3^-$	745	53 ± 7	$0, 3^-$	650	51
	$?, 3^-$	1040	31 ± 8	$1, 3^-$	1078	0.06
	$?, 3^-$	1150	16 ± 6	$2, 3^-$	905	29
^{238}U				$3, 3^-$	1165	10
	$0, 3^-$	732	64 ± 6	$0, 3^-$	778	44
	$?, 3^-$	998	24 ± 5	$1, 3^-$	1161	0.7
	$?, 3^-$	1169	28 ± 7	$2, 3^-$	922	18
^{238}Pu				$3, 3^-$	1236	11
	$0, 3^-$	661	71 ± 12	$0, 3^-$	912	48
				$1, 3^-$	1186	0.0
				$2, 3^-$	1031	9
^{240}Pu				$3, 3^-$	1273	9
	$0, 3^-$	649	41 ± 6	$0, 3^-$	878	53
				$1, 3^-$	1183	0.0
				$2, 3^-$	939	4
^{242}Pu				$3, 3^-$	1221	12
	$0, 3^-$	833	42 ± 7	$0, 3^-$	881	12
	$?, 3^-$	1020	45 ± 7	$1, 3^-$	1137	4
				$2, 3^-$	791	41
^{246}Cm				$3, 3^-$	1123	9
	$1, 3^-$	1128	≤ 131	$0, 3^-$	1293	9
				$1, 3^-$	890	1.5
				$2, 3^-$	774	32
			$3, 3^-$	1271	12	

**OXYGEN-16 COULOMB EXCITATION IN THE
ACTINIDE REGION WITH THE ENGE
MAGNETIC SPECTROMETER**

C. E. Bemis, Jr.¹ R. L. Robinson
F. K. McGowan P. H. Stelson
W. T. Milner J. L. C. Ford, Jr.

Static electric quadrupole moments of excited nuclear states may be determined by the use of the reorientation effect in Coulomb excitation, especially when using heavy-ion projectiles, as the influence of the static

moment on the excitation probability for a given state can be quite large. The octupole states in the deformed actinide region lie at quite low excitation energies, in contrast to the rare-earth deformed region. For the even-mass radium and thorium isotopes, the $K = 0$ octupole band is only a few hundred keV above the ground state. Measurements of the static quadrupole moments for the $KJ^\pi = 03^-$ states for these nuclei could lead to a more complete understanding of the exact nature of these states and their relation to the deformation properties of the nuclear ground state, that is, octupole vibrations built on the ground state or

permanent octupole deformations as suggested recently by Möller, Nilsson, and Sheline.²

We have investigated the possibilities for use of the Enge split-pole magnetic spectrograph in Coulomb excitation studies in the actinide region using ^{16}O ions from the EN tandem Van de Graaff. Using line-shaped targets of ^{230}Th (about $15\ \mu\text{g}/\text{cm}^2$) on $20\text{-}\mu\text{g}/\text{cm}^2$ carbon backings as prepared in an isotope separator, we investigated the resolution characteristics of the Enge magnet equipped with a 60-cm-long position-sensitive proportional counter of the Borkowski-Kopp type. The elastic and inelastic scattering of 39.0-MeV ^{16}O ions was observed at an angle of 150° (lab) for a variety of ^{230}Th targets and under various experimental conditions in order to optimize the energy resolution for the scattered ions. The observed scattered ion charge-state distribution, $I_{5+}:I_{6+}:I_{7+}:I_{8+}$, was 1.0:9.5:17.7:6.8 for the ^{16}O scattering from ^{230}Th at 150° (lab). The energy resolution was about 60 keV FWHM for the elastic peak and was primarily determined by the position resolution of the counter. Although the position or energy resolution could possibly be improved by substituting a 20-cm version of the counter, the primary limitation to experiments of this type is the length of time required to complete an experiment because of the relatively small excitation cross sections for the higher states. As thin targets are required to optimize the energy resolution, the small solid angle of the Enge magnet (about 3 m-sr) and the beam current limitations of the EN tandem essentially govern the experimental data rate.

We are attempting to perform experiments of the type mentioned above, namely, the determination of static quadrupole moments for excited states in the actinide region in reorientation experiments, by the use of the thick-target gamma-ray technique in coincidence with backscattered heavy ions.

1. Chemistry Division.
2. P. Möller, S. G. Nilsson, and R. K. Sheline, *Phys. Lett.* **40B**, 329 (1972).

COULOMB-NUCLEAR INTERFERENCE FOR ALPHA PARTICLES ON DEFORMED NUCLEI

C. E. Bemis, Jr.¹ W. T. Milner
 F. K. McGowan R. L. Robinson
 P. H. Stelson J. L. C. Ford, Jr.
 W. Tuttle²

The pronounced influence of direct nuclear excitation on Coulomb excitation at incident projectile energies well below the classical Coulomb barrier has prompted

us to investigate these effects using alpha particles for four even-mass targets which span the rare-earth deformed region, ^{154}Sm , ^{166}Er , ^{182}W , and include ^{234}U , in the actinide deformed region. We were particularly interested in the sensitivity of the derived electric quadrupole and electric hexadecapole transition moments, under the assumption of pure Coulomb excitation, to incident projectile energy as well as the influence of the sign of the hexadecapole charge deformation parameter, β_{40}^c , on the Coulomb-nuclear interference effect.

Since the majority of our precision Coulomb excitation studies in the even-even actinides were performed with 17-MeV alpha particles scattered at a laboratory angle of 150° ,^{3,4} it was necessary to verify that Coulomb excitation was the predominant reaction mechanism and that possible interferences with direct reactions did not influence the analyses. Measurements were performed for ^{234}U , a typical even-mass actinide target, at energies in the range 16 to 19 MeV. The results of these experiments are shown in Fig. 1, where

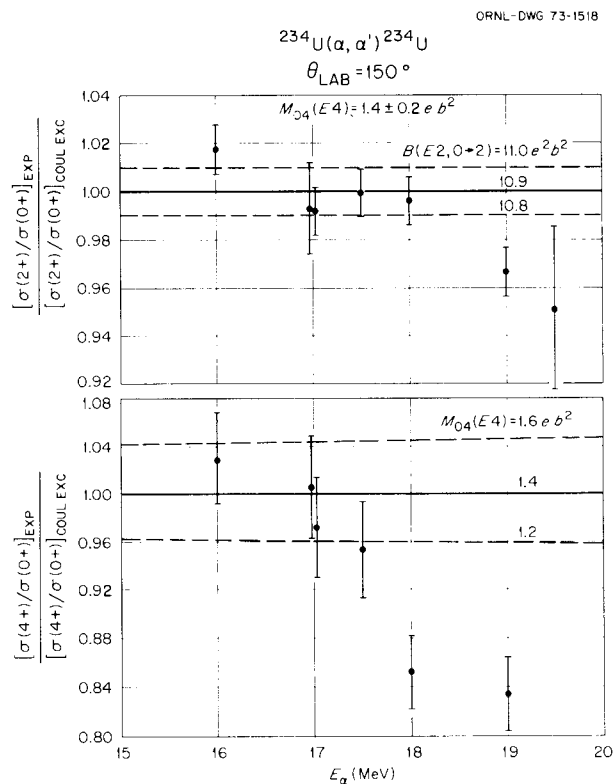


Fig. 1. Experimental excitation probabilities for the 2^+ and 4^+ states in ^{234}U relative to the elastic scattering as a function of bombarding energy. The results are presented in units of the probabilities for pure Coulomb excitation with $B(E2, 0 \rightarrow 2) = 10.9\ e^2 b^2$ and $M_{04}(E4) = 1.4\ eb^2$.

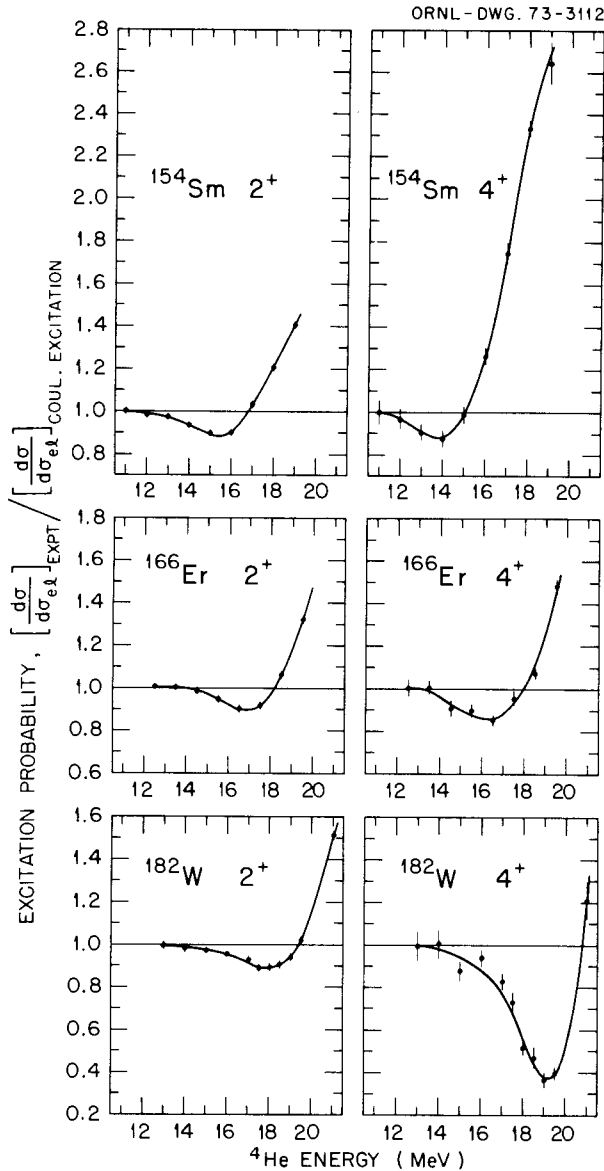


Fig. 2. Curves for the ratios of experimental 2^+ and 4^+ excitation probabilities for ^4He ions to the calculated excitation probability expected for pure Coulomb excitation for ^{154}Sm , ^{166}Er , and ^{182}W . Measurements were performed at 150° (lab).

we have plotted the experimental excitation probabilities, $d\sigma_{2^+}/d\sigma_{e1}$ and $d\sigma_{4^+}/d\sigma_{e1}$, relative to calculated excitation probabilities assuming pure Coulomb excitation as a function of ^4He ion bombarding energy. For pure Coulomb excitation, the ratio of experimental to calculated probability is 1.00. It is clear that a noticeable deviation for the 4^+ state occurs at 17.5 MeV, but the deviations for the 2^+ state occur at somewhat higher energies. However, it is also clear that at 17 MeV, our measurements are slightly affected, if at all, by the direct-reaction interference.

In order to explore further the Coulomb-excitation–direct-reaction interference, we have performed similar experiments in the rare-earth deformed region for ^{154}Sm , ^{166}Er , and ^{182}W . In these nuclei the projectile energies required to surpass the Coulomb barrier are lower and within the range of our model EN tandem Van de Graaff accelerator. Scattered alpha particles from thin ($25 \mu\text{g}/\text{cm}^2$) targets on carbon backings ($40 \mu\text{g}/\text{cm}^2$) were observed at a laboratory angle of 150° with an Enge split-pole magnetic spectrometer. A position-sensitive proportional counter was used in the focal plane. Excitation functions were measured in 0.5- or 1.0-MeV steps in the energy range 11.0 to 21.0 MeV, which spans the classical Coulomb-barrier region for these targets.

Figure 2 shows the ratios of experimental 2^+ and 4^+ excitation probabilities to calculated probabilities for pure Coulomb excitation (combined $E2$ and $E4$ excitations). In contrast to a previous result,⁵ we observe interferences for the 4^+ state as well as the 2^+ state. In fact, a most interesting feature is the exceedingly strong interference for the 4^+ state of ^{182}W . This nucleus has a negative β_{40} value. The much stronger experimental effect for a negative β_{40} is just the opposite from the situation for pure Coulomb excitation, where positive β_{40} values are more easily detected. The derived matrix elements and calculated deformation parameters using the lowest-energy data are listed in Table 1. These Coulomb-nuclear interference results for ^{154}Sm ,

Table 1. Experimental transition moments and charge deformation parameters derived from Coulomb excitation measurements with ^4He ions for ^{154}Sm , ^{166}Er , and ^{182}W

Errors include, in addition to the usual statistical uncertainties, an uncertainty corresponding to a ± 50 -keV possible error in the incident beam energy

	$\langle 2^+ M(E2) 0^+ \rangle$ (eb)	$\langle 4^+ M(E4) 0^+ \rangle$ (eb ²)	Uniform distribution		Deformed Fermi distribution	
			β_{20}	β_{40}	β_{20}	β_{40}
^{154}Sm	2.063 ± 0.015	$+0.58 \pm 0.14$	0.274 ± 0.012	$+0.112 \pm 0.039$	0.301 ± 0.012	$+0.112 \pm 0.040$
^{166}Er	2.378 ± 0.011	$+0.32 \pm 0.16$	0.301 ± 0.011	$+0.020 \pm 0.039$	0.329 ± 0.012	$+0.019 \pm 0.040$
^{182}W	2.053 ± 0.015	$-0.63^{+0.34}_{-0.16}$	0.266 ± 0.009	-0.181 ± 0.060	0.290 ± 0.010	-0.187 ± 0.062

^{166}Er , and ^{182}W were the subject of a recent publication,⁶ and the results for ^{234}U were included in ref. 4.

1. Chemistry Division.
2. U.S. Public Health Service Fellow in Radiological Health Physics from the University of Tennessee, Knoxville, Tenn.
3. F. K. McGowan, C. E. Bemis, Jr., J. L. C. Ford, Jr., W. T. Milner, P. H. Stelson, and R. L. Robinson, *Phys. Div. Annu. Progr. Rep. Dec. 31, 1972*, ORNL-4844, p. 91.
4. C. E. Bemis, Jr., F. K. McGowan, J. L. C. Ford, Jr., W. T. Milner, P. H. Stelson, and R. L. Robinson, *Phys. Rev. C8*, 1466 (1973).
5. W. Brückner, J. G. Merdinger, D. Pelte, V. Smilansky, and K. Traxel, *Phys. Rev. Lett.* 30, 57 (1973).
6. C. E. Bemis, Jr., P. H. Stelson, F. K. McGowan, W. T. Milner, J. L. C. Ford, Jr., R. L. Robinson, and W. Tuttle, *Phys. Rev. C8*, 1934 (1973).

BETA, GAMMA, AND OCTUPOLE VIBRATIONAL STATES AND HEXADECAPOLE DEFORMATIONS IN $^{156,158}\text{Gd}$

J. H. Hamilton¹ A. V. Ramayya¹
 R. M. Ronningen¹ G. Garcia-Bermudez¹
 L. L. Riedinger² R. L. Robinson
 P. H. Stelson

Coulomb excitation of states of $^{156,158}\text{Gd}$ has been carried out, and for ^{160}Gd , data are being analyzed to study the systematics of the β , γ , and octupole vibrational states. Many data on the gamma-ray branching ratios from these bands in the softly deformed nuclei in the region $A = 152$ to 158 , as summarized in a recent review,³ have shown that the rotational model even with second-order perturbational corrections does not explain these ratios for the β bands, although there is rather reasonable agreement for the γ bands. The $B(E2)_{\text{exc}}$ strengths provide additional helpful information on these nuclei. Of particular interest is the presence of two $K^\pi = 0^+$ bands in $^{156,158}\text{Gd}$ and the possible interactions of these bands.⁴

A second problem of interest is the hexadecapole deformation in these nuclei. The β_4 deformations

provide significant tests of various models of nuclear deformation.⁵ While the β_4 deformation is measured in $^{158,160}\text{Gd}$, it is interesting to test the predicted⁵ increase in β_4 as one moves down in neutron number to ^{156}Gd .

Thin high-purity targets (about $25 \mu\text{g}/\text{cm}^2$) of $^{156,158,160}\text{Gd}$ were prepared at ORNL with a magnetic isotope separator. Coulomb excitation of these nuclei was studied by magnetic analysis at 90° (to enhance the vibrational states) and at 150° (to enhance the $E4$ moments) of inelastically scattered alpha particles with energies of 11.5 to 12.5 (150°) and 14 to 15 (90°) MeV. The alpha particles were detected in the focal plane of an Enge split-pole spectrograph by a 20-cm-long position-sensitive proportional counter.

The results for the $B(E2)_{\text{exc}}$'s for the 2^+ ground and the $2^+\gamma$, $2^+\beta$, 2^+o (second $K^\pi = 0^+$ band), and 3^- octupole vibrational states are given in Table 1. One sees the same pattern for the ground, β , and γ bands as for the hafnium isotopes,⁶ namely, the ground- and γ -band 2^+ energies and $B(E2)_{\text{exc}}$ values are quite similar, while for the β band the energies move up and the $B(E2)$ values go down rapidly with increasing neutron number. As noted in our hafnium work,⁶ this similarity is somewhat surprising in the sense that in going to lighter masses in hafnium one goes toward the region of more highly deformed nuclei, while in the gadolinium nuclei the reverse occurs and one moves away from highly deformed ones. This difference in deformation with neutron number change shows up in the small increase in the ground-state $B(E2)_{\text{exc}}$ with increasing N as predicted⁵ for $^{156,158}\text{Gd}$.

There is a marked difference in the comparison of the β -band branching ratios in the two regions. In the more strongly deformed hafnium nuclei, there is reasonable agreement with theory for the β bands, particularly in the lighter-mass ones, while no agreement for the branching ratios is found for any of the β bands in the gadolinium nuclei. The second $K^\pi = 0^+$ band, which in ^{156}Gd lies very close to the beta level, seems to have little interaction with the β -type states. In ^{156}Gd our

Table 1. Results of Coulomb excitation of $^{156,158}\text{Gd}$ via (α, α') studies

	2^+ ground	$2^+\gamma$	$2^+\beta$	2^+o	3^-
^{156}Gd					
Energy (keV)	89.0	1154.1	1129.4	1258.0	1276.2
$B(E\lambda)$ ($e^2\text{b}^\lambda$)	4.53 ± 0.03	0.126 ± 0.006	0.014 ± 0.004	0.008	0.16(4)
^{158}Gd					
Energy (keV)	79.5	1187.1	1517.3	1259.9	
$B(E2)$ ($e^2\text{b}^2$)	4.90 ± 0.04	0.084 ± 0.009	<0.02	<0.02	

data indicate that the second $K^\pi = 0^+$ band has considerably less $E2$ strength to the ground state, as suggested by measurement of the $E2/M1$ mixing ratios,⁷ which show the $2^+_{\text{o}} \rightarrow 2^+_{\text{g}}$ transition to be predominantly $M1$, while the $2^+_{\beta} \rightarrow 2^+_{\text{g}}$ transition is essentially $E2$. Thus these $K^\pi = 0^+$ bands must be quite different in character to mix so little in ^{156}Gd . The decrease in the $B(E2)_{\text{exc}}$ for the γ band in going from ^{156}Gd to ^{158}Gd may be related to the softness of nuclei around 158–160 to γ vibrations.

The analysis of the Coulomb excitation of the 4^+ state leads to $M_{04}(E4)$ values of (0.48 ± 0.07) and (0.39 ± 0.15) eb^2 for $^{156,158}\text{Gd}$ respectively. Our findings for the excitation of the 2^+_{g} and 4^+_{g} states in ^{158}Gd are in agreement with those of Erb et al.⁸ Our data in ^{156}Gd are in agreement with the increases in β_4 predicted⁵ as one goes down in N from ^{160}Gd to ^{158}Gd .

1. Vanderbilt University, Nashville, Tenn.
2. Consultant to ORNL from the University of Tennessee, Knoxville, Tenn.
3. J. H. Hamilton, *Izv. Akad. Nauk SSSR, Ser. Fiz.* **36**, 17 (1972).
4. A. F. Kluk, N. R. Johnson, and J. H. Hamilton, *Z. Phys.* **253**, 1 (1972).
5. U. Gotz, H. C. Pauli, K. Alder, and K. Junker, *Nucl. Phys.* **A192**, 1 (1972).
6. J. H. Hamilton, L. Varnell, R. M. Ronningen, A. V. Ramayya, J. Lange, L. L. Riedinger, R. L. Robinson, and P. H. Stelson, "Coulomb Excitation of $^{176,178,180}\text{Hf}$," this report.
7. W. E. Collins, J. H. Hamilton, J. Lange, A. V. Ramayya, N. R. Johnson, and J. J. Pinajian, to be published.
8. K. A. Erb, J. E. Holden, I. Y. Lee, J. Z. Saladin, and T. K. Saylor, *Phys. Rev. Lett.* **29**, 1010 (1972).

COULOMB EXCITATION OF $^{176,178,180}\text{Hf}$

J. H. Hamilton ¹	J. Lange ¹
L. Varnell ²	L. L. Riedinger ³
R. M. Ronningen ¹	R. L. Robinson
A. V. Ramayya ¹	P. H. Stelson

The properties of rotational and vibrational levels in well-deformed nuclei provide important tests of the collective model.⁴ We have been involved in determining properties of such states in the hafnium nuclei through alpha-particle-induced Coulomb excitation studies. Of particular interest is the systematic behavior of these states with neutron number. Fourteen-MeV alpha particles inelastically scattered through an angle of 150° from thin targets (about $25 \mu\text{g}/\text{cm}^2$) enriched in $^{176,178,180}\text{Hf}$ were magnetically analyzed and detected by a 20-cm-long position-sensitive proportional counter. Gamma rays following bombardment of

a thick ^{180}Hf target with 13- and 15-MeV alpha particles were also measured.

The results for the $B(E\lambda)_{\text{exc}}$'s for the 2^+ ground, the $2^+ \gamma$, $2^+ \beta$ type, and 3^- octupole vibrational states are given in Table 1. The ^{174}Hf results are those of ref. 5, and our ^{176}Hf results are compared with those of Hammer et al.⁶

The ground-band 2^+ states are very similar in energy and $B(E2)_{\text{exc}}$. The $2^+, K^\pi = 0^+$ β -type vibrational states show a sharp rise in energy and marked decrease in $B(E2)_{\text{exc}}$ as one moves from the light to the heavy hafnium nuclei, with no $K^\pi = 0^+$ state observed in ^{180}Hf below 1.5 MeV. In ^{178}Hf a second $K^\pi = 0^+$ band is known,⁷ but its 2^+ member has little collective strength to the ground state. A similar result for this 2^+ level at 1277 keV is found here. The $K^\pi I = 0^+ 2$ vibrational states in ^{178}Hf will be studied more carefully, but it seems clear that the small β -type strength in ^{178}Hf is in the 1496-keV 2^+ level. The relative branching ratios for transitions out of these $K^\pi I = 0^+ 2$ states in $^{174,176}\text{Hf}$ are the only cases where agreement is found with the predictions of the rotational model with perturbational corrections of band mixing. It is interesting to note that when the large (61%) $M1$ admixture in the $2 \rightarrow 2$ transition from the 1496-keV level is subtracted, the branching ratios for this level in ^{178}Hf also essentially agree⁷ with the rotational model with perturbational corrections, while those for the 1277-keV level still do not. The latter level is presumably more quasi-particle in character, but it is not clear why the rotational model does not predict the correct branching ratios. In the gadolinium nuclei, the same trend with neutron number is observed for the energies and $B(E2)$'s for the $K^\pi I = 0^+ 2$ states, but no agreement⁸ with the theory is found for the β -band branching ratios in $^{154,156,158}\text{Gd}$. Also, in contrast to the hafnium nuclei, gadolinium nuclei move farther from the strongly deformed region with decreasing mass.

From our gamma-ray data, the relative $B(E2)$ values for the 1200.5-, 1107.2-, and 892-keV transitions are, respectively, $73 \pm 7 / 100 / 10 \pm 4$ from the 1200.5-keV level in ^{180}Hf . From $B(E2; 2\gamma \rightarrow 0g)/B(E2; 2\gamma \rightarrow 2g)$ a band-mixing parameter $Z_2 = -(7 \pm 20) \times 10^{-3}$ for the mixing of the γ and ground-state bands was obtained for the γ band in ^{180}Hf . This value indicates less mixing than in ^{178}Hf , where $Z_2 = (23 \pm 10) \times 10^{-3}$ was observed,⁹ but of course these two values overlap within errors. In any case, however, the rotational model with little perturbational correction works for the γ band in ^{180}Hf .

Table 1. Properties of states in the hafnium nuclei from (α, α') studies

	^{174}Hf	^{176}Hf	^{178}Hf	^{180}Hf
Ground-band 2^+ state				
Energy (keV)	91 ^a	88.3	93.1	93.3
$B(E2; 0 \rightarrow 2)$ ($10^{-48} \times e^2 \text{cm}^4$)	5.35 ± 0.35^a	5.14 ± 0.05 5.78 ± 0.23^b	4.84 ± 0.05	4.64 ± 0.05
β 2^+ state				
Energy (keV)	901 ^a	1226.6	(1496)	
$B(E2; 0 \rightarrow 2)$ ($10^{-48} \times e^2 \text{cm}^4$)	0.062 ± 0.010^a	0.030 ± 0.003 0.025 ± 0.005^b	0.027 ± 0.010	
γ 2^+ state				
Energy (keV)	1229 ^a	1341.3	1174.6	1200.5
$B(E2; 0 \rightarrow 2)$ ($10^{-48} \times e^2 \text{cm}^4$)	0.138 ± 0.020^a	0.124 ± 0.005 0.076 ± 0.006^b	0.113 ± 0.012	0.104 ± 0.009
$Z_2 \times 10^3$			23 ± 10^c	-7 ± 20
δ			$-(32^{+32}_{-12})^c$	$9.6^{+22}_{-5.8}$
$K = 2, 3^-$ state				
Energy (keV)	(1324) ^a	1313.3	1322.5	
$B(E2; 0 \rightarrow 3)$ ($10^{-74} \times e^2 \text{cm}^6$)		13 ± 3	9 ± 2	

^aH. Ejire and G. B. Hagemann, *Nucl. Phys.* **A161**, 449 (1971).

^bT. Hammer et al., *Nucl. Phys.* **A202**, 321 (1973).

^cL. Varnell et al., *Phys. Rev.* **C3**, 1265 (1971).

Our analysis of the $E4$ moments yields $\beta_4 = 0.0 \pm 0.03$ for ^{178}Hf , which is consistent with the small negative value predicted.¹⁰

1. Vanderbilt University, Nashville, Tenn.
2. Vanderbilt University. Present address: Yale University, New Haven, Conn.
3. Consultant to ORNL from the University of Tennessee, Knoxville, Tenn.
4. A. Bohr and B. R. Mottelson, *Kgl. Dan. Vidensk. Selsk., Mat.-Fys. Medd.* **27**, No. 16 (1953); B. R. Mottelson, *J. Phys. Soc. Japan Suppl.* **24**, 87 (1968).
5. H. Ejiri and G. B. Hagemann, *Nucl. Phys.* **A161**, 449 (1971).
6. T. Hammer, H. Ejiri, and G. B. Hagemann, *Nucl. Phys.* **A202**, 321 (1973).
7. P. E. Little, J. H. Hamilton, A. V. Ramayya, and N. R. Johnson, *Phys. Rev.* **C5**, 252 (1972).
8. J. H. Hamilton, *Izv. Akad. Nauk SSSR, Ser. Fiz.* **36**, 17 (1972).
9. L. Varnell, J. H. Hamilton, and R. L. Robinson, *Phys. Rev.* **C3**, 1265 (1971).
10. U. Gotz, H. C. Pauli, K. Alden, and K. Junken, *Nucl. Phys.* **A192**, 1 (1972).

NEUTRON PHYSICS

SEARCH FOR AN ELECTRIC DIPOLE MOMENT OF THE NEUTRON, AND OTHER COLD-NEUTRON EXPERIMENTS AT THE INSTITUTE LAUE-LANGEVIN, GRENOBLE, FRANCE

P. D. Miller W. B. Dress

The question of the existence of an electric dipole moment (EDM) of elementary particles has interested physicists for nearly 25 years. The first experimental search for an EDM of the neutron was undertaken as a test of parity conservation at the ORNL Graphite Reactor in 1950, and resulted in an upper limit for the dipole distance of 5×10^{-20} cm.¹ After the discovery of CP violation in the decay of the long-lived neutral K in 1964,² there followed a renewal of interest in experiments and theoretical predictions for the neutron EDM. Since 1967, a series of more sensitive experiments at ORNL^{3,4} have succeeded in decreasing the upper limit for the dipole distance to 1.0×10^{-23} cm.

A great many of the more recent theoretical predictions of the size of the neutron EDM are in the neighborhood of this present upper limit.^{5,6} In order to pursue this search for a neutron EDM at a more sensitive level, in 1972, the magnetic resonance spectrometer was moved from ORNL to the Institute Laue-Langevin at Grenoble, France. The High Flux Reactor at the Institute is comparable in flux to the HFIR in Oak Ridge, but it possesses the unique advantage of utilizing a liquid deuterium secondary moderator and neutron-conducting guide tubes to provide a beam of very slow neutrons ($\langle V \rangle = 150$ m/sec), several hundred times more intense than any beam of comparable velocity elsewhere. The modifications to the equipment and methods of taking data and the results to date will be discussed.

During our assignment to the institute, two additional experiments have been proposed. Both of these experiments utilize much of the equipment from the neutron EDM experiment, and their costs and time requirements are minimal. (1) The magnetic moment of the neutron is presently known to only one part in 30,000. It appears to be quite feasible to redetermine this fundamental value with an improvement between a factor of 10 and 100. (2) An experiment to search for two-gamma emission in $n + p$ capture has been suggested by Adler in a series of papers,⁷ and a first experiment to search for this decay mode was made at NBS.⁸ Their result using small NaI(Tl) detectors was $\sigma_{2\gamma} < 1.0$ mb. This is approximately a factor of 20 larger than the cross section suggested by Adler. We will discuss how we propose to detect or to set an upper limit for this cross section, lower than that calculated by Adler.

SEARCH FOR AN ELECTRIC DIPOLE MOMENT OF THE NEUTRON

W. B. Dress P. Perrin¹
P. D. Miller N. F. Ramsey²

The magnetic resonance spectrometer used to search for an electric dipole moment (EDM) of the neutron at ORNL³ was moved to the High Flux Reactor at the Institute Laue-Langevin in 1972. The background of this experiment was discussed in the introductory summary. The mechanical arrangement of the experiment is shown in Fig. 1. The intensity at our detector in Grenoble is approximately 1000 to 2000 times the intensity that we had in Oak Ridge at the ORR. In order to take full advantage of this increase, we have had to make several modifications to our equipment and methods of collecting data.

1. It is hopeless to attempt to use proportional counters as we had used in Oak Ridge at counting rates of a few million counts per second, so we developed a detector using ⁶Li-loaded glass scintillators and fast 5-cm photomultipliers. With this system, we have been able to get a fairly flat plateau up to a counting rate of 5×10^6 counts/sec. The monitor is similar to the detector and monitors the beam entering the polarizing magnet.

2. Figure 2 shows a typical magnetic resonance with the phase shift between the two rf coils set at $\pi/2$. If this phase shift is reversed, then the slope of the resonance is also reversed. In Oak Ridge we accumulated data by reversing the phase shift daily and reversing the polarity of the electric field about every 200 sec. We thus required stability of the magnetic field over a period of 200 sec such as to not appreciably change the counting rate compared with statistics. This stability requirement would be much more difficult with 2000 times the intensity. Our solution to this problem was to reverse the rf phase every second, recording the counting rate in a PDP-11 computer each cycle. Thus the period over which we require stability is reduced to 1 sec. This solution also is a great aid in compensating for slow drifts in the magnetic field. The calculated errors for each electric field cycle, including a real-time compensation for magnetic field drifts, have been quite comparable with those expected from statistics.

3. The PDP-11 computer furnished by the Institute and the CAMAC electronics furnished by the CENG

1. J. H. Smith, Ph.D. thesis, Harvard University, 1951 (unpublished).

2. J. H. Christenson, J. W. Cronin, V. L. Fitch, and R. Turlay, *Phys. Rev. Lett.* **13**, 138 (1964).

3. P. D. Miller, J. K. Baird, W. B. Dress, and N. F. Ramsey, *Phys. Rev. Lett.* **19**, 381 (1967).

4. W. B. Dress, P. D. Miller, and N. F. Ramsey, *Phys. Rev. D* **7**, 3147 (1973).

5. T. D. Lee, Columbia University report CO-2271-9 (unpublished).

6. A. Pais and J. R. Primack, Rockefeller University report COO-2232B-21 (unpublished).

7. R. J. Adler, *Phys. Rev.* **C6**, 1964 (1972).

8. R. G. Arnold, B. T. Chertok, I. G. Schroder, and J. L. Alberi, *Phys. Rev.* **C8**, 1179 (1973).

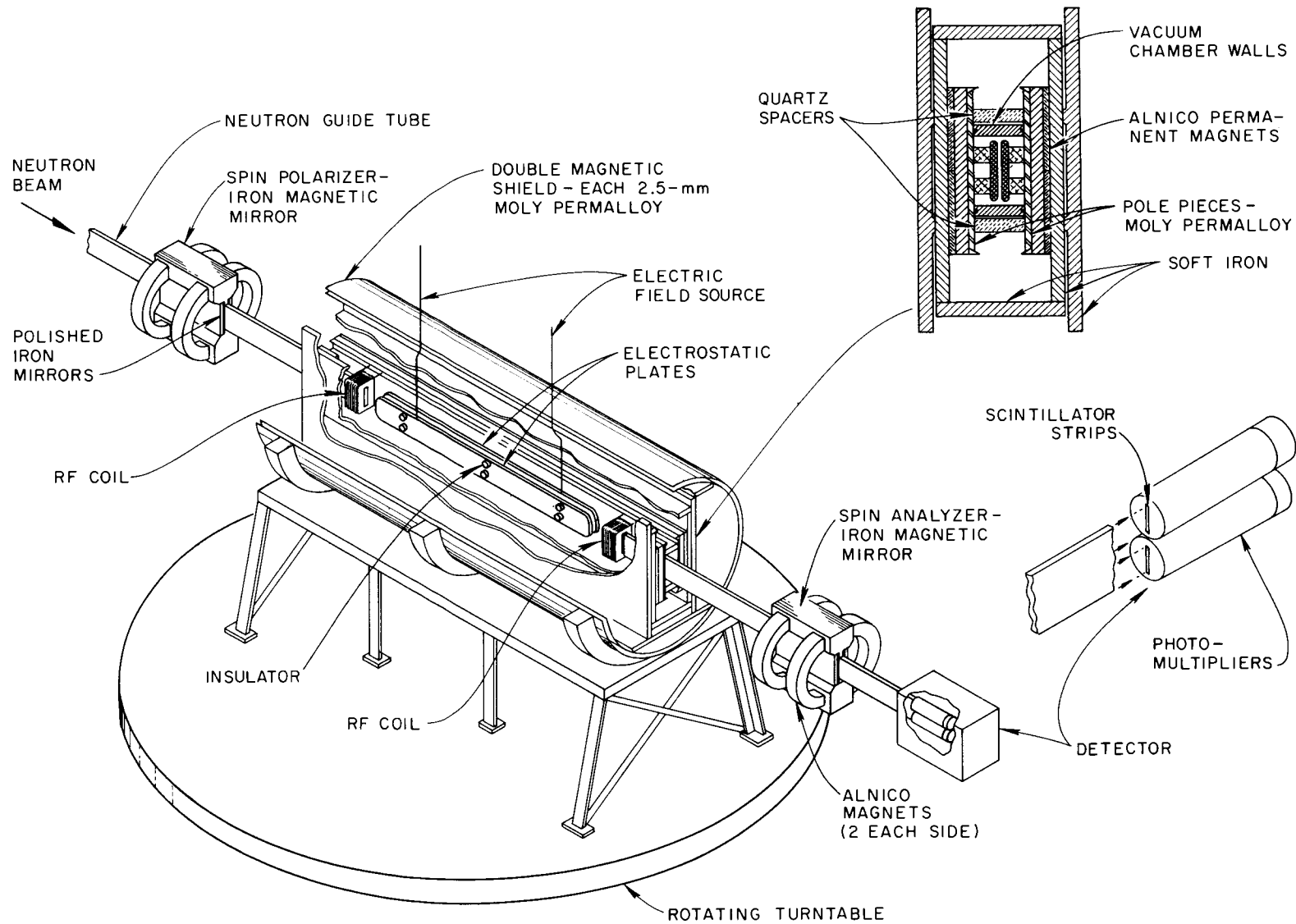


Fig. 1. Mechanical arrangement of the neutron electric dipole moment experiment.

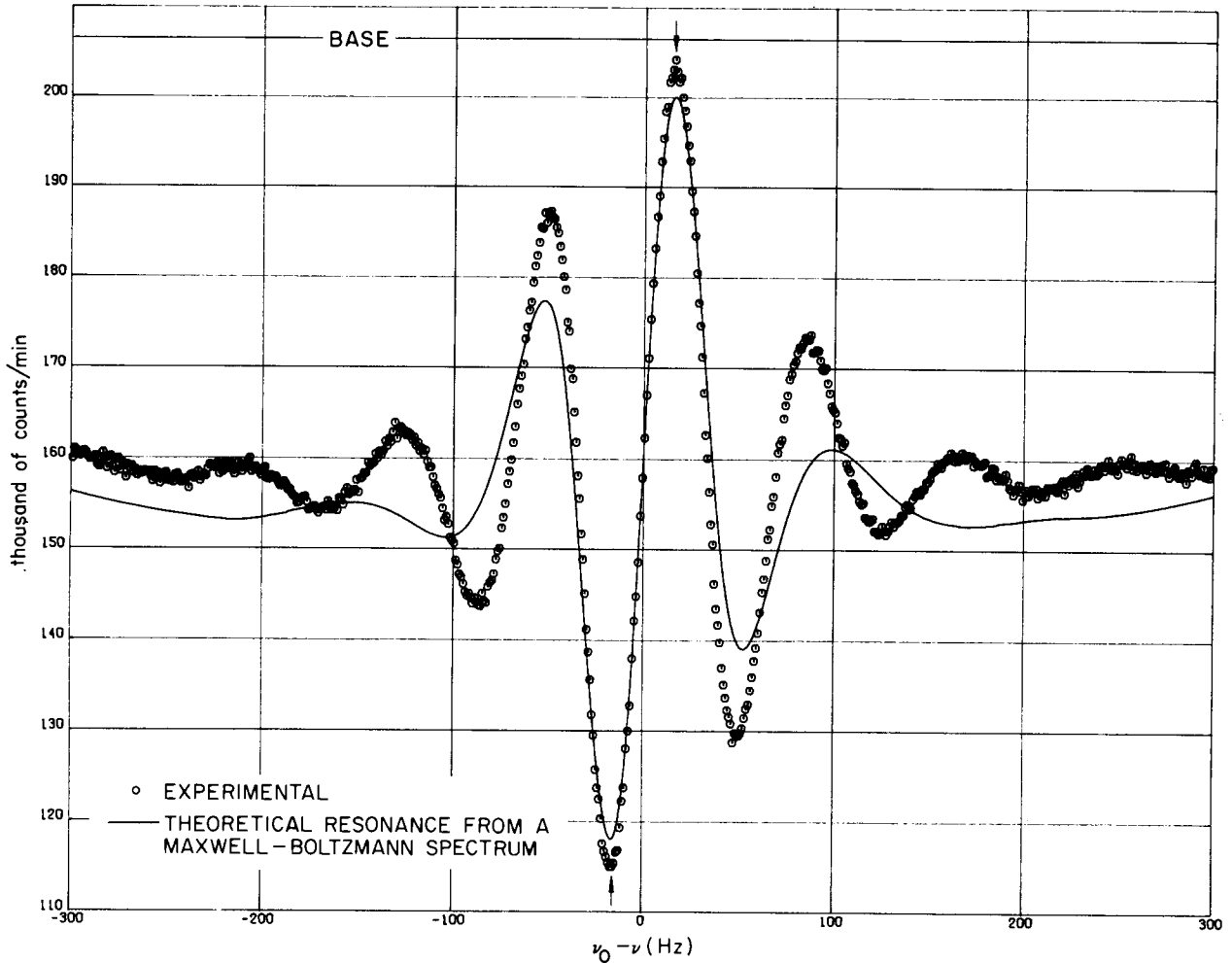


Fig. 2. Typical neutron magnetic resonance with phase shift $\sigma = +\pi/2$ between the two rf coils.

also allow us to monitor vacuum conditions, resonance drift, and other experimental parameters, and to control the electric field and the oscillator frequency. These control functions are essential with the great sensitivity that we have at such high fluxes.

4. The most difficult problem encountered is the problem of the *stability* of the angle between the electric and magnetic fields. The electric and magnetic fields are, in principle, parallel, but any error in the parallelism is reflected as a systematic error due to the interaction of the neutron's magnetic moment μ with the electric field \mathbf{E} through a term in the Hamiltonian

$$H_E = \mu \cdot \frac{\mathbf{v}}{c} \times \mathbf{E},$$

where \mathbf{v} is the neutron's velocity. Our method of dealing with this systematic effect is to turn the

apparatus end for end every few days so as to reverse \mathbf{v} . This method is only useful if the angle between the electric and magnetic fields remains constant in time. During our first series of measurements during November and December 1973, we accumulated 25 days of data which included six velocity reversals. The result of the first 18 days was

$$D = (3.0 \pm 6.3) \times 10^{-25} \text{ cm},$$

$$\beta = 2^\circ \pm \frac{1}{3}^\circ,$$

where β is the angle between the fields. During the following seven days the results fluctuated greatly compared with statistics and indicated a large and changing β .

We believe that this problem originated with the guide fields that maintain the neutron polarization in the

region between the polarizing magnet and the magnetic shields surrounding the spectrometer, and between these shields and the analyzing magnet. In Oak Ridge and for this first set of data in Grenoble, we always removed the guide fields and disconnected the spectrometer from the polarizing and analyzing magnets each time we reversed the direction of the spectrometer. It is believed that the fluctuating results during December were due to changes in the guide fields, and perhaps changes in the fringing fields from the polarizing and analyzing magnets. In order to alleviate this problem the polarizing and analyzing magnets and the Helmholtz coils providing the guide fields have been rigidly mounted so as to rotate *with* the spectrometer. Thus when the spectrometer is rotated end for end, more of the magnetic world which might perturb the internal uniform magnetic field is rotated with the spectrometer, and one of the potentially most serious sources of the systematic $\mathbf{v} \times \mathbf{E}$ effect will remain fixed and, in principle, measurable. The hardware for this modification has been constructed, and the modifications will be carried out in the first part of January 1974. During February and March, we will attempt to obtain 30 or 40 days of useful data, which should again bring us into the 5×10^{-25} cm range. We should obtain an overall sensitivity of about 4×10^{-25} cm, or about 25 times better than the previous measurement at ORNL.

-
1. CENG, Grenoble, France.
 2. Harvard University, Cambridge, Mass.
 3. W. B. Dress, P. D. Miller, and N. F. Ramsey, *Phys. Rev. D7*, 3147 (1973).

PROPOSAL TO REDETERMINE THE MAGNETIC MOMENT OF THE NEUTRON

W. B. Dress N. F. Ramsey¹
 P. D. Miller P. Perrin²
 C. Guet³

Since the proton magnetic moment is known to some few parts in 10^9 and the electron moment even better, it is of some interest to improve the present knowledge of the neutron moment. The most recent determination⁴ of the neutron magnetic moment is accurate to only one part in 30,000.

The presently existing spectrometer described in the previous paper was carefully constructed to provide a long and homogeneous magnetic field. From all our measurements, we have established that the field is homogeneous to at least one part in 10^4 , since our neutron resonance is not detectably washed out; see

Fig. 2 of the preceding paper. Thus, except for the magnitude of the magnetic field, we have an ideal instrument for measuring the neutron's magnetic moment: (1) large gap for proton probe (9 cm), (2) long apparatus (2 m), thus a (3) narrow neutron resonance (42 Hz width), and (4) facility to reverse velocity. Calculations show that we can increase the magnetic field some 50 times to around 950 G; this means we will have a width-to-frequency ratio

$$\Delta\nu/\nu \approx 15 \times 10^{-6}$$

A measurement of the resonant frequency to a part in 100 of the line width is probably feasible. Thus we can expect to obtain a measurement of the apparent resonant frequency to perhaps 2 to 4 parts in 10^7 .

Point 4 mentioned above is perhaps the unique feature in this proposed measurement. Most of the error in determining the true Larmor frequency comes from distortions and asymmetries of the neutron resonance. It can be shown that most (if not all) of these distortions can be symmetrized by reversing the direction of the velocity; for example, the shift caused by the Doppler effect is clearly such a one. A figure based on current results would indicate that a relative precision of 10^{-7} could be obtained in about 15 min of measuring time, so the problem is to obtain a proton nmr probe which can approach this accuracy and to calibrate the uniform magnetic field with it.

As of the present time, we have ordered the necessary magnets through ORNL, obtained the verbal commitment of M. Servoz-Gavin of the CENG to provide us with proton probes and electronics, and obtained the necessary budget from the CENG to build the required number of amplifiers. The time involved for this experiment will be essentially the time necessary to rebuild the spectrometer to accommodate an appropriate proton probe and to install the new magnets.

-
1. Harvard University, Cambridge, Mass.
 2. CENG, Grenoble, France.
 3. ISN, Université Grenoble, Grenoble, France.
 4. N. Corngold, "The Neutron Magnetic Moment," Ph.D. thesis, Harvard University (1954), unpublished.

SEARCH FOR DOUBLY RADIATIVE np CAPTURE

P. Perrin¹ W. B. Dress
 C. Guet² P. D. Miller

This experiment was suggested by Adler³ in the latest of a series of papers seeking to understand the 8% discrepancy between experimental measurements and

theoretical calculations of the np capture cross section. Adler's calculations were based on the possibility of an anomalously large overlap integral between the 3S continuum np state and the ground state of the deuteron as suggested by Breit.⁴

The basis of the experiment is to search for gamma rays from a suitable hydrogen target which are in fast coincidence and which sum to 2.223 MeV. Five-inch-by-five-inch NaI(Tl) crystals, fast photomultipliers, and all of the analog electronic equipment were taken to Grenoble from ORNL. With a weak ^{60}Co source we have achieved $2\frac{1}{2}$ nsec time resolution with $7\frac{1}{2}\%$ pulse-height resolution. With this system it should be possible to achieve a sensitivity of $10\ \mu\text{b}$, compared with $43\ \mu\text{b}$ calculated by Adler¹ and compared with the most sensitive experiment previously reported,⁵ which set a limit $\sigma_{2\gamma} < 1.0\ \text{mb}$.

A first quick experiment is being done in January of 1974 to evaluate shielding problems. The final experiment will be done during April or May while the magnetic resonance spectrometer is being modified as described in the previous paper.

-
1. CENG, Grenoble, France.
 2. ISN, Université Grenoble, Grenoble, France.
 3. R. J. Adler, *Phys. Rev.* C6, 1964 (1972).
 4. G. Breit and M. L. Rustgi, *Nucl. Phys.* A161, 337 (1971).
 5. R. G. Arnold, B. T. Chertok, I. G. Schroder, and J. L. Alberi, *Phys. Rev.* C8, 1179 (1973).

LIGHT-ION REACTIONS AND INTERNAL CONVERSION COEFFICIENTS

LOW-LYING STATES IN ^{111}In AND ^{113}In

H. J. Kim R. L. Robinson

There is considerable experimental evidence indicating that ^{115}In and ^{117}In have a rotational band which coexists with spherical states below 1.6-MeV excitation.¹⁻⁷ The spherical states are attributed to the single proton hole in the $Z = 50$ major shell closure and its interaction with the vibration of the $Z = 50$ core;^{3,4} the deformed states are thought to belong to the $K = \frac{1}{2}^+$ [431] rotational band.^{1,2} Although not as extensive, there is some evidence indicating that a similar situation may prevail in ^{111}In and ^{113}In .^{8,9}

Low-lying states of ^{111}In and ^{113}In were investigated in the present work via the (p,n) and $(p,n\gamma)$ reactions on ^{111}Cd and ^{113}Cd targets for an incident energy range $2.7 \leq E_p \leq 5.2$ MeV. These reactions are particularly suitable for a comprehensive study of the low-lying states because at low projectile energies the

dominant mechanism is the compound-nuclear reaction. Unlike a one-step process, a compound-nuclear reaction is an efficient tool for exciting most residual states without regard for their detailed structure.¹⁰ Excitation energies, decay modes, half-lives, and spin-parities for the levels below 1.62 MeV were determined from the neutron time-of-flight spectra, gamma-ray spectra, and gamma-ray time distributions relative to the pulsed proton beam initiating the (p,n) reaction. For the $^{111}\text{Cd}(p,n)^{111}\text{In}$ reaction the enhanced resonance yields of neutrons at the 0^+ isobaric analog resonance, which provided additional information for the spin-parity assignments, were also measured. This technique has been discussed previously.¹¹

The principal decay mode of all excited states below 1.62 MeV is by gamma-ray decay to either the $\frac{9}{2}^+$ ground state or the $\frac{1}{2}^-$ isomeric state for both ^{111}In and ^{113}In . A similar situation prevails for ^{115}In and ^{117}In . The decays to these two states are compared in Figs. 1 and 2.

The $\frac{9}{2}^+$ ground state and the two negative-parity states occurring systematically in the odd indium isotopes (see Fig. 1) have been attributed to the configuration of a single proton hole in the $Z = 50$ major shell closure,^{12,13} but a comparable explanation for the systematic occurrence of the pair of positive-parity states is as yet unavailable. As a way of interpreting the highly enhanced $B(E2)$ values for the $\frac{3}{2}^+ \rightarrow \frac{1}{2}^+$ transition in ^{115}In and ^{117}In , Backlin et al.¹ proposed these positive-parity states to be the low-spin members of the $K = \frac{1}{2}^+$ [431] rotational band. An alternative interpretation of these $\frac{1}{2}^+$ and $\frac{3}{2}^+$ states is suggested by the systematic observation of the $\frac{9}{2}^+$, $\frac{1}{2}^-$, and $\frac{3}{2}^-$ proton-hole states in odd-mass antimony nuclei.¹⁴ These states are believed to arise from the addition of a proton pair to the ground and first two excited states of the odd-mass indium nuclei, that is, two-particle, one-hole states.¹⁴ If this is the case, it is reasonable to speculate that the closely separated $\frac{1}{2}^+$ and $\frac{3}{2}^+$ pair of states, together with $\frac{5}{2}^+$ and $\frac{7}{2}^+$ states, that characterize the low energy levels of odd-mass antimony nuclei,¹⁵ would appear in the odd-mass indium nuclei (i.e., two-hole, one-particle state).

Coupling of the $g_{9/2}$ proton hole to the 2^+ vibration of the $Z = 50$ core can account for one each of the $\frac{5}{2}^+$, $\frac{7}{2}^+$, and $\frac{9}{2}^+$ states shown in Fig. 2. The remaining states are left for some other mode of excitation. The $K = \frac{1}{2}^+$ rotational band and the single proton-hole state ($\frac{5}{2}^+$ and $\frac{7}{2}^+$) of the odd-mass antimony nuclei appearing as two-hole, single-particle states are possible explanations for the excess of high-spin states. But as noted by Sergeev et al.,¹⁶ if they belong to the rotational band,

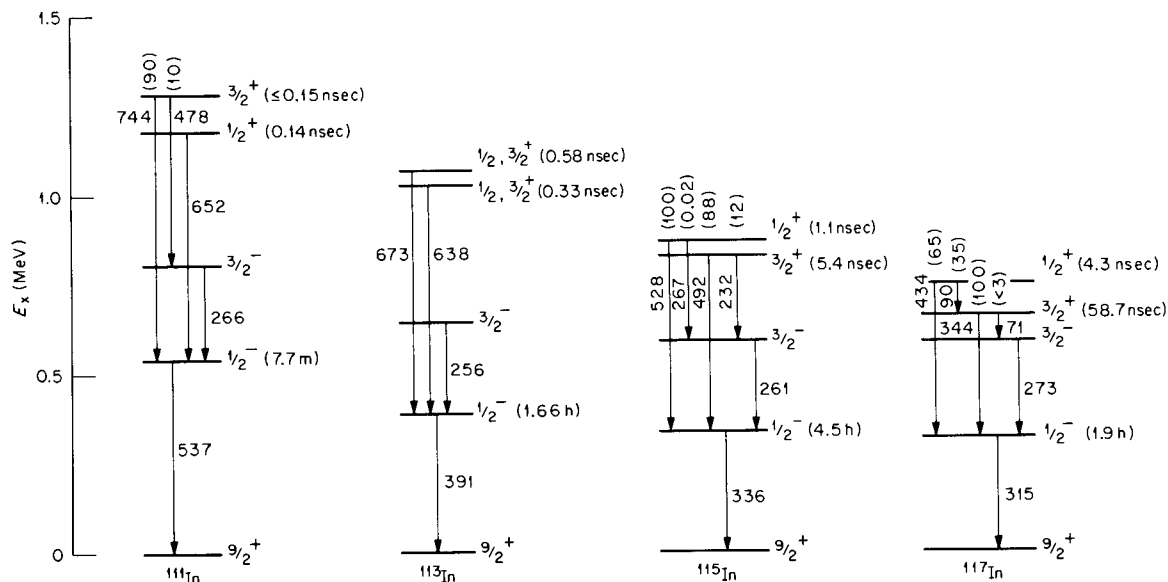


Fig. 1. Comparison of the low-spin states in the odd-mass indium nuclei. The results for ^{111}In and ^{113}In are based on the present work and that of H. J. Kim and W. T. Milner [*Nucl. Instrum. Methods* 95, 429 (1971)]. The ^{115}In results are from A. Backlin et al. [*Nucl. Phys.* A96, 539 (1967)] and V. Sergeev et al. [*Nucl. Phys.* A202, 385 (1973)]. The ^{117}In results are from A. Backlin et al. [*Nucl. Phys.* A96, 539 (1967)] and S. Hara and R. N. Horoshko [*Nucl. Phys.* A183, 161 (1972)].

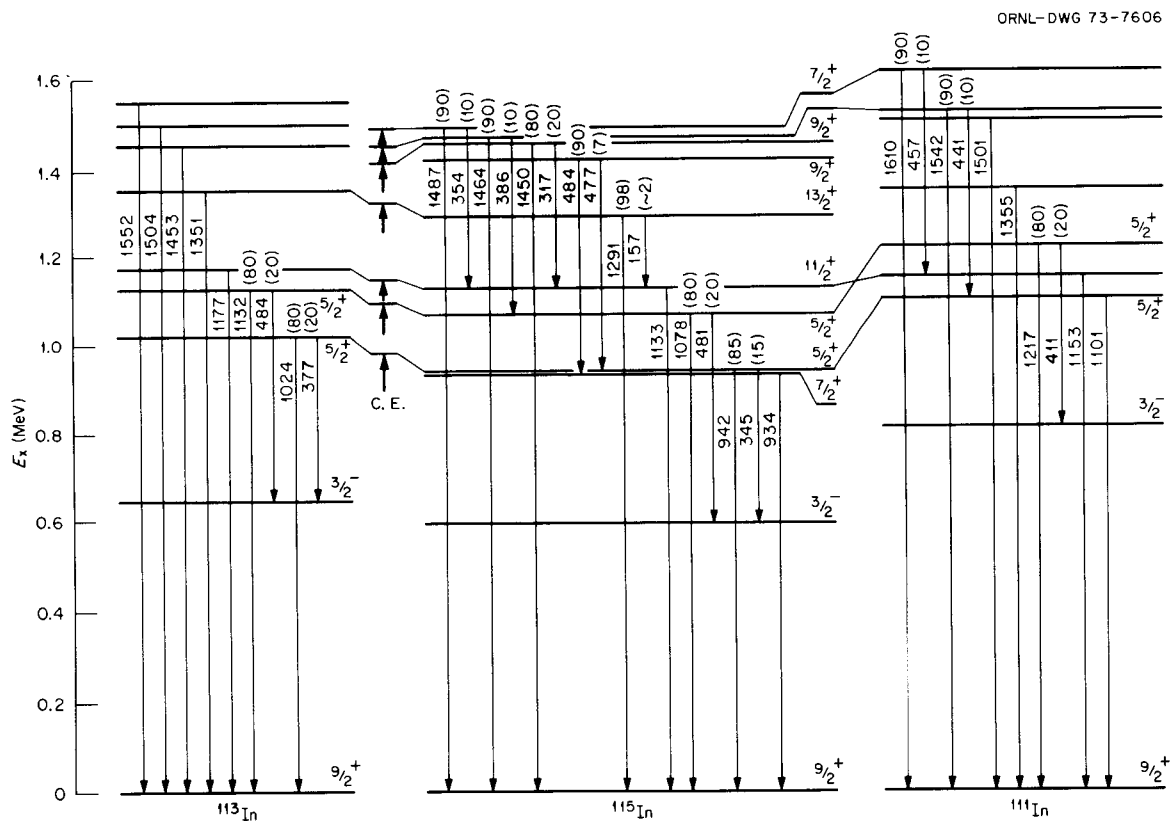


Fig. 2. Comparison of the high-spin states in the odd-mass indium nuclei. The upward bold arrows show the levels Coulomb-excited.

their energies are very much shifted from those predicted by the simple rotational model.

1. A. Backlin, B. Fogelberg, and S. M. Malmskog, *Nucl. Phys.* **A96**, 539 (1967).
2. V. R. Pandharipande, K. G. Prasad, R. P. Sharma, and B. V. Thosar, *Nucl. Phys.* **A109**, 81 (1968).
3. J. McDonald, D. Porter, and D. Stewart, *Nucl. Phys.* **A104**, 177 (1967).
4. F. S. Dietrich, B. Herskind, R. A. Naumann, G. Stokstad, and G. E. Walker, *Nucl. Phys.* **A155**, 209 (1970).
5. R. S. Raghavan and P. Raghavan, *Phys. Rev. Lett.* **28**, 54 (1972).
6. H. Haas and D. A. Shirley, University of California Radiation Laboratory report No. 20426, p. 208, 1970 (unpublished).
7. B. I. Atalay and L. W. Chiao-Yap, *Phys. Rev.* **C5**, 369 (1972); A. Covello, V. R. Manfredi, and N. Nazziz, *Nucl. Phys.* **A201**, 215 (1973).
8. E. M. Bernstein, G. G. Seaman, and J. M. Palms, *Nucl. Phys.* **A141**, 67 (1970).
9. H. J. Kim and W. T. Milner, *Nucl. Instrum. Methods* **95**, 429 (1971).
10. H. J. Kim, R. L. Robinson, C. H. Johnson, and S. Raman, *Nucl. Phys.* **A142**, 35 (1970).
11. R. L. Kernell, H. J. Kim, R. L. Robinson, and C. H. Johnson, *Nucl. Phys.* **A176**, 449 (1971).
12. M. Conjeaud, S. Hara, and E. Thuriere, *Nucl. Phys.* **A129**, 10 (1969).
13. C. V. Weiffenbach and R. Tickle, *Phys. Rev.* **C3**, 1668 (1971).
14. R. L. Auble, J. B. Ball, and C. B. Fulmer, *Nucl. Phys.* **A116**, 14 (1968).
15. M. Conjeaud, S. Hara, and Y. Cassagnou, *Nucl. Phys.* **A117**, 449 (1968).
16. V. Sergeev, J. Becker, L. Ericksson, L. Gidefeldt, and L. Holmberg, *Nucl. Phys.* **A202**, 385 (1973).

PROTON SIZE RESONANCES IN TIN ISOTOPES

C. H. Johnson J. K. Bair
C. M. Jones

Proton optical-model parameters can be deduced from measurements on elastic scattering, polarization, and total absorption cross sections, but only the latter is useful at sub-Coulomb energies. As a result, very little proton optical-model work has been done below the Coulomb barrier. That is unfortunate. Special features can be observed at low energies because the single-particle states, quasi bound by the barrier, produce broad resonances in strength functions vs energy. Similar resonances do not occur above the barrier.

The paucity of observed strength function resonances in the literature stems in part from the need for precision to reveal the effects in the presence of the Coulomb barrier. In 1969, Johnson and Kernell¹ first

observed these resonances in isotopes of tin. But those results were not entirely convincing because of contaminant yields at lower energies and inadequate data above the resonant peak.

We repeated those measurements with higher accuracy to bombarding energies extending well above the peaks. Experimental details are in an earlier report.² Briefly, carefully prepared targets of ¹¹⁷Sn, ¹¹⁸Sn, ¹¹⁹Sn, ¹²⁰Sn, ¹²²Sn, and ¹²⁴Sn were bombarded by 3- to 7-MeV protons, and neutrons were detected in 4 π geometry by a counter calibrated to better than $\pm 1\%$.

We have made small corrections as shown for ¹²⁴Sn in Fig. 1 for (a) neutrons from the target backing, (b and c) neutrons from (p,n) reactions in contaminants of copper and chlorine, (d) room background, (e) detector energy response, and (f) nonlinearity of the excitation function. Dead-time corrections are not shown; they were less than 0.8%. The point of this figure is that the corrections are small and the uncertainties smaller. It is a precision experiment.

In Figs. 2 and 3 the observed cross sections are plotted as ratios to a smooth empirical function. Table 1 lists values of the function; interpolation can be done by plotting $\ln \sigma$ vs E^{-1} .

Strength functions can be deduced from these data by dividing out the Coulomb effects and correcting for emission of gamma rays and protons from the compound nucleus. We have not completed the Hauser-Feshbach calculations on the gamma-ray and proton emission. Our earlier report² showed that removal of the Coulomb effects reveals a sequence of resonant maxima in approximate agreement with predictions. The optical-model code GENOA will be used to interpret these resonances.

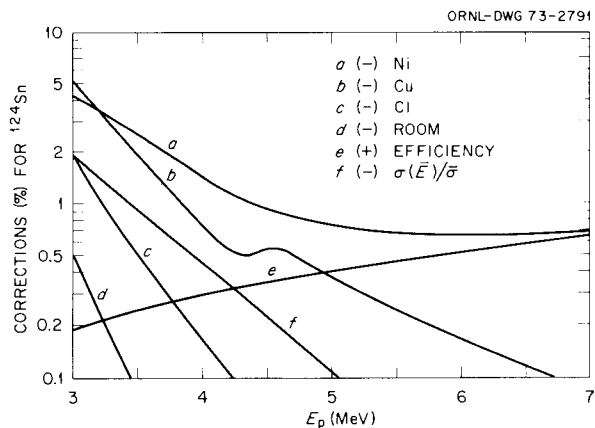


Fig. 1. Corrections to the observed ¹²⁴Sn(p,n) yields.

1. C. H. Johnson and R. L. Kernell, *Phys. Rev.* **C2**, 639 (1970).

2. D. W. Smith, J. K. Bair, C. M. Jones, and C. H. Johnson, *Phys. Div. Annu. Progr. Rep. Dec. 31, 1970*, ORNL-4659, p. 59.

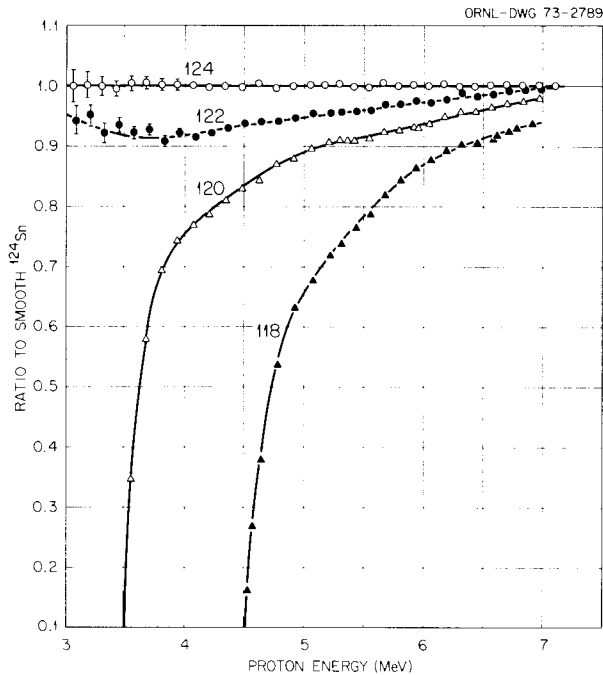


Fig. 2. Even-isotope ratios of (p,n) cross sections to a smooth curve from Table 1.

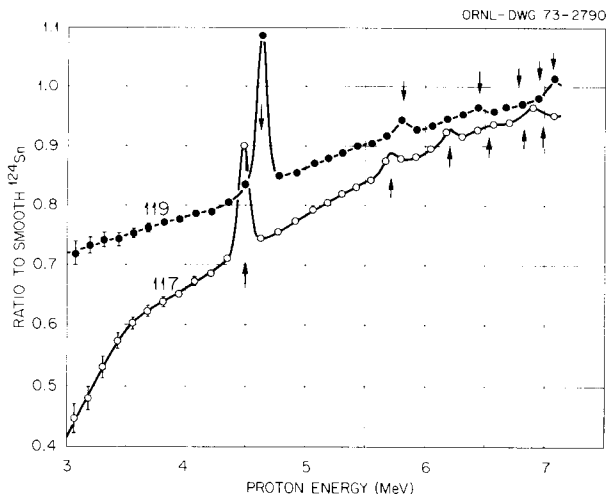


Fig. 3. Odd-isotope ratios of (p,n) cross sections to smooth curve from Table 1. Arrows indicate energies of known analog states.

Table 1. Smoothed cross section for $^{124}\text{Sn}(p,n)$

E (MeV)	σ (mb)
3.00	0.0865
3.50	0.576
4.00	2.51
4.25	4.74
4.50	8.10
5.00	20.53
5.50	43.15
6.00	77.40
6.50	121.8
7.00	174.2
7.20	198.7

M4 CONVERSION COEFFICIENTS AND E5 TRANSITIONS

S. Raman T. A. Walkiewicz¹
R. L. Auble R. Gunnink²
W. T. Milner B. Martin³

It is generally believed that the theory of internal conversion is in broad agreement with experiment. There exist several tabulations of calculated internal conversion coefficients. The tables of Hager and Seltzer⁴ are widely used now. How good are these conversion coefficients? Can they, for instance, reliably predict conversion coefficients as large as 1000, which are confirmed by experiments? Can we trust them to, say, 3% accuracy?

To answer these questions, we have refined a little-used trick to measure conversion coefficients. When an isomer deexcites via two transitions in cascade, it is possible to deduce the ratio of the two total conversion coefficients by measuring photon intensities only. Consider, for example, the case of $^{123}\text{Te}^m$ decay, shown in Fig. 1. The 88.5-keV transition (γ_1) is M4, and the 159.0-keV transition (γ_2) is M1 + <1.3% E2. We can write

$$I_{\gamma_1}(1 + \alpha_1) = I_{\gamma_2}(1 + \alpha_2); \quad \alpha = I_{ce}/I_{\gamma}$$

If the photon intensity ratio, $I_{\gamma_2}/I_{\gamma_1}$, is measured and if α_2 is small (say less than 0.2) and is set equal to the theoretical value,⁴ α_1 can be readily obtained. We have employed this technique and high-resolution Ge(Li) detectors to determine one of the largest ($\alpha = 1076 \pm 42$ for the 88.5-keV, M4 transition⁵ in ^{123}Te) and one of the most accurately known ($\alpha = 46.40 \pm 0.25$ for the

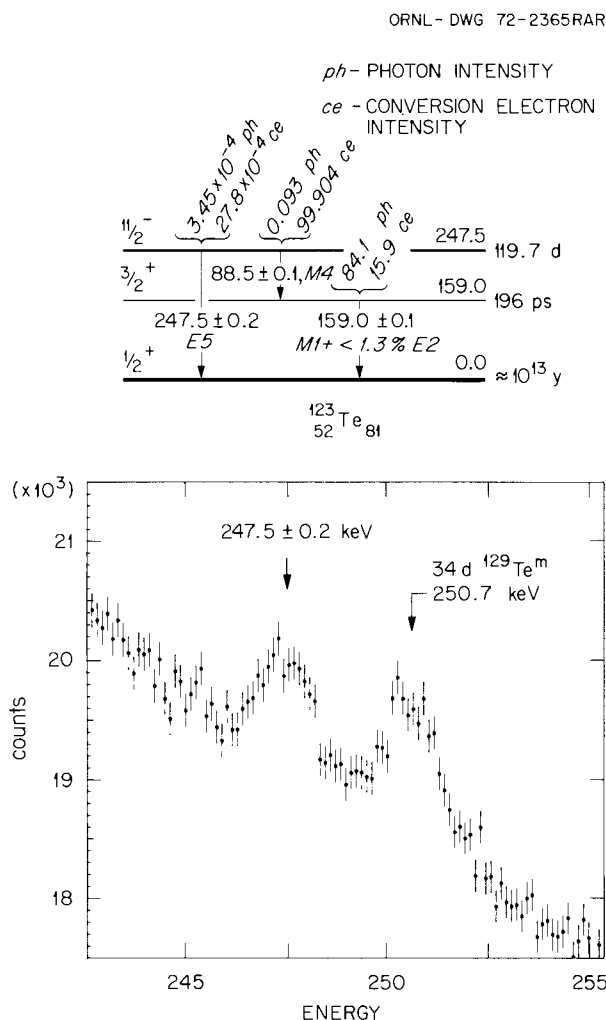


Fig. 1. $^{123}\text{Te}^m$ decay scheme. The intensities given are per 100 decays of $^{123}\text{Te}^m$. See also S. Raman, *Nucl. Instrum. Methods* **103**, 407 (1971); S. Raman et al., *Phys. Lett.* **47B**, 19 (1973).

156.0-keV, $M4$ transition⁶ in ^{117}Sn) conversion coefficients.

In ^{123}Te , the measured value, $\alpha = 1076 \pm 42$, can be compared with $\alpha = 1152$ predicted by Hager and Seltzer.⁴ In ^{117}Sn , the measured and predicted values are 46.40 ± 0.25 and 47.8 respectively. The discrepancy

from the theoretical value is $-2.9 \pm 0.6\%$. This discrepancy prompted us to examine the literature for all $E3$ and $M4$ conversion coefficients experimentally determined to better than 5% accuracy. The results of our survey are shown in Fig. 2. We found that the theoretical values were *systematically* 2 to 3% higher than the experimental values. We attempted to understand possible reasons for the discrepancy by calculating α_K and α values with screening functions different from those employed by Hager and Seltzer.⁴ Our values agreed with the Hager and Seltzer values. Therefore, we do not have a simple explanation for the observed discrepancy.

The existing experimental information on $E5$ transitions is limited. In the course of our measurements with $^{123}\text{Te}^m$, we observed an extremely weak 248-keV, $E5$ transition. The measured photon intensity is given in Fig. 1. The $E5$ partial gamma half-life was deduced as 3.0×10^{12} sec, compared with the Weisskopf single-particle estimate of 1.5×10^{11} sec, or a hindrance factor of 20.

In Fig. 3, we show a log-log plot of enhancement factor vs energy for all known $E5$ transitions.⁷ The enhancement factor appears to increase smoothly with the transition energy. This trend can be qualitatively understood as follows. Collective (particle-hole) core excitation states have energies of at least 3 to 4 MeV in medium and heavy nuclei. As the transition energy increases and approaches the core excitation energy, the isomeric state from which the $E5$ transition originates is expected to mix more strongly with the core excitation states or states with configurations consisting of core excitations coupled to low-energy states. Such a condition would induce $E5$ enhancement, as is apparently borne out by the available data.

1. Edinboro State College, Edinboro, Pa.
2. Lawrence Livermore Laboratory, Livermore, Calif.
3. Max-Planck-Institut für Kernphysik, Heidelberg, Germany.
4. R. S. Hager and E. C. Seltzer, *Nucl. Data* **A9**, 119 (1971).
5. S. Raman, *Nucl. Instrum. Methods* **103**, 407 (1971).
6. S. Raman, T. A. Walkiewicz, R. Gunnink, and B. Martin, *Phys. Rev. C* **7**, 2531 (1973).
7. S. Raman, R. L. Auble, and W. T. Milner, *Phys. Lett.* **47B**, 19 (1973).

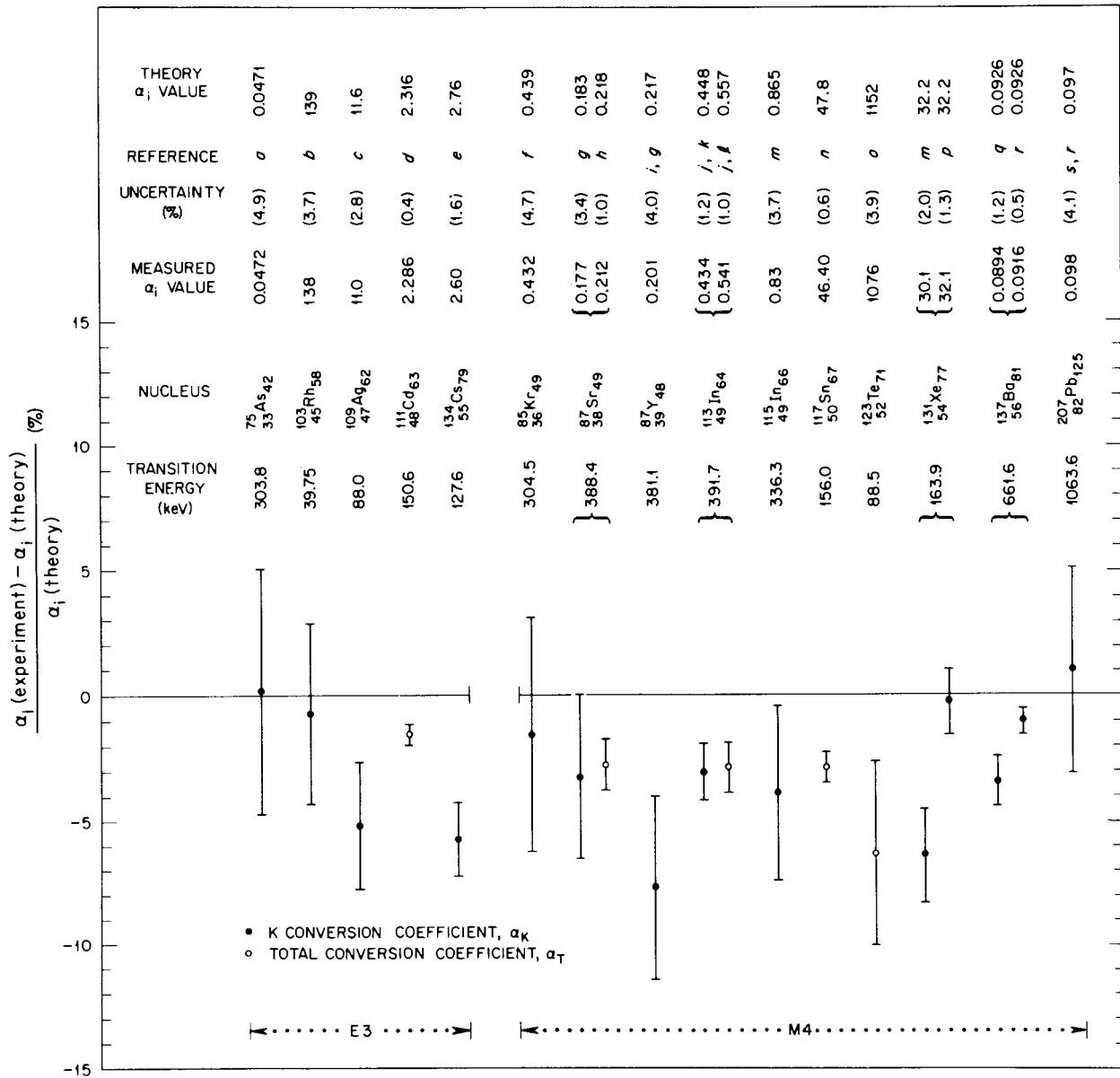


Fig. 2. Comparison between precisely measured E3 and M4 conversion coefficients and theoretical (Hager and Seltzer) values. For additional details, see S. Raman et al., *Phys. Rev. C7*, 2531 (1973).

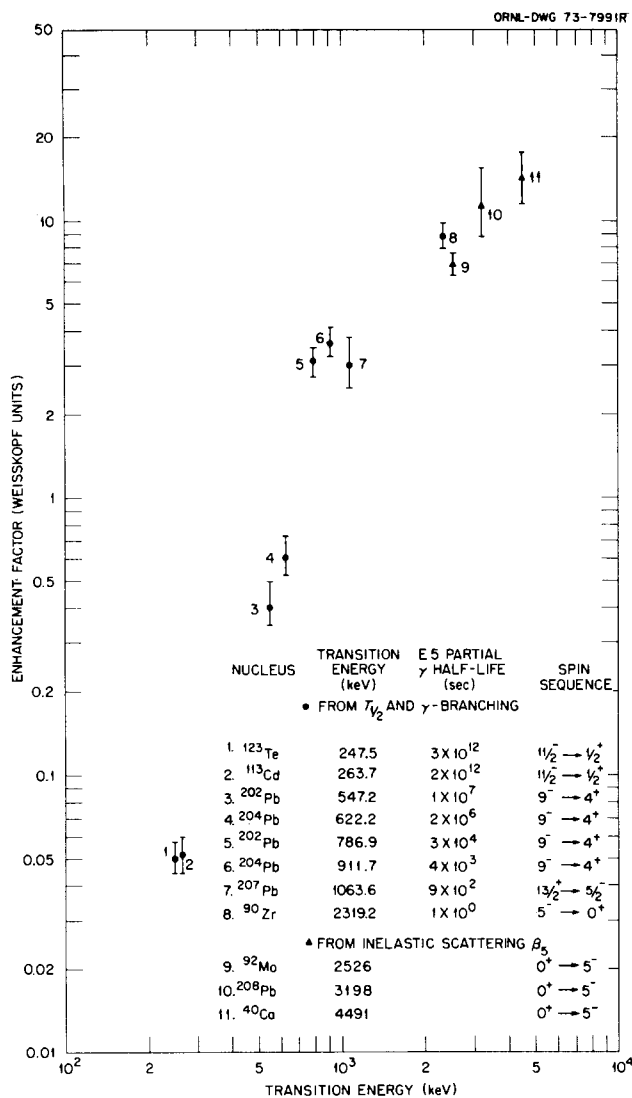


Fig. 3. Summary of known E5 transitions and their enhancement factors. For additional details, see S. Raman et al., *Phys. Lett.* 47B, 19 (1973).

ATOMIC AND SOLID-STATE PHYSICS

ATOMIC STRUCTURE AND COLLISIONS EXPERIMENTS

I. A. Sellin ¹	P. M. Griffin
H. H. Haselton ¹	M. D. Brown ²
R. Laubert ¹	Sheldon Datz ³
J. Richard Mowat ¹	Bailey Donnally ⁴
D. J. Pegg ¹	R. Kauffman ²
R. S. Peterson ¹	J. R. Macdonald ²
R. S. Thoe ¹	P. Richard ²
W. W. Smith ⁵	

Our principal research activity concerns the atomic structure and collision phenomena of highly stripped

ions in the range $Z = 10$ to 35. The primary objective of our research is the study of atomic structure of highly ionized heavy ions and their modes of formation and destruction in collisions. The decay of excited states of these ions, by radiative and also by electron emission processes, is the phenomenon we use in carrying out these experiments. Our principal tools are the various heavy-ion accelerators at ORNL; x-ray, soft x-ray, and extreme ultraviolet spectrometers; electron spectrometers; and a variety of peripheral equipment associated with these devices.

The principal themes of our work during 1973 were: (1) Study of metastable states of simple ions – those that contain a small number of electrons. Because many relatively forbidden deexcitation processes involving excited states of these ions occur at higher rates than in their low- Z counterparts because of increased magnetic interactions, it is possible to study these rates to an accuracy which is competitive with theoretical structure calculation. Only the few-electron systems are amenable to sufficiently detailed theoretical analysis. Hence, our structure experiments tend to concern the most elementary, few-electron heavy ions. A number of these ions are fairly abundant constituents of the solar corona and of other plasmas of similar temperature, so that our work frequently contributes something of interest to solar plasma physics as well. (2) While studying metastable states of few-electron chlorine and argon ions through their x-ray decay channels, we discovered strong dependence of x-ray production cross sections on incident ion charge state, as these ions were passed through thin gas targets. (3) In recent experiments on hydrogen atoms formed by passage of protons through carbon foils at energies on the order of 200 keV, we discovered fore-aft asymmetries in the electron charge distribution of the emergent atom. (4) In higher-resolution experiments, we discovered that very highly ionized target atom lines are produced by impact of energetic, highly ionized heavy ions on lighter gas targets – for example, 150-MeV Ar^{15+} on neon. This raises the possibility of under some circumstances avoiding the large Doppler shifts and spreads normally associated with beam-foil spectroscopy.

Electron Spectroscopy on Metastable Ion States

As an example of the first activity, Fig. 1 exhibits a spectrum of autoionization electrons emitted by foil-excited 6-MeV fluorine ions undergoing decay in flight. Spectra *b* and *c* refer to time delays of 0.1 and 0.4 nsec, respectively, with respect to *a*. Energies for both laboratory frame and rest frame of the emitting ion are

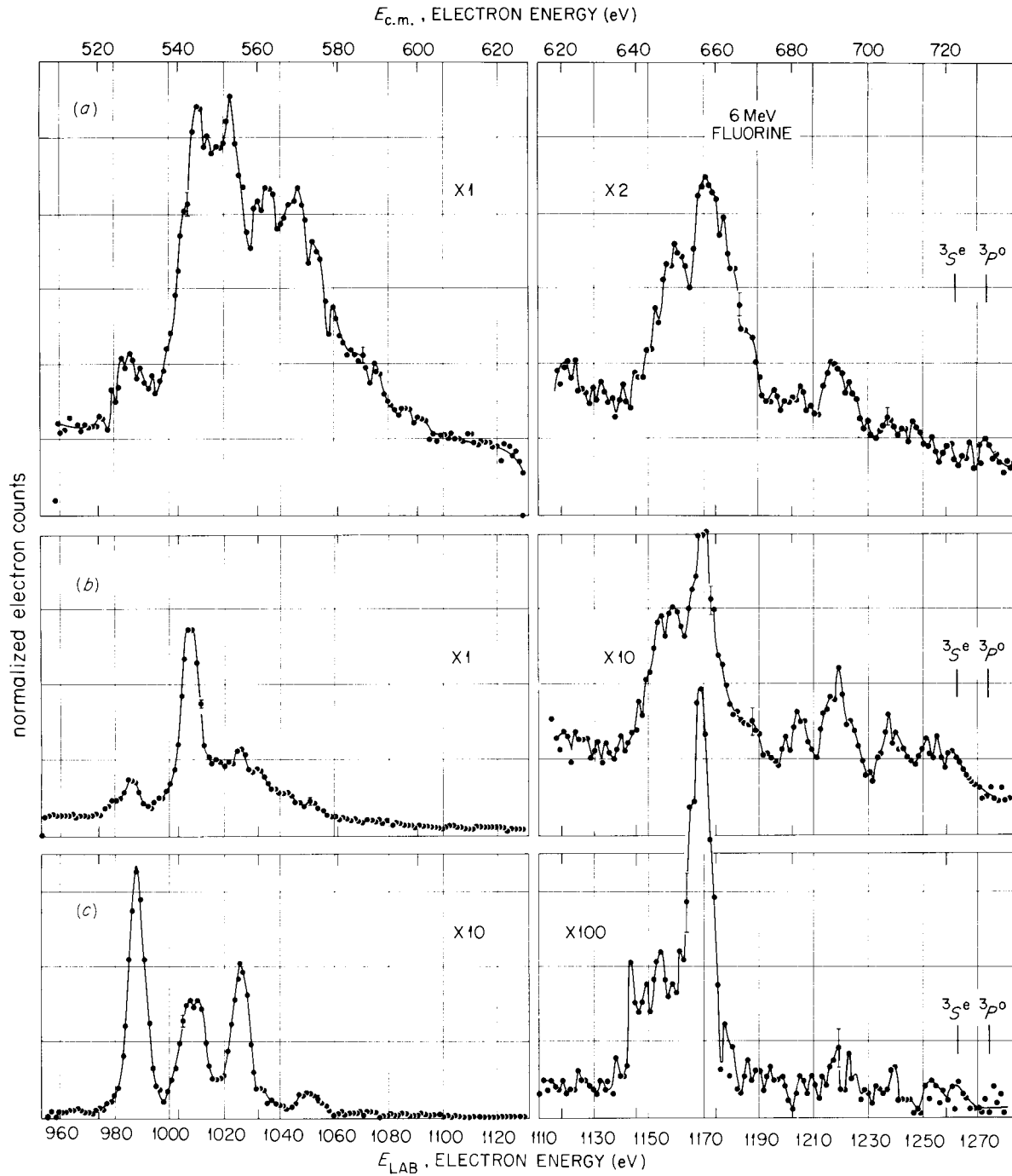


Fig. 1. Spectra of autoionization electrons emitted by 6-MeV fluorine ions undergoing decay in flight. Spectra *b* and *c* refer to time delays of 0.1 and 0.4 nsec, respectively, with respect to *a*. For other information, see caption to Fig. 4.

shown. The energy scale is divided, separating the "low" and "high" energy group of peaks. The expansion factors shown normalize the intensity scales to that of the spectrum in the top left-hand corner. We note that several long-lived features survive translation of the foil target to upstream locations. Corresponding time delays are long compared with usual autoionization lifetimes. A variety of metastable autoionizing states thus appear in the spectrum. The three most prominent peaks in *c* are associated with the $1s2s2p$ and $1s2p^2 \ ^4P$ and the $1s2p^2 \ ^2P$ states of three-electron ions respectively. The $J = 5/2$ component of the leftmost peak, which corresponds to complete spin alignment and maximum total angular momentum of an emergent lithium-like ion, typically has a lifetime in the nano-second region and survives at separations of the target from the spectrometer viewing region of $\gtrsim 10$ cm. The open circles in Fig. 2 correspond to results obtained on the lifetime of this particular state during the past two years, as a function of the screened Z of the incident ion. Increasing departures from the simple scaling law (solid line) from the work of investigators at the Columbia Radiation Laboratory are noted at higher values of Z . At the higher values, this is due in part to the opening of a magnetic quadrupole radiative decay channel to the $1s^2 2s$ state, which competes with the autoionizing transition. In the autoionizing case, the final state of the system is a helium-like ion in its ground state plus a free electron emitted in an F state, with total angular momentum $5/2$. Some reasonably general conclusions can be drawn from our experience with this type of experiment. Multiply excited states of high excitation energy and high angular momentum –

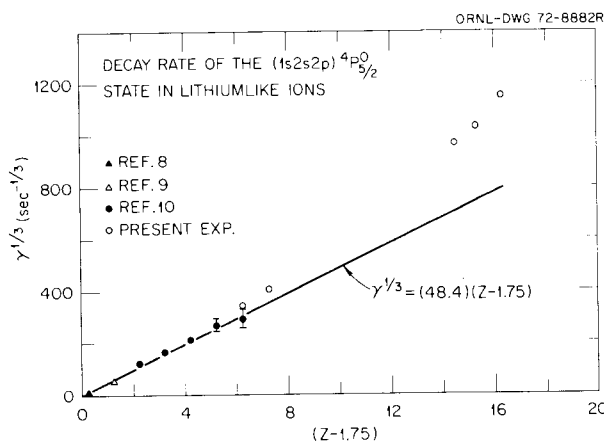


Fig. 2. Total decay rate (inverse lifetime) of the $(1s2s2p) \ ^4P_{5/2}^o$ level in some three-electron ions taken to the one-third power and plotted against an effective nuclear charge of $Z - 1.75$. Open circles represent present work.

both spin angular momentum and orbital angular momentum – are sufficiently abundantly formed to make such experiments attractive. In many cases the radiative decay channels are so weak that only the autoionizing channels can be observed. Methods akin to the ones in use by us appear to be the only means of getting information on such states at present.

Metastable X-Ray-Emitting States

There are many metastable x-ray-emitting states as well. Historically, the observation of helium-like inner combination lines in the emission spectra of highly stripped ions in both laboratory plasmas and the solar corona stimulated attempts to compute the associated decay rates. It was found that singlet-triplet mixing by the relativistic spin-orbit interactions allows the 2^3P_1 to decay to the ground state by electric dipole emission. We have made earlier measurements of the decay rate of this state in helium-like oxygen for comparison with the theoretical results of Elton and of Drake et al.,⁶ obtaining results in rough agreement with theory. In the present experiments, we were able to extend this measurement to helium-like fluorine, in which the use of a Si(Li) detector made an advance in accuracy possible because of its high solid-angle–efficiency product. The Z dependence of this transition probability is so strong that a change of Z of only one unit ($Z = 8$ to 9) is accompanied by more than a threefold increase in the decay rate. The results of the fluorine experiment are in excellent agreement with the theoretical predictions mentioned. Figure 3 exhibits a decay curve obtained from this experiment. In addition to the upstream portion of this curve, from which a value of the intercombination line transition probability can be derived, one sees a long-lived tail which might be due to nuclear hyperfine mixing of another 3P state. Work on this possibility is under way.

Charge-State Dependence of Characteristic X-Ray Production

Concerning theme 2, we have done a number of experiments related to the exponential projectile charge dependence of K -shell x-ray production by highly ionized heavy ions in thin gas targets. These initial results were mentioned in the 1972 Physics Division report. The work arose from our discovery that neon K x-ray yields were strongly dependent upon the charge state of incident highly stripped argon ions which were passed through a thin neon target. This collision system is different from most previously studied collision

systems in several respects. It falls outside the scope of the plane-wave Born approximation because $Z_1 > Z_2$ (projectile and target charges) and because the projectile contains tightly bound electrons. The experiment also involves velocities greater than those for which electron promotion models are thought to be valid. Figure 4 presents some representative data from our experiments. X-ray yields are plotted vs projectile charge state for an 80-MeV argon beam incident on a thin neon target. One notes an exponential rise of the neon K yield and a faster than exponential rise in the argon K yield. The x-ray spectral distribution from both the neon and the argon particles (not shown) indicates that in most cases at least half of the neon electrons are ejected in each single collision. Lines near the Lyman series limit of one-electron neon have in fact been observed in our spectra, so that multiple electron ejection processes are dominant rather than rare.

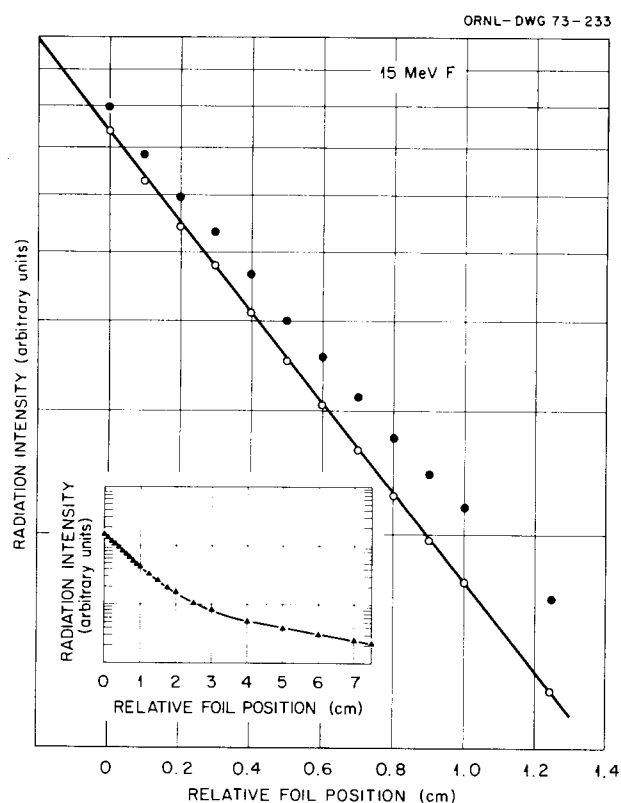


Fig. 3. Experimental decay curve at 15 MeV beam energy. The inset shows the full curve fitted to a sum of two decaying exponentials (solid line). Closed circles are uncorrected data, and open circles are data after subtraction of the apparent background, which has been represented to a useful degree of accuracy by a single exponential. The statistical counting errors are smaller than the circles. The solid line passing through the open circles is a least-squares fit to a single decaying exponential.

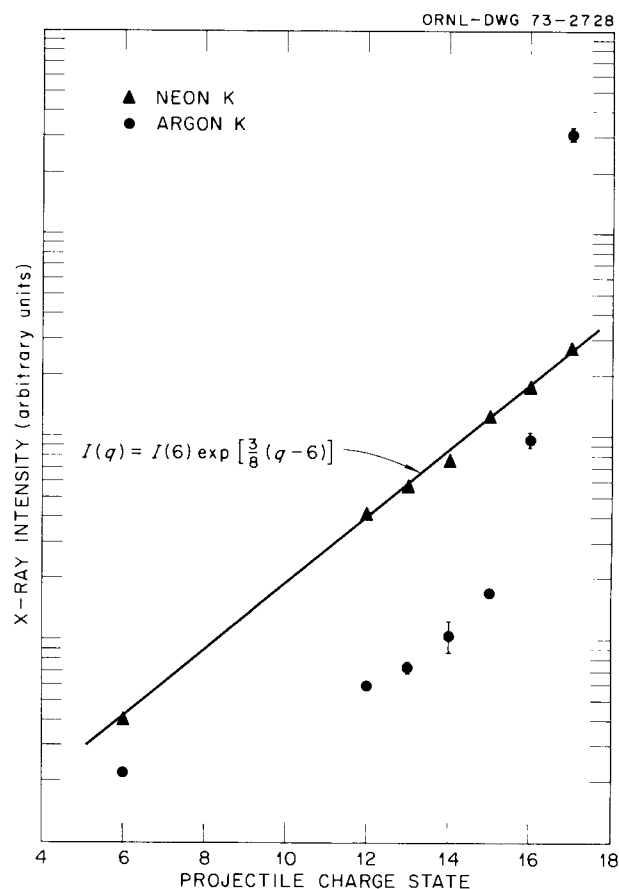


Fig. 4. Neon and argon K x-ray yield vs projectile charge state. The data have been normalized to the same gas-cell pressure and to the same number of incident projectiles. In all cases the statistical counting errors are smaller than the point symbol, as is the scatter of data from run to run except where otherwise indicated.

Fluorescence yields are well known to rise with an increasing degree of ionization of an ion, but the maximum possible theoretical rise in these yields is insufficient to explain either the neon yield data or the argon yield data. One expects rearrangement collisions — electron capture — to become increasingly probable for the higher incident-ion charge states. While it is clear that electron capture does play an increasing role in the case of the highest incident-ion charge states, it is also becoming clear that electron capture alone is not a satisfactory mechanism to explain the observed data.

Coherent Excitation of Atoms by Foils

Topic 3 concerns the observation of coherent electron density distribution oscillations in collision-averaged foil excitation of the $N=2$ hydrogen levels. Using foil-excited hydrogen beams (80 to 400 keV), we have

applied a simple technique recently proposed by Eck⁷ to unambiguously separate genuine excitation coherence in emergent hydrogen atoms from that induced by fine structure at probe fields. We find compelling evidence for strong excitation coherence and have studied quantities related to the collision-averaged S - P phase coherence angle. Using Eck's theory, the data exhibit coherent fore-aft oscillations of the electron cloud with respect to the proton. Basically, the technique depends on the use of electric probe fields respectively parallel and antiparallel to the beam to exploit the fact that the excitation coherence signal is odd under field reflection, whereas other experimental signals are not. A number of investigations have dealt with observable excited-state coherence in simple excited systems induced by the fine-structure interaction, when initial magnetic substate population asymmetry (alignment) prevails. These observations do not demonstrate true excitation coherence, since axial symmetry in the Russell-Saunders coupling approximation requires that only states of the same M_L and M_S can be coherently excited, while states of different J but the same L can still interfere because of the fine-structure interaction. A simple physical picture of the relationship between true excitation coherence and field reversal is as follows. If there is an initial displacement of an electron charge cloud with respect to the proton, or one develops in time due to an inequality in proton and average electron axial velocity, the displacement will be enhanced or diminished depending on the direction of E relative to that of the charge displacement. Incoherent coupling and quenching effects, light intensity anisotropies, etc., depend on the magnitude of E , but not on whether the electric field is parallel or antiparallel to the quantization axis defined by the common axis ($+Z$) of the beam and E . Figure 5 displays a field-free Lyman α decay signal, together with the sum signal (top curve) for E respectively parallel and antiparallel to the beam, as well as a difference signal for the same field conditions. The strong difference signal is clearly evident, and the significance of the first minimum in the difference signal is thought to represent peak concentration of the electron cloud in the backward hemisphere at a time substantially after the exit of the atom through the foil. Thereafter, the charge distribution asymmetry continues to ring periodically between the two limits, as is evident from the exponentially damped wave form observed. The frequency of the oscillation shown is basically that of the Stark-perturbed Lamb shift, the amplitude at $t = 0$ (at the foil) is related to the initial charge cloud distortion of the system, and the development of subsequent

minima and maxima is related to the corresponding lag and lead of the average axial velocity of the electron cloud with respect to the proton. There is a complete analogy between the charge distribution asymmetry at $t = 0$ and thereafter to conditions of the initial position and velocity of the classical oscillator. In effect, the physical content of the difference oscillations in Fig. 5 is the suggestion that while the initial dipole charge distribution may be reasonably small, the initial collision-average electron cloud velocity is not small, and furthermore the initial cloud velocity lags that of the proton, since, according to Eck's theory, the electron concentration initially grows in the backward hemisphere.

Instrument Development

In addition to the research results described in previous paragraphs, we have been carrying on a number of equipment development projects. The work has been shared between the University of Tennessee and the Oak Ridge National Laboratory. A new

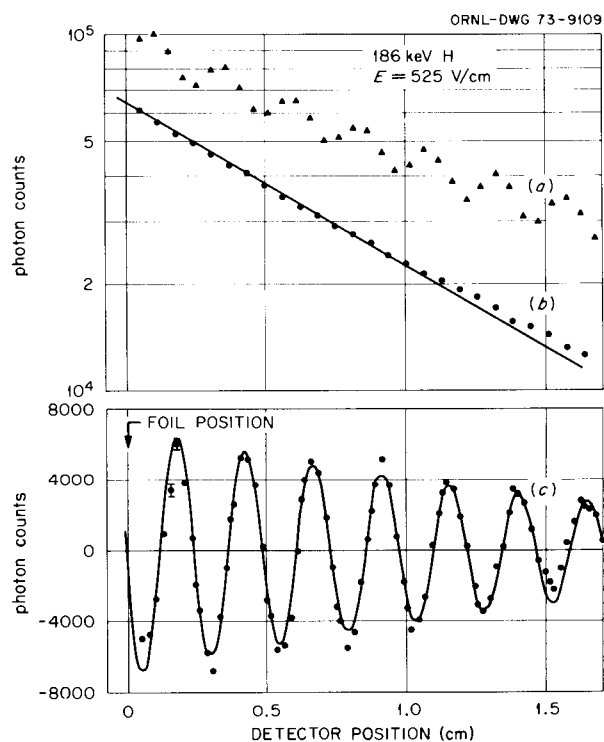


Fig. 5. Variation of signal strengths with distance downstream at 525 and 0 V/cm and 186 keV beam energy. The raw data for zero field are shown with an arbitrarily normalized straight line superposed, whose slope corresponds to τ_{2p} (b). The sum of the signals for E parallel and antiparallel to the field is plotted in the top curve, a, and the difference signal ($E_{\text{par}} - E_{\text{antipar}}$) is plotted in the bottom curve, c.

cylindrical electron spectrometer was designed and its construction started. The overall length of the instrument is approximately 15 in., and its resolving power should exceed 1000. Because of the cylindrical symmetry of this device with respect to an incident ion beam, the instrument should have a significantly higher *étendue* than other electrostatic spectrometers of comparable resolution. This is a critical feature for doing experiments on electrons emitted from ions as they undergo decay in flight. Because of kinematic broadening of the Auger lines from moving emitters, it is necessary to restrict the polar angle of electron emission with respect to incident ion beam very severely in order to achieve desired resolutions. It is for this reason that the cylindrical capacitor design was chosen. In addition, a high-vacuum system has been procured to house the new spectrometer, and provisions have been made for a triple-layered magnetic shield.

Another new instrument acquired during 1973 is a 2-m grazing-incidence x-ray spectrometer. This large spectrometer was purchased jointly by the University of Tennessee Physics Department and the Oak Ridge National Laboratory. The spectrometer support frame and target chamber fixturing have been constructed in the University of Tennessee shops. A good deal of design help and advice was provided by staff members of ORNL. The new instrument has been mounted at the ORNL tandem Van de Graaff facility, and initial ion beam test runs have been made. The instrument is currently undergoing final calibrations.

Other new instruments being developed include a bent-crystal soft-x-ray spectrometer, designed to cover the range 5 to 50 Å, and a half-meter visible-region spectrometer for complementary use in the corresponding spectral range. An existing Seya instrument has also been refurbished for use in our experiments. With the four photon spectrometers already mentioned, we therefore cover the entire range from visible wavelengths to those for which Si(Li) detectors are useful. Since many of the ion excited states we study decay preferentially by electron emission as opposed to photon emission, the new electron spectrometer provides us with the auxiliary means for studying these decay channels as well.

1. University of Tennessee, Knoxville, Tenn. (Sellin and Pegg are consultants to ORNL).

2. Kansas State University.

3. Associate Director, Chemistry Division, ORNL.

4. Lake Forest College.

5. University of Connecticut.

6. R. C. Elton, *Astrophys. J.* **148**, 573 (1967); G. W. F. Drake and A. Dalgarno, *Astrophys. J.* **157**, 459 (1969).

7. T. G. Eck, *Phys. Rev. Lett.* **31**, 270 (1973).

INFLUENCE OF IONIC CHARGE STATE ON THE STOPPING POWER OF 27.8- AND 40-MeV OXYGEN IONS IN THE [011] CHANNEL OF SILVER

C. D. Moak M. D. Brown²
 B. R. Appleton¹ S. Datz³
 J. A. Biggerstaff H. F. Krause³
 T. S. Noggle¹

In many cases, it has been assumed that the stopping power of an ion is not strongly influenced by its ionic charge because screening electrons would largely mask the effect of charge-state differences. Usually it is difficult to tell whether an ion moving through a solid is highly stripped but highly screened or less highly stripped and screened. Earlier experiments had demonstrated that fast prestripped oxygen ions are able to survive passage through crystal channels of about 1 μm length and more without electron capture or loss. An experiment to detect slight differences in screening which would cause small differences in the stopping powers of O⁸⁺, O⁷⁺, and O⁶⁺ ions has been performed with 27.8- and 40-MeV oxygen ions in the [011] channel of a silver crystal with 0.8 μm path length. The differences are not small. The stopping powers follow the simple relation $S = kq^2$. The result in this case indicates that dynamic screening by conduction electrons plays no significant role in equalizing stopping powers. The results appear to contradict the conclusion of Brandt et al.⁴ that dynamic screening by conduction electrons occurs within a very short distance (0.04 μm) compared with our crystal thickness.

The experimental arrangement is shown in Fig. 1. Input ion charge states were selected by means of a

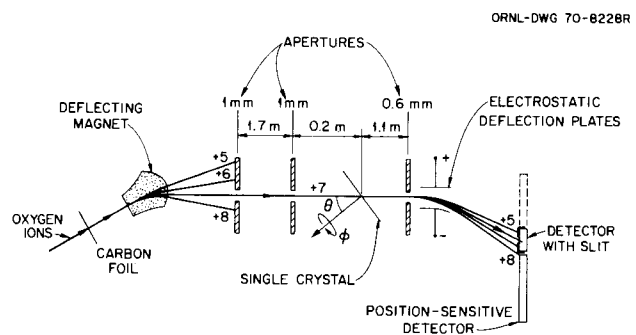


Fig. 1. Experimental arrangement.

deflecting magnet, and emerging ion charge states were selected by means of an electrostatic analyzer. Stopping powers were measured for various combinations of input and output charge. Part of the data is shown in Fig. 2. Clearly the stopping powers are different, and thus it can be said that conduction electrons do not dynamically screen out the differences in charge and

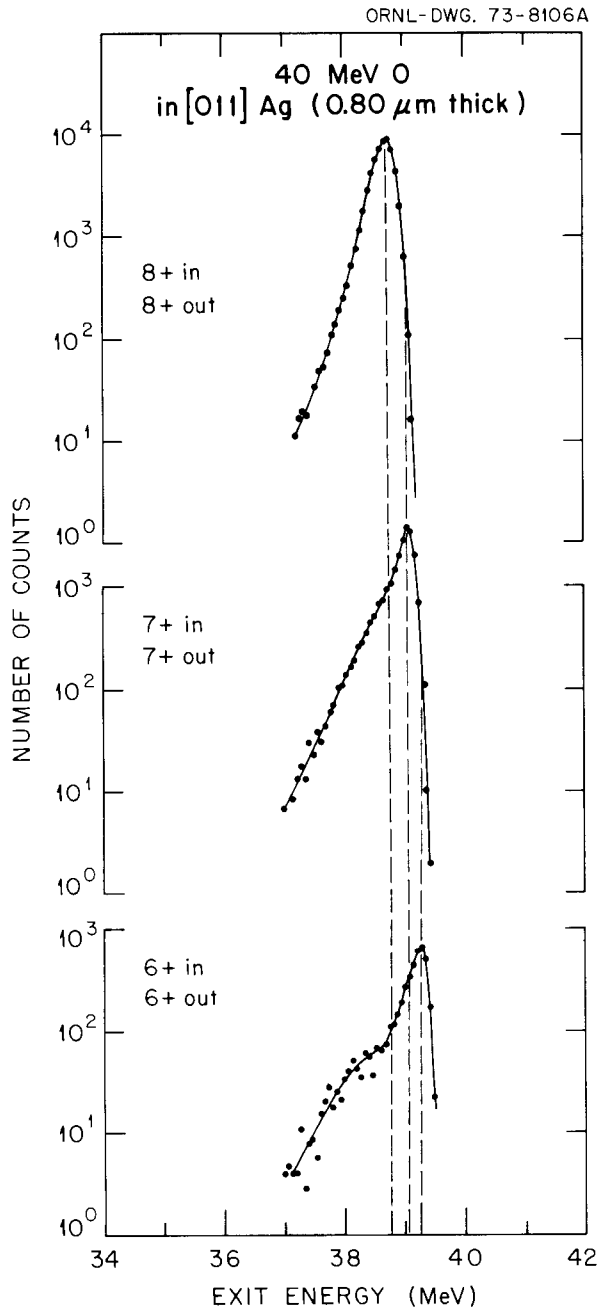


Fig. 2. Emergent energy spectra. 40-MeV oxygen ions, 0.8 μm path length in [011] channel in silver. $\Delta q = 0$.

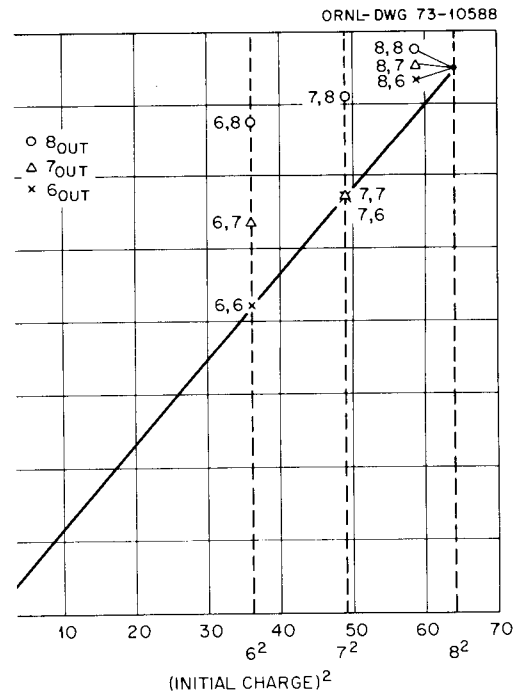


Fig. 3. Stopping powers of 40-MeV oxygen ions, [011] axis in silver, for various charge-state combinations, q_{in} and q_{out} .

stopping power. As shown in Fig. 3, the stopping powers of those ions which did not change charge are proportional to the square of the ion charge. A complete analysis of all the data is being prepared for publication.

1. Solid State Division.
2. Visiting Scientist under AEC Contract AT(11-1)-2130, Kansas State University, Manhattan, Kan.
3. Chemistry Division.
4. W. Brandt, R. Laubert, M. Morino, and A. Schwarzchild, *Phys. Rev. Lett.* 30, 358 (1973).

VELOCITY DEPENDENCE OF THE STOPPING POWER OF CHanneled IODINE IONS

C. D. Moak J. A. Biggerstaff
B. R. Appleton¹ S. Datz²
T. S. Noggle¹

Recent measurements of some uranium ion stopping powers, in the energy range 30 to 90 MeV,³ in polycrystalline targets, together with earlier data for bromine ions and iodine ions, have shown that, in the energy region where the theories of Lindhard, Scharff, and Shiøtt⁴ and Firsov⁵ predict that electronic stopping should obey the relation $S_e = kE^{1/2}$, the data show that $S_e = a + bE^{1/2}$. Figure 1 is illustrative of the

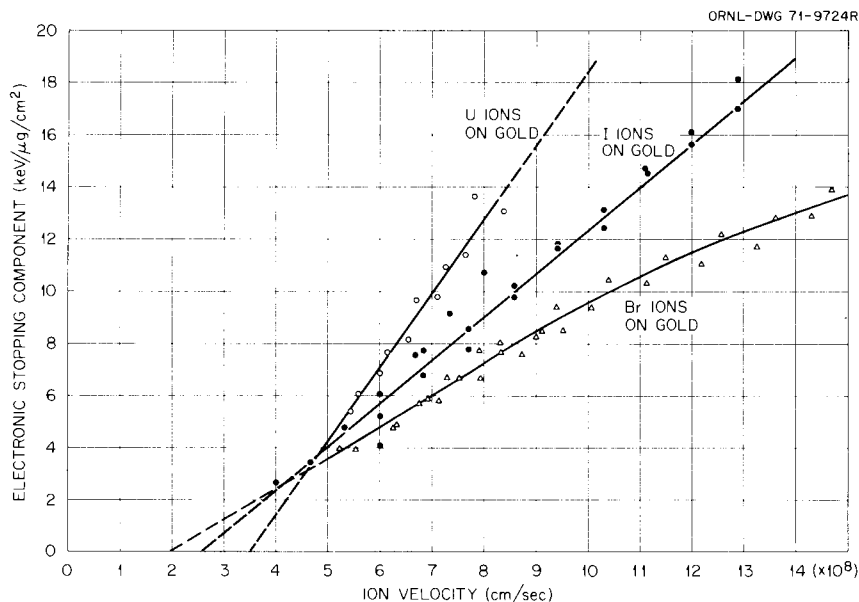


Fig. 1. Stopping power of uranium, iodine, and bromine ions in gold.

fact that heavier ions show a larger value of a than that for light ions. Presumably this effect would be unimportant for ions as light as oxygen. In particular, stopping power data for uranium ions have been compared with the theoretical predictions of the theories of Lindhard and Firsov for carbon, nickel, and gold, respectively, as shown in Figs. 2–4. The important point is that the data cannot be reconciled with theory by a simple change of slope.

It was expected that ions moving in crystal channels and having no close collisions with atoms might show the $S_e = kE^{1/2}$ behavior. Some data taken by Eriksson, Davies, and Jespersgaard⁶ with very low energy xenon ions in tungsten crystals do appear to follow this relationship. At higher energy, 21.6- to 32.5-MeV iodine ion stopping powers have been measured for particles hyperchanneled⁷ in the $\langle 100 \rangle$ axis of a crystal of silver. The results are shown in Fig. 5. Polycrystalline stopping powers measured by Moak and Brown⁸ are shown as measured and, slightly below, adjusted to remove the estimated contribution of nuclear stopping.⁹ Channeling data have not been adjusted for nuclear stopping since there is strong evidence for the conclusion that nuclear stopping is negligible for channeled ions.¹⁰ The energy loss pattern for iodine ions hyperchanneled in the $[011]$ axis in silver is shown schematically in Fig. 5. Beginning with particles showing the least energy loss (and running nearest the center of the channel) and including particles which fall in the class of ordinary axially channeled particles and finally

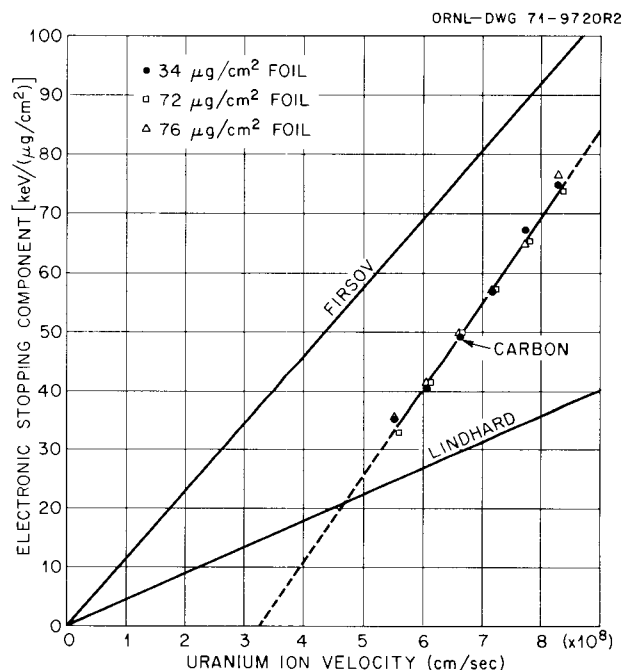


Fig. 2. Comparison of uranium ion stopping power in carbon with theoretical estimates.

including particles which run in the $\langle 100 \rangle$ planar channels, the behavior of the stopping power does not obey the relation $S = kE^{1/2}$. The data given by Eriksson, Davies, and Jespersgaard have been included in the figure, even though both the ion and the stopping

medium are different. At higher energies, where the iodine measurements were made, the stopping powers follow the relation $S_e = a + bE^{1/2}$. The data suggest that, below 21.6 MeV, there is a velocity region where the stopping-power curve is more complicated and that some additions must be made to the theory for this velocity range.

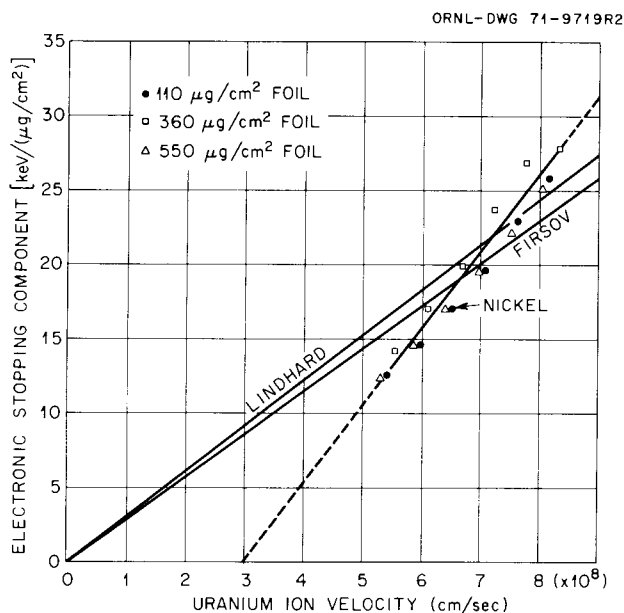


Fig. 3. Comparison of uranium ion stopping power in nickel with theoretical estimates.

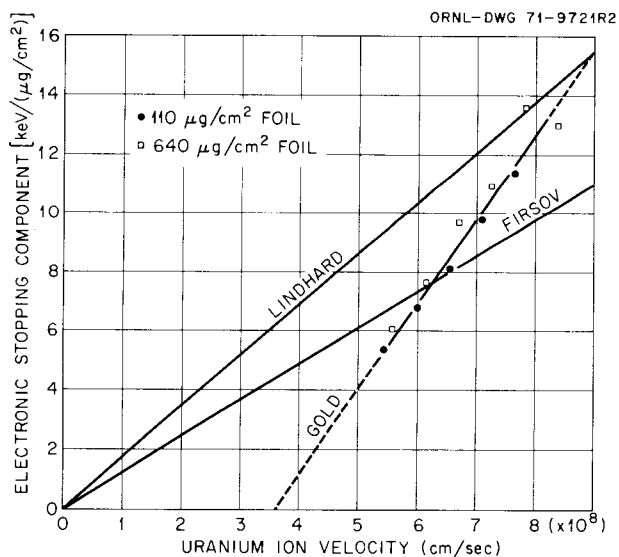


Fig. 4. Comparison of uranium ion stopping power in gold with theoretical estimates.

1. Solid State Division.
2. Chemistry Division.
3. M. D. Brown and C. D. Moak, *Phys. Rev.* **B6**, 90 (1972).
4. J. Lindhard, M. Scharff, and H. E. Shiøtt, *Kgl. Dan. Vidensk. Selsk., Mat.-Fys. Medd.* **33**, 14 (1963).
5. O. B. Firsov, *Zh. Eksp. Teor. Fiz.* **36**, 1517 (1959) [*Sov. Phys. JETP* **9**, 1076 (1959)].
6. L. Eriksson, J. A. Davies, and P. Jespersgaard, *Phys. Rev.* **161**, 219 (1967).
7. B. R. Appleton, C. D. Moak, T. S. Noggle, and J. H. Barrett, *Phys. Rev. Lett.* **28**, 1307 (1972).
8. C. D. Moak and M. D. Brown, *Phys. Rev.* **149**, 224 (1966).
9. J. Lindhard, V. Nielsen, and M. Scharff, *Kgl. Dan. Vidensk. Selsk., Mat.-Fys. Medd.* **36**, 10 (1968).
10. C. D. Moak, J. W. T. Dabbs, and W. W. Walker, *Rev. Sci. Instrum.* **37**, 1131 (1966).

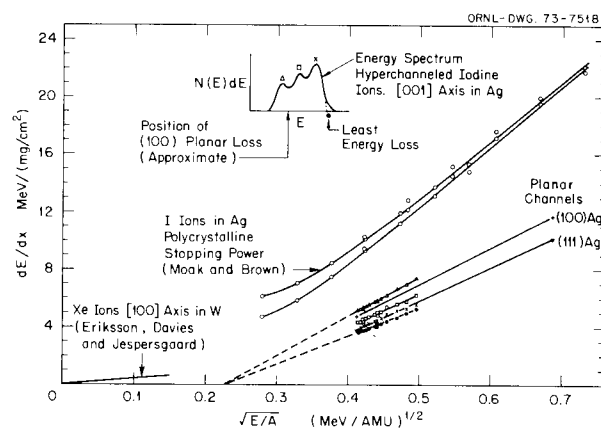


Fig. 5. Stopping power of iodine ions in various crystal channels.

HYPERCHANNELING: I. INVESTIGATIONS FOR HIGH-ENERGY HEAVY IONS IN SILVER¹

B. R. Appleton² C. D. Moak
 J. H. Barrett² S. Datz³
 J. A. Biggerstaff T. S. Noggle²

When a beam of energetic ions enters a single crystal parallel to an axial direction, those which enter most nearly the center of the channel receive the smallest deflections. Some small fraction will acquire trajectories which remain within the confines of one particular axis (i.e., the open region surrounded by nearest neighbors), while a larger fraction will be axially channeled, but wander from one particular axis to another. Those ions confined to a particular axial channel will have two distinguishing characteristics: (1) they will be populated over a much smaller range of angles than regular axial channeling and (2) they will have a much lower rate of

energy loss. It is this particular axial channeling phenomenon which we call hyperchanneling. Although this effect was recognized to exist in the 1963 paper by Robinson and Oen⁴ which initiated present-day channeling studies, it was not until 1966 that the first experimental observation was reported by Eisen.⁵ He attributed a high-energy tail for 375-keV protons transmitted through 2.2- μm silicon crystals along the [110] direction to protons which remained within a single axial channel (hyperchanneling) in traversing the crystals. The effect was not, however, sufficiently prominent to investigate in detail. No further investigations of this phenomenon were reported until 1972, when Appleton, Moak, Noggle, and Barrett^{6,7} observed hyperchanneling for high-energy heavy ions. For 21.6-MeV iodine ions transmitted through thin silver single crystals near the [011] axis, they observed a distinct hyperchanneled group of ions with much lower energy loss rates than regular axial channeling and with a characteristic critical angle well within the axial critical angle. Because of the prominence of this effect for high-energy heavy ions, it was possible to study the details of hyperchanneling phenomena.

Recently the investigations for high-energy heavy ions were extended to include measurements for the [001] directions as well as the [011], and these results were

compared with model calculations. Although the main features of the hyperchanneling measurements could be understood in terms of the model, several new and unexpected features appeared. Perhaps the most interesting of these can be understood with the aid of Fig. 1. The two sets of data shown in this figure were obtained by measuring the transmitted energy spectra of 21.6-MeV iodine ions incident at various angles, $\Delta\psi$, relative to the [001] (left-hand figure) and [011] (right-hand figure). The spectra were measured by an energy-sensitive detector in line with the incident beams, but with an acceptance angle of only $\pm 0.012^\circ$. Consider first the data for the [011] axis. The features in these spectra are well understood in terms of the hyperchanneling model. The intense peak at lowest energy loss, near $\Delta\psi = 0$, results from hyperchanneled ions; the smaller peak at lower dE/dx which grows as $|\Delta\psi|$ increases can be identified as axially channeled ions which are wandering from one particular axis to another. These same two peaks can be identified in the spectra for the [001] axis, but in addition, group structure which cannot be understood in terms of the model calculations at all appears at intermediate energy loss values. Although more work is required to identify the nature of this structure, it appears likely that it results from discrete oscillations supported within a

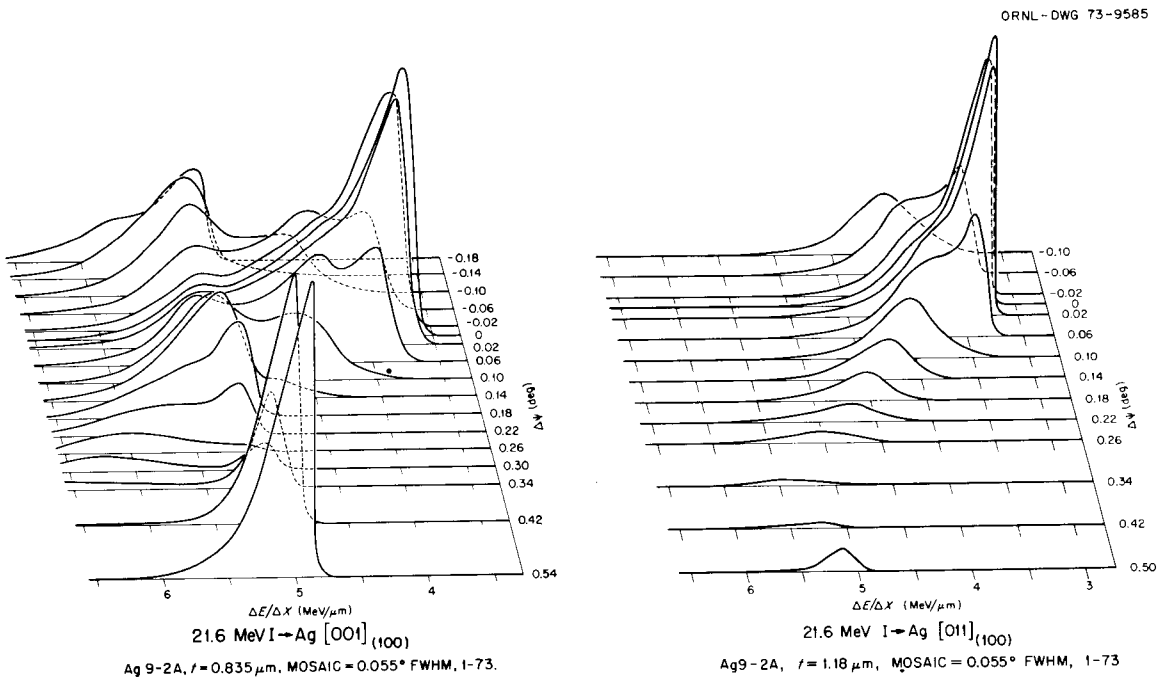


Fig. 1. Comparison of normalized transmitted energy-loss distributions for 21.6-MeV iodine ions incident at various angles to [001] in (100) (path length, 0.835 μm ; mosaic spread, 0.055 $^\circ$ FWHM) and to [011] in (100) (path length, 1.18 μm ; mosaic spread, 0.055 $^\circ$).

[001] hyperchannel. It clearly is a fine-structure effect which will be valuable in studying the ion-solid interaction potential.

1. Summary of paper to be published.
2. Solid State Division.
3. Chemistry Division.
4. M. T. Robinson and O. S. Oen, *Phys. Rev.* **132**, 2385 (1963).
5. F. H. Elsen, *Phys. Lett.* **23**, 401 (1966).
6. B. R. Appleton, C. D. Moak, T. S. Noggle, and J. H. Barrett, *Phys. Rev. Lett.* **28**, 1307 (1972).
7. B. R. Appleton, J. H. Barrett, T. S. Noggle, and C. D. Moak, *Radiat. Eff.* **13**, 171 (1972).

K AND L X-RAY PRODUCTION CROSS SECTIONS FROM HEAVY-ION BOMBARDMENT

Jerome L. Duggan¹ P. D. Miller

The group was composed of P. D. Miller and the following outside users:

Jerome L. Duggan	North Texas State University
Tom J. Gray	North Texas State University
J. Lin	Tennessee Technological University
R. F. Carlton	Middle Tennessee State University
J. D. McCoy	University of Tulsa
E. L. Robinson	University of Alabama (Birmingham)
Ram Chaturvedi	State University of New York, Cortland, N.Y.
George Pepper	Ph.D student, North Texas State University
R. A. Gallman	M.S. thesis done on tandem; degree received June 1973 (University of Tennessee)

The group has been primarily concerned with the measurement of x-ray production cross sections induced by oxygen and carbon ions. These measurements have all been made for targets that can be considered thin for the incident ions. Measurements have been made for *K* x rays for a variety of target materials between calcium and antimony for incident oxygen energies between 16 and 44 MeV and for carbon ions in the 11-to-32-MeV region. The measured cross sections have been compared with the predictions of the binary encounter approximation (BEA) which has been proposed by Garcia et al.² for an interaction of this type.

Figure 1 shows the x-ray production cross section dependence on atomic number. Figure 2 shows the yield curve for six elements for incident oxygen ions between 8 and 32 MeV. The lines in the figure are not theoretical fits; rather, they are only to guide the eye. Figure 3 shows a universal curve for six elements. In this representation, U is the binding energy of the *K* electron, Z is the charge of the projectile, and λ is the ratio of the oxygen mass to the electron mass. Calculations are being made for these data which improve the theoretical fit. These calculations, which have recently been proposed by McGuire et al.,³

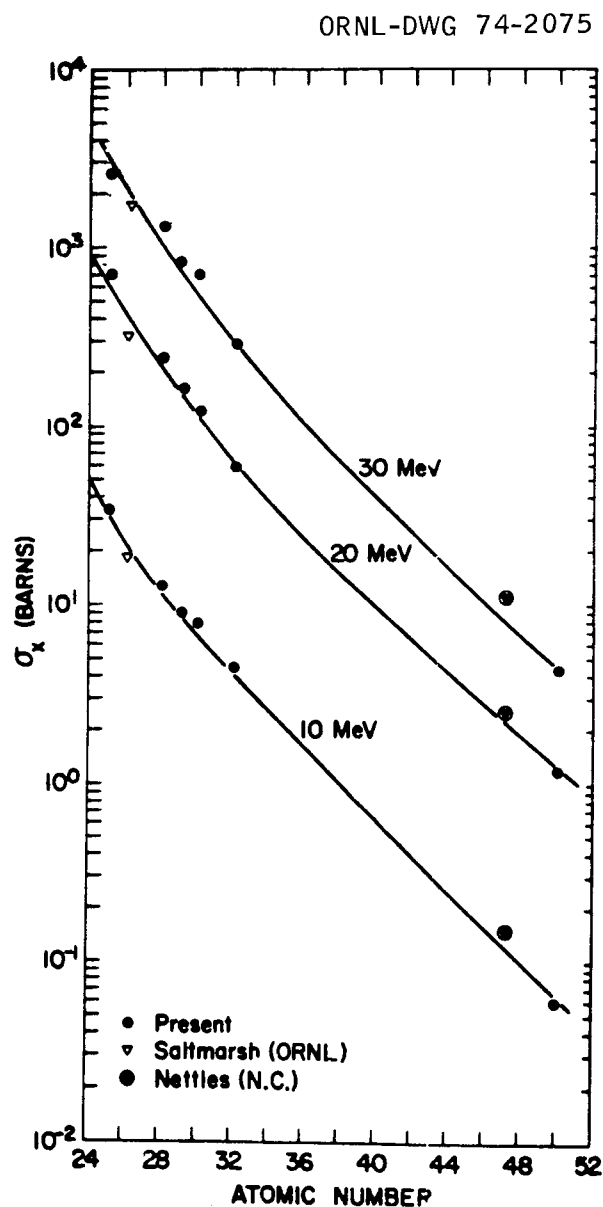


Fig. 1. σ_x vs Z for 10-, 20-, and 30-MeV oxygen ions.

ORNL-DWG 74-2076

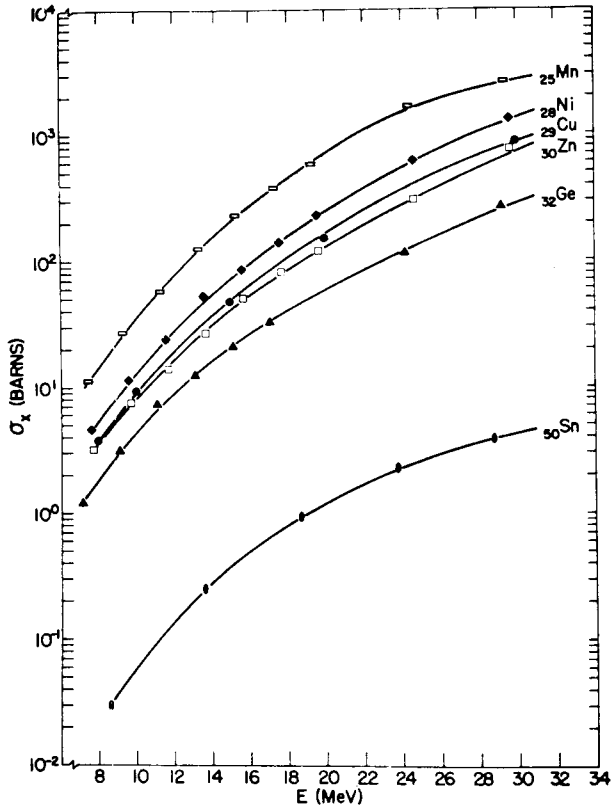
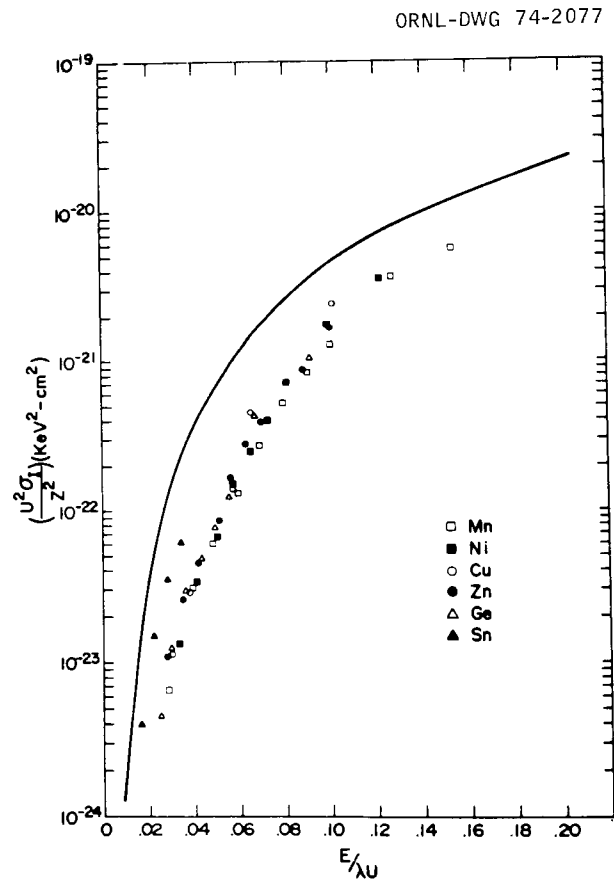


Fig. 2. X-ray production cross section by oxygen bombardment on Mn, Ni, Cu, Zn, Ge, and Sn. Solid curves drawn through experimental points.

Fig. 3. K shell ionization by oxygen impact. The solid curve is the prediction of the binary encounter model.



ORNL-DWG 74-2077

account for the fact that multiple ionization is a pronounced effect for heavy-ion reactions of this type. The model being used is a modified BEA calculation. The presence of satellite lines in high-resolution spectra and energy shifts in the characteristic spectra all tend to indicate that these multiple ionization effects are important. Figure 4 shows a typical energy shift for nickel $K\alpha$ and $K\beta$. Figure 5 shows these energy shifts as a function of bombarding energy for three elements. Figure 6 shows the $K\alpha/K\beta$ ratios for six elements as a function of energy.

We have also measured K and L x-ray cross sections for ten elements measured in the range from calcium ($Z = 20$) to

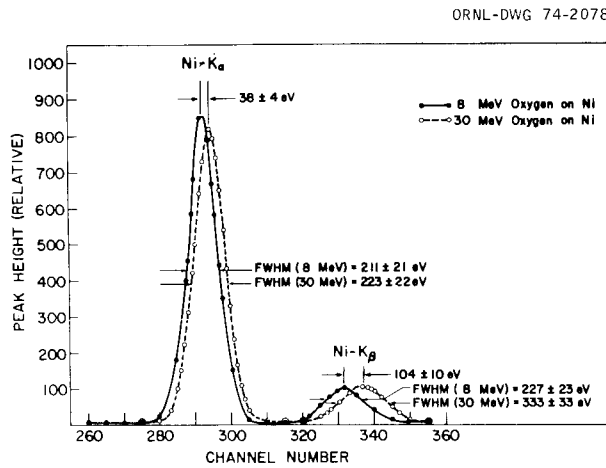


Fig. 4. K x-ray energy shift for 8- and 30-MeV oxygen impact on nickel.

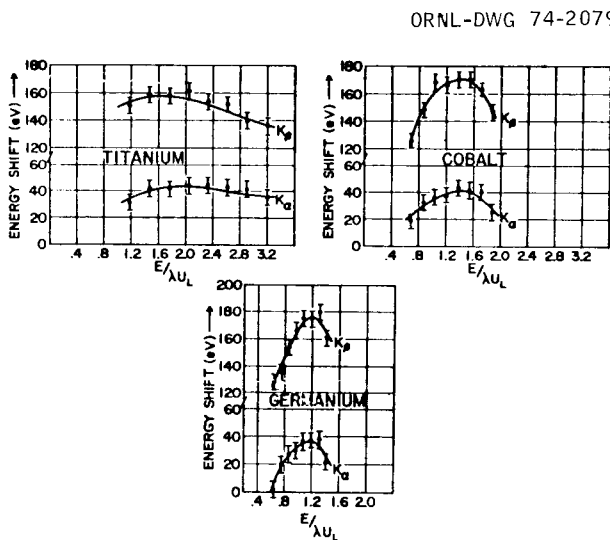


Fig. 5. $K\alpha$ and $K\beta$ x-ray energy shifts vs reduced oxygen ion energy.

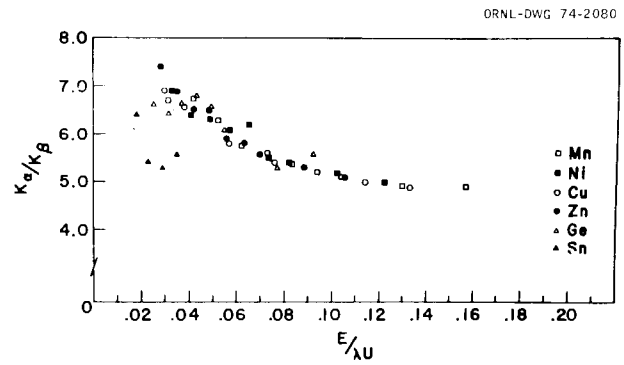


Fig. 6. $K\alpha/K\beta$ ratios for oxygen bombardment on Mn, Ni, Cu, Zn, Ge, and Sn.

palladium ($Z = 46$) for incident carbon ions from 11 to 32 MeV. The data are being analyzed in terms of the recent McGuire theory.³

1. North Texas State University, Denton, Tex.
2. J. D. Garcia, R. J. Fortner, and T. M. Kavanagh, "Inner Shell Vacancy Production in Ion Atom Collisions," *Rev. Mod. Phys.* 45, 111 (1973).
3. J. H. McGuire and P. Richard, *Phys. Rev.* A8, 1374 (1973).

ACCELERATOR OPERATION, DEVELOPMENT, AND APPLICATIONS

STATUS REPORT ON THE TANDEM VAN DE GRAAFF ACCELERATOR

G. F. Wells	N. F. Ziegler
R. L. Robinson	G. K. Werner
F. A. DiCarlo	D. M. Galbraith
J. W. Johnson ¹	R. P. Cumby ¹

The tandem ion source facility has undergone a major change during the spring and early summer of 1973. The original ion source, vacuum housing, and electronics provided with the accelerator in 1960 were removed and a more flexible arrangement of ion sources installed. Two new ion source injection positions were added to the existing pulsed ion source and polarized proton source. A new injection magnet was added to bring beams from any of the four positions onto the accelerator beam injection line. Two sets of controls, local and remote, may be switched simultaneously to control off-ground power supplies pertinent to each of the six types of ion sources now available.

The two new ion source positions are equipped with modular-designed off-ground vacuum housings and "accel" tubes. Each can accommodate a variety of ion sources and provide additional acceleration energy of

100 kV to the energy at which negative ions are produced. They are designed so that (1) an ion source assembly may be removed from the vacuum housing and replaced by another, (2) the ion source assembly, vacuum housing, and accel tube may be replaced as a unit, or (3) the entire system may be replaced by another without undue effort. Handling of ion source assemblies can be done manually. Handling of larger components is done with an overhead crane hoist. Simplified alignment adjustments are built into the support stand.

An improved model of the charge-exchange ion source, built by ORNL, is mounted in one of the two

new positions. It has commonly produced H^- , He^- , C^- , O^- , F^- , S^- , Cl^- , Br^- , and I^- beams in the past. Improved performance with regard to reliability, increased beam intensity, and increased beam transmission have resulted.

Three new ion sources have been purchased for use on the other new position. Thus far the Cs^+ sputter-cone source of Middleton² has reliably produced C^- , O^- , Cu^- , Ni^- , and Au^- beams of 1 to 20 μa intensity and Al^- , Fe^- , and Bi_2^- beams of 0.3 to 1.0 μa intensity. Experience with the Hortig-type³ sputter ion source and the Heinicke⁴ Penning discharge ion source is insufficient to report.

Table 1. Research activities on the tandem Van de Graaff accelerator

Type	Projectile	Investigators	Percent of research time
($^{16}O, \alpha$), ($^{16}O, d$), ($^{16}O, ^6Li$)	^{16}O	Ford, Del Campo, ^a Robinson, Thornton, ^b and Stelson	6
($^{16}O, X$) in-beam gamma	^{16}O	Robinson, Kim, Sayer, ^c Smith, ^d Milner, Singhal, ^c J. Wells, ^e Lin, ^e Hamilton, ^c and Ramayya ^c	25
(O, n) and (C, n) cross sections	$^{16,18}O, ^{12,13}C$	Bair and Stelson	0.7
(O, X) cross section	$^{16,18}O$	Robinson, J. Wells, ^e Kim, Ford, Plendl, ^f Holub, ^f Zeller, ^f and DeMeijer ^f	5
Short-lived radioactivities	$^{16}O, p$	Ramayya, ^c Ronnigan, ^c Garcia-Bermudez, ^c Lange, ^c Carter, Raman, Gove, ^g and Walkiewicz ^h	5
Elastic scattering	^{16}O	Raman, Stelson, and Saltmarsh	0.3
Coulomb excitation	$\alpha, ^{16}O$	McGowan, Bemis, Milner, Robinson, Stelson, Ford, Hamilton, ^c Ronnigan, ^c Garcia-Bermudez, ^c Ramayya, ^c Raman, Dagenhart, ⁱ Tuttle, ^j and Riedinger ^j	20
Hydrogen contaminations on metallic surfaces	p	Saltmarsh and Wolfenden ^k	0.6
Channeling	I	Moak, Biggerstaff, Appleton, ^l Noggle, ^l Datz, ^m Brown, ⁿ and Krause ^m	8
Heavy-ion atomic physics	O, F, Cl, Al	Sellin, ^j Laubert, ^o Haselton, ^j Pegg, ^j Thoe, ^j Peterson, ^j Mowat, ^j Griffin, and Brown ⁿ	19
X-ray studies	^{16}O	Duggan, ^p Chaturvedi, ^q Gray, ^q Kauffman, ⁿ Pepper, ^p Light, ^p E. Robinson, ^r Miller, Lin, ^e McCoy, ^s and Carlton ^t	8
High-charge-state studies	I	Miller, Moak, Biggerstaff, Alton, Jones, Kessel, ^u Bridwell, ^v and Wehring ^w	3

^aUniversity of Mexico, Mexico City.

^bUniversity of Virginia.

^cVanderbilt University.

^dORAU Postdoctoral Fellow.

^eTennessee Technological University.

^fFlorida State University.

^gComputer Sciences Division.

^hEdinboro College.

ⁱIsotopes Division.

^jUniversity of Tennessee.

^kMetals and Ceramics Division.

^lSolid State Division.

^mChemistry Division.

ⁿKansas State University.

^oNew York University.

^pNorth Texas State University.

^qSUNY College, Cortland.

^rUniversity of Alabama.

^sUniversity of Tulsa.

^tMiddle Tennessee State University.

^uUniversity of Connecticut.

^vMurray State University.

^wUniversity of Illinois.

Other developments include the installation of a more sophisticated beam control system of HVEC⁵ design, a new technique by J.W. Johnson for cutting belt charging system screens that produces more uniform screen-belt contact,⁶ and an improved bearing mounting for drive motor and terminal generator bearings that is providing longer operating life for them.

The principal failures of the year are (1) the burnout of a switching magnet coil, disabling the experimental legs beyond it (except for the straight-through port) in one experimental room; (2) a charging system belt failure, which required two replacements before satisfactory operations were resumed; (3) continued unreliability of the quadrupole power supplies (these are in process of replacement by all-solid-state supplies); (4) a drive motor and terminal generator replacement (the presently installed units, with improved bearing mountings in both, are now exceeding 4000 hr operating time).

Research activities and utilization of the operational time of the Van de Graaff accelerator are summarized in Tables 1 and 2.

1. Instrumentation and Controls Division.
2. R. Middleton and C. Adams, University of Pennsylvania, Philadelphia, Pa.
3. M. Mueller and G. Hortig, *IEEE Trans. Nucl. Sci.* NS-16, p. 38 (1969).
4. E. Heinicke, K. Bethge, and H. Baumann, *Nucl. Instrum. Methods* 58, 125 (1968).
5. High Voltage Engineering Corp., Burlington, Mass.
6. The screen is cut along a bias line instead of a warp or woff line.

Table 2. Utilization of scheduled operation and maintenance support time^a

Function	Hours	Percent of time
Maintenance	844	21
Changeover ^b	168	4
Development	1648	42
Research ^c	1292	33
Total	3952	100

^a16 hr per day, five days a week.

^bTime required to change from one experiment to another.

^c1392 hr of additional research was performed in non-scheduled time (between midnight and 8 AM and on weekends and holidays). This gives a utilization factor of

$$\frac{2684 \text{ research hours}}{3952 \text{ scheduled support hours}} = 0.68.$$

TANDEM DATA-LOGGING SYSTEM

J. A. Biggerstaff W. T. Milner
N. F. Ziegler

Accumulation of typical operating data for the tandem accelerator under varying beam conditions has been a repetitious and time-consuming task. An automatic data-logging system is being implemented which should remove much of the drudgery and improve the accuracy of the data. An existing PDP-11 computer, analog-to-digital converter, and 20-channel multiplexer will be used in the system. An analog signal-conditioning unit has been constructed which presently contains 18 channels. The number of channels may be easily expanded to the full capacity of the multiplexer, which is in turn expandable to 32 channels. The computer has been programmed to display the data on a cathode ray tube output. When the system is completed, hard copy of the data will be provided by an existing line printer.

TANDEM CONTROL SYSTEM

N. F. Ziegler

Continued difficulty in maintaining beam current with "normal" disturbances of the accelerating voltage has led to the installation of a voltage-stabilizing system on the EN tandem accelerator. The stabilizer is a commercial unit manufactured by High Voltage Engineering Corporation and has proven to be very popular with accelerator operators, since maintaining the beam on target no longer requires their constant attention. A block diagram of the system is shown in Fig. 1. Three modes of operation are provided: slit, GVM (generating voltmeter), and auto. In the auto mode the slit signals normally provide the error input to the stabilizer, but in the event of beam loss and/or terminal voltage excursion the system automatically switches to the GVM mode. When slit signals are again acquired, the system switches back to the slit mode. Thus, in most instances, operator action is unnecessary when a voltage breakdown occurs in the accelerating system. The corona current supplied by the control tube, however, is limited, and under heavy beam loading the stabilizer may lose control when the loading ceases abruptly. To alleviate this situation a new belt charge regulator has been designed which will maintain the corona tube current at a fixed value through variation of the terminal charging current. This device, when installed, should maintain control of the accelerator under all "normal" operating conditions. Spark-detection circuits

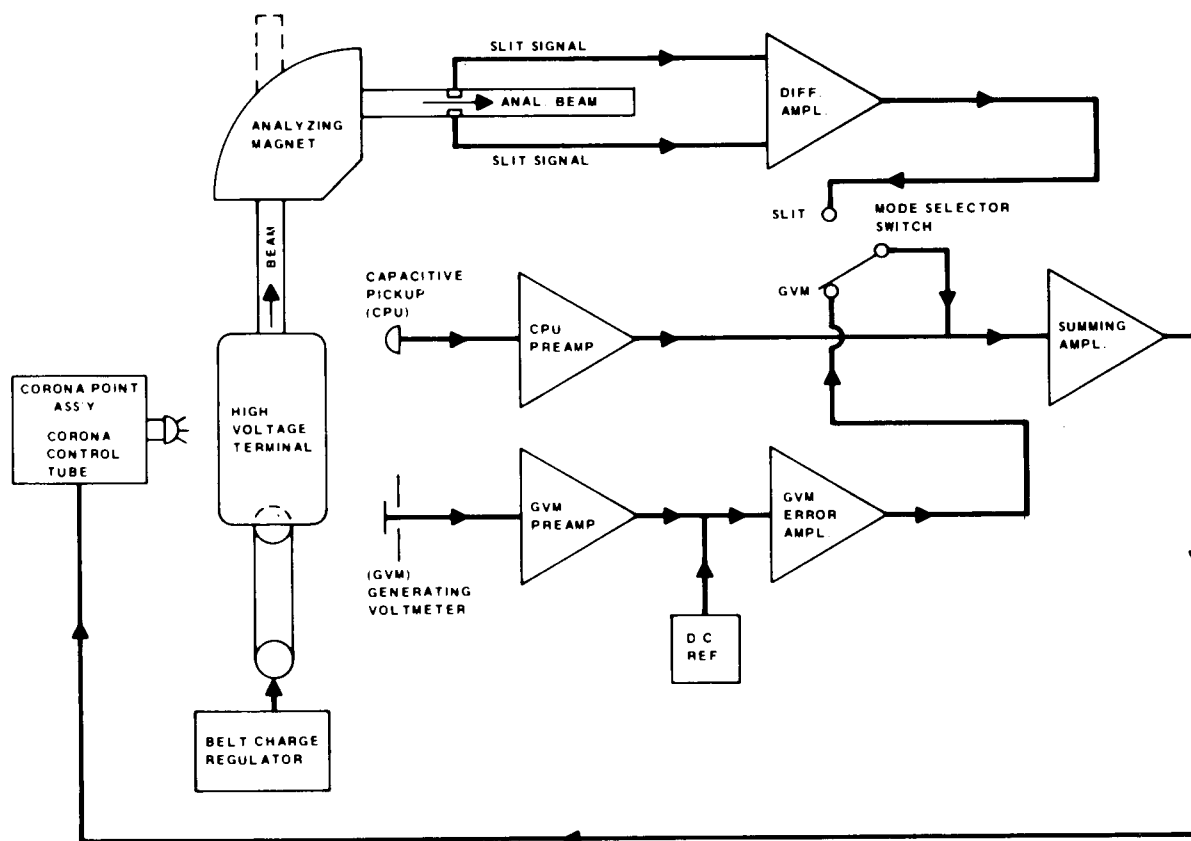


Fig. 1. Typical voltage stabilizer system.

have been included in the regulator to prevent overshoot in terminal voltage and to remove belt charge after a selected number of sparks.

DEVELOPMENTS IN COMPUTER AND DATA ACQUISITION SYSTEMS

J. A. Biggerstaff J. W. McConnell¹
W. T. Milner N. F. Ziegler

Although the permanent Van de Graaff Laboratory staff has decreased considerably within the last few years, the load on the data acquisition and computer facilities continues to increase because there is a growing number of outside researchers in both nuclear and atomic physics. In addition, as experiments become steadily more sophisticated and the researcher becomes more aware of the capability and potential of the computer and the computer-based data acquisition systems, their usage increases, and a demand for further developments is created.

The present system consists of the following list of major components: (1) a CDC-3200 computer with 32K words of memory and standard peripherals, (2) an interface to three multichannel analyzer data transmission terminals, (3) a PDP-11/20-based Tennecomp data acquisition system, (4) 22 million 8-bit bytes of disk storage accessible from both computers, (5) a 20-input multiplexed ADC linking the PDP-11 to analog signals measuring tandem operating parameters, and (6) a memory-to-memory data transmission link between the PDP-11 and the CDC-3200.

Capabilities of the Current System

1. All single-parameter data acquired in this laboratory are maintained either on immediately accessible disk files or on magnetic tape. At the present time, between 1 and 1.5 million channels of single-parameter data are always immediately available to both the PDP-11 and the CDC-3200. One million channels of two-parameter data are also immediately accessible. The

single-parameter tape file now contains about 12,000 spectra, or approximately 18 million channels. About 10 million channels of two-parameter data have been acquired within the last eight months. Any of these data can be made available to both the CDC-3200 and the PDP-11 within about 2 to 5 min.

2. The CDC-3200 handles all data transmissions from the multichannel analyzer terminals via a background program and is therefore always available for batch job processing (processing data, doing computations, etc.). Either the CDC-3200 or the PDP-11 is used for all of our data processing.

3. Data acquired via the PDP-11 system are transferred into the permanent data base without intervention by the CDC-3200.

4. The PDP-11 system can acquire single-parameter data at rates above 50K events per second and acquire multiple-parameter data at rates up to at least 2000 events per second.

5. Two-parameter data arrays up to one million channels in size can be maintained via the use of both the PDP-11 and the CDC-3200 (to sort the data) at data rates up to 1000 events per second.

6. We have at our disposal a rather powerful base for PDP-11 software development. Programs are developed, off line, by the use of a CDC-3200 program (written at this laboratory) which assembles programs written in PDP-11 assembly language, produces listings and diagnostics, and writes PDP-11 loader-compatible code on disk. Systems routines available on the CDC-3200 provide for convenient storage, editing, and use of source files.

Developments within the Past Year

Programs have been developed which provide for the disk communication necessary to load programs, store and retrieve one- and two-parameter data, and store multiple-parameter data. The data-taking and spectrum analysis programs, supplied by Tennecomp Systems Inc., have been completely rewritten and improved.

One of the great strengths of a computer-based data acquisition system is its ability to do event-by-event processing in real time, thus reducing the amount of data storage required. We have developed software to process the two signals from a position-sensitive detector (energy and energy times position) which reduces an 8K by 8K input array to a single-parameter spectrum of 512 channels. The flexibility of the system provides many options as to just what additional information is extracted from each event.

A multiple-parameter data-taking system has been developed which utilizes both computers. When operated in the two-parameter mode, it keeps a one million channel array on disk updated in nearly real time (less than 10 min lag). Single-parameter spectra corresponding to gates in either direction can be retrieved into the CDC-3200 and gates in one direction can be retrieved into the PDP-11 concurrently with data taking. Event-by-event tapes (with up to six parameters) can be produced simultaneously and scanned, off line, to yield up to fifty 4096-channel spectra per pass.

Hardware and software have been developed and implemented which provide for the bidirectional transmission of data and interrupts between the PDP-11 and the CDC-3200 computers. This means that the user can develop his own data reduction program on the CDC-3200 (in FORTRAN) and execute it, as well as send data to it and receive results from it, from the PDP-11, while data taking is in progress.

A comprehensive "computer users handbook" (about 100 pages) has been produced which gives explicit directions for the use of some 20 of the most frequently used CDC-3200 and PDP-11 programs as well as some general operating instructions for both computer systems. The text of this manual is on punched cards and is edited and updated as often as system changes require.

At the present time, we are in the process of deriving the necessary analog signals required to monitor a number of tandem operating parameters. A general-purpose multiplexed analog-to-digital converter (with 32 inputs possible) interfaced to the PDP-11 is used to read digital values associated with these parameters into the PDP-11 for display purposes.

Plans for Next Year

More interactive data reduction software, utilizing the CDC-3200-PDP-11 communications link, will be developed in the near future. The PDP-11/20 research computer will be replaced with a much more powerful PDP-11/45. The PDP-11/20 will then be assigned to monitor and control the tandem Van de Graaff accelerator, since it has become impossible to maintain full-time operator coverage. In addition, developments in this area should be invaluable in the event that a larger electrostatic accelerator is funded in the future.

PROTON MICROANALYSIS USING A LITHIUM ION BEAM

J. A. Biggerstaff

Accurate measurements of hydrogen concentrations on and near the surface of solids have such diverse applications as analysis of lunar surface materials for water and trapped solar protons and studies of hydrogen-embrittlement failure of titanium aircraft structures. A promising new technique for making these measurements using an intense ${}^7\text{Li}$ ion beam from the CN Van de Graaff accelerator is being developed by a group from Grumman Aircraft Corporation headed by G. M. Padawer. Lithium ions from the accelerator slowing down in a hydrogen-bearing sample excite a strong narrow resonance at 3.07 MeV lithium ion energy in the ${}^7\text{Li}(p,\gamma)$ reaction. The depth in the sample at which this takes place is controlled by varying the initial ion energy. The reaction is extremely exoergic, producing 15- and 17-MeV gamma rays which are easily detected. Depths up to 30 μm can be probed with about 0.1 μm resolution, and hydrogen concentrations of a few parts per million can be detected.

THE HEAVY-ION SOURCE PROGRAM

MULTIPLY CHARGED HEAVY-ION SOURCE SYSTEM STUDIES

G. D. Alton C. M. Jones
E. D. Hudson M. L. Mallory

In order to identify promising areas of study for the multiply charged heavy-ion source physics program, we have attempted to make a fairly thorough analysis of the physical processes which lead to multiply charged heavy ions. The result of this study is a set of conclusions and viewpoints which enabled us to develop a strategy for this program. In this contribution, we will try to very briefly summarize some of these ideas and also to discuss several aspects of our work which do not fit naturally into other contributions.

One can divide ion source systems into three basic types, namely, those which function by the interaction of photons, electrons, and ions with atoms or molecules. The first of these, photon bombardment, has received relatively little attention. This fact motivated us to make a careful study of concepts based on photon-induced ionization. In particular, we have made a conceptual study of the idea of producing an intense x-ray beam by electron bombardment,¹ and then using this beam to produce multiply charged ions by inner-shell vacancy production followed by cascade proc-

esses.² The essential result is that even with a well-optimized geometry, the expected ionization rates are less than those which would be obtained with an electron beam of an intensity used to produce the x-ray beam in question.

This conceptual study was corroborated by experimental measurements in which an existing calutron source³ was modified so as to approximate the concept described above. Our conclusion is that x-ray bombardment might be an attractive element of an ion containment source, either as the principal ionizing mechanism or as a supplemental ionizing mechanism. However, it also seems clear that a simple source in which a given atom is subjected to only one photon collision before extraction is not attractive.

The second mechanism listed above, electron bombardment, is the basis for virtually all the devices which we normally think of as "ion sources."⁴ These range from the Penning and duoplasmatron sources now in use on heavy-ion accelerators to such novel concepts as laser-produced plasmas. Two simple considerations are helpful in thinking about electron bombardment sources. The first is yield. In general, we wish to have a source which will produce at least particle microamperes of the ion in question. This consideration immediately rules out "crossed beam" devices and forces consideration of more sophisticated concepts. The second consideration might be called "practicality." By this, we mean that a useful source must have properties which allow it to be used with an accelerator. For example, we require high macroscopic duty cycle and high brightness (the latter implies low ion temperature, preferably less than a few tens of electron volts).

The result of these considerations is that we have chosen to focus our effort on two types of ion containment sources, namely, Penning sources and the class of device represented by the INTEREM machine. The first choice was straightforward. Penning sources are used in virtually all heavy-ion accelerators employing multiply charged sources, and even small incremental improvements in their properties will have immediate and widespread consequences. More detailed accounts of our work on Penning sources⁵ and a Penning source test facility⁶ are given in other contributions.

The INTEREM machine is a plasma containment device originally built as part of the thermonuclear program. It has, for us, two important features: a magnetic containment geometry consisting of superimposed cylindrical mirror and quadrupole fields and electron cyclotron resonance heating. Without going into detail given elsewhere in this report,⁷ we believe that a device of this type may have the potential for

long ion containment lifetime, a feature which we believe is necessary for dramatic improvement in the yield of highly charged ions.

The third mechanism listed above, ion-atom interactions, is the process we normally call "stripping." The essence of our conclusions about stripping is that under suitable circumstances, simple systems based on stripping compare very favorably with conventional ion sources. We cite two examples. The first is the tandem Van de Graaff accelerator. In small sizes, the tandem accelerator can be an attractive ion source,⁸ while in large sizes it becomes an attractive accelerator in its own right. In both of these applications, a high-yield, high-brightness negative ion source and optimized terminal stripper systems are important factors in obtaining the performance which is inherent in the accelerator. The second example is the "recycle" concept suggested by Hudson, Mallory, and Lord.⁹ In this case, stripping techniques, as well as positive source technology, are important factors in the successful realization of the idea. Motivated by these considerations, we have begun an active program to study negative ion sources and the physics of stripping.

One of the principal short-term goals of our negative source program is the construction of a negative ion source test facility. This facility, now being designed, will use an existing magnetic analyzer and have the following parameters: acceleration voltage, up to 100 kV; acceptance (full area), 10 cm-milliradians; nominal resolution, 400 to 1500, depending on object size; mass dispersion at 240 amu, 0.3 cm; design operating pressure, less than 10^{-7} torr. Completion of this facility is expected in 1974. We expect that it will be used not only for ion source diagnostics but also as a source of negative beams for subsequent experiments.

Additional work on negative sources has included a careful assessment of what is known about multiply negative ions and construction of a locally designed cesium surface ionization source.

Our work on stripper physics has been concentrated on the phenomenology of stripping at nonzero angles. It is described in detail in another contribution.¹⁰ It should be emphasized that this work has potential application not only to tandem accelerators and recycle but to any accelerator system utilizing stripping.

Finally, we have become increasingly aware of the importance of beam transport, especially with respect to extraction from sources and injection of an extracted beam into an accelerator. This realization has motivated us to begin to develop a greater capability in two other areas — ion optics and low-energy charge-changing cross sections for ion-atom collisions. This work is also described in greater detail in other contributions.^{11,12}

1. E. Storm, H. I. Israel, and D. W. Lier, *Bremsstrahlung Emission Measurement from Thick Tungsten Targets in the Energy Range 12–300 kV*, Los Alamos Scientific Laboratory report No. LA-4624.

2. T. A. Carlson, W. E. Hunt, and M. O. Krause, *Phys. Rev.* **151**, 41 (1966).

3. L. O. Love and W. A. Bell, ORNL-3606 (1963).

4. A good review is given in the proceedings of the International Conference on Multiply Charged Heavy Ion Sources and Accelerating Systems, held in Gatlinburg, Tennessee, October 1971 [*IEEE Trans. Nucl. Sci.* NS-19(2) (1972)].

5. E. D. Hudson, M. L. Mallory, R. S. Lord, J. E. Mann, J. A. Martin, R. K. Goosie, and F. Irwin, "Heavy-Ion Beam Development," this report.

6. M. L. Mallory, E. D. Hudson, C. M. Jones, and S. W. Mosko, "Penning Ion Source Test Facility," this report.

7. H. Tamagawa, C. M. Jones, N. H. Lazar, and W. M. Good, "Measurements on INTEREM," this report.

8. For example, a 6-MV tandem accelerator using an oxygen terminal stripper and a carbon stripper at ground potential can produce a beam of Br^{17+} at an intensity of about 1.5 particle- μA when the injected beam is 100 μA .

9. E. D. Hudson, M. L. Mallory, and R. S. Lord, to be published in *Nuclear Instruments and Methods*; E. D. Hudson, M. L. Mallory, R. S. Lord, J. E. Mann, J. A. Martin, R. K. Goosie, and F. Irwin, "Heavy-Ion Beam Development," this report.

10. P. D. Miller, C. M. Jones, B. Wehring, J. A. Biggerstaff, G. D. Alton, C. D. Moak, Q. C. Kessel, and L. B. Bridwell, "Absolute Yields of High Charge States for 20-MeV Iodine Ions Small-Angle-Scattered from Xenon and Argon," this report.

11. G. Alton and H. Tamagawa, "Ion Optics Capabilities," this report.

12. E. W. Thomas, "Charge-Changing Cross Sections for Multiply Charged Heavy Ions at Low Velocity," this report.

ABSOLUTE YIELDS OF HIGH CHARGE STATES FOR 20-MeV IODINE IONS SMALL-ANGLE-SCATTERED FROM XENON AND ARGON

P. D. Miller	G. D. Alton
C. M. Jones	C. D. Moak
B. Wehring ¹	Q. C. Kessel ²
J. A. Biggerstaff	L. B. Bridwell ³

The production of highly charged beams of heavy ions has occupied an important position in accelerator technology for several years. In the case of tandem electrostatic accelerators, singly charged negative ions are accelerated to the energy given by the terminal voltage and then are stripped to multiply charged positive ions. Conventionally, stripping has been accomplished through the use of carbon foils or gas in differentially pumped cells. The present experiment was undertaken to determine if there is a sufficient yield of highly charged ions from small-angle scattering to serve

as a basis for the design of a new type of terminal stripper.

Charge-state fractions have been measured at low pressure by Kessel⁴ for 1.5- to 12-MeV iodine ions scattered by xenon through angles between 2.5° and 8° . Kessel found that the relative fraction of high charge states rises sharply with angle, even at small angles where cross sections are high; no absolute cross sections or yields were measured.

In the present work, an energy of 20 MeV was chosen because of the relevance to electrostatic accelerators with terminal voltages in the 20-to-30-MV range. The pressure range used was 10^{-3} to 1.0 torr in a 2-cm-long differentially pumped cell, corresponding to the range 7×10^{13} to 7×10^{16} atoms/cm². Lowest pressures correspond to the single-scattering region. At the highest pressures, near-equilibrium charge-state distributions were observed. Absolute yields of iodine ions of each charge state per incident I^{6+} ion were measured from 0° to 1.5° over this pressure range.

The experimental arrangement is shown in Fig. 1. A 20-MeV I^{6+} beam was defined by two apertures placed 154 cm apart. The first aperture was 3 mm in diameter, and the second, which defined the beam, was $\frac{1}{2}$ mm in diameter. The monitor, described previously by Appleton et al.,⁵ consisted of a surface-barrier detector for particles scattered at 60° from a chemically milled annular film around the first aperture. Some details of the differentially pumped target cell and electrostatic analyzer are included in the figure. The gas cell served as the pivot for rotation of the charge-state analyzer system. The charge-state analyzer system was mounted

on the table of a milling machine so that the table position could be used to determine the scattering angle. The analyzer itself, consisting of a vertical electrostatic analyzer and a position-sensitive detector, has been described previously.⁶ The monitor efficiency was calibrated by measuring the beam intensity at 0° vs monitor counts, with the cell evacuated.

Only the xenon data will be discussed here since it was found that the yield of high charge states was systematically 2 to 3 times greater than that for argon at all pressures and angles. Yields were measured as a function of pressure for angles of 0.3° and 1.5° . At both angles the yield of high charge states had maxima at pressures in the range of 0.02 to 0.1 torr. For this interesting pressure range, absolute yields vs angle were measured at pressures of 0.02, 0.05, and 0.1 torr. Figure 2 shows the yield of some representative charge states as a function of angle for a pressure of 0.1 torr. In this figure the absolute yield is expressed in units of particles (incident particle)⁻¹ (deg)⁻¹, so that integration over some suitable angular range gives the fraction of the incident beam. For example, the yield of iodine ions of charge 18 is of order 10^{-3} for an angular range from 0.2 to 1.5° . Continuing this example, if one could build a suitable focusing system and gas cell in the terminal of a 20-MV tandem accelerator, a 100-particle-nanoampere beam of 380-MeV iodine ions could be obtained, starting with a negative ion current of 100 μ A.

The above results appear promising, and additional measurements are being made. Preliminary experiments with iron ions scattered by xenon indicate that appre-

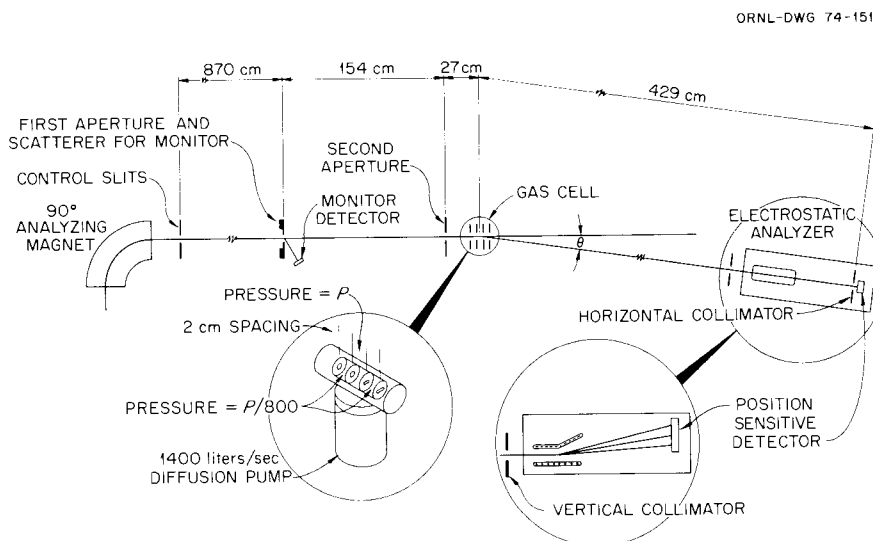


Fig. 1. Experimental arrangement.

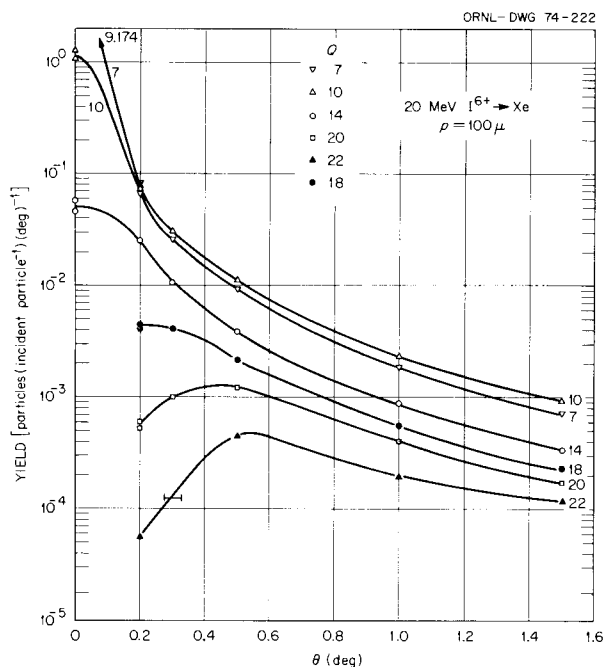


Fig. 2. Yields of some representative high charge states for 20-MeV I^{6+} ions scattered at small angles from xenon.

ciable yields of high charge states may be obtained. The effect of incident charge state upon yields is being investigated, and yields at higher energies and with other incident ions and stripping gases will be measured.

1. University of Illinois, Urbana, Ill.
2. University of Connecticut, Storrs, Conn.
3. Murray State University, Murray, Ky.
4. Q. C. Kessel, *Phys. Rev. A2*, 1881 (1970).
5. B. R. Appleton, J. H. Barrett, T. S. Noggle, and C. D. Moak, *Radiat. Eff.* **13**, 171 (1972).
6. C. D. Moak, H. O. Lutz, L. B. Bridwell, L. C. Northcliffe, and S. Datz, *Phys. Rev.* **176**, 427 (1968).

ION OPTICS CAPABILITIES

G. D. Alton H. Tamagawa¹

The SLAC Electron Optics Computer Program² (FORTRAN version) has been modified for local use on the IBM 360 system. The code is designed to calculate charged-particle trajectories in electrostatic and magnetostatic fields. Poisson's equation is solved by finite-difference methods using boundary conditions determined by specification of the position and types of boundaries for the actual electrodes comprising the lens system. Particle trajectories are then calculated using the fields obtained by differentiating the computed potential distributions. Cylindrical or Cartesian coordi-

nate systems may be used. Space-charge and self-magnetic-field effects are taken into account by the program.

The program is designed to produce a combination of printed and plotted output data and typically uses 300K bytes of total storage. The output data include all input data, trajectories, and equipotential plots. Immediate application of the code will be made in optimizing the electrode design for the recently constructed cesium surface ionization source.

A code has also been written to calculate particle trajectories through electromagnetic fields which can be expressed analytically or in discrete-point fashion. Cartesian or cylindrical coordinate systems may be used. Particle trajectories are calculated by numerically integrating the time-dependent second-order differential equation for each of three mutually perpendicular directions. Space-charge or self-magnetic-field effects are not included.

The program output is in printed and plotted form. Typically, the program uses 270K bytes of total storage. Applications of this code have included calculation of the trajectories of charged particles emitted from the INTEREM plasma containment device and design of a two-dimensional lens system for the negative ion source test facility. This lens will be used to improve ion transmission through the magnetic pole gap of the system.

1. Visiting scientist from Nagoya University, Nagoya, Japan.
2. W. B. Herrmannsfeldt, SLAC report No. 166 (1973).

MEASUREMENTS ON INTEREM

H. Tamagawa¹ N. H. Lazar²
C. M. Jones W. M. Good

Our work on the INTEREM machine is motivated by the following idea. Ions contained in a plasma for a sufficiently long time will be subjected to a number of collisions with electrons of the plasma. Each of these collisions can result in removal of one and occasionally several atomic electrons. Under proper conditions, this process can lead to a plasma in which there is a significant number of highly charged ions. Given successful extraction, such a plasma can then be the basis for a multiply charged heavy-ion source.

A simple way to think about this process is to assume that only one atomic electron is removed in each electron-ion collision. Then, as shown, for example, by Daugherty et al.,³ plasma parameters which give interesting results can be determined. In summary, two conditions are important. First, the electron tempera-

ture should have a value which maximizes ionization rates. In general, this value is a few keV. Second, the product n_e (electron density) times τ_i (ion containment lifetime) should be high. For example, $n_e\tau_i \approx 10^{10}$ sec/cm³ should give 50% ionization with elements whose masses are near the low end of the periodic table.⁴ Actually this value is conservative when the electron temperature is high, since in this case multiply ionizing events are energetically possible.⁵

Specific motivations for study of INTEREM-like devices have been discussed by Herbert and Wiesemann.⁶ In particular, the INTEREM⁷ device has two important features. The first is a magnetic containment geometry consisting of superimposed cylindrical mirror and quadrupole fields. This geometry allows stable operation at low neutral densities, a condition which is a necessary but not sufficient condition for long ion containment lifetimes. The second is electron cyclotron resonance heating, a feature which permits simultaneous achievement of high electron temperature and low ion temperature.

Typical operating parameters for INTEREM with hydrogen are $n_e = 3 \times 10^{11}$ /cm³ and $\tau_i = 1 \times 10^{-3}$ sec. The latter is anomalously long and cannot be explained by simple trapping in the mirror field. Lazar⁸ has postulated ion confinement due to trapping in an electrostatic space potential, but this mechanism has not been conclusively demonstrated.

Our work to date has been concentrated on development of a spectrometer with which we plan to measure the charge-state spectra of ions leaking from the end of the machine. This work proceeded in two steps. In the first, we investigated the possibility of using the external magnetic field of the INTEREM device as a magnetic analyzer. After carefully mapping the field, we determined analytically that this technique would not yield sufficient resolution. The second step has been modification of a commercial quadrupole mass filter to serve as a charge-state analyzer. Specifically, we have built an ultrahigh vacuum system to house the mass filter and a system of energy-sensitive einzel lenses which allow only ions of a known energy to enter the filter. The energy resolution, $\Delta E/E$, of this lens system is about 9%. This lens system will allow us to measure charge-state distributions as a function of ion energy. It is also necessary to achieve good resolution with the mass filter. In particular, at mass 4 ($m/q = 4$) we observe a resolution of $\Delta m < 0.1$. For calibration purposes, a simple coaxial electron bombardment ion source has been placed on axis between the INTEREM plasma chamber and the mass filter.

This system has been fabricated, assembled, and tested. In the coming year, it will be installed on the

INTEREM machine and be used for the measurement of charge-state spectra. Our hope is that these measurements not only will serve as a measurement of the ion yield from INTEREM but also will help to illuminate some of the unresolved plasma physics problems associated with this type of device and thereby help in making an assessment of its ultimate potential as a heavy-ion source.

1. Visiting scientist from Nagoya University, Nagoya, Japan.
2. Thermonuclear Division.
3. J. D. Daugherty, L. Grodzins, G. S. Janes, and R. H. Levy, *Phys. Rev. Lett.* **20**, 369 (1968).
4. T. H. Stix, *IEEE Trans. Nucl. Sci.* **NS-19**(2), 150 (1972).
5. See, for example, R. L. Darling and R. H. Davis, *Rev. Sci. Instrum.* **44**, 375 (1973); A. Van der Woude, *IEEE Trans. Nucl. Sci.* **NS-19**(2), 187 (1972). (This is an account of previous work at ORNL on a similar device, ELMO. The motivation for this work was the idea that it might be possible to produce interesting yields with a plasma in which the predominant mechanism for production of highly charged ions was inner-shell vacancy production followed by cascade processes.)
6. H. C. Herbert and K. Wiesemann, "The Production of Highly Charged Ions in a Plasma with High Electron Temperature," paper presented at the GSI Conference on Ion Sources for Highly Charged Heavy Ions, Heidelberg, 1971.
7. R. A. Dandl, J. C. Dunlap, H. O. Eason, P. H. Edmonds, A. C. England, W. J. Herrmann, and N. H. Lazar, *Third International Conference on Plasma Physics and Controlled Fusion Research*, vol. II, IAEA, Vienna (1968), p. 435.
8. N. H. Lazar, ORNL-4545, p. 38 (1969).

PENNING ION SOURCE TEST FACILITY

M. L. Mallory C. M. Jones
E. D. Hudson S. W. Mosko

In 1973 we began construction of a facility for the testing and development of ion sources which satisfy the needs of ORIC in particular and ORIC-like accelerators in general. The heavy-ion performance of ORIC is strongly dependent on the performance of its ion source. Ion source performance in terms of current for high charge-to-mass ratios and source lifetime is a limiting factor in ORIC performance, and further improvements of ion source parameters would yield substantial benefits. In addition, the ion source facility can be thought of as a low-energy-high-charge-state accelerator. For example, it can provide high-intensity beams of $^{40}\text{Ar}^{9+}$ which can be useful in atomic physics experiments. Another proposed use of the facility is the measurement of cross sections for capture and loss of electrons in hydrogen gas for various ions (O^{n+} or C^{n+}). This information is important for controlled thermonuclear experiments, where plasma cooling and loss are very dependent on impurity ions.

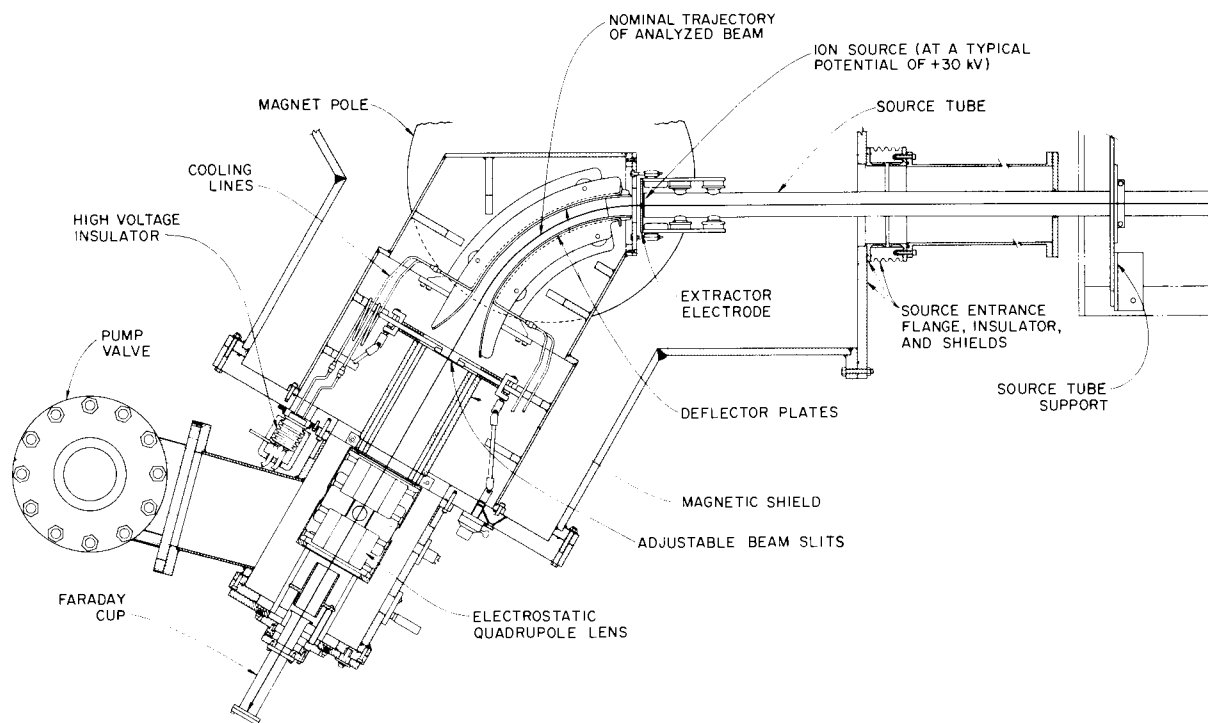


Fig. 1. A schematic drawing showing a median plane view of the Penning ion source test facility. The ion source is inserted from the right and is floated to positive potentials. The ions are extracted from the 30-in.-diam magnet by a set of curved electrostatic plates followed by a slit system which provides single-charge-state extraction. An electrostatic quadrupole lens then allows focusing of the single-charge-state beam into a Faraday cup.

The ion source test facility is composed of a 30-in.-diam magnet having a variable gap. The ion source in the facility is floated to +36 kV, allowing acceleration of ions to an energy of up to $36q$ keV. Floating the source to high potential necessitates operation of the 75-kW ion source power supply at high potential. A cross-field channel provides substantial q/m dispersions (0.5 in. for $^{40}\text{Ar}^{9+}$ at an acceleration voltage of 10 kV) and extraction of the ions. This combination of curved electrostatic field and magnetic field leads to a focused beam at the deflector plate exit. A slit system is provided at this focus point and allows single-charge-state extraction. The ions after extraction are again focused by an electrostatic quadrupole lens. The lens can then be followed by any piece of experimental equipment mounted at ground potential. Figure 1 is a drawing of the facility showing the ion source and the beam extraction system.

During the months of October to December the facility was used to test the new rotating-cathode ion source described in another contribution.¹ We expect this facility to be operating full time in 1974, allowing ion source research to proceed at a rapid pace.

1. E. D. Hudson, M. L. Mallory, R. S. Lord, J. E. Mann, J. A. Martin, R. K. Goosie, and F. Irwin, "Heavy-Ion Beam Development," this report.

CHARGE-CHANGING CROSS SECTIONS FOR MULTIPLY CHARGED HEAVY IONS AT LOW VELOCITY

E. W. Thomas¹

In the past year we have completed a survey of existing information on ionization and charge-transfer cross sections for low-velocity heavy ions incident on gaseous and solid targets. Particular emphasis has been placed on reactions involving species that are three or more times ionized and on the energy range from 10 eV to 25 keV per nucleon. Our principal interest has been in experimental measurements, but we have also considered theoretical calculations wherever these can lead to useful predictions of cross sections. It was found that the available information is generally fragmentary. While there is satisfactory coverage of the stripping of many electrons from singly charged atoms, there is very

little information on how multicharged species gain or lose electrons. Theoretical predictions are, likewise, inadequate. The energy range considered was too low to permit application of the Born approximation, so that the few useful methods of prediction are based upon semiempirical or statistical models.

1. Consultant to ORNL Thermonuclear Division and Physics Division from Georgia Institute of Technology, Atlanta, Ga.

ELASTIC SCATTERING OF POSITRONS BY HYDROGEN

G. D. Alton M. Reeves¹
W. R. Garrett²

In the projection operator approach of Feshbach³ to the scattering problem, the elastic channel is projected out of the total Schrödinger equation, and all other channels are included in a complex nonlocal optical-potential operator. Perhaps the most significant feature of the technique is that it offers theoretical means of calculating total cross sections which present the least difficulty to the experimenter.

The theoretical study of low-energy electron scattering from hydrogen was recently made by the authors.⁴ Both real and virtual first-order transitions to discrete and continuum target states were included in the nonlocal potential. Although exchange was neglected in the analysis, good agreement with experimental results was obtained.

Measured total cross sections for positron scattering from helium have been recently reported by Canter et al.⁵ A monotonically decreasing cross section with decreasing positron energy was observed. Such a result is explainable in our treatment by the fact that (for the case of positrons on hydrogen) the static and first-order real potentials are of opposite signs. Therefore the positrons pass through a minimum in potential at low energies. The results obtained for positron scattering from hydrogen are shown in Fig. 1 and display a minimum in cross section at about 1.2 eV. The importance of atomic distortion, even at very low energies, is readily seen. Only first-order contributions to the nonlocal potential were included, and the effects produced by positronium formation were excluded from the analysis. Second-order contributions to the nonlocal potential are presently being evaluated, and the results of this study will be reported in the near future.

1. Computer Sciences Division.

2. Health Physics Division.

3. H. Feshbach, *Ann. Phys.* 19, 287 (1962).

4. G. D. Alton, W. R. Garrett, M. Reeves, and J. E. Turner, *Phys. Rev. A* 6, 2138 (1972).

5. K. F. Canter, P. G. Coleman, T. C. Griffith, and G. R. Heyland, *J. Phys.* B5, L167 (1972).

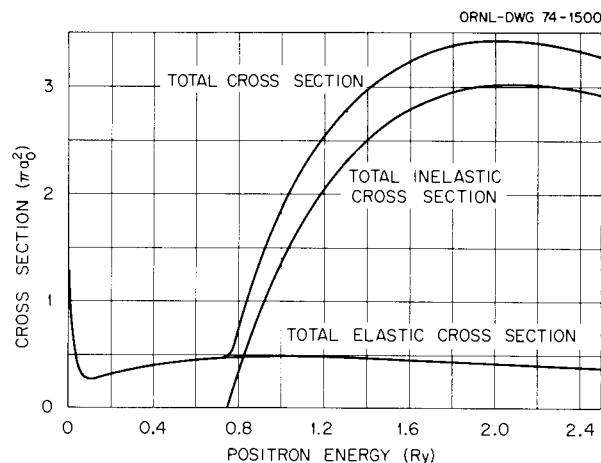


Fig. 1. Calculated total elastic, total inelastic, and total interaction cross sections for positron collisions with atomic hydrogen.

THEORETICAL SHUNT IMPEDANCE MODEL FOR SPIRALLY LOADED RF RESONANT CAVITIES

P. Z. Peebles, Jr.¹ C. M. Jones

A recently discovered resonant rf cavity structure which appears useful for heavy-ion linear accelerators is the spirally loaded cavity² (SLC) shown in Fig. 1. During 1973, a theoretical model was developed which gives the bare shunt impedance for this type of cavity when the spiral is loosely wound. From the equations of the model, optimum cavity dimensions may be found to maximize shunt impedance.

For loosely wound spirals it may be argued that the shunt impedance of a SLC is the same as a quarter-wavelength section of shorted transmission line having a center conductor, with the same cross section as that of the SLC spiral, which is placed between two infinite parallel planes separated by the axial length of the SLC. Developing this model shows that shunt impedance Z is given by

$$Z = \frac{8Z_0}{L\alpha} \quad (1)$$

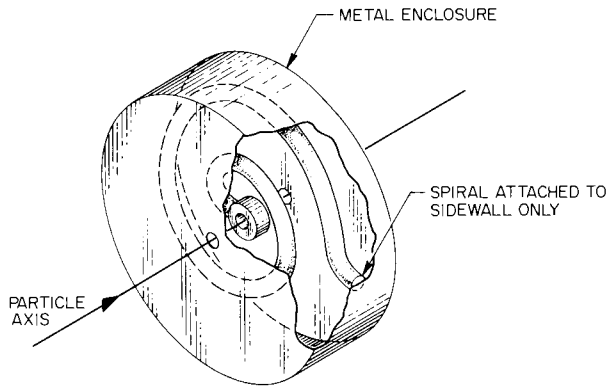
Here l is the length of the quarter-wavelength spiral (m), L is the axial length of the cavity (m), Z_0 is the characteristic impedance of the model line, and α is the attenuation constant of the model line (nepers/m).

Developing (1) for spirals having circular cross section (diameter d_0) gives

$$\frac{R_s \epsilon_r Z}{\pi^3 (60)^2} = \frac{16 \ln^2(L/d_0)}{\pi^2 (1 + L/d_0)} \quad (2)$$

Here R_s is the surface resistance (Ω) and ϵ_r is the dielectric constant of the material filling the cavity (usually air or vacuum). For copper,

ORNL-DWG 74-1251



SPIRALLY-LOADED CAVITY

Fig. 1. Pictorial view of a spirally loaded resonant cavity.

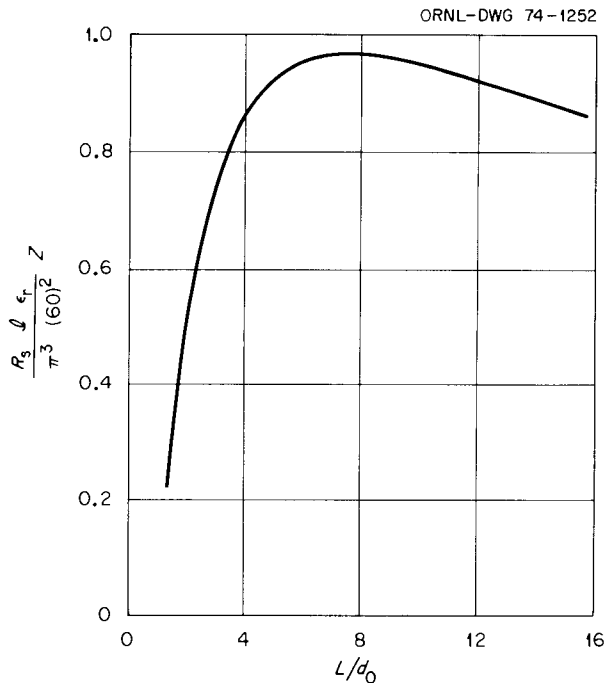


Fig. 2. Normalized bare shunt impedance for spirally loaded cavities using spirals with circular cross section.

$$R_s = 2.61(10^{-7}) \sqrt{f}, \quad (3)$$

where f is the frequency (Hz). A plot of the left side of (2) vs L/d_0 is shown in Fig. 2.

The optimum value of L/d_0 in Fig. 2 is 7.57. Assuming this value, an air dielectric, and copper surfaces, the optimum shunt impedance is $Z = 5560 \sqrt{f}$ Ω/m . For 100 MHz, $Z = 55.6$ M Ω/m is possible.

Curves similar to Fig. 2 have been found for spirals with rectangular cross section. Optimum shunt impedance occurs for the square cross section and is approximately 13.4% less than the corresponding optimum for a circular cross section.

Having developed a model which indicates the possibility of obtaining large shunt impedances from the SLC, a measurement program has been undertaken. During 1974, some 15 SLC's will be measured. These data should not only verify Fig. 2 but provide additional insight into the behavior of SLC's for tightly wound spirals.

1. Consultant to ORNL from the University of Tennessee, Knoxville, Tenn.

2. G. J. Dick and K. W. Shepard, private communication.

SUPERCONDUCTING RESONANT CAVITIES

J. P. Judish P. Z. Peebles, Jr.¹
C. M. Jones W. T. Milner

In the past several years there has been widespread technological and theoretical interest in the rf surface resistance of superconducting materials. On one hand, the availability of materials with surface resistance as low as 10^{-6} times that of normal conductors has important implications in the technology of accelerators and certain types of electronic devices. On the other hand, comparison of measured values of surface resistance with predictions based on the Bardeen, Cooper, and Schrieffer theory of superconductivity have provided a valuable check on this theory. Although agreement between experiment and theory has been good at higher temperatures and frequencies, measured and theoretical results have always diverged greatly at lower temperatures and frequencies. In this so-called residual resistance region, no theory has yet been presented which can explain the measured results.

These considerations have motivated us to continue our work on rf superconductivity. Specifically, the three-transmission-line measurement system reported last year² has been used for a series of careful measurements on a new lead-plated helically loaded cavity whose geometry is similar to that used in our

previously reported measurements.³ In particular, we have measured the surface resistance of lead as a function of temperature at low field levels and frequencies of 136.7, 233.9, 316.5, 395.9, and 471.6 MHz, a frequency region in which there have been relatively few measurements.

At 4.2°K, our results are greater than predictions of the theory⁴ by a factor as high as 1.8 at 136.7 MHz down to a factor as low as 1.2 at 471.6 MHz. These factors almost certainly arise from the fact that a small fraction of the surface currents flow through the indium gaskets used for making the vacuum seals between the cavity parts. This is evident from the break in the curve of Fig. 1 at 3.4°K, the critical temperature of indium. Figure 1 shows the measured and theoretical surface resistance at 136.7 MHz as a function of temperature at maximum surface fields of about 6 G. The shapes of the curves are typical of the measured

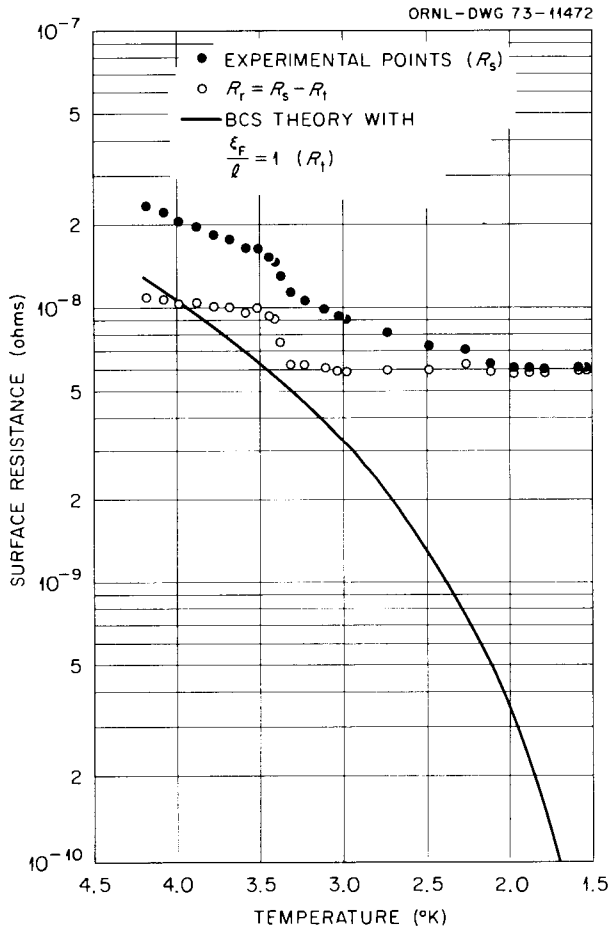


Fig. 1. Surface resistance vs temperature for a frequency of 136.7 MHz. The cavity stored energy for these measurements was 2.5×10^{-5} J.

results at the remaining frequencies. Figure 1 also shows the difference between experiment and theory.

The contribution to the observed surface resistance of the currents through the indium is surely negligible at 1.5°K, yet the theoretical and experimental results disagree by a factor as high as 120 at 136.7 MHz down to a factor of 58 at 471.6 MHz. Despite this disagreement, we believe 4.6×10^{-9} Ω , the measured surface resistance at 136.7 MHz and maximum surface fields of 2 G, is the lowest ever observed for lead and, for our cavity, corresponds to a Q of 1.77×10^9 .

Figure 2 shows a plot of the measured surface resistance at 1.5°K as a function of frequency and compares it with predictions of a theory due to Passow.⁵ Passow has developed an expression whose first term is meant to predict, for an ideal superconductor, the surface resistance component due to losses suffered by current transport electrons. His second term predicts the surface resistance component due to losses caused by phonon generation resulting from interaction

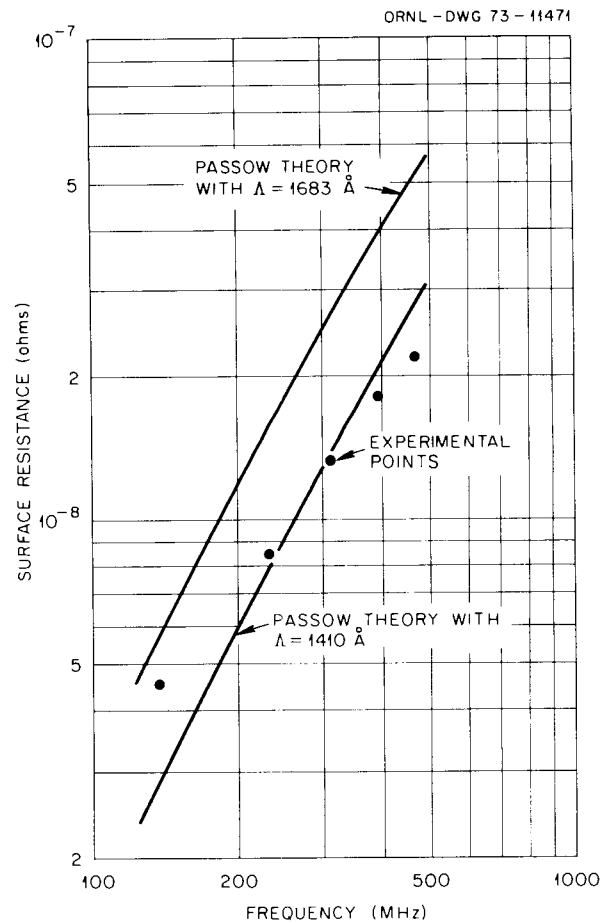


Fig. 2. Surface resistance vs frequency for a fixed temperature of 1.5°K and cavity stored energy of 1×10^{-6} J.

of the electromagnetic field and lattice ions. The first term should dominate at higher temperatures, the second at lower. Furthermore, the second term should provide a lower bound for the surface resistance in the absence of other loss mechanisms.

Theoretical results depend on Λ , a number derived from the values assigned to the London penetration depth and the coherence length, two of the superconductor's material parameters. With Passow's choice of these values, which makes $\Lambda = 1680 \text{ \AA}$, his prediction for the lower bound of the surface resistance is seen to lie above our results. If Λ were, instead, 1410 \AA , Passow's theory would predict results closer to those measured by us. However, the first term of Passow's expression predicts, for surface resistance at 4.2°K , values which are ten times higher than those calculated

from the exact theoretical expressions⁴ based on the Bardeen, Cooper, and Schrieffer theory. Such a large discrepancy leads us to suspect that Passow's second term may also overestimate the contribution of phonon generation to surface resistance.

1. Consultant to ORNL from the University of Tennessee, Knoxville, Tenn.

2. J. P. Judish, C. M. Jones, F. K. McGowan, and P. Z. Peebles, Jr., *Phys. Div. Annu. Progr. Rep. Dec. 31, 1972*, ORNL-4844, p. 140.

3. C. M. Jones, J. P. Judish, R. F. King, F. K. McGowan, W. T. Milner, and P. Z. Peebles, Jr., *Particle Accel.* 3, 103-13 (1972).

4. J. Halbritter, *Z. Phys.* 238, 466 (1970).

5. G. Passow, *Phys. Rev. Lett.* 28, 427 (1972).

3. Electron Linear Accelerator (ORELA)

INTRODUCTION

J. A. Harvey

1. ORELA neutron time-of-flight facility. ORELA has continued to demonstrate that it is an excellent, reliable facility for neutron spectroscopy. During the past year, many unique neutron measurements requiring excellent neutron energy resolution and high neutron intensity have been performed over an energy range of more than seven decades (from about 1 to more than 10^7 eV). Although the accelerator has been in operation for over four years and most experiments were started two or three years ago, changes in equipment, instrumentation, and programs for acquiring data and analysis of the data are made constantly. Considerable improvements have been achieved in the performance of liquid scintillators by eliminating optical interfaces with the phototube. Not only do the measurements span a wide neutron energy range, they also cover a wide range of masses. Often a nuclide is investigated by several processes, such as neutron total, capture, and fission cross-section measurements and gamma-ray spectra from neutron capture or inelastic scattering. Capture and total measurements have complemented each other in many cases, such as the isotopes of Ca, Zr, Pb, etc.

2. Light nuclides. For light nuclides, high-resolution precise total cross-section measurements from about 0.1 to a few MeV can be analyzed to give not only the details of the excited states but also the potential phase shifts, as was done for ^{16}O . This past year, excellent total cross-section measurements have been made upon ^{40}Ca , and the data have been carefully analyzed to give the neutron widths, spins, and parities of the resonances and the phase of the potential scattering for each partial wave as a function of neutron energy. The magnitude and energy dependence of these phase shifts can be related to the scattering from an energy-dependent Saxon-Woods real potential with spin-orbit coupling. To complete this study, similar measurements and analysis will be made on other light nuclides such as ^{28}Si , ^{32}S , etc.

3. Gamma-ray spectra from neutron capture. The principal goal of capture gamma-ray spectra investigations the past few years has been to confirm, deny, or find evidence for nonstatistical effects (in particular, valency capture) in medium-weight nuclides. In the mass region of 90 to 100 (i.e., Zr and Mo), several nuclides do show valency capture over a limited energy range. However, early conclusions based on insufficient data have often been modified or contradicted due to the greater quantity and quality of data from the improved resolution at ORELA. Measurements have been made of the energy of the gamma rays from neutron capture in several resonances in ^{57}Fe . The energy levels of ^{58}Fe and their branching ratios derived from these data are in excellent agreement with shell-model calculations. A careful study of many of the isotopes of tin is in progress in order to determine the level schemes of these nuclides at high excitation.

4. Capture cross sections and nucleosynthesis. The emphasis of the capture cross-section program is on measurements of nuclides of interest to nucleosynthesis. For

example, the capture of ^{32}S is relevant to the theory of weak *s*-process element formation. The energy range of interest is a Maxwellian average for $kT \sim 30$ keV. In this capture work the spins and parities of many of the resonances can be identified, and average spacings and strengths for both *s*- and *p*-wave resonances can be obtained. The average *s*-wave radiation width is three times that of *p*-wave resonances. From capture measurements on the isotopes of calcium, the radiation widths of the *s*-wave resonances are found to be 4 to 7 times those for non-*s*-wave resonances for the even isotopes and a factor of 2 greater for ^{43}Ca . The data on the calcium isotopes also have astrophysical interest. Whereas the abundances of ^{40}Ca and ^{42}Ca are accounted for by explosive oxygen burning, it has been suggested that ^{43}Ca is formed by slow neutron capture. Unstable ^{41}Ca is of primary importance for the production of $A \geq 43$, and cross sections for this isotope must be estimated from the systematics derived for the other isotopes.

5. Subthreshold fission and spin determination. Subthreshold fission for many of the heavy nuclides is undoubtedly the most striking example of intermediate structure. From the strengths, shapes, and spacings of the subthreshold fission clusters a great deal can be learned about the properties of the first and second potential wells, such as barrier heights, differences between well depths, coupling between the states of the two wells, etc. ^{234}U was considered to be one of the more interesting nuclides to study. In addition to subthreshold fission clusters, several vibrational levels in the second well were found. These vibrational levels give the fission strength to the class II levels in the second well, which in turn give the fission strength to the class I fine-structure levels. Perhaps the most difficult and expensive neutron experiment ever attempted on an accelerator or reactor was the measurement of the spins of the resonances in ^{237}Np and ^{235}U using polarized neutrons and polarized nuclei. From both transmission and fission measurements upon ^{237}Np , all nine members of the 40-eV group of subthreshold fission resonances were shown to have the same spin and to arise from a single class II level of spin 3 in the second well. All resonances in each higher energy cluster have the same spin, although the various clusters have different spins. The measurements upon ^{235}U determined the spins of more resonances than had been determined by all other techniques in the past ten years and also showed that assignments from other techniques were often wrong.

6. Total cross-section measurements. The *M1* giant resonance arising from spin-flip transitions is strongest near closed shells and should occur at an excitation near the neutron separation energy. From photoneutron data upon ^{208}Pb , claims had been made that almost the complete *M1* strength for ^{208}Pb was located at 7.9 MeV with a width of about 700 keV. High-resolution, accurate total cross-section data obtained with ORELA show that *s*-wave resonances are present corresponding to levels observed in the photoneutron work and hence are excited by *E1* transitions. Thus, there is now no evidence for an *M1* giant resonance in ^{208}Pb . Total cross-section data taken on ^{90}Zr and ^{91}Zr have also been valuable in interpreting the photoneutron reactions on ^{91}Zr and ^{92}Zr . Recently, it was reported that a "resonance peculiarity" had been observed in $^{207}\text{Pb} + n$ at 16.8 MeV which was thought to be due to an analog state. Total cross-section measurements were made up to about 30 MeV, but this resonance was not found. Results from total cross-section measurements are still of interest in determining *s*- and *p*-wave strength functions for the medium-weight nuclides. High-resolution measurements have been completed up to about 500 keV for the isotopes of Si, S, K, Ca, Ti, Fe, Zr, and Pb, and the data are now being analyzed.

7. Standard neutron cross sections and applied problems. In addition to these basic nuclear physics experiments, some effort is expended on applied problems. Standard neutron cross sections are needed since most partial cross-section measurements are made relative to a standard such as the capture cross section of gold. Careful measurements have been made of the capture cross section of gold from 3 to 550 keV relative to $^6\text{Li}(n,\alpha)$, which will decrease the uncertainty in the gold standard. Accurate total

cross-section measurements (about 1% accuracy) made upon ${}^6\text{Li}$ should give an accurate curve for the (n,α) reaction in the 100-to-300-keV region. Requested priority neutron capture cross-section measurements for which analysis is not complete include ${}^{238}\text{U}$, Na, Sc, Zr, Nb, Mo, and Ta. Other capture data taken but not yet analyzed (on about 30 stable nuclides) include important fission product reactor poisons and vanadium, a potential construction material for thermonuclear reactors. Measurements of the ${}^{249}\text{Cf}$ fission cross section and the determination of neutron absorption by ${}^{248}\text{Cm}$ up to about 1500 eV from transmission measurements may be of interest from a waste disposal viewpoint.

8. Cooperative programs with other laboratories and universities. In order to supplement our research staff, we have welcomed nuclear physicists from other laboratories and other divisions at ORNL to collaborate with us on joint experiments. During the past year, physicists from Savannah River, Aerojet Nuclear, Brookhaven, Los Alamos, Chalk River, Harwell, Nationalist China, Denison University, University of Missouri, Centenary College, and Columbia University have visited ORELA for cooperative experiments.

SUBTHRESHOLD AND THRESHOLD NEUTRON FISSION OF ${}^{234}\text{U}$

J. W. T. Dabbs G. D. James¹ N. W. Hill²

One of the few nuclides which exhibit the phenomenon of grouping of fission resonances well below the fission threshold is ${}^{234}\text{U}$. This phenomenon is closely related to the presence of class II levels in the second minimum in the fission potential barrier. A complete analysis of the phenomenon can be obtained only if both the fission cross section and the total cross section are known for each of the contributing resonances.

The high intensity of neutron bursts at ORELA provides the possibility for measurements of much higher accuracy and detail than previous work.^{3,4} The present measurement is complementary to a measurement of total cross section at ORELA.⁵ Taken together, these measurements have shown that the spacing of class II intermediate structure levels is only about 2.1 keV, rather than 7 keV,³ and has enabled estimates to be made of the parameters of the double-humped fission barrier in ${}^{234}\text{U} + n$.

Figure 1 illustrates a few of the levels which contribute to the lowest energy intermediate structure, which extends to about 1000 eV. The arrow indicates a level with very small Γ_n but very large Γ_f . Such levels occur near the center of the structure. Figure 2 shows the distribution of Γ_f vs E_n below 1500 eV.

The threshold region is illustrated in Fig. 3, where the intermediate structure levels are superimposed on broad underlying vibrational levels. The analysis of these levels is of necessity tentative but leads to not unreasonable parameters for the fission barrier. A detailed report on

these results is nearly complete and will be published elsewhere.⁶

1. Visiting scientist 1972-1973 from AERE, Harwell, England.
2. Instrumentation and Controls Division.
3. G. D. James and E. R. Rae, *Nucl. Phys.* **A118**, 313 (1968).
4. G. D. James and G. G. Slaughter, *Nucl. Phys.* **A139**, 471 (1969).
5. J. A. Harvey, G. D. James, N. W. Hill, and R. H. Schindler, "Neutron Total Cross Section of ${}^{234}\text{U}$ from 3 to 3000 eV," this report.
6. G. D. James et al., to be published.

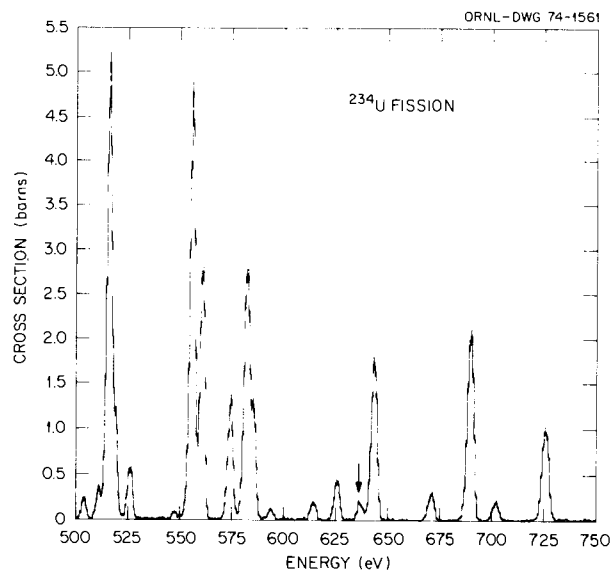


Fig. 1. A small sample of resonances which contribute to the lowest energy intermediate structure. The arrow indicates a level whose Γ_n value is extremely small compared with its neighbors.

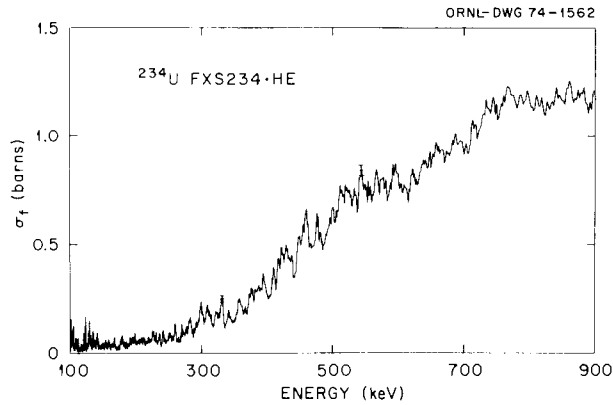


Fig. 2. Γ_f vs E_n for ^{234}U below 1500 eV. The solid curve is a single-peak fit centered at 650 eV; a better fit is obtained with two peaks, one at 550 eV and the second at about 1100 eV.

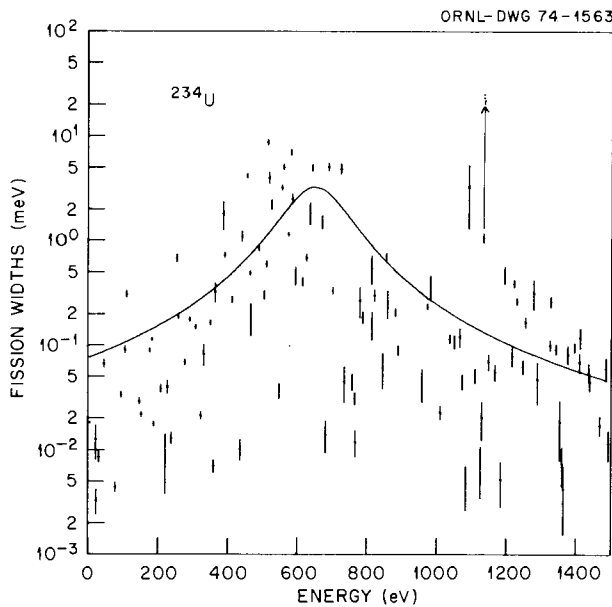


Fig. 3. Fission threshold region in ^{234}U . Intermediate structure levels are superimposed on assumed broad underlying vibrational levels.

NEUTRON TOTAL CROSS SECTION OF ^{234}U FROM 3 TO 3000 eV

J. A. Harvey N. W. Hill²
G. D. James¹ R. H. Schindler³

In order to extract the fission widths of the resonances from subthreshold fission cross section measurements upon ^{234}U , it is necessary to know the neutron widths of the resonances. This is because fission measurements yield only the quantity $\Gamma_n \Gamma_f / \Gamma$ except

for resonances where Γ_f is large compared with Γ_γ and the experimental neutron energy resolution. The nuclide ^{234}U is of particular interest as it was expected that this nuclide might be a good example of "moderate coupling" between the excited states in the two potential wells. For this coupling, in addition to a Lorentzian distribution of fission widths with a width of about 100 eV centered at each class II level (which have a few keV spacing), a single resonance in each cluster might be identified as the class II level if it should have a very large fission width and a very small neutron width. The total cross-section data can also be analyzed to give the average *s*-wave level spacing, *s*-wave strength function, and parameter distributions to compare with the Wigner level spacing distribution and the Porter-Thomas neutron width distribution.

Neutron time-of-flight transmission measurements were performed at ORELA using a 5.69-g sample of $^{234}\text{U}_3\text{O}_8$ (6.45×10^{-3} atom/b). The sample was cooled to liquid nitrogen temperature to reduce the Doppler broadening of the resonances. With a ^6Li glass scintillation detector (1.27 cm thick and 11.1 cm in diameter) located 78.203 m from the neutron target and with 28-nsec pulses from the accelerator, the energy resolution is 0.08%. More than 120 resonances were observed up to 1500 eV. These have been analyzed by the area analysis program of Atta and Harvey⁴ to give the neutron widths of the resonances based on an assumed radiation width of 25 meV. The *s*-wave level spacing (D_I) was determined to be 10.7 ± 0.5 eV and the *s*-wave neutron strength function, $\bar{\Gamma}_n^0/D_I$, $(0.86 \pm 0.11) \times 10^{-4}$. These are in good agreement with values reported by James and Slaughter⁵ based on transmission measurements up to 800 eV. Also, they are consistent with values for other nuclides in this mass region, such as ^{238}U , for which $D_I = 17.7 \pm 0.7$ eV and $\bar{\Gamma}_n^0/D_I = (1.1 \pm 0.1) \times 10^{-4}$. The details of the fission parameters are reported by Dabbs et al.⁶ A complete paper on this work is being prepared for publication.⁷

1. Visiting scientist 1972–1973 from AERE, Harwell, England.

2. Instrumentation and Controls Division.

3. Summer research student from University of Rochester.

4. S. E. Atta and J. A. Harvey, *Numerical Analysis of Neutron Resonances*, ORNL-3205 (1961) and Addendum (1963).

5. G. D. James and G. G. Slaughter, *Nucl. Phys.* **A139**, 471 (1969).

6. J. W. T. Dabbs, G. D. James, and N. W. Hill, "Subthreshold and Threshold Neutron Fission of ^{234}U ," this report.

7. G. D. James et al., to be published.

**POLARIZED-NEUTRON, POLARIZED-TARGET
FISSION OF ^{235}U AND ^{237}Np AT ORELA**

G. A. Keyworth¹ F. T. Seibel¹
J. W. T. Dabbs N. W. Hill²

Results of the measurements described in the last annual report³ have now been analyzed and published.⁴⁻⁶ The experimental setup is shown schematically in Fig. 1.

The difficulty of spin determination by methods less direct than the present one is well known. The present method is absolute within a sign, which has been resolved without difficulty here; thus the method affords a standard of comparison with the less direct approaches.

In the ^{235}U measurements,⁴ 65 resonances below 60 eV were assigned as either 3^- or 4^- . The agreement with other determinations was poor in general with notable exceptions.

Table 1 summarizes the status of agreement. It is seen that only one of four capture measurements and the other polarization measurements (previously restricted to $E_n < 15$ eV) are in complete agreement with the present work. The number of spins assigned is also significantly larger in the present work than for any of the other methods.

Figure 2 shows the $^{235}\text{U} + n$ resonances between 50 and 60 eV. The spin assignments of the seven largest resonances are definite; those of the resonances at 50.6 and 53.4 eV are uncertain and were not reported.⁴ A remeasurement of ^{235}U is planned, and a very substan-

tial improvement in detector background and counting rate has been attained in tests toward this end.

The final analysis of the $^{237}\text{Np} + n$ data⁵ demonstrates conclusively that all nine members of the 40-eV group of subthreshold fission resonances have spin 3, thus verifying the idea that all these resonances undergo fission via a single class II level of spin 3 in a second well in the fission barrier potential. This result thus corroborates the Strutinski model of the fission barrier. In addition, spins of 14 other isolated intermediate structure fission resonance groups below 1 keV were assigned. Of these, four had at least two resonances, three apparently contained only a single resonance, and seven above 400 eV probably consisted of unresolved

Table 1. Agreement with present work, 65 resonances below 60 eV

Type of measurement	Number in agreement/total number measured
Other polarization	13/13 ^a
Capture	4/5, 8/18, 13/13, ^b 1/2
Gamma multiplicity	12/23
Scattering	11/14, 2/4
Mass asymmetry	18/29 (9/10 below 30 eV)

^aR. I. Schermer et al., *Phys. Rev.* **167**, 1121 (1968); E. R. Reddinghuis, H. Postma, C. E. Olsen, D. C. Rorer, and V. L. Sailor, "Spins of Low Energy Neutron Resonances in ^{235}U ," to be published.

^bF. Corvi et al., *Nucl. Phys.* **A203**, 145 (1973).

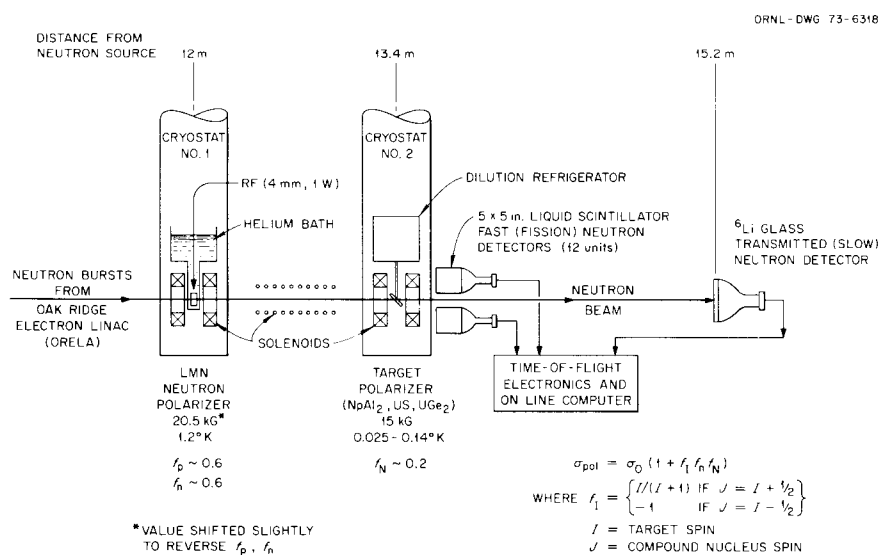


Fig. 1. Schematic of experiments. No transmission detector was used in the ^{235}U measurements.

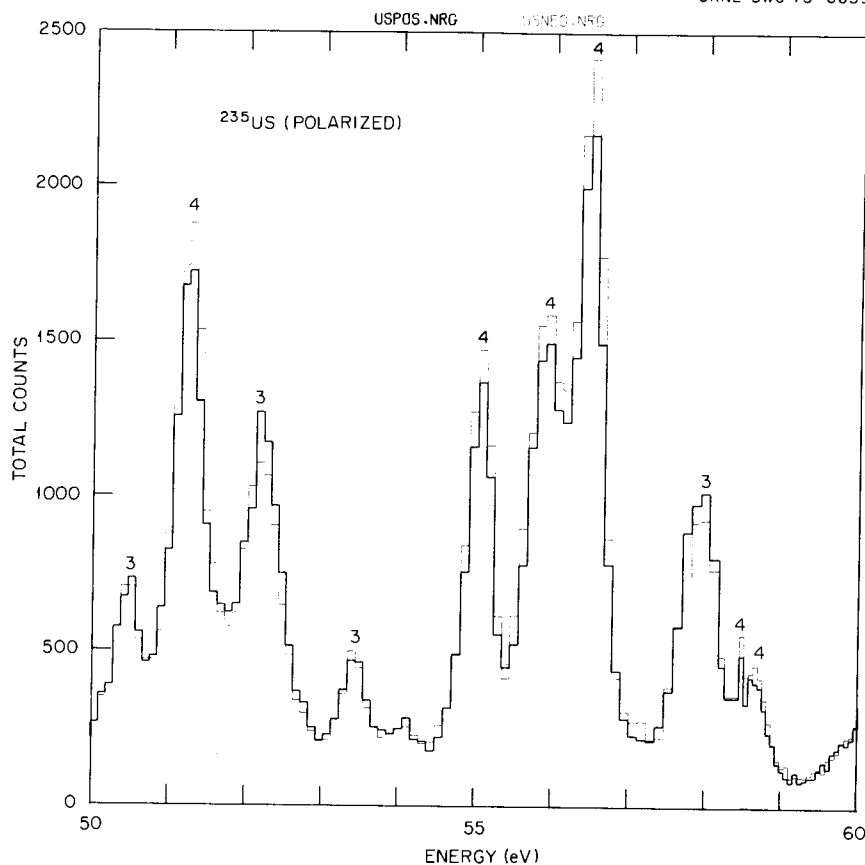


Fig. 2. Example of $^{235}\text{U} + n$ resonances. Spin assignments of resonances at 50.6 and 53.4 eV are uncertain. The patriotic compound uranium monosulfide was used.

resonances. The assignment of only one level at 283 eV remains tentative. Spin assignments were also made using the transmission effect in the total cross section for 92 resonances below 101.5 eV. Of these, 12 remain tentative. Confirmation of the spins of 8 of the 9 resonances observed in fission between 26.6 and 50.4 eV was obtained in the transmission measurement. A comparison of the present results with those of Kuiken et al.⁷ indicates that $K = 2$ is predominant for both $J = 2$ and $J = 3$ with some contribution from $J:K = 3:3$ and $J:K = 2:1$ states. A $2J + 1$ distribution of spins was found in the total cross section spin determinations.

5. G. A. Keyworth, J. R. Lemley, C. E. Olsen, F. T. Seibel, J. W. T. Dabbs, and N. W. Hill, *Phys. Rev. C* **8**, 2352 (1973).

6. G. A. Keyworth, J. R. Lemley, C. E. Olsen, F. T. Seibel, J. W. T. Dabbs, and N. W. Hill, *Proc. 3rd Int. IAEA Conf. Phys. and Chem. of Fission, Rochester, Aug. 13-17, 1973*, IAEA, Vienna (to be published).

7. R. Kuiken, N. J. Pattenden, and H. Postma, *Nucl. Phys. A* **196**, 389 (1972).

NEUTRON TOTAL CROSS SECTIONS OF TRANSURANIUM NUCLIDES

J. A. Harvey	C. E. Ahlfeld ²
N. W. Hill ¹	F. B. Simpson ³
R. W. Benjamin ²	O. D. Simpson ³

Four years ago a program to measure the neutron total cross sections of transuranium nuclides was initiated in collaboration with physicists from Savannah River Laboratory and Idaho Nuclear Corporation. The interest at the time was the need for accurate neutron cross-section data for nuclides in the production chain

1. Los Alamos Scientific Laboratory, Los Alamos, N.M.
2. Instrumentation and Controls Division.
3. G. A. Keyworth, J. W. T. Dabbs, F. T. Seibel, N. W. Hill, and J. M. Anaya, *Phys. Div. Annu. Progr. Rep. Dec. 31, 1972*, ORNL-4844, pp. 94-99.
4. G. A. Keyworth, C. E. Olsen, F. T. Seibel, J. W. T. Dabbs, and N. W. Hill, *Phys. Rev. Lett.* **31**, 1077 (1973).

to ^{252}Cf . To optimize the ^{252}Cf yield it is necessary to know the thermal and resonance-energy cross sections for both capture and fission and to carry out the irradiations in the appropriate neutron flux. Obviously a neutron energy region where nuclides have a small capture cross section or a large fission cross section should be avoided as much as possible. This past year the neutron total cross section of ^{248}Cm has been measured from 2 to about 3000 eV. The neutron total cross section of ^{241}Pu has also been measured from 1 eV to 500 keV. Accurate cross-section data of this nuclide are needed for the LMFBR program. In previous years the nuclides ^{242}Pu , ^{243}Am , and ^{244}Cm have been measured.

Recently considerable interest has been aroused in the cross sections of these heavy actinide elements because of the large amounts of the actinides which will be produced in the power reactors of the future. Since most fission products have half-lives less than about 1000 years, it seems acceptable to store them in deep geological formations. However, many of the actinides have half-lives much longer than 1000 years, and it has been suggested⁴ that these objectional nuclides be recycled in a high-flux reactor to burn them up via fission. Of particular interest are the fission and capture cross sections of the isotopes of americium, curium, and neptunium.

This past year the parameters for 47 resonances in ^{248}Cm were obtained from transmission measurements at ORELA. Although only 13 mg of ^{248}Cm was available, meaningful measurements could be made up to about 3000 eV with an energy resolution ($\Delta E/E$) of 0.3%. The samples were cooled to liquid nitrogen temperature to reduce the Doppler broadening. This reduced Doppler broadening permits a more accurate determination of the widths of the low-energy resonances and gives an improved effective energy resolution for higher energy resonances. The three lowest energy resonances were analyzed by shape analysis to obtain the radiation and neutron widths of the resonances. The parameters E_0 (eV), Γ_γ (meV), and Γ_n (meV) obtained for these three resonances are as follows: $(7.247 \pm 0.005, 23.3 \pm 1.0, 1.78 \pm 0.06)$, $(26.90 \pm 0.02, 32 \pm 3, 19.6 \pm 0.9)$, $(35.01 \pm 0.03, 30 \pm 3, 11.7 \pm 0.5)$. These three values for Γ_γ are consistent with a constant value for $\bar{\Gamma}_\gamma$ of 26 ± 2 meV, which is the value assumed for the higher energy resonances. Figure 1 shows some of the transmission data and the theoretical fits for the higher energy resonances. The observed shapes of the resonances are determined mainly by the energy resolution and Doppler broadening. After applying a small correction for small reso-

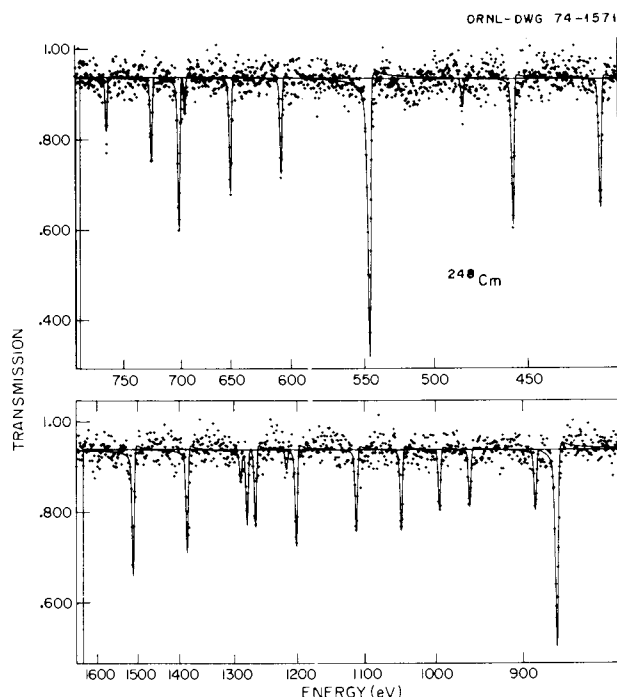


Fig. 1. Transmission of ^{248}Cm vs neutron energy and the theoretical fit to the data in the keV energy region.

nances which would not have been observed because they were smaller than the limit of detectability, we obtained a value of 40 ± 5 eV for the average s -wave level spacing, D , and an s -wave neutron strength function $\bar{\Gamma}_n^0/D$ of $(1.2 \pm 0.2) \times 10^{-4}$. This value for D for ^{248}Cm is considerably larger than those of ^{244}Cm and ^{246}Cm , which are 14 ± 2^5 and about 30^5 eV respectively. Also, the average radiation width of 26 ± 2 meV for ^{248}Cm is lower than those of ^{244}Cm and ^{246}Cm , which are 36 ± 2^5 and 35 ± 2^5 meV. These variations of D and Γ_γ are probably due to the decrease in the neutron separation energy rather than the effect of a nuclear subshell. A paper giving the details of the measurements and analysis has been prepared and will soon be submitted for publication.

The total cross-section measurements on ^{241}Pu are complete but have not been analyzed to obtain resonance parameters. The measurements were made from about 1 to 3000 eV using a ^6Li glass scintillator at an 80-m flight path with an energy resolution of 0.08%. Above 30 keV the NE-110 detector was used, but no detailed structure is observed since the Doppler broadening and resolution widths are greater than the level spacing. Since fission is large in the resonances, it will be necessary to make a multilevel multichannel analysis to obtain meaningful parameters of the resonances.

1. Instrumentation and Controls Division.
2. Savannah River Laboratory, Aiken, S.C.
3. Aerojet Nuclear Co., Idaho Falls, Idaho.
4. H. C. Claiborne, *Neutron-Induced Transmutation of High-Level Radioactive Waste*, ORNL-TM-3964 (December 1972).
5. S. F. Mughabghab and D. I. Garber, *Neutron Cross Sections*, vol. 1, *Resonance Parameters*, BNL-325, 3d ed. (June 1973);

NEUTRON-INDUCED FISSION OF ^{249}Cf

J. W. T. Dabbs N. W. Hill³
 C. E. Bemis, Jr.¹ M. S. Moore⁴
 G. D. James² A. N. Ellis⁴

This measurement has demonstrated the possibilities of ORELA as a pulsed neutron source for σ_f measurements on very small samples of easily fissionable isotopes with short alpha half-lives. Such measurements have previously been done only with underground nuclear explosions as the neutron source and are restricted to energies above about 20 eV because of the small neutron flux at lower energies from the explosion.

The use of thin (125 μm) diffused-junction silicon fragment detectors directly in the beam and in close proximity to the fissionable sample (approximately 2π geometry) permits a large gain in counting rate. For short alpha half-lives (352 years in this case), it is necessary to use a current-sensitive preamplifier with fast rise and fall times (3 and 15 ns respectively here) to avoid alpha pulse pileup to levels above the smallest fission fragment pulses. The alpha count rate was 10^7 per second in the present measurements.

The analysis of these measurements is now complete, and 11 resonances below 20 eV have been found (see Table 1). A multilevel analysis was performed up to 70 eV with results between 20 eV and 70 eV in substantial agreement with Silbert's results from the Physics-8 underground explosion. Comparable resolution was obtained, although there was a factor of about 24 in the flight paths used. By far the most interesting finding was a resonance at 0.71 eV with σ_f of about 5400 b and a total width of 160 meV (see Fig. 1). This resonance alone accounted for about 75% of the total fission count recorded and is responsible for some 85% of the resonance integral of 1630 b.⁵ In this case the lower limit of

$$\text{R.I.} = \int_{0.55 \text{ eV}}^{2 \text{ MeV}} \sigma_f dE/E, \quad (1)$$

which is the "standard" definition of the resonance integral,⁶ falls on the side of the resonance, with

disastrous results for all cadmium-shielded determinations made in the past.⁷ Large errors in correcting the lower end point come from assuming a $1/v$ cross section in this neighborhood. The fact that the resonance integral was large and unaccounted for by Silbert's measurements was a major factor in the decision to measure this cross section. It is conceivable that this large resonance, and one which should appear in ^{251}Cf , may be useful in "burnout" of long-lived

Table 1. Summary of ^{249}Cf resonances below 20 eV ($\Gamma_\gamma = 40 \text{ meV}$ assumed)

E_0 (eV)	Γ_n^0 (meV)	Γ_f (meV)
0.708	0.741	119.6
3.90	0.115	44.9
5.08	0.268	154.3
7.52	0.063	83.4
8.66	0.115	146.0
9.52	0.362	97.1
10.35	0.078	252.2
11.90	0.037	242.4
13.63	0.403	205.1
16.06	0.159	325.4
16.82	0.420	162.9

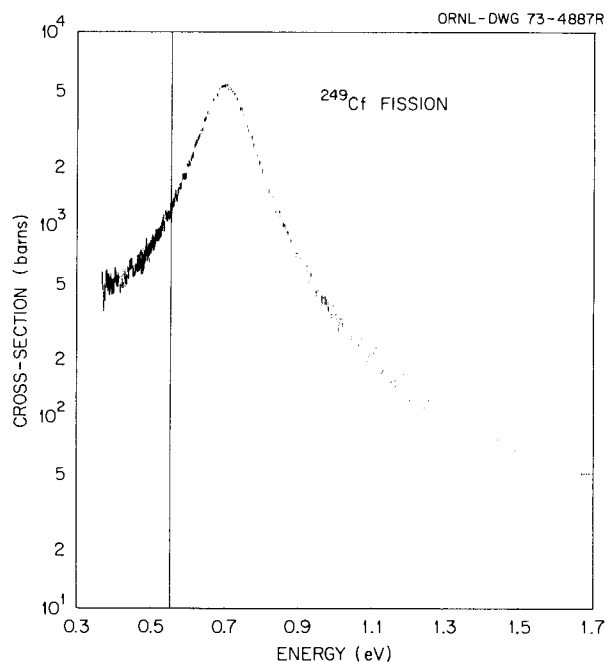


Fig. 1. Fission cross section of ^{249}Cf vs energy in the neighborhood of the largest low-energy resonance. The vertical line is the lower limit of the resonance integral (see text).

actinides to fission products of shorter half-lives, thus reducing the storage problem of radioactive wastes in nuclear energy production.

The present approach affords a less expensive and repeatable way to carry out measurements of σ_f on approximately 100- μg samples than underground nuclear explosions in selected cases. Where the spontaneous fission half-life is less than about 10^8 years, the explosion approach is probably superior; alpha-decay half-lives as short as 100 years can probably be tolerated, provided somewhat faster amplifiers (which appear feasible) are developed. The use of semiconductor detectors is not indicated in these cases because of radiation damage; for this reason, development work on fast ionization (methane) chambers has been undertaken and used.⁸

1. Chemistry Division.
2. Visiting scientist 1972-1973 from AERE, Harwell, England.
3. Instrumentation and Controls Division.
4. Los Alamos Scientific Laboratory, Los Alamos, N.M.
5. Value obtained from direct integration of present results.
6. H. Goldstein et al., EANDC-12 (1961).
7. R. W. Benjamin, K. W. MacMurdo, and J. D. Spencer, *Nucl. Sci. Eng.* 47, 203 (1972).
8. See "Subthreshold and Threshold Neutron Fission of ^{234}U " by J. W. T. Dabbs, G. D. James, and N. W. Hill, this report.

OPTIMIZED DETECTION OF FISSION NEUTRONS WITH LARGE LIQUID SCINTILLATORS

N. W. Hill¹ J. W. T. Dabbs H. Weaver²

A new performance test for pulse shape discrimination systems has been found to be about 10 times more sensitive than the usual tests using ^{252}Cf as a fission neutron source. A beam of neutrons from ORELA was passed through 20 in. of iron. The well-known "windows" in iron (narrow regions of low total cross sections) give a discrete spectrum extending from 25 keV to about 1.5 MeV. The usual lower neutron energy cutoff falls in this region and can therefore be easily ascertained. Such a beam is also essentially free of gamma rays. Neutrons which are misidentified as gamma rays are much more easily seen than in ^{252}Cf tests, since they exhibit the time-of-flight structure associated with the iron windows. It is also possible to determine susceptibility to gamma pileup with an auxiliary gamma source.

A test of a commercial 5×5 in. liquid scintillator cell with a quartz light pipe coupling to an unselected RCA 4522 photomultiplier tube showed 7.4% and 23%

misidentification for 700 keV and 300 keV neutron biases respectively. These results were much worse than anticipated on the basis of ^{252}Cf source tests made previously. A conventional fast anode pulse start, slow (0.4 μsec) DDL amplifier crossover stop was used with a time-to-amplitude converter. These findings led to efforts to improve the system, principally in the area of light collection from the liquid scintillator.

Photocathode response can be strongly nonuniform; in the outer 20% of the photocathode area, it can be reduced by as much as 50%, while in the inner 80%, the response to red light can vary $\pm 10\%$, and to blue light, $\pm 20\%$.³ Losses in each light coupling interface can be as large as 20%.⁴

Light intensity calculations have been developed for liquid scintillator systems and are embodied in a Monte Carlo code called O5S.⁵ Each calculation is for a specific incident neutron energy and includes neutron attenuation, but does not include light transport to the photocathode. Only one reference to measured attenuation of light in such systems has been found;⁶ this indicates that substantial attenuation occurs in practice. Calculations covering the range 0.5 MeV to 5.5 MeV were weighted according to a fission spectrum and made for a number of liquid scintillator sizes. A crude attenuation model was used to estimate an optimum size for the liquid scintillator. This size is 2 to 3 in. thick by 4.5 in. in diameter for a 5-in. photomultiplier.

A specially fabricated open-ended cell was sealed to an RCA 4522 photomultiplier with an indium O-ring. The tube was selected for uniformity and quantum efficiency. The NE-213 liquid scintillator was deoxidized by argon bubbling before filling. This open-ended cup configuration permits the use of curved photocathodes (as in the RCA 4522) without a light pipe and its attendant losses. The experimental tests verified that this approach gives much superior pulse shape discrimination. The iron filter tests showed only 0.7% misidentified neutrons at 700 keV neutron bias. Figure 1 shows the response obtained with a ^{252}Cf source (approximately 3-in. lead filter). The excellence of the separation is evident. Further improvement may be expected with selected GaP first dynode tubes and operation of the liquid scintillator at an optimum temperature.

1. Instrumentation and Controls Division.
2. Neutron Physics Division.
3. R. Schaeffer, RCA, Lancaster, Pa., private communication.
4. H. R. Krall, RCA, Lancaster, Pa., private communication.
5. R. E. Textor and V. V. Verbinski, ORNL-4160 (1968). A copy of this code was kindly furnished by G. L. Morgan.
6. Kuiper et al., *Nucl. Instrum. Methods* 42, 56 (1966).

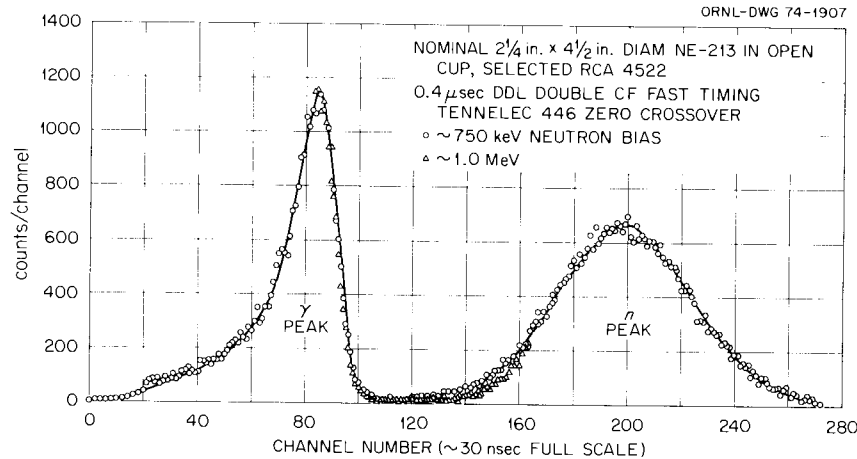


Fig. 1. Pulse shape discrimination; time response of open-cup liquid scintillator to ^{252}Cf .

GOLD NEUTRON CAPTURE CROSS SECTION FROM 3 TO 550 keV

R. L. Macklin J. Halperin¹

The capture cross section of gold has been used as a neutron standard for over 20 years, and its accuracy is still being improved. The need for accurate measurements of this cross section is covered under priority 1 requests² (No. 394) for primary standards, including individual and average resonance parameter analysis of the data.

A recent series of measurements with the ORELA total gamma energy detector (TED) of the gold neutron capture cross section from 3 to 550 keV is being prepared for publication. The saturated resonance technique has been used for calibration (4.9-eV gold, confirmed by 3.9-eV holmium and 6.7-eV ^{238}U). The calibration is also within 7% of that calculated from geometries, detector composition, Compton (and other photon) cross section, ^6Li content of the monitor scintillation glass, etc. The results depend on the shape of the $^6\text{Li}(n,\alpha)$ cross section as a function of energy, which has been taken from recent work of Poenitz,³ also agreeing with recent results from England and France as to the peak cross section near 250 keV.

Our energy resolution below 90 keV is a little better than 0.2%, allowing isolated resonance parameter extraction below 5 keV or so and fluctuation analysis for *s*-wave and *p*-wave average parameters. That work is not yet complete, but the average cross section has been fitted to strength functions; $S^0 = 1.6 \times 10^{-4}$ (taken as a $2J + 1$ average from the *AIP Handbook*⁴), $S^1 = 0.6 \times 10^{-4}$, $S^2 = 0.7 \times 10^{-4}$, and $\Gamma_\gamma/D_{\text{obs}} = 0.125/15.5$ following the definitions and scheme of Gibbons et al.⁵

This fit and a histogram of the data are shown in Fig. 1. Also shown is the Poenitz evaluation curve from Fig. 1 of his paper at the October 1970 ANL Symposium⁶ (CONF-701002, pp. 320–326), which overlaps the fitted curve from 23 to 120 keV. Our data from 120 to 550 keV agree more closely with the recent data of Le Rigoleur et al.⁷ than with the evaluation. Corrections have been applied to our sample yield data for average scattering of neutrons, self-absorption of capture gamma rays, and, above 240 keV, inelastic gamma ray yield.

At 30 keV the strength function fit (579 mb) and the evaluation curve (576 mb) are in excellent agreement.

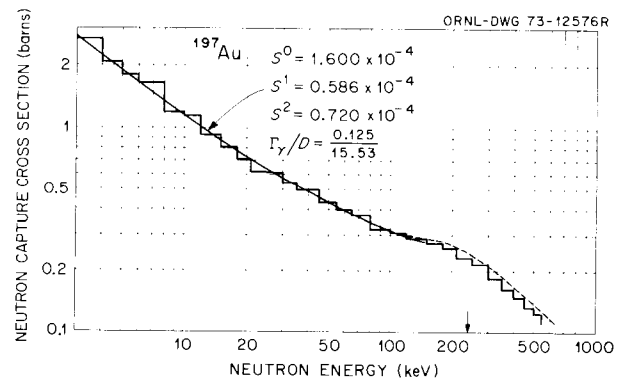


Fig. 1. Histogram of $^{197}\text{Au}(n,\gamma)$ cross section. The sample yields have been corrected for average resonance self-protection, multiple scattering, and gamma-ray self-absorption. A correction for inelastic scattering has been applied at energies above the threshold indicated by the arrow. The dotted curve (coincident with the solid line *s*, *p*, *d* wave strength function fit from 23 to 120 keV) is from an evaluation of earlier measurements by Poenitz. Recent data from Le Rigoleur et al. above 70 keV agree well with ours.

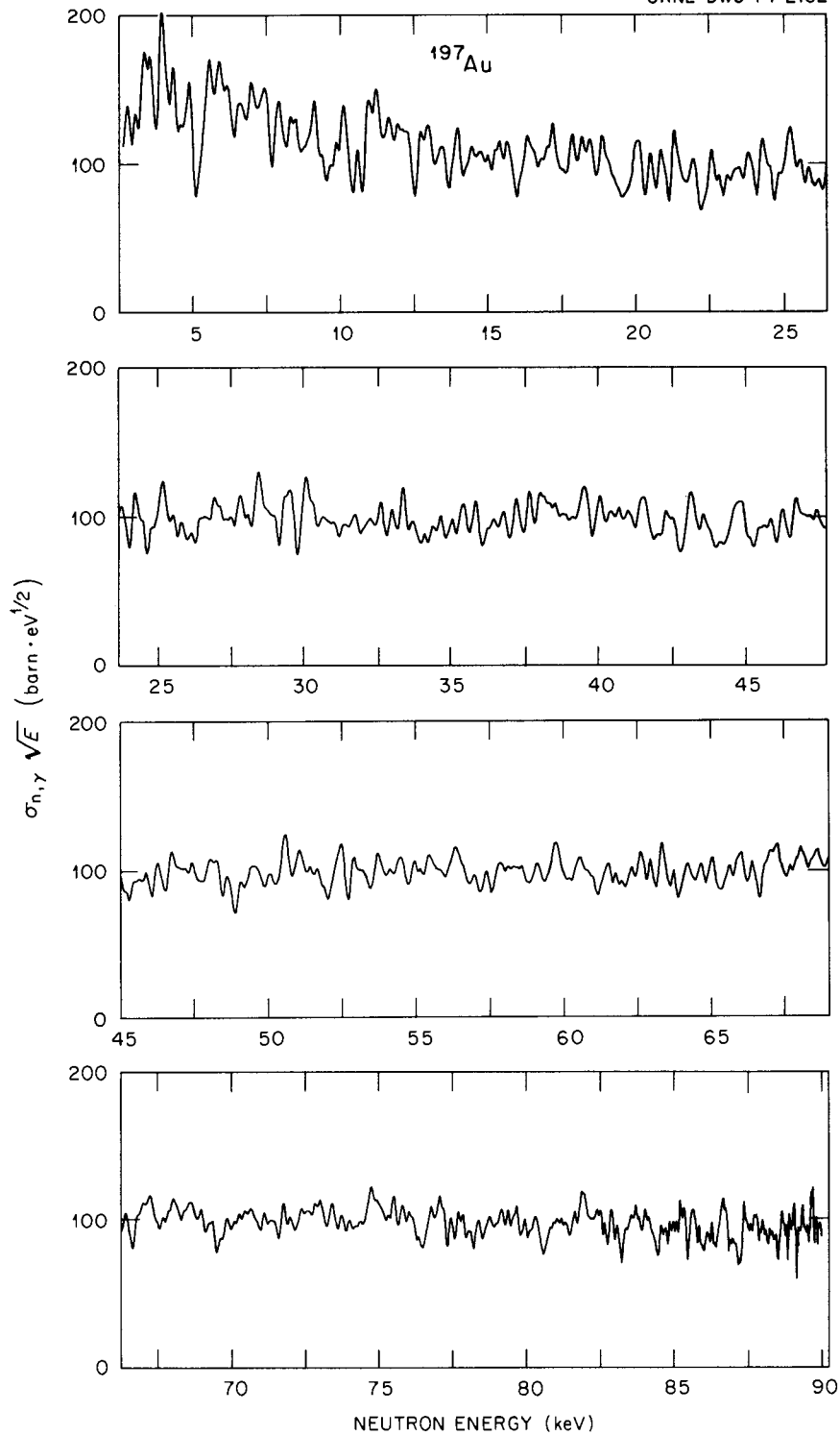


Fig. 2. Gold capture data smeared to a constant Gaussian resolution (175 eV full width at half maximum) to average over tens of compound nucleus resonances. The fluctuations remaining can be analyzed for evidence of intermediate structure. Likewise, the departure of the cross section from smooth behavior over energy bands less than a few keV wide (as used in other earlier measurements of the cross section) can be evaluated.

For comparison with ${}^7\text{Li}(p,n)$ threshold source measurements, our high-resolution data have been integrated over the total yield spectra for uniform lithium (metal, fluoride, or silicate, for example) targets as a function of incident proton energy. The results indicate a 1% higher value for protons half a keV above threshold than for incident protons several keV above threshold. Thus the long-suspected influence of the gold resonance structure is not large for this neutron source reaction. For the narrower 24-keV iron filter neutron spectrum the effect is 9% compared with the strength function fit of Fig. 1. Figure 2 shows the fluctuations still present when the high-resolution data are averaged over tens of resonances (Gaussian averaging, 175 eV full width at half maximum). The smoothness near 55 keV may be interpreted as indicating a local clustering of levels, while the large fluctuations near 5 keV correspondingly indicate a gap.

-
1. Chemistry Division.
 2. L. Stewart et al., "Compilation of Requests for Nuclear Data," USNDC-6 report, June 1973.
 3. W. P. Poenitz, "Measurements of the ${}^6\text{Li}(n,\alpha)\text{T}$ Cross Section in the keV Energy Range," submitted to JNE, October 1973.
 4. J. A. Harvey and M. D. Goldberg, chap. 8f, *American Institute of Physics Handbook*, McGraw-Hill Book Company (D. E. Gray, Coordinating Editor), pp. 8-218–8-253 (1972), 3rd Edition.
 5. J. H. Gibbons et al., *Phys. Rev.* **122**, 182–201 (1961).
 6. W. P. Poenitz in *Neutron Standards and Flux Normalization*, A. B. Smith, Coordinator, AEC Symposium Series Report 23 (August 1971).
 7. C. Le Rigoleur et al., *Mesure de la Section Efficace de Capture Radiative des Neutrons par l'Or Entre 75 keV et 550 keV*, report CEA-N-1662 (Aout 1973).

NEUTRON CAPTURE IN SULFUR TO 1100 keV

J. Halperin¹ R. L. Macklin R. R. Winters²

Neutron time-of-flight radiative capture data for a sample of natural sulfur (95% ${}^{32}\text{S}$, 0.026 atom/b) have been taken at the Oak Ridge National Laboratory electron linear accelerator and have been analyzed for single-level resonance parameters. Detailed descriptions

of the experimental arrangement and data handling have been given previously.³ Figure 1 illustrates the structure discernible in a plot of capture cross section (mb) vs energy (keV) and the adequacy of the background corrections. Some 52 resonances to 1100 keV have been identified and are listed in Table 1, including about 25 resonances not previously reported. Resonances appear not to have been missed up to about 500 keV, as judged by a plot of the cumulative number of observed resonances vs energy.

On the basis of seven identified s -wave resonances, an upper limit may be placed for the average level spacing of $D(l=0) \leq 160$ keV. The average reduced s -wave neutron width and strength function are found to be $\langle g\Gamma_n^0 \rangle = 13 \pm 5$ eV and $S^0 = (0.86 \pm 0.40) \times 10^{-4}$ respectively. For some 44 resonances assigned to p -wave neutron capture we obtain an average level spacing of $D(l=1) = 25$ keV. On the basis of 17 resonances for which widths are available from our resolved resonances or from transmission measurements⁴ an upper limit to the p -wave reduced neutron width can be estimated as $\langle g\Gamma_n^1 \rangle \leq 10.3$ eV. Further, the average s - and p -wave radiation widths can be similarly estimated as 5.9 ± 2.2 eV and 2.3 ± 0.6 eV.

The current evaluation of the capture gamma area for the 30.38-keV resonance is about 50% greater than reported earlier.⁵ The effect of this resonance is relevant to the theory of weak s -process element formation since ${}^{32}\text{S}$ serves as a seed nucleus and Maxwellian averages for $kT \cong 30$ keV neutrons are of course sensitive to this resonance.⁶ The 30-keV Maxwellian average cross section is computed as 4.95 ± 0.50 mb.

-
1. Chemistry Division.
 2. Denison University, Granville, Ohio.
 3. B. J. Allen, R. L. Macklin, R. R. Winters, and C. Y. Fu, *Phys. Rev.* **C8**, 1504 (1973).
 4. S. Cierjacks, P. Forti, D. Kopsch, L. Kropp, J. Nebe, and H. Unseld, "High Resolution Total Neutron Cross Sections between 0.5-30 MeV", Gesellschaft für Kernforschung M.B.H., Karlsruhe, June 1968.
 5. S. F. Mughabghab and D. I. Garber, *Neutron Cross Sections*, vol. 1, *Resonance Parameters*, BNL-325, Third Edition, available from National Technical Information Service, U.S. Dept. Commerce, June 1973.
 6. J. G. Peters, W. A. Fowler, and D. D. Clayton, *Astrophys. J.* **173**, 637 (1972).

Table 1. Resonance parameters for $^{32}\text{S}(n,\gamma)^{33}\text{S}$

E_n (keV)	J	l	$g\Gamma_n\Gamma_\gamma/\Gamma$ (eV)	$g\Gamma_\gamma$ (eV)	$g\Gamma_n$ (eV)	$g\Gamma_n^0$ (eV)	$g\Gamma_n^1$ (eV)
30.38	$\frac{3}{2}$	1	1.27	0.64 ₂	46.9		10.9
43.12			0.066 ₃				
46.82			0.045 ₂				
97.52	$\frac{1}{2}$	1	0.46 ₁	0.46	310		13.3
102.9	$\frac{1}{2}$	0	9.0 ₀	9.0	17,000	52.9	
112.2	$\frac{1}{2}$	1	0.55 ₀	0.55	840		29.5
145.2			0.24 ₂				
160.3			0.81 ₂				
172.8			0.77 ₅				
202.4	$\frac{1}{2}$	1	0.31 ₂	0.31	1,300		20.2
261.4			1.46				
272.3	$\frac{1}{2}$	1	2.11	2.1	1,170		12.2
288.5	$\frac{1}{2}$	1	3.62	3.6	1,140		11.0
309.4			2.32				
312.7			1.76				
321.2			1.61				
346.1			1.57				
353.6			3.27				
378.9			1.33	1.3	1,500		10.2
380.0	$\frac{1}{2}$	0	0.47	0.47	4,800	7.85	
382.5			0.63 ₄				
401.6			1.28				
413.0			1.52				
426.2			0.40				
460.2			1.91				
463.3			1.13				
514.1			2.24				
533.9			2.21				
577.0			1.82				
587.0	$\frac{5}{2}$	2	4.67	1.56	1,800		(107) ^a
649.1			3.76	3.76	1,200		4.29
667.1			1.89				
676.5			1.31	1.31	1,200		4.09
694.0			1.01				
700.0	$\frac{1}{2}$	0	1.36	1.36	10,000	12.0	
726.0			1.41	1.41	5,000		15.6
741.1			1.62	1.62	2,500		7.68
778.6	$\frac{1}{2}$	0	2.05	2.05	2,500	2.85	
785.7			2.39				
820.1			0.85	0.867	1,600		4.40
835.6			3.74				
868.7			5.83	5.83	3,000		7.70
886.6			16.71				
903.4			1.27				
921.9	$\frac{1}{2}$	0	9.89	9.9	3,200	3.35	
948.4			1.16	1.16	2,500		5.88
987	$\frac{1}{2}$	0	3.57	3.57	10,000	10.1	
1011			1.99	1.99	3,000		6.59
1049	$\frac{1}{2}$	0	15.0	15.0	5,400	5.26	
1060			5.06	5.06	3,000		6.28
1069			7.64				
1089			7.79	7.79	3,000		6.11

^aReduced neutron width ($g\Gamma_n^2$) for d -wave resonance.

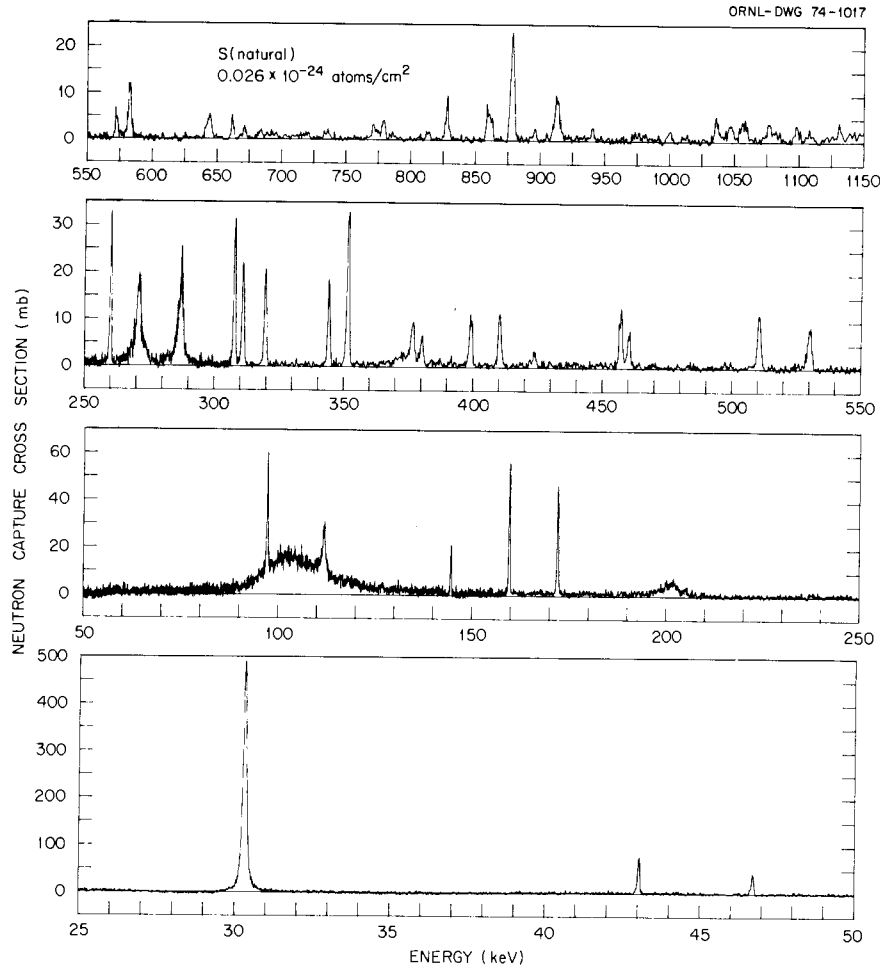


Fig. 1. Radiative capture yield of ^{32}S (95%). No resonances were seen below 25 keV except for two resonances at 17.6 and 23.9 keV attributable to the minor ($^{3/4}\%$) isotope ^{33}S . Resolution drops from $E_n/600$ (FWHM) at the lower energies to $E_n/250$ at 1000 keV.

NEUTRON TOTAL CROSS SECTION OF ^6Li FROM 100 eV TO 1 MeV

J. A. Harvey N. W. Hill¹

One of the more useful neutron standards in the energy region below 1 MeV is the $^6\text{Li}(n,\alpha)$ reaction, since fast, efficient, stable neutron detectors utilizing this reaction can readily be constructed. Although much effort has been spent to measure this (n,α) cross section accurately, a recent evaluation by Uttley et al.² lists an uncertainty in some energy regions as large as 15% and about 5% in the energy region of the large resonance at 247 keV. Neutron total cross sections have also been analyzed to give the (n,α) cross section in the 247-keV energy region. However, the most recent total cross-section measurements³ give a resonance energy of

255 keV, about 8 keV higher than the value accepted by Uttley.² The energy calibration for this measurement was based on the $^7\text{Li}(p,n)$ and $^{11}\text{B}(p,n)$ thresholds. The present measurements were made to determine this resonance energy at ORELA and to obtain accurate total cross-section data which could be analyzed to obtain the (n,α) cross section in the 100-to-400-keV energy region.

Transmission measurements were made upon two samples of ^6Li (98.72%) with inverse thicknesses of 11.84 and 2.585 b/atom. Data were obtained with a ^6Li glass scintillator and an NE-110 proton recoil detector 78.203 m from the neutron target at ORELA. The neutron energy resolution $\Delta E/E$ was about 0.1%, or 0.2 keV at 247 keV. Since no fine structure was observed, the data with the thin sample using the NE-110 detector shown in Fig. 1 have been averaged to give

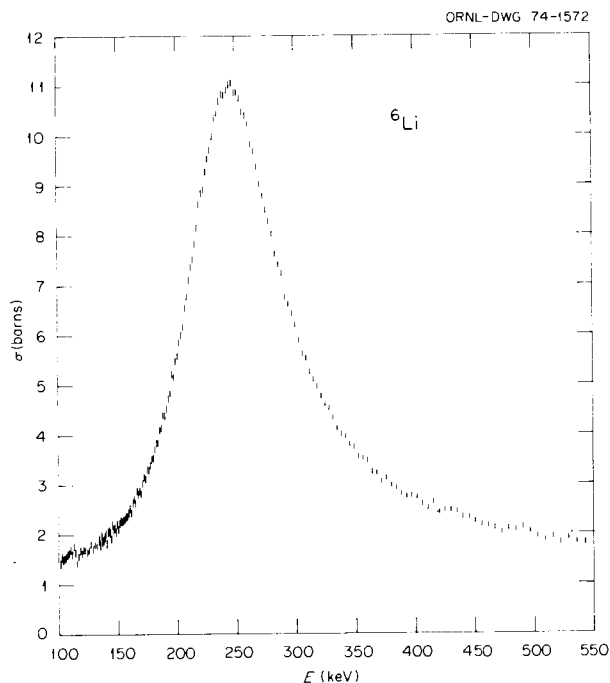


Fig. 1. Total cross section of ${}^6\text{Li}$ vs neutron energy.

about 2-keV resolution. The statistical accuracy on these averaged points is about 0.05 b. The backgrounds (room and 2.23-MeV gamma rays from neutron capture in the water of the moderator) were less than 1% in this energy region. Other systematic errors arising from uncertainties in the neutron monitor are estimated to produce much less than 0.1 b uncertainty. The observed peak cross section is 11.0 ± 0.1 b, in good agreement with values reported in refs. 2 and 3. The data obtained with the thin sample and the ${}^6\text{Li}$ glass detector are in excellent agreement (within 0.1 b and 0.5 keV) with the data shown in Fig. 1. The energy scale is accurate to within about 0.1%. The resonance energy obtained by the method of diameters is 246 ± 1 keV, in good agreement with the time-of-flight measurements of Uttley² (247 keV). Energy values from Van de Graaff measurements on this nuclide are about 5 keV too high. In the energy region from 300 to 10,000 eV the data from the thin sample are in excellent agreement (within about 0.05 b or about 1%) with the formula proposed by Uttley,² namely, $\sigma_T = 0.70 + 149.5/\sqrt{E}$. We plan to make a phase-shift analysis of these data using the program of Johnson⁴ to obtain parameters of this p-wave resonance at 247 keV and hence the ${}^6\text{Li}(n,\alpha)$ cross section in the 100-to-400-keV energy region.

1. Instrumentation and Controls Division.
2. C. A. Uttley, M. G. Sowerby, B. H. Patrick, and E. R. Rae, *Proceedings of Conference on Neutron Standards and Flux Normalization*, AEC Symposium Series 23 (1971), p. 80.
3. J. W. Meadows and J. F. Whalen, *Nucl. Sci. Eng.* **48**, 221 (1972).
4. C. H. Johnson, *Phys. Rev.* **C7**, 561 (1973).

THE ${}^57\text{Fe}(n,\gamma){}^58\text{Fe}$ REACTION AND SHELL-MODEL CALCULATIONS OF ${}^58\text{Fe}$ LEVELS

S. Raman J. A. Harvey
 G. G. Slaughter J. B. McGrory
 W. M. Good D. Larson¹

We have known for some time that shell-model calculations work well in the case of ${}^58\text{Fe}$, but how well is the next question. A great deal of experimental information already exists concerning ${}^58\text{Fe}$ levels, but there are also some gaps. In particular, gamma-ray studies following resonance neutron capture in ${}^57\text{Fe}$ have not been attempted before, probably due to the nonavailability of enriched samples in sufficient amounts and due to the fact that the neutron resonances lie in the several keV range. We were fortunate in obtaining the loan of a 100-g 86% enriched ${}^57\text{Fe}$ metal target from W. C. Koehler of the ORNL Solid State Division. We then exploited the unique capabilities of the Oak Ridge Electron Linear Accelerator, which can provide sufficient intensity of neutrons in the keV range. The capture gamma-ray studies led to a level scheme for ${}^58\text{Fe}$. This information was combined with the already existing data and compared with the results of a shell-model calculation as discussed below.

Neutron resonances in the ${}^57\text{Fe} + n$ system were identified via both transmission and capture gamma-ray studies. The resonances are shown in Fig. 1. The gamma spectra from neutron capture in the first three resonances are shown in Fig. 2. A total of 23 primary gamma rays were observed from our study of 12 resonances below 30 keV. The level scheme based on these measurements is shown in Fig. 3. A more complete level scheme for levels below 4.5 MeV, based on all available data, is shown in Fig. 4.

We have carried out detailed shell-model calculations of ${}^58\text{Fe}$ levels with the Oak Ridge-Rochester shell-model code. An inert ${}^{48}\text{Ca}$ core was assumed. Protons were restricted to the $f_{7/2}$ shell and neutrons to the $p_{3/2}$, $f_{5/2}$, and $p_{1/2}$ orbits. The Hamiltonian includes proton-proton, neutron-neutron, and neutron-proton interactions. For the two-body matrix elements of the

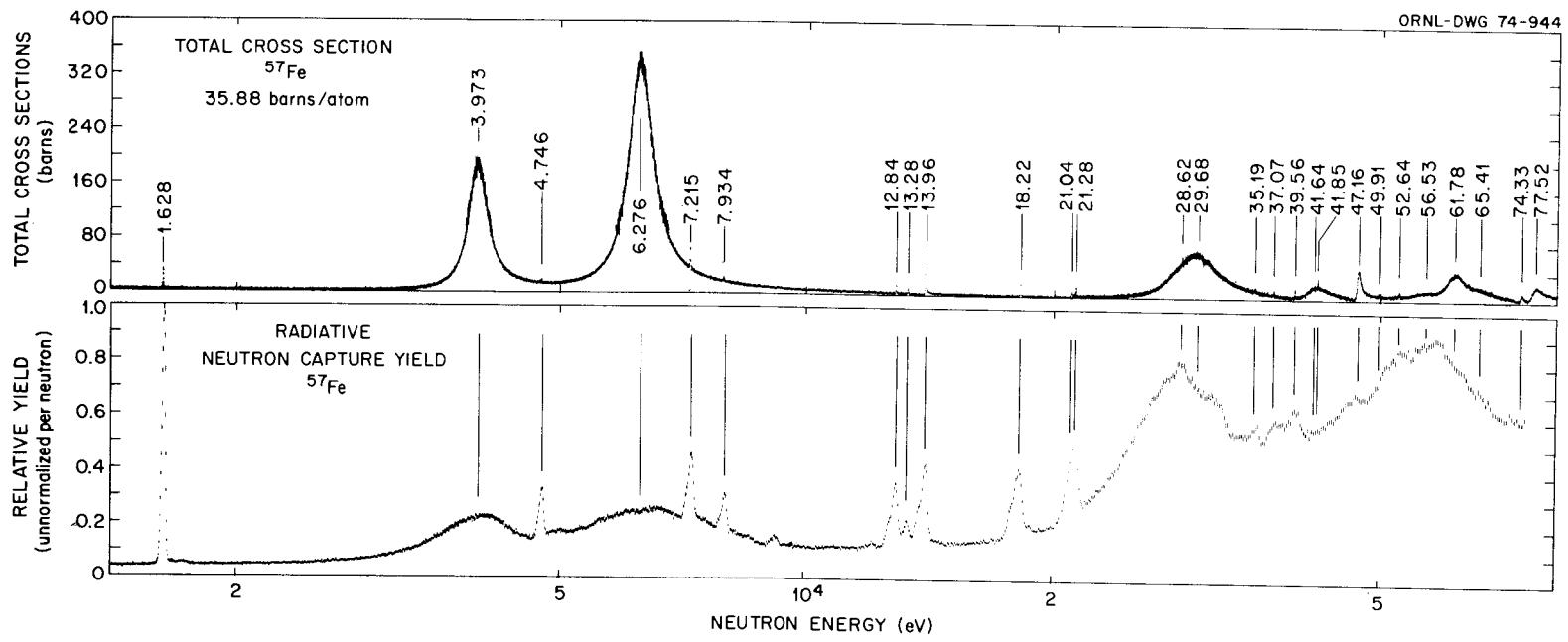


Fig. 1. Neutron resonances in the $^{57}\text{Fe} + n$ system observed in transmission and capture gamma-ray measurements.

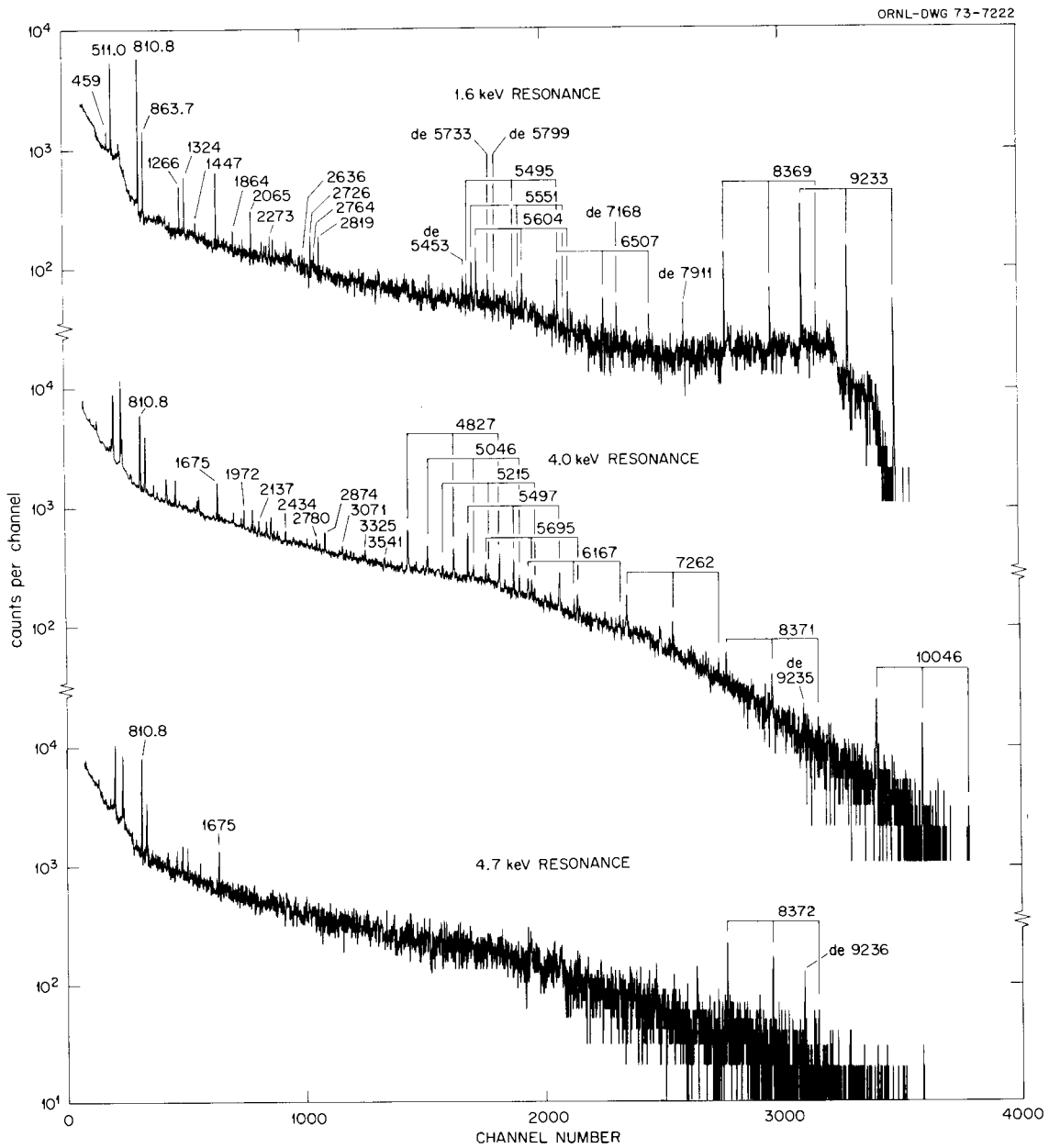
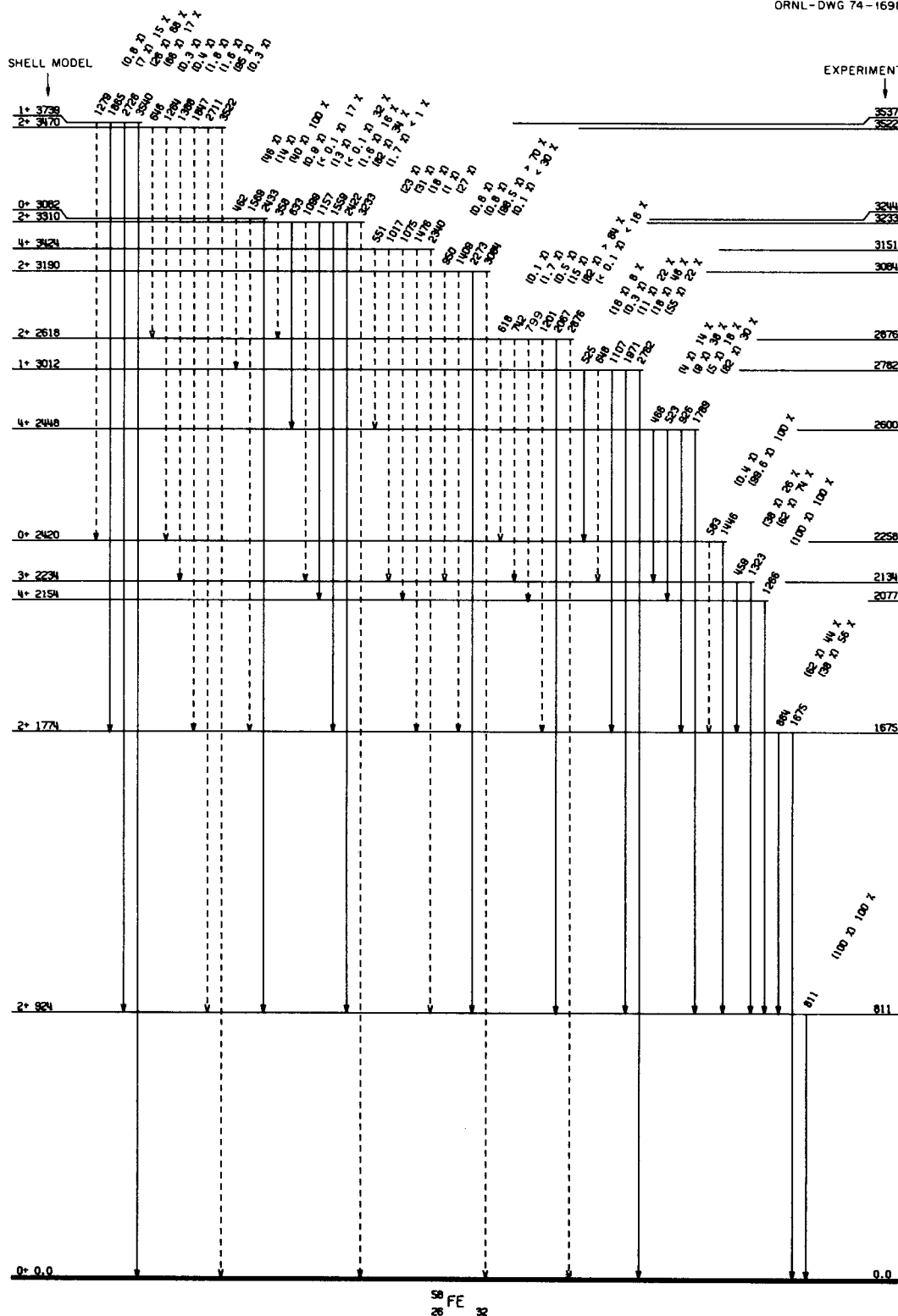


Fig. 2. Typical gamma-ray spectra from the first three neutron resonances. The 4.0-keV resonance is known to be 0^- from transmission measurements. The observation of the 10,046-keV gamma ray in the middle spectrum is due to the low-energy tail of the 6.3-keV, $J^\pi = 1^-$ resonance.



proton-proton interaction, we use the experimentally known energies of the lowest 2^+ , 4^+ , and 6^+ states in ^{54}Fe . The neutron-neutron interaction is taken from the work of Cohen et al.² For the neutron-proton two-body matrix elements, we use an interaction proposed by Vervier.³

Figure 4 shows the comparison between the experimental and calculated energy levels. The agreement is very good. For the first 12 experimental levels, the average difference between the two sets is only 150 keV. The wave functions increase in dimensionality from 48 terms for the 0^+ states to 216 terms for the 4^+ states.

A more rigorous test of the predictive power of these calculations is provided by gamma-ray branching ratios, which we employ in the absence of experimental lifetime measurements. The necessary single-particle matrix elements were calculated with unrenormalized free-nucleon values for the $M1$ operator, an effective proton charge of 1.2 (total proton charge of 2.2), and an effective neutron charge of 1.9. These effective charges were chosen so that good agreement is obtained for the $B(E2)\uparrow$ value in the two-proton-hole case of ^{54}Fe and the two-neutron-particle case of ^{58}Ni . The calculated gamma branchings are given in parentheses in Fig. 5, where they have been compared with the experimental values. We note that for the excited 2^+ states above 2 MeV, theory predicts very small intensities for the gamma transitions to the ground state, in accord with experiment. The overall agreement between the experimental and calculated gamma branching ratios is less satisfactory. In particular, it appears that we need to decrease the $B(M1)$ operator by about a factor of 2. Calculations are presently under way to determine an effective $M1$ operator that will result in improved agreement between the experiment and theory.

-
1. Neutron Physics Division.
 2. S. Cohen, R. D. Lawson, M. H. Macfarlane, S. P. Pandya, and M. Soga, *Phys. Rev.* **160**, 903 (1967).
 3. J. Vervier, *Nucl. Phys.* **78**, 497 (1966).

SEARCH FOR A NEUTRON RESONANCE IN ^{207}Pb AT 16.8 MeV

J. A. Harvey N. W. Hill¹
W. M. Good R. H. Schindler²

At the Budapest Conference³ in 1972 a "resonance peculiarity" with a width of about 150 keV was reported in the neutron total cross section of ^{207}Pb at

16.8 MeV. It was suggested that it might be an isobaric analog resonance. Since this type of intermediate structure had not been observed previously, we attempted to verify its existence by measurements at ORELA. All our previous transmission measurements at ORELA have been made with a tantalum target and a water moderator. For this measurement we used a beryllium target irradiated with bremsstrahlung from a tantalum converter. This target produces more high-energy neutrons above 10 MeV, and the gamma flash problem is much less severe.

A 1-in.-diam ^{207}Pb sample (92.4%, 253 g, $1/N = 6.865$ b/atom) was placed 9 m from the beryllium target. With a 78.185-m flight path and 5-nsec electron bursts, the neutron resolution was 0.5% at 16 MeV. An NE-110 plastic scintillation detector (3 in. in diameter and 3 in. long) was used. Transmission data with about 3% statistical uncertainty were obtained in a few days of linac operation. The resulting total cross section in the energy range of interest is shown in Fig. 1. The data points have been averaged by fives (resulting in an energy resolution of about 120 keV) in order to improve the statistics. The well-known rise (about 0.7

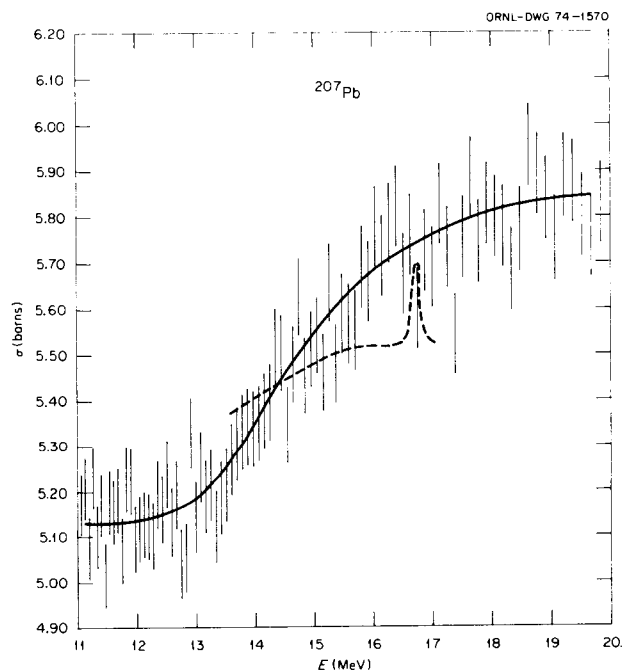


Fig. 1. Total cross section of ^{207}Pb vs neutron energy. The dashed curve is from B.A. Benetzky, V. V. Nefedov, I. M. Frank, and I. V. Shtanikh, "Interaction of 13–17 MeV Neutrons with the Pb Isotopes," *Proceedings of Budapest Conference on Nuclear Structure Studies with Neutrons* (Budapest, Hungary, August 1972), to be published; *J. Nucl. Sci.* **17**, 21 (1973).

b) from 12 to 18 MeV is observed, but there is no evidence for a resonance at 16.8 MeV. With improvements in the experimental setup, the counting statistics could be improved. However, this particular cross section has also been investigated recently at Livermore in the energy range from 16.3 to 17.1 MeV with about 55 keV energy resolution using a (d,T) source. A smooth energy variation of the transmission to about 1% was found over the energy range studied. Hence, this resonance at 16.8 MeV has not yet been confirmed.

1. Instrumentation and Controls Division.

2. Undergraduate Research Trainee at ORNL during summer 1973 from the University of Rochester, Rochester, N.Y. (trainee program administered by Oak Ridge Associated Universities).

3. B. A. Benetzky, V. V. Nefedov, I. M. Frank, and I. V. Shtranikh, "Interaction of 13-17 MeV Neutrons with the Pb Isotopes," *Proceedings of Budapest Conference on Nuclear Structure Studies with Neutrons* (Budapest, Hungary, August 1972), to be published; *J. Nucl. Sci.* 17, 21 (1973).

NONEXISTENCE OF A GIANT $M1$ RESONANCE IN ^{208}Pb

J. A. Harvey N. W. Hill¹
W. M. Good R. H. Schindler²

In 1970, Bowman et al.³ reported a concentration of $M1$ strength in ^{208}Pb at an excitation energy of 7.9 MeV with a width of about 700 keV from threshold photoneutron and angular-distribution measurements on ^{208}Pb . From these measurements and from total cross-section data, seven states in ^{208}Pb were determined to be 1^+ ($M1$ excitation leading to p -wave neutron emission). The $M1$ strength of the five strongest transitions was 51 eV, or about 50% of the total $M1$ strength predicted from shell-model calculations of spin-flip transitions in the $i_{13/2}$ neutron shell and $h_{11/2}$ proton shell (or about 100% if polarization effects are included). However, if these excited states had negative parity (1^- states), they would be excited by $E1$ transitions leading to s -wave emission, and their strengths would be normal.

Recently Toohey and Jackson⁴ repeated these photonuclear measurements with better neutron energy resolution and have questioned the positive parity assignment by Bowman et al.³ of three of these five 1^+ states. They showed that a small d -wave admixture in the s -wave yield would give an asymmetric angular distribution which could be similar to p -wave neutron emission. Above 400 keV they concluded that the parities could not be determined from photoneutron data alone. However, they concluded that the 181-keV

resonance had positive parity since a large anisotropy was observed and the d -wave width of this resonance should be very small. Also, they accepted the positive assignment to the 318-keV resonance made by Bowman et al.³ who claimed that this resonance was "symmetrical in neutron data, and had a peak height several times the theoretical maximum neutron total cross section for an $l = 0$ resonance; thus, it must have positive parity." The parity of this resonance could not be assigned from photoneutron data. Toohey and Jackson concluded that the presence of an $M1$ giant resonance was probable but by no means certain.

In order to check the 1^+ assignment of the 181- and 318-keV resonances and possibly the higher energy resonances, we have made high-resolution total cross-section measurements on ^{207}Pb ($\Delta E/E \approx 0.05\%$). The standard tantalum water-moderated neutron target and 5-nsec bursts were used with an NE-110 detector at the 200-m flight station. In the energy range below 1 MeV, more than 100 resonances have been observed. Although several obvious s -wave resonances were observed at 41.2, 101.8, 231, 256, 372, 443, 462, 492, 542, and 554 keV, symmetrical p -wave resonances predominate. An order of magnitude more resonances are observed than were found in the (γ,n) threshold work. Also, several resonances were observed in the vicinity of the levels claimed to be excited by $M1$ transitions in the (γ,n) work. For example, three resonances were observed in the 181-keV energy region, a small s -wave resonance with spin 1^- at 181.5 keV, and two probably p -wave resonances at 181.1 and 180.9 keV. Hence, the neutron peak at 181 keV⁴ in the photoneutron work in this energy region may be due to a normal-strength $E1$ transition to this 1^- state and not a strong $M1$ transition.

Figure 1 shows the total cross section in the 318-keV energy region. It is obvious that the large resonance at 319 keV is not symmetrical, as claimed by Bowman et al.³ but is quite complex. From a cursory analysis, we judge that it consists of several resonances, a wide s -wave resonance of spin 1^- , a large p -wave resonance of spin 2^+ , and a small (possibly s -wave) resonance at 317 keV. Thus the neutron peak at 315 keV in the photoneutron reaction is probably not due to a strong $M1$ transition but a normal $E1$ transition to one of these s -wave resonances.

The total cross-section data in the region of 610 and 850 keV are even more complicated, and it will be necessary to do a multilevel phase-shift analysis of these data (and also the lower energy data) in order to determine if s -wave resonances are present in these energy regions which would account for the strong

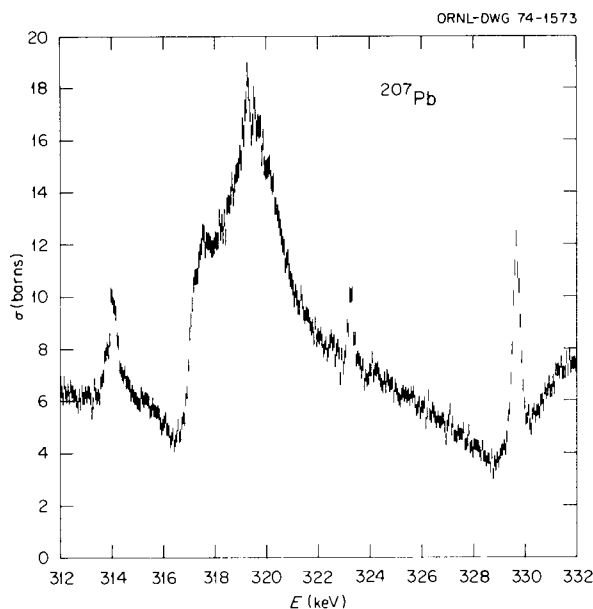


Fig. 1. Neutron total cross section of ^{207}Pb vs energy.

gamma-ray strengths in the photoneutron measurements.

A high-resolution measurement of the neutron total cross section of ^{207}Pb has also been made recently at LLL.⁵ Their data are now being analyzed, and parity assignments are not yet conclusive.⁶

In conclusion, there is now no evidence of strong $M1$ transitions in ^{208}Pb , and there will not be unless high-resolution total cross-section data can prove there are no s -wave neutron resonances at 608, 619, 657, and 854 keV.

1. Instrumentation and Controls Division.

2. Undergraduate Research Trainee at ORNL during summer 1973 from the University of Rochester, Rochester, N.Y. (trainee program administered by Oak Ridge Associated Universities).

3. C. D. Bowman, R. J. Baglan, B. L. Berman, and T. W. Phillips, *Phys. Rev. Lett.* **25**, 1302 (1970).

4. R. E. Toohey and H. E. Jackson, *Phys. Rev.* **C6**, 1440 (1972).

5. T. W. Phillips and B. L. Berman, *Bull. Amer. Phys. Soc.* **18**, 539 (1973).

6. B. L. Berman, private communication.

THE $^{16}\text{O} + n$ TOTAL CROSS SECTION: DIAGNOSTICS AND REFINEMENTS

C. H. Johnson L. A. Galloway²
J. L. Fowler¹ N. W. Hill³

The scattering by oxygen of neutrons of a few MeV has been studied at so many laboratories, including

ORNL,⁴ that there is little incentive related to nuclear physics for further measurements. But the very fact that total cross sections are available and have been fitted in detail⁵ makes oxygen ideal for checking out equipment.

Figure 1 shows the oxygen total cross section observed for 50- to 2000-keV neutrons at the ORELA 200-m flight path. The scatterer was beryllium oxide, with matching beryllium, and the detector was NE-110. The circuitry included background discrimination by pulse height but not pulse shape. The backgrounds are small and mostly from gamma rays.

The overall energy resolution, including effects of the 5-nsec bursts and the size of source and detector, ranges from about 0.03 keV at 50 keV to 2.2 keV at 2 MeV. The points in the figure are averaged over several resolution widths, except near the 1651- and 1833-keV resonances.

Those narrow resonances provide vehicles for comparing the present resolution with the best achieved at the ORNL Van de Graaff laboratory by Fowler et al.⁴ Their peak for the first one was 7.2 b, somewhat less than the 8 b observed here, but their peak for the second one was only slightly less than here. On the other hand, the present resolution does not reveal the narrow 2889-keV peak observed at the Van de Graaff facility. Thus the crossover between the two facilities is

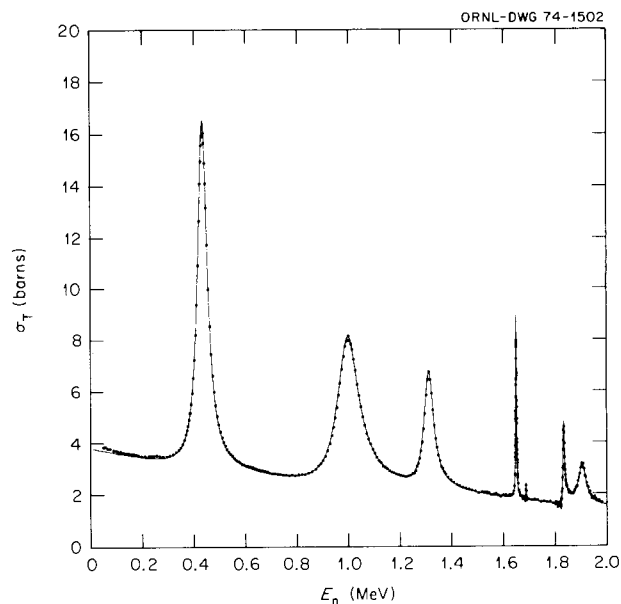


Fig. 1. Total neutron cross section of oxygen. The curve is a previously published R -matrix fit [C. H. Johnson, *Phys. Rev.* **C7**, 561 (1973)] except that the first resonance peak has been shifted from 443 to 435 keV.

about 2 MeV. Below that, ORELA is a superb instrument.

The solid curve in the figure is Johnson's⁵ R -matrix fit except for the energy shift discussed below for the first resonance. The curve is an excellent fit and, in some regions, constitutes a prediction of the R -matrix theory. For example, the curve for the 1-MeV resonance, having been deduced⁵ more from precision⁴ off-resonant points than from the less precise resonant data, predicts the observed resonance almost exactly. We have little motivation to adjust parameters to improve the fit, but we do anticipate future detailed measurements on other nuclei. Analyses of such data will allow us to deduce the potential phase shifts as well as the usual resonant parameters.

The curve below 600 keV is an exception to the good fit. The published curve⁵ was based on a resonant energy⁶ of 442 keV. But we find the peak at 435 ± 1 keV, corresponding to a resonant energy of 434 ± 1 keV. The curve shown is based on this new energy.

More serious discrepancies occur below 300 keV, as shown on an expanded scale in Fig. 2. The curve should be a good prediction because it is tied to the well-known cross section at thermal. We understand the discrepancy in part. The slight peak at 257 keV is a resonance with magnitude corresponding to the known 0.4 at. % of lithium in the scatterer. But we do not understand the deviation below 200 keV. It is too large

and has the wrong energy dependence for credible amounts of hydrogen.

1. On assignment 1973–1974 to AERE, Harwell, England.
2. Centenary College, Shreveport, La.
3. Instrumentation and Controls Division.
4. J. L. Fowler, C. H. Johnson, and R. M. Feezel, *Phys. Rev. C8*, 545 (1973).
5. C. H. Johnson, *Phys. Rev. C7*, 561 (1973).
6. A. Okazaki, *Phys. Rev. 99*, 55 (1955).

POTENTIAL SCATTERING OF NEUTRONS BY CALCIUM

J. L. Fowler¹ C. H. Johnson

The usual optical model for the interaction of nucleons with nuclei has several parameters, at least ten. Even so, it usually has no dependence on angular momentum, other than the spin-orbit term. Perhaps that is because the model has been derived mostly from data at high energies, where many partial waves are active. Recent low-energy data^{2,3} do indicate an orbital dependence.

Individual partial waves can be studied by scattering neutrons near isolated resonances. The "signature" of potential-resonance interference in total cross sections reveals the phase for a particular partial wave, and this phase can be interpreted in terms of scattering from a potential. But meaningful measurements require excellent energy resolution, particularly for narrow resonances of higher partial waves. Extensive data do exist at low energies, where s waves dominate, but are limited to a region of a few hundred keV, where p and d waves become active.

The 200-m flight path and associated NE-110 detector at ORELA may presently be the best facility anywhere for such studies. Figures 1 and 2 show the calcium total cross sections which we obtained at this facility. The burst width was 5 nsec, and the overall resolution ranges from 30 eV at 50 keV to 1 keV at 1050 keV. The cross sections show broad s -wave resonances and much narrower p -, d -, and f -wave peaks. The s -wave resonances show clear interference, and some of the narrow resonances have sufficient width to give a "signature" of potential-resonant interference. For these narrow resonances we have deduced the potential phase shift, as well as the resonant width and J value, by least-squares-fitting a single-level formula convoluted with a Gaussian resolution function.

Figure 3 shows preliminary phases for $J = \frac{1}{2}$ to $\frac{7}{2}$, not including s waves. The curves are for scattering from an energy-dependent Saxon-Woods real well with a spin-orbit term with parameters consistent with the

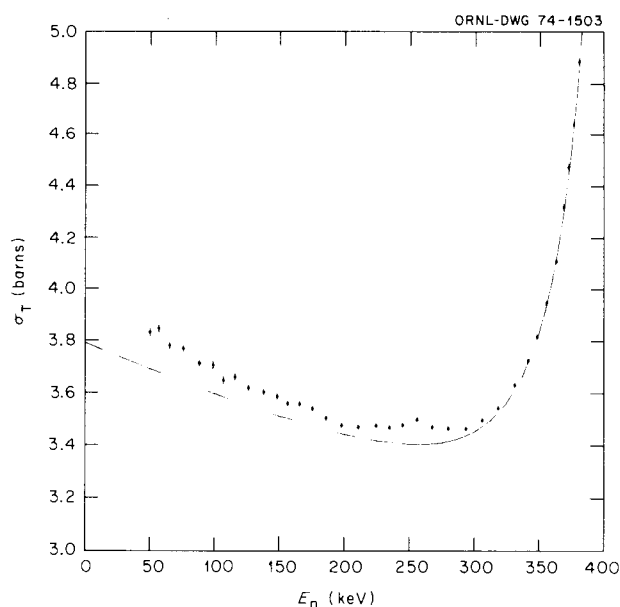


Fig. 2. Expanded view of $^{16}\text{O}(n,n)$ total cross section, showing 257-keV resonance of lithium contaminant and unexplained discrepancy below 200 keV.

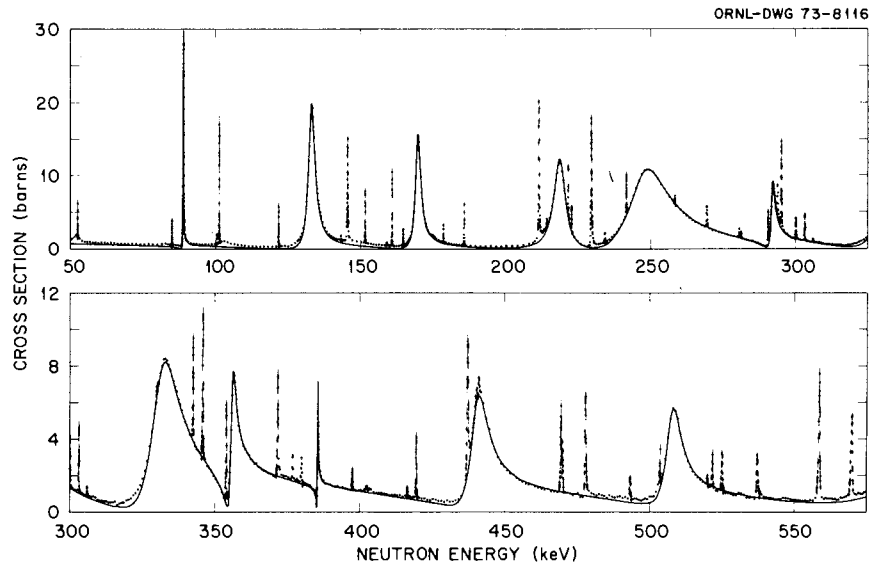


Fig. 1. Total neutron cross section of calcium. The curve is a visual *R*-function fit to *s* waves only.

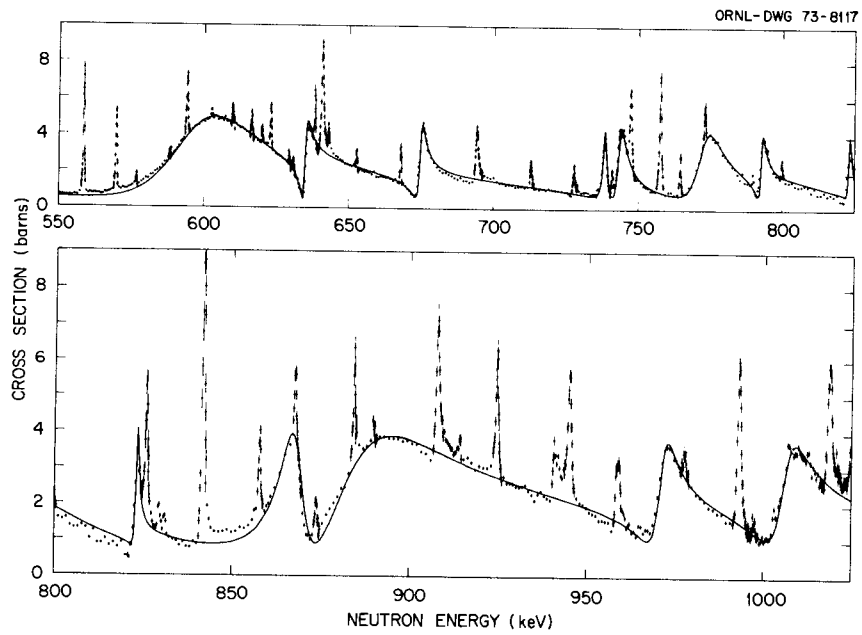


Fig. 2. Total neutron cross section of calcium.

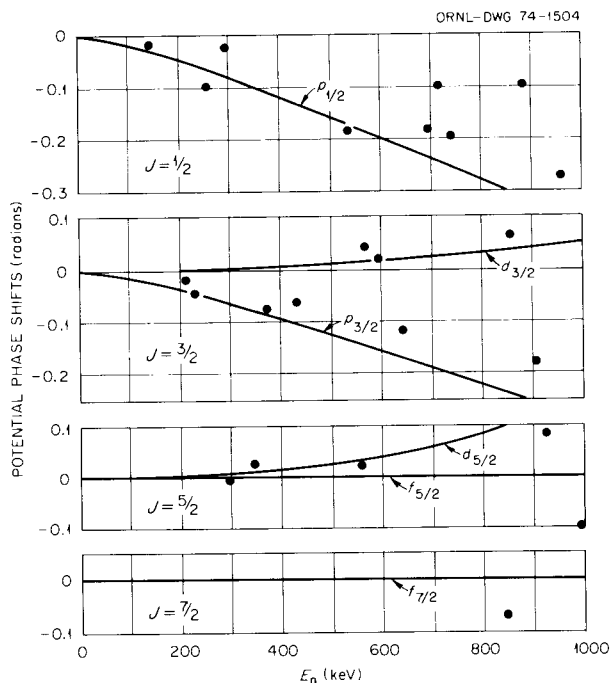


Fig. 3. Potential phase shifts near narrow neutron resonances in calcium. The curves are phases for scattering from a real well.

energies of known bound states and with nucleon scattering at much higher energies. Each potential phase is expected to be continuous with energy. Thus, we expect to identify the partial wave for each resonance simply by the continuity of the potential phase shifts. (There will be fluctuations due to multilevel interference.) For example, we assign $p_{3/2}$ to all resonances with negative phase with $J = 3/2$, and $d_{3/2}$ to all with positive phase. Beyond the assignment of l values, we hope to determine the magnitude of the potential phase and to make appropriate adjustments in the model potential. But that will require a careful analysis, possibly including multilevel effects.

(The two negative points for $J = 5/2$ and $7/2$ are anomalies because the centrifugal barrier rules out such large values for f waves. We tentatively assume these peaks are not single levels.)

The negative s -wave potential phase required for the multilevel R -function curve in Fig. 1 is much smaller than predicted by the model for the curves in Fig. 3. But we do not expect the calculated s -wave phases to be right because absorptive spreading of the $3s$ state has been ignored. We plan to include such effects in the analysis.

1. On assignment 1973–1974 to AERE, Harwell, England.
2. C. H. Johnson, *Phys. Rev. C* **7**, 561 (1973).
3. H. S. Camarda, *Phys. Rev. C* **9**, 28 (1974).

NEUTRON TOTAL CROSS SECTIONS IN THE keV ENERGY RANGE

W. M. Good J. A. Harvey N. W. Hill¹

Neutron total cross sections can be measured with high resolution, and the resonances observed can be analyzed to give the neutron widths and often the spins and parities of the corresponding energy states. The resonant spacing and width distributions and the s -wave strength functions have been determined for heavy nuclides, and the results are in agreement with the statistical model of the nucleus. However, for medium-weight nuclides below mass 90, deviations from the statistical model occur which are associated with the doorway-state concept.

ORELA, with its associated data acquisition and analysis system, is the best of a generation of instruments that possess energy resolutions which are an order of magnitude or more better than was available when many of the last experiments were made, especially for those mass nuclides for which level spacings are of the order of 1 keV (roughly below mass 90 and a few heavy nuclides). We have reported total cross-section measurements to be in progress on the isotopes of Si, S, K, Ca, Ti, Fe, and Pb up to about 300 keV. Measurements are made with at least two sample thicknesses and with a ^6Li detector below about 50 keV and a NE-110 detector above about 20 keV. Some of the data have been analyzed using single-level analysis, but for some cases a multilevel analysis which includes more than one channel will be needed. We have, however, partially analyzed our results in two special cases: the narrow resonances in $^{57}\text{Fe} + n$ below about 50 keV and the resonances in $^{41}\text{K} + n$ for 55 keV $< E_n < 90$ keV.

The $^{57}\text{Fe} + n$ results also provide information for a study of the resonant radiative capture spectra which is reported elsewhere in this report.² Table 1 supplemented by information from BNL-325 (3d ed.) summarizes the results of this partial analysis. The small resonances had not been seen before in transmission although they had been observed in capture.

Recently resonance parameters have been reported from Columbia Nevis³ from the total cross-section measurements upon normal potassium. The isotopic identity of the resonances was based on transmission

measurements on isotopic compounds ^{39}KCl and ^{41}KCl at ORELA using a ^6Li glass detector. The original data permitted assignment of the resonances in potassium and chlorine up to 100 keV. Figure 1 shows results for ^{41}K which consist of the ^6Li detector data below about 25 keV and of an improved measurement (with the NE-110 detector and shorter neutron bursts) above about 25 keV. Two types of differences are observed between our results and those of Columbia: (1) Resonances in the 93% abundant ^{39}K obscure resonances in ^{41}K in the Columbia data in the energy interval $25 \text{ keV} < E_n < 80 \text{ keV}$. The resonances not observed by Columbia are given together with the results of our analysis in Table 2.⁴ (2) Our data indicate that three levels in ^{41}K previously listed as single by Columbia are probably double, namely, 38.48 and 38.67, 74.93 and 75.51, 79.40 and 79.87 keV.

There has been considerable interest in the total neutron cross sections of isotopes of zirconium for both fundamental and practical reasons. The reported *s*-wave strength functions have considerable uncertainties because of the doubtful assignment of some sizable resonances and because zirconium is in the region of anomalously small *s*-wave strength functions. Total cross-section measurements have been completed with an energy resolution of 0.1% or better up to about 300 keV and are shown in Fig. 2. Analysis of the data is in progress.

1. Instrumentation and Controls Division.

2. S. Raman, G. G. Slaughter, W. M. Good, J. A. Harvey, J. B. McGrory, and D. Larson, "The $^{57}\text{Fe}(n,\gamma)^{58}\text{Fe}$ Reaction and Shell-Model Calculations of ^{58}Fe Levels," this report.

3. U. N. Singh et al., *Phys. Rev. C*8, 1833 (1973).

4. Figure 1 identifies very narrow levels which are not listed in Table 2. These levels appeared in the more recent higher resolution measurements and have not been analyzed.

Table 1. Parameters of resonances in $^{57}\text{Fe} + n$

E_0 (keV)	J	l	Γ	$g\Gamma_n$ (eV)	$\frac{2g\Gamma_n\Gamma_\gamma}{\Gamma}$ (eV)
1.628			0.5	0.05	0.10
3.973	0	0		50 ^a	1.14 ^b
4.746				0.5	0.10
6.276	1	0		307 ^a	1.32 ^b
7.218				0.05	0.72
7.936				0.18	0.36
12.85				1.3	0.86
13.29				0.70	
13.97	1	0		10	1.4
18.06					
18.23				4.8	1.17
21.05				1.9	
21.29				4.5	2.18
28.62					
29.72	1	0		2435 ^a	4 ^b
35.19					
37.08					
39.36					
41.64	0, 1 ^a	0		675 ^a	
41.96					
47.16					
49.92 ^c	1	0	262	262 ^a	

^aFrom BNL-325, 3d ed.

^b Γ_γ .

^cBNL-325, 3d ed., quotes 45.5 keV.

Table 2. Resonances in $^{41}\text{K} + n$ not observed by Columbia

E_0 (keV)	J	l	Γ_n (eV)
28.34			
42.36	2	1	180
58.20	2	1	140
63.22	1	1	63
67.08	1	1	250
70.45	0	1	270

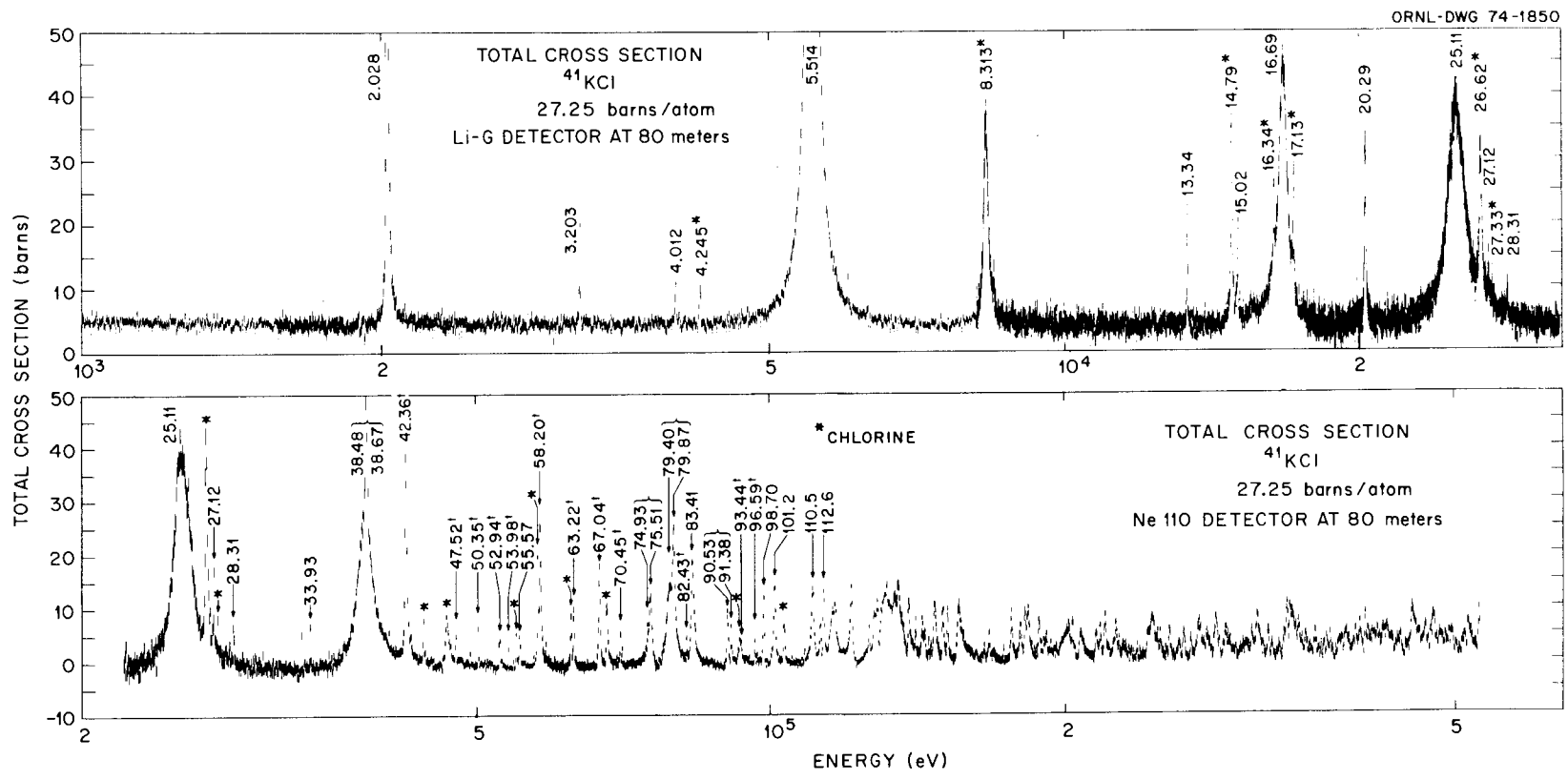


Fig. 1. Neutron total cross section of ^{41}KCl . *, chlorine; †, new resonance. Braces indicate doublets previously reported single.

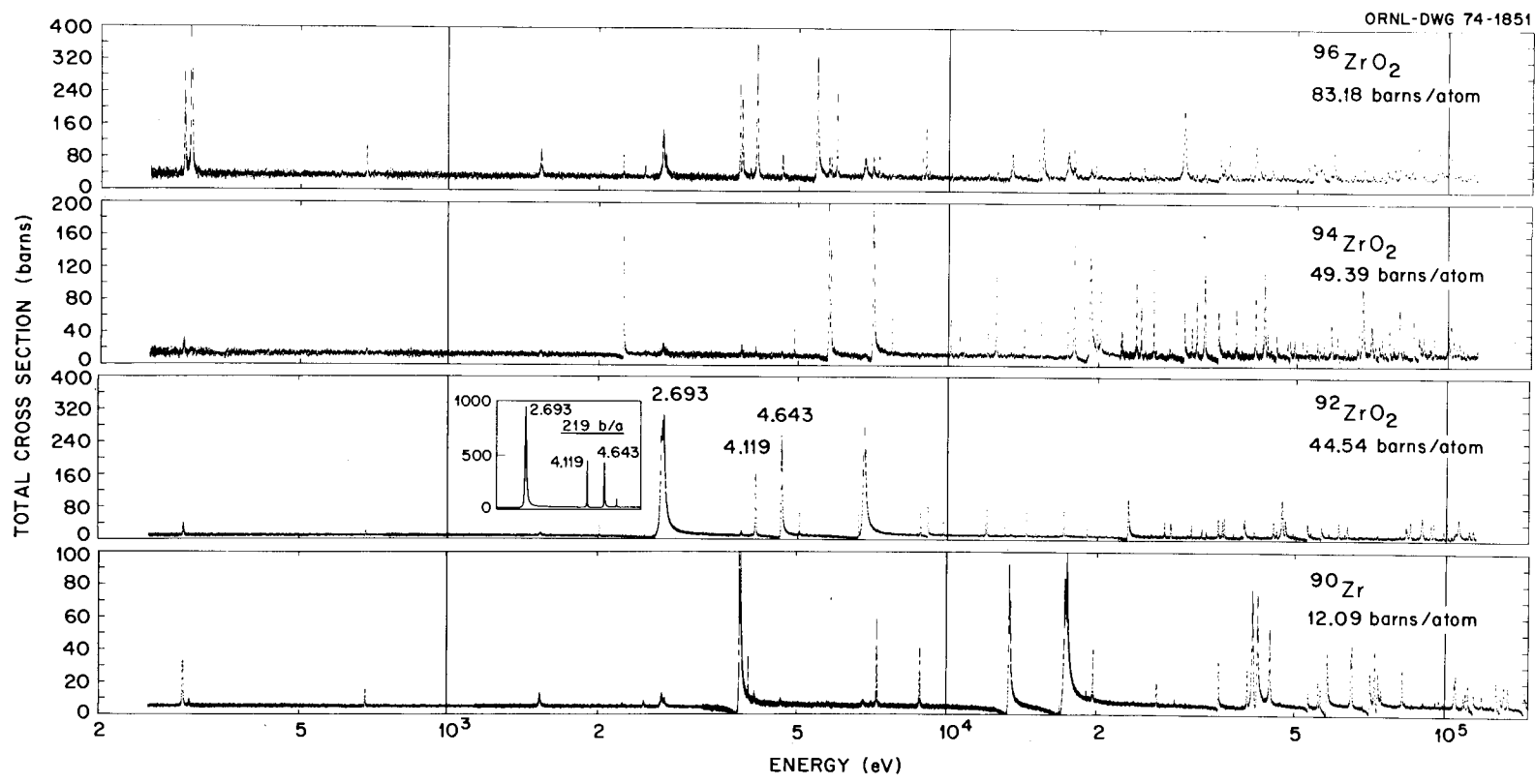


Fig. 2. Neutron total cross sections of $^{90,92,94,96}\text{Zr}$.

STATUS REPORT ON THE OAK RIDGE ELECTRON LINEAR ACCELERATOR (ORELA)

J. A. Harvey T. A. Lewis²
F. C. Maienschein¹ H. A. Todd²
 J. G. Craven³

Accelerator operation and development. During the past year, ORELA was operated for experimenters for 4548 hr. However, since an average of four or five experimenters take data when the accelerator is operating, this represents about 20,000 experimenter hours. The slight decrease in accelerator hours for experimenters from the previous year was a result of the decrease in operating funds and a deliberate decision to schedule a reasonable amount of time for accelerator engineers for accelerator development and improvement. Also, in order to reduce the consumption of spare parts and reduce the operating costs of the accelerator, an upper limit of 40 kW on target was imposed.

There were three major unscheduled shutdowns during the year, and during these periods, many modifications and changes were made in addition to remedying the cause of the shutdown. On November 27, 1973, the accelerator and modulator rooms and underground experimental areas were flooded to a depth of 27 in. due to unprecedented heavy rains. Damage was obviously more extensive than was caused by the 9-in. flood in December 1972, and the accelerator was down for nearly four weeks. In January 1973 a hole was burned in the beryllium-clad water-cooled target while operating at 55 kW after 5300 hr total operating time, and the accelerator was down 22 days.

In February 1973 the main chilled-water feed lines were fractured due to construction of a new flight station, and the accelerator was down 23 days.

Klystrons have continued to operate exceedingly well, as indicated by Table 1. One of the original klystrons has operated nearly 24,000 hr. Not one klystron has failed during the year.

The original electron guns, by contrast, have generally given rather short service. Therefore, the Isotope Development Group (headed by J. Tracy and R. L. Johnson) has developed, over a period of time, an improved electron gun. The first ORNL gun installed on the accelerator performed exceedingly well. It produced peak currents of over 20 A on the target and lasted over 3900 hr. This gun was removed from the accelerator because a vacuum failure in the accelerator poisoned the cathode, rather than any fault of the gun. It is hoped that a newly designed electron gun with greatly increased pumping speed will permit the use of higher gun accelerating voltages (up to 160 kV), and peak currents greater than 25 A on target are expected.

The development and testing of improved electron guns were made possible by the use of the old gun tank as an injection-system test stand. This test stand not only allows for the investigation of techniques for pulse bunching but permits conditioning and testing new electron guns. This operation previously required several days of accelerator time for the installation of each new gun.

A number of equipment changes were made during the year in order to upgrade the performance of the linac and remove demonstrated weak links. For example, the neutron monitor, which was originally

Table 1. Klystron lifetimes at ORELA, 1973

Klystron No.	High-voltage hours	Date
2002	1,447	Original—Nov. 3, 1969 ^a
2003	23,800.4	Original—Dec. 31, 1973 ^b
2004R1	12,896.8	Sept. 1971—Dec. 31, 1973 ^b
2006R1	120.9	Dec. 17, 1973—Dec. 31, 1973 ^b
2007	7,850.0	Dec. 1969—Apr. 27, 1971 ^a
2009	3,106.3	Sept. 30, 1970—Apr. 27, 1971 ^a
2010	5,726.9	Apr. 27, 1971—Apr. 25, 1972 ^a
2011	2,327.4	Apr. 27, 1971—Sept. 1, 1971 ^a
2012	9,418.8	Apr. 25, 1972—Dec. 17, 1973 ^a
2014	1,323.3	Sept. 1, 1973—Dec. 31, 1973 ^b

^aSpare.

^bStill in accelerator.

assembled from available components, has been replaced. The new system, which was designed for the purpose, incorporates dual channels based upon detection of neutrons by ^{235}U fission chambers. These chambers can be calibrated accurately, and they are intended to have sufficient flexibility to provide an accurately reproducible indication of the neutron level both to the experimenters and to the accelerator operators. Filters were added to the ORELA chilled-water system to prevent the deposition in the heat exchanger of precipitated phosphates, which were used as additives in the antifreeze solution used in the system.

Data handling system. The phase I data acquisition system which is used for acquiring data at ORELA was brought to its full complement during the past year. This system is based on the use of small computers with a fast cycle time (about 750 nsec), each equipped with a large (0.4 to 1×10^6 words) disk storage for experimental data. A third SEL 810B computer was accepted from the manufacturer in August 1973 and is in limited operation. Each of the computers can be shared by from one to four experimenters; thus the number of simultaneous experiments at ORELA is no longer limited by the availability of data acquisition equipment.

Development of software continues for the phase II data analysis system, which consists basically of a PDP-10 computer with large mass store and a series of interactive displays and Teletypes. Three of the four interactive displays are located at ORELA for use by the experimenters there. Very widespread use of the system for time sharing is made throughout ORNL, and only about 20% of this use occurs at ORELA. In general, the PDP-10 performs only minor computations in addition to serving the interactive displays, but it provides direct block transfer for substantial computations to the IBM-360-75 and -91 computers at ORNL.

Increasingly significant use of the data analysis system has been made by experimenters during the past year, although the development of specialized software for specific experiments will continue indefinitely. The goal for experimenters is to provide a short-turnaround capability for the various steps in the analysis of experimental data. The analysis of most experimental data usually requires interaction with the experimenter at several stages during the analysis. Most of the data from ORELA reported in this report have been analyzed using this system.

-
1. Neutron Physics Division.
 2. Instrumentation and Controls Division.
 3. Computer Sciences Division.

4. Theoretical Physics

INTRODUCTION

G. R. Satchler

The theoretical physics program serves two functions. One is to provide broad theoretical support and stimulus for the experimental programs. This ranges from providing computer codes and assistance in their use, for the comparison of experimental results with the predictions of various nuclear models, to active cooperation and the suggestion of new experiments of significance. The other function (not unrelated!) is to do basic research, primarily into nuclear structure and nuclear reactions, although some work is done in other areas such as astrophysics, condensed matter, and atomic and molecular physics. Important parts of the latter are T. A. Welton's efforts related to the electron microscope project, both with respect to design theory and the information processing of the micrographs.

The type of research pursued is influenced somewhat by the extensive computing facilities available at ORNL. Elaborate computer programs have been developed or adapted by the theory group to explore intensively and in detail the consequences of models of nuclear structure and reactions, as well as to extend basic studies of the Brueckner type. The existence of these facilities has also helped to alleviate somewhat the manpower shortage by encouraging participation by people from other national laboratories and universities, both in this country and elsewhere. These include consultants and guest visitors. In this way, the group, small though it is, has managed to maintain active contact with most areas of current interest in nuclear physics.

The nuclear physics research may be categorized as:

1. Brueckner-Hartree-Fock studies of basic nuclear structure (primarily R. L. Becker and K. T. R. Davies), which in a sense provide underpinning for
2. shell-model calculations (orchestrated by Edith C. Halbert and J. B. McGrory) of the properties of low-lying nuclear states in terms of a few valence nucleons;
3. investigations of more collective properties, such as nuclear fission, heavy-ion collisions, exotic nuclear configurations, etc. (mainly by R. Y. Cusson,¹ D. Kolb,² T. A. Welton, and C. Y. Wong), and
4. direct nuclear reaction studies (principally by G. R. Satchler), both to understand the reaction mechanism and as a tool for extracting nuclear structure information from experimental data.

None of these categories is independent, as to either physics or personnel. For example, category 1 is closely related to category 2 in providing the effective interactions to be used in shell-model calculations, and Davies, currently on assignment at the Los Alamos Scientific Laboratory, is preparing to work on the microscopic understanding of collective motions.

The past year has seen more attention paid to the physics of heavy-ion collisions. Various computer codes were adapted to handle heavy-ion scattering and reactions, and a detailed analysis was made of the data from ORIC on single-nucleon transfer reactions between ^{11}B and ^{208}Pb . Work was begun on the structure aspects of two-nucleon and alpha-particle transfers. Initial studies were made of shock-wave effects in high-energy encounters.

No new results were obtained on the theory of the recently discovered giant resonances, but the first steps were taken in a program to study various microscopic models of these excitations and their effects on inelastic proton scattering.

The work on nuclei with exotic shapes (bubbles and toroids) was carried over to the other extreme of physical dimensions and applied to stellar and galactic objects. The experience gained there promises to be of value in the original application to heavy nuclei. The original suggestion of nuclei as incipient bubbles received some support from a number of Hartree-Fock calculations.

More detailed reports on current work follow this introduction, and references to completed work are listed in the back of this report.

¹Consultant from Duke University, Durham, N. C.

²Guest assignee to ORNL during summer 1973 from Duke University, Durham, N.C. Present address: Yale University, New Haven, Conn.

DEVELOPMENTS IN MANY-BODY THEORY OF NUCLEI

Richard L. Becker Franz Mohling³
R. W. Jones¹ L. W. Owen²
N. M. Larson² M. R. Patterson²
R. J. Philpott⁴

a. Introduction: Current Emphasis on Improving the Self-Consistent Field

Richard L. Becker

Prime goals of the fundamental many-body approach to nuclear phenomena, employing realistic nuclear forces, are to show how the phenomenological nuclear models can arise as approximate descriptions, to derive values of the basic parameters of the models, and to provide refined theories going beyond the models. The decisive step, which allowed a realistic many-body theory to develop, was Keith Brueckner's demonstration that a many-body perturbation theory could be obtained by eliminating the nearly singular nucleon-nucleon interaction in favor of a renormalized or "effective" interaction, Brueckner's reaction matrix. The lowest order terms of the perturbation expansion yield the Brueckner-Hartree-Fock self-consistent-field approximation, which already provides a derivation of the shell model: the field is the shell-model single-particle (s.p.) potential, the eigenfunctions of the s.p. Hamiltonian are the shell-model orbitals, and the reaction matrix is the shell-model "residual" interaction.

In going beyond the Brueckner approximation, one is faced with a perturbation series for any quantity to be calculated. We have argued⁵ that, whenever possible, it would be desirable to include higher order effects by changing the self-consistency conditions of the field. Not all correlation effects can be included in this way, but many can be, namely, "factorizable self-energy" processes. This point of view places great merit in achieving a realistic self-consistent field. Improvements in the field would be valuable in giving better predictions of nuclear properties in several ways: (1) different fields may lead to different orderings of levels, hence different ground-state configurations (particularly for deformed nuclei, for which s.p. levels cross as a function of deformation); (2) in shell-model matrix diagonalizations, s.p. energies of the active orbits are required, and self-consistency of the orbitals is assumed; (3) the s.p. radial wave functions determine the values of the first approximation to matrix elements of all s.p. operators (moments, electromagnetic and beta decay rates, and form factors for direct reactions); (4) the energies and wave functions of normally empty s.p. states have a strong influence on the effective interaction. We want a field sufficiently accurate to predict s.p. properties not only of existing nuclei but also of so-far unobserved ones, such as those out of the valley of stability and superheavy ones.

A desirable feature of Hartree-Fock theory, widely exploited in atomic and molecular theory, is the property known as Koopmans' theorem, that the s.p. energies are very nearly equal to the separation energies

of the shells. The Brueckner-Hartree-Fock approximation does not have this property: there are very large “rearrangement energy” differences between the s.p. and separation energies. Over the past few years we have concentrated on overcoming this problem by exploiting a second renormalization of the theory, namely, a modification of the propagator of nucleons as they travel through the nucleus. This involves taking into account the fact that when two nucleons interact, they are temporarily knocked out of the normally occupied shell-model states. Consequently, the interaction with a given shell is weighted by the “true” fractional occupation probability of the shell. While these considerations are concerned with correlations, they have their most striking effect in a weakening of the self-consistent s.p. potential. In the propagator-renormalized Brueckner-Hartree-Fock (RBHF) approximation⁵ the s.p. energies are equal to mean separation energies (a generalization of Koopmans’ theorem).⁶ This fact makes RBHF a considerable improvement over the BHF approximation.

We have hoped that the RBHF approximation would play a role in nuclear theory similar to that of the Hartree-Fock approximation in atomic theory. Unfortunately, the RBHF approximation has not succeeded in overcoming another difficulty of the BHF approximation, the “saturation problem.”

The *saturation problem* is the fact that with the best available nuclear forces it has not been possible to obtain both the binding energy and the radius of nuclei to sufficient accuracy. Alterations which improve the binding energy worsen the radius, and conversely. In infinite nuclear matter, calculations with the Reid soft-core interaction which give the semiempirical value (about 16 MeV) of the binding per nucleon yield a saturation density about 25% too large, which corresponds to a nuclear radius about 8% too small.⁷ Similar results from some RBHF calculations made at ORNL are shown in Table 1.

There are two ways in which the saturation problem might be overcome. One is to alter the assumed nucleon-nucleon interaction without upsetting the agreement with two-body data. Such attempts have been unsuccessful up till now. The other is to argue that our present level of many-body theory is inadequate. Numerous authors have investigated correlation corrections to the theoretical nuclear radius, and have found them to contribute only 1 or 2%. We believe that the most likely solution of the saturation problem would be to refine once again the definition of the self-consistent field.

In searching for guides to the needed improvements we have tried a variety of things, which are reported

Table 1. Saturation properties obtained in RBHF calculations

Ratios of calculated to experimental binding energy per nucleon and rms radius of the proton distribution are cited

Nucleus	BE /A	R_p	Reference
¹⁶ O	99%	92.5%	a
	66%	97.5%	b
⁴⁰ Ca	125	81.5	b
	58	90.0	b
²⁰⁸ Pb	124	76.8	b
	32	88.4	b

^aR. L. Becker, K. T. R. Davies, and M. R. Patterson, *Phys. Rev. C* (March 1974, to be published).

^bK. T. R. Davies and R. J. McCarthy, *Phys. Rev. C*, 4, 81 (1971).

below in Sects. b–e. First the adequacy of the RBHF theory was tested in a new way by calculating the real part of the optical potential. The capability of calculating optical potentials from reaction matrix elements is of intrinsic interest for understanding nucleon scattering from nuclei. Next, the controversial question of the first-order potential for normally excited s.p. states was investigated formally in a Green’s function formulation. A modified RBHF approximation containing this potential was developed. Second-order terms were investigated in two ways: diagonal second-order and also third-order terms (“rearrangement” energies) were calculated, and comparisons with experimental quasi-particle energies were made; and finally, off-diagonal particle-hole second-order terms were calculated. Definite progress in improving the saturation properties has been achieved by incorporating second-order terms into the field.

b. Calculation of the Real Part of the $n + {}^{16}\text{O}$ Optical Potential in the Renormalized Brueckner-Hartree-Fock Approximation

Richard L. Becker R. J. Philpott⁴
L. W. Owen²

In order to extend the scope of Brueckner theory from stable bound states to unstable states and nuclear reactions, we have initiated microscopic calculations of the optical potential, the self-consistent field for nucleons in the continuum. Because our RBHF calculations are carried out by matrix diagonalization in a harmonic oscillator basis, all RBHF s.p. states are bound states, even those of high energy. This is appropriate for calculating stable nuclear states but not for nucleon

emission or scattering. We have achieved the needed coupling to the nuclear exterior by matching interior RBHF wave functions with channel wave functions on a sphere of radius slightly larger than the nuclear radius, as in Wigner's R -matrix theory of nuclear reactions.

A few calculations⁸ of the real part of the optical potential have been made in the Hartree-Fock approximation, employing a nonsingular phenomenological nucleon-nucleon interaction. In the calculation by MacKellar et al.,⁸ employing the Tabakin two-term factorable interaction, a second-order ladder term was also included. We report here the first calculations made using reaction matrices, that is, summing ladders of all orders. The case of neutrons on ^{16}O was treated because of the new ORNL data of Fowler, Johnson, and Feezel⁹ together with its multilevel analysis by Johnson.¹⁰ The Hamada-Johnston nucleon-nucleon interaction was used to generate the reaction matrix elements, which were then used to calculate both the RBHF orbitals of the target¹¹ and the optical potential.

A special interest in generalizing the theory of the optical potential from the Hartree-Fock to the Brueckner-Hartree-Fock approximation is to find out if the opposite energy dependences of the reaction matrix elements and the empirical optical-model potential can be reconciled. The individual matrix elements in the oscillator basis become more negative as the projectile energy is increased, whereas the empirical Woods-Saxon potential becomes shallower. The calculated phase shifts are in fairly good agreement with experiment (see Fig. 1). The explanation is that, as the projectile energy is increased, the projectile wave function has decreasing overlaps with the low-lying oscillator orbitals and increasing overlaps with the higher oscillator states. The higher oscillator states have less negative (or positive) matrix elements.

We have calculated the neutron $s_{1/2}$, $d_{5/2}$, and $d_{3/2}$ optical-model phase shifts for neutron energies in the c.m. system from zero to 16 MeV. The simplest to discuss is the s -wave phase shift shown in Fig. 1. The triangles are the "experimental" nonresonant phase shifts obtained by Cleland Johnson¹⁰ by an R -matrix analysis of the ORNL data.⁹ The four dots are phase shifts calculated in the Hartree-Fock approximation by Vautherin and Veneroni⁸ with the phenomenological effective interaction $B1$ of Brink and Boeker. Our three theoretical curves are describable as follows: the solid one is for the unrenormalized BHF potential calculated with the Hamada-Johnston interaction; the dashed-dotted curve is the corresponding RBHF calculation; and the dashed curve is for an RBHF calculation with the Reid soft-core interaction. The rate of decrease

of the s -wave phase shift is strongly correlated with the s.p. energy of the $1s_{1/2}$ bound state. This calculated energy is -5.46 MeV (from the potential giving the solid curve), -1.83 (dashed), -1.46 (dashed-dotted), and -0.14 (from Vautherin's and Veneroni's poten-

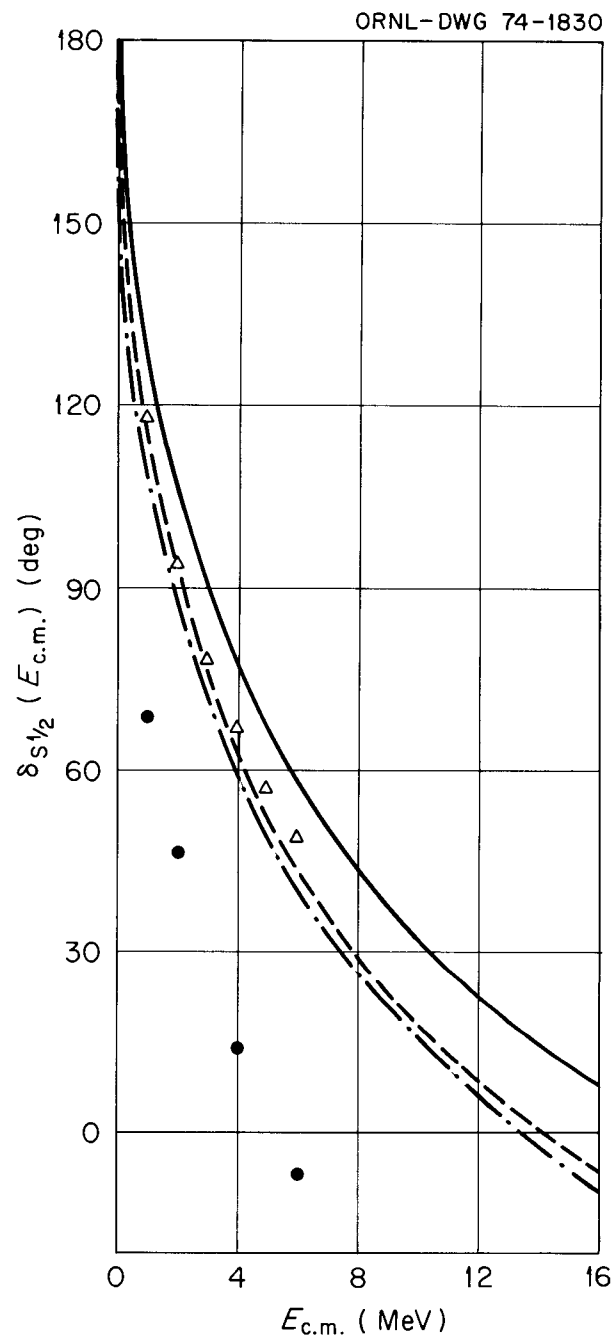


Fig. 1. S -wave nonresonant phase shift for neutrons on ^{16}O from 0 to 16 MeV in the c.m. system. The curves and points are as described in the text.

tial⁸). The experimental separation energy is -3.27 MeV.

It is planned to continue this work in various directions. A very interesting possibility, involving a major effort, would be to try to reproduce the compound nuclear resonances (not shown in the figure) by including two-particle-one-hole “doorway” states in the calculations.

c. A Renormalized Brueckner-Hartree-Fock Approximation Containing the Quasi-Particle Separation-Energy Field

Richard L. Becker R. W. Jones¹
Franz Mohling³

In recent years the most satisfactory version of Brueckner theory from the formal point of view has been the generalized-time-ordered (g.t.o.) series of Brandow. In this formalism the Brueckner-Hartree-Fock (BHF) self-energy for normally empty (“particle”) states does not factorize, and for this reason it is not included in the single-particle (s.p.) potential, U . This feature of the theory leads to differences: (1) between s.p. energies and the separation energies of quasi-particle states and (2) between U and the real part of the optical potential. Employing the formalism of energy-dependent s.p. Green functions, $G(\omega)$, we have achieved more extensive factorization, with the consequence that U can be defined to include the on-energy-shell BHF potential for particles.^{1,2}

The simplest stationary truncation of the expansion is a renormalized BHF approximation similar to that for Brandow’s expansion⁵ but differing from it by containing (1) the RBHF potential for “particle” states, which implies a smaller energy gap and greater diffuseness at the Fermi surface, and (2) propagator renormalization factors which contain s.p. density matrices plus “folded” terms. This formulation allows a close connection between “virtual” and “valence” s.p. states, while staying close to the computationally successful framework of the older formulations of Brueckner theory and avoiding complex energies.

In the present RBHF approximation the total nuclear binding energy is

$$E = \sum_k v_k \langle k|T|k \rangle + \frac{1}{2} \sum_{jk'k'} \langle jk|t_A(e_{jk})|j'k' \rangle \times \left[v_j v_k \delta_{jj'} \delta_{kk'} - P^{(2)}_{j'j} P^{(2)}_{k'k} \right],$$

where v_k is the shell-model occupation probability of s.p. state k (equal to 1 for normally occupied and 0 for

normally empty states), t_A is an antisymmetrized Brueckner reaction matrix for which the “starting energy” e_{jk} is the sum of the s.p. energies $e_j + e_k$, and $P^{(2)}$ is the second-order contribution to the line-weighting factor,

$$P^{(2)}_{k'k} = \frac{1}{2} \left[P^{\dagger(2)}_{k'k} + P^{(2)}_{kk'} \right],$$

with

$$P^{\dagger(2)}_{k'k} = -\frac{1}{2} v_{k'} v_k \sum_{lmn} v_l (1 - v_m) (1 - v_n) \times \frac{\langle k'l|t_A(e_{k'l})|mn \rangle \langle mn|t_A(e_{kl})|kl \rangle}{(e_{kl} - e_{mn})(e_{k'l} - e_{mn})} + (1 - v_{k'}) v_k \sum_l v_l \times \frac{\langle k'l|t_A(e_{kl}) - \text{Re}[t_A(e_{k'l})]|kl \rangle}{e_k - e_{k'}}.$$

The s.p. potential is

$$\langle k|U|k' \rangle = \frac{1}{2} [\langle k|U^{\dagger}|k' \rangle + \langle k'|U^{\dagger}|k \rangle],$$

with

$$\langle k|U^{\dagger}|k' \rangle = \sum_{l'l'} \langle kl|t_A(e_{kl})|k'l' \rangle \left[v_l \delta_{l'l'} + P^{\dagger(2)}_{l'l'} \right].$$

It is planned to make numerical calculations with this theory in the hope that certain failures of the g.t.o.-RBHF approximation cited in Sect. a may be overcome.

d. Rearrangement Energies in Brueckner Theory

Richard L. Becker M. R. Patterson²

RBHF approximations contain only the terms in the renormalized Brueckner expansion which are of first order in the effective interaction. Higher order terms do contribute, in principle, to the definition of the self-consistent field in modern formulations (see ref. 12) of Brueckner theory. Because the higher order terms are more difficult to calculate than those of first order, a useful first step is to calculate such a term as a perturbation. Perturbative corrections to single-particle energies are referred to as rearrangement energies.

Whereas the RBHF single-particle energies correspond to mean separation energies, the sum of single-particle and rearrangement energies gives the theoretical energy of a particular eigenstate of a nucleus, $A \pm 1$, with one

valence “particle” or hole relative to the core. This eigenstate is the one describable as an elementary excitation or quasi-particle state.¹² Mean removal and addition energies are not so well known experimentally as are separation energies for specific states. Thus, the comparison of theoretical quasi-particle separation energies with experimental “eigen-separation energies” offers a good test of the theory.

We have computed renormalized second- and third-order rearrangement energies (the diagrams for which are given in ref. 11) for several nuclei. The results for ¹⁵N and ¹⁷F are shown in Table 2. One sees generally good agreement for the holes, but a deficit of binding for *s-d* shell “particles” by about 3 MeV. We believe that this problem is closely related to the “saturation problem” discussed in Sect. a and hope that modifications of the self-consistent field may provide the needed additional binding.

e. New, Second-Order Approximation in Renormalized Brueckner Theory

Richard L. Becker N. M. Larson²

The renormalization of the Brueckner-Hartree-Fock approximation with occupation probabilities lowers the central density and increases the rms radius^{11,13,14} but not enough to give radii in sufficiently good agreement with experiment (see Table 1, Sect. a, and Fig. 2). Because the improvement in radii resulting from renormalization is primarily associated with the particle-hole elements of the s.p. potential,^{11,13} we suspected that the inclusion of second-order terms in the particle-hole matrix elements of the self-consistent potential would result in significant changes in the radii. Preliminary results shown in Fig. 2 show a smoothing and an expansion of the density distribution and a resulting increase in the radius.

The figure contains the “shell-model” proton density calculated from the s.p. orbitals. The center-of-mass

density has not been unfolded. The two curves containing a dip in the density at the origin are for the first-order theory. One sees that the RBHF density has an rms radius (2.41 fm) which is 7½% greater than that of the unrenormalized (BHF) calculation.^{11,13} An “experimental” value of the “shell-model” radius may be defined by

$$R_{SM}^2 = R_{chg}^2 - R_{proton}^2 + R_{cm}^2,$$

where R_{chg} is the experimental charge radius, $R_{proton} = 0.80$ fm is the experimental proton radius, and R_{cm} is the rms of the c.m. distribution calculated from the determinant of s.p. wave functions. For the RBHF determinant, $R_{cm} = 0.48$ fm. Two recent measurements of the charge radius of ¹⁶O, by H. A. Bentz and by I. Sick, lead to $R_{SM}^{exp} = 2.59$ and 2.65, respectively, for

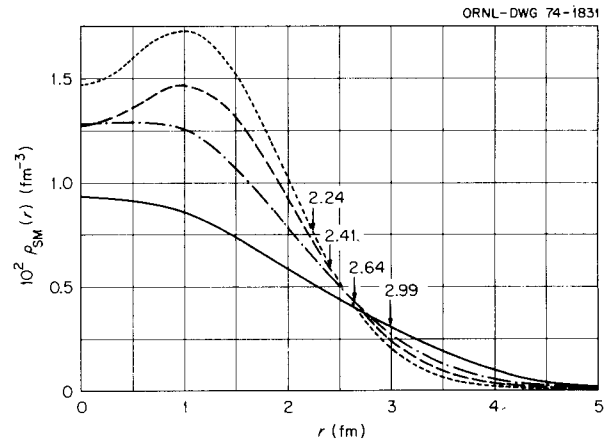


Fig. 2. Plot of the “shell-model” proton density calculated from the single-particle orbitals. The center-of-mass density has not been unfolded. The arrows indicate r.m.s. “shell-model” radii. The curves are distinguished as follows: the dotted curve is for the BHF calculation, the dashed curve gives the RBHF density, the dashed-dotted curve is for BHF + $U_{ph}^{(2)}$, and the solid curve is for the RBHF + $U_{ph}^{(2)}$ calculation.

Table 2. Rearrangement and quasi-particle separation energies of protons in ¹⁷F and proton holes in ¹⁵N

See R. L. Becker, K. T. R. Davies, and M. R. Patterson, *Phys. Rev. C* (March 1974, to be published)

	$0s_{1/2}$	$0p_{3/2}$	$0p_{1/2}$	$0d_{5/2}$	$1s_{1/2}$	$0d_{3/2}$
$E_{rear}^{(2)}$	13.7	2.1	2.4	1.1	1.4	1.9
$E_{rear}^{(3)}$				-1.1	-1.0	-1.0
$E_{q.p.}$ (calc.)	-31.8	-16.5	-12.5	2.5	3.1	7.6
$E_{q.p.}$ (exp.)	-31 ± 3	-18.5	-12.1	-0.6	-0.1	4.5

the RBHF density. One sees that the calculated $R_{SM} = 2.41$ is 7% and 9% smaller than the two "experimental" values, respectively.

The third and fourth curves in the figure were calculated by diagonalizing the Hamiltonian containing the first-order terms plus the particle-hole elements of the second-order potential. The latter was calculated using the s.p. energies and wave functions of the first-order self-consistent calculation (BHF or RBHF). Thus, these preliminary results are not fully self-consistent. The second-order terms are calculated only perturbatively. Consequently, the changes produced by the second-order terms are expected to overshoot those of the fully self-consistent calculations, which are now in progress. The effect of the second-order terms on the density is similar to our expectations: the density is smoother and has a larger radius. For the unrenormalized calculation the radius increased by 17%, and for the renormalized calculation the increase was 24%.

For consistency, and in particular in order to have a stationary truncation (see ref. 12), the new formulation is being completed to include the factorizable second-order particle-particle matrix elements. The diagonal particle-particle matrix elements are just the second-order valence-particle rearrangement energies calculated as perturbations in the preceding section. We are developing also the self-consistent second-order renormalized Brueckner approximation for the expansion containing the quasi-particle field (Sect. c). This contains self-consistently also the hole-state rearrangement energy.

The aim of the rather difficult extension from the first-order (RBHF) to the second-order approximation of renormalized Brueckner theory is to obtain a self-consistent field theory, calculated from first principles, adequate to provide the energies and orbitals needed for shell-model and direct-reaction calculations, and to provide a guide to more phenomenological approaches, such as density-dependent field theory or density-dependent Hartree-Fock, which can be used for a great variety of nuclei including the superheavies.

-
1. University of South Dakota, Vermillion, S.D.
 2. Computer Sciences Division.
 3. University of Colorado, Boulder, Colo.
 4. Florida State University, Tallahassee, Fla.
 5. R. L. Becker, *Phys. Rev. Lett.* **24**, 400 (1970); *Phys. Lett.* **32B**, 263 (1970); *Proceedings, Symposium on the Nuclear Many-Body Problem, Rome, 1972* (to be published).
 6. R. L. Becker and M. R. Patterson, *Nucl. Phys.* **A178**, 88 (1971).
 7. H. A. Bethe, *Ann. Rev. Nucl. Sci.* **21**, 93 (1971).

8. D. Vautherin and M. Veneroni, *Phys. Lett.* **25B**, 175 (1967) and **26B**, 552 (1968); A. D. MacKellar, J. F. Reading, and A. K. Kerman, *Phys. Rev.* **C3**, 460 (1971).

9. J. L. Fowler, C. H. Johnson, and R. M. Feezel, *Phys. Rev.* **C8**, 545 (1973).

10. C. H. Johnson, *Phys. Rev.* **C7**, 561 (1973).

11. R. L. Becker, K. T. R. Davies, and M. R. Patterson, *Phys. Rev. C* (March 1974, to be published).

12. R. W. Jones, F. Mohling, and R. L. Becker, *Nucl. Phys.* (March 1974, to be published).

13. R. L. Becker and M. R. Patterson, *Phys. Div. Annu. Progr. Rep. Dec. 31, 1968*, ORNL-4395, pp. 107-15.

14. K. T. R. Davies and R. J. McCarthy, *Phys. Rev. C* **4**, 81(1971).

LARGE UNCERTAINTIES IN NUCLEAR PROTON DENSITIES PERMITTED BY ELASTIC SCATTERING DATA

Richard L. Becker James A. Smith¹

One of the most useful results of nuclear self-consistent field calculations (e.g., those of ref. 2) is a set of single-particle radial wave functions ("orbitals"). Such orbitals can be employed in calculations of electromagnetic moments, beta decay rates, nucleon transfer, the optical potential, and effective interactions for nuclear spectroscopy. Unfortunately, experiments do not exist which could test the radial wave functions very directly. Only some crude experimental information on the momentum distribution in individual shells is available from high-energy knockout reactions [(*p,2p*) and (*e,e'p*)]. However, a weighted sum of the absolute squares of the proton orbitals is the proton density in the approximation of the independent-particle model. Accurate information has been obtained on the form factor of the total proton density from elastic electron scattering, supplemented by muonic x-ray data. Given the orbitals, one can calculate the absolute square of the form factor and compare it with the corresponding experimental function. We have attempted to test in this way the quality of the proton densities given by self-consistent *renormalized Brueckner-Hartree-Fock* (RBHF) calculations.² Unfortunately it was found difficult to use comparisons of squared form factors as a guide to possible improvements in the theory. It would be advantageous to be able to "invert the data" and make a comparison of theoretical and experimental densities. Somewhat to our surprise, this program has been impeded by our discovery that the proton densities inferred from the existing data are subject to very great uncertainties, particularly near the center of the nucleus. This is demonstrated below for the alpha particle. Only certain low moments, such as the rms radius, are accurately determined. Consequently, we

must settle for the comparison of theoretical and experimental squared form factors as the best available test of proton densities.

The large uncertainties in proton densities stem from two sources: (1) the uncertainties in charge densities arising from the upper limit on the momentum transfers obtained by elastic electron scattering and (2) the magnification of uncertainties in going from the charge density to the proton density, which occurs because the proton density is more rapidly varying than the charge density, the latter being the convolution of the proton density with the density of charge within a proton.

The method we propose in order to exhibit the uncertainties in proton densities may be described as follows: First, obtain an analytical charge form factor, $f_{\text{chg}}^{(0)}(q)$, which fits the data, provides a standard extrapolation to all momentum transfers beyond those of the data, and corresponds to a rather conventional charge density, $\rho_{\text{chg}}^{(0)}$; do this both for the nucleus

under investigation and for a single proton. Second, divide the charge form factor by the form factor of a single proton to obtain an analytical "body" form factor, and invert it to obtain a proton (or "body") density in the nucleus. Third, vary the charge form factor, essentially only for values of momentum transfer greater than those reached by the data, by adding $\pm \Delta f_{\text{chg}}(q)$, $q \gtrsim q_{\text{max}}$; calculate the corresponding $f_{\text{body}}^{(0)} \pm \Delta f_{\text{body}}$, $\rho_{\text{chg}}^{(0)} \pm \Delta \rho_{\text{chg}}$, and $\rho_{\text{body}}^{(0)} \pm \Delta \rho_{\text{body}}$.

In the figures are shown the results of this procedure for ${}^4\text{He}$, for which data exist out to $q_{\text{max}}^2 \approx 20 \text{ fm}^{-2}$, which is greater than for most other nuclei. Figure 1 contains the data of Frosch et al.,³ the analytical $f_{\text{chg}}^{(0)}(q)$ obtained by them, and the body form factor obtained from it by dividing out Wilson's double-pole form factor for a proton. The corresponding charge and proton densities are given in Fig. 2. Figure 3 shows modified charge form factors compatible with the data. The corresponding charge densities appear in Fig. 4, and the body densities in Fig. 5. One sees that a 5% change in the charge density at the origin results in a 100% change in proton density there. This magnification makes possible a very sensitive test of theoretical proton densities, but it will require data to considerably higher momentum transfers than presently available.

Further investigations of uncertainties in charge and proton densities are in progress. It should be mentioned that a fundamental question, affecting all comparisons between experimental and theoretical densities, deserves attention, namely, whether or not the charge density of a single proton is appreciably modified when the proton enters a nucleus.

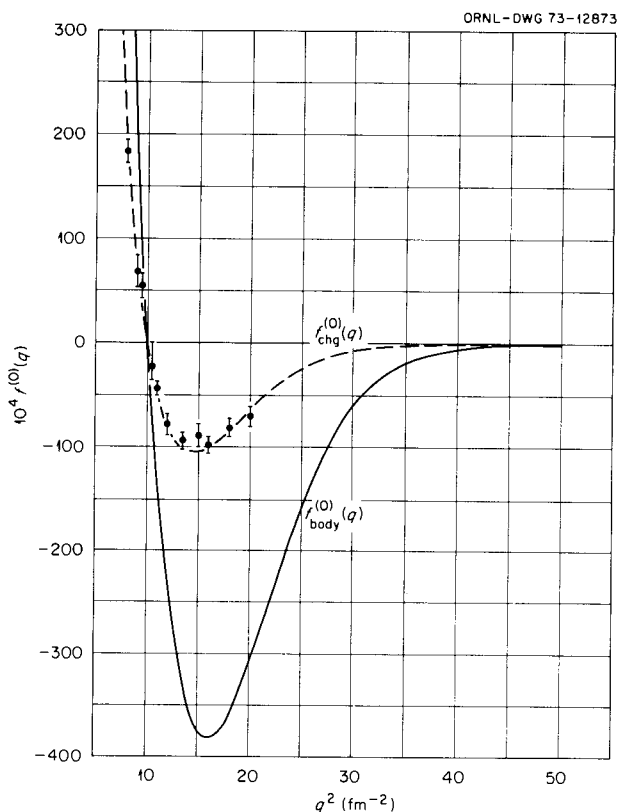


Fig. 1. Analytical charge form factor, $f_{\text{chg}}^{(0)}$, of Frosch et al. [*Phys. Rev.* 160, 874 (1967)] (dashed line), which gives a good fit to their measured form factor for elastic electron scattering from ${}^4\text{He}$. Data points represent $\pm |f_{\text{chg}}^{\text{exp}}(q)|$. The analytical body form factor, $f_{\text{body}}^{(0)}(q)$, has been obtained from $f_{\text{chg}}^{(0)}$ by dividing by the charge form factor of the proton.

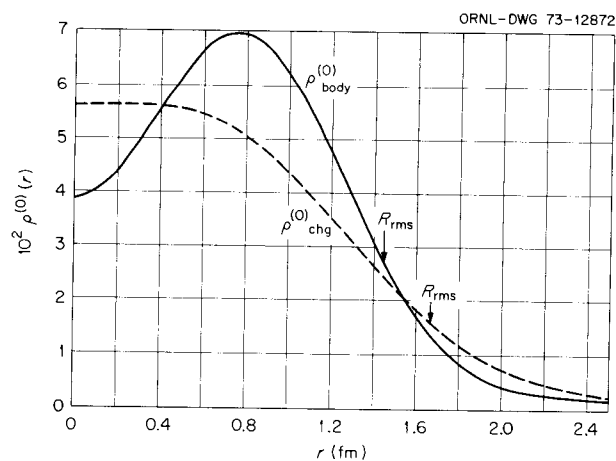


Fig. 2. Analytical charge density (dashed line) and proton density of ${}^4\text{He}$ corresponding to the analytical charge and body form factors of Fig. 1.

1. Undergraduate Research Trainee at ORNL during summer 1973 from New College, Sarasota, Fla. (trainee program administered by Oak Ridge Associated Universities).

2. R. L. Becker, *Phys. Rev. Lett.* 24, 400 (1970); R. L. Becker, K. T. R. Davies, and M. R. Patterson, *Phys. Rev. C* (March 1974); R. L. Becker in *Proceedings Int. Symp. Nucl. Many-Body Problem, Rome, 1972* (in press); K. T. R. Davies and R. J. McCarthy, *Phys. Rev. C* 4, 81 (1971).

3. R. F. Frosch, J. S. McCarthy, R. E. Rand, and M. R. Yearian, *Phys. Rev.* 160, 874 (1967).

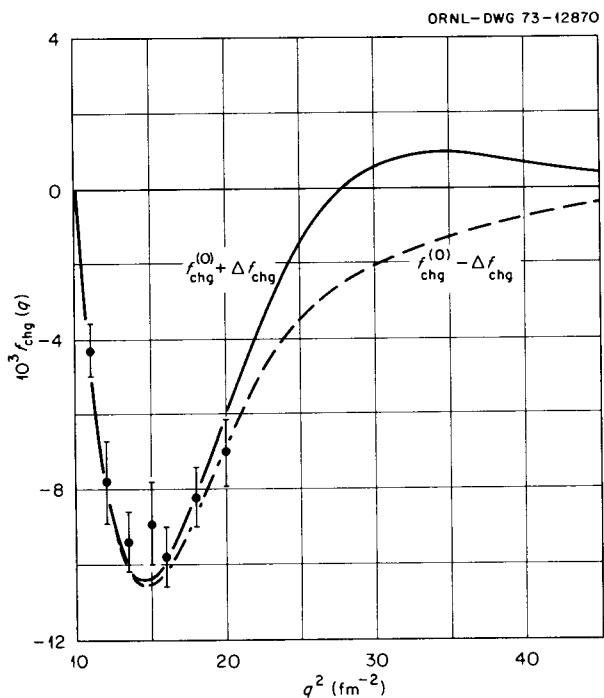


Fig. 3. Modified analytical charge form factors, $f_{\text{chg}}^{(0)}(q) \pm \Delta f_{\text{chg}}(q)$, which differ significantly from $f_{\text{chg}}^{(0)}(q)$ only for momentum transfers q greater than those reached in the experiments of Frosch et al. [*Phys. Rev.* 160, 874 (1967)].

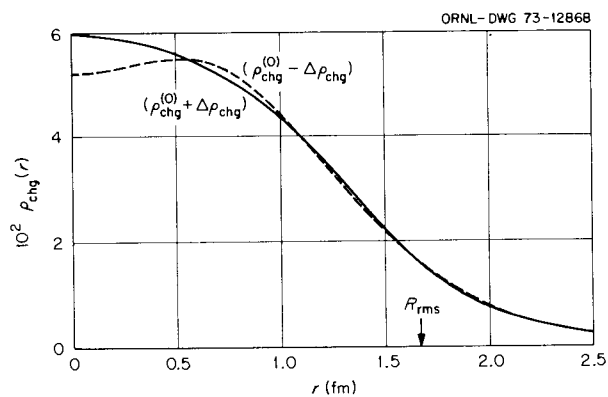


Fig. 4. Analytical charge densities of ^4He corresponding to the charge form factors of Fig. 3, which are compatible with the existing data.

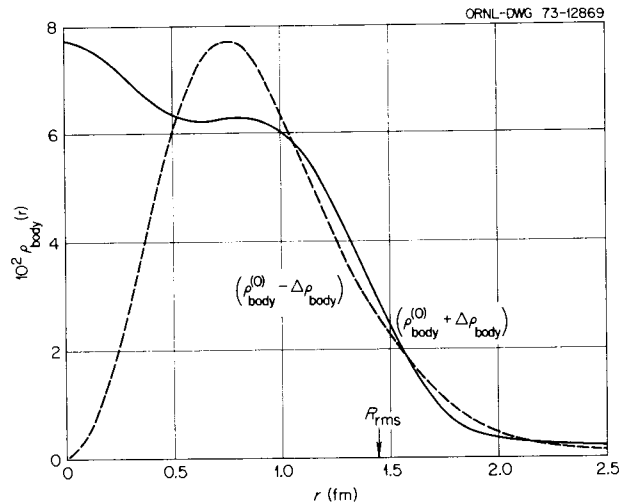


Fig. 5. Analytical proton densities, $\rho_{\text{body}}^{(0)}(r) \pm \Delta \rho_{\text{body}}(r)$, corresponding to the charge form factors, $f_{\text{chg}}^{(0)}(q) \pm \Delta f_{\text{chg}}^{(0)}(q)$, of Fig. 3.

SHOCK WAVES IN HEAVY-ION COLLISIONS

T. A. Welton C. Y. Wong

The acceleration of heavy nuclei to high energies can lead to interesting new frontiers and phenomena unique in nuclear physics. For example, the energy can be so high that the relative velocity of two nuclei after contact is greater than the speed with which a density disturbance in a nucleus transmits itself. The latter speed is the speed of sound in nuclear matter, which we find to be about 10 MeV per nucleon.^{1,2} When the relative velocity after contact exceeds this sound speed, a density perturbation will not have enough time to propagate to the other parts of the nuclei, but density will continue to pile up because of the relative motion. What one then obtains is a shock-wave front characterized by a near discontinuity in density, pressure, and velocity, a phenomenon well known in fluid mechanics and well understood in the collision of two identical stars.³ Of course, the application of this to heavy-ion collisions is useless if the actual thickness of the approximate discontinuity is not small compared with the sizes of the nuclei. A simple rule is that the thickness of any such transition region is approximately equal to the mean free path of a nucleon in nuclear matter, which is roughly 0.7 fm, after due consideration of the Pauli exclusion effect. In ref. 2, we worked out a simple illustrative example for the collision of two slabs of nuclear matter to reveal the important features such as shock wave velocity, density increase, energy increase, and the Mach number at which dissociation of

nucleons would occur. We are now pursuing this further to consider a full hydrodynamical calculation of two spherical nuclei in head-on collisions. In such a hydrodynamical calculation, a sharp surface with tensional force leads to technical difficulties because the natural choice for coordinate mesh surfaces is not necessarily the same as the nuclear surface. The difficulty is avoided by considering a continuum of nuclear matter in a nucleus without a sharp surface and simulating the surface tension with an attractive Yukawa potential between different fluid elements. In such a formulation, the method used in ref. 3 in the collision of two identical stars can be carried over directly. Of particular interest is to see, in analogy with the collision of stars, whether in a nuclear collision the recoiling shock waves will also emerge in the forward and backward directions and carry with them dissociated nucleons in these directions. If so, the detection of these nucleons would be a way to trace out the shock waves. It is also of interest to find the minimum energy at which a heavy nucleus may be punctured by a smaller nucleus, thereby leaving a remnant with a hole in it, and minimal excitation. This possibility was one of the main motives for exploring the stability of toroidal nuclei.⁴

1. A. E. Glassgold, W. Heckrotte, and K. M. Watson, *Ann. Phys. (N.Y.)* **6**, 1 (1959).

2. C. Y. Wong and T. A. Welton, submitted to *Physics Letters*.

3. F. G. P. Seidl and A. G. W. Cameron, *Astrophys. Space Sci.* **15**, 44 (1972).

4. C. Y. Wong, *Phys. Lett.* **41B**, 448 (1972); *Phys. Lett.* **41B**, 451 (1972); *Ann. Phys. (N.Y.)* **77**, 279 (1973).

ADAPTATION OF DIRECT REACTION COMPUTER CODES FOR USE WITH HEAVY IONS

L. W. Owen¹ G. R. Satchler

Nuclear reactions involving heavy ions are distinguished by much larger angular momenta and shorter wavelengths than are usually encountered in light-ion reactions. Consequently computer codes which are quite adequate for the latter need to be redimensioned, etc., for use with heavy ions so as to be able to handle, for example, several hundred partial waves and large numbers of radial integration steps. Other modifications may also be required or useful.

The codes which have been adapted are Perey's GENOA² (optical-model search code for elastic scattering), Kunz's DWUCK³ (DWBA code suitable for inelastic scattering and "zero-range" transfer reactions),

and DeVries' LOLA⁴ (for exact finite-range DWBA calculations of transfer reactions). Each was initially modified to take the very general Tamura-Saclay Coulomb wave function subroutine.⁵ Naturally the codes were carefully checked against each other and against earlier versions as well as other codes such as JULIE.⁶ All such checks were satisfied, although of course there always remains the possibility of unsuspected errors when a new region of parameter space is being explored. Various options were also added to the codes; for example, the new GENOA includes the facility of using "folded" potentials instead of the usual Woods-Saxon shape.

These codes are now available on disk at the IBM 360-91/75, and instructions for using them may be obtained from the above authors. Another version of GENOA is being developed which is oriented toward searching on excitation functions at one or a few angles instead of angular distributions at one or a few energies. The code SATURN-MARS was also made available by Tamura⁷ and is currently being adapted. This also performs exact finite-range DWBA calculations of transfer reactions; results from this and the LOLA code compare very well. SATURN-MARS also has the capability of doing CCBA calculations, that is, of including inelastic plus transfer reactions. It is hoped to include this facility in our version in the future.

We are indebted to the original authors for making their codes available and for their advice and assistance in adapting them.

1. Computer Sciences Division.
2. F. G. Perey, Neutron Physics Division (unpublished).
3. P. D. Kunz, University of Colorado (unpublished).
4. R. DeVries, University of Washington report (1973) (unpublished); *Phys. Rev.* **C8**, 951 (1973).
5. T. Tamura, *Comput. Phys. Commun.* **3**, 73 (1972).
6. R. M. Drisko, R. H. Bassel, and G. R. Satchler, ORNL report 3240 (1962) (unpublished).
7. T. Tamura and K. S. Low, *Phys. Rev. Lett.* **31**, 1356 (1973).

VISCOSITY AND FUSION REACTIONS

H. H. K. Tang¹ C. Y. Wong

In heavy-ion reactions, the fusion mechanism requires some understanding of the viscous property of nuclei. We undertook to study the classical problem of the vibration of a viscous charged liquid drop. Previously, a characteristic equation for the vibration of a viscous gravitational globe was obtained by Chandrasekhar.² The same equation was found to apply for a viscous liquid drop under the restoring force of surface tension.³ We have proved⁴ that it also applies to all

combinations of gravitational attraction, surface tension, and Coulomb repulsion with surface or volume charge distribution. We evaluated complex solutions to this Chandrasekhar equation corresponding to the periodic motion with damping, which have not been found up to now but are called for in a large class of physical problems. In addition, some solutions for higher aperiodic modes of decay are also evaluated. From the solution of the characteristic equation, an upper bound on the kinematic viscosity of nuclear matter has been found to be $\nu = 0.019$ fm-c.

1. Student guest at ORNL during summer and fall 1973 from Kalamazoo College, Kalamazoo, Mich.
2. S. Chandrasekhar, *Proc. London Math. Soc.* (3) 9, 141 (1959).
3. W. H. Reid, *Proc. London Math. Soc.* (3) 9, 388 (1959); *Quart. Appl. Math.* 18, 86 (1960).
4. H. H. K. Tang and C. Y. Wong, *J. Phys. A* (in press).

CALCULATION OF SINGLE-NUCLEON TRANSFER REACTIONS WITH HEAVY IONS ON ^{208}Pb

L. W. Owen¹ G. R. Satchler

The ORNL version of the exact finite-range code LOLA² was used to study the single-nucleon transfer reactions induced by 72-MeV ^{11}B ions incident on ^{208}Pb as measured at ORIC.³ To obtain optical-model parameters, the elastic scattering data⁴ obtained at ORIC for ^{11}B and ^{12}C on ^{208}Pb were analyzed extensively using the new version of the code GENOA. The results of these analyses are presented elsewhere in this report. As part of this work, the structures of the transfer calculations are being studied in detail, both for their intrinsic interest and to determine how to do the DWBA calculations as economically as possible without loss of accuracy. (An accuracy of about 1% or better was aimed for.)

Consider the reaction $A(a,b)B$, where $a = b + x$, $B = A + x$; thus x is the transferred particle. An important step in the calculation⁵ is to obtain the multipoles

$$g_K(r_{aA}, r_{bB}) = \int_{-1}^1 d\mu P_K(\mu) u_1(r_{xA}) u_2(r_{xb}) V(r_{xb}), \quad (1)$$

where $\mu = \cos \theta$ and θ is the angle between r_{aA} and r_{bB} (see Fig. 1). Also, u_1 is the bound state of x to A and u_2 of x to b , while V is the b - x binding potential. Evaluation of the g_K was the most time-consuming part of the calculation with the original finite-range code.⁶

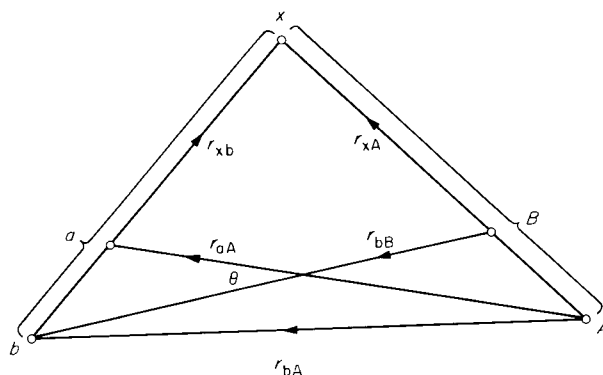


Fig. 1. Vector diagram for transfer reaction.

LOLA uses the Gauss-Legendre integration method; when the full range $-1 \leq \mu \leq 1$ was used, a high order of Gauss-Legendre integration was required, of the order of four times K_{\max} , before an accurate result was obtained. However, in many cases the integrand in (1) is concentrated near $\mu = 1$ or $\theta = 0$. For $^{11}\text{B} + ^{208}\text{Pb}$ we found that $\theta \lesssim 2$ or 3° was adequate, although the calculations reported used $\theta_{\max} = 5^\circ$. This allows a low order of Gauss-Legendre integration to be used even for large K (the number of $K \approx$ the number of partial waves) and such an increase in speed that now the g_K evaluation takes only a small fraction of the total time.

The remainder of the calculation involves two-dimensional integrals of the form⁵

$$\int dr_{aA} \int dr_{bB} \chi_{L_b}(r_{bB}) \times F_{L_a L_b}(r_{aA}, r_{bB}) \chi_{L_a}(r_{aA}), \quad (2)$$

where the χ are partial distorted waves in the entrance and exit channels and the $F_{L_a L_b}$ are linear combinations of the g_K involving angular momentum coupling coefficients.⁵ Examination of the form factors $F_{L_a L_b}(r_{aA}, r_{bB})$ shows them in many cases to be concentrated along the diagonal $r_{aA} \approx r_{bB}$. For $^{11}\text{B} + ^{208}\text{Pb}$ we find that this band is only about 1 fm wide or less; very good accuracy was obtained by restricting the integration to a bandwidth of 2 fm. Further, the wave numbers involved in the χ are generally large (for $^{208}\text{Pb} + ^{11}\text{B}$ at 72 MeV, $k \approx 6 \text{ fm}^{-1}$), and this would seem to require very small (and hence very many) steps in r_{aA} and r_{bB} in the integral (2). Fortunately, the Coulomb barrier and strong absorption ensure that the important grazing collision partial waves vary relatively slowly in the region where the transfer takes place.

Again for the $^{11}\text{B} + ^{208}\text{Pb}$ case, a step length of 0.1 fm across the ridge in $F_{lL_aL_b}$ gave good accuracy; the remaining integration could then use steps two or three times larger without loss of accuracy.

The strong absorption associated with heavy ions allows a further economy. Contributions from radii less than some lower cutoff value R_{\min} (approximately equal to the target nuclear radius) and from partial waves with L less than the corresponding angular momentum L_{\min} are negligible. ($^{11}\text{B} + ^{208}\text{Pb}$ at 72 MeV allows $R_{\min} \approx 8$ fm, $L_{\min} \approx 20$. The distribution in L for a ($^{11}\text{B}, ^{10}\text{Be}$), reaction is illustrated in Fig. 2.)

These various considerations allow the computing time to be reduced enormously. Very roughly, the computing time on the IBM-360/91 is

$$\tau \cong (\text{NRA} \times \text{NRB})[(\text{NG} \times \text{NK})\tau_{\text{GK}}^{\circ} + \text{NL}(l+1)(2l_1+1)(2l_2+1)\tau_L^{\circ}],$$

where NRA, NRB are the number of radial steps in the r_{aA} , r_{bB} directions, NG is the order of Gauss-Legendre chosen, NK is the number of g_K required, NL is the number of partial waves, l is the l transfer, and l_1, l_2 are the bound orbitals. Then $\tau_{\text{GK}}^{\circ} \approx 3 \times 10^{-6}$ sec, $\tau_L^{\circ} \approx 2 \times 10^{-5}$ sec.

The way the contributions to the transfer amplitudes (2) are distributed in space is of interest. (We refer here

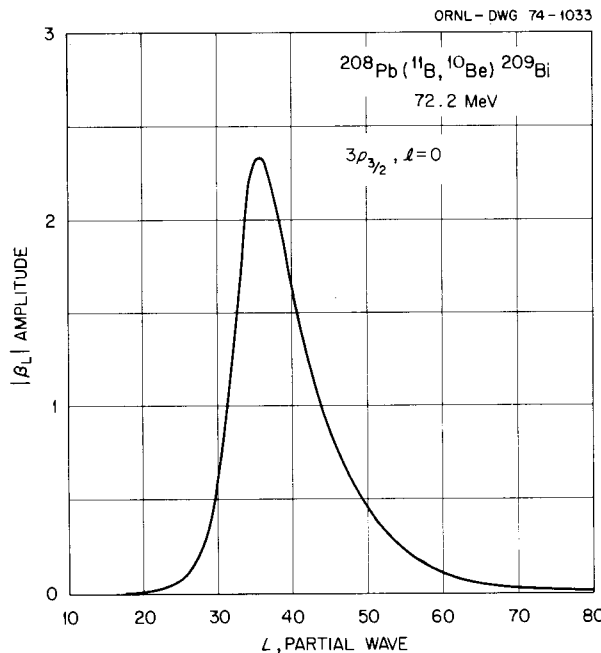


Fig. 2. Distribution of contributions from various partial waves for $l = 0$ angular momentum transfer.

again to $^{11}\text{B} + ^{208}\text{Pb}$ at 72 MeV.) First we note that the strong absorption radius obtained from the elastic scattering in the entrance channel is about 12.2 fm and corresponds to $L \approx 37$. (The L values close to this also give the largest transfer probabilities; see Fig. 1.) When the post interaction V_{xb} is used, the integrand of Eq. (1) peaks strongly, with a width of about 2 fm, for $r_{xb} \approx 2.3$ fm, $r_{xA} \approx 9.9$ when x is on the line joining the centers of the two nuclei (i.e., $\mu = 1$ or $\theta = 0$), and the centers are 12.2 fm apart. When x moves off the line of centers ($\theta > 0$), the integrand rapidly decreases; for $\theta = 1^\circ$, x has moved off about 2 fm. It is these off-line contributions ($\theta > 0$) which allow the nonnormal-parity l transfers (l for which $\Delta\pi \neq (-)^l$) which do not appear in the no-recoil approximation. Typically these nonnormal-parity cross sections are an order of magnitude smaller than the normal-parity ones allowed in a given transition for these $^{11}\text{B} + ^{208}\text{Pb}$ reactions, but in some cases they can be much more important. For example, in the transfer of a nucleon from an orbit with l_1 in ^{208}Pb to a $1p$ orbit in the projectile, transfers with $l = l_1, l_1 \pm 1$ are possible in general. The nonnormal $l = l_1$ has a cross section comparable with the smaller, normal, $l = l_1 - 1$; then if $l = l_1 + 1$ is forbidden, the nonnormal contributes a large fraction of the cross section. This occurs if $j_1 = l_1 - 1/2$ and the nucleon enters a $1p_{1/2}$ orbit.

Equation (1) contains the post form of the interaction; one may also use the prior form, $V(r_{xA})$, which binds x to A . The complete post and prior interactions would give identical results, but the leading terms chosen represent approximations for which post-prior identity cannot be expected in general. In particular, it is usual to omit the Coulomb parts of V . A comparison of post and prior results for ^{11}B on ^{208}Pb has shown relatively small differences (about 20%) for neutron transfer, but large differences (prior approximately 1.6 times post) for proton transfer. Switching off all Coulomb forces in the distorted waves and bound states, however, leads to post and prior cross sections agreeing to better than 1% on the peak, showing that the neglected *nuclear* interaction terms do not induce a major post-prior discrepancy. Calculations are under way to see the effect of including the Coulomb part of the binding potentials $V(r_{xb})$ or $V(r_{xA})$.

1. Computer Sciences Division.
2. R. DeVries, University of Washington report, 1973 (unpublished).
3. J. L. C. Ford, Jr., K. S. Toth, D. C. Hensley, R. M. Gaedke, P. J. Riley, and S. T. Thornton, contributed paper to *Symposium on Heavy Ion Transfer Reactions, March 1973*, Argonne National Laboratory report PHY-1973B, vol. II.

4. J. L. C. Ford, Jr., K. S. Toth, D. C. Hensley, R. M. Gaedke, P. J. Riley, and S. T. Thornton, *Phys. Rev. C* **8**, 1912 (1973).

5. N. Austern, R. M. Drisko, E. C. Halbert, and G. R. Satchler, *Phys. Rev.* **133B**, 3 (1964).

6. R. M. Drisko, "The Code FANNY," 1962 (unpublished); R. M. Drisko, G. R. Satchler, and R. H. Bassel, Proc. Third Conf. on Reactions between Complex Nuclei (1963).

STUDIES WITH "REALISTIC" INTERACTIONS FOR INELASTIC NUCLEON SCATTERING

K. T. R. Davies¹ W. G. Love²
G. R. Satchler

As part of the ongoing program³ to study the usefulness of various "realistic" effective nucleon-nucleon interactions, we have used the Skyrme-type interactions, which have experienced a revival of popularity for nuclear structure problems.⁴ Although these forces are simple, almost schematic, they have been very successful in correlating a number of nuclear properties, and it is of interest to forge another link between the forces used in structure studies and those used to describe inelastic scattering.

For convenience, the momentum dependence of the Skyrme force was converted into an equivalent finite-range Gaussian with a Majorana exchange term. Particular attention was given to the three-body contact potential; this can often be replaced by an equivalent density-dependent two-body term, but its strength and exchange character depend on the context within which it is to be used.

Calculations were made for the $^{40}\text{Ca}(p,p')$ reaction, using transition densities normalized to give the observed $B(EL)$ values. Figure 1 compares with experiment the results for several Skyrme-type interactions whose parameters were determined by fitting to various nuclear properties. Considering the simple nature of the forces, the agreement is remarkably good.

Further studies are in progress using the forces of Banerjee and Sprung,⁵ which are intended to be equivalent to the sophisticated effective interactions of Negele derived from Brueckner-Bethe-type calculations. These have the advantage of being local and expressible as sums of Gaussians.

Other calculations have been started using microscopic wave functions for the giant resonances which have aroused interest recently⁶ in order to compare the results with the collective model which has been used so far. These wave functions may be obtained from RPA-type calculations⁷ or from simple models such as

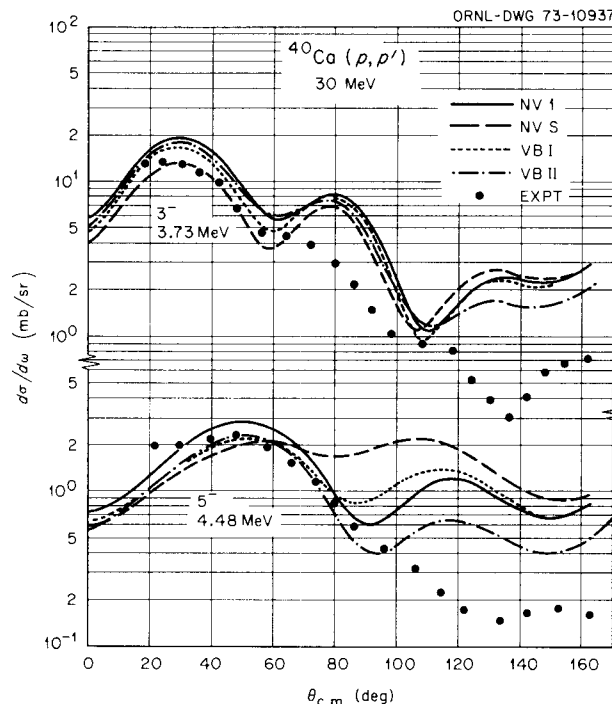


Fig. 1. Comparison between experiment and predictions for various Skyrme-type forces.

acting on the ground state with the corresponding multipole operator.

1. On assignment at the Los Alamos Scientific Laboratory, September 1973 through August 1974.

2. University of Georgia, Athens, Ga.

3. G. R. Satchler, *Z. Phys.* **260**, 209 (1973).

4. C. B. Dover and N. Van Giai, *Nucl. Phys.* **A190**, 373 (1972).

5. D. W. L. Sprung and P. K. Banerjee, *Nucl. Phys.* **A168**, 273 (1971).

6. G. R. Satchler, ORNL report TM-4347 (1973); *Rev. Mod. Phys.*, to be published.

7. D. J. Rowe and C. Ngo Trong, private communication.

GAUSSIAN POTENTIALS EQUIVALENT TO THE "SUSSEX" MATRIX ELEMENTS

R. H. Tookey¹ G. R. Satchler

The "Sussex" matrix elements² form a set of matrix elements of the nucleon-nucleon interaction in harmonic oscillator representation which were deduced directly from nucleon-nucleon scattering phase shifts without going through the intermediary of an explicit coordinate representation of the potential. This is very convenient input for many nuclear structure calcula-

tions. However, in some cases, especially the microscopic description³ of the inelastic scattering of nucleons from nuclei, it is important to have the potential in a coordinate representation, and in a form which can easily be expanded into multipoles. Partly for this reason, and partly to facilitate comparison with other simple nucleon-nucleon forces which have been used, we undertook to find simple Gaussian potentials which would reproduce closely the Sussex matrix elements.

First, the Sussex matrix elements were rearranged by a standard Racah transformation⁴ to separate out the central, spin-orbit, and tensor force contributions. These were then fitted separately by the matrix elements of an interaction of the form

$$v = v^{(0)} + v^{(1)}2L_{12} \cdot (\sigma_1 + \sigma_2) + v^{(2)}S_{12},$$

where

$$v^{(k)} = \sum_i V_i^{(k)} \exp(-\gamma_i^{(k)} r^2) \quad \text{for } k = 0, 1$$

or

$$v^{(2)} = \sum_i V_i^{(2)} (\gamma_i^{(2)} r^2) \exp(-\gamma_i^{(2)} r^2) \quad \text{for } k = 2.$$

The degree of fit was determined by a least-squares search.

So far, only one term in the sum over Gaussians has been used for the spin-orbit and tensor parts, and this seems to be adequate. Indeed, only the ¹S and ³S matrix elements appear to require more than one term for their central parts. Only preliminary results are available at the present. The ¹P odd-state potential is very close to that obtained earlier,² with $V^{(0)} \approx 430$ MeV, $\gamma^{(0)} \approx 1.365 \text{ fm}^{-2}$. The ²P central component is weak and poorly determined, the spin-orbit term has $V^{(1)} \approx -70$ MeV, $\gamma^{(1)} \approx 1.8 \text{ fm}^{-2}$, and the tensor term has $V^{(2)} \approx -20$ MeV, $\gamma^{(2)} \approx 0.6 \text{ fm}^{-2}$.

Because Yukawa-type interactions (and regularized OPEP for the tensor term) are also often used in other calculations, we plan to obtain fits using these forms as well. The code can also be used to find simple interactions equivalent to other sets of matrix elements, such as those resulting from Brueckner calculations.

Finally, we note that a similar but more limited study was published recently.⁵ Our results indicate that the even-state interaction obtained there is not unreasonable, but their odd-state interaction is nowhere near the optimum one and gives a poor fit to the corresponding Sussex matrix elements.

1. Student guest at ORNL during fall 1973 from DePauw University, Greencastle, Ind. (assignment through Great Lakes Colleges Association Program administered by Oak Ridge Associated Universities).

2. J. P. Elliott et al., *Nucl. Phys.* **A121**, 241 (1968).

3. W. G. Love and G. R. Satchler, *Nucl. Phys.* **A159**, 1 (1970); G. R. Satchler, *Z. Phys.* **260**, 209 (1973).

4. D. M. Brink and G. R. Satchler, *Angular Momentum*, Oxford Univ. Press, 1971.

5. K. P. Joshi and Y. R. Waghmare, *Phys. Rev.* **C7**, 874 (1973).

TARGET-SPIN EFFECTS ON ELASTIC SCATTERING CROSS SECTIONS

W. G. Love¹ G. R. Satchler
C. B. Fulmer

The angular distributions of 50-MeV alphas elastically scattered from ⁵⁹Co and ⁶⁰Ni show significant differences.² Compared with ⁶⁰Ni, the ⁵⁹Co distribution has appreciably less deep minima. When a projectile has spin, the introduction of a spin-orbit coupling term into the optical potential often has a similar effect. This led to the suggestion that in alpha scattering it was due to an analogous coupling between the spin of the target nucleus and the relative orbital motion, which clearly would be absent for ⁶⁰Ni but could be present for ⁵⁹Co with its spin of $\frac{7}{2}^-$. However, estimates of the magnitude of this coupling suggested it was much too small to account for the data. These estimates were based upon microscopic calculations using the alpha-nucleon spin-orbit interaction and an effective spin-orbit term arising from nucleon exchange between the alpha and the target. The latter dominates over the former.

Nonetheless, the target spin is the simplest feature distinguishing these two nuclei. It allows ⁵⁹Co to have a quadrupole moment, and it was suggested some years ago³ that scattering from the quadrupole moment could lead to odd-even differences just of the kind observed. Consequently this was explored further using a simple model which makes use only of empirical results. The odd nucleus is considered as a single particle (or hole) in an orbit j coupled to core states with spin L , where the core is taken to be the adjacent even nucleus. The odd ground state, for example, is then

$$|\text{odd}, IM\rangle = \alpha_I |(\text{even}, 0), j = I; IM\rangle + \sum_{Lj} \beta_{LjI} |(\text{even}, L), j; IM\rangle. \quad (1)$$

The even-parity core-excited terms, with $j = I$, allow a contribution to the elastic scattering cross section which is of order β^2 and which is proportional to the inelastic scattering cross sections for the corresponding even nucleus. (It can be argued³ that other kinds of contributions of order β^2 contribute roughly equally for odd and even targets.) Then

$$\sigma_{el}(\text{odd}) - \sigma_{el}(\text{even}) \approx \sum_L \frac{(2\alpha_L \beta_{LII})^2}{2L+1} \sigma_{inel}(\text{even}, 0^+ \rightarrow L^+). \quad (2)$$

Since for strongly absorbed particles, σ_{inel} for normal-parity states with $L = \text{even}$ oscillates out of phase with σ_{el} as a function of angle, this extra term will fill in the minima for $\sigma_{el}(\text{odd})$ relative to $\sigma_{el}(\text{even})$.

Now $\sigma_{inel}(\text{even})$ can be measured, and the coefficient can be deduced from the measured multipole moments of the odd-nucleus ground state and the measured $B(EL)$ for excitation of the state in the even nucleus. For example, for $L = 2$ the quadrupole moment corresponding to (1) is

$$Q = \alpha^2 Q_{val}(j=I) + \alpha_I \beta_{2II} \left[\frac{64\pi I(2I-1)}{5(I+1)(2I+3)} \right]^{1/2} \langle 2 || r^2 Y_2 || 0 \rangle \dots,$$

where the odd nucleon contributes

$$Q_{val}(j=I) = -[(2I-1)/2(I+1)] \langle r^2 \rangle_{j=I}$$

and the core matrix element is given by the transition rate in the even nucleus,

$$B(E2)_{2 \rightarrow 0} = e^2 |\langle 2 || r^2 Y_2 || 0 \rangle|^2.$$

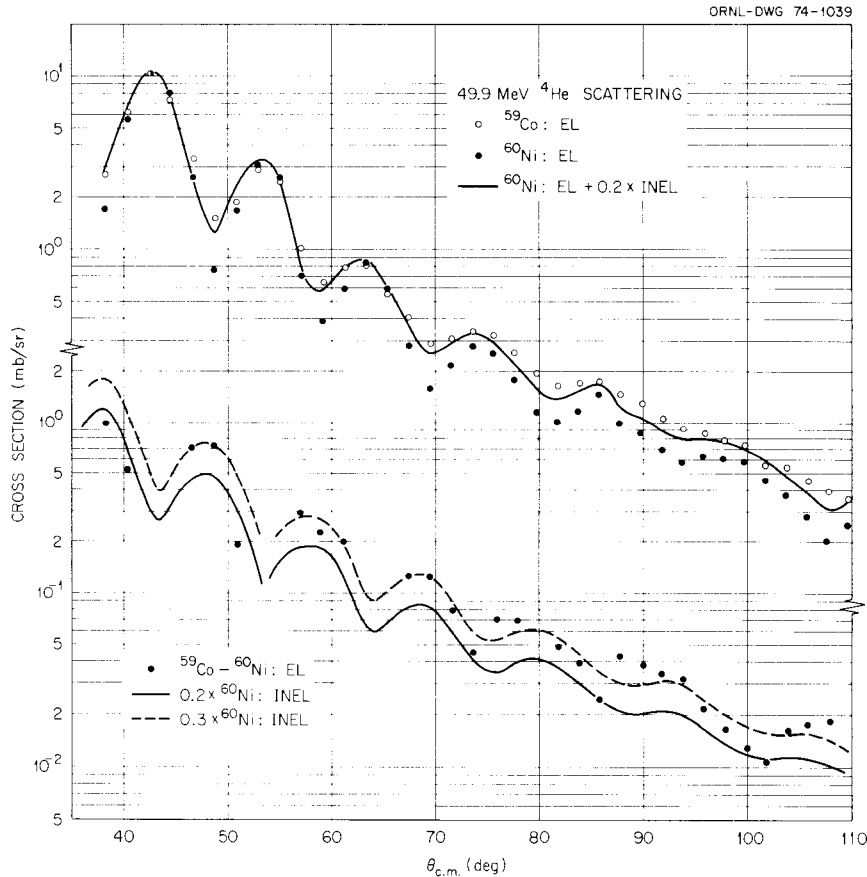


Fig. 1. Scattering of 49.9-MeV alpha particles. The upper part compares cross sections for ^{59}Co and ^{60}Ni . The solid line is obtained by adding one-fifth of the inelastic cross sections for the 2^+ state in ^{60}Ni to the elastic cross sections from ^{60}Ni . The lower part compares the differences between the ^{59}Co and ^{60}Ni elastic cross sections with one-fifth of the inelastic cross sections. Error bars are omitted for clarity.

We have applied this model to the pair ^{59}Co and ^{60}Ni , where $j = I = 7/2$ and is assumed due to a $1f_{7/2}$ proton hole. Only $L = 2$ and the first excited state of ^{60}Ni were considered. Taking $Q = 40 \text{ fm}^2$ and $B(E2) = 200 e^2 \text{ fm}^4$, we find $(2\alpha\beta) \approx 1$ so that

$$\sigma_{el}(59) \approx \sigma_{el}(60) + \frac{1}{5}\sigma_{inel}(60, 0^+ \rightarrow 2^+).$$

Figure 1 shows the results for 50-MeV alphas; clearly the core-excitation contribution accounts for most of the differences between the two targets. The lower half of the figure emphasizes this by comparing the actual differences with one-fifth of the observed inelastic cross section. This comparison suggests that more core excitation would improve the fit. This is not surprising since we have only included the contribution from the lowest 2^+ state in ^{60}Ni ; in particular, it was necessary to use an effective charge of $2e$ for the valence proton hole in order to reproduce the observed Q , and this implies that there are other core excitation terms, such as the giant quadrupole state of ^{60}Ni .

The elastic scattering of ^3He also shows systematic odd-even differences,⁴ and Fig. 2 shows that for ^{59}Co ,

^{60}Ni these again are largely explained by the core excitation effect. In this case the observed differences oscillate more strongly with angle than does the corresponding inelastic scattering from ^{60}Ni , but the average magnitude is in good agreement.

Previous experiments have shown essentially no odd-even differences for proton scattering, so it is important to see if this is consistent with our model. Indeed, 40-MeV proton scattering⁵ shows very similar results for ^{60}Ni and ^{59}Co , and at the same time the inelastic scattering from ^{60}Ni is much smaller relative to the elastic.

1. University of Georgia, Athens, Ga.
2. C. B. Fulmer and J. C. Hafele, *Electronuclear Div. Annu. Rep. Dec. 31, 1970*, ORNL-4649.
3. G. R. Satchler, *Nucl. Phys.* **45**, 197 (1963).
4. C. B. Fulmer and J. C. Hafele, *Phys. Rev.* **C7**, 631 (1973).
5. M. P. Fricke, E. E. Gross, B. J. Morton, and A. Zucker, *Phys. Rev.* **156**, 1207 (1967).

ASYMMETRIC FISSION OF ^{236}U IN A SELF-CONSISTENT K -MATRIX MODEL

D. Kolb¹ R. Y. Cusson² H. W. Schmitt³

The phenomenological single-particle Hamiltonian of Meldner was rederived as a renormalized single-particle K matrix.⁴ The parameters of this deformation- and atomic-number-independent model were obtained by fitting to the experimental properties of ^{16}O , ^{40}Ca , ^{48}Ca , and ^{208}Pb . It was then used to calculate the properties of ^{236}U on the fission path from the ground state to scission into asymmetric fragments. Substantial radial density fluctuations or incipient "bubble" shapes were observed (see Fig. 1), as well as a displacement of the neutron center of mass relative to that of the protons. It was also found that the presence of a broad third minimum and saddle near scission can be observed for one of the parameter sets of the interaction. These results can then be used to illustrate the essential importance of using a nonorthogonal two-oscillator basis as well as taking into account the properties of nuclear matter.

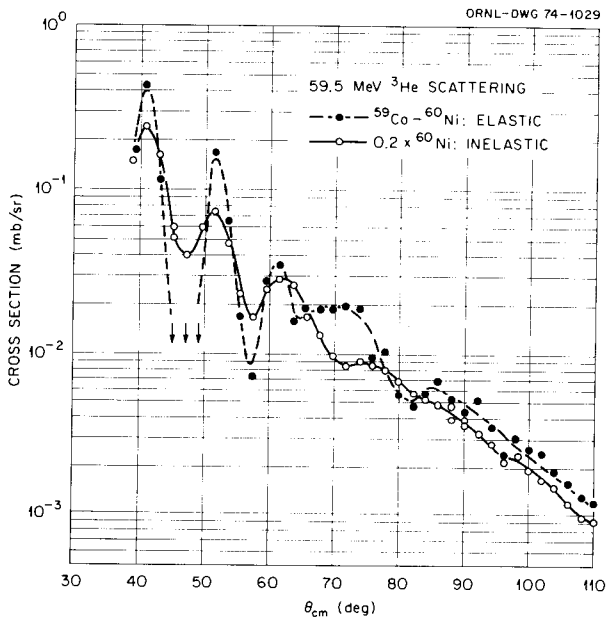
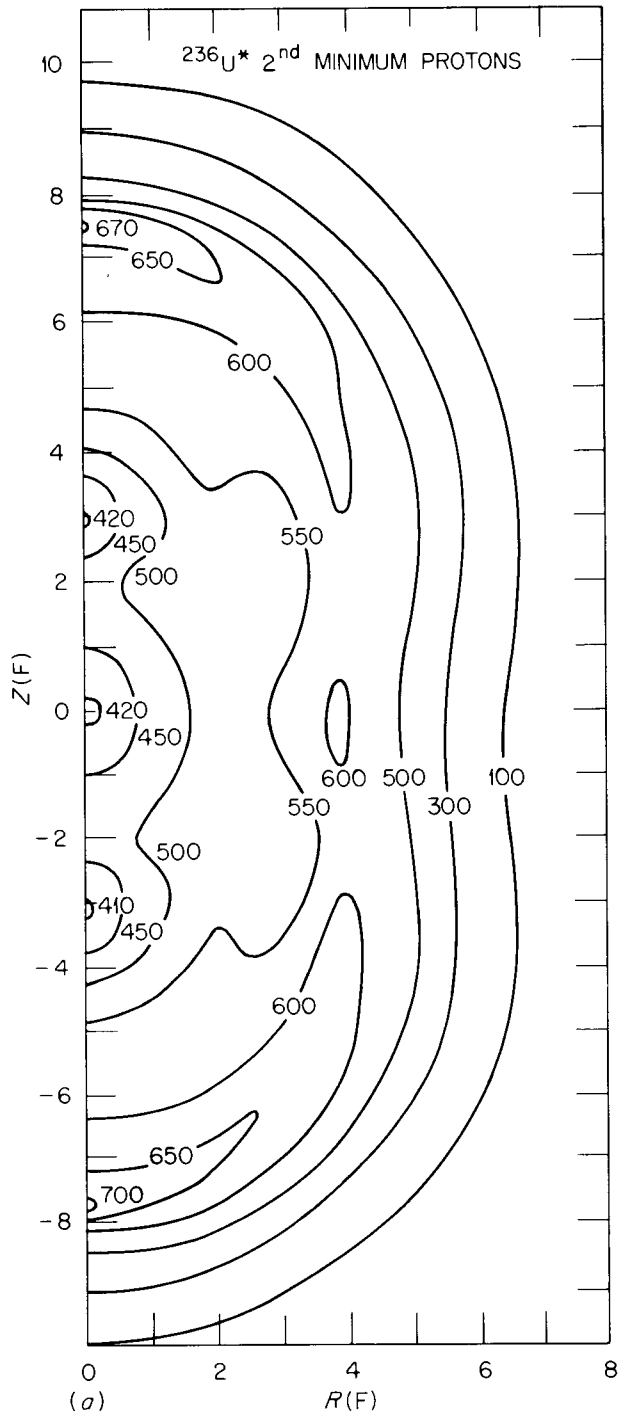


Fig. 2. Scattering of 59.5-MeV ^3He . Comparison of the differences between the ^{59}Co and ^{60}Ni elastic cross sections with one-fifth of the inelastic cross section to the 2^+ state in ^{60}Ni . Error bars are omitted for clarity.

1. Guest assignee to ORNL during summer 1973 from Duke University, Durham, N.C. Present address: Yale University, New Haven, Conn.
2. Consultant to ORNL from Duke University, Durham, N.C.
3. On leave of absence from ORNL. Present address: Environmental Systems Corp., Knoxville, Tenn.
4. D. Kolb, R. Y. Cusson, and M. Harvey, *Nucl. Phys.* **A250**, 1 (1973).

ORNL-DWG 73-11492



ORNL-DWG 73-11490

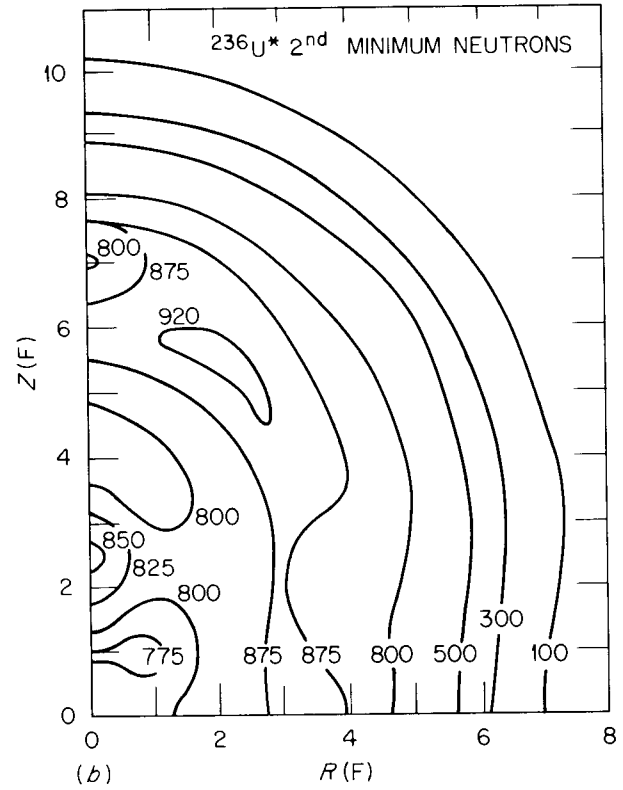


Fig. 1. Density contours of ^{236}U in the second potential minimum. (a) Protons; (b) neutrons.

A STRONG-COUPLING APPROACH TO THE TRUNCATION OF LARGE SHELL-MODEL CALCULATIONS

L. B. Hubbard¹ J. B. McGroary

The usefulness of large shell-model calculations in analyzing and understanding observed low-energy nuclear phenomena is generally accepted. The computational difficulties of extending such calculations to more than five or six particles beyond a "closed shell" are also well known. Thus, one question of interest has always been to find useful means of truncating shell-model spaces. One such approach is based on more or less well-known strong-coupling ideas. We have developed a code based on a strong-coupling model to be used in conjunction with our conventional shell-model computer programs.² The basic idea is sketched out here. Suppose that the shell-model space can be divided into two inequivalent spaces (i.e., antisymmetrization between the two can be ignored). Then

$$H = H_{1-1} + H_{2-2} + H_{1-2},$$

where H_{1-1} is the complete Hamiltonian in space 1, H_{2-2} is the same in space 2, and H_{1-2} represents the interaction between spaces 1 and 2. Suppose the problems represented by H_{1-1} and H_{2-2} can be solved exactly. This leads to a set of energies and eigenvalues, E_i and $|\psi_i\rangle$, for each space:

Space 1	Space 2
_____ E_{n_1}	_____ E_{n_2}
_____	_____
_____	_____
_____	_____
_____	_____ E_3
_____ E_2	_____ E_2
_____ E_1	_____ E_1

The full space, 1 + 2, is spanned by the set of states $|\psi_{12}\rangle = |\psi_1\rangle \times |\psi_2\rangle$, where $|\psi_1\rangle$ and $|\psi_2\rangle$ are all states in space 1 and space 2. For spin-independent forces, the interaction Hamiltonian H_{1-2} can be expanded in terms of spherical harmonics; that is, schematically,

$$H_{12} = \sum_L C_L(r_1, r_2) Y^L(1) \cdot Y^L(2).$$

The matrix elements of H_{12} between product states $|\psi_{12}\rangle$ can be written, very schematically, as

$$\langle \psi_{12} | H_{12} | \psi'_{12} \rangle = \sum_L C'_L(r_1, r_2) \times \langle \psi_1 || Y^L(1) || \psi'_1 \rangle \langle \psi_2 || Y^L(2) || \psi'_2 \rangle.$$

From this it follows that only states which are strongly connected by the spherical harmonic operators are strongly mixed when H_{12} is diagonalized. Such states are "strongly" coupled. This suggests the following general approach to the shell-model problem. Do the problem in neutron-proton formalism (n.p.). Treat H_{nn} and H_{pp} exactly. From the resulting two subspaces, select only the lowest few neutron and proton states, and those excited states that are strongly coupled to these lowest few states by the spherical harmonic operators. One way to do this is to select the lowest few states in the neutron spectrum, form the set of states obtained by acting on these states with the spherical harmonic operators, and from all these states form an orthonormal basis. Programs are now available for carrying out all these operations.

Such an approach should be useful where the neutron-proton interaction is expected to be weak. This may be particularly true when there is a reasonable neutron excess. We have made a preliminary study of the practicality of such an approach to nuclei in the f - p shell. In particular, we have studied the nucleus ^{44}Ti , and treated it as the result of coupling two-neutron states (^{42}Ca) to two-proton states (^{42}Ti), in a model where we assume an inert ^{40}Ca core. We have used the realistic effective f - p shell two-body interaction of Kuo and Brown,³ and single-particle energies derived from the observed spectrum of ^{41}Ca . We have then carried out calculations in ^{44}Ti in the space spanned by coupling together various sets of low-lying states in the two-particle systems. We first included only the lowest four states in the two-particle space ($J = 0, 2, 4, 6$). We next calculated the four-particle space spanned by all couplings of the two lowest $J = 0, 2, 4$, and 6 states. Next we included these eight states plus the third 2^+ , third 4^+ , and lowest 5^+ state. There are relatively few two-particle states in our spaces, and the states generated with the spherical harmonic operators are very similar to the eigenstates of our two-body Hamiltonian. As we go to larger spaces, this approach should be more useful. The resulting calculated spectra are compared with the exact shell-model diagonalization of the $T = 0$ states of four particles in the f - p shell in Fig. 1. Above the line representing the ground state in each spectrum is given the absolute binding energy of the ground state

relative to ^{40}Ca . (The $f_{7/2}$ binding energy in ^{41}Ca is set to 0, so the binding energies shown in Fig. 1 are essentially the two-body contributions to the binding energy.) The numbers under each spectrum give the number of two-particle states included in the basis space as discussed above. We consider these results reasonably encouraging. We also include in this figure the spectrum of low-lying two-particle states which are used to generate our four-particle basis. When 8 states are included in the two-particle space, the excitation energies of most of the 12 states in the "exact" spectrum of ^{44}Ti are reproduced reasonably well. The main effect of introducing 3 states to go from 8 states to 11 states is to add 500 keV binding energy.

This result is particularly encouraging because it is for a case where neutrons and protons occupy the same orbits, and the n - p interaction is not weak. The approach should be more useful where there is a neutron excess. We have made one calculation for the

nucleus ^{93}Nb with this same approach which suggests the strong coupling is quite good there. ^{93}Nb can be characterized as one neutron outside a ^{92}Mo core. We have treated ^{93}Nb in an exact shell-model calculation where protons occupy the $p_{1/2}$ and $g_{9/2}$ orbits and neutrons occupy the $d_{5/2}$, $s_{1/2}$, and $d_{3/2}$ orbits. We then repeated the calculation in our strong-coupling approach, where we couple a neutron in the $d_{5/2}$, $s_{1/2}$, or $d_{3/2}$ orbit to the lowest $J = 0^+$, 2^+ , and 4^+ states in the calculated ^{92}Mo spectrum. The results are summarized in Fig. 2. There we show the exact shell-model results for states with $J \leq 9/2$, for ^{92}Mo , ^{89}Sr , and ^{93}Mo , the weak-coupling results (i.e., each ^{93}Mo state is exactly one neutron state coupled to one proton state, and the neutron-proton interaction is ignored), and the strong-coupling results. In this figure, the numbers in parentheses in the "exact" spectrum indicate the intensity of the exact wave function which is in our strong-coupling basis. We see that many of the

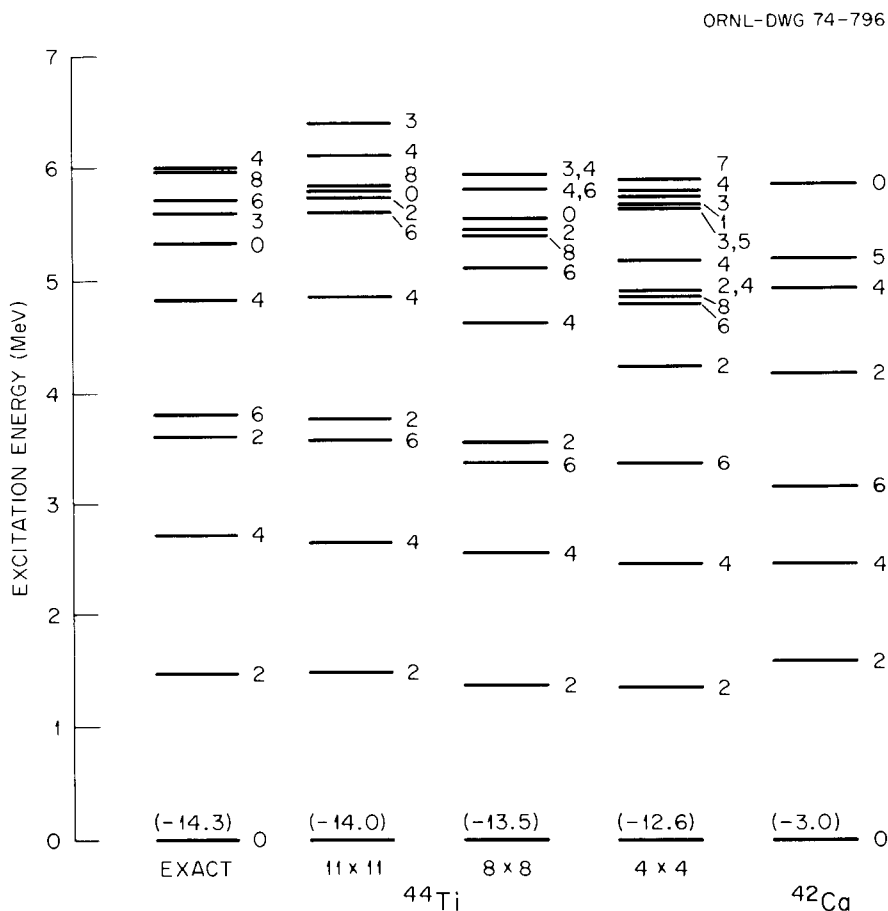


Fig. 1. Calculated spectra of ^{44}Ti in various approximations. The numbers $a \times a$ under each column indicate the number of two-particle states included in the calculation of that spectrum.

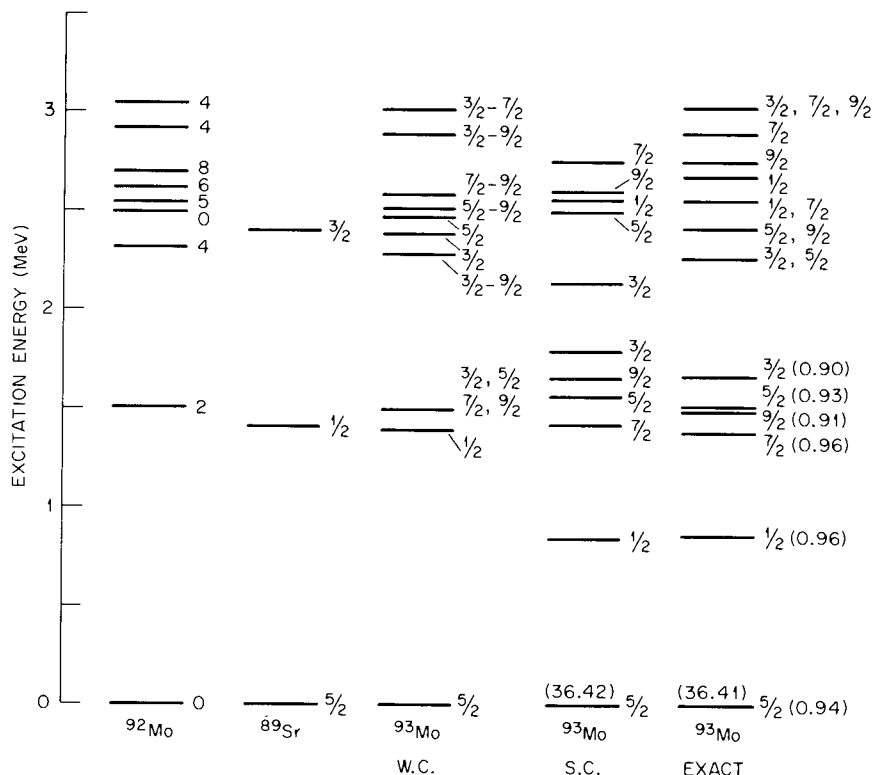


Fig. 2. Calculated spectra of ^{93}Nb in various strong- and weak-coupling approximations.

low-lying states in ^{93}Mo are well accounted for by this strong-coupling approach.

Our first application of these programs to nuclei where we cannot do the exact shell-model calculations will be to some of the $A = 46-50$ $f-p$ shell nuclei, and in particular to a four-particle, four-hole calculation of the semimagic nucleus ^{56}Ni .

1. Furman University, Greenville, S.C.
2. J. B. French, E. C. Halbert, J. B. McGrory, and S. S. M. Wong, *Advances in Nuclear Physics*, vol. 3, eds. M. Baranger and E. Vogt, Plenum Press, New York, 1969, pp. 193-257.
3. T. T. S. Kuo and G. E. Brown, *Nucl. Phys.* **A114**, 241 (1968).

EXTENSION OF THE CAPABILITIES OF THE SHELL-MODEL COMPUTER PROGRAMS

E. C. Halbert J. B. McGrory

The Oak Ridge-Rochester shell-model computer programs are being extended in two ways. At present, no more than six single-particle orbits can be active in any given calculation. Also, the upper half of the symmetric energy matrix to be diagonalized must fit into the computer core; this limits the size of the matrix which

can be handled on our present machines to approximately 750×750 . We are in the process of relaxing these two restrictions. The main shell-model program, which constructs and "diagonalizes" the model energy matrix, is being modified so that up to 30 different single-particle orbits can be treated at one time. The changes are being made so that if there is ever any conceivable reason for wanting more than 30 shells, only very simple dimension changes will be required to achieve this additional capability. The first application of the extended program will probably be to make detailed studies of collective multipole states in ^{16}O and ^{40}Ca , in a model space which includes all $2\hbar\omega$ excitations of 16- or 40-particle systems, and with spurious center-of-mass motion properly eliminated.

In order to relax the restriction that half the symmetric matrix must fit into the core, a program has been developed in the Computer Sciences Division which obtains the lowest few eigenvalues of arbitrarily large matrices. The method is a variation of the power method, wherein the principal operation is the calculation of the product of the matrix times a trial eigenvector. This method can be applied very conveniently by storing each row of the matrix on a disk and

then bringing each row into the core sequentially as the multiplication is effected. This program has already been applied to a test matrix of order 1200. Four converged eigenvalues and two converged eigenvectors were obtained in less than 5 min on the IBM 360 model 91 computer.

An integral part of the shell-model programs is the set of single-shell matrix elements which are read from precalculated tapes at execution. These tapes are lengthy, and it is often useful to generate special tapes which can be used more efficiently. The programs to generate these tapes have been appropriately revised so that they are now safely exportable, and they will be made available to the various groups now using the shell-model codes. Similarly, the auxiliary programs for calculating various electromagnetic transition rates are now being made readily "exportable."

SUPERCHARGED NUCLEI AND EXOTIC SHAPES

R. Y. Cusson¹ K. T. R. Davies²
 D. Kolb³ S. J. Krieger⁴
 C. Y. Wong

The collision of two very heavy nuclei may result in a compound system with excessive charge such that the fissility parameter x exceeds unity. We know that $x = 1.0$ is the limit of stability for spherical nuclei in the liquid-drop model. Some superheavy nuclei with x slightly greater than unity may be stable because of nuclear shell effects.⁵ What of other nuclei with different shapes? Would they be energetically more favorable? Are there also shell effects for these nuclei?

Our previous studies⁶ of toroidal and bubble shapes showed that indeed for x greater than about 1.05 a toroidal nucleus is energetically more favored than a spherical nucleus. As x increases to $x \geq 2.1$, a spherical bubble begins to be energetically more favored than a spherical nucleus. However, when one compares all three configurations, the toroid is still the one with the lowest energy as x exceeds 1.05. It was for this reason that Wheeler⁷ many years ago suggested that superheavy nuclei might be in the shape of a toroid. In the liquid-drop model, when these shapes are stable against expansion and contraction, they are unstable against various types of shape distortion. However, in the shell model, shells appear in the expansion and contraction degree of freedom. Simple calculations of the Strutinsky type show that the shell effects can in many cases be large enough to overcome the liquid drop instabilities and render the nucleus stable against expansional and contractional motion.

As the Strutinsky-type calculations we performed were qualitative in nature, we also studied such nuclei in a Hartree-Fock calculation.⁸ We found with the Nestor force⁹ that for those nuclei expected to have a density depression in the center, Hartree-Fock calculations indeed give such solutions. Similar solutions have been found with the Sprung-Banerjee interaction,¹⁰ the Rouben-Pearson-Saunier interaction,^{11,12} and the Kolb-Cusson-Schmitt interaction,^{13,14} but not with the Skyrme interaction,^{10,12,15} for which the nuclear incompressibility is large.

Another interesting subject related to the bubble nuclei is the density and shape of the mercury isotopes, for which an anomalous isotope shift between 185 and 187 has been reported.¹⁶ This shift was interpreted as possibly due to a change from a spherical to a deformed configuration¹⁶ or from an oblate to prolate deformation¹⁷ and could also be interpreted as the onset of a bubble configuration.¹⁸ The interpretation as the onset of large deformation is not without difficulty, as recent measurements of neighboring even-even nuclei show little change in the lowest two states for the isotopes from ²⁰⁰Hg to ¹⁸⁴Hg.^{19,20} We investigated¹⁴ the bubble configurations of these isotopes in the Brueckner reaction matrix formulation with the Kolb-Cusson-Schmitt interaction.¹³ Spherical solutions with a centrally depressed proton density have been obtained for all these isotopes and found to lie between 2 and 6 MeV higher than the ground oblate solution, while the nearby prolate solution comes down to within about 0.5 MeV of the ground oblate state for ¹⁸⁴Hg and ¹⁹⁶Hg (Fig. 1). The change in the rms radius between the oblate and the prolate solution in ¹⁸⁴Hg is, however, only about 1%, while the experimental change between ¹⁸⁵Hg and ¹⁸⁷Hg is about 2.5%. Thus, it appears that the interpretation of the anomalous isotope shift data depends strongly on the core polarization effect of the unpaired neutron.

The emergence of bubble structures at $x = Z^2/50A \geq 2.1$ has been considered in an energy density formalism²¹ and can be checked in the realistic single-particle K -matrix model.¹³ We have investigated²² several spherical extraheavy nuclei which are beta stable and stable under particle emission. These requirements so far have confined us to values of $x \approx 1.6$. Yet a significant central depletion was observed (Fig. 2). For example, ⁵⁷⁰₁₈₀X_H₃₉₀ shows a central proton depletion of 40%, while ⁶⁸⁰₂₂₀X_H₄₆₀ shows a 55% depletion. Note the persistence of shell effects which manifest themselves as density oscillations with a wavelength of about 3 F. We are presently investigating nuclei where the proton single-particle energy is positive but substan-

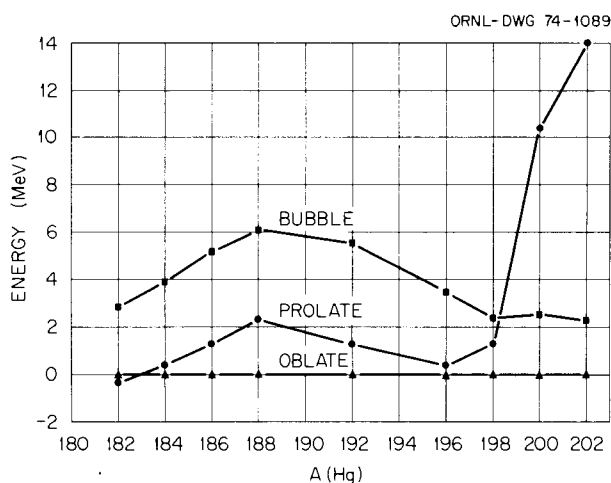


Fig. 1. Energies of the various minima relative to the oblate minima for different isotopes of mercury. Lines are joined between calculated points to guide the eyes only.

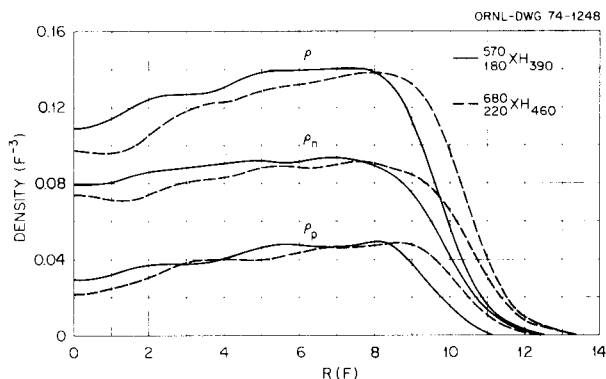


Fig. 2. Proton density, neutron density, and total density for extraheavy nuclei ${}_{180}^{570}\text{XH}_{390}$ and ${}_{220}^{680}\text{XH}_{460}$.

tially below the Coulomb barrier, in order to increase the fissility parameter and develop an explicit bubble structure. Although these species will exhibit beta decay and weak proton emission, the major decay models may still be fission modes. It remains to be seen whether shell effects can really stabilize these extraheavy nuclei.

For the toroidal nuclei, our previous liquid-drop model dealt with a toroid with a circular meridian.⁶ The meridian of a toroidal nucleus in equilibrium is not circular; it is elongated elliptically parallel to the symmetry axis. It is desirable to evaluate the shape of the meridian so as to determine more accurately when a toroidal shape begins to compete energetically with the spherical shape and how this additional degree of freedom would affect other instability properties. We

calculated^{2,3} this meridian from the equilibrium condition that the sum of the pressure due to surface tension and the potential must be constant over the surface of equilibrium. The potential and the shape are to be self-consistently related. Fortunately, our previous experience with the toroidal figures of equilibrium encountered in astrophysics²⁴ was helpful in providing most of the mathematical technique for such a solution. In particular, the evaluation of the potential and the potential energies for a toroidal figure is the same whether the interaction is gravitational or Coulombic. One eventually ends up with a second-order differential equation with volume conservation as a constraint. Detailed calculations are in progress.

1. Consultant to ORNL from Duke University, Durham, N.C.
2. On assignment at the Los Alamos Scientific Laboratory, September 1973 through August 1974.
3. Guest assignee to ORNL during summer 1973 from Duke University, Durham, N.C. Present address: Yale University, New Haven, Conn.
4. Consultant to ORNL from the University of Illinois at Chicago Circle, Chicago, Ill. Presently on leave to Oxford University, Oxford, England.
5. See, for example, M. Brack, J. Damgaard, A. S. Jensen, H. C. Pauli, V. M. Strutinsky, and C. Y. Wong, *Rev. Mod. Phys.* **44**, 320 (1972), and references therein.
6. C. Y. Wong, *Phys. Lett.* **41B**, 448 (1972); *Phys. Lett.* **41B**, 451 (1972); *Ann. Phys. (N.Y.)* **77**, 279 (1973).
7. J. A. Wheeler, private communication.
8. K. T. R. Davies, C. Y. Wong, and S. J. Krieger, *Phys. Lett.* **41B**, 455 (1972); K. T. R. Davies, S. J. Krieger, and C. Y. Wong, *Nucl. Phys.* **A216**, 250 (1973).
9. C. W. Nestor, K. T. R. Davies, S. J. Krieger, and M. Baranger, *Nucl. Phys.* **A113**, 14 (1968).
10. X. Campi and D. W. L. Sprung, *Phys. Lett.* **46B**, 291 (1973).
11. B. Rouben, J. M. Pearson, and G. Saunier, *Phys. Lett.* **42B**, 385 (1972).
12. G. Saunier, B. Rouben, and J. M. Pearson, preprint.
13. D. Kolb, R. Y. Cusson, and H. Schmitt, to be published.
14. D. Kolb and C. Y. Wong, to be published.
15. C. Y. Wong, to be published.
16. J. Bonn, G. Huber, H. J. Kluge, L. Kugler, and E. W. Otten, *Phys. Lett.* **38B**, 308 (1972).
17. A. Faessler, U. Götz, B. Slavor, and T. Lederberger, *Phys. Lett.* **39B**, 579 (1972).
18. P. Hornshøj, P. G. Hansen, B. Johnson, A. Lindahl, and O. B. Nielsen, *Phys. Lett.* **43B**, 377 (1973).
19. D. Proetel, R. M. Diamond, P. Kienle, J. R. Leigh, K. H. Maier, and F. S. Stephens, *Phys. Rev. Lett.* **31**, 896 (1973).
20. N. Rud, D. Ward, H. R. Andrews, R. L. Graham, and J. S. Geiger, *Phys. Rev. Lett.* **31**, 1420 (1973).
21. R. M. Krishnan and W. W. T. Pu, *Phys. Lett.* **47B**, 225 (1973).
22. R. Y. Cusson and C. Y. Wong, to be published.
23. C. Y. Wong, to be published.
24. C. Y. Wong, submitted to the *Astrophysical Journal*.

NUCLEI WITH DISCRETE SYMMETRIES

H. H. K. Tang¹ C. Y. Wong

If one takes Wheeler's 1937 molecular viewpoint² in nuclear structure to the extreme, one is led to construct a model of a nucleus consisting of superclusters ($A > 4$) with configurations satisfying point groups of higher symmetry. The validity of such a model for a light cluster such as an alpha particle has recently been reexamined.^{3,4} We are studying⁵ the single-particle states in a nucleus with tetrahedral symmetry. The symmetry of the configuration is exploited in selecting a set of harmonic oscillator basis states by employing group theoretical techniques. The single-particle potential is taken to be the sum of four Woods-Saxon potentials centered at the cluster points, and this potential is expanded in tetrahedral harmonics whose matrix elements can be easily evaluated with the basis functions. The single-particle Hamiltonian is diagonalized with the usual technique. Calculations are in progress.

-
1. Student guest at ORNL during summer and fall 1973 from Kalamazoo College, Kalamazoo, Mich.
 2. J. A. Wheeler, *Phys. Rev.* **52**, 1083 (1937).
 3. D. M. Brink, H. Friedrich, A. Weiguny, and C. W. Wong, *Phys. Lett.* **33B**, 143 (1970).
 4. International Conference on Clustering Phenomena in Nuclei (IAEA, Bochum, 1970).
 5. H. H. K. Tang and C. Y. Wong, to be published.

ASTROPHYSICS: TOROIDAL GALAXIES AND TOROIDAL STARS

S. D. Blazier¹ C. Y. Wong

As the gravitational and Coulomb interactions are identical except for a sign and a strength, our results on the Coulomb potential and Coulomb energy in a toroidal nucleus² find application directly in the investigation of the stability of a self-gravitating toroidal mass where the attractive gravitational force is balanced by the force due to centrifugal acceleration. Such an investigation³ is useful as the experience we gain can help in the development of similar problems in nuclear physics. Already, the technique we have developed in the astrophysical case has been incorporated in a more precise determination of the energies and shapes of toroidal nuclei around $x \sim 1.0$, as mentioned in another report.

The subject of the stability of a toroidal mass is also worthy of review. The last comprehensive theoretical

work was done in the last century,⁴⁻⁶ when approximate expansions were used and the effects of self-consistency of the potential and shape were not considered. On the other hand, there exist toroidal galaxies such as plates 146 and 147 of Arp's catalogue of peculiar galaxies.⁷ A toroidal star has also been inferred as the unseen component of epsilon Aurigae⁸ and suggested as the faint component of BM Orionis.⁹ Recent measurements on the neutral hydrogen,¹⁰⁻¹³ continuum radiation,^{1,4} emission nebulae,^{1,5} and mass distribution^{1,6} of galaxy M31 (Andromeda galaxy) also showed peculiar density distributions of a toroidal type. Toroidal structures have also been inferred¹¹ in a number of "normal spiral galaxies." Furthermore, Chandrasekhar^{1,7} and Bardeen^{1,8} showed recently that a flattened spheroid of equilibrium (Maclaurin spheroid) is unstable against distortions leading to a toroidal shape when the angular momentum is larger than a certain limit. It was therefore of interest to investigate whether toroidal figures of equilibrium play any role in the evolution of mass systems with large angular momenta and whether the observed toroidal mass is one step in their path of evolution.

Following Poincaré, Dyson, and Kowalewsky, we idealize for simplicity to a uniform and incompressible mass distribution rotating with respect to the central symmetry axis of the toroid. The angular velocity is assumed to be independent of position. The case where the toroidal mass is restricted to have circular meridians is first considered, since we already have the analytic solutions for the gravitational potential.² Next, the meridian is allowed to be flattened. The equilibrium configuration is then obtained in a self-consistent manner. We found that the set of toroidal figures of equilibrium forms a sequence which begins when the angular momentum L is given by

$$(25/12)(4\pi/3)^{1/3} L^2 \rho^{1/3} / GM^{10/3} = 0.8437(5).$$

The corresponding Maclaurin spheroid having such a critical angular momentum would have an eccentricity $e = 0.9817(1)$. The toroidal sequence and the Maclaurin sequence do not join on each other directly but are inferred to be connected by an unstable sequence with intermediate shapes. The properties of the toroidal sequence under beaded displacements, in which the toroid becomes thicker in some meridians but thinner in some others, is studied for two cases where the flow pattern is assumed known. Stability against these displacements is found to depend on the flow pattern, which is affected by the dissipative mechanism. Finally, we point out that evolution from a flattened disk to a

toroid with subsequent breakup provides a plausible scenario for the evolution of a rapidly rotating galaxy or star and may lead to the formation of multiplet galactic and stellar systems.

It is a simple matter to generalize our calculation to the case where there is a point mass located in the center of the toroid. Such a calculation is of interest as the mass in the nucleus of galaxy M31 is not completely zero but only about $1/2_0$ of the outer toroidal mass. Our result¹⁻⁹ shows that with a small central nucleus, there is an increase in the initial critical angular momentum of the toroid above which toroidal figures of equilibrium are possible.

In order to help in the identification of a toroidal star, if it ever exists, we evaluate the variation of luminosity when a precessing toroidal star eclipses itself.²⁻⁹ The star is idealized to be rotating rapidly so as to assume its proper toroidal figure of equilibrium, and the surface brightness is assumed to be uniform. The effect of limb darkening is properly taken into account. Our result indicates that for some combinations of precession and tilt angles, the light curves have double minima of equal magnitude, while for some other combinations, there appear secondary maxima inside the minima. These characteristics in the light curves are quite different from those of ordinary binary stars and allow simple identification of precessing toroidal stars.

1. Undergraduate student from the University of Tennessee, Knoxville, Tenn. in ORNL Cooperative Educational Program.
2. C. Y. Wong, *Ann. Phys. (N.Y.)* **77**, 279 (1973).
3. C. Y. Wong, submitted to the *Astrophysical Journal*.
4. H. Poincaré, *Bull. Astron.*, 1885.
5. F. W. Dyson, *Phil. Trans. Roy. Soc.* **184A**, 43 (1892); *Phil. Trans. Roy. Soc.* **184A**, 1041 (1893).
6. S. Kowalewsky, *Astron. Nachr.* **111**, 37 (1885).
7. H. Arp, *Atlas of Peculiar Galaxies*, California Institute of Technology Press, 1966.
8. R. E. Wilson, *Astrophys. J.* **170**, 529 (1971).
9. D. S. Hall, *Int. Astron. Union Colloquium* **15**, Bamberg, 1971, p. 217.
10. B. F. Burke, K. C. Turner, and M. A. Tuve, in Annual Report of the Director, Dept. of Terrestrial Magnetism, 1963-64, *Carnegie Institution of Washington Yearbook* **63**, p. 341.
11. M. S. Roberts, *Astrophys. J.* **144**, 639 (1966); M. S. Roberts, *Int. Astron. Union Symposium* No. 31, ed. H. Van Woerden, London, Academic Press, p. 189.
12. W. D. Brundage and J. D. Kraus, *Science* **153**, 411 (1966).
13. S. T. Gottesman, R. D. Davies, and V. C. Reddish, *Mon. Notic. Roy. Astron. Soc.* **133**, 359 (1966).
14. G. G. Pooley, *Mon. Notic. Roy. Astron. Soc.* **144**, 101 (1969).
15. H. Arp, *Astrophys. J.* **139**, 1045 (1963).
16. V. C. Rubin and W. K. Ford, *Astrophys. J.* **159**, 379 (1970).

17. S. Chandrasekhar, *Astrophys. J.* **142**, 1513 (1965); *Astrophys. J.* **147**, 3341 (1967).
18. J. M. Bardeen, *Astrophys. J.* **167**, 425 (1971).
19. C. Y. Wong, to be published.
20. S. D. Blazier and C. Y. Wong, to be published.

AN IMPROVED METHOD FOR CONSTRUCTING A FILTER FUNCTION FOR PROCESSING HIGH-COHERENCE ELECTRON MICROGRAPHS

T. A. Welton

Wiener¹ has given an elegant mathematical procedure for the processing of electrical signals, corrupted by transmission distortion and by addition of random noise, to obtain an optimum estimate of the uncorrupted input signal. As shown by the author,² this procedure offers a most attractive method of recovering object structure to spatial resolution of 1 Å (or better) from electron micrographs which, to the eye, would appear to contain only about 3 Å spatial information. This surprising recovery of spatial detail has been convincingly demonstrated by the author through the use of simulated micrographs,^{3,4} and the Oak Ridge High Coherence Microscope (described elsewhere in this report) is the culmination of a program aimed at practical realization of this theoretical possibility.

In order to facilitate the necessarily difficult transition from theoretical data to real data, a large amount of work has been done with simple micrographs, very carefully made with a conventional microscope.⁵ At the same time, several generations of computer programs have been produced and rather stringently tested. The experience thereby gained appears to be sufficiently extensive so that the high-coherence data, now beginning to appear, can be fully exploited.

In ref. 2 it is shown that the optical density in a micrograph [image function $I(\mathbf{x})$] for an electron microscope working in the phase-contrast mode is related to the object structure $O(\mathbf{x})$ by an integral equation of simple form

$$I(\mathbf{x}) = \int d\mathbf{x}' P(\mathbf{x} - \mathbf{x}') O(\mathbf{x}') + R(\mathbf{x}), \quad (1)$$

where R is a random function containing the counting errors and P is the point spread function determined by the instrumental parameters. Wiener's algorithm then states that the best linear estimate for $O(\mathbf{x})$ is

$$O(\mathbf{x}) = \int d\mathbf{x}' W(\mathbf{x} - \mathbf{x}') I(\mathbf{x}') \quad (2)$$

with

$$W(\xi) = \frac{1}{4\pi^2} \int d\mathbf{k} W(\mathbf{k}) e^{i\mathbf{k}\cdot\xi} \quad (3)$$

and

$$W(\mathbf{k}) = \frac{P(\mathbf{k})}{P^2(\mathbf{k}) + N^2(\mathbf{k})/S^2(\mathbf{k})}. \quad (4)$$

The quantity $P(\mathbf{k})$ is simply the Fourier transform of P , while $N^2(\mathbf{k})$ and $S^2(\mathbf{k})$ are "power spectra" of the noise function and the object function.

The functions $P(\mathbf{k})$ and $N(\mathbf{k})$ are simple concepts, but are not necessarily simple to evaluate, while $S(\mathbf{k})$ is elusive both in concept and value. Fortunately every properly obtained micrograph contains the information which determines whether processing will be useful, and further permits estimates of the above functions to be made. The simplest micrograph for this purpose is that

of a uniform (randomly deposited) thin carbon film, although it is devoid of external interest. Although films containing objects of interest have been studied, the results are more difficult to assess for reasons which will be apparent. Conventional electron microscopy yields much more satisfying pictures if a thin carbonaceous set of objects are embedded in a heavy, strongly scattering material (by vacuum evaporation, or by evaporation of a solution). If such pictures with enhanced contrast are used, the estimates of P , N , and S are badly confused by the distribution of scattering power between the heavy-metal atoms and the substrate carbon atoms. If, on the other hand, no enhancement is used, the contrast obtained usually is too low to allow a satisfactory signal-to-noise ratio, for purposes of computation by reasonably efficient available procedures.

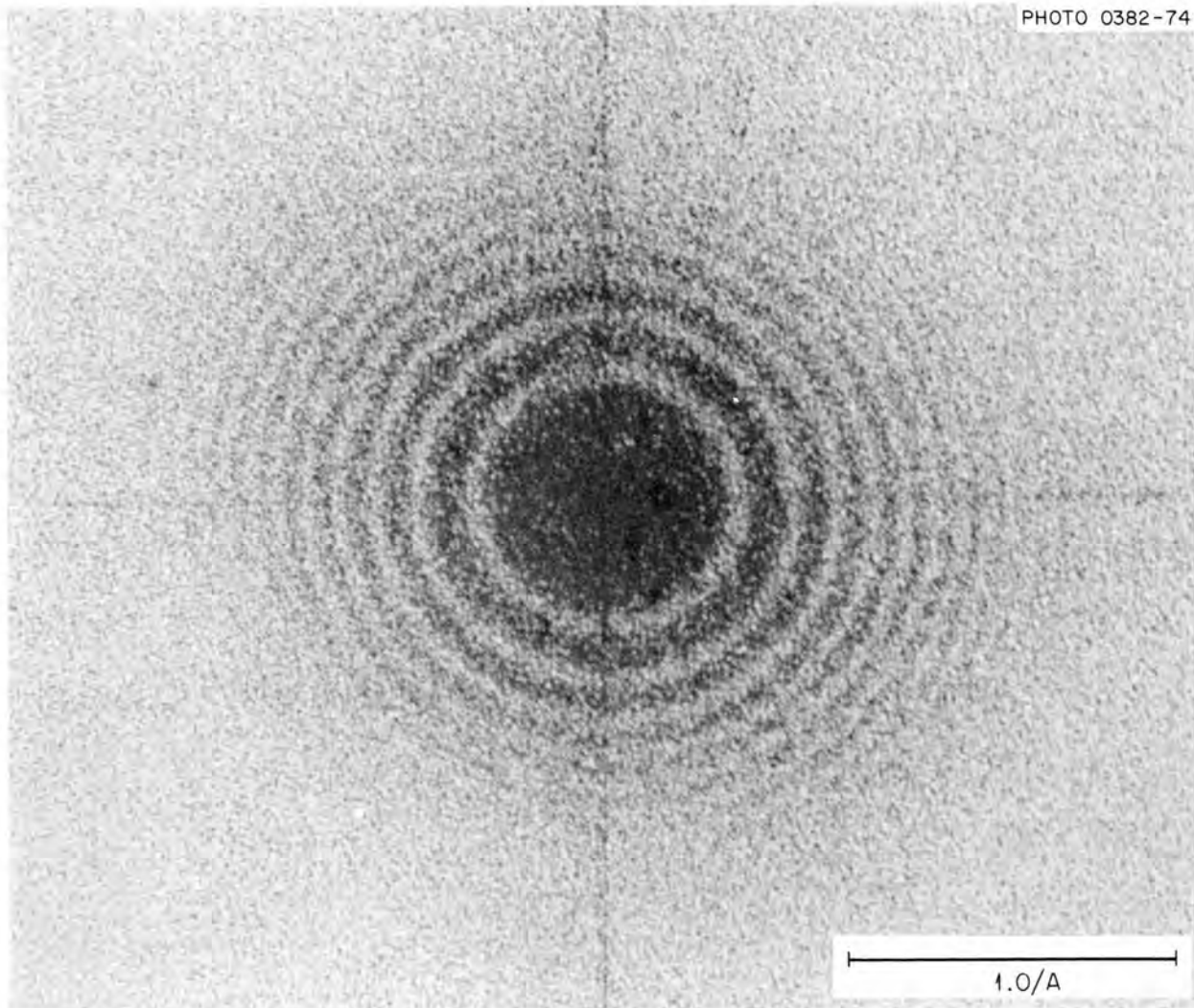


Fig. 1. Fourier transform of portion of micrograph.

A complete theory of the relation between microscope parameters and the function $P(\mathbf{k})$ has been given by the writer.² Unfortunately, these constants are not accurately known a priori, and must be determined from the micrograph itself. Schiske⁶ has described a nonlinear least-squares fitting procedure for carrying out this work, although the class of functions used was not actually broad enough to give good results for work with high-coherence micrographs. The writer has made extensive use of displays of $|I(\mathbf{k})|^2$, as computed from $I(\mathbf{x})$ (put into digital form by a scanning microdensitometer), or the equivalent Fraunhofer diffraction pattern (diffractogram) of the micrograph, to attempt to determine an analytic form for $P(\mathbf{k})$. Figure 1 shows such a display, derived from a micrograph, a portion of which is shown in Fig. 2. The sample is negatively stained (phosphotungstic acid) tobacco mosaic virus on a thin carbon film, and is not fully appropriate for our analysis, since the scattering power is strongly divided between carbon and tungsten atoms and the maximum phase shift is substantial. As will be seen, however, the measurement problems are much reduced by insertion of the heavy atoms.

The dark rings of Fig. 1 correspond to lines where $|P(\mathbf{k})|^2$ vanishes, since it can be shown that

$$\langle |I(\mathbf{k})|^2 \rangle = \langle |O(\mathbf{k})|^2 \rangle |P(\mathbf{k})|^2 + N^2(\mathbf{k}), \quad (5)$$

where the angle brackets indicate a roughly defined ("eyeball") smoothing of the display. As a plausible (but unrigorous) assumption, we equate $\langle |O(\mathbf{k})|^2 \rangle$ to $S^2(\mathbf{k})$. It can also be made plausible that for samples of not too pathological a structure,

$$S^2(\mathbf{k}) = S^2(0) \frac{|F(\mathbf{k})|^2}{|F(0)|^2} \quad (6)$$

where $F(\mathbf{k})$ is the electron scattering amplitude for momentum transfer $\hbar\mathbf{k}$ from a typical sample atom.

We can now find $N(\mathbf{k})$ for any \mathbf{k} near the center of a dark band by writing

$$N^2(\mathbf{k}) = \langle |I(\mathbf{k})|^2 \rangle_{\text{dark}}, \quad (7)$$

and N can presumably be estimated by interpolation at other points. In particular, it is known that $|P(\mathbf{k})|^2$ has

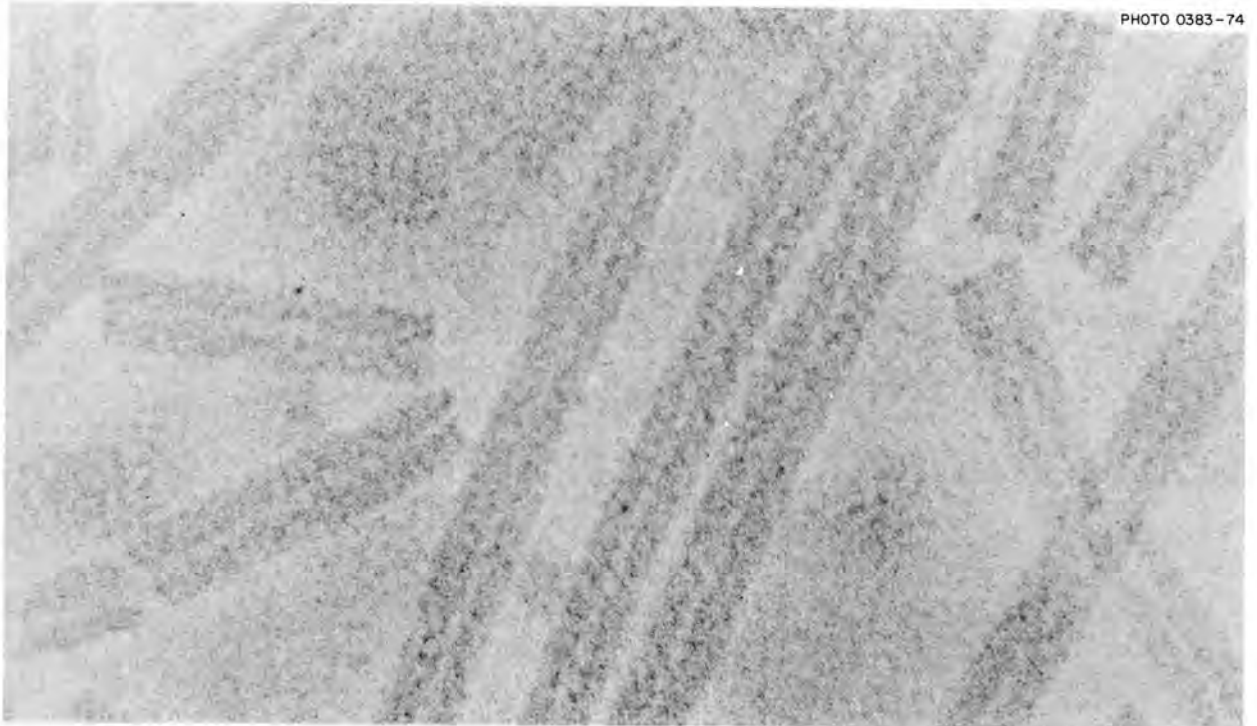


Fig. 2. Portion of micrograph of negatively stained tobacco mosaic virus.

unit value near the centers of the first few light rings (excluding the center of the central light area). Thus, $S^2(0)$ can be determined from

$$\langle |I(\mathbf{k}_n)|^2 \rangle = S^2(0) \frac{|F(\mathbf{k}_n)|^2}{|F(0)|^2} + N^2(\mathbf{k}_n), \quad (8)$$

where \mathbf{k}_n is any point on the center of the n th light ring. Since $F(\mathbf{k})$ is a known function, $\langle |I(\mathbf{k})|^2 \rangle$ is a known estimate from the noisy data, and $N(\mathbf{k})$ is obtained by interpolation from the adjoining dark rings, (8) gives a series of estimates for $S(0)$. The cleanest situation obtains when the first few of these estimates agree reasonably well, but if they do not, the first light ring should be used. Finally, using the fact that $P(\mathbf{k})$ is real, we have

$$P(\mathbf{k}) = \pm \left\{ \left[\langle |I(\mathbf{k})|^2 \rangle - N^2(\mathbf{k}) \right] \frac{|F(0)|^2}{|F(\mathbf{k})|^2} \right\}^{1/2} / S(0). \quad (9)$$

From its definition $P(\mathbf{k})$ will reverse sign as each dark ring is crossed, and the \pm must be so resolved.

In Fig. 3 is shown a renormalized logarithmic plot of the function $\langle |I(\mathbf{k})|^2 \rangle$ with the abscissa chosen proportional to k^2 and normalized so that a damped sinusoidal oscillation appears (only the peaks and valleys are shown). The points are noisy, but would be very much worse if averages around the rings had not been taken, in addition to a little radial averaging. A simple analytical function of a theoretically possible form for $P(\mathbf{k})$ was chosen so that (9) would be reasonably well satisfied, and the filtered picture was calculated by the Wiener algorithm, Eq. (4), and displayed as in Fig. 4. The result is not strikingly improved over the original, but some interesting enhancement has resulted.

In an attempt to obtain a cleaner test of the method, several samples were used which had no heavy elements present. Reasonable appearing diffractograms were obtained, but quantitative work of the type described above never gave a detectable peak-to-valley ratio to use in setting up $W(\mathbf{k})$. The difficulty appears to be in the weak signal arising from the presence of carbon atoms only. The diffractograms accordingly have too little contrast, and the crude averaging procedures described above seem inadequate to extract a useful result for $W(\mathbf{k})$.

To meet this problem, a computer realization has been written for a concept known in communications work as the "adaptive equalizer," which is simply a Wiener filter for an output signal voltage which adjusts itself to (or "adapts" to) the statistical properties of the signal.

In the case of image filtering, we do a simple filter operation on $|I(\mathbf{k})|^2$ to smooth it by an easily performed linear operation. Specifically, the autocorrelation function for $I(\mathbf{x})$ is first constructed by Fourier transforming $|I(\mathbf{k})|^2$. Thus

$$G(\xi) = \int d\mathbf{k} e^{i\mathbf{k} \cdot \xi} |I(\mathbf{k})|^2 \quad (10)$$

Finally, contributions to $G(\xi)$ for values of $|\xi|$ large enough so that $G(\xi)$ is down to noise level are excluded and an inverse transform performed. Thus

$$\langle |I(\mathbf{k})|^2 \rangle = \frac{1}{4\pi^2} \int d\xi F(\xi) e^{-i\mathbf{k} \cdot \xi} G(\xi). \quad (11)$$

The function $F(\xi)$ is zero for values of ξ such that

$$|\xi| \geq \xi_m$$

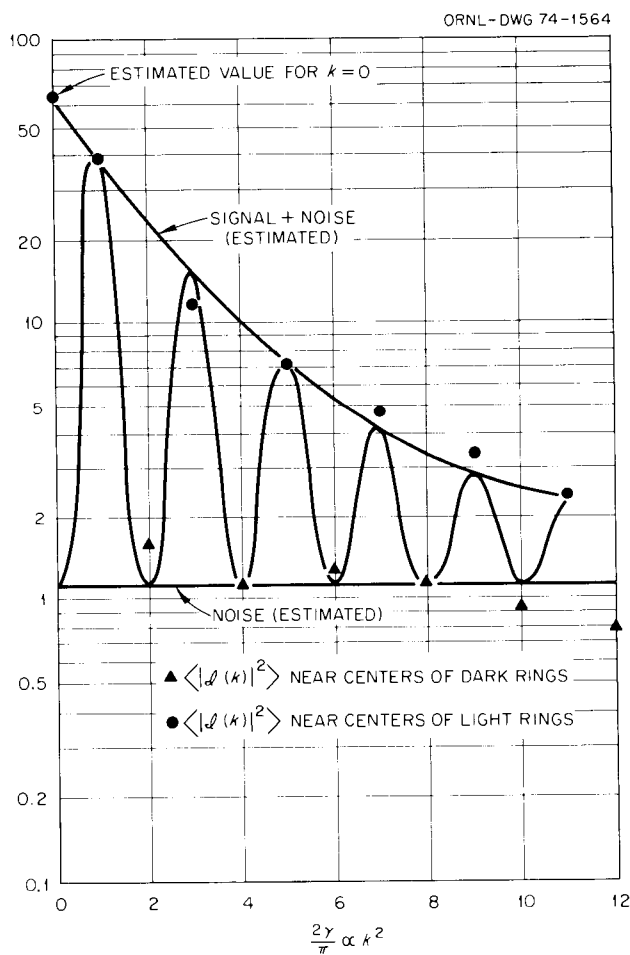


Fig. 3. Plot of $\langle |I(\mathbf{k})|^2 \rangle$.

PHOTO 0384-74



Fig. 4. Filtered micrograph.

and is unity inside this radius. A simple calculation shows that ξ_m should be roughly twice the transverse coherence length of the illumination system of the microscope. Following this rule, extraordinarily smooth and useful tabular representations of $\langle |I(\mathbf{k})|^2 \rangle$ have been obtained, an example being Fig. 5, from a micrograph which was apparently hopeless by the earlier techniques. It is anticipated that this algorithm will be of great value in processing high-coherence micrographs, where the diffractogram ring system becomes very complex and where use of heavy-metal stains will produce undesirable degradation of the performance potential of the microscope.

1. N. Wiener, *The Interpolation, Extrapolation, and Smoothing of Stationary Time Series*, John Wiley & Son, New York, 1949.

2. T. A. Welton, *Proceedings of Workshop Conference on Microscopy of Cluster Nuclei in Defected Crystals* (Chalk River, Canada, September 1971), CRNL-622-1, ed. by J. R. Parsons (1972).

3. T. A. Welton, in *Proceedings 29th Annual Meeting of Electron Microscopy Society of America, Baton Rouge, La., August 1971*, Claitor's Publishing Division, Baton Rouge, 1971, p. 94.

4. J. Frank, *Advanced Techniques in Biological Electron Microscopy*, Springer-Verlag, Berlin, Heidelberg, and New York, 1973, p. 242.

5. All micrographs used have been provided through the kindness of W. W. Harris of the Physics Division and Frances Ball of the Molecular Anatomy Program.

6. P. Schiske, in *Proceedings Fourth European Regional Conference on Electron Microscopy, Rome, 1968*, vol. 1, pp. 145-46.

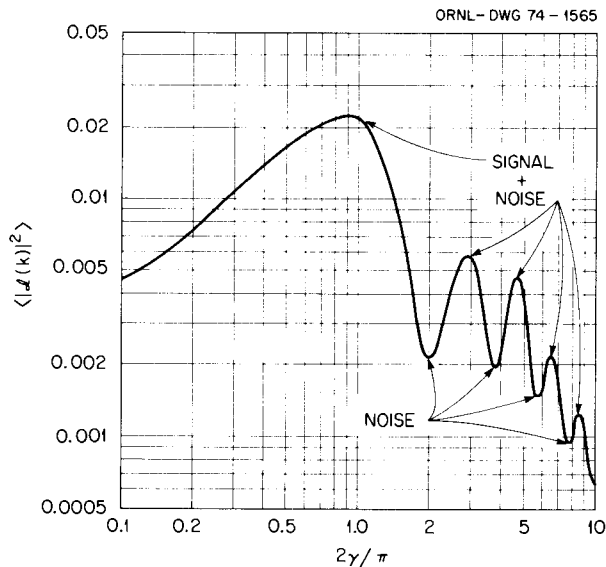


Fig. 5. Smoothed $\langle |I(\mathbf{k})|^2 \rangle$ for micrograph of a carbon film.

5. Status Report of the Nuclear Data Project

R. L. Auble	B. Harmatz	M. J. Martin
J. B. Ball	D. J. Horen	F. K. McGowan
F. E. Bertrand	H. J. Kim	W. T. Milner
Y. A. Ellis	D. C. Kocher ¹	S. Raman
W. B. Ewbank	M. B. Lewis	M. R. Schmorak

Introduction

The major effort of the Data Project during the calendar year 1973 has centered on the program to update the existing mass-chain compilations, many of which are out of date. This past year has seen a growing amount of time devoted to providing assistance to the NSF-NIRA Program in various forms as discussed below. The NIRA Program, now entering its third year, is beginning to make a significant impact on the "catch-up" compilation effort.

Although the evaluated nuclear structure properties, level schemes, etc., which are the end result of these compilations, are oriented toward workers doing basic research in nuclear physics, they also provide a base of knowledge that will prove increasingly important to many applied fields (breeder reactor technology, environmental monitoring, nuclear medicine, etc.). Thus, a strong effort is being made to establish the data base in a manner that will serve a wide variety of users and to provide, on request, special evaluations for applied programs. Currently, selected special compilations are being used as a testing ground for storage and retrieval of a computer-based data bank which has grown from the production of *Nuclear Data Sheets*. When fully implemented, this data base will provide a very flexible system to provide special information to both basic and applied programs. Already in operation is a computerized bibliographic reference system which can be searched to provide special reference lists for specific nuclei, specific reactions, etc. Some of these points are discussed in more detail below.

Revised A-Chains

During the calendar year, 30 evaluated mass chains were prepared, in photoready form, for publication in *Nuclear Data Sheets*.

A = 71, K. R. Alvar¹
A = 72, K. R. Alvar¹
A = 77, P. P. Urone,¹ L. L. Lee, Jr.,² and S. Raman
A = 94, D. C. Kocher¹
A = 97, L. R. Medsker¹
A = 98, L. R. Medsker¹
A = 100, D. C. Kocher¹
A = 101, R. R. Todd,¹ W. H. Kelly,³ F. M. Bernthal,³
and W. C. McHarris³
A = 124, F. E. Bertrand
A = 126, R. L. Auble
A = 128, R. L. Auble
A = 141, R. L. Auble
A = 142, J. F. Lemming¹ and S. Raman
A = 153, L. A. Kroger¹ and C. W. Reich⁴
A = 157, J. K. Tuli¹
A = 159, J. K. Tuli¹
A = 164, A. Buyrn¹
A = 165, A. Buyrn¹
A = 168, L. R. Greenwood¹
A = 169, B. Harmatz
A = 174, M. M. Minor¹
A = 181, Y. A. Ellis
A = 188, M. R. Schmorak
A = 190, M. R. Schmorak
A = 191, M. B. Lewis
A = 192, M. R. Schmorak
A = 213, C. Maples¹
A = 217, C. Maples¹
A = 221, C. Maples¹
A = 225, C. Maples¹

Recent References

Bibliographic data on publications dealing with all aspects of nuclear structure properties are stored in a computer-retrievable system. Existing programs are capable of searching this system to provide specialized lists of references. This system is used to prepare a list of new entries, ordered by A-value and specific isotope, of articles appearing in recent journals and reports, etc. Such a list is published three times a year as part of

Nuclear Data Sheets. This year a section has been added which tabulates references according to specific nuclear reactions studied. Such lists demonstrate very clearly the potential utility of the computerized reference system.

“Recent References (September 1972–December 1972),” D. C. West, W. B. Ewbank, F. W. Hurley, and M. R. McGinnis

“Recent References (January 1973–April 1973),” W. B. Ewbank, F. W. Hurley, and M. R. McGinnis

“Recent References (May 1973–August 1973),” R. N. Dietrich, W. B. Ewbank, F. W. Hurley, and M. R. McGinnis

National Science Foundation–Nuclear Information Research Associate (NIRA) Program

The NIRA Program completed its second year in October 1973 and has entered into its third and final year. The program has involved some 21 postdoctoral appointments, most working under a university sponsor, preparing mass-chain evaluations in the $A > 45$ region. The Data Project has participated by supplying references, reviewing and editing compilations, consulting (in some cases coauthoring), and publishing in *Nuclear Data Sheets*. By January 1, 1974, this program had resulted in 20 published A-chains, 7 more A-chains in print, 6 being readied for publication, and 16 A-chains in various stages of review. Some 45 A-chains remain to be evaluated of those originally assigned to the NIRA Program.

Special Compilations

These compilations usually are of two types. In the first, a special evaluation may be prepared to answer specific interests of a requester – often this may be from an applied field that requires a special treatment or special presentation of the data. An example of this is the *Supplement to Radioactive Atoms*,⁵ which summarized nuclear and atomic data for 15 nuclear species of particular importance in monitoring gaseous effluents from nuclear reactors. This compilation was prepared in response to a request from the Regulatory Branch of the USAEC. Presently, an evaluation is being prepared in response to a similar request for information on some 85 additional radioisotopes. Also under preparation, for inclusion in a forthcoming handbook of the National Bureau of Standards, is a summary of decay properties of 190 nuclei of special interest for nuclear medicine and industrial applications.

The second type of special compilation deals with correlating a specific nuclear property over a wide range of nuclei and is generally termed a “horizontal” compilation. Two examples of such a compilation were published during the past year. One of these dealt with log ft values and rules for deriving spin-parity assignments,⁶ and the other presented a comparison of theoretical and experimental $E3$ and $M4$ conversion coefficients.⁷ Currently in progress is a compilation of $B(E2)$ values for exciting the lowest 2^+ levels of all even-even nuclei.

Research Papers, Verbal Presentations, Etc.

Several members of the Data Project participate actively in the research program of the division. Writeups of this work are included elsewhere in this annual report. From these activities, there resulted 11 papers submitted for publication and 19 papers presented at scientific meetings (4 of these being invited talks).

Nuclear Level Schemes

A collection of the level scheme figures taken from *Nuclear Data Sheets* was prepared as a separate volume summarizing level scheme information for nuclei from $A = 45$ to 257 and published in book form by Academic Press.

Charged-Particle Reaction Data

A reaction list for charged-particle-induced nuclear reactions has been prepared from the journal literature for the period from July 1972 through June 1973. Each published experimental paper is listed under the target nucleus in the nuclear reaction with a brief statement of the type of data in the paper. The nuclear reaction is denoted by $A(a,b)B$, where $M_a \geq 1$ (one nucleon mass). There is no restriction on energy. Nuclear reactions involving mesons in the outgoing channel are not included. Theoretical papers which treat directly with the analysis of nuclear reaction data and results are included in the reaction list. These reaction lists, which were originally published in *Nuclear Data Tables A*, will in the future appear in *Atomic Data and Nuclear Data Tables*, a journal published by Academic Press.

Professor H. Ikegami of Osaka University recently made a study of the usefulness of *Nuclear Data Tables A*. From a sample of 23 leaders in experimental nuclear spectroscopy and reaction physics, Professor Ikegami found that 62% of the nuclear physicists had used the reaction lists for charged-particle-induced nuclear reac-

tions and that 22% made frequent use of the reaction lists.

A reaction list summarizing the charged-particle-induced nuclear reaction data appearing in the literature from 1948 through June 1971 was prepared and published in the *Reprint Series of Atomic and Nuclear Data*.

The cross-section data file (3×10^5 cross sections) has been maintained, and cross-section data were supplied to the following requests: Cyclotron Lab at Harvard University, Stanford, Rochester, Princeton, Rutgers, and New Mexico Universities, Los Alamos,

BNL, Jet Propulsion Lab, Ohio State University Hospital, Massachusetts General Hospital, Karlsruhe, Aktiebolaget Atomenergi Sweden, and CTR Division of AEC.

-
1. Nuclear Information Research Associate (NIRA).
 2. State University of New York at Stony Brook, Stony Brook, N.Y.
 3. Michigan State University, East Lansing, Mich.
 4. National Reactor Testing Station, Idaho Falls, Idaho.
 5. M. J. Martin, ORNL-4923 (1973).
 6. S. Raman and N. B. Gove, *Phys. Rev. C7*, 1995 (1973).
 7. S. Raman, T. A. Walkiewicz, R. Gunnink, and B. Martin, *Phys. Rev. C7*, 2531 (1973).

6. High Energy Activities

H. O. Cohn R. D. McCulloch¹ W. M. Bugg² G. T. Condo² E. L. Hart³

Introduction

This past year the high-energy physics group has been analyzing data from several bubble chamber experiments: (1) π^+D interaction at 8 GeV/c obtained with the BNL 80-in. bubble chamber, (2) interaction of stopping \bar{p} and K^- in carbon, titanium, tantalum, and lead plates placed inside the 30-in. BNL hydrogen bubble chamber, and (3) γ -D interaction at 3 GeV/c, film obtained at SLAC with the laser beam and 82-in. bubble chamber. We have also obtained new film which is being scanned and measured at the present time: (1) 8-GeV/c π^- on hydrogen in the 82-in. SLAC bubble chamber and (2) 15-GeV/c π^+ on deuterium in the same chamber.

Further, we have been actively involved in a hybrid PWC—bubble-chamber experiment at NAL. Our contribution to this collaborative effort has concentrated in two areas. We have built and installed the 16 downstream 1-ft-square wire proportional counters, and we have written several computer programs for the survey and analysis problems.

Proposals for future experiments have been submitted to accelerator review committees.

Investigation of Nuclear Periphery of Heavy Elements

In October 1971, we received a 100,000-picture exposure of the BNL 30-in. hydrogen bubble chamber fitted with thin flat plates of carbon, titanium, tantalum, and lead. The incident beam was \bar{p} 's (70,000 pictures) and K^- mesons (30,000 pictures) with the entrance momenta at the chamber selected to maximize the number of incident particles stopping in the plates. Both experiments have been completed during the past year.

The analysis of the \bar{p} data⁴ indicated that as Z of the target increases, the ratio of $\bar{p}n$ to $\bar{p}p$ interactions increased more rapidly than the neutron-to-proton

ratio. Since it has been well documented that the nuclear absorption of slow heavy negative particles occurs far out in the nuclear fringe,⁵ our experiment constitutes the most conclusive evidence, to date, for the existence of a neutron halo in heavy nuclei. The hypothesis of a neutron-rich nuclear surface in heavy elements had first been put forth by Johnson and Teller⁶ in 1954.

The analysis of the K^- data⁷ reached virtually the same conclusion as did that of the \bar{p} data with respect to the existence of a neutron fringe in the heavy nuclei. The only significant discrepancy between the two bodies of data concerned tantalum, for which the K^- experiment implied a much stronger neutron halo than did the \bar{p} data. We have subsequently suggested⁸ that this could well be due to a substantial amount of interior (as opposed to peripheral) capture by the tantalum nucleus. The large quadrupole moment of tantalum, presumably, could sufficiently alter the atomic capture so that the capture occurs in the more central regions of the tantalum nucleus.

In the future, we plan a systematic study of the interaction products from the K^- and \bar{p} interactions in the four elemental plates. Since the nucleus with which the K^- or \bar{p} interacts is unambiguously known, such quantities as the pion momentum spectra from the \bar{p} interactions in each element, the dependence of the K^- multinucleon reaction rate on nuclear size, the rate of heavy hyperfragment production from K^- interactions, etc., should be of interest.

Earlier plans to repeat these experiments with different targets have run afoul since no chambers exist which have access to slow beams of heavy negative particles.

π^+D Interaction at 7.87 GeV/c

The data consist of 305,000 pictures taken over an extended period (starting in 1968 and ending in 1973).

Collaborators are from the University of Cincinnati and, in the early stage, from BNL.

This experiment has yielded five articles,⁹⁻¹³ and several others are in various stages of preparation. Evidence suggesting that the four-pion decay of the f^0 (1260) was nonexistent with an upper limit of 3.3% of the dipion decay at 90% confidence limit was published.¹³ In addition, $\rho\Delta$ production in π^+D was found to be inconsistent with isovector exchange. This could imply the importance of exotic exchange to the $\rho\Delta$ production process. Other $\rho\Delta$ production data were examined, and we find that inconsistencies with isovector exchange are not uncommon.

Currently we are investigating our data for evidence of the $\omega\pi\pi$ decay modes of the A_2 and ϕ (1660) mesons. While voluminous ω production is observed in the 5π channels ($\pi^+n \rightarrow \rho\pi^+\pi^+\pi^-\pi^0$), our data do not appear to be consistent with the large branching ratios recently reported for the $\omega\pi\pi$ channel.¹⁴

γ -D Interactions at 3 GeV/c

Measurement of about 13,000 events obtained in an exposure of a polarized 3-GeV/c gamma beam to the SLAC deuterium-filled 82-in. bubble chamber has been completed this past year. Analysis of the data is under way. Due to a malfunction of the film clamping mechanism in the cameras, an exposure obtained earlier has been rejected from inclusion in the analysis. If in the future we can ascertain which photographs were distortion free (by measuring all the fiducials), we may be able to improve the statistics of this experiment. A systematic survey of medium-energy γ -D interaction will be done. We will also study the nondiffractive ρ photoproduction and investigate the contribution of exotic exchange to Δ isobar formation.

Hybrid PWC-Bubble-Chamber Experiment

We are members of a consortium that has proposed to study very high energy phenomena at NAL with a hybrid system of wire proportional counters (PWC) and the 30-in. bubble chamber. Our contribution to date has been in (1) design and construction of the downstream PWC counters and (2) data analysis and programming for track reconstruction through the system. The counters built at ORNL consist of sixteen 1-ft-square active area counters with wire separation of 2 mm. These are placed in groups of three at 120° in four separate enclosures, to be placed at various distances downstream from the bubble chamber. Some of the units are staggered to form effective 1-mm wire spacing

counters. Analysis has been completed of test runs at NAL in the proportional wire chamber-30-in. bubble chamber hybrid system. Run 1 (16,000 200-GeV protons, 5000 bubble chamber pictures) was conducted prior to installation of the final downstream PWC chambers. For run 2 (2,000 300-GeV protons) the entire downstream PWC system had been installed, but no bubble chamber pictures were obtained. Beam tracks have been used to locate the PWC chambers and to connect the PWC coordinate system to the bubble chamber system. The average plane efficiency for the downstream counters in a test run with π^- at 150 GeV has been found to be 99.5%. This compares favorably with the 99.3% design efficiency, meaning that such efficiency is of acceptable level for track reconstruction through the system. The PWC system has been used as a moderately high resolution spectrometer for determination of the momentum of the beam. Momentum resolution is approximately $3/4\%$ for run 1 and improves by a factor of 3 with the complete downstream system in place.

New Experiments

As part of a larger exposure of 8-GeV/c π^- to the 82-in. hydrogen bubble chamber, we have obtained 800,000 pictures, in a run completed in July 1973. This run was in collaboration with MIT and Tohoku University. We will measure all events on our one-third share of this film and provide the data to our collaborators in return for their data. A few thousand events have already been measured on the spiral reader. We will investigate possible isovector exchange violations by selecting reactions where isoscalar exchange or diffractive production is excluded, thus avoiding pitfalls encountered in invoking such violations to explain the observed ratios of ρ and A_2 production off nucleons. The experiment also will yield a high-statistics study of the A_2^- production, which is of interest in the light of the A_2 splitting controversy.

-
1. Mathematics Division.
 2. Consultant to ORNL from the University of Tennessee, Knoxville, Tenn.
 3. Guest assignee to ORNL from the University of Tennessee, Knoxville, Tenn.
 4. W. M. Bugg, G. T. Condo, E. L. Hart, and H. O. Cohn, *Phys. Rev. Lett.* **31**, 475 (1973).
 5. E. H. S. Burhop, in *High Energy Physics*, ed. by E. H. S. Burhop (Academic, New York, 1969), vol. III, p. 228.
 6. M. H. Johnson and E. Teller, *Phys. Rev.* **93**, 357 (1954).
 7. W. M. Bugg, G. T. Condo, E. L. Hart, and H. O. Cohn, *Nucl. Phys.* **B64**, 29 (1973).

8. W. M. Bugg, G. T. Condo, E. L. Hart, and H. O. Cohn, *Phys. Rev. C* (to be published).
9. A. M. Cnops, P. V. C. Hough, F. R. Huson, I. R. Kenyon, J. M. Scarr, I. O. Skillicorn, H. O. Cohn, R. D. McCulloch, W. M. Bugg, G. T. Condo, and M. M. Nussbaum, *Phys. Rev. Lett.* **21**, 1609 (1968).
10. A. M. Cnops, P. V. C. Hough, F. R. Huson, I. R. Kenyon, J. M. Scarr, I. O. Skillicorn, H. O. Cohn, R. D. McCulloch, W. M. Bugg, G. T. Condo, and M. M. Nussbaum, *Phys. Lett.* **29B**, 45 (1969).
11. I. R. Kenyon, J. B. Kinson, J. M. Scarr, I. O. Skillicorn, H. O. Cohn, W. M. Bugg, G. T. Condo, and M. M. Nussbaum, *Phys. Rev. Lett.* **23**, 146 (1969).
12. W. M. Bugg, G. T. Condo, E. L. Hart, H. O. Cohn, R. D. McCulloch, M. M. Nussbaum, R. Endorf, and C. P. Horne, *Phys. Rev.* **6D**, 3047 (1972).
13. W. M. Bugg, G. T. Condo, E. L. Hart, H. O. Cohn, R. D. McCulloch, R. J. Endorf, C. P. Horne, and M. M. Nussbaum, *Phys. Rev.* **7D**, 3264 (1973).
14. J. Diaz et al., *Phys. Rev. Lett.* **32**, 260 (1974).

7. Electron Spectroscopy Program

INTRODUCTION

T. A. Carlson

In the last few years the use of electron spectroscopy for the study of chemical bonding and as an analytical tool has grown enormously. The field of electron spectroscopy was born out of the needs of basic research in physics. It has been our principal goal to extend the usefulness of electron spectroscopy, in part by improvements in technology but in the main through the expansion of its phenomenological basis. For example, in the more detailed reports given below we (1) have tried to develop the quantitative use of photoelectron data and (2) have examined the relationship between satellite structure in photoelectron spectroscopy and chemical bonding. In addition, a number of explorative studies have been carried out to evaluate the possible uses of electron spectroscopy for applied problems. Our purpose has been to build bridges between basic and applied science and to be responsive to specific needs in the laboratory. This is a two-way street. Not only have we helped to supply answers, but the questions have stimulated new areas of research.

A secondary goal of our program has been the long-standing interest in the basic nature of excitation and ionization. This goal is joined with our primary goal when satellite lines in x-ray photoelectron spectroscopy are studied. In addition to the report given below on solids, measurements have been carried out on gases. Work on satellite lines in the x-ray photoelectron spectroscopy of the rare gases was completed last year and will appear soon as a publication.¹ To accompany these studies, calculations² on the total amount of electron shake-up plus shake-off were carried out for each subshell of the rare gases. Satellite structure in some simple free molecules has also been studied.³

Contributions during the year for exploration of applied uses include the following: (1) The evaluation of x-ray photoelectron spectroscopy and Auger electron spectroscopy for analysis of particulates in the air was completed.⁴ (2) Various samples of coal were examined by x-ray photoelectron spectroscopy, with particular emphasis on the analysis of the oxidation state of sulfur, which for the most part was found to be consistent with that expected for organic heterocyclics, although sulfate was found in some samples. The use of x-ray photoelectron spectroscopy in coal research would appear to have a substantial potential. (3) The binding-energy shifts of nitrogen in morphine and morphine derivatives were determined in order to evaluate molecular orbital calculations.⁵ Large chemical shifts were noted between the free bases and the corresponding salts, while only small shifts were observed between the various protonated species, in confirmation of calculated electron densities. (4) Assistance was given the Analytical Chemistry Division⁶ in corrosion studies of a ten-year-old smokestack which had spontaneously disintegrated. With the combination of x-ray photoelectron spectroscopy and scanning electron microscopy, it was determined that the intergranular boundaries consisted of silicon, in the form of silicides and silicates, and sulfur in the form of sulfates. (5) Preliminary

studies⁷ are in progress for the possible use of electron spectroscopy in the thermonuclear program. In particular it is desired to learn about surface emanation of ions from the containment walls that could poison the hot plasma.

1. D. P. Spears, H. J. Fischbeck, and T. A. Carlson, *Phys. Rev. A* (in press).
2. T. A. Carlson and C. W. Nestor, Jr., *Phys. Rev. A* 8, 2887 (1973).
3. D. P. Spears, thesis, University of Oklahoma (1974).
4. W. J. Carter III, G. K. Schweitzer, T. A. Carlson, L. D. Hulett, and B. Fish (to be published).
5. This work was carried out in collaboration with W. S. Koski and J. Kaufman of the Johns Hopkins University.
6. In collaboration with L. D. Hulett, Analytical Chemistry Division.
7. In collaboration with C. F. Barnett, Thermonuclear Division.

QUANTITATIVE MODEL FOR ESCA

W. J. Carter III¹ T. A. Carlson
G. K. Schweitzer²

The use of x-ray photoelectron spectroscopy has developed in recent years into an important analytical tool. It is frequently known by the acronym ESCA (electron spectroscopy for chemical analysis). By the use of monochromatic x rays (for example, aluminum and magnesium $K\alpha$ x rays of respectively 1487 and 1254 eV), photoelectrons can be ejected from the core shells of atoms. An electron spectrometer may be used to determine the kinetic energy of these photoelectrons, from which measurement the binding energies can be evaluated. Since the core binding energies are characteristic of the atom, x-ray photoelectron spectroscopy provides a means for elemental analysis. ESCA has three important properties: (1) It can measure any element that has a core shell, which is to say all elements of $Z > 2$. (2) The ejected photoelectrons have a small mean free path in solids, the order of 10 to 20 Å, and thus the analysis deals with the surface and near-surface layers of solids. (3) Changes in the chemical environment cause slight shifts in the binding energy of the core shell electrons. These shifts can be interpreted in terms of the electrostatic potential that surrounds each atom, which in turn is related to the oxidation state and nature of the chemical bonding.

Though much attention has been paid to the photoelectron energies and their use in qualitative analysis, there has been relatively only a small effort expended in using the intensities of the photoelectron peaks for quantitative analysis.^{3,4} By means of a simple model, we have employed recent calculations of Scofield⁵ on atomic photoelectron cross sections to determine the relative atomic percent from photoelectron spectra of a homogeneous solid.

Simple Model for Quantitative Analysis

Figure 1 shows schematically the basic problems involved in the use of x-ray photoelectron spectroscopy for quantitative analysis. First, it must be realized that the mean free path for kilovolt x rays in matter is several orders of magnitude greater than for the ejected photoelectrons. Thus, the depth to which the sample is studied is determined by the probability for an electron escaping without inelastic collisions, and the x-ray beam is essentially unattenuated over the escape depth. The probability for photoejecting an electron from a given subshell per unit volume is

$$N_0 = \sigma n F, \quad (1)$$

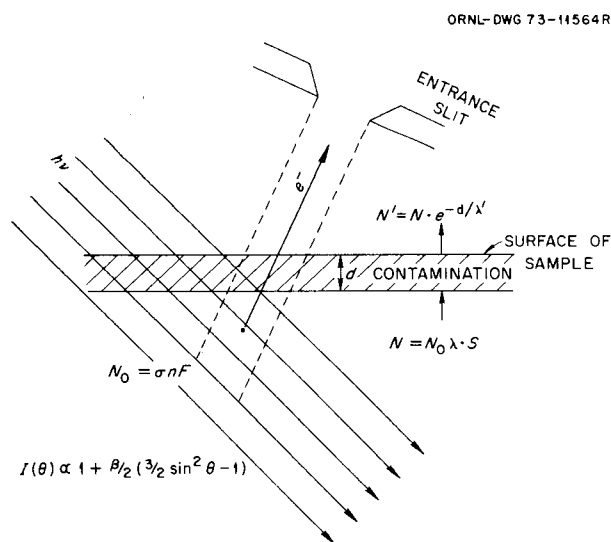


Fig. 1. Schematic representation of problems involved in quantitative evaluation of x-ray photoelectron spectroscopy of solids. See text for description of symbols. If sample is homogeneous without contamination layer, $e^{-d/\lambda'} = 1$.

where σ is the photoelectron cross section for a given subshell of a given element, F is the x-ray flux, and n is the concentration of the element in terms of atoms per unit volume.

Second, the angular distribution of the photoelectron needs to be considered. This is given by

$$N(\theta) = 1 + \frac{\beta}{2} \left(\frac{3}{2} \sin^2 \theta - 1 \right), \quad (2)$$

where θ is the angle between the direction of the photon beam and the direction of the ejected photoelectron. The angular parameter, β , can vary from -1 to $+2$ and is dependent on the photoelectron energy and the nature of the atomic orbital. Manson⁶ has made comprehensive calculations of β as a function of element. At higher photoelectron energies, this value approaches an asymptotic value for a given angular momentum, and corrections for relative intensities measured at a fixed angle are not large. For example, the intensity integrated over all angles to that measured at 90° is about 10% higher for p orbitals than for s orbitals. In solids the angular correction is reduced by the leveling effect of elastic collisions. To remove the angular effect, one may measure the intensity at 54.7° , at which angle the intensity is independent of β . Our simple model assumes that any problem related to angular distribution has been corrected.

Third, the probability for escape of the electron from the material must be considered. It requires that the photoelectron emerges without any energy loss due to an inelastic collision, passes through the spectrometer, and is detected, which leads to

$$dN = N_0 e^{-x/\lambda} dx \cdot S,$$

where $1/\lambda$ is the reciprocal of the mean free path, or the cross section for inelastic scattering, x is the distance below the surface, and S is the spectrometer factor. The total signal integrated from the surface to an infinite depth is

$$N = \int_0^\infty N_0 e^{-x/\lambda} dx = \lambda \cdot \sigma n F \cdot S. \quad (3)$$

The relative intensity for two different photoelectron peaks from the same sample is

$$\frac{N_1}{N_2} = \frac{\sigma_1 n_1 \lambda_1 S_1}{\sigma_2 n_2 \lambda_2 S_2}. \quad (4)$$

From empirical observations the mean free path, λ , over the energy range of interest to ESCA (100 to 1500 eV) is approximately

$$\lambda \propto \sqrt{E},$$

where E is the kinetic energy of the electron.

For a given spectrometer the spectrometer factor will be the same except for a possible dependence on the kinetic energy of the ejected electron. This energy dependence can usually be determined. In our spectrometer, which is an electrostatic analyzer without predeceleration, the intensities need only be corrected by dividing by the window width, E . Our simple model for quantitative analysis in ESCA assumes that the energy dependence of the spectrometer coefficient has been accounted for and $S_1 = S_2$. The object of the calculation is to obtain the expected intensities in the photoelectron spectra for equal molar concentration, so that $n_1 = n_2$. The choice of elements and subshell for a standard is arbitrary, and we have chosen the 1s peak of carbon. The final form of the calculation thus becomes

$$\frac{N_{Z,nl}}{N_{C,1s}} = \frac{\sigma_{Z,nl} \sqrt{h\nu - E_B(Z, nl)}}{\sigma_{C,1s} \sqrt{h\nu - 285}}, \quad (6)$$

where $N_{Z,nl}$ is the integrated intensity of the photoelectron peak associated with subshell nl of element Z , $h\nu$ is the x-ray energy, and E_B is the binding energy of the atomic orbital, which has been taken from an experimental collation of Siegbahn.⁷

The photoelectron cross sections used in Eq. (6), $\sigma_{Z,nl}$, have been calculated by Scofield.⁵ His calculations are based on relativistic Hartree-Fock-Slater wave functions and are for each subshell of each atom. The values should be reliable so long as one is not too close to the threshold for photoionization, a condition which has been avoided in the use of Eq. (6). The calculated cross sections were checked by studying the relative intensities of photoelectric peaks observed in the gas phase of some simple molecules, and agreement between experiment and theory was found to be satisfactory.

Results of Calculations for Quantitative Analysis

Using Eq. (6), we have calculated the relative intensities expected for photoelectron peaks for at least one subshell of every element from $Z = 3$ to 92 for both aluminum $K\alpha$ and magnesium $K\alpha$ x rays. For example,

Fig. 2 gives the ratios for aluminum $K\alpha$ radiation. The subshells chosen for calculations are those most likely to be used in ESCA. This frequently means that the subshells have the highest angular momentum for a given principal quantum number. This is so because vacancies in such orbitals cannot be filled by Coster-Kronig transitions, which can drastically shorten the half-life of such states and thus broaden the photoelectron peak. To effect a quantitative analysis, the measured photoelectron intensities for different elements in a homogeneous sample need only be divided by ratios such as given in Fig. 2.

In Table 1 are listed the relative intensities for elements in different solid compounds as determined from experimentally determined ratios of photoelectron intensities for known compounds, together with ratios calculated from Eq. (6). Although some scattering occurs among the different data, agreement between theory and experiment is quite satisfactory.

Chemical Effects and Inhomogeneity

The simple model as seen above would appear to give a reasonable basis for quantitative analysis. In the future, improvements in both theory and experiment ought to be obtainable, but there are intrinsic diffi-

culties which will prevent ultimate agreement of better than about 5%. For example, it has been noted that the intensities of photoelectron peaks of the same element separated by chemical shifts do not always follow the stoichiometric formula.⁸ This has been attributed to differences in electron shake-up and shake-off.

More important are the problems of nonhomogeneity. Sometimes variation from expected behavior for homogeneous material can be of help in characterizing the nature of the surface of a material. For example, if a homogeneous material containing two elements of known concentration lies below the surface of a contaminant layer, the observed intensity will be

$$\frac{N_1}{N_2} = \frac{N_1'}{N_2'} e^{d(1/\lambda_2' - 1/\lambda_1')}, \quad (7)$$

where N_1'/N_2' is the ratio of intensities expected for a homogeneous substance, which can be obtained with the aid of Eq. (6). If $1/\lambda_2' - 1/\lambda_1'$ is known or can be estimated, this thickness of the contamination layer may be obtained. As another example, variations in the intensities of tungsten and tungsten oxide were used to characterize the anodization of a tungsten metal surface.⁹

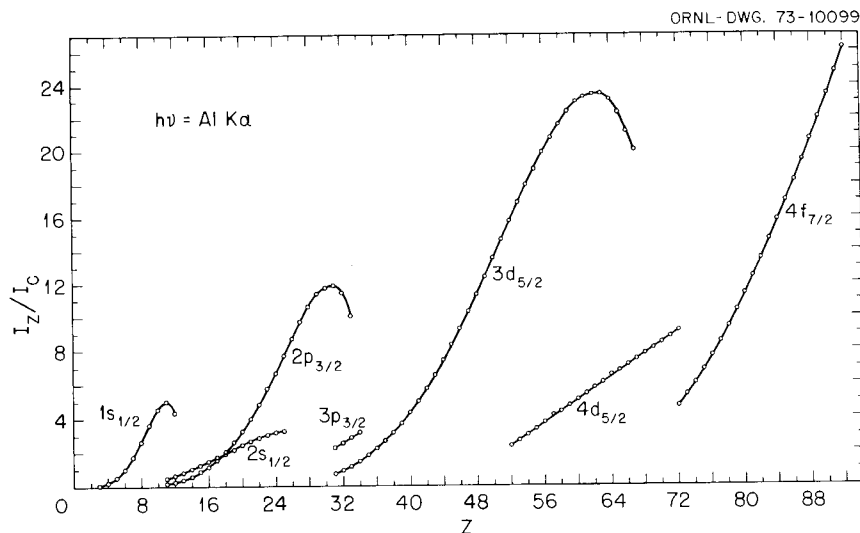


Fig. 2. Calculated intensities of photoelectron peaks from x-ray photoelectron spectra of solid. Results given are relative to the 1s peak of carbon for equal atomic concentrations. Calculations are for studies made with aluminum $K\alpha$ x rays, $h\nu = 1487$ eV. Values are given for each element for different atomic subshells.

Table 1. Comparison of relative intensities for photoelectron peaks in solids
Aluminum $K\alpha$ x rays

Ratio	Relative intensity				
	Wagner ^a	Carter ^b	Nefedov ^c	Average	Theory ^d
C(1s)/F(1s)	0.24	0.29	0.24	0.26	0.277
C(1s)/Na(1s)	0.61	0.53	0.35	0.50	0.522
Na(1s)/F(1s)	2.09	1.44	1.89	1.80	1.39
Si(2p _{3/2})/F(1s)	0.17	0.23	0.15	0.18	0.161
P(2p _{3/2})/Na(1s)	0.26	0.18	0.12	0.19	0.167
S(2p _{3/2})/Na(1s)	0.33	0.30	0.18	0.27	0.232
Cl(2p _{3/2})/Na(1s)	0.46	0.43	0.25	0.38	0.312
K(2p _{3/2})/F(1s)	0.85	1.03	0.83	0.90	0.723
Ca(2p _{3/2})/F(1s)	1.01	1.06	0.98	1.02	0.903
Pb(4f _{7/2})/F(1s)	4.10	4.12		4.11	3.74
Na(2s)/Na(1s)	0.065	0.145	0.077	0.096	0.0919

^aC. D. Wagner, *Anal. Chem.* **44**, 1050 (1972).

^bData from this report.

^cV. I. Nefedov, N. P. Sergushin, I. M. Band, and M. B. Trzhaskovskaya, *J. Electron Spectrosc. Related Phenomena* **2**, 383 (1973).

^dCalculated from Eq. (6).

Conclusion

A simple model has been developed with the help of photoelectron cross sections from Scofield to enable one to convert x-ray photoelectron spectroscopy of solids into a quantitative technique. This model can be used with effectiveness over the whole periodic table. Though accurate to only about 10%, it means that the usefulness of x-ray photoelectron spectroscopy to surface analysis and chemical shifts can be supplemented with quantitative evaluation of the relative intensities of the elements present. The model is based on a homogeneous distribution of sample. Deviation from expectations may be used to evaluate the non-homogeneity of the surface layers.

1. Oak Ridge Associated Universities Laboratory Graduate Fellow from the University of Tennessee, Knoxville, Tenn.

2. University of Tennessee, Knoxville, Tenn.

3. C. D. Wagner, *Anal. Chem.* **44**, 1050 (1972).

4. V. I. Nefedov, N. P. Sergushin, I. M. Band, and M. B. Trzhaskovskaya, *J. Electron Spectrosc. Related Phenomena* **2**, 383 (1973).

5. J. H. Scofield, Lawrence Livermore Laboratory report UCRL-51326 (1973). Specific values at $h\nu = 1254$ and 1487 eV were kindly supplied to us by the author.

6. S. T. Manson, *J. Electron Spectrosc. Related Phenomena* **1**, 413 (1972/73).

7. K. Siegbahn et al., "ESCA," *Nova Acta Regiae Soc. Sci. Upsal.* [4] **20** (1967).

8. U. Gelius in *Electron Spectroscopy*, ed. by D. A. Shirley (North-Holland Pub. Co., Amsterdam, 1972), p. 311; D. P. Spears, thesis, University of Oklahoma (1974).

9. T. A. Carlson and G. E. McGuire, *J. Electron Spectrosc. Related Phenomena* **1**, 161 (1972).

SATELLITE STRUCTURE IN X-RAY PHOTOELECTRON SPECTROSCOPY OF TRANSITION-METAL COMPOUNDS

T. A. Carlson L. J. Saethre²

J. C. Carver¹ F. García Santibáñez³

G. A. Vernon⁴

In the photoionization process, all the energy of the photon is expended in the ejection of a photoelectron according to the energy relationship

$$E_e = h\nu - E_B, \quad (1)$$

where E_e is the kinetic energy of the photoelectron, $h\nu$ is the energy of the photon, and E_B is the binding energy, which may be defined

$$E_B = T_f - T_i,$$

where T_i is the total energy of the initial neutral species and T_f is the total energy of the resultant ion. The binding energy of a given orbital is thus expressed by Eq. (1) if the ion has the configuration where a single vacancy has been created in that orbital. For a monochromatic source of photons, there is a series of photoelectron peaks corresponding to the binding energies of the atomic and molecular orbitals.

In photoionization, there is also the possibility that additional ionization or excitation will occur simultaneously with photoelectron ejection. When this happens, the total energy for the final state becomes T_f^* , and satellite structure will be observed with a kinetic energy lower than the "normal" photoelectron peak by the amount $T_f^* - T_f$. The study of satellite structure in x-ray photoelectron spectroscopy is important for three reasons: (1) One must be able to characterize the entire photoelectron spectrum, (2) satellite structure will teach us about the basic nature of excitation as the result of photoionization, and (3) there is a large potential for the use of satellites for elucidating the nature of chemical bonding.

We are currently engaged in several different points of attack on the study of satellite structure in the photoelectron spectra of transition-metal compounds. These fall into three areas: (1) the use of data on the 1s shell of the first-row transition metals in order to determine the relative importance of electron shake-up and multiplet splitting, (2) the systematic study of satellite structure in the 2p shell of transition-metal compounds, which is interpreted as involving monopole excitation of the valence-shell electrons, and (3) the study of splitting in the photoelectron spectrum of the 3s shell of $\text{NiFe}_x\text{Cr}_{2-x}\text{O}_4$ spinels and its relationship to Mössbauer data. Each of these efforts will be discussed briefly below.

A. Study of 2p Shell of Transition-Metal Compounds

1. Multiplet splitting or electron shake-up? There are two possible sources that appear most likely for the explanation of satellite structure found in the photoelectron spectrum of the 2p shell for transition-metal ions: (1) multiplet splitting arising from the coupling of the 2p shell in which a vacancy has been created by the photoionization process with the unfilled 3d shell of the metal ion and (2) shake-up which is the result of monopole excitation caused by a sudden change in the central potential as a shielding electron is photoejected. Most workers in the field feel that the latter effect is the reason for at least most of the satellite structure found with 2p photoionization. This belief is based on the contention that the energy spread in multiplet splitting would be rather small for the 2p subshell and that the satellite structure is not proportional to the number of unpaired spins in the 3d shell, as is the case with multiplet splitting from photoionization in the s shell. However, Nestor et al. have calculated multiplet splitting using Hartree-Fock free-ion calculations (cf.

Table 1) and have found that it is not negligible, although multiplet splitting for p ionization is much more complicated than for s shells.

One way to test the question of the relative importance of multiplet splitting vs electron shake-up is to look at the satellite structure associated with the 1s shell of the transition metals, since the energy of multiplet splitting has been calculated to be negligible (cf. Table 1), while the energy of excitation due to electron shake-up is nearly independent of the core vacancy and the intensity will also be nearly the same or slightly larger. Thus, experiments were carried out with copper $K\alpha$ radiation on the K shell of some iron compounds [FeCl_3 , FeBr_3 , $\text{K}_3\text{Fe}(\text{CN})_6$, and $\text{K}_4\text{Fe}(\text{CN})_6$]. The photoelectron lines are considerably less well resolved over what is observed with the 2p shell using aluminum and magnesium $K\alpha$ x rays because of the greater widths of the copper $K\alpha$ x rays and the larger natural width of the K shell. However, the presence of satellite structure can easily be detected, and it appears to closely follow that observed for the 2p shell, thus confirming that at least for these compounds, satellite structure in the 2p shell of iron is primarily due to electron shake-up.

Table 1. Calculation^a of multiplet splitting for iron and manganese with initial configurations of $3d^5 4s^0$ as a function of inner shell vacancy

Inner shell vacancy	Final state	Intensity (%)		Relative energy (eV)	
		Mn ³⁺	Fe ⁴⁺	Mn ³⁺	Fe ⁴⁺
3s	7S	58	58	0.0	0.0
3s	5S	42	42	14.2	15.7
2s	7S	58	58	0.0	0.0
2s	5S	42	42	6.1	7.2
1s	7S	58	58	0.0	0.0
1s	5S	42	42	0.08	0.10
3p	7P	58	58	0.0	0.0
3p	5P	42	42	17.3	18.9
3p	$^5P(1)^b$	28	28	4.0	4.6
3p	$^5P(2)^b$	0	0	9.4	10.5
3p	$^5P(3)^b$	14	14	24.0	26.4
2p	7P	58	58	0.0	0.0
2p	5P	42	42	6.1	7.2
2p	$^5P(1)^b$	24	23	3.2	3.6
2p	$^5P(2)^b$	0	0	7.7	8.7
2p	$^5P(3)^b$	19	18	10.0	11.7

^aCalculated by C. W. Nestor, Jr., J. C. Carver, and T. A. Carlson from nonrelativistic Hartree-Fock code of C. Froese Fischer. Energies are taken from the total energy of the ion for the given term value.

^bWith configuration interaction.

2. Transition-metal compounds. A comprehensive study of satellite structure has been made for each of the halides (fluorides, chlorides, bromides, and a few iodides) of the first-row transition-metal compounds: Sc, Ti, V, Cr, Mn, Fe, Co, Ni, Cu, and Zn, as well as a number of hexacyano complexes and other miscellaneous compounds. In addition, a comprehensive study has been made on a series of metal acetylacetonates and corresponding sulfur analogs. For example, see Fig. 1. The following generalizations can be made. The satellite structure is strongly dependent on the nature of the

metal ion, the ligand, and the structure of the complex. The most intense satellite structure is usually found with paramagnetic compounds. However, satellite structure is still found when the $3d$ shell is formally completely empty (e.g., Sc(III) and Ti(IV) compounds) or when the compound is diamagnetic but with a metal $3d$ shell that is only partially filled, as with cobalt oxalate. Very little satellite structure is seen with a completely filled $3d$ shell. The principal requirement for satellite structure is for the $3d$ metal subshell not to be completely filled.

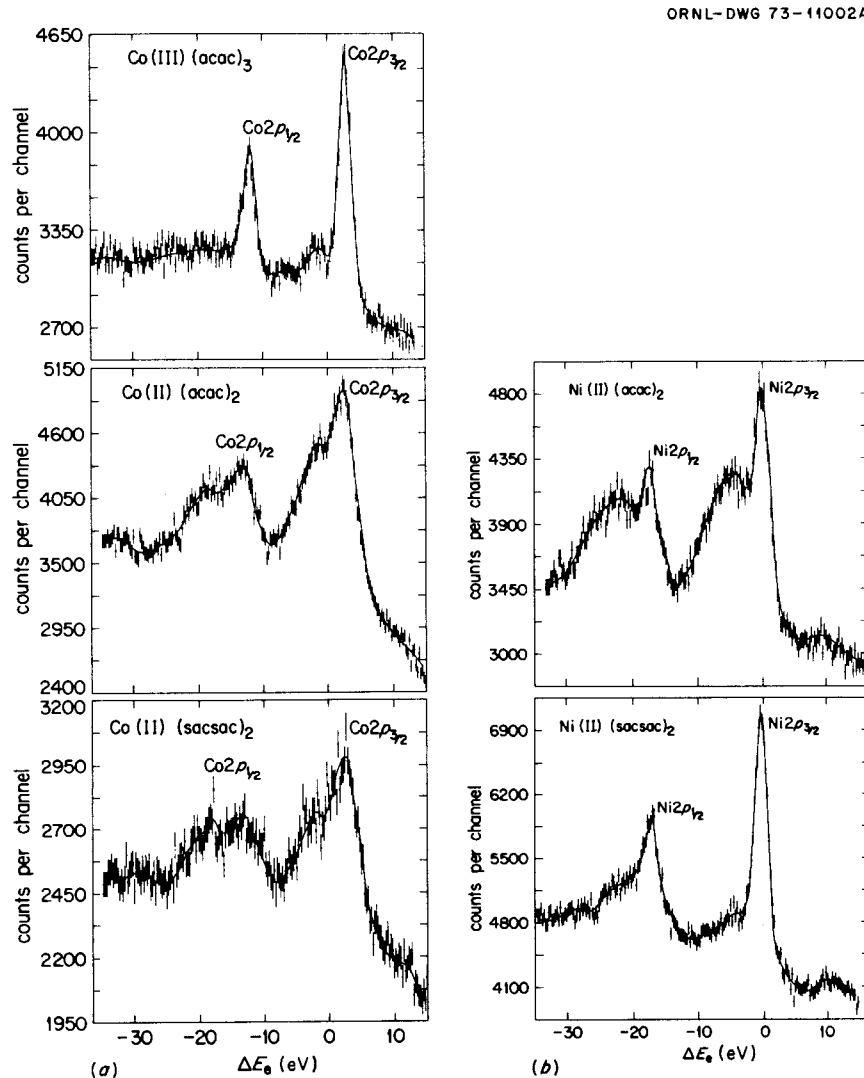


Fig. 1. Photoelectron spectra using aluminum $K\alpha$ x rays of the $2p$ shell of (a) cobalt and (b) nickel compounds. In addition to the normal $2p_{1/2}$ and $2p_{3/2}$ peaks, there appears substantial satellite structure in the case of Co(II)(acac)_2 , Co(II)(sacsac)_2 , and Ni(II)(acac)_2 , but little or no satellite structure is seen for Co(III)(acac)_3 and Ni(II)(sacsac)_2 . It is to be noted that the former complexes are known to be paramagnetic, while the latter are diamagnetic.

The above generalization may be understood with the aid of Fig. 2, which shows possible monopole transitions in an inorganic complex. The diagram is for an octahedral structure, but the arguments can be taken in a more general sense. In atoms the selection rules for monopole transitions are

$$\Delta L = \Delta S = \Delta J = 0;$$

$$\Delta l = \Delta s = \Delta j = 0.$$

That is, the angular momentum and spin remain unchanged, and the angular momentum and spin of the individual electron also remain constant. Electron shake-up involves only a change in principal quantum number. In molecules, we anticipate that the parity and symmetry of the molecule will remain constant as the result of monopole excitation.

Let us consider first the excitation involving molecular orbitals derived from $3d$ atomic orbitals of the metal ion. Such transitions as $e_g \rightarrow e_g$ (corresponding to the atomic transition $3d \rightarrow 4d$) can in principle take place, but the absence of strong satellite structure when the

$3d$ shell is filled suggests that this transition is not very important. Matienzo et al.⁵ propose such transitions as the $e_g \rightarrow a_g$, which corresponds to the atomic transition $3d \rightarrow 4s$. The selection rule $\Delta l = 0$ is violated (this, however, is of less importance to a molecular orbital), but if L for the $3d$ electron is *not* 0, then transitions can take place where $\Delta L = \Delta S = 0$. The requirement that $L \neq 0$ for the ground state explains why diamagnetic compounds with filled d shells do not show satellites. Alternatively, excitation may occur via charge exchange between the ligand and $3d$ orbitals such as $e_g \rightarrow e_g$ or $t_{2g} \rightarrow t_{2g}$. These transitions are certainly monopole, and they require only that there be empty $3d$ orbitals. This not only explains why paramagnetic compounds show satellite structure but also why compounds with formally empty d shells show such structure. Through further experimental and molecular orbital calculations we hope to ascertain the exact nature of the transition. In turn, these studies should provide a potentially powerful tool for determining the chemical structure for transition-metal complexes.

B. Multiplet Splitting of Spinels and Its Relationship to Mössbauer Magnetic Hyperfine Interactions

Magnetic hyperfine fields can arise from two principal sources: (1) that due to the Fermi contact interaction and (2) that due to the orbital magnetic moment. In x-ray photoelectron spectroscopy, multiplet splitting can occur as the result of coupling a core vacancy with an unfilled valence shell. In the case of $3s$ photoionization, two peaks occur with a splitting arising from an exchange potential. Changes in the multiplet splitting should be directly proportional to that part of the magnetic field if due entirely to the Fermi contact interaction, and in certain instances this has been verified experimentally.⁶ Recently, Love and Obenshain⁷ have studied the hyperfine field by Mössbauer experiments on ^{61}Ni for a series of spinels with the formula $\text{NiFe}_x\text{Cr}_{2-x}\text{O}_4$. Two sites of quite different hyperfine fields are detected, and these fields were studied as a function of composition. Results of multiplet splitting in the $3s$ shell of nickel were obtained by ourselves on the same compounds. The multiplet splitting did not seem to change appreciably over the entire Fe-Cr concentration range. One must thus assume that the substantial change in the hyperfine field is due *not* to a large change in contact interaction but rather to some other causes such as an alteration in the field arising from the orbital magnetic moment.

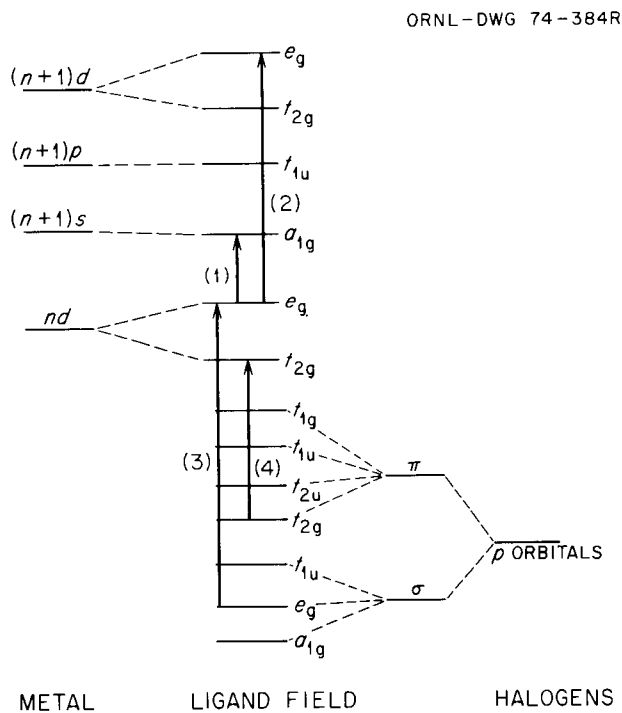


Fig. 2. Schematics of molecular orbitals in a hexahalide complex (octahedral structure). Arrows show possible monopole transitions. Transitions 1 and 2 involve only metal-ion orbitals, while transitions 3 and 4 are charge-exchange transitions between ligand and metal-ion orbitals.

-
1. Work done in part while a student at the University of Tennessee, Knoxville, Tenn., and in part while Postdoctoral Research Associate at the University of Georgia, Athens, Ga.
 2. Guest assignee from the University of Bergen, Bergen, Norway, supported by a Royal Norwegian Council for Scientific and Industrial Research fellowship.
 3. Guest assignee from Physics Instituté, National University of México, supported by Science and Technology National Council, México City, México.
 4. Oak Ridge Associated Universities Laboratory Graduate Fellow from the University of Illinois, Urbana, Ill.
 5. L. J. Matienzo, L. I. Yin, S. O. Grim, and W. E. Swartz, Jr., *Inorg. Chem.* **12**, 2762 (1973).
 6. S. Hufner and G. K. Wertheim, *Phys. Rev. B* **7**, 2333 (1973).
 7. J. C. Love and F. E. Obenshain, "⁶¹Ni Mössbauer Studies of Substituted Ni Spinels," proceedings of 19th Conference on Magnetism and Magnetic Materials, Boston, Mass., Nov. 13–16, 1973 (to be published in the American Institute of Physics Conference Proceedings series).

8. Hyperfine Interactions in Solids

Felix E. Obenshain	J. C. Love ³
J. O. Thomson ¹	J. C. Williams ⁴
P. G. Huray ¹	R. Graetzer ⁵
J. Thompson ²	P. Scholl ⁶

INTRODUCTION

Experimental techniques of nuclear physics applied to solid state, chemical, and biophysics have provided a large body of information about the environment of the nucleus in metals, alloys, and compounds. Among these techniques are nuclear gamma resonance (NGR or Mössbauer effect), perturbed angular correlation (PAC), and time differential perturbed angular correlation (TDPAC). Each of these methods is in a sense complementary to the others, and they give information about nuclear physics as well as solid state physics. The importance of these methods derives from the fact that they are local measurements, as contrasted with bulk measurements, and they reflect in three distinct ways the changes in local behavior of the material under investigation. These are: (1) the electric monopole interaction (isomer shift), which shows changes in the electronic charge density, (2) the magnetic dipole interaction, which is a measure of the magnetic properties of the solid, and (3) the electric quadrupole interaction, which reflects the charge symmetry of the crystalline structure. When this information is combined with ESCA, neutron diffraction and inelastic scattering, magnetic susceptibility, and nuclear magnetic resonance data, a very complete description of solids emerges. All of these methods may be used in conjunction with charged-particle accelerators to produce the excited nuclear state of interest, and this greatly widens the scope of the methods.

A major part of the present activity is directed toward the magnetic interactions in solids and the local behavior of the electronic charge distribution. These investigations require experimental techniques which involve high magnetic fields (a superconducting magnet capable of producing fields of the order of 150 kG is now being constructed in the Thermonuclear Division) and a wide range of temperatures, from above room temperature to 0.015°K. The very low temperature apparatus is a ³He-⁴He dilution refrigerator in which the temperature is continuously variable to 0.015°K and has just become operational this past year at the University of Tennessee. This equipment allows, for example, the observation of the formation of local magnetic moments of 3d transition elements iron, cobalt, and manganese in nonmagnetic materials such as palladium, silver, and gold. These local moments exist even at concentrations of the order 1 ppm of the transition element, where direct interaction, that is, near-neighbor interactions, is not very likely and the interaction would have to communicate information over many tens of lattice spacings. Initial efforts with this equipment are directed to the study of magnetic impurities in metals as a function of temperature and applied magnetic field in an attempt to understand the conditions under which magnetic moments may appear.

Among the classical methods of characterization of magnetic properties of compounds and alloys, magnetic susceptibility measurements have played a major role. However, the magnetic properties of the heavier elements (protactinium, plutonium, californium, etc.) have not been studied in any detail due to the small quantities of materials available. A SQUID (superconducting quantum interference device) is presently being tested and will be used as a highly sensitive magnetometer. This device will be highly suitable for susceptibility measurements of very small samples, for example, microgram quantities.

1. Consultant to ORNL from the University of Tennessee, Knoxville, Tenn.
2. University of Tennessee, Knoxville, Tenn.
3. Florida Institute of Technology, Melbourne, Fla.
4. Memphis State University, Memphis, Tenn.
5. Research Participant under appointment with Oak Ridge Associated Universities during summer 1973 from Pennsylvania State University, University Park, Pa.
6. Undergraduate Research Trainee at ORNL during summer 1973 from Transylvania University, Lexington, Ky. (trainee program administered by Oak Ridge Associated Universities).

⁵⁷Fe MÖSSBAUER MEASUREMENTS OF IRON-COBALT ALLOYS

An impurity atom introduced into an otherwise pure metallic matrix will cause a redistribution of electronic charge around the impurity atom and the neighboring atoms of the host matrix. In the case of magnetic materials, in this instance cobalt in a pure iron matrix, the screening is accomplished by the 3*d* electrons, due to the large density of *d*-electron states, as well as the 4*s* electrons. Spin density fluctuations of the 3*d* electrons will change the value of the magnetic hyperfine field at the iron sites, and the combination of the *d* and *s* electrons will effect a change in the isomer shift at these sites.

Precision measurements of both these quantities for ⁵⁷Fe as a function of the cobalt concentration (0.1% to 10.0%) have been carried out. The data are shown in Table 1. To ensure that the observed changes were due to the introduction of cobalt alone, each sample was carefully analyzed, and all other impurities were found to be less than a few parts per million.

The change in the magnetic hyperfine field at an iron atom in a given coordination sphere *k* may be described by the simple model^{1,2}

$$\Delta H_{\text{hf}}^k = \Delta H_{\text{cep}}^k + \Delta H_{\text{cp}}^k,$$

where ΔH_{cp} is the change in the core polarization field and ΔH_{cep} is the change in the conduction electron polarization. The former follows very closely the change in the local magnetic moment as determined, for example, by neutron diffraction and diffuse scattering measurements,³ and the latter is proportional to the polarization of the conduction electrons and is related

in some cases to the average magnetization of the material.

NGR spectra were taken with a ⁵⁷Co in copper source, and the absorbers were various concentrations of cobalt in iron. This combination of source and absorber yields a six-line spectrum for the iron matrix, and it is assumed that the change in the magnetic hyperfine field in the *k*th coordination sphere can be treated as a six-line spectrum with a splitting which increases or decreases according to the sign of ΔH_{hf}^k and that the total spectrum is a superposition of all these spectra. The alloys are assumed to be random, and the weight given to each spectrum is obtained from a binomial distribution.

Since only a line broadening is observed when cobalt is added to iron, the spectra were analyzed in terms of the first and second coordination spheres. The absolute value of the field increases as cobalt is added to the iron matrix, and the local magnetic moment also increases.

Table 1. Magnetic fields and isomer shifts for cobalt in iron

Cobalt concentration (at. %)	Magnetic hyperfine field (kOe)	Isomer shift ^a (μm/sec)
0	-333	0
0.1		-0.31 (15)
0.5	-334.3 (1.7)	+0.48 (13)
1.0	-334.8 (1.7)	+0.96 (16)
2.5	-336.2 (1.7)	+2.58 (22)
5.0	-341.1 (1.7)	+5.87 (35)
10	-350.3 (1.7)	(+14 (2))

^aRelative to pure iron.

Therefore, one may assume that the negative contribution to the field increases and is proportional to the local magnetic moment. In addition, the average magnetic moment also increases, so that the conduction electron polarization is increasing, and this contribution has a positive sign, so that the net change in H_{hf} is relatively small, a few kilogauss per percent cobalt. It is still an open question to which coordination shell to attribute the changes in H_{hf} , and one objective of these measurements is to make this determination using an improved analysis program to unfold the spectra. Preliminary results indicate reasonable agreement with the two measurements of Vincze and Campbell² at 1.5% and 3% Co. The contribution at the first neighbor is about 13 kG and the second is about 6 kG.

Determination of the isomer shift is more difficult than the magnetic interaction due to small value of the shift, which is about $+1.2 \mu\text{m}/\text{sec}$ per percent cobalt. Isomer shifts of this magnitude are nearly impossible to measure using the source-absorber arrangement mentioned above due to the very large magnetic hyperfine splitting, which removes the absorption lines far from zero velocity and causes an effective loss of resolution of the overall system.

One method of measurement to overcome this difficulty is to replace the ^{57}Co in copper source by a ^{57}Co in iron source, so that the emission as well as the absorption spectrum is composed of six lines. When the two spectra are convoluted, an absorption minimum will occur near zero velocity, and the spectrometer may be tuned to include only the zero-velocity line, which yields all the relevant isomer shift information. This procedure gives an effective increase in resolution of about 50, and another factor about 10 comes from the larger number of counts distributed over just one line.

We measure positive shifts for cobalt in iron relative to pure iron for concentrations equal to and greater than 0.5% Co. Since the sign of the nuclear radius change $\Delta R_N/R_N$ is negative, the change in the s -electron density at the nucleus must also be negative, which indicates a decrease in the conduction s electrons and/or an increase in the d -electron occupancy, which would effectively shield the conduction electrons. A change in the d electrons is the more likely effect, since the local magnetic moments are also increasing, indicating an increase in the spin-down d -electron occupancy. This is also consistent with the change in H_{hf} .

The isomer shift for 0.1% Co in iron is *not* positive, but negative. While the associated error is not small, it is two standard deviations (σ) from zero shift and nearly 3σ from the expected value given by a linear interpola-

tion. The interaction must be long range because of the low concentration and indicates a conduction s -electron deficiency at iron sites as proposed above.

1. G. K. Wertheim, V. Jaccarino, J. H. Wernick, and D. N. E. Buchanan, *Phys. Rev. Lett.* **12**, 24 (1964).

2. I. Vincze and I. A. Campbell, *J. Phys. F: Metal Phys.* **3**, 647 (1973).

3. M. F. Collins and G. G. Low, *Proc. Phys. Soc.* **85**, 535 (1965).

MAGNETIC BEHAVIOR OF IRON AND COBALT IMPURITIES IN SILVER

We have studied the magnetization of ^{57}Fe and ^{57}Co impurities in silver metal at a concentration level of the order of 1 ppm as a function of applied magnetic field, H_{app} , up to 60 kG and as a function of temperature, T , from 0.025°K to 18.5°K . These studies were performed by measuring the internal field H_i at the nuclei of these impurities using the Mössbauer effect. The iron fields were obtained by the line spacing of the Mössbauer spectra, while the cobalt fields were determined from the line intensity asymmetry of the same spectra (caused by the nuclear polarization of the parent ^{57}Co).

We find within our experimental errors that the cobalt impurity is nonmagnetic below 0.1°K for fields up to 60 kG; the cobalt field is characterized by a positive Knight shift, $K = 0.27 \pm 0.07$, that is, $H_i = H_{\text{app}}(1 + K)$. The small positive hyperfine field, H_{hf} , for cobalt, $H_{\text{hf}} = KH_{\text{app}}$, is opposite in sign to that found for magnetic cobalt atoms but is similar to that found at very low temperature for ^{60}Co in gold by Weyhmann et al.¹ This behavior is characteristic of a dilute magnetic impurity in a metallic host at temperatures far below the Kondo temperature of the system.

From our studies of H_i for iron, we find that the ^{57}Fe impurities are nonmagnetic at the lowest temperatures, and this is characteristic of the Kondo state; the Kondo temperature, T_K , determined from spectra taken below 0.03°K is $T_K = 1.9 \pm 0.2^\circ\text{K}$. These data are in excellent agreement with earlier Los Alamos results taken in similar fields but at temperatures above 1°K .^{2,3} At present there is no theory of the Kondo effect which holds over wide ranges of both temperature and field to compare with our extensive experimental results, which range from the low-temperature, low-field nonmagnetic region to temperatures and fields substantially larger than those required to break up the Kondo state. Kitchens and Taylor³ have offered a semiempirical model to correlate results on hyperfine

field measurements for impurities in Kondo alloys:

$$H_{\text{hf}} = H_{\text{sat}} B J \frac{g J \mu_B H_{\text{app}}}{k_B (T + T_K)}$$

All of our data may be correlated by this equation to within a mean deviation of about 1 kG for $J = 2$, $g = 2$, $T_K = 1.9^\circ\text{K}$, and $H_{\text{sat}} = -40.0$ kG. We have, however, also fitted our data to other saturating functions with comparable success.

1. R. J. Holliday and W. Weyhmann, *Phys. Rev. Lett.* **25**, 243 (1970).

2. T. A. Kitchens, W. A. Stegart, and R. D. Taylor, *Phys. Rev.* **138**, A467 (1965).

3. T. A. Kitchens and R. D. Taylor, *Phys. Rev.* **B9**, 344 (1974).

⁶¹Ni MÖSSBAUER STUDIES OF SUBSTITUTED NICKEL SPINELS

The ⁶¹Ni nuclear gamma resonance (NGR) spectrum of the spinel NiCr₂O₄ shows the largest magnetic hyperfine (hf) interaction yet reported.^{1,2} The effective magnetic field of 440 kOe for the tetrahedrally coordinated (*A*-site) Ni²⁺ ion in the chromite may be compared with values obtained for octahedrally coordinated nickel oxides, such as NiO (100 kOe)³ and NiFe₂O₄ (94 kOe).¹ The source of the large field in NiCr₂O₃ has been ascribed to a large orbital contribution, since the electronic ground state of *A*-site Ni²⁺ is orbitally degenerate in cubic symmetry. However, this ion displays a strong Jahn-Teller (J-T) effect, and tetragonal ($c/a > 1$) distortions below 310°K lead to a singlet ground state and large reductions of orbital contributions to the g factor and the hf field.⁴ Thus, any orbital moment that may be present at low temperatures results from a balance between J-T and spin-orbit interactions, and other effects, and is not easily estimated a priori.

In order to investigate the origin of this large field experimentally, we measured ⁶¹Ni NGR spectra at 4.2°K of powdered absorbers for the series of mixed spinels NiFe_{*x*}Cr_{2-*x*}O₄ ($0 \leq x \leq 2$), which spans the range from the "anomalous" NiCr₂O₄ to the ferrite NiFe₂O₄. These materials have interesting magnetic properties and have been the subject of several investigations.⁵⁻¹¹ It is known that Cr³⁺ is found only on the *B* sites, whereas Fe³⁺ is found on both sites. It is believed that Ni²⁺ also tends to seek *B* sites, but direct evidence is difficult to obtain because of the almost equal scattering factors of iron and nickel for both neutrons and x rays.

Low-temperature x-ray studies^{5,8} of this series show tetragonal distortions with the J-T signature ($c/a > 1$) for the range $0 \leq x \leq 0.18$, orthorhombic structure for compositions $0.2 < x < 0.28$, and tetragonal ($c/a < 1$) for $0.28 \leq x < 1.0$. Goodenough⁹ has interpreted this complicated structure as due to competitive J-T and spin-orbit interactions at *A*-site Ni²⁺. The spin-orbit interaction produces a tetragonal ($c/a < 1$) distortion of the site and stabilizes the ion in a ground state with unquenched orbital moment ($J = |L - S| = |1 - 1| = 0$), in contrast to the effect of J-T interaction. One may expect that the ⁶¹Ni hyperfine field at *A*-site ions will exhibit large changes with composition in this region ($0 \leq x < 1.0$); this provides the motivation for the present experiments.

Representative spectra are shown in Fig. 1. For $x = 0$, the single-valued field 440 kOe is measured and may be associated with the *A* sites, which are exclusively occupied by nickel. For both $x = 1.5$ and 2.0, only a small-field pattern is seen, and it is known that nickel occupies *B* sites in these samples. For intermediate values of x , two distinct hf patterns are seen, with the "small"-field component growing in intensity at the expense of the "large"-field component as x is increased. The large field is in fact a *distribution* of field values, as would be expected in mixed systems such as this, whose average value and width both increase as x increases. The average value for the large component reaches the value of $|H_{\text{hf}}^A| = 630$ kOe for $x = 0.5$, and a similar result is found for the related compound NiFe_{0.5}V_{1.5}O₄ (see Fig. 1*b*).

There are a large number of effects displayed by these spectra, including distributions of fields and quadrupole interactions for the two sites, and we have not attempted least-squares fittings of sufficient flexibility to take them into account. Rather, rough estimates of average fields were obtained by fittings with two unique hf patterns, one for each site, with variable line widths. Such estimates are listed in Table 1.

Preliminary measurements to determine the sign of H_{hf} have been carried out with an applied field of 35 kG, and these indicate that the large-field component is positive. The large hf fields at *A*-site Ni²⁺ ions are difficult to understand without invoking orbital contributions. The contact field due to core polarization (cp) by the 3*d* spin has been estimated by Watson and Freeman¹² to be -332 kOe for the free ion and -275 kOe for a simple cubic environment (an octahedral array of point-charge ligands). If we adopt the value $H_{\text{cp}} = -300$ kOe as an estimate, which is consistent with the preliminary ESCA measurements of Carlson et al.,¹³ then rather large additional contributions are

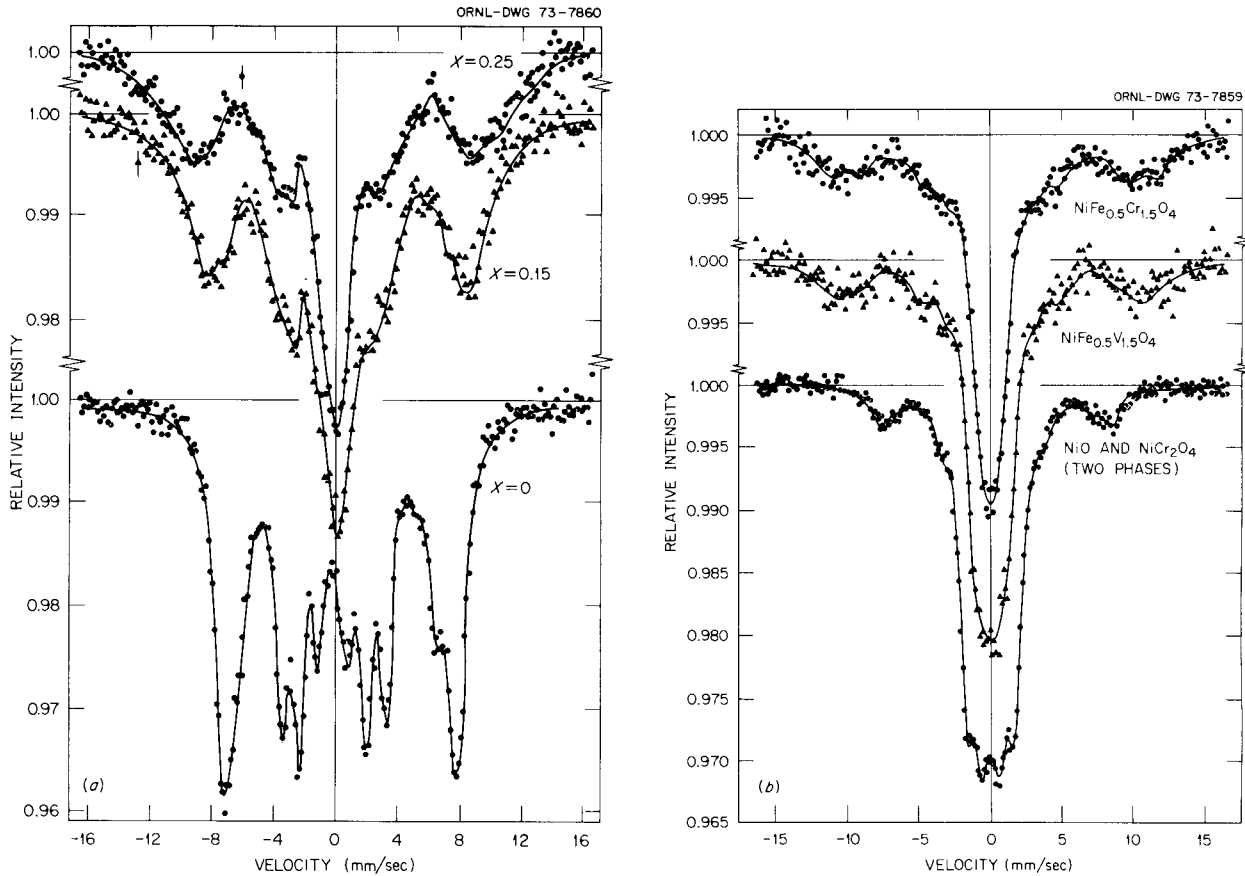


Fig. 1. ^{61}Ni NGR spectra for $\text{NiCr}_x\text{Fe}_{2-x}\text{O}_4$ spinels. The absorption dip at zero velocity is the B-site component.

Table 1. Lattice constants and ^{61}Ni hf fields at tetrahedral (A) and octahedral (B) sites in $\text{NiFe}_x\text{Cr}_{2-x}\text{O}_4$ and $\text{NiFe}_x\text{V}_{2-x}\text{O}_4$

x	H_A (kOe)	H_B (kOe)	Lattice constant at room temperature (Å)
$\text{NiFe}_x\text{Cr}_{2-x}\text{O}_4$			
0	440		8.3162
0.15	506	20	8.3115
0.25	560	20	8.3167
0.50	617	48	8.3112
0.50	631	49	(annealed)
0.50	609	44	8.3057
0.50	623	48	(annealed)
1.50		84	8.3160
2.0		94	8.3375
$\text{NiFe}_x\text{V}_{2-x}\text{O}_4^a$			
(0.5)	639	71	
1.0			8.3568

^aPreliminary results.

needed to explain the values of (+)440 kOe ($x = 0$) and (+)630 kOe ($x = 0.5$); specifically, these are +740 kOe for $x = 0$ and +930 kOe for $x = 0.5$. We may, however, eliminate several possible sources for these contributions, including variations in transferred hf interaction¹⁴ due to the large B-sublattice spin as iron replaces chromium (one expects $\Delta H < 40$ kOe due to this factor) and spin dipole fields (only the lattice contributes, therefore negligible). Covalency-overlap effects are harder to estimate but probably tend to reduce the magnitude of H_{CP} by (say) 10% or less, since oxides of the spinel type are predominantly ionic.¹⁵

As Watson and Freeman point out, the core field is the result of partial cancellation of large opposing 2s and 3s terms, and, as such, it should be sensitive to environment. However, it has been shown empirically that the core field per unit spin is (almost) constant over the 3d series for a range of ionicities and ligand bond lengths,^{16,17} and again this is consistent with the recently obtained ESCA data. Moreover, the Watson and Freeman calculation has been shown to be in

excellent agreement with data for several octahedrally coordinated Ni^{2+} fluorides and oxides.^{3,17}

For these cases of octahedral coordination, the orbital fields are accurately estimated from the shift of the electronic g value (from EPR data) from the spin-only value of 2.0023, because both quantities are due to second-order spin-orbit perturbations of the ${}^3A_{2g}$ orbital singlet ground state and are given by the same matrix elements to within a constant factor. Such estimates yield large *positive* orbital fields (typically +200 kOe for Δg about 0.28) that nearly cancel the negative cp component and give net fields of the order of -100 kOe, such as the B -site fields reported here. Unfortunately, the 3T_1 ground state appropriate to the (cubic) A site is orbitally degenerate, and one expects no simple relation between g shifts and orbital hf fields. We may estimate the g values for A -site Ni^{2+} in NiCr_2O_4 for the cubic (high T) and J-T distorted phases (low T) by comparing with the susceptibility data of NiRh_2O_4 , a compound isostructural with the chromite, in which Ni^{2+} is the only magnetic ion. From Blasse's¹⁸ data, we obtain $g(c/a = 1) = 3.2 \mu_B$ and $g(c/a > 1) = 2.5 \mu_B$. The latter value is then to be associated with the pure chromite ($x = 0$), and the former value is applied to A -site nickel in the composition $x = 0.5$, since the cubic and spin-orbit-distorted A -site ions should have about the same values for $\langle L_z \rangle$. The large g values would allow for the huge positive orbital fields that are needed.

1. H. Sekizawa, T. Okada, S. Okamoto and F. Ambe, *J. Phys.* **32**, C326, Suppl. 2-3 (1971).
2. J. Goring, *Z. Naturforsch.* **A26**, 1929 (1971).
3. J. C. Love, F. E. Obenshain, and G. Czjzek, *Phys. Rev.* **B3**, 2827 (1971).
4. F. S. Ham, *Phys. Rev.* **138A**, 1727 (1965).
5. T. R. McGuire and S. Greenwald, *Proc. International Conf. on Solid State Physics, Brussels 1958* (Academic Press, New York, 1960), vol. 3.
6. F. C. Romeijn, *Philips Res. Rep.* **8**, 304 (1953).
7. I. S. Jacobs, *J. Phys. Chem. Solids* **15**, 54 (1960).
8. R. J. Arnott, A. Wold, and D. B. Rogers, *J. Phys. Chem. Solids* **25**, 161 (1964).
9. J. B. Goodenough, *J. Phys. Soc. Jap.* **17**, Suppl. B-1, 185 (1962).
10. J. Chappert and R. B. Frankel, *Phys. Rev. Lett.* **19**, 570 (1967).
11. V. F. Belov et al., *Sov. Phys. - Solid State* **13**, 747 (1971).
12. R. E. Watson and A. J. Freeman, *Phys. Rev.* **120**, 1125, 1134 (1960).
13. T. A. Carlson et al., "Satellite Structure in X-Ray Photoelectron Spectroscopy of Transition-Metal Compounds," this report.
14. A. J. Heeger and T. W. Houston, *Proc. Int. Conf. on Magnetism, Nottingham, England, 1964*, p. 395.

15. D. S. McClure, *J. Phys. Chem. Solids* **3**, 311 (1957).

16. R. E. Watson and A. J. Freeman in *Hyperfine Interactions*, ed. by A. J. Freeman and R. B. Frankel (Academic Press, 1967), p. 53.

17. S. Geschwind in *Hyperfine Interactions*, ed. by A. J. Freeman and R. B. Frankel (Academic Press, 1967), p. 225.

18. G. Blasse, *Philips Res. Rep.*, Suppl. (1964), No. 3 (see p. 66); independent data by S. Miyahara and S. Horiuti, *Proc. Int. Conf. on Magnetism, Nottingham, England, 1964*, p. 550.

${}^{61}\text{Ni}$ MÖSSBAUER EFFECT IN NICKEL COMPOUNDS

The magnitudes of the isomer shifts and magnetic hyperfine fields have been measured for a series of nickel compounds. The effect of covalent bonding on the magnetic properties of the transition-metal ion has been studied in some cases, and these have shown reasonable correlation with the observed magnetic hyperfine fields. There have been many studies made which correlate isomer shifts with electronegativities of the ligand ions. In most cases it is shown that there is a linear correlation between them as long as the coordination of the ligands is approximately the same. The octahedral compounds of nickel also show this correlation. However, it is doubtful that such correlations have any physical significance, and a more fruitful approach may be in correlating the isomer shifts and bond energies of the ions of interest.

Nuclear gamma resonance spectroscopy with ${}^{61}\text{Ni}$ was used to study hyperfine interactions at ${}^{61}\text{Ni}$ in some selected nickel compounds.¹ The absorption spectra were computer fitted with a line-shape function (transmission integral) having parameters related to physical properties of the source and absorbers. From these spectra we have deduced absorber recoilless fractions, energy shifts, and magnetic hyperfine fields. The results are tabulated in Table 1. The main contributions to the magnetic hyperfine field of transition-metal ions in magnetically ordered compounds are the core polarization field H_{cp} , the orbital field H_o , and, for ions at lattice sites of lower than cubic symmetry, the dipolar field. An additional contact field can arise from overlap and covalent mixing of ligand and metal $4s$ orbitals. The core polarization is given approximately by $H_{cp} = -332 \langle S_z \rangle$, where the value -332 is from Watson and Freeman's calculation² for free Ni^{2+} ions and $\langle S_z \rangle$ is the expectation value of the spin. The orbital field is given by $H_o = 125 \cdot \Delta g \cdot \langle r^{-3} \rangle \langle S_z \rangle$, where $\Delta g = g - 2.0023$ and is a measure of the unquenched orbital angular momentum. The expectation value for the spin is reduced from unity for two reasons: (1) Spin density is transferred to the ligand anions by covalent admixture. (2) Zero-point

Table 1. Properties of nickel compounds

Q	Formal charge state
$\Delta\epsilon$	Electronegativity difference
f_A	Recoilless fraction for compounds
δ_{SOD}	Second-order Doppler shift calculated from lattice dynamics and/or from the recoilless fraction must be subtracted from observed energy shifts to obtain the isomer shift
IS	Isomer shift
T_N	Néel temperature
g	Ni gyromagnetic ratio
H_{hf}	Observed magnetic hyperfine field
$H_{\text{hf}}^{\text{cal}}$	Calculated magnetic hyperfine field

Compound	Q	$\Delta\epsilon$	f_A (%)	δ_{SOD} (μ/sec)	IS (μ/sec)	T_N ($^\circ\text{K}$)	g	$ H_{\text{hf}} $ (kOe)	$H_{\text{hf}}^{\text{cal}}$ (kOe)
NiF ₂	+2	2.2	13.8	-112	+34 (12)	73.2	2.31	45 (1)	-45
KNiF ₃	+2	(1.82)	14.8	-112	+24 (12)	25.3	2.29	64 (2)	-64
NiO	+2	1.7	11.5	-103	+19 (9)	52.3	2.23	100 (2)	-104
NiCl ₂ ·6H ₂ O	+2	(1.4)	3.4	-65	+11 (26)	5.34		46 (1)	
NiCl ₂	+2	1.2	3.5	-65	+8 (20)	52		33 (1)	
Ni(NO ₃) ₂ ·6H ₂ O	+2	(1.02)	4.0	-68	-6 (20)	52			
NiSO ₄ ·7H ₂ O	+2	(0.42)	0.32	-38	-40 (21)				
(NH ₄) ₁₂ [NiMo ₉ O ₃₂] ₂ ·13H ₂ O	+4	(0.16)	18.5	-138	-48 (21)				
Ni[P(OC ₂ H ₅) ₃] ₄	0	(0.17)	4.6	-71	-63 (22)				
K ₄ Ni ₂ (CN) ₆	+1	(~0)	0.25	-37	-94 (23)				

motion of an antiferromagnetically ordered spin system in its ground state reduces the net average spin on any ion. Measurements of Δg and $\langle S_z \rangle$ have been reported for NiF₂,³ KNiF₃,⁴ and NiO.⁵ Calculations for H_{hf} using these parameters are shown in the last column of the table. The agreement with the measured values is excellent if the sign of the field is assumed to be negative. The necessary parameters are not available for NiCl₂ and NiCl₂·6H₂O, but, assuming that $\langle S_z \rangle \cong 0.8$, about the same as for the other three compounds, values for Δg may be obtained. They are 0.33 for NiCl₂ and 0.28 for NiCl₂·6H₂O.

The electronegativity differences, $\Delta\epsilon$, in parentheses in column 2 of the table were obtained by assuming that the values for NiF₂, NiO, and NiCl₂ are those given by Pauling, 2.2, 1.7, and 1.2 respectively. By plotting the square of $\Delta\epsilon$ vs isomer shift, one observes that there is a linear correlation between them. Assuming this relationship, the remaining values of $\Delta\epsilon$ are obtained and the ionicities may be calculated. Since the bond energies are proportional to the squares of the electronegativity differences, this type of correlation may be more satisfactory than the simple correlation with the ligand electronegativities. On this basis the ionicity for NiF₂ is 0.7, corresponding to a $3d^8 4s^{0.3}$ configuration for Ni, and for K₄Ni₂(CN)₆ it is approximately zero and would indicate a $3d^8 4s^2$ configuration. With the calculations of s -electron densities a scale for the nickel

isomer shifts may be established, and a prediction for the electronic configuration of nickel in nickel metal may be made from the isomer shift. It is $3d^9 4s^1$, in agreement with minimum polarity models.

1. J. C. Love, F. E. Obenshain, and G. Czjzek, *Phys. Rev.* **B3**, 2827 (1971).
2. R. E. Watson and A. J. Freeman, *Phys. Rev.* **120**, 1125, 1134 (1960).
3. R. G. Shulman, *Phys. Rev.* **121**, 125 (1961).
4. M. T. Hutchings and H. S. Guggenheim, *J. Phys.* **3**, 1303 (1970).
5. B. E. F. Fender, A. J. Jacobsen, and F. A. Wedgewood, *J. Chem. Phys.* **48**, 990 (1968).

MAGNETIC SUSCEPTIBILITY MEASUREMENTS

An apparatus has been constructed for measurement of the bulk magnetic susceptibility and electrical resistivity of solids. The equipment is based on SQUID (superconducting quantum interference device) electronics for extremely high sensitivity and is intended particularly for use with limited quantities of heavy elements, their compounds, and alloys and for very dilute gold alloys. The design sensitivity would detect a change in the dimensionless magnetic susceptibility ($4\pi\chi$) of 1 part in 10^7 for a 50- μg quantity of material and an applied field of 4 kG. Sample temperature is variable and controllable between 4.2°K and room

temperature, and the external magnetic field may range from 0 to 60 kG. The field is produced by a superconducting magnet operated in a persistent mode and is stable to 1 part in 10^5 for 1 hr. The susceptibility measurements may be made in either a dc or ac fashion, and the electrical resistivity determination is obtained from the out-of-phase susceptibility in the ac technique.

Operating in a dc mode, the SQUID electronics act as a fluxmeter with digital and printed readout of temperature, applied field, and static magnetic susceptibility.

Operating in an ac mode, the SQUID electronics act up to 10 kc as null detector for in-phase and quadrature components of an ac bridge circuit. The measurement sensitivity is in this case much less than for the dc

measurements (by a factor of about 10^3), but the magnetic susceptibility may be determined as a function of applied field.

The equipment will initially be used for the measurement of impurity contribution to the magnetic susceptibility of the gold(X) alloys. The information is complementary to the Mössbauer electron charge density determinations and electrical resistivity measurements which have previously been obtained for these alloys. A systematic picture of the potentials provided by impurity atoms to the conduction electrons of metallic alloys is being established for the *s-p* (Ag, Cd, In, Sn, Sb, Cu, Zn, Ga, and Ge) and transition-metal (Ca, Sc, Ti, V, Cr, Mn, Fe, Co, and Ni) impurities. A similar study will be made for the *5f* alloy impurities in metals.

9. Molecular Spectroscopy

MILLIMETER AND SUBMILLIMETER SPECTRA OF TRITIUM-SUBSTITUTED WATER AND AMMONIA

H. W. Morgan F. DeLucia¹
P. A. Staats P. Helminger¹
W. Gordy¹

The absorption spectra of water and ammonia, and their isotopic species, have been the subject of intensive study by molecular spectroscopists. Both are simple molecules from which isotopic data can be expected to yield valuable information; both are basic molecules of importance in terrestrial and extraterrestrial biochemistry. Thorough study of these molecules substituted with tritium is providing the maximum in structural data which can be obtained by present technology.

The water molecule is the lightest asymmetric rotor which is chemically stable, and the effects of centrifugal distortion are appreciable. Earlier studies^{2,3} provided an accurate evaluation of the distortion effects and molecular constants for H₂O, D₂O, and HDO. This study has given similar information on T₂O, and spectra have been obtained from which these data are being evaluated for HTO and DTO. These studies provide the basis for improved prediction of the complete spectra of these six isotopic species and for the prediction of centrifugal distortion effects in the spectra of other molecules.

NH₃ and ND₃ have been extensively studied by microwave spectroscopy, but no previous microwave measurements have been made on NT₃. Infrared studies^{4,5} of both the vibrational and pure rotational spectra of NT₃ have been made, but neither the inversion doubling nor the *K* splitting has been resolved. Consequently the molecular constants from these studies are not accurate. Theoretical efforts⁶ to derive the inversion splitting in NT₃ have not been successful. Our studies have measured the rotation-inversion transitions of NT₃ in the ground state, from which the rotational constants as well as the inversion splitting

have been accurately determined. These constants, combined with those for NH₃ and ND₃, should allow an accurate prediction of the spectra of the seven mixed isotopic species.

Based on the experience in tritium chemistry at ORNL, samples were prepared and transported to Duke University in sealed systems which contained a section of specially designed waveguide. These self-contained systems allowed filling the waveguide to any desired pressure, and changing samples when necessary. The spectrometer covers the submillimeter wave region to above 800 GHz, and employs a liquid-helium-cooled InSb detector.⁷

Forty-six transitions of the asymmetric rotor T₂O were measured. For light asymmetric rotors a large number of distortion parameters are necessary to fit the spectrum to the experimental uncertainty. Watson's formulation of a reduced Hamiltonian was used as a model for the analysis. From this study, the following spectroscopic rotational constants were obtained for T₂O: *A* = 338,815.81 MHz, *B* = 145,639.72 MHz, and *C* = 100,280.22 MHz. Based upon these data, and averaging over the variations due to the inertial defect, the structure of T₂O is given in Table 1, together with structures for H₂O and D₂O obtained in a similar manner.

The structures and distortion constants of THO and TDO, when fully evaluated, will be combined with the data on HDO and the data described above to give a complete picture of the water molecule as can be obtained, and certainly with an accuracy which should be more than adequate for theoretical work in the foreseeable future.

Table 1. Effective structures obtained from averaged values of ground-state structural parameters

	H ₂ O	D ₂ O	T ₂ O
Bond length	0.9650 Å	0.9631 Å	0.9623 Å
Bond angle	104.8°	104.6°	104.6°

In the NT_3 study, the transitions $J = 0 \rightarrow 1$, $1 \rightarrow 2$, and $2 \rightarrow 3$ were measured. The ^{14}N hyperfine structure was well resolved only in the $J = 0 \rightarrow 1$ transition, giving $eqQ = -4.170 \pm 0.049$ MHz. The rotational constants for $^{14}\text{NT}_3$ are as follows: $B_0 = 105,565.373 \pm 0.034$ MHz, $D_J = 2.5981 \pm 0.0024$ MHz, and $D_{JK} = -4.472 \pm 0.006$ MHz. These are the familiar terms to describe normal symmetric top molecules without inversion, where B_0 is the rotational constant and D_J and D_{JK} are centrifugal distortion constants. Structures can be determined only through use of moment values from spectra containing ^{15}N and H, D. The values expected to be closest to NT_3 are: bond length, 1.0128 Å; bond angle, $107^\circ 02'$.

The inversion problem in the ammonias is of great interest because NH_3 , ND_3 , and NT_3 represent the only symmetric isotope sequence with inversion splitting of the vibrational states sufficiently large to permit accurate measurement. Although there is much theoretical work on inversion doubling, no one has attempted to predict the splitting in NT_3 with any success. Swalen and Ibers⁸ used a potential function in the form of a harmonic oscillator with a Gaussian barrier to fit the splittings in NH_3 and ND_3 . We have performed a similar calculation for NT_3 , based on this function, which gives $\nu_i = 0.01 \text{ cm}^{-1}$, or 300 MHz, for the ground state. This is in remarkably good agreement with the experimental values for $^{14}\text{NT}_3$, shown in Table 2, where C_1 and C_2 represent effects of centrifugal distortion on the inversion transition frequency.

Table 2. Inversion constants of $^{14}\text{NT}_3$

$(\nu_i)_0$	305.89 ± 0.11 MHz
C_1	-0.557 ± 0.020 MHz
C_2	0.971 ± 0.038 MHz

The data from the three symmetric isotopic ammonias should allow prediction of the rotational spectra of the seven asymmetric mixed isotopic species with considerable accuracy, and assist considerably in the assignment of the infrared and microwave spectra of these molecules.

1. Duke University, Durham, N.C.
2. F. C. DeLucia, P. Helminger, R. L. Cook, and W. Gordy, *Phys. Rev.* **A5**, 487 (1972); **A6**, 1324 (1972).
3. F. C. DeLucia, R. L. Cook, P. Helminger, and W. Gordy, *J. Chem. Phys.* **55**, 5334 (1971).
4. R. S. McDowell and L. H. Jones, *J. Mol. Spectrosc.* **9**, 79 (1962).
5. K. N. Rao, W. W. Brim, J. M. Hoffman, L. H. Jones, and R. S. McDowell, *J. Mol. Spectrosc.* **7**, 362 (1961).
6. T. P. Norris and J. M. Dowling, *Can. J. Phys.* **39**, 1220 (1961).
7. P. Helminger, F. C. DeLucia, and W. Gordy, *Phys. Rev. Lett.* **25**, 1397 (1970).
8. J. D. Swalen and J. A. Ibers, *J. Chem. Phys.* **36**, 1914 (1962).

10. High Resolution Electron Microscopy Program

R. E. Worsham W. W. Harris J. E. Mann E. G. Richardson N. F. Ziegler

Introduction

The principal factor that limits resolution to about 3 Å in an electron microscope is the spherical aberration of the objective lens. The only other lens aberration of significance is chromatic. In addition, however, certain practical limitations are imposed by mechanical vibration, contamination forming on the specimen, and specimen drift. A third type of limit occurs because of the destruction of the specimen itself as a result of the electron irradiation. There is strong evidence that this last limit can be extended by a factor of about 5 in many biological specimens by cooling the specimens to liquid-helium temperature. Contamination can be eliminated by ultrahigh vacuum. Mechanical vibration and specimen drift are design and construction problems that appear to be quite solvable. Chromatic aberration can be reduced to about 0.2 Å if the accelerating voltage and objective lens current are stable to a few parts in 10^7 with 100 to 150 kV operation. The only disturbing factor necessarily remaining — and the most difficult one — is the spherical aberration of the objective. Ultimately, a very complex set of lenses consisting of at least four quadrupoles and three octupoles is necessary to correct the aberration, thereby improving the resolution directly in the microscope to less than 1 Å. However, a simpler method has been proposed by Welton.¹ If the illuminating beam has a transverse coherence length of about 1000 Å, a microscope that is limited only by spherical aberration could give micrographs with detailed information of the specimen down to less than 1 Å. Although the finest details are scrambled, the information can be extracted from the micrograph using, most practically, a digital computer.

The immediate purpose of this project has been, then, the development of a microscope with a highly coherent source and with no limitation in resolution to more than a few tenths of an angstrom except spherical

aberration. The apparatus was developed along three somewhat independent lines to be combined into the so-called high-coherence microscope. First, a microscope column (called microscope I) that used some parts from a Siemens I commercial microscope was built with a liquid-helium-cooled specimen carrier, stage, and objective lens. The lens coil was made superconducting. Second, techniques were developed for utilizing the enormous brightness of a field-emission source. A field-emission gun capable of the required 1000 Å coherence length while maintaining short exposure times was constructed. Third, a 150-kV power supply with a stability of $\frac{1}{4}$ to $\frac{1}{3}$ ppm was developed. Construction of these three components was completed in 1972.² Testing of each was sufficiently complete by March 1973 to permit their assembly into the high-coherence column. Further commissioning has continued since that time.

The following paragraphs summarize the work that was completed in 1973.

Field-Emission Gun

The techniques for making and operating field-emission tips were developed before this report period. All of the emitters were made with either (310)- or (111)-oriented tungsten wire of 5-mil diameter welded to a filament wire made from ordinary tungsten of 9-mil diameter. A set of jigs is required for the assembly.

A study of accelerating lens aberrations was completed as the first step in gun design. The geometry chosen — evident in Fig. 1 — has low aberrations besides lending itself to simple magnetic shielding for the beam and to rugged mechanical construction. The use of either an einzel or a magnetic lens between the tip and the accelerating lens that would eliminate the axial adjustment (Z) of the tip was found to lead always to a larger spot size from the gun. Since the rays of the

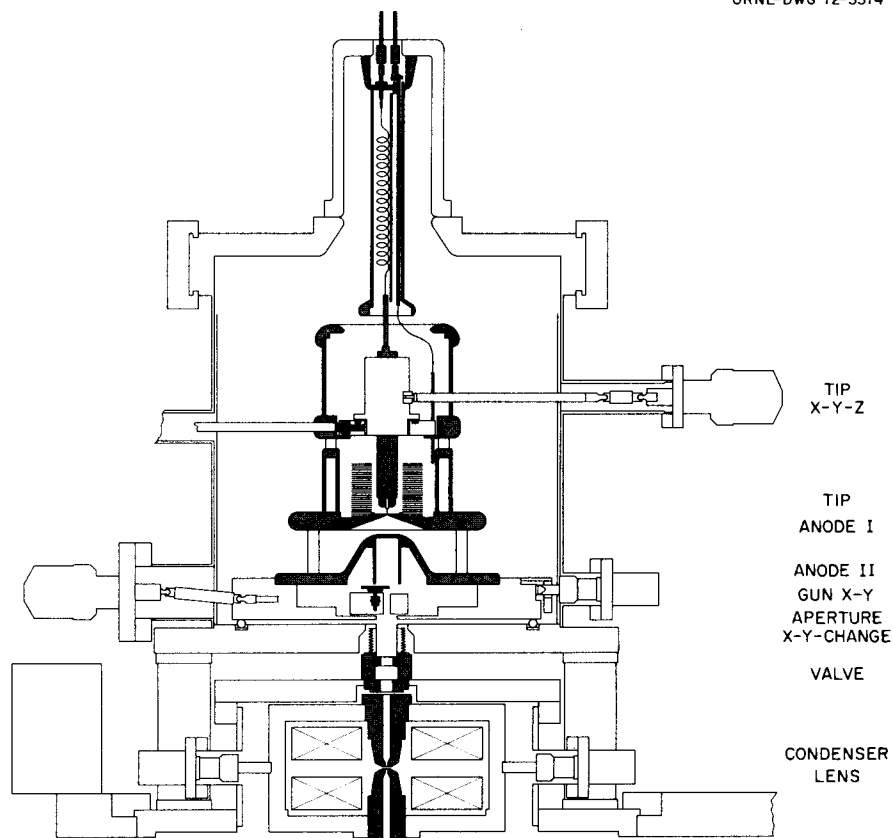


Fig. 1. Sectional diagram of the field-emission gun-illuminating system. The tip is held in the X-Y-Z adjustable carrier at high voltage. All other elements can be aligned independently in the horizontal (x-y) plane.

illuminating beam at the specimen should ideally be parallel to the axis ($\geq 1000 \text{ \AA}$ coherence requires the aperture angle to be $\leq 1.3 \times 10^{-5}$ radian entering the second-zone objective lens), a single condenser lens is needed to reduce the angular aperture of the rays from the gun. This lens has a minimum focal length of 3 mm. The aperture to eliminate nonparaxial rays was located as close as possible to anode II — the final electrode of the accelerating lens. Aberrations in the condenser have negligible effect compared with those of the accelerating lens.

The gun, which requires ultrahigh vacuum for reliable field emission, is enclosed in a 16-in.-diam, 16-in.-high bakeable stainless steel tank. A 400-liter/sec sputter-ion pump along with an 8-hr bakeout at about 200°C gives an ultimate pressure below 2×10^{-11} torr. When the valve into the cryostat is opened, the pressure rises to 1 or 2×10^{-10} torr. The field-emission tips can be operated at these pressures for 1 to 3 hr before recleaning is required.

High-voltage terminal. A high-voltage terminal contains the power supplies needed for tip operation, all of which must be insulated for the 150-kV accelerating voltage. As shown in Fig. 2, it is mounted above and to the rear of the gun tank, permitting it and the gun high-voltage insulator to be surrounded by insulating gas — Freon-12 or sulfur hexafluoride. The supplies are: (1) a 0-to-5-kV supply for field emission that is applied between the tip and anode I, (2) a negative 0-to-10-kV supply for tip forming, (3) a flashing supply for cleaning the tip by heating its support filament white hot momentarily, (4) a 0-to-1500-V supply for voltage focusing. All of these supplies are operated with insulated control shafts. Those needed while the image is being observed are motor driven.

Gun testing. Initial testing of the gun was completed with a temporary setup. The brightness of the tip emission was measured as $1.6 \times 10^7 \text{ A cm}^{-2} \text{ sr}^{-1}$ at 35 kV, which is in the range expected — about 10^3 times as large as that of a thermionic emitter. The high-

voltage terminal and gun electrodes were operated at voltages up to 160 kV without corona.

After combining the gun with microscope I, the smallest spot size of the beam at the specimen with the condenser off was measured as 1000 Å. With the

condenser on and the gun operating with the first crossover at the focal point of the condenser, the spot size was measured there as 400 Å. Micrographs were made with holey films that showed interference of different sets of Fresnel fringes over a distance greater

ORNL-DWG 74-3414

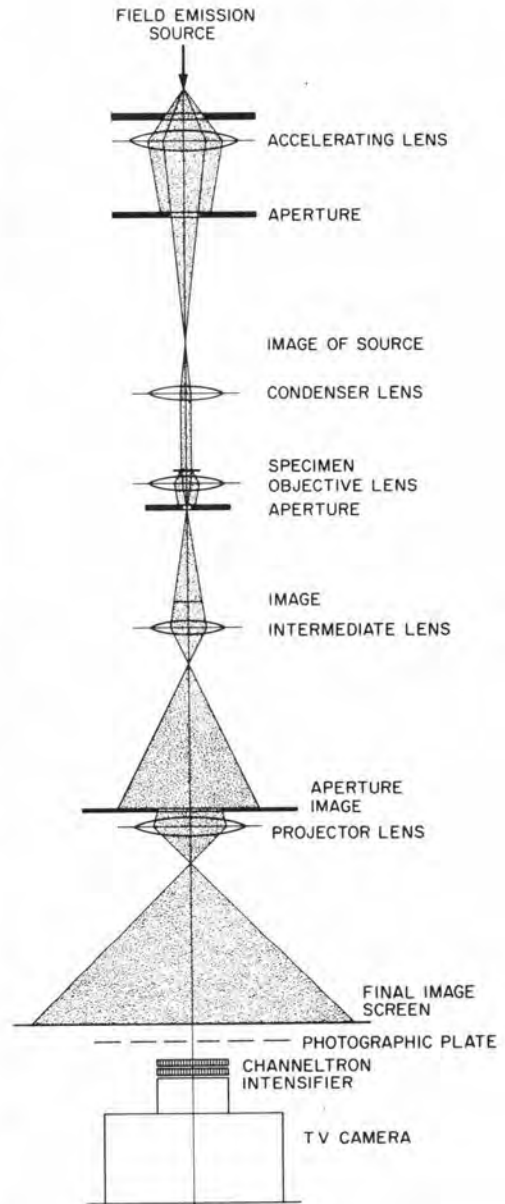
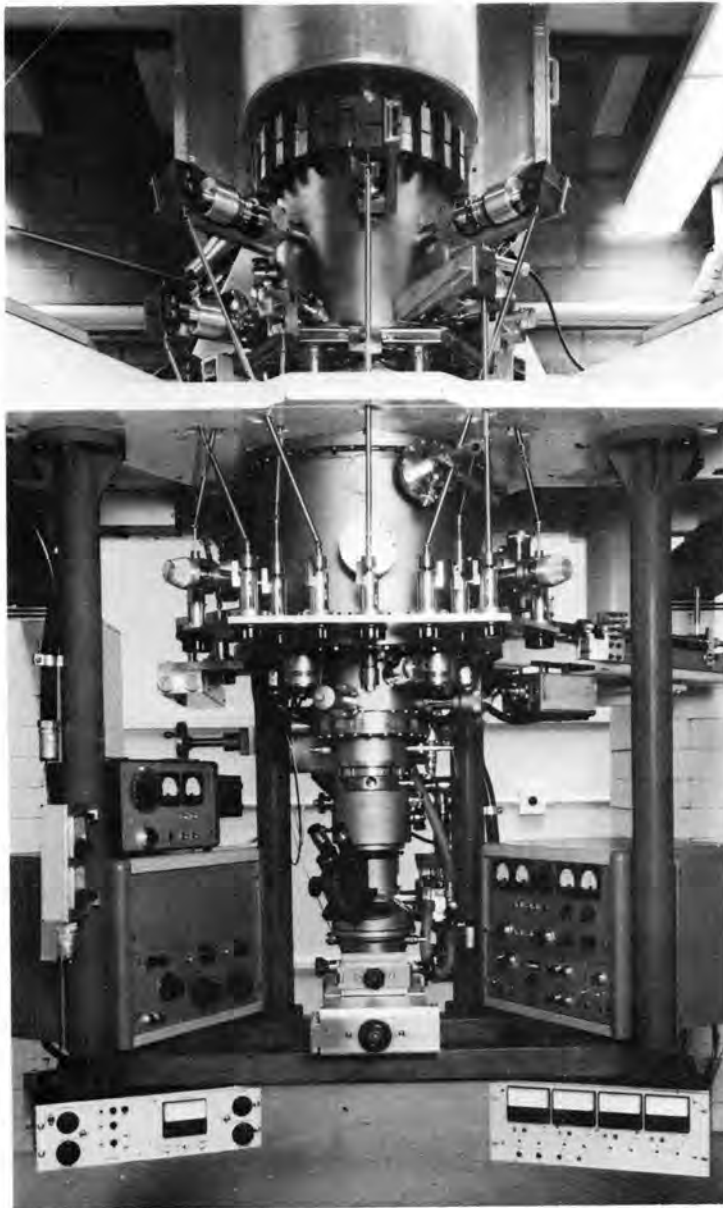


Fig. 2. The high-coherence microscope. The gas-insulated 150-kV terminal is the aluminum housing at the top of the column directly above the field-emission gun. The gun mechanical controls are extended through drive shafts down to a level suitable for the operator. The white support structure is bolted on at the condenser-top of cryostat level. The specimen insertion mechanism is visible at the right side of the cryostat. The three sputter-ion pumps, which are located behind the column, are supported directly from the frame.

than 1000 Å. This value more than met the requirement for high coherence. These values all are within the design requirements or expectations.

150-kV high-voltage supply. Further measurements at 100 kV of the stability and noise of the output voltage showed a peak-to-peak variation of $1/4$ to $1/3$ ppm.

Preparation Laboratory

Basic laboratory facilities for sample preparation and screening of biological materials and specimens were established adjacent to the high-coherence microscope. This facility includes a high-quality commercial electron microscope (Siemens IA), an optical diffractometer, and the essential ancillary equipment needed for high-resolution work. Test specimens were prepared and evaluated both for the high-coherence microscope and the Siemens IA as needed for development of the image-processing software. Most of this work was with ultrathin carbon films. Biological specimens available include tobacco mosaic virus, T4, and catalase crystals.

Microscope I

The construction of this microscope column, which was modified to test all parts in the high-coherence column below the gun, was completed in 1972. Tests were completed in early 1973. A simple specimen carrier was added in the intermediate lens so that at $k^2 \sim 3$ a magnification of 17,000 could be achieved. It was used to evaluate performance of all components other than the objective without having to cool the cryostat to liquid-helium temperature. The Channeltron TV camera was shown to be useful for setting up the microscope column at minimum beam currents – to minimize specimen damage. With the chevron-mounted double unit, clear images were obtained on the TV monitor for current densities below 10^{-13} A/cm². Under such illumination, the normal screen would be dark. Because of the TV system, the gray scale was somewhat inferior, however.

The resolution was measured, using Fresnel fringes at the edges of holes in carbon films, as 17 to 20 Å without astigmatism correction. Upon correcting astigmatism, slightly lower values were observed. Vibration was clearly recognized as a large factor, most of which appeared to come from the motion of the thermionic gun. The power supply used with the thermionic gun contributed about 7 parts in 10^5 peak-to-peak noise on the high voltage, a value that would lead to about 10 Å of chromatic aberration. Once the column had been tested completely and its limitation in resolution had been traced to the thermionic gun and to the support

structure, testing was stopped. The needed parts were combined with the field-emission gun into the high-coherence column.

High-Coherence Microscope

The field-emission gun was taken over into this new column without modification. The principal modifications made to microscope I were:

Support. A heavy framework of 4 X 6 in. box beams supports the column at a point above the center of gravity. The entire structure then sits on rubber isolation pads on top of the four concrete block posts. The lower part of the column, including the controls, is rigidly clamped in a rectangular frame up to the main support.

Film vacuum lock. A lock to permit rapid removal of exposed film and to return to the approximately 2×10^{-7} torr operating vacuum in the lower unit was added. A Polaroid camera or a Channeltron TV camera may be mounted on the lock.

Vacuum system. The Orb-Ion pumps, with their ac fields and water cooling, were replaced with sputter-ion pumps. The Vacsorb roughing pumps were mounted on a cart that is easily removable from the column.

Controls and power supplies. All of the controls were mounted directly on the frame of the microscope, leading to a smaller number of wires required from external units. All of the supplies other than the high voltage and lens currents are furnished from batteries. All ac equipment is well removed from the microscope.

Additional modifications. In the course of commissioning the microscope, the following principal additions have been made:

1. An electrostatic stigmator was added in anode II of the gun. This unit corrects the astigmatism of the gun itself.
2. The objective lens stage drives were modified so that the mechanical connection between shield I (20 to 30°K) and the stage itself (4°K) could be opened to reduce a possible source of specimen drift, both mechanical and thermal.
3. A beam shutter was added below the intermediate lens that can control film exposure time with little mechanical motion.
4. Several of the power supplies and their controls were modified to improve stability or to ease control. The vernier power supply used for voltage focusing was found to introduce excessive vibration because of its motor drive. The 150-kV supply was modified without affecting the noise on its output to allow the small changes required for focusing.

5. An additional set of deflection coils were designed to align the beam between the gun and the condenser lens.
6. Liquid nitrogen cryopumping was found to be highly effective in pumping the lower section (including the film chamber) and, of course, the cryostat. The installation of a larger trap that can be removed for cleaning was designed.

Field-emission tip and gun operation. About one dozen tips have been used to date. Four failed following sparks in the high voltage. At least three appear to have failed from damage due to excessive current in the gun. The other tips were replaced after an emission pattern that was not bright along the tip axis appeared following the cleaning-forming operation.

Most of the gun operation has been with the tip in closer to anode I than would be implied from the ray pattern of Fig. 1, so that the condenser sees a virtual source above or near the tip position. The condenser, then, runs as a weak lens to bring the rays to a spot on the specimen. This spot diameter is, typically, about $\frac{1}{4}$ μ .

Specimen stability. Specimen drift has been large at times; however, it appears to be just a matter of thermal equilibrium that is made more difficult by the operation at liquid-helium temperatures. Generally, drift will stop within a few minutes after a specimen is inserted.

Vibration. Sources of sharp noise can be seen to shake the image. Coupling is through both building vibrations and the air. The column has two resonant frequencies: at about 20 Hz and about 300 Hz. Both, however, are heavily damped, so that their time constants are less than 0.5 sec. A pneumatic vibration isolation system to reduce coupling from building vibrations has been ordered.

Resolution, coherence, magnification. Figure 3 illustrates some of the results obtained. A value of coherence exceeding the 1000- \AA value required for image processing was obtained in the earliest micrographs. As shown, more recently, by the diffractographs, however, the coherence was not uniform in all directions. Attempts to eliminate the source(s) of this fault are in progress. The maximum magnification was checked as approximately 1.25×10^6 times, for which the image of a carbon smoke specimen showed no variation above about 8 \AA in a 30-sec exposure. Resolution values down to 3.9 \AA have been measured in thick carbon-Formvar films using the diffractographs as illustrated.

1. T. A. Welton, *Phys. Div. Annu. Progr. Rep. Dec. 31, 1970*, ORNL-4659, pp. 6-13.

2. R. E. Worsham et al., *Phys. Div. Annu. Progr. Rep. Dec. 31, 1972*, ORNL-4844, pp. 132-33.

PHOTO 0816-74

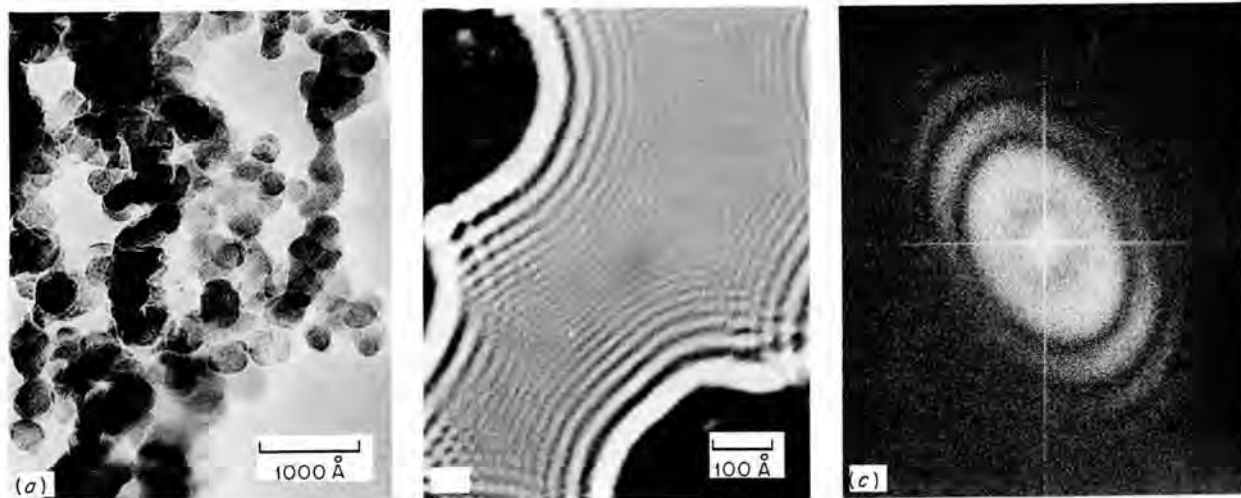


Fig. 3. Examples of micrographs. *A* is an example of carbon smoke made at 60,000 \times with 2 to 3 sec exposure. The phase-grain structure is evident. *B* is an example of the Fresnel fringes around carbon smoke particles. This micrograph was made at about 450,000 \times with a 15-sec exposure and a total field-emission tip current of about 0.5 μA . *C* is an optical diffractogram of a micrograph made using a carbon-Formvar film (about 200 \AA thick). The effect of nonuniform coherence is evident.

11. Publications

Prepared by Wilma L. Stair

The following listing of publications includes primarily those articles by Physics Division staff members and associates¹ which have appeared in print during 1973. It is not possible to include open-literature publications for the entire calendar year, however, as some journals for 1973 will be received only after this report has gone to press; thus six 1972 open-literature publications not previously reported in an annual report are included, and a few 1973 articles yet to be published will be listed in the next report for the period ending December 31, 1974.

Note: Articles pending publication and/or published early in 1974 are listed on pp. 272–275 of this report.

BOOK, JOURNAL, AND PROCEEDINGS ARTICLES

- Allen, B. J., and R. L. Macklin, "ORELA Neutron Capture and Stellar Nucleosynthesis," *Atomic Energy in Australia* **16**, 14–21 (1973).
- Allen, B. J., and R. L. Macklin, "Fast Neutron Capture Cross Sections for Silicon," pp. 291–292 in *Proceedings International Conference on Photonuclear Reactions and Applications (Pacific Grove, California, March 1973)*, ed. by B. L. Berman, USAEC Conf-73-0301, 1973.
- Allen, B. J., R. L. Macklin, C. Y. Fu, and R. R. Winters, "Comments on the Doorway State in ^{206}Pb ," *Phys. Rev. C7* (Comments & Addenda), 2598–2600 (1973).
- Allen, B. J., R. L. Macklin, R. R. Winters, and C. Y. Fu, "Neutron Capture Cross Sections of the Stable Lead Isotopes," *Phys. Rev. C8*, 1504–1517 (1973).
- Appleton, B. R., J. H. Barrett, T. S. Noggle, and C. D. Moak, "Orientation Dependence of Intensity and Energy Loss of Hyperchanneled Ions," pp. 391–401 in *Atomic Collisions in Solids IV. Physics of Channeling and Related Phenomena*, ed. by S. Andersen, K. Björkqvist, B. Domeij, and N. G. E. Johansson, Gordon & Breach Science Publishers, London, 1972.
- Appleton, B. R., C. D. Moak, T. S. Noggle, and J. H. Barrett, "Hyperchanneling — an Axial Channeling Phenomenon," pp. 98–102 in *Monograph on Hyperchanneling*, Physical Society of Japan, 1973 [reprinted from *Phys. Rev. Lett.* **28**, 1307–1311 (1972)].
- Auble, R. L., "Nuclear Data Sheets for $A = 126$," *Nucl. Data Sheets* **9**, 125–156 (February 1973).
- Auble, R. L., "Nuclear Data Sheets for $A = 128$," *Nucl. Data Sheets* **9**, 157–194 (February 1973).
- Auble, R. L., "Nuclear Data Sheets for $A = 141$," *Nucl. Data Sheets* **10**, 151–204 (August 1973).
- Auble, R. L., F. E. Bertrand, Y. A. Ellis, and D. J. Horen, "Nuclear Spectroscopy of ^{109}Ag from the $^{108}\text{Pd}(^3\text{He},d)$ Reaction," *Phys. Rev. C8*, 2308–2312 (1973).
- Bair, J. K., "Absolute Neutron Yields from Thick Target $^{14}\text{C}(\alpha,n)$," *Nucl. Sci. Eng. (Technical Note)* **51**, 83 (1973).

¹ Associates include consultants, guest assignees, graduate students, members of other ORNL divisions, faculty member collaborators, etc.

- Bair, J. K., "Total Neutron Yields from the Proton Bombardment of $^{17,18}\text{O}$," *Phys. Rev.* **C8**, 120–123 (1973).
- Bair, J. K., and H. M. Butler, "Neutron Yield from a Small High Purity $^{238}\text{PuO}_2$ Source," *Nucl. Technol. (Technical Note)* **19**, 202–203 (1973).
- Bair, J. K., and F. X. Haas, "Total Neutron Yield from the Reactions $^{13}\text{C}(\alpha, n)^{16}\text{O}$, and $^{17,18}\text{O}(\alpha, n)^{20,21}\text{Ne}$," *Phys. Rev.* **C7**, 1356–1364 (1973).
- Ball, J. B., C. B. Fulmer, J. S. Larsen, and G. Sletten, "Energy Levels of ^{94}Ru Observed with the $^{96}\text{Ru}(p, t)$ Reaction," *Nucl. Phys.* **A207**, 425–432 (1973).
- Ball, J. B., J. J. Pinajian, J. S. Larsen, and A. C. Rester, "Study of ^{82}Sr , ^{84}Sr , and ^{86}Sr with the (p, t) Reaction," *Phys. Rev.* **C8**, 1438–1447 (1973).
- Bemis, C. E., Jr., F. K. McGowan, J. L. C. Ford, Jr., W. T. Milner, P. H. Stelson, and R. L. Robinson, " E_2 and E_4 Transition Moments and Equilibrium Deformations in the Actinide Nuclei," *Phys. Rev.* **C8**, 1466–1480 (1973).
- Bemis, C. E., R. J. Silva, D. C. Hensley, O. L. Keller, Jr., J. R. Tarrant, L. D. Hunt, P. F. Dittner, R. L. Hahn, and C. D. Goodman, "X-Ray Identification of Element 104," *Phys. Rev. Lett.* **31**, 647–650 (1973).
- Bemis, C. E., Jr., P. H. Stelson, F. K. McGowan, W. T. Milner, J. L. C. Ford, Jr., R. L. Robinson, and W. Tuttle, "Interference between Direct Nuclear and Coulomb Excitation with Alpha Particles on ^{154}Sm , ^{166}Er , and ^{182}W ," *Phys. Rev.* **C8**, 1934–1937 (1973).
- Bertrand, F. E., "Nuclear Data Sheets for $A = 124$," *Nucl. Data Sheets* **10**, 91–150 (August 1973).
- Bertrand, F. E., M. B. Lewis, G. R. Satchler, D. J. Horen, D. C. Kocher, R. W. Peelle, E. E. Gross, and E. Newman, "Excitation of a Giant Resonance in the Nuclear Continuum by Inelastic Proton Scattering," p. 711 in *Proceedings International Conference on Photonuclear Reactions and Applications (Pacific Grove, California, March 1973)*, ed. by B. L. Berman, USAEC Conf-73-0301, 1973.
- Bertrand, F. E., and R. W. Peelle, "Complete Hydrogen and Helium Particle Spectra from 30- to 60-MeV Proton Bombardment of Nuclei from $A = 12$ to 209 and Comparison with the Intranuclear Cascade Model," *Phys. Rev.* **C8**, 1045–1064 (1973).
- Bhatt, K. H., J. C. Parikh, and J. B. McGrory, "On the Collective Structure of Some Shell Model States," p. 130 in Vol. 1 of *Proceedings International Conference on Nuclear Physics (Munich, Germany, August–September 1973)*, ed. by J. de Boer and H. J. Mang, North-Holland/American Elsevier, 1973.
- Bingham, C. R., and G. T. Fabian, "Neutron Shell Structure in ^{93}Zr , ^{95}Zr , and ^{97}Zr by (d, p) and $(\alpha, ^3\text{He})$ Reactions," *Phys. Rev.* **C7**, 1509–1519 (1973).
- Bingham, C. R., and D. L. Hillis, "Neutron Shell Structure in ^{125}Sn by (d, p) and $(\alpha, ^3\text{He})$ Reactions," *Phys. Rev.* **C8**, 729–736 (1973).
- Bingham, C. R., D. U. O'Kain, K. S. Toth, and R. L. Hahn, "Measurement of Alpha-Decay Branching Ratios for $^{150,151}\text{Dy}$ and $^{149\text{m}}\text{Tb}$," *Phys. Rev.* **C7**, 2575–2579 (1973).
- Bird, J. R., B. J. Allen, I. Bergqvist, and J. A. Biggerstaff, "Compilation of keV-Neutron-Capture Gamma-Ray Spectra," *Nucl. Data Tables* **11**, 433–529 (May 1973).
- Bloom, S. D., J. B. McGrory, and S. A. Moszkowski, "Analog and Configuration States in ^{49}Sc ($J^\pi = 3/2^-$ and $1/2^-$) and the Low-Lying Level Structure in ^{48}Sc ," *Nucl. Phys.* **A199**, 369–385 (1973); also, UCRL-73391, Rev. 1, August 1972.
- Brown, M. D., "The Response of a Silicon Surface Barrier Detector to Bromine, Iodine, and Uranium Ions," *Nucl. Instrum. Methods* **106**, 141–145 (1973).
- Bugg, W. M., G. T. Condo, E. L. Hart, H. O. Cohn, and R. D. McCulloch, "Evidence for a Neutron Halo in Heavy Nuclei from Antiproton Absorption," *Phys. Rev. Lett.* **31**, 475 (1973).
- Bugg, W. M., G. T. Condo, E. L. Hart, H. O. Cohn, and R. D. McCulloch, "Interactions of Stopping K^- Mesons with Nuclei and the Neutron Halo Question," *Nucl. Phys.* **B64**, 29–33 (1973).
- Bugg, W. M., G. T. Condo, E. L. Hart, H. O. Cohn, R. D. McCulloch, R. J. Endorf, C. P. Horne, and M. M. Nussbaum, "Four Pion Decay of the f^0 Meson," *Phys. Rev.* **D7**, 3264–3266 (1973).

- Burton, J. W., J. O. Thomson, P. G. Huray, and L. D. Roberts, "Magnetic Hyperfine Structure Coupling and Mössbauer Isomer Shift for ^{197}Au in Au-Ni and Cu-Ni-Au Alloys," *Phys. Rev.* **B7**, 1773–1782 (1973).
- Butler, H. M., K. M. Wallace, and C. B. Fulmer, "Half-Value Thicknesses of Ordinary Concrete for Neutrons from Cyclotron Targets," *Health Phys.* **24**, 438–439 (1973).
- Carlson, T. A. (invited paper), "Present and Future Applications of Auger Spectroscopy," pp. 2274–2304 in Vol. 4 of *Proceedings International Symposium on Future Applications of Inner Shell Ionization Phenomena (Atlanta, Georgia, April 1972)*, ed. by R. W. Fink et al., USAEC Conf-720404 (1973).
- Carlson, T. A., and G. E. McGuire, "Angular Distribution of the Photoelectron Spectrum of CO_2 , COS , CS_2 , N_2O , H_2O , and H_2S ," *J. Electron Spectrosc.* **1**, 209–217 (1973).
- Carlson, T. A., and C. W. Nestor, Jr., "Calculation of Electron Shake-Off Probabilities as the Result of X-Ray Photoionization of the Rare Gases," *Phys. Rev.* **A8**, 2887–2894 (1973).
- Carlson, T. A., and R. M. White (invited paper), "Study of the Angular Distribution for the Photoelectron Spectra of Halogen Substituted Methane Molecules," *Trans. Faraday Soc.* **54**, 285–291 (1972) (Proceedings General Discussion on Photoelectron Spectroscopy of Molecules, Sussex, England, September 1972).
- Cheng, K. L., J. C. Carver, and T. A. Carlson, "X-Ray Photoelectron Spectra of Ethylenediaminetetraacetic Acid and Its Metal Complexes," *Inorg. Chem.* **12**, 1702–1704 (1973).
- Christensen, P. R., I. Chernov, E. E. Gross, R. Stokstad, and F. Videbaek, "The Interference of Coulomb and Nuclear Excitation in the Scattering of ^{16}O from ^{58}Ni , ^{88}Sr , and ^{142}Nd ," *Nucl. Phys.* **A207**, 433 (1973).
- Coker, W. R., J. Lin, J. L. Duggan, and P. D. Miller, "Multistep Contributions to $^{11}\text{B}(h,\alpha)^{10}\text{B}$ from 8.0 to 12.0 MeV," *Phys. Lett.* **45B**, 321–323 (1973).
- Datz, S., B. R. Appleton, and C. D. Moak, "Detailed Studies of Channeled Ion Trajectories and Associated Channeling Potentials and Stopping Powers," pp. 153–179 in *Channeling*, Chap. VI, ed. by D. V. Morgan, John Wiley & Sons, Ltd., Sussex, England, 1973.
- Datz, S., F. W. Martin, C. D. Moak, B. R. Appleton, and L. B. Bridwell, "Charge-Changing Collisions of Channeled Oxygen Ions in Gold," pp. 87–93 in *Atomic Collisions in Solids IV. Physics of Channeling and Related Phenomena*, ed. by S. Andersen, K. Björkqvist, B. Domeij, and N. G. E. Johansson, Gordon & Breach Science Publishers, London, 1972.
- Datz, S., C. D. Moak, T. S. Noggle, B. R. Appleton, and H. O. Lutz, "Potential-Energy and Differential-Stopping-Power Functions from Energy-Loss Spectra of Fast Ions Channeled in Gold Single Crystals," pp. 86–97 in *Monograph on Hyperchanneling*, Physical Society of Japan, 1973 (reprinted from *Phys. Rev.* **179**, 315–326 (1969)).
- Davies, K. T. R., S. J. Krieger, and C. Y. Wong, "Generalized Shells in Nuclei: Hartree-Fock Calculations of Bubble Nuclei," *Nucl. Phys.* **A216**, 250–270 (1973).
- Davies, K. T. R., R. J. McCarthy, and P. U. Sauer, "Higher-Order Corrections to Brueckner-Hartree-Fock Binding Energies and Radii," *Phys. Rev.* **C7**, 943–951 (1973).
- de Lange, J. C., J. Bron, A. van Poelgeest, H. Verheul, and W. B. Ewbank, "New Activities Produced with the AVF Cyclotron of the Free University (Amsterdam): ^{91}Tc and $^{93\text{m}}\text{Ru}$," p. 220 in Vol. 1 of *Proceedings International Conference on Nuclear Physics* (Munich, Germany, August–September 1973), ed. by J. de Boer and H. J. Mang, North-Holland/American Elsevier, 1973.
- De Lucia, F. C., P. Helminger, W. Gordy, H. W. Morgan, and P. A. Staats, "Millimeter and Submillimeter Wave Spectrum and Molecular Constants of T_2O ," *Phys. Rev.* **A8**, 2785–2791 (1973).
- Deye, J. A., R. L. Robinson, and J. L. C. Ford, Jr., "The ^{110}Pd , $^{166}\text{Cd}(p,p'\gamma)$ Reactions," *Nucl. Phys.* **A204**, 307–320 (1973).
- Dress, W. B., P. D. Miller, and N. F. Ramsey, "Improved Upper Limit for the Electric Dipole Moment of the Neutron," *Phys. Rev.* **D7**, 3147–3149 (1973).

- Eichler, E., N. R. Johnson, R. O. Sayer, D. C. Hensley, and L. L. Riedinger, "Sign of the Hexadecapole Moments of ^{232}Th and ^{238}U Nuclei," *Phys. Rev. Lett.* **30**, 568–571 (1973).
- Ellis, Y. A., "Nuclear Data Sheets for $A = 181$," *Nucl. Data Sheets* **9**, 319–399 (April 1973).
- Ewbank, W. B., "Appendix, L -Subshell Conversion Ratios," pp. 238–243 in Vol. 1, *Atomic and Nuclear Data Reprints*, ed. by Katherine Way, Academic Press, Inc., New York, 1973.
- Ewbank, W. B., F. W. Hurley, and M. R. McGinnis, "Recent References (January 1973 through April 1973)," *Nucl. Data Sheets* **9**, 515–669 (June 1973).
- Ferguson, R. L., F. Plasil, H. Freiesleben, C. E. Bemis, Jr., and H. W. Schmitt, "Fragment Kinetic Energy in ^{18}O -Induced Fission of ^{232}Th and ^{246}Cm ," *Phys. Rev.* **C8**, 1104–1108 (1973).
- Ferguson, R. L., F. Plasil, Frances Pleasonton, S. C. Burnett, and H. W. Schmitt, "Systematics of Fragment Mass and Energy Distributions for Proton-Induced Fission of ^{233}U , ^{235}U , and ^{238}U ," *Phys. Rev.* **C7**, 2510–2522 (1973).
- Ferrer, J. C., J. Rapaport, and S. Raman, "Decay of ^{51}Mn ," *Z. Phys.* **265**, 365–369 (1973).
- Ford, J. L. C., Jr., K. S. Toth, D. C. Hensley, R. M. Gaedke, P. J. Riley, and S. T. Thornton, "Single-Nucleon Transfer Reactions and Inelastic Scattering Induced by ^{11}B Ions Incident on ^{208}Pb ," *Proceedings Symposium on Heavy-Ion Transfer Reactions (Argonne, Illinois, March 1973)*, ANL Informal Report PHY-1973B, Vol. II, 495–502 (1973).
- Ford, J. L. C., Jr., K. S. Toth, D. C. Hensley, R. M. Gaedke, P. J. Riley, and S. T. Thornton, "Inelastic Scattering and Single Nucleon Transfer Reactions with ^{11}B Ions Incident on ^{208}Pb ," p. 381 in Vol. 1 of *Proceedings International Conference on Nuclear Physics (Munich, Germany, August–September 1973)*, ed. by J. de Boer and H. J. Mang, North-Holland/American Elsevier, 1973.
- Ford, J. L. C., Jr., K. S. Toth, D. C. Hensley, R. M. Gaedke, P. J. Riley, and S. T. Thornton, "Interference between Coulomb and Nuclear Excitation in the Inelastic Scattering of ^{11}B Ions from ^{208}Pb ," *Phys. Rev.* **C8**, 1912–1915 (1973).
- Fowler, J. L., C. H. Johnson, and R. M. Feezel, "The Level Structure of ^{17}O from Neutron Total Cross Sections," *Phys. Rev.* **C8**, 545–562 (1973).
- Fowler, J. L., C. H. Johnson, and N. W. Hill, "Total Neutron Cross Section of Calcium," p. 525 in Vol. 1 of *Proceedings International Conference on Nuclear Physics (Munich, Germany, August–September 1973)*, ed. by J. de Boer and H. J. Mang, North-Holland/American Elsevier, 1973.
- Fulmer, C. B., and J. C. Hafele, "Spin-Orbit and Target-Spin Effects in Helion Elastic Scattering," *Phys. Rev.* **C7**, 631–637 (1973).
- Fulmer, C. B., and J. C. Hafele, "Optical-Model-Family Ambiguity Resolved for ^3He Elastic Scattering from ^{60}Ni ," *Phys. Rev.* **C8**, 172–177 (1973).
- Fulmer, C. B., J. C. Hafele, and C. C. Foster, "Energy Dependence of the Optical Model for Helion Scattering from ^{60}Ni ," *Phys. Rev.* **C8**, 200–205 (1973).
- Geramb, H. F., and J. B. McGrory, "Correlation Effects in the Microscopic Analysis of $^{12}\text{C}(p,p')$ Reactions," p. 386 in Vol. 1 of *Proceedings International Conference on Nuclear Physics (Munich, Germany, August–September 1973)*, ed. by J. de Boer and H. J. Mang, North-Holland/American Elsevier, 1973.
- Gomez del Campo, J., J. L. C. Ford, Jr., R. L. Robinson, P. H. Stelson, J. B. McGrory, and S. T. Thornton, "Population of High Spin States in ^{22}Na by Means of the $^{10}\text{B}(^{16}\text{O},\alpha)$ Reaction," *Phys. Lett.* **B46**, 180–182 (1973).
- Gomez del Campo, J., J. L. C. Ford, Jr., S. T. Thornton, R. L. Robinson, and P. H. Stelson, "High Spin States in ^{22}Na ," p. 167 in Vol. 1 of *Proceedings International Conference on Nuclear Physics (Munich, Germany, August–September 1973)*, ed. by J. de Boer and H. J. Mang, North-Holland/American Elsevier, 1973.
- Grabowski, Z. W., and R. L. Robinson, "Properties of the $2'$ and $2''$ States in $^{106,112}\text{Cd}$ and ^{114}Cd ," *Nucl. Phys.* **A206**, 633–640 (1973).
- Haas, F. X., and J. K. Bair, "Total Neutron Yield from the (α,n) Reaction on $^{21,22}\text{Ne}$," *Phys. Rev.* **C7**, 2432–2436 (1973).

- Halbert, M. L., D. C. Hensley, and H. G. Bingham, " ${}^6\text{Li}({}^3\text{He},t)$ Reaction and the Solar Neutrino Puzzle," *Phys. Rev.* **C8**, 1226–1229 (1973).
- Halbert, M. L., P. Paul, K. A. Snover, and E. K. Warburton, "Radiative Capture of Protons by Deuterium," pp. 531–534 in *Few-Particle Problems in the Nuclear Interaction* (Proceedings International Conference, Los Angeles, California, August–September 1972), ed. by Ivo Slaus, North-Holland Publishers, Amsterdam, Netherlands, 1973.
- Halbert, M. L., A. van der Woude, and N. M. O'Fallon, "Sequential Reactions Induced by Alpha Particles on ${}^3\text{He}$," *Phys. Rev.* **C8**, 1621–1628 (1973).
- Hamilton, J. H., A. V. Ramayya, W. E. Collins, L. Varnell, J. Lange, G. Garcia-Bermudez, R. Ronningen, R. L. Robinson, P. H. Stelson, J. L. C. Ford, Jr., N. R. Johnson, A. Kluk, J. Pinajian, L. L. Riedinger, H. Yamada, T. Katoh, M. Fujioka, M. Sekikawa, and S. H. Ahn, "Properties of $K^\pi = 2^+$ and 0^+ Bands in ${}^{156,158}\text{Gd}$ and ${}^{176,178,180}\text{Hf}$," p. 294 in Vol. 1 of *Proceedings International Conference on Nuclear Physics* (Munich, Germany, August–September 1973), ed. by J. de Boer and H. J. Mang, North-Holland/American Elsevier, 1973.
- Harmatz, B., "Nuclear Data Sheets for $A = 169$," *Nucl. Data Sheets* **10**, 359–426 (October 1973).
- Harris, E. G., P. G. Huray, F. E. Obenshain, J. O. Thomson, and R. A. Villecco, "Experimental Test of Weyl's Gauge Invariant Geometry," *Phys. Rev.* **D7**, 2326–2330 (1973).
- Helton, V. D., J. C. Hiebert, and J. B. Ball, "Neutron Hole States in ${}^{138}\text{La}$ and ${}^{140}\text{Pr}$," *Nucl. Phys.* **A201**, 225–246 (1973).
- Hensley, D. C., "List or Sort? – Some Experience with the ORIC Multiparameter Data Acquisition System," *IEEE Trans. Nucl. Sci.* **NS-20**, No. 1, 334–341 (1973) (Proceedings 1972 Nuclear Science Symposium, Miami Beach, Florida, December 1972).
- Horen, D. J., "Nuclear Data Project: Operations, Status, and Plans," pp. 325–333 in Vol. II of *Proceedings of IAEA Symposium on Applications of Nuclear Data in Science and Technology* (Paris, France, March 1973), International Atomic Energy Agency, Vienna, 1973.
- Horen, D. J., W. B. Ewbank, R. L. Auble, F. E. Bertrand, Y. A. Ellis, B. Harmatz, M. B. Lewis, M. J. Martin, S. Raman, and M. R. Schmorak, *Nuclear Level Schemes, $A = 45$ through $A = 257$ from the Nuclear Data Sheets*, ed. by the Nuclear Data Group, Academic Press, Inc., 1973, 866 pp.
- Horen, D. J., and A. M. Weinberg (keynote address), "Criteria of Choice for Compilations of Nuclear Data," pp. 3–11 in Vol. 1 of *Nuclear Data in Science and Technology* (Proceedings Symposium, Paris, France, March 1973), International Atomic Energy Agency, Vienna, Austria, 1973.
- Hudson, E. D., R. S. Lord, C. A. Ludemann, M. L. Mallory, J. A. Martin, W. T. Milner, S. W. Mosko, P. H. Stelson, and A. Zucker, "A Multi-Accelerator System for Heavy Ions," *IEEE Trans. Nucl. Sci.* **NS-20**, No. 3, 168–172 (June 1973) (Proceedings 1973 Particle Accelerator Conference, San Francisco, California, March 1973).
- Hudson, E. D., M. L. Mallory, R. S. Lord, and A. Zucker, "Energy Multiplication by Beam Recycling in an Isochronous Cyclotron," *IEEE Trans. Nucl. Sci.* **NS-20**, No. 3, 173–177 (June 1973) (Proceedings 1973 Particle Accelerator Conference, San Francisco, California, March 1973).
- Hutcherson, J. W., and P. M. Griffin, "Self-Broadened Absorption Line Widths for the Krypton Resonance Transitions," *J. Opt. Soc. Amer.* **63**, 338–341 (1973).
- Ichimura, M., A. Arima, E. C. Halbert, and T. Terasawa, "Alpha-Particle Spectroscopic Amplitudes and the SU(3) Model," *Nucl. Phys.* **A204**, 225–278 (1973).
- Johnson, C. H., "Unified R -Matrix-Plus-Potential Analysis for ${}^{16}\text{O} + n$ Cross Sections," *Phys. Rev.* **C7**, 561–573 (1973).
- Jones, C. M., "Feasibility and Cost of a Superconducting Heavy Ion Linear Accelerator," *Particle Accel.* **5**, 45–60 (1973).
- Jones, C. M., J. L. Fricke, B. Piosczyk, and J. E. Vetter, "A Slow Tuner for Superconducting Helically Loaded Resonant Cavities," *Proceedings 1972 Proton Linear Accelerator Conference (Los Alamos, New Mexico, October 1972)*, LASL-5115, 163–167 (1972).

- Keller, O. L., Jr., C. W. Nestor, Jr., T. A. Carlson, and B. Fricke, "Predicted Properties of the Superheavy Elements. II. Element 111, Eka-Gold," *J. Phys. Chem.* **77**, 1806–1809 (1973).
- Keyworth, G. A., J. R. Lemley, C. E. Olsen, F. T. Seibel, J. W. T. Dabbs, and N. W. Hill, "Spin Determination of Intermediate Structure in the Subthreshold Fission of ^{237}Np ," *Phys. Rev.* **C8**, 2352–2363 (1973).
- Keyworth, G. A., C. E. Olsen, F. T. Seibel, J. W. T. Dabbs, and N. W. Hill, "Spin Determination of Resonances in the Neutron-Induced Fission of ^{235}U ," *Phys. Rev. Lett.* **31**, 1077–1080 (1973).
- Kim, H. J., R. L. Robinson, and W. T. Milner, "High-Spin States of ^{42}Ca via the $^{28}\text{Si}(^{16}\text{O}, 2p\gamma)$ Reaction," p. 172 in Vol. 1 of *Proceedings International Conference on Nuclear Physics* (Munich, Germany, August–September 1973), ed. by J. de Boer and H. J. Mang, North-Holland/American Elsevier, 1973.
- Ko, C. M., T. T. S. Kuo, and J. B. McGrory, "Weak-Coupling Model for ^{212}Pb and ^{204}Pb ," *Phys. Rev.* **C8**, 2379–2389 (1973).
- Kocher, D. C., "Nuclear Data Sheets for $A = 94$," *Nucl. Data Sheets* **10**, 205–308 (September 1973).
- Kocher, D. C., F. E. Bertrand, E. E. Gross, R. S. Lord, and E. Newman, "Excitation of Giant Resonances in ^{58}Ni via Inelastic Scattering of Polarized Protons," p. 654 in Vol. 1 of *Proceedings International Conference on Nuclear Physics* (Munich, Germany, August–September 1973), ed. by J. de Boer and H. J. Mang, North-Holland/American Elsevier, 1973.
- Kocher, D. C., F. E. Bertrand, E. E. Gross, R. S. Lord, and E. Newman, "Excitation of Giant Resonances in ^{58}Ni via Inelastic Scattering of Polarized Protons," *Phys. Rev. Lett.* **31**, 1070–1073 (1973).
- Krieger, S. J., K. T. R. Davies, and C. Y. Wong, "Generalized Shells in Nuclei: HF Calculations of Bubble Nuclei," p. 56 in Vol. 1, *Proceedings International Conference on Nuclear Physics* (Munich, Germany, August–September 1973), ed. by J. de Boer and H. J. Mang, North-Holland/American Elsevier, 1973.
- Lanford, W. A., and J. B. McGrory, "Two-Neutron Pickup Strengths on the Even Lead Isotopes. The Transition from Single-Particle to 'Collective,'" *Phys. Lett.* **45B**, 238–240 (1973).
- Larsen, J. S., J. B. Ball, and C. G. Fulmer, "Level Structure of ^{92}Mo and ^{94}Mo Studied with the (p,t) Reaction," *Phys. Rev.* **C7**, 751–760 (1973).
- Lemming, J. F., and S. Raman, "Nuclear Data Sheets for $A = 142$," *Nucl. Data Sheets* **10**, 309–357 (October 1973).
- Lewis, M. B., "Nuclear Data Sheets for $A = 191$," *Nucl. Data Sheets* **9**, 435–514 (1973).
- Lewis, M. B., "Giant Resonances in the High-Energy Helium Inelastic Scattering," *Phys. Rev.* **C7**, 2041–2043 (1973).
- Lewis, M. B., "Can We Generalize the Giant Resonance Idea?" pp. 685–694 in *Proceedings International Conference on Photonuclear Reactions and Applications (Pacific Grove, California, March 1973)*, ed. by B. L. Berman, USAEC Conf-730301, 1973.
- Lewis, M. B., F. E. Bertrand, and C. B. Fulmer, "Investigation of the $^{208}\text{Pb}(p,p')$ Reaction at $E = 54$ MeV," *Phys. Rev.* **C7**, 1966–1972 (1973).
- Lewis, M. B., F. E. Bertrand, and D. J. Horen, "Corroboration of the Quadrupole Assignment for the 11-MeV Giant Resonance in ^{208}Pb ," *Phys. Rev.* **C8**, 398–400 (1973).
- Ludemann, C. A., J. M. Domaschko, S. W. Mosko, and K. Hagemann, "Computer Control of the Oak Ridge Isochronous Cyclotron," *IEEE Trans. Nucl. Sci.* **NS-20**, No. 3, 618–620 (June 1973) (Proceedings 1973 Particle Accelerator Conference, San Francisco, California, March 1973).
- Macklin, R. L., and R. R. Winters, "Neutron Capture in Fluorine below 1500 keV," *Phys. Rev.* **C7**, 1766–1769 (1973).
- Malik, F. B., and M. G. Mustafa, "A Pedestrian Approach to the Intermediate Structure in Photonuclear Reaction in Light Nuclei," pp. 124–162 in *Proceedings Fifth Symposium on the Structure of Low-Medium Mass Nuclei* (Lexington, Kentucky, October 1973), ed. by J. P. Davidson and B. D. Kern, University of Kentucky Press, 1973.

- Mallory, M. L., E. D. Hudson, and R. S. Lord, "Cyclotron Internal Ion Source with DC Extraction," *IEEE Trans. Nucl. Sci.* **NS-20**, No. 3, 147–150 (June 1973) (Proceedings 1973 Particle Accelerator Conference, San Francisco, California, March 1973).
- McGowan, F. K., "Some Nuclear Structure Results from Coulomb Excitation," pp. 38–54 in *Proceedings Heavy-Ion Summer Study (Oak Ridge, Tennessee, June 1972)*, USAEC Conf-720669 (1973).
- McGowan, F. K., and W. T. Milner, "Charged-Particle Reaction List, 1948–1971," pp. 1–547 in Vol. 2, *Atomic and Nuclear Data Reprints*, ed. by Katherine Way, Academic Press, New York & London, 1973.
- McGrory, J. B., "Shell Model Spectroscopy of *f-p*-Shell Nuclei with $A \leq 44$," *Phys. Rev.* **C8**, 693–710 (1973).
- McGrory, J. B., and B. H. Wildenthal, "Shell Model Calculations for $A = 18, 19$, and 20 Nuclei with Core Excitation Included Explicitly," *Phys. Rev.* **C7**, 974–993 (1973).
- McGuire, G. E., G. K. Schweitzer, and T. A. Carlson, "Study of Core Electron Binding Energies in Some Group IIIA, VB and VIB Compounds," *Inorg. Chem.* **12**, 2450–2453 (1973).
- Mosko, S. W., "A New RF System for the ORIC," *IEEE Trans. Nucl. Sci.* **NS-20**, No. 3, 416–417 (June 1973) (Proceedings 1973 Particle Accelerator Conference, San Francisco, California, March 1973).
- Mowat, J. R., I. A. Sellin, D. J. Pegg, R. S. Peterson, M. D. Brown, and J. R. Macdonald, "Exponential Projectile Charge Dependence of Ar *K* and Ne *K* X-Ray Production by Fast, Highly-Ionized Argon Beams in Thin Neon Targets," *Phys. Rev. Lett.* **30**, 1289–1292 (1973).
- Mowat, J. R., I. A. Sellin, D. J. Pegg, R. S. Peterson, M. D. Brown, and J. R. Macdonald, "Exponential Projectile Charge Dependence of Ar *K* and Ne *K* X-Ray Production by Fast, Highly-Ionized Argon Beams in Neon Targets," pp. 727–728 in Vol. 2, *Electronic and Atomic Collisions* (Proceedings Conference, Belgrade, Yugoslavia, July 1973), ed. by B. C. Cobic and M. V. Kurepa, Institute of Physics, Belgrade, 1973.
- Mowat, J. R., I. A. Sellin, R. S. Peterson, D. J. Pegg, M. D. Brown, and J. R. Macdonald, "Mean Life of the Metastable 2^3P_1 State of the Two-Electron Fluorine Ion," *Phys. Rev.* **A8**, 145–150 (1973).
- Muga, M. L., G. L. Griffith, H. W. Schmitt, and H. E. Taylor, "Thin Film Detector Response to the Passage of Accelerated Heavy Ions," *Nucl. Instrum. Methods* **3**, 581–585 (1973).
- Mustafa, M. G., U. Mosel, and H. W. Schmitt, "Asymmetry in Nuclear Fission," *Phys. Rev.* **C7**, 1519–1532 (1973).
- Mustafa, M. G., and H. W. Schmitt, "Potential Energy Surface for the Fission of the Superheavy Nucleus $^{298}_{114}\text{X}_{184}$," *Phys. Rev.* **C8**, 1924–1928 (1973).
- Newman, E., K. S. Toth, and I. R. Williams, "Decay of 5.9-Day ^{145}Eu to Levels in ^{145}Sm ," *Phys. Rev.* **C7**, 290–296 (1973).
- Nugent, L. J., and K. L. Vander Sluis, "Electron-Transfer Bands in the Absorption Spectrum of CfCl_3 ," *J. Chem. Phys.* **59**, 3440–3441 (1973).
- Peebles, P. Z., Jr., "Resonant Frequency Control of Superconducting RF Cavities," *IEEE Trans. Nucl. Sci.* **NS-20**, No. 3, 113–115 (June 1973) (Proceedings 1973 Particle Accelerator Conference, San Francisco, California, March 1973).
- Pegg, D. J., P. M. Griffin, I. A. Sellin, and W. W. Smith, "Electron Spectroscopy of Foil-Excited Chlorine Beams," *Nucl. Instrum. Methods* **110**, 489–492 (1973) (Proceedings Third International Conference on Beam-Foil Spectroscopy, Tucson, Arizona, October 1973).
- Pegg, D. J., P. M. Griffin, I. A. Sellin, W. W. Smith, and B. Donnally, "Metastable States of Highly Excited Heavy Ions," pp. 327–333 in *Atomic Physics 3*, Plenum Press, London (1973) (Proceedings Third International Conference on Atomic Physics, Boulder, Colorado, August 1972).
- Pegg, D. J., I. A. Sellin, R. Peterson, J. R. Mowat, W. W. Smith, M. D. Brown, and J. R. Macdonald, "Electron Decay-in-Flight Spectra from Autoionizing States of Highly Stripped Oxygen, Fluorine, Chlorine, and Argon Ions," *Phys. Rev.* **A8**, 1350–1364 (1973).

- Plasil, F., R. L. Ferguson, Frances Pleasonton, and H. W. Schmitt, "Fission of ^{209}Bi by 36.1 MeV Protons: Search for an Asymmetric Component in the Mass Distribution, and Neutron Emission Results," *Phys. Rev.* **C7**, 1186–1193 (1973).
- Pleasonton, Frances, "Prompt Gamma Rays Emitted in the Thermal-Neutron Induced Fission of ^{233}U and ^{239}Pu ," *Nucl. Phys.* **A213**, 413–425 (1973).
- Pleasonton, Frances, R. L. Ferguson, F. Plasil, and C. E. Bemis, Jr., "Fragment Mass and Kinetic Energy Distributions from the Spontaneous Fission of ^{246}Cm ," *Phys. Rev.* **C8**, 1018–1022 (1973).
- Raman, S., R. L. Auble, and W. T. Milner, "An $E5$ Transition in ^{123}Te and $E5$ Transitions, in General," *Phys. Lett.* **B47**, 19–20 (1973).
- Raman, S., J. L. Foster, Jr., O. Dietzsch, D. Spalding, L. Bimbot, and B. H. Wildenthal, "Energy Levels in ^{142}Nd ," *Nucl. Phys.* **A201**, 21–40 (1973).
- Raman, S., and N. B. Gove, "Rules for Spin and Parity Assignments Based on Log ft Values," *Phys. Rev.* **C7**, 1995–2009 (1973).
- Raman, S., H. J. Kim, T. A. Walkiewicz, and M. J. Martin, "The Disintegration Energy of ^{133}Sn – Why Have P_L/P_K Measurements Yielded Incorrect Values?" *Phys. Lett.* **44B**, 255–256 (1973).
- Raman, S., P. H. Stelson, G. G. Slaughter, J. A. Harvey, T. A. Walkiewicz, G. J. Lutz, L. G. Multhauf, and K. G. Tirsell, "Gamma Transitions between Low-Lying Levels in ^{119}Sn ," *Nucl. Phys.* **A206**, 343–352 (1973).
- Raman, S., T. A. Walkiewicz, R. Gunnink, and B. Martin, "How Good Are the Theoretical Internal Conversion Coefficients?" *Phys. Rev.* **C7**, 2531–2535 (1973).
- Rao, C. L., M. Reeves III, and G. R. Satchler, "Target Excitations and the Optical Potential for Protons Scattering from Nuclei," *Nucl. Phys.* **A207**, 182–208 (1973).
- Rapaport, J., J. B. Ball, and R. L. Auble, "The $^{48}\text{Ti}(p,t)^{46}\text{Ti}$ Reaction," *Nucl. Phys.* **A208**, 371–380 (1973).
- Saltmarsh, M. J., A. van der Woude, and C. A. Ludemann, "Energy Shifts and Relative Intensities of K X-Rays Produced by Swift Heavy Ions," pp. 1395–1405 in Vol. 2 of *Proceedings International Conference on Inner Shell Ionization Phenomena (Atlanta, Georgia, April 1972)*, ed. by R. M. Fink et al., USAEC Conf-720404 (1973).
- Satchler, G. R., "Non-Locality Effects on Charge-Exchange and Inelastic Scattering," *Phys. Lett.* **B44**, 13–15 (1973).
- Satchler, G. R., "Nuclear Giant Resonances, Sum Rules, Effective Charges and Such-Like," *Comments Nucl. Particle Phys.* **6**, 145–151 (1973).
- Satchler, G. R., "Some Aspects of the DWBA as Applied to Heavy-Ion Transfer Reactions," pp. 145–159 in Vol. 1, *Proceedings Symposium on Heavy-Ion Transfer Reactions (Argonne, Illinois, March 1973)*, ANL Informal Report PHY-1973B (1973).
- Satchler, G. R., "The Folding and Deformed Potential Models for Inelastic Scattering," *Phys. Lett.* **39B**, 495–498 (1972).
- Satchler, G. R., "Exchange Effects on the Excitation of ^{20}Ne by Protons," *Particles Nucl.* **5**, 77–88 (1973).
- Satchler, G. R., "Effective Interactions and the $^{40}\text{Ca}(p,p')$ Reaction," *Z. Phys.* **260**, 209–230 (1973).
- Satchler, G. R., "New Giant Resonances in Nuclei," *Nature "News & Views"* **244**, 541 (1973).
- Satchler, G. R., "Excitation of Giant Monopole Resonances by Proton Scattering," *Particles Nucl.* **5**, 105–118 (1973).
- Schmidt-Ott, W.-D., and R. L. Mlekodaj, "He-Jet Ion Source of the UNISOR Mass Separator," pp. 445–450 in *Proceedings Eighth International Conference on Low Energy Ion Accelerators and Mass Separators* (Billingshus, Skövde, Sweden, June 1973), ed. by G. Andersson and G. Holmen in Gothenberg, Sweden, 1973.
- Schmidt-Ott, W.-D., R. L. Mlekodaj, and C. R. Bingham, "The Measurement of the Absolute Transport Efficiency for Recoils from Heavy Ion Reactions with He-Jet Systems," *Nucl. Instrum. Methods* **108**, 13–21 (1973).

- Schmorak, M. R., "Nuclear Data Sheets for $A = 192$," *Nucl. Data Sheets* **9**, 195–228 (February 1973).
- Schmorak, M. R., "Nuclear Data Sheets for $A = 190$," *Nucl. Data Sheets* **9**, 401–433 (April 1973).
- Schmorak, M. R., "Nuclear Data Sheets for $A = 188$," *Nucl. Data Sheets* **10**, 553–671 (December 1973).
- Sellin, I. A., "Autoionization of Atoms Produced in Heavy-Ion Collisions," pp. 551–563 in *Proceedings Heavy-Ion Summer Study (Oak Ridge, Tennessee, June 1972)*, USAEC Conf-720669 (1973).
- Sellin, I. A. (invited paper), "Metastable Autoionizing States," *Nucl. Instrum. Methods* **110**, 477–487 (1973) (Proceedings Third International Conference on Beam-Foil Spectroscopy, Tucson, Arizona, October 1972).
- Sellin, I. A., J. R. Mowat, R. S. Peterson, P. M. Griffin, R. Laubert, and H. H. Haselton, "Observation of Coherent Electron-Density-Distribution Oscillations in Collision-Averaged Foil Excitation of the $n = 2$ Hydrogen Levels," *Phys. Rev. Lett.* **31**, 1335–1337 (1973).
- Sewell, P. T., J. C. Hafele, C. C. Foster, N. M. O'Fallon, and C. B. Fulmer, "Straight-Back Elastic Alpha Scattering from ^{48}Ti , ^{52}Cr , ^{53}Cr , and ^{58}Ni ," *Phys. Rev.* **C7**, 690–694 (1973).
- Silberman, E., J. R. Lawson, and H. W. Morgan, "Vibrational Determination of Crystal Structures," pp. 92–101 in Vol. I, *Advances in Raman Spectroscopy* (Proceedings Third International Conference, Reims, France, September 1972), Heyden & Son, Ltd., London, 1973.
- Smith, W. W., B. Donnally, D. J. Pegg, M. Brown, and I. A. Sellin, "Beam Fractions in the Lowest-Quartet Metastable Autoionizing State for O^{5+} and F^{6+} Beams after Passage through Foils," *Phys. Rev.* **A7**, 487–491 (1973).
- So, Y. K., W. T. Pinkston, and K. T. R. Davies, "Nucleon Transfer Form Factors Calculated with Realistic Interactions," *Particles Nucl.* **6**, 1–31 (1973).
- Spejewski, E. H., R. L. Mlekodaj, H. K. Carter, W.-D. Schmidt-Ott, E. L. Robinson, R. W. Fink, J. M. Palms, W. H. Brantley, B. D. Kern, K. J. Hofstetter, E. F. Zganjar, A. R. Quinton, F. T. Avignone, W. M. Bugg, C. R. Bingham, F. Culp, J. Lin, J. H. Hamilton, A. V. Ramayya, M. A. Ijaz, J. A. Jacobs, J. L. Duggan, W. G. Pollard, R. S. Livingston, C. E. Bemis, E. Eichler, N. R. Johnson, R. L. Robinson, and K. S. Toth, "The UNISOR Project," pp. 318–323 in *Proceedings Eighth International Conference on Low Energy Ion Accelerators and Mass Separators* (Billingeus, Skövde, Sweden, June 1973), ed. by G. Andersson and G. Holmen in Gothenberg, Sweden, 1973.
- Stelson, P. H., C. E. Bemis, Jr., F. K. McGowan, W. T. Milner, J. L. C. Ford, Jr., R. L. Robinson, and W. Tuttle, "Coulomb-Nuclear Interference for Alpha-Particles on Rare-Earth Nuclei," p. 378 in Vol. 1, *Proceedings International Conference on Nuclear Physics* (Munich, Germany, August–September 1973), edited by J. de Boer and H. J. Mang, North-Holland/American Elsevier, 1973.
- Stelson, P. H., S. Raman, J. A. McNabb, R. W. Lide, and C. R. Bingham, "Search for a Zero-Phonon Gamma-Ray Transition in ^{108}Pd and ^{134}Ba ," *Phys. Rev.* **C8**, 368–374 (1973).
- Stoughton, R. W., J. Halperin, C. E. Bemis, and H. W. Schmitt, "Neutron Multiplicity Distributions in the Spontaneous Fission of ^{246}Cm , ^{248}Cm , and ^{252}Cf ," *Nucl. Sci. Eng.* **50**, 169–171 (1973).
- Stoughton, R. W., J. Halperin, J. S. Drury, F. G. Perey, R. L. Macklin, R. V. Gentry, C. B. Moore, J. E. Noakes, R. M. Milton, J. H. McCarthy, and D. W. Sherwood, "A Search for Superheavy Elements in Nature by Neutron Emission Measurements," *Nature (Physical Sciences)* **246**, 26–28 (1973).
- Thornton, S. T. (editor), *Proceedings of Heavy-Ion Summer Study (Oak Ridge, Tennessee, June 1972)*, USAEC Conf-720669, 638 pp. (1973).
- Toth, K. S., R. L. Hahn, C. R. Bingham, M. A. Ijaz, and R. F. Walker, Jr., "Study of Hafnium Alpha-Emitters: New Isotopes, ^{159}Hf , ^{160}Hf , and ^{161}Hf ," *Phys. Rev.* **C7**, 2010–2018 (1973).
- Toth, K. S., and E. Newman, "High-Lying 2^+ States in ^{148}Sm Observed in the Decay of 5^-^{148}Eu ," *Phys. Rev. (Comments & Addenda)* **C7**, 460–463 (1973).
- Urone, P. P., L. L. Lee, Jr., and S. Raman, "Nuclear Data Sheets for $A = 77$," *Nucl. Data Sheets* **9**, 229–318 (March 1973).

- van der Woude, A., M. J. Saltmarsh, C. A. Ludemann, R. L. Hahn, and E. Eichler, "On the Z^2 -Dependence of the X-Ray Production Cross Section by 5 MeV/amu Heavy Ions," pp. 1388–1394 in Vol. 2, *Proceedings International Conference on Inner Shell Ionization Phenomena (Atlanta, Georgia, April 1972)*, ed. by R. W. Fink et al., USAEC Conf-720404 (1973).
- Wasson, O. A., and B. J. Allen, " P -Wave Resonances in $^{111}\text{Cd}(n,\gamma)^{112}\text{Cd}$," *Phys. Rev. C7*, 780–787 (1973).
- Wasson, O. A., B. J. Allen, R. R. Winters, R. L. Macklin, and J. A. Harvey, "Neutron Resonance Parameters of ^{92}Mo ," *Phys. Rev. C7*, 1532–1541 (1973).
- Wasson, O. A., and G. G. Slaughter, "Valency Neutron Capture in $^{92}\text{Mo}(n,\gamma)^{93}\text{Mo}$," *Phys. Rev. C8*, 297–314 (1973).
- Welton, T. A., Frances L. Ball, and W. W. Harris, "Wiener Processing of Phase Contrast Electron Micrographs," pp. 270–271 in *Proceedings Thirty-First Annual Electron Microscopy Society of America Meeting (New Orleans, Louisiana, August 1973)*, ed. by Claude J. Arceneaux, Claitor's Publishing Division, Baton Rouge, 1973.
- West, D. C., W. B. Ewbank, F. W. Hurley, and M. R. McGinnis, "Recent References (September 1972–December 1972)," *Nucl. Data Sheets 9*, 1–124 (January 1973).
- Wildenthal, B. H., and J. B. McGrory, "Shell-Model Calculation for Masses 27, 28, and 29: General Methods and Specific Applications to ^{27}Al , ^{28}Si , and ^{29}Si ," *Phys. Rev. C7*, 714–732 (1973).
- Wong, C. Y., "Fusion Threshold Energy in Heavy-Ion Reactions," *Phys. Lett. 42B*, 186–190 (1972).
- Wong, C. Y., "Toroidal and Spherical Bubble Nuclei," *Ann. Phys. (N.Y.) 77*, 279–353 (1973).
- Wong, C. Y., "Interaction Barrier in Charged-Particle Nuclear Reactions," *Phys. Rev. Lett. 31*, 766–769 (1973).
- Worsham, R. E., J. E. Mann, E. G. Richardson, and N. F. Ziegler, "An Electron Microscope with Highly Coherent Illumination," pp. 260–261 in *Proceedings Thirty-First Annual Electron Microscopy Society of America Meeting (New Orleans, Louisiana, August 1973)*, ed. by Claude J. Arceneaux, Claitor's Publishing Division, Baton Rouge, 1973.
- Wu, R. R., R. L. Dangle, M. M. Duncan, J. L. Duggan, P. D. Miller, and J. Lin, "A Study of the $^{11}\text{B}(^3\text{He},p)^{13}\text{C}$ Reaction at 12, 10, 8, 6, and 4 MeV," *Nucl. Phys. A199*, 23–30 (1973).

Pending Publications as of February 15, 1974
(References Included If Known)

- Allen, B. J., A. R. de L. Musgrove, D. M. Chan, and R. L. Macklin, "Neutron Capture Cross Sections of the Calcium and Barium Isotopes," *Proceedings Kiev Conference on Neutron Physics (Kiev, USSR, May–June 1973)*.
- Allen, B. J., A. R. de L. Musgrove, D. M. Chan, and R. L. Macklin, "Neutron Capture Cross Sections of the Isotopes of Calcium," *Nucl. Phys.*
- Appleton, B. R., J. A. Biggerstaff, T. S. Noggle, S. Datz, C. D. Moak, M. D. Brown, H. F. Krause, R. H. Ritchie, and V. N. Neelavathi, "Radiative Electron Capture by Channeled Oxygen Ions," *Proceedings Fifth International Conference on Atomic Collisions in Solids (Gatlinburg, Tennessee, September 1973)*.
- Bair, J. K., and F. X. Haas, "Averaged $^{21,22}\text{Ne}(\alpha,n)$ Cross Sections: Correction and Comment," *Phys. Rev.*
- Barrett, B. R., E. C. Halbert, and J. B. McGrory (invited paper), "Effective Three-Body Forces in Truncated Shell-Model Calculations," *Proceedings Symposium on Correlations in Nuclei (Balatonfured, Hungary, September 1973)*.
- Becker, R. L., "The Renormalized Brueckner-Hartree-Fock Approximation," *Proceedings International Symposium on Present Status and Novel Developments in the Nuclear Many-Body Problem (Rome, Italy, September 1972)*.
- Becker, R. L., K. T. R. Davies, and M. R. Patterson, "Renormalized Brueckner-Hartree-Fock Calculations of ^4He and ^{16}O with Center-of-Mass Corrections," *Phys. Rev.*
- Behar, M., Z. W. Grabowski, and S. Raman, "Angular Correlation Studies in ^{144}Nd ," *Nucl. Phys.*
- Bertrand, F. E., "Nuclear Data Sheets for $A = 105$," *Nucl. Data Sheets 11*, 449–494 (April 1974).

- Bhatt, K. H., J. C. Parikh, and J. B. McGrory, "The Quadrupole Collectivity and Possible Existence of Macroscopic SU_3 Symmetry in Some Collective Shell Model States," *Nucl. Phys.*
- Boyce, J. R., T. D. Hayward, R. Bass, H. W. Newson, E. G. Bilpuch, F. O. Purser, and H. W. Schmitt, "Absolute Cross Sections for Proton Induced Fission of the Uranium Isotopes," *Nucl. Phys.*
- Carlson, T. A., "Primary Processes in Hot Atom Chemistry," *Nuclear Transformations in Solids*, ed. by Harbottle and Maddock, North-Holland Publishing Company, Amsterdam, Netherlands.
- Carlson, Thomas A. (invited paper), "Creation of Excited States as the Result of X-Ray Photoionization," Proceedings Eighth International Conference on the Physics of Electronic and Atomic Collisions (Belgrade, Yugoslavia, July 1973).
- Cohen, S., F. Plasil, and W. J. Swiatecki, "Equilibrium Configurations of Rotating Charged or Gravitating Liquid Masses with Surface Tension." Part II, *Ann. Phys. (N.Y.)*.
- Collins, W. E., J. H. Hamilton, R. L. Robinson, H. J. Kim, and J. L. C. Ford, Jr., "Levels in ^{72}Se Populated by ^{72}Br ," *Nucl. Phys.*
- Datz, S., B. R. Appleton, J. A. Biggerstaff, M. D. Brown, H. F. Krause, C. D. Moak, and T. S. Noggle, "Charge State Dependence of Stopping Power for Oxygen Ions Channeled in Silver," Proceedings Fifth International Conference on Atomic Collisions in Solids (Gatlinburg, Tennessee, September 1973).
- Davies, K. T. R., and G. R. Satchler, "Inelastic Proton Scattering with Skyrme Forces," *Nucl. Phys.*
- Dietrich, R. N., W. B. Ewbank, F. W. Hurley, and M. R. McGinnis, "Recent References (May 1973 through August 1973)," *Nucl. Data Sheets* **11**, 1-119 (January 1974).
- Dietrich, R. N., W. B. Ewbank, F. W. Hurley, and M. R. McGinnis, "Recent References (September through December 1973)," *Nucl. Data Sheets* **12**, 1-137 (May 1974).
- Fielding, H. W., S. D. Scherry, D. A. Lind, C. D. Zafaritos, and C. D. Goodman, "Widths of Analog States in Heavy Elements from (p,n) Spectra," *Phys. Rev. (Comments & Addenda)*.
- Ford, W. F., R. C. Braley, R. L. Becker, and M. R. Patterson, "Deformed Brueckner-Hartree-Fock Calculations," Proceedings Symposium on Present Status and Novel Developments in the Many-Body Problem (Rome, Italy, September 1972).
- Ford, J. L. C., Jr., J. Gomez del Campo, R. L. Robinson, P. H. Stelson, and S. T. Thornton, "States in ^{24}Mg Populated by the $^{10}\text{B}(^{16}\text{O},d)^{24}\text{Mg}$ and $^{12}\text{C}(^{16}\text{O},\alpha)^{24}\text{Mg}$ Reactions," *Nucl. Phys.*
- Ford, J. L. C., Jr., J. Gomez del Campo, R. L. Robinson, P. H. Stelson, and S. T. Thornton, "Excitation of Rotational Bands in ^{20}Ne by the $^{10}\text{B}(^{16}\text{O},^6\text{Li})$ Reaction," *Phys. Rev.*
- Gomez del Campo, J., J. L. C. Ford, Jr., R. L. Robinson, P. H. Stelson, and S. T. Thornton, "Study of the $^{10}\text{B}(^{16}\text{O},\alpha)^{22}\text{Na}$ Reaction," *Phys. Rev.*
- Goodman, C. D., "Isospin," *Encyclopedia of Physics*, second edition.
- Gutbrod, H. H., F. Plasil, H. C. Britt, B. H. Erkkila, R. H. Stokes, and M. Blann, "Fission and Complete Fusion Measurements in ^{40}Ar Bombardments of ^{58}Ni and ^{109}Ag ," Proceedings Third Symposium on the Physics and Chemistry of Fission (Rochester, New York, August 1973).
- Hamilton, J. H., A. V. Ramayya, W. T. Pinkston, R. M. Ronningen, G. Garcia Bermudez, H. K. Carter, R. L. Robinson, H. J. Kim, and R. O. Sayer, "Evidence for Coexistence of Spherical and Deformed Shapes in ^{72}Sr ," *Phys. Rev. Lett.* **32**, 239-243 (1974).
- Helminger, P., F. C. De Lucia, W. Gordy, H. W. Morgan, and P. A. Staats, "Microwave Rotation-Inversion Spectrum of NT_3 ," *Phys. Rev.* **A9**, 12-16 (1974).
- Holub, R., M. G. Mustafa, and H. W. Schmitt, "Calculation of Charge Vibration in Fission with Strutinsky Shell Correction," *Nucl. Phys.*
- Horen, D. J., F. E. Bertrand, and M. B. Lewis, "Comparison of the Inelastic Scattering of Protons by $^{144,154}\text{Sm}$ in the Region of Giant Resonances," *Phys. Rev.*

- Horen, D. J., and B. Harmatz, "Nuclear Data Sheets for $A = 171$," *Nucl. Data Sheets* **11**, 549–602 (April 1974).
- Hubbard, L. B., "Absorbed Fractions for Small Bodies – The Cube Root of Mass Dependence," *Radiat. Res.* **57**, 1–8 (1974).
- Hudson, E. D., M. L. Mallory, and R. S. Lord, "An Ion Source for High Intensity Metal Ions," *Nucl. Instrum. Methods*.
- Jones, R. W., F. Mohling, and R. L. Becker, "Perturbation Theory of a Many-Fermion System. II. Expansions in Reaction Matrices," *Nucl. Phys.*
- Keyworth, G. A., J. R. Lemley, C. E. Olsen, F. T. Seibel, J. W. T. Dabbs, and N. W. Hill, "Determination of Spins of Intermediate Structure Resonances in Subthreshold Fission," Proceedings Third IAEA Symposium on the Physics and Chemistry of Fission (Rochester, New York, August 1973).
- Kim, H. J., and R. L. Robinson, "Low-Lying States in ^{111}In and ^{113}In ," *Phys. Rev.*
- Kocher, D. C., "Nuclear Data Sheets for $A = 100$," *Nucl. Data Sheets* **11**, 337–447 (February 1974).
- Krewald, S., K. W. Schmid, A. Faessler, and J. B. McGrory, "A Comparison between Shell-Model Configuration Mixing Calculations and the MCHF-Model in the Ground State Rotational Spectra of ^{20}Ne , ^{22}Ne , and ^{24}Mg ," *Nucl. Phys.*
- Lewis, M. B., "Empirical Spreading Widths of Deep Lying Hole States in ^{207}Pb ," *Phys. Rev. Lett.*
- Lewis, M. B., "Damping Widths, Semidirect Reactions, and Direct Excitation of Giant Resonances in the Nuclear Continuum," *Phys. Rev.*
- Lewis, M. B., "Collective Multipole Expansion of the Inelastic Scattering Continuum," *Phys. Rev.*
- Love, J. C., and F. E. Obenshain, " ^{61}Ni Mössbauer Studies of Substituted Ni Spinels," Proceedings Nineteenth Conference on Magnetism and Magnetic Materials (Boston, Massachusetts, November 1973), AIP Conference Proceedings.
- McGowan, F. K., and W. T. Milner, "Reaction List for Charged-Particle-Induced Nuclear Reactions $Z = 1$ to 98 (H to Cf)," *At. Data Nucl. Data Tables*.
- McGowan, F. K., and P. H. Stelson, "Coulomb Excitation," Chapter VII.A in *Nuclear Spectroscopy*, II, ed. by Joseph Cerny, Academic Press, Inc., New York.
- McGrory, J. B. (invited paper), "Nuclear Structure Studies with Large Shell Model Calculations," Proceedings International Conference on Nuclear Physics (Munich, Germany, August–September 1973).
- McGrory, J. B., "Shell Model Predictions of Three- and Four-Particle Cluster Transfer Spectroscopic Factors in Some s - d and f - p Shell Nuclei," *Phys. Lett.*
- Moak, C. D., B. R. Appleton, J. A. Biggerstaff, S. Datz, and T. S. Noggle, "Velocity Dependence of the Stopping Power of Channeled Iodine Ions," Proceedings Fifth International Conference on Atomic Collisions in Solids (Gatlinburg, Tennessee, September 1973).
- Monard, Joyce A., P. G. Huray, and J. O. Thomson, "Mössbauer Studies of Electric Hyperfine Interactions in ^{234}U , ^{236}U , ^{238}U ," *Phys. Rev.*
- Mowat, J. R., B. R. Appleton, J. A. Biggerstaff, S. Datz, C. D. Moak, and I. A. Sellin, "Charge State Dependence of Si K X-Ray Production in Solid and Gaseous Targets by MeV Oxygen Ion Impact," Proceedings Fifth International Conference on Atomic Collisions in Solids (Gatlinburg, Tennessee, September 1973).
- Mowat, J. R., I. A. Sellin, P. M. Griffin, D. J. Pegg, and R. S. Peterson, "Projectile Charge State Dependence of K X-Ray Production by 1–4 MeV/amu Heavy Ions in Gases," *Phys. Rev.*
- Mustafa, M. G., and F. B. Malik, "A Theory of Intermediate Structure, Overlapping Resonances and Photonuclear Reactions in Light Nuclei," *Ann. Phys.* (N.Y.).
- Newman, E., K. S. Toth, D. C. Hensley, and W.-D. Schmidt-Ott, "Levels in $^{146,147,148}\text{Gd}$ Observed Following the Decay of Their Terbium Parents; New Isotope, ^{146}Tb ," *Phys. Rev.*

- Nugent, L. J., K. L. Vander Sluis, B. Fricke, and J. B. Mann, "On the Electronic Configuration in the Ground State of Atomic Lawrencium," *Phys. Rev.*
- Obenshain, F. E., "Nuclear Gamma Resonance with ^{61}Ni ," Mössbauer Effect Data Index.
- Pegg, D. J., H. H. Haselton, P. M. Griffin, R. Laubert, J. R. Mowat, R. Peterson, and I. A. Sellin, "Lifetime and Binding Energy of the Metastable $(1s2s2p)^4 p_{5/2}^o$ State in ^{13}S ," *Phys. Rev.*
- Plasil, F., R. L. Ferguson, and Frances Pleasonton, "Neon-Induced Fission of Silver," Proceedings Third Symposium on the Physics and Chemistry of Fission (Rochester, New York, August 1973).
- Raman, S., R. L. Auble, and F. F. Dyer, "Weak Gamma Transitions in 129-d $^{123}\text{Sn}^g$ Decay," *Phys. Rev.* **C9**, 426–427 (1974).
- Roberts, W. J., E. E. Gross, and E. Newman, "Test of Isospin Conservation by a Comparison of $^3\text{H}(^3\text{He}, ^4\text{He})^2\text{H}$ and $^3\text{He}(^3\text{He}, ^4\text{He})2p$ at 16.0 MeV c.m.," *Phys. Rev.* **C9**, 149–155 (1974).
- Robinson, R. L., H. J. Kim, and J. L. C. Ford, Jr., "Absolute Cross Sections for the $^{58,60}\text{Ni}(^{16}\text{O}, \chi)$ Reactions," *Phys. Rev.*
- Satchler, G. R. (invited paper), "Direct Reactions with Light Ions," Proceedings International Conference on Nuclear Physics (Munich, Germany, August–September 1973).
- Satchler, G. R. (invited paper), "Calculations of the Imaginary Part of the Optical Potential," Proceedings Symposium on Correlations in Nuclei (Balatonfured, Hungary, September 1973).
- Satchler, G. R., "New Giant Resonances in Nuclei – An Interim Review," *Rev. Mod. Phys.*
- Satchler, G. R., and F. G. Perey (invited paper), "The Optical Model," Proceedings Conference on Nuclear Structure Study with Neutrons (Budapest, Hungary, July–August 1972).
- Sayer, R. O., E. Eichler, N. R. Johnson, D. C. Hensley, and L. L. Riedinger, "Coulomb Excitation of Ground Bands in $^{160,162,164}\text{Dy}$ with ^{20}Ne and ^{35}Cl Ions," *Phys. Rev.*
- Schmidt-Ott, W.-D., K. S. Toth, E. Newman, and C. R. Bingham, "Alpha-Decay Branching Ratios for High- and Low-Spin Isomers in $^{151,152,153,154}\text{Ho}$," *Phys. Rev.*
- Schmitt, H. W., and M. G. Mustafa, "Potential Energy Surfaces and Dependence of Fission Mass Asymmetry on the Internal Excitation Energy of the Fissioning Nucleus," Proceedings Third Symposium on Physics and Chemistry of Fission (Rochester, New York, August 1973).
- Spears, D. P., H. J. Fischbeck, and T. A. Carlson, "Satellite Structure in the X-Ray Photoelectron Spectra of Rare Gases and Alkali Metal Halides," *Phys. Rev.*
- Staats, P. A., and O. C. Kopp, "Studies on the Origin of the 3400 cm^{-1} Region Infrared Bands of Synthetic and Natural Alpha-Quartz," *J. Phys. Chem. Solids*.
- Tang, H. H. K., and C. Y. Wong, "Vibration of a Viscous Liquid Sphere," *J. Phys.*
- Vander Sluis, K. L., and L. J. Nugent, "Ionization Energies of Doubly and Triply Ionized Lanthanides by a Linearization Technique," *J. Chem. Phys.*
- Vander Sluis, K. L., and L. J. Nugent, "Systematics in the Relative Energies of Some Low-Lying Electron Configurations in the Gaseous Atoms and Free Ions of the Lanthanide and Actinide Series," *J. Opt. Soc. Amer.*
- Varnell, L., J. H. Hamilton, and R. L. Robinson, "Coulomb Excitation in ^{180}Hf ," *Phys. Rev.*
- White, R. M., T. A. Carlson, and D. P. Spears, "Angular Distribution of the Photoelectron Spectra for Ethylene, Propylene, Butene, and Butadiene," *J. Electron Spectrosc.* **3**, 59–71 (1974).
- Wong, C. Y., "Toroidal Figures of Equilibrium," *Astrophys. J.*
- Wong, C. Y., and T. A. Welton, "Supersonic Heavy-Ion Collisions," *Phys. Lett.*
- Ziegler, N. F., "A 100 KV Regulator with $1/4$ PPM Stability," Proceedings Conference on Precision Electromagnetic Measurements (London, England, July 1974).

THESES

- Gomez del Campo, Jorge, "Estudia de la Reaccion $^{10}\text{B}(^{16}\text{O},\alpha)^{22}\text{Na}$," Ph.D. thesis, November 1973, National University of Mexico.
- Lukuba, Z. L. T., "Cyclotron Yields of Radionuclides for Medical Applications," M.S. thesis, December 1973, University of Tennessee.
- Roberts, W. J., "A Test of Isospin Conservation by a Comparison of the Reactions $^3\text{H}(^3\text{He},^4\text{He})^2\text{H}$ and $^3\text{He}(^3\text{He},^4\text{He})2p$," Ph.D. thesis, March 1973, University of Tennessee.
- Spears, D. P., "Satellite Structure in the Photoelectron Spectra of Rare Gases, Some Simple Gaseous Molecules, and Alkali Metal Halides," Ph.D. thesis, December 1973, University of Oklahoma.

NOTE: The above includes only theses by M.S. degree and Ph.D. degree candidates who received their degrees during 1973 and who were engaged in full-time research with the Physics Division for a specified period of time. For further information on thesis research activity in the Division during 1973, see two later sections of this report entitled "Ph.D. Thesis Research" and "M.S. Thesis Research."

ANNUAL REPORT

- Fowler, J. L., G. R. Satchler, P. H. Stelson, and F. E. Obenshain (editor), *Physics Division Annual Progress Report for the Period Ending December 31, 1972*, ORNL-4844 (May 1973).

TOPICAL REPORTS

- Bertrand, F. E., and R. W. Peelle, *Cross Sections for Hydrogen and Helium Particles Produced by 61-, 39-, and 29-MeV Protons on Carbon and Oxygen*, ORNL-4799 (July 1973).
- Castle, J. G., Jr., and R. B. Dickinson, *On the Use of Proton Beams for Radiotherapy: A Summer Study at ORIC*, ORNL-TM-4166 (April 1973).
- Macklin, R. L., *Neutron Capture in Reactor Structure Materials*, ORNL-TM-4128 (February 1973).
- Martin, M. J., *Radioactive Atoms – Supplement I*, ORNL-4923 (October 1973).
- Satchler, G. R., *New Giant Resonances in Nuclei – An Interim Review*, ORNL-TM-4347 (August 1973).

12. Papers Presented at Scientific and Technical Meetings

Prepared by Wilma L. Stair

American Physical Society Meeting, New York, New York, January 29–February 1, 1973

F. E. Bertrand, G. R. Satchler, M. B. Lewis, and D. J. Horen, "Inelastic Proton Excitation of Giant Resonances in the Nuclear Continuum," *Bull. Amer. Phys. Soc.* **18**, 68 (1973).

G. W. Cole, R. E. Chrien, R. C. Byrd, S. F. Mughabghab, J. A. Harvey, and G. G. Slaughter, "Validity of the Valence Neutron Model for ^{98}Mo ," *Bull. Amer. Phys. Soc.* **18**, 96 (1973).

C. C. Foster, N. M. O'Fallon, J. C. Hafele, and C. B. Fulmer, "Excitation Functions for 180° Elastic Alpha Scattering from ^{27}Al and ^{28}Si in the 13 to 28 MeV Energy Range," *Bull. Amer. Phys. Soc.* **18**, 118 (1973).

J. L. Fowler, "Lunar Magnetic Fields: Possible Dipole Sources," *Bull. Amer. Phys. Soc.* **18**, 101 (1973).

C. M. Ko, T. T. S. Kuo, and J. B. McGrory, "Generalized Pairing Vibrational Model for ^{212}Pb and ^{204}Pb ," *Bull. Amer. Phys. Soc.* **18**, 138 (1973).

J. C. Love and F. E. Obenshain, "Giant Magnetic Hyperfine Fields at ^{61}Ni on Tetrahedral Sites of Spinel," *Bull. Amer. Phys. Soc.* **18**, 114 (1973).

F. E. Obenshain, J. E. Tansil, and G. Czjzek, "Magnetic Hyperfine Fields at ^{61}Ni Nuclei in Dilute Pd:Ni Alloys," *Bull. Amer. Phys. Soc.* **18**, 114 (1973).

N. M. O'Fallon, C. C. Foster, J. C. Hafele, and C. B. Fulmer, "Excitation Functions for 180° Elastic Helion Scattering from ^{58}Ni , ^{59}Co , and ^{60}Ni between 22 and 31 MeV," *Bull. Amer. Phys. Soc.* **18**, 118 (1973).

W. J. Roberts, E. E. Gross, and E. Newman, "Test of Isospin Conservation by a Comparison of $^3\text{H}({}^3\text{He}, {}^4\text{He})^2\text{H}$ and $^3\text{He}({}^3\text{He}, {}^4\text{He})2p$," *Bull. Amer. Phys. Soc.* **18**, 18 (1973).

G. R. Satchler, F. E. Bertrand, and M. B. Lewis, "Possible Giant Monopole Resonances in Proton Inelastic Scattering," *Bull. Amer. Phys. Soc.* **18**, 68 (1973).

G. G. Slaughter (invited paper), "A Sufficiency of Well-Timed Neutrons," *Bull. Amer. Phys. Soc.* **18**, 12 (1973).

K. S. Toth, R. L. Hahn, C. R. Bingham, M. A. Ijaz, and R. F. Walker, Jr., "Study of Hafnium Alpha-Emitters; New Isotopes, ^{159}Hf , ^{160}Hf , and ^{161}Hf ," *Bull. Amer. Phys. Soc.* **18**, 37 (1973).

Joint Nuclear Division Meeting of German and Dutch Physical Societies, Heidelberg, Germany, February 1973

U. Mosel, M. G. Mustafa, and H. W. Schmitt, "Asymmetry in Nuclear Fission."

A. C. Rester, J. B. Ball, J. J. Pinajian, and J. S. Larsen, "A Study of the $^{86}\text{Sr}(p,t)^{84}\text{Sr}$ Reaction at 31 MeV."

1973 Particle Accelerator Conference, San Francisco, California, March 5–7, 1973

E. D. Hudson, R. S. Lord, C. A. Ludemann, M. L. Mallory, J. A. Martin, W. T. Milner, S. W. Mosko, P. H. Stelson, and A. Zucker, "A Multi-Accelerator System for Heavy Ions."

E. D. Hudson, M. L. Mallory, R. S. Lord, A. Zucker, H. G. Blosser, and D. A. Johnson, "Energy Multiplication by Beam Recycling in an Isochronous Cyclotron."

C. A. Ludemann, J. M. Domaschko, S. W. Mosko, and K. Hagemann, "Computer Control of the Oak Ridge Isochronous Cyclotron."

M. L. Mallory, E. D. Hudson, and R. S. Lord, "Cyclotron Internal Ion Source with DC Extraction."

J. A. Martin and P. H. Stelson, "Ion Stripping Considerations for Tandem-Cyclotron Heavy-Ion Accelerator Design."

S. W. Mosko, "A New RF System for the ORIC."

P. Z. Peebles, Jr., "Resonant Frequency Control of Superconducting RF Cavities."

IAEA Symposium on Applications of Nuclear Data in Science and Technology, Paris, France, March 12–16, 1973

D. J. Horen, "Nuclear Data Project: Operations, Status, and Plans."

D. J. Horen and A. M. Weinberg, "Criteria of Choice for Compilations of Nuclear Data."

Symposium on Heavy-Ion Transfer Reactions, Argonne, Illinois, March 15–17, 1973

J. B. Ball, P. R. Christensen, O. Hansen, J. S. Larsen, D. Sinclair, F. Videbaek, R. A. Broglia, R. Liotta, and B. Nilsson, " ^{16}O Induced Transfer Reactions on ^{26}Mg , ^{27}Al , and ^{30}Si ."

J. L. C. Ford, Jr., K. S. Toth, D. C. Hensley, R. M. Gaedke, and P. J. Riley, "Single-Neutron Transfer Reactions and Inelastic Scattering Induced by ^{11}B Ions Incident on ^{208}Pb ."

G. R. Satchler (invited paper), "DWBA Survey."

International Conference on Photonuclear Reactions and Applications, Pacific Grove, California, March 26–30, 1973

B. J. Allen and R. L. Macklin, "Fast Neutron Capture Cross Sections for Silicon."

F. E. Bertrand, M. B. Lewis, G. R. Satchler, D. J. Horen, D. C. Kocher, R. W. Peelle, E. E. Gross, and E. Newman, "Excitation of Giant Resonance in the Nuclear Continuum by Inelastic Proton Scattering."

M. B. Lewis (invited paper), "Can We Generalize the Giant Resonance Idea?"

American Physical Society Meeting, Washington, D.C., April 23–26, 1973

R. L. Becker, "Predicted Intermediate Structure in Deep-Hole Spectra, II. Importance of Elimination of Spurious Excitations of the Center of Mass," *Bull. Amer. Phys. Soc.* **18**, 576 (1973).

R. W. Benjamin, C. E. Ahlfeld, J. A. Harvey, and N. W. Hill, "The Neutron Total Cross Section of ^{248}Cm ," *Bull. Amer. Phys. Soc.* **18**, 539 (1973).

W. M. Bugg, G. T. Condo, E. L. Hart, A. Pevsner, R. Sard, A. Snyder, R. Hulsizer, V. Kistiakowsky, P. Trepagnier, H. O. Cohn, R. D. McCulloch, M. Mills, and D. Dauwe, "Data Analysis of Primary Tracks in the NAL-PWC-Bubble Chamber Hybrid System," *Bull. Amer. Phys. Soc.* **18**, 564 (1973).

G. T. Condo, W. M. Bugg, E. L. Hart, H. O. Cohn, and R. D. McCulloch, "Nuclear Structure from Stopping \bar{p} Annihilations in Heavy Nuclei," *Bull. Amer. Phys. Soc.* **18**, 692 (1973).

S. Datz, B. R. Appleton, J. A. Biggerstaff, M. G. Menendez, and C. D. Moak, "Electron Production in Collisions of 21.6–60 MeV ^{127}I Ions," *Bull. Amer. Phys. Soc.* **18**, 662 (1973).

W. W. Eidson, R. G. Rasmussen, C. C. Foster, N. M. O'Fallon, C. B. Fulmer, and D. C. Hensley, " 180° Inelastic Alpha Particle Scattering to the 3^+ Unnatural Parity State in ^{24}Mg ," *Bull. Amer. Phys. Soc.* **18**, 667 (1973).

C. C. Foster, N. M. O'Fallon, W. W. Eidson, J. C. Hafele, and C. B. Fulmer, " $\sigma(\theta)$ near 180° for Inelastic Alpha Scattering to the 1.78 MeV (2^+) State of ^{28}Si in the 14 to 28 MeV Range," *Bull. Amer. Phys. Soc.* **18**, 667 (1973).

H. Freisleben, F. Plasil, R. L. Ferguson, C. E. Bemis, and H. W. Schmitt, "Fragment Kinetic Energies from ^{18}O -Induced Fission of ^{246}Cm ," *Bull. Amer. Phys. Soc.* **18**, 628 (1973).

C. B. Fulmer, D. C. Hensley, W. W. Eidson, and J. C. Hafele, "Large Angle Elastic Alpha Scattering at 28.3 and 39.8 MeV," *Bull. Amer. Phys. Soc.* **18**, 667 (1973).

- J. Gomez del Campo, J. L. C. Ford, Jr., S. T. Thornton, R. L. Robinson, and P. H. Stelson, "Investigation of the $^{10}\text{B}(^{16}\text{O},\alpha)$ Reaction," *Bull. Amer. Phys. Soc.* **18**, 599 (1973).
- M. B. Greenfield, D. L. McShan, G. Vourvopoulos, and S. Raman, "The $^{58}\text{Ni}(p,t)^{56}\text{Ni}$ Reaction at 40 MeV," *Bull. Amer. Phys. Soc.* **18**, 653 (1973).
- G. B. Hagemann, D. C. Hensley, N. R. Johnson, W. T. Milner, and L. L. Riedinger, "Lifetime Measurements of 8^+ , 10^+ , and 12^+ Rotational States in ^{164}Dy ," *Bull. Amer. Phys. Soc.* **18**, 581 (1973).
- M. L. Halbert, D. C. Hensley, and H. G. Bingham, "Search for a $^3\text{He} + ^3\text{He}$ Resonance near Threshold," *Bull. Amer. Phys. Soc.* **18**, 651 (1973).
- J. H. Hamilton, A. V. Ramayya, L. L. Riedinger, P. H. Stelson, and R. L. Robinson, "Coulomb Excitation of ^{156}Gd ," *Bull. Amer. Phys. Soc.* **18**, 655 (1973).
- C. H. Johnson, J. L. Fowler, and N. W. Hill, "Total Cross Section of Calcium," *Bull. Amer. Phys. Soc.* **18**, 538 (1973).
- H. J. Kim, R. L. Robinson, W. T. Milner, J. C. Wells, Jr., and J. Lin, "In-Beam Gamma Rays from the $^{28}\text{Si}(^{16}\text{O},2p)^{42}\text{Ca}$ Reaction," *Bull. Amer. Phys. Soc.* **18**, 600 (1973).
- J. R. Mowat, I. A. Sellin, R. S. Peterson, D. J. Pegg, M. D. Brown, and J. R. MacDonald, "Mean Life of the Metastable 2^3P_1 State of the Two-Electron Fluorine Ion," *Bull. Amer. Phys. Soc.* **18**, 610 (1973).
- M. G. Mustafa, H. W. Schmitt, and U. Mosel, "Fission Properties of Superheavy Nucleus, $Z = 114$ and $N = 184$," *Bull. Amer. Phys. Soc.* **18**, 627 (1973).
- F. Plasil and M. Blann, "Fission-Imposed Limits on Angular Momentum in Heavy-Ion Reactions," *Bull. Amer. Phys. Soc.* **18**, 600 (1973).
- Frances Pleasonton, R. L. Ferguson, F. Plasil, and C. E. Bemis, Jr., "Mass and Total Kinetic Energy Distributions from the Spontaneous Fission of ^{246}Cm ," *Bull. Amer. Phys. Soc.* **18**, 628 (1973).
- Frances Pleasonton, R. L. Ferguson, and H. W. Schmitt, "Prompt Gamma Rays Emitted in the Thermal-Neutron Induced Fission of ^{233}U , ^{235}U , and ^{239}Pu and the Spontaneous Fission of ^{252}Cf ," *Bull. Amer. Phys. Soc.* **18**, 626 (1973).
- A. V. Ramayya, G. Garcia-Bermudez, R. M. Ronningen, J. H. Hamilton, R. L. Robinson, H. J. Kim, H. K. Carter, and E. Collins, "Lifetime of the 937 keV 0^+ State in ^{72}Se ," *Bull. Amer. Phys. Soc.* **18**, 721 (1973).
- L. L. Riedinger, P. H. Stelson, G. B. Hagemann, D. C. Hensley, R. L. Robinson, N. R. Johnson, E. Eichler, and R. O. Sayer, "Rotational Band Excitation of ^{164}Yb in (H.I.,xn)," *Bull. Amer. Phys. Soc.* **18**, 580 (1973).
- G. R. Satchler (invited paper), "Direct Excitation of Giant Nuclear Multipoles," *Bull. Amer. Phys. Soc.* **18**, 614 (1973).
- M. R. Schmorak, "Systematics of Nuclear Structure for $A = 188, 190, 192$," *Bull. Amer. Phys. Soc.* **18**, 700 (1973).
- P. H. Stelson, G. B. Hagemann, D. C. Hensley, R. L. Robinson, L. L. Riedinger, and R. O. Sayer, "High Spin States in ^{164}Yb and ^{160}Er ," *Bull. Amer. Phys. Soc.* **18**, 581 (1973).
- A. Stolovy, A. I. Namenson, and J. A. Harvey, "Further Search for Intermediate Structure in the Re Isotopes," *Bull. Amer. Phys. Soc.* **18**, 592 (1973).
- S. T. Thornton, J. L. C. Ford, Jr., J. Gomez del Campo, R. L. Robinson, and P. H. Stelson, "The $^{10}\text{B}(^{16}\text{O},d)$ and $^{10}\text{B}(^{16}\text{O},^6\text{Li})$ Reactions," *Bull. Amer. Phys. Soc.* **18**, 599 (1973).
- K. S. Toth, J. L. C. Ford, Jr., D. C. Hensley, R. M. Gaedke, and P. J. Riley, "Single-Nucleon Transfer Reactions Induced by ^{11}B Ions Incident on ^{208}Pb ," *Bull. Amer. Phys. Soc.* **18**, 714 (1973).
- T. Watts, T. Ou, D. Fong, H. Lucas, I. Pless, P. Trepagnier, J. Wolfson, R. D. McCulloch, W. M. Bugg, and T. Ludlam, "Secondary Track Measurement Using Multiwire Proportional Counters with the NAL 30" Bubble Chamber," *Bull. Amer. Phys. Soc.* **18**, 564 (1973).

J. C. Wells, Jr., J. Lin, R. L. Robinson, H. J. Kim, and J. L. C. Ford, Jr., "Cross Sections for $^{61}\text{Ni}(^{16}\text{O},\chi)$ Reactions," *Bull. Amer. Phys. Soc.* **18**, 712 (1973).

R. R. Winters, O. A. Wasson, and R. L. Macklin, "Valency Model of Radiative Neutron Capture in $^{88}\text{Sr}(n,\gamma)^{89}\text{Sr}$," *Bull. Amer. Phys. Soc.* **18**, 591 (1973).

C. Y. Wong, "Toroidal Liquid Stars," *Bull. Amer. Phys. Soc.* **18**, 644 (1973).

R. Yamamoto, P. Marcato, I. Pless, B. Wadsworth, J. Wolfson, E. Alyea, H. Martin, R. Burnstein, R. Robertson, C. Chien, V. Bogert, H. Brashear, H. O. Cohn, T. Devlin, R. Plano, H. Sanders, T. Watts, D. Dauwe, and H. Taft, "Hybrid Bubble Chamber – Spectrometer System for Use with the NAL 30" Bubble Chamber," *Bull. Amer. Phys. Soc.* **18**, 564 (1973).

1973 Annual American Industrial Hygiene Association Conference, Boston, Massachusetts, May 20–25, 1973

H. M. Butler, K. M. Wallace, and C. B. Fulmer, "Half-Value Thickness Measurements of Ordinary Concrete for Neutrons from Cyclotron Targets."

Kiev Conference on Neutron Physics, Kiev, USSR, May 28–June 3, 1973

B. J. Allen, A. R. de L. Musgrove, D. M. H. Chan, and R. L. Macklin, "Neutron Capture Cross Sections of the Calcium and Barium Isotopes."

Twenty-Eighth Annual Symposium on Molecular Structure and Spectroscopy, Columbus, Ohio, June 11–15, 1973

F. C. DeLucia, P. Helminger, W. Gordy, P. A. Staats, and H. W. Morgan, "Millimeter and Submillimeter Spectroscopy of Tritiated Water."

P. Helminger, F. C. DeLucia, W. Gordy, H. W. Morgan, and P. A. Staats, "Microwave Rotation-Inversion Spectrum of NT_3 ."

International Conference on Low Energy Ion Accelerators and Mass Separators, Billingeus, Skovde, Sweden, June 12–15, 1973

W.-D. Schmidt-Ott and R. L. Mlekodaj, "He-Jet On-Line Ion Source of the UNISOR Mass Separator."

E. H. Spejewski, R. L. Mlekodaj, H. K. Carter, W.-D. Schmidt-Ott, E. L. Robinson, R. W. Fink, J. M. Palms, W. H. Brantley, B. D. Kern, K. J. Hofstetter, E. F. Zganjar, A. R. Quinton, F. T. Avignone, W. M. Bugg, C. R. Bingham, F. Culp, J. Lin, J. H. Hamilton, A. V. Ramayya, M. A. Ijaz, J. A. Jacobs, J. L. Duggan, W. G. Pollard, R. S. Livingston, C. E. Bemis, E. Eichler, N. R. Johnson, R. L. Robinson, and K. S. Toth, "The UNISOR Project."

1973 Society of Nuclear Medicine Meeting, Miami, Florida, June 14, 1973

D. J. Horen (invited paper), "Precursors for Nuclear Data Compilations for Medical Applications."

Gordon Research Conference on Nuclear Structure Physics, New London, New Hampshire, June 18–22, 1973

F. E. Bertrand (invited paper), "Excitation of Giant Resonances in Nuclei."

Gordon Research Conference on Nuclear Chemistry, New London, New Hampshire, June 25–29, 1973

F. E. Bertrand (invited paper), "Inelastic Scattering Studies of Giant Quadrupole Resonances."

M. L. Mallory (invited paper), "Cyclotron Beam Recycling."

E. H. Spejewski (invited paper), "The UNISOR Project."

Eighth International Conference on the Physics of Electronic and Atomic Collisions, Belgrade, Yugoslavia, July 16–20, 1973

T. A. Carlson (invited paper), "Creation of Excited States as the Result of X-Ray Photoionization."

J. R. Mowat, I. A. Sellin, D. J. Pegg, R. S. Peterson, M. D. Brown, and J. R. Macdonald, "Exponential Projectile Charge Dependence of Ar K and Ne K X-Ray Production by Fast, Highly-Ionized Argon Beams in Neon Targets."

Third Symposium on the Physics and Chemistry of Fission, Rochester, New York, August 13–17, 1973

J. W. T. Dabbs, C. E. Bemis, N. W. Hill, G. D. James, M. S. Moore, and A. N. Ellis, "Neutron Fission Cross-Section of ^{249}Cf ."

H. H. Gutbrod, F. Plasil, H. C. Britt, B. H. Erkkila, R. H. Stokes, and M. Blann, "Fission and Complete Fusion Measurements in ^{40}Ar Bombardments of ^{58}Ni and ^{109}Ag ."

G. A. Keyworth, J. R. Lemley, C. E. Olsen, F. T. Seibel, J. W. T. Dabbs, and N. W. Hill, "Determination of Spins of Intermediate Structure Resonances in Subthreshold Fission."

F. Plasil, R. L. Ferguson, and Frances Pleasonton, "Heavy-Ion-Induced Fission of Nuclei in the Region of Silver."

Frances Pleasonton, R. L. Ferguson, and H. W. Schmitt, "Prompt Gamma Rays Emitted in the Thermal-Neutron Induced Fission of ^{233}U , ^{235}U , and ^{239}Pu ."

H. W. Schmitt and M. G. Mustafa, "Potential Energy Surfaces and Dependence of Fission Mass Asymmetry on the Internal Excitation Energy of the Fissioning Nucleus."

Joint Meeting Electron Microscopy Society of America and Electron Probe Analysis Society of America, New Orleans, Louisiana, August 13–17, 1973

T. A. Welton, Frances L. Ball, and W. W. Harris, "Wiener Processing of Phase Contrast Electron Micrographs."

R. E. Worsham, J. E. Mann, E. G. Richardson, and N. F. Ziegler, "An Electron Microscope with Highly Coherent Illumination."

International Conference on Nuclear Physics, Munich, Germany, August 27–September 1, 1973

K. H. Bhatt, J. C. Parikh, and J. B. McGrory, "On the Collective Structure of Some Shell Model States."

J. L. C. Ford, Jr., K. S. Toth, D. C. Hensley, R. M. Gaedke, P. J. Riley, and S. T. Thornton, "Inelastic Scattering and Single Nucleon Transfer Reactions with ^{11}B Ions Incident on ^{208}Pb ."

J. L. Fowler, C. H. Johnson, and N. W. Hill, "Total Neutron Cross Section of Calcium."

H. V. Geramb and J. B. McGrory, "Correlation Effects in the Microscopic Analysis of $^{12}\text{C}(p,p')$ Reactions."

J. Gomez del Campo, J. L. C. Ford, Jr., S. T. Thornton, R. L. Robinson, and P. H. Stelson, "High Spin States in ^{22}Na ."

J. H. Hamilton, A. V. Ramayya, W. E. Collins, L. Varnell, J. Lange, G. Garcia-Bermudez, R. Ronningen, R. L. Robinson, P. H. Stelson, J. L. C. Ford, Jr., N. R. Johnson, A. Kluk, J. Pinajian, L. L. Riedinger, H. Yamada, T. Katoh, M. Fujioka, M. Sekikawa, and S. H. Ahn, "Properties of $K^\pi = 2^+$ and 0^+ Bands in $^{156,158}\text{Gd}$ and $^{176,178,180}\text{Hf}$."

H. J. Kim, R. L. Robinson, and W. T. Milner, "High-Spin States of ^{42}Ca via the $^{28}\text{Si}(^{16}\text{O}, 2p\gamma)$ Reaction."

D. C. Kocher, F. E. Bertrand, E. E. Gross, R. S. Lord, and E. Newman, "Excitation of Giant Resonances in ^{58}Ni via Inelastic Scattering of Polarized Protons."

S. J. Krieger, K. T. R. Davies, and C. Y. Wong, "Generalized Shells in Nuclei: HF Calculations of Bubble Nuclei."

J. B. McGrory (invited paper), "Studies of Nuclear Structure with Large Shell Model Calculations."

G. R. Satchler (invited paper), "Direct Reactions."

D. Sinclair, J. B. Ball, Ole Hansen, J. S. Larsen, and F. Videbaek, "The $^{26}\text{Mg}(^{16}\text{O}, ^{15}\text{N})^{27}\text{Al}$ Reaction at Small Angles."

P. H. Stelson, C. E. Bemis, Jr., F. K. McGowan, W. T. Milner, J. L. C. Ford, Jr., R. L. Robinson, and W. Tuttle, "Coulomb-Nuclear Interference for Alpha-Particles on Rare-Earth Nuclei."

Symposium on Correlations in Nuclei, Balatonfured, Hungary, September 3–8, 1973

G. R. Satchler (invited paper), "Calculations of the Imaginary Part of the Optical Potential."

Twenty-Fourth International Congress on Pure and Applied Chemistry, Hamburg, Germany, September 3–8, 1973

H. W. Morgan, P. A. Staats, and E. Silberman, "Chemical Reactions in Alkali Halide Solid Solutions."

Fifth International Conference on Atomic Collisions in Solids, Gatlinburg, Tennessee, September 24–28, 1973

B. R. Appleton, J. A. Biggerstaff, T. S. Noggle, S. Datz, C. D. Moak, M. D. Brown, H. F. Krause, R. H. Ritchie, and V. N. Neelavathi, "Radiative Electron Capture by Channeled Oxygen Ions."

S. Datz, B. R. Appleton, J. A. Biggerstaff, M. D. Brown, H. F. Krause, C. D. Moak, and T. S. Noggle, "Charge State Dependence of Stopping Power for Oxygen Ions Channeled in Silver."

C. D. Moak, B. R. Appleton, J. A. Biggerstaff, S. Datz, and T. S. Noggle, "Velocity Dependence of the Stopping Power of Channeled Iodine Ions."

J. R. Mowat, B. R. Appleton, J. A. Biggerstaff, S. Datz, C. D. Moak, and I. A. Sellin, "Charge State Dependence of Si K X-Ray Production in Solid and Gaseous Targets by 40 MeV Oxygen Ion Impact."

Heavy-Ion Workshop, Copenhagen, Denmark, October 15–20, 1973

E. E. Gross (invited paper), "The Heavy-Ion Program at ORIC."

American Physical Society Meeting, Bloomington, Indiana, November 1–3, 1973

R. L. Auble, S. Raman, W. T. Milner, and F. F. Dyer, "Gamma-Ray Spectroscopy of $A = 123$," *Bull. Amer. Phys. Soc.* **18**, 1425 (1973).

J. B. Ball, D. Sinclair, J. S. Larsen, F. Videbaek, and O. Hansen, "A Study of the ($^{16}\text{O}, ^{15}\text{N}$) Reaction at Small Angles," *Bull. Amer. Phys. Soc.* **18**, 1414 (1973).

H. G. Bingham, M. L. Halbert, D. C. Hensley, E. Newman, K. W. Kemper, and L. A. Charlton, "($^6\text{Li}, ^3\text{He}$) and ($^6\text{Li}, t$) Reactions on ^{12}C at 60 MeV," *Bull. Amer. Phys. Soc.* **18**, 1389 (1973).

C. C. Foster, N. M. O'Fallon, S. A. Gronemeyer, C. B. Fulmer, D. C. Hensley, W. W. Eidson, and R. G. Rasmussen, "Isotope Effect in 40 MeV Elastic Alpha Scattering from ^{28}Si , ^{29}Si , and ^{30}Si ," *Bull. Amer. Phys. Soc.* **18**, 1427 (1973).

W. M. Good, J. A. Harvey, and N. W. Hill, "Neutron Resonances in ^{39}K and ^{41}K ," *Bull. Amer. Phys. Soc.* **18**, 1401 (1973).

C. D. Goodman, H. W. Fielding, and D. A. Lind, "Differential Cross Sections for $^{10}\text{B}(p,n)^{10}\text{C}$ and $^{11}\text{B}(p,n)^{11}\text{C}$," *Bull. Amer. Phys. Soc.* **18**, 1419 (1973).

N. B. Gove and S. Raman, "Angular Correlation with One Ge(Li) Detector?" *Bull. Amer. Phys. Soc.* **18**, 1413 (1973).

E. E. Gross, H. G. Bingham, M. L. Halbert, D. C. Hensley, and M. J. Saltmarsh, "Coulomb-Nuclear Interference in $^{22}\text{Ne} + ^{88}\text{Sr}$ Inelastic Scattering," *Bull. Amer. Phys. Soc.* **18**, 1388 (1973).

M. W. Guidry, R. J. Sturm, N. R. Johnson, E. Eichler, G. D. O'Kelley, G. B. Hagemann, D. C. Hensley, R. O. Sayer, and L. L. Riedinger, "Multiple Coulomb Excitation of ^{236}U ," *Bull. Amer. Phys. Soc.* **18**, 1405 (1973).

M. L. Halbert, C. B. Fulmer, S. Raman, M. J. Saltmarsh, A. H. Snell, and P. H. Stelson, "Elastic Scattering of ^{16}O by ^{16}O ," *Bull. Amer. Phys. Soc.* **18**, 1387 (1973).

J. H. Hamilton, G. Garcia-Bermudez, A. V. Ramayya, L. L. Riedinger, C. R. Bingham, E. F. Zganjar, E. H. Spejewski, R. L. Mlekodaj, H. K. Carter, and W.-D. Schmidt-Ott, "Evidence for a New Thallium Isotope of Mass 188," *Bull. Amer. Phys. Soc.* **18**, 1379 (1973).

J. A. Harvey, W. M. Good, N. W. Hill, and R. Schindler, "Neutron Total Cross Section of ^{207}Pb from 5 to 35 MeV," *Bull. Amer. Phys. Soc.* **18**, 1403 (1973).

D. C. Hensley, C. B. Fulmer, M. B. Lewis, C. C. Foster, N. M. O'Fallon, S. A. Gronemeyer, W. W. Eidson, and R. G. Rasmussen, "Anomalous Effects in Back Angle Inelastic Scattering of Alpha-Particles from 2+ Levels in ^{60}Ni ," *Bull. Amer. Phys. Soc.* **18**, 1427 (1973).

D. J. Horen, F. E. Bertrand, and M. B. Lewis, "Excitation of Giant Resonances in $^{144,154}\text{Sm}$ by Inelastic Proton Scattering," *Bull. Amer. Phys. Soc.* **18**, 1386 (1973).

C. H. Johnson and J. L. Fowler, "Ordering of Single-Particle Levels from Neutron Total Cross Section of Calcium," *Bull. Amer. Phys. Soc.* **18**, 1401 (1973).

N. R. Johnson, R. J. Sturm, M. W. Guidry, E. Eichler, R. O. Sayer, N. C. Singhal, G. D. O'Kelley, J. S. Smith III, and D. C. Hensley, "Lifetimes of Rotational States in ^{232}Th ," *Bull. Amer. Phys. Soc.* **18**, 1405 (1973).

H. J. Kim, R. L. Robinson, and W. T. Milner, "High Spin States of ^{39}K via the $^{28}\text{Si}(^{16}\text{O},\alpha\gamma)^{39}\text{K}$," *Bull. Amer. Phys. Soc.* **18**, 1405 (1973).

D. C. Kocher, F. E. Bertrand, E. E. Gross, R. S. Lord, and E. Newman, "Excitation of Giant Resonances via Inelastic Scattering of Polarized Protons," *Bull. Amer. Phys. Soc.* **18**, 1386 (1973).

R. S. Lee, A. V. Ramayya, J. H. Hamilton, K. S. R. Sastry, E. H. Spejewski, R. L. Mlekodaj, H. K. Carter, W.-D. Schmidt-Ott, J. Lin, C. R. Bingham, L. L. Riedinger, E. F. Zganjar, J. L. Weil, B. D. Kern, A. Xenououlos, and R. W. Fink, "Study of Some Neutron Deficient $A = 117$ Isobars," *Bull. Amer. Phys. Soc.* **18**, 1425 (1973).

M. B. Lewis, "Giant Hole State Resonances in ^{207}Pb ," *Bull. Amer. Phys. Soc.* **18**, 1387 (1973).

E. Newman, K. S. Toth, D. C. Hensley, and W.-D. Schmidt-Ott, "Levels in $^{146,147,148}\text{Gd}$ Observed Following the Decay of Their Terbium Parents: New Isotope, ^{146}Tb ," *Bull. Amer. Phys. Soc.* **18**, 1425 (1973).

S. Raman, L. G. Multhauf, and K. G. Tirsell, "Potassium-48," *Bull. Amer. Phys. Soc.* **18**, 1407 (1973).

K. S. R. Sastry, A. V. Ramayya, R. S. Lee, J. H. Hamilton, R. L. Mlekodaj, and N. R. Johnson, "Precession of Gamma-Gamma Correlation in ^{126}Xe ," *Bull. Amer. Phys. Soc.* **18**, 1425 (1973).

W.-D. Schmidt-Ott, K. S. Toth, E. Newman, and C. R. Bingham, "Alpha-Decay Branching Ratios for High- and Low-Spin Isomers in $^{151,152,153,154}\text{Ho}$," *Bull. Amer. Phys. Soc.* **18**, 1378 (1973).

G. G. Slaughter and O. A. Wasson, "Test of Valency Neutron Capture in $^{90}\text{Zr}(n,\gamma)^{91}\text{Zr}$," *Bull. Amer. Phys. Soc.* **18**, 1402 (1973).

R. J. Sturm, N. R. Johnson, M. W. Guidry, R. O. Sayer, E. Eichler, N. C. Singhal, and D. C. Hensley, "Lifetime of the 10^+ State in ^{154}Sm ," *Bull. Amer. Phys. Soc.* **18**, 1405 (1973).

K. S. Toth, J. L. C. Ford, Jr., D. C. Hensley, R. M. Gaedke, P. J. Riley, and S. T. Thornton, "Inelastic Scattering and Single-Nucleon Transfer Reactions with ^{11}B Ions Incident on ^{208}Pb ," *Bull. Amer. Phys. Soc.* **18**, 1414 (1973).

G. Vourvopoulos, M. B. Greenfield, D. L. McShan, and S. Raman, "The $^{60}\text{Ni}(p,t)^{58}\text{Ni}$ Reaction at 40 MeV and Further Investigation of the Particle-Hole Structure of the Ni Isotopes," *Bull. Amer. Phys. Soc.* **18**, 1407 (1973).

A. Xenououlos, K. R. Baker, G. Gowdy, J. L. Wood, R. W. Fink, E. H. Spejewski, R. L. Mlekodaj, H. K. Carter, W.-D. Schmidt-Ott, J. Lin, C. R. Bingham, L. L. Riedinger, E. F. Zganjar, J. Weil, B. D. Kern, K. S. R. Sastry, A. V. Ramayya, and J. H. Hamilton, "On-Line Mass Separator Study of ^{116}Xe and ^{116}I Decays," *Bull. Amer. Phys. Soc.* **18**, 1424 (1973).

C. Y. Wong and T. A. Welton, "Supersonic Heavy-Ion Collisions," *Bull. Amer. Phys. Soc.* **18**, 1383 (1973).

Fifth Symposium on Engineering Problems of Fusion Research, Princeton, New Jersey, November 5–9, 1973

M. Roberts, P. N. Haubenreich, D. D. Cannon, and R. S. Lord, "Conceptual Design Study for the ORMAK F/BX Facility."

Southeastern Section Meeting American Physical Society, Winston-Salem, North Carolina, November 8–10, 1973

T. A. Carlson (invited paper), "Industrial Application of Electron Spectroscopy for Chemical Analysis (ESCA)," in press, *Bull. Amer. Phys. Soc.*

D. C. Hensley (invited paper), "Element 104: An Application of an X-Ray Technique," in press, *Bull. Amer. Phys. Soc.*

J. Lin, F. T. Avignone, E. H. Spejewski, R. L. Mlekodaj, H. K. Carter, W.-D. Schmidt-Ott, K. R. Baker, J. L. Wood, A. C. Xenoulos, G. M. Gowdy, R. W. Fink, B. D. Kern, J. Weil, K. J. Hofstetter, C. Bingham, L. L. Riedinger, and L. Harwood, "On-Line Study of Short-Lived Activities for $A = 115$," in press, *Bull. Amer. Phys. Soc.*

J. B. McGrory (invited paper), "The Shell Model Is Still Alive and Kicking," in press, *Bull. Amer. Phys. Soc.*

H. W. Morgan, P. A. Staats, and E. Silberman, "Chemical Reactions in Alkali Halide Solid Solutions," in press, *Bull. Amer. Phys. Soc.*

J. R. Mowat (invited paper), "Projectile Charge State Effects in Heavy-Ion Induced K X-Ray Production," in press, *Bull. Amer. Phys. Soc.*

R. L. Robinson (invited paper), "Neutron Deficient Nuclei Produced by Heavy-Ion Induced Reactions," in press, *Bull. Amer. Phys. Soc.*

R. Ronningen, J. H. Hamilton, A. V. Ramayya, G. Garcia-Bermudez, L. L. Riedinger, R. L. Robinson, and P. H. Stelson, "Coulomb Excitation of ^{158}Gd ," in press, *Bull. Amer. Phys. Soc.*

W.-D. Schmidt-Ott, R. L. Mlekodaj, and E. H. Spejewski, "He-Jet Ion Source of the UNISOR Mass Separator," in press, *Bull. Amer. Phys. Soc.*

E. F. Zganjar, B. D. Kern, J. L. Weil, K. J. Hofstetter, H. K. Carter, W.-D. Schmidt-Ott, R. L. Mlekodaj, E. H. Spejewski, C. R. Bingham, L. L. Riedinger, J. L. Wood, G. Gowdy, R. W. Fink, J. H. Hamilton, and A. V. Ramayya, "Confirmation of a New Thallium Isotope of Mass 189," in press, *Bull. Amer. Phys. Soc.*

Nineteenth Annual Conference on Magnetism and Magnetic Materials,
Boston, Massachusetts, November 13–16, 1973

J. C. Love and F. E. Obenshain, " ^{61}Ni Mössbauer Studies of Substituted Ni Spinel."

Eastern Analytical Symposium, New York, New York, November 14–16, 1973

T. A. Carlson (invited paper), "Experimental Evaluation of a Simple Model for Quantitative Analysis in ESCA."

American Physical Society Meeting, New Haven, Connecticut, December 10–12, 1973

T. A. Carlson (invited paper), "Electron Shake-Up as Observed in X-Ray Photoelectron Spectroscopy," *Bull. Amer. Phys. Soc.* **18**, 1511 (1973).

S. Datz, J. R. Mowat, I. A. Sellin, B. Appleton, J. A. Biggerstaff, and C. D. Moak, "Effective Charge State of Heavy Ions Penetrating Solids Deduced from Comparing X-Ray Yields in Gases and Solids," *Bull. Amer. Phys. Soc.* **18**, 1508 (1973).

H. Haselton, D. J. Pegg, P. M. Griffin, R. Laubert, J. R. Mowat, R. Peterson, and I. A. Sellin, "Binding Energy and Lifetime of the $(1s2s2p)^4 P_{5/2}^o$ State in Lithium-Like Sulfur," *Bull. Amer. Phys. Soc.* **18**, 1527 (1973).

J. R. Mowat, I. A. Sellin, P. M. Griffin, D. J. Pegg, and R. S. Peterson, "Projectile Structure Effects in Heavy-Ion-Induced K X-Rays: Target X-Rays," *Bull. Amer. Phys. Soc.* **18**, 1508 (1973).

D. J. Pegg, I. A. Sellin, R. Peterson, and J. R. Mowat, "Electron Spectra from the Decay-in-Flight of Metastable Autoionizing States Associated with Highly Excited Heavy Ions," *Bull. Amer. Phys. Soc.* **18**, 1528 (1973).

R. S. Peterson, J. R. Mowat, P. M. Griffin, H. Haselton, R. Laubert, and I. A. Sellin, "Observation of Coherently Excited Dipole Charge Distribution Oscillations in Collision-Averaged Foil Excitation of the $n = 2$ H Levels," *Bull. Amer. Phys. Soc.* **18**, 1528 (1973).

I. A. Sellin, J. R. Mowat, P. M. Griffin, D. J. Pegg, and R. S. Peterson, "Projectile Structure Effects in Heavy-Ion-Induced K X-Rays: Projectile X-Rays," *Bull. Amer. Phys. Soc.* **18**, 1508 (1973).

American Physical Society Meeting, Berkeley, California, December 27–29, 1973

F. E. Bertrand (invited paper), "Excitation of Giant Resonances by Inelastic Proton Scattering," *Bull. Amer. Phys. Soc.* **18**, 1568 (1973).

Seventh European Conference on Physics and Chemistry of Complex Nuclear Reactions,
Kibbutz Ginosar, Sea of Galilee, Israel, December 31, 1973–January 4, 1974

F. Plasil, "Heavy Ion Induced Fusion and Fission."

13. Omniana

Prepared by J. A. Martin and Audrey B. Livingston

ANNOUNCEMENTS

P. H. Stelson was appointed Director of the Physics Division effective July 1, 1973.

R. L. Robinson was appointed Associate Director of the Van de Graaff Laboratory.

PERSONNEL ASSIGNMENTS

During 1973 the Physics Division was host to approximately 35 guests from the United States and from abroad. Many of these were short-term assignments such as are often sponsored by Oak Ridge Associated Universities. Longer appointments may extend for a year or more and are usually sponsored by fellowships or the home institution of the individual. Several Physics Division staff members have been guests of other laboratories, both in the United States and abroad. A list of guests and various staff assignments follows:

Guest Assignees from Abroad

- F. G. Garcia Santibanez, National University of Mexico – Electron Spectroscopy Program (began one-year assignment in August 1973)
- G. Hagemann, Niels Bohr Institute, University of Copenhagen, Denmark – Nuclear Physics Program (completed one-year assignment in July 1973)
- K. A. Hagemann, Niels Bohr Institute, University of Copenhagen, Denmark – Nuclear Physics Program (completed one-year assignment in July 1973)
- G. D. James (Exchange Assignee), Atomic Energy Research Establishment, Harwell, England – Oak Ridge Electron Linear Accelerator Program and part time with Molecular Anatomy Program of Director's Division (completed one-year assignment in October 1973)

- R. J. Griffiths, University of London, King's College, London, England – Nuclear Physics Program (completed two-month assignment in September 1973)
- L. J. Saethre, on leave of absence from the University of Bergen, Norway – Electron Spectroscopy Program (began one-year assignment in August 1973)
- W.-D. Schmidt-Ott, University of Goettingen, Goettingen, Germany – University Isotope Separator at Oak Ridge Program (began assignment in June 1972)
- H. Tamagawa, Nagoya University, Nagoya, Japan – Van de Graaff Program (began one-year assignment in March 1973)

Guest Assignees from the United States

- J. Arbo, Columbia University – Oak Ridge Electron Linear Accelerator Program (completed three-week assignment in November 1973)
- R. W. Benjamin, Savannah River Laboratory – Oak Ridge Electron Linear Accelerator Program (completed two-week assignment in January 1973)
- G. W. Cole, Brookhaven National Laboratory – Oak Ridge Electron Accelerator Program (completed one-week assignment in July 1973)
- R. K. Cole, University of Southern California – Nuclear Physics Program (completed five-months assignment in July 1973)

J. Felvinci, Columbia University – Oak Ridge Electron Accelerator Program (completed three-week assignment in November 1973)

Reinhard Graetzer,¹ Pennsylvania State University – Mössbauer Experimental Program (completed two-month assignment in August 1973)

E. L. Hart, University of Tennessee – High Energy Physics Program (continued part-time assignment begun in October 1969)

H. H. Haselton, University of Tennessee – Van de Graaff Program (began one-year assignment June 1973)

G. A. Keyworth, Los Alamos Scientific Laboratory – Oak Ridge Electron Linear Accelerator Program (completed six-month assignment in January 1973)

D. Kolb, Duke University – Theoretical Physics Program (completed three-month assignment in August 1973)

Roman Laubert, University of Tennessee – Van de Graaff Program (began seven-month assignment in August 1973)

E. Melkonian, Columbia University – Oak Ridge Electron Linear Accelerator Program (completed three-week assignment in November 1973)

J. R. Mowat, University of Tennessee – Van de Graaff Program (continued appointment begun in June 1972)

R. O. Sayer, Vanderbilt University (on leave from Furman University) – Van de Graaff Program (began nine-month assignment September 1973)

F. T. Seibel, Los Alamos Scientific Laboratory – Oak Ridge Electron Linear Accelerator Program (completed six-month assignment in January 1973)

F. B. Simpson, Aerojet Nuclear Company – Oak Ridge Electron Linear Accelerator Program (completed three-week assignment April 1973)

N. Singhal, Vanderbilt University (postdoctoral assignment) – Nuclear Chemistry (Chemistry Division)

G. J. Smith (received Ph.D. from Purdue University) – ORIC Program (began one-year assignment as Oak Ridge Postdoctoral Fellow in September 1973)

R. S. Thoe, University of Tennessee – Van de Graaff Program (began one-year assignment in September 1973)

O. A. Wasson, Brookhaven National Laboratory – Oak Ridge Electron Linear Accelerator Program (completed one-week assignment in April 1973)

B. Wehring, University of Illinois – Ion Source Physics (began five-month assignment in September 1973)

*University Isotope Separator
at Oak Ridge (UNISOR)*

E. H. Spejewski, Oak Ridge Associated Universities (indefinite appointment)

R. L. Mlekodaj, Oak Ridge Associated Universities (indefinite appointment)

H. K. Carter, Vanderbilt University (began one-year appointment in June 1973)

Jung Lin, Tennessee Technological University (completed two-month appointment in August 1973)

Kandula Sastry, University of Massachusetts (completed two-month assignment in August 1973)

E. F. Zganjar, Louisiana State University (began nine-month assignment in September 1973)

Staff Assignments

J. B. Ball – Nuclear Physics. Completed in July 1973 one-year exchange assignment to Niels Bohr Institute, Copenhagen, Denmark

K. T. R. Davies – Theoretical Physics Program. Began in August 1973 a one-year assignment with the Los Alamos Scientific Laboratory

W. B. Dress – Van de Graaff Program. Continued through 1973 an assignment with the Institute Laue-Langevin, Grenoble, France

J. L. C. Ford – Van de Graaff Program. Began in September 1973 a one-year assignment with Max-Planck Institut für Kernphysik, Heidelberg, Germany

J. L. Fowler – Nuclear Physics Program. Began in September 1973 a one-year exchange assignment with the Atomic Energy Research Establishment, Harwell, England

C. B. Fulmer – Nuclear Physics. Completed two-month exchange assignment to University of London, King's College, London, England

C. D. Goodman – Nuclear Physics. Completed in August 1973 a one-year assignment at University of Colorado, Boulder, as visiting professor of physics

¹ Research participant sponsored by Oak Ridge Associated Universities.

- D. J. Horen – Nuclear Data Project. Began in September 1973 a nine-month assignment with the Institut des Sciences Nucléaires, University of Grenoble, Grenoble, France
- H. J. Kim – Van de Graaff Program. Completed in August 1973 a 14-month assignment with the Centre d'Etudes Nucléaires, Saclay, France
- P. D. Miller – Van de Graaff Program. Completed in August 1973 a 14-month assignment with the Institute Laue-Langevin, Grenoble, France
- S. Raman – Nuclear Data Project. Completed in June 1973 a three-month assignment to Institute for Nuclear Studies, University of Tokyo, Tokyo, Japan
- M. J. Saltmarsh – Nuclear Physics. Completed in August a two-month assignment to Los Alamos Scientific Laboratory, New Mexico, to participate in the initial calibration and setup of the Low-Energy Pion Channel at the Los Alamos Meson Physics Facility
- H. W. Schmitt – Physics of Fission Program. Began in May 1973 a leave of absence; presently affiliated with Environmental Systems Corp., Knoxville, Tennessee

Staff Appointees – Intralaboratory Loans

- R. S. Lord (Cyclotron Development and Operations) – part-time loan to Thermonuclear Division for preparing a conceptual design of a feasibility/burning experiment (F/BX)
- M. B. Marshall (Cyclotron Operations) – part-time loan to Thermonuclear Division for design of power supplies for the toroidal field coils of the “High Field Ormak”
- S. W. Mosko (Cyclotron Development and Operations) – part-time loan to Thermonuclear Division for

design of power supplies for the toroidal field coils of the “High Field Ormak”

- E. Newman (Cyclotron Laboratory, Nuclear Physics Program) – began on October 1, 1973, a one-year assignment with the Director's Division, Program Planning and Analysis

Personnel Changes

- G. D. Alton – transfer from Isotopes Division to Physics Division
- T. A. Carlson – transfer from Chemistry Division to Physics Division; previously on loan from Chemistry Division (1960)
- W. W. Harris – transfer from Molecular Anatomy Program to Physics Division
- M. L. Mallory – transfer from Chemistry Division to Physics Division
- M. G. Mustafa – temporary employee and consultant until August 1973. Presently at the University of Maryland, College Park, Maryland
- A. W. Riikola – retired from ORNL Physics Division in May 1973
- H. W. Schmitt – began in May 1973 a two-year leave of absence for industrial development. Currently president of Environmental Systems Corp., Knoxville, Tennessee
- W. R. Smith – transfer from ORNL Physics Division in June 1973 to Estimating Department of Engineering Division, Y-12
- G. F. Wells – transfer from Instrumentation and Controls Division to Physics Division
- D. C. West – resigned from the Physics Division in March 1973

MISCELLANEOUS PROFESSIONAL ACTIVITIES OF DIVISIONAL AND ASSOCIATED PERSONNEL

Staff members and their associates who use the accelerators and other facilities of the Division are involved in numerous professional activities which are incidental to their primary responsibilities. Such activities during 1973 are included in the following:

- G. D. Alton – cochairman for Physics Division Seminar
- J. B. Ball – acting ex officio member, U.S. Nuclear Data Committee; acting chairman, USNDC Sub-

committee on Materials Analysis, Environmental Matters, and Safeguards; reviewer for *Nuclear Physics*; referee for *The Physical Review* and *Physical Review Letters*

- R. L. Becker – reviewer for *The Physical Review*, *Physical Review Letters*, and *Nuclear Physics*; part-time faculty member of the Department of Physics of the University of Tennessee, lecturing in the Oak Ridge Resident Graduate Program

- T. A. Carlson – reviewer for *The Physical Review*, *Inorganic Chemistry*, and *Analytical Chemistry*; joint Editor-in-Chief of the *Journal of Electron Spectroscopy*; lecturer at NSF short course on “Chemical Applications of Photoelectron and Auger Spectroscopies” given at the University of Tennessee, June 18–30, 1973
- H. O. Cohn – member of Accelerator Users Groups at National Accelerator Laboratory, Stanford Linear Accelerator Center, Brookhaven National Laboratory, and Argonne National Laboratory
- J. W. T. Dabbs – member, Oak Ridge Chamber of Commerce Industrial Development Division; president of the Mobile Steam Society; reviewer for *Nuclear Physics* and *The Physical Review*.
- E. Eichler (Chemistry Division) – chairman of 1973 Gordon Research Conference on Nuclear Chemistry; completed one-year assignment in Program Planning and Analysis Office (Director’s Division); reviewer for *The Physical Review* and *Physical Review Letters*
- J. L. Fowler – member of Executive Committee of Council of the American Physical Society (1970–1973); representative of the American Physical Society on the Governing Board of the American Institute of Physics (1972–1974); member of the Manpower Statistics Advisory Committee of the American Institute of Physics (1972–1973); member of Publications Committee of the Council of the American Physical Society (1970–1973) and chairman (1973); Divisional Councilor of the American Physical Society for the Division of Nuclear Physics (1970–1973); chairman of the American Physical Society Fellowship Appeals Committee (1973); member of Executive Committee of Division of Nuclear Physics of the American Physical Society (1970–1973); member of Program Committee for the Division of Nuclear Physics of the American Physical Society (1972–1973); chairman of the Publications Committee for the Division of Nuclear Physics of the American Physical Society for *The Physical Review C* and *Physical Review Letters* (1972–1973); secretary of the Commission on Nuclear Physics of the International Union of Pure and Applied Physics and ex officio member of U.S. National Committee for the International Union of Pure and Applied Physics (1972–1975); referee for *The Physical Review* and *Physical Review Letters*
- C. B. Fulmer – member of the ORNL Accelerator and Radiation Sources Review Committee; referee for *The Physical Review*
- W. M. Good – member of U.S. Nuclear Data Committee Isotope Subcommittee
- C. D. Goodman – member of the Advisory Committee to the Information Services Division of the American Institute of Physics; referee for *The Physical Review C* and *Physical Review Letters*
- E. E. Gross – member of the Technical Advisory Panel for the Los Alamos Meson Factory; referee for *The Physical Review*, *Physical Review Letters*, and *Nuclear Physics*; secretary of the ORIC Program Committee; member of UNISOR Executive Committee
- Edith Halbert – referee for *The Physical Review* and *Physical Review Letters*; chairman of Physics Division Seminars (January–September 1973)
- M. L. Halbert – reviewer for *The Physical Review C* and *Physical Review Letters*
- J. A. Harvey – secretary-treasurer of the Division of Nuclear Physics of the American Physical Society (1967–1974); member of the editorial board of *Atomic and Nuclear Data Tables*, a journal published by Academic Press; reviewer for *The Physical Review* and *Nuclear Science and Engineering*; labor coordinator for the Physics Division
- C. H. Johnson – chairman of Accelerator and Radiation Sources Review Committee at ORNL; reviewer for *The Physical Review*
- N. R. Johnson (Chemistry Division) – reviewer for *The Physical Review*, *Physical Review Letters*, and *Nuclear Physics*
- M. B. Lewis – referee for *Physical Review Letters*
- C. A. Ludemann – Physics Division representative to Union Carbide Division Affirmative Action Program; consultant to Thermonuclear Division in a computer control application
- R. L. Macklin – member of the Oak Ridge Gaseous Diffusion Plant Nuclear Safety Committee; member of the Subcommittee on Neutron Data Applications of the U.S. Nuclear Data Committee; reviewer for *Il Nuovo Cimento*, *The Physical Review*, *Nuclear Physics*, *Physical Review Letters*, *Nuclear Instruments and Methods*, *Astrophysical Journal*, *Nuclear Applications*, *Nuclear Science and Engineering*, and *Nuclear Science and Technology*
- J. A. Martin – president of the Nuclear and Plasma Sciences Society of the Institute of Electrical and Electronics Engineers; member of the Administrative Committee of the IEEE Nuclear and Plasma Sciences

- Society (1971–1975); member of the Technical Committee on Particle Accelerator Science and Technology of the IEEE-NPSS; member of Editorial Advisory Board of *Particle Accelerators*; reviewer for *Particle Accelerators*; consultant to the National Science Foundation Physics Section as a member of the Visiting Committees for the Indiana University Cyclotron Project and the Columbia University Synchrotron Improvement Project; consultant to Columbia University Synchrocyclotron Improvement Project; member of the Organizing Committee for the 1975 Particle Accelerator Conference (Washington, D.C., 1975)
- F. K. McGowan – member, Editorial Board of *Atomic Data and Nuclear Data Tables*, journal published by Academic Press; member of Subcommittee on Nuclear Data for Materials Analysis, Safeguards, and Environmental Matters of the United States Nuclear Data Committee; reviewer for *The Physical Review* and *Physical Review Letters*; member of Committee for International Conference on Reactions between Complex Nuclei (Nashville, Tennessee, June 10–14, 1974)
- J. B. McGrory – referee for *The Physical Review* and *Physical Review Letters*; co-chairman for Physics Division Seminars
- P. D. Miller – reviewer for *The Physical Review*
- C. D. Moak – member of Organizing Committee for the 4th Beam Foil Spectroscopy Conference (to be held in 1975); member of the Organizing Committee for Atomic Physics Collaboration, Oak Ridge (APCOR); member of Local Committee and Program Committee and Editorial Board for Proceedings of the 5th International Conference on Atomic Collisions in Solids (Gatlinburg, September 1973); reviewer for *Reviews of Scientific Instruments* and *Physical Review Letters*
- S. W. Mosko – member of the Ad Hoc Committee (USAEC intralaboratory committee) for preparing “Safety Guidelines for Working on Energized Electrical Equipment”
- E. Newman – member of the ORNL Graduate Fellow Selection Panel; reviewer for *The Physical Review* and *Physical Review Letters*
- F. E. Obenshain – part-time faculty member with the Department of Physics, University of Tennessee; reviewer for *The Physical Review* and *Physical Review Letters*
- F. Plasil – reviewer for *Nuclear Physics*; member of ORNL Ph.D. Recruiting Team
- S. Raman – reviewer for *The Physical Review* and *Physical Review Letters*
- R. L. Robinson – reviewer for *The Physical Review* and *Physical Review Letters*; secretary for the Conference on Reactions between Complex Nuclei (Nashville, Tennessee, June 1974)
- G. R. Satchler – member of Editorial Board of *Particles and Nuclei*, a journal published by F.U. Research Institute, Athens, Ohio; member of Editorial Board of *Atomic Data and Nuclear Data Tables*, a journal published by Academic Press; reviewer for *The Physical Review*, *Physical Review Letters*, *Nuclear Physics*, and *Physics Letters*; member of organizing committee of the Conference on Reactions between Complex Nuclei (Nashville, Tennessee, June 1974)
- I. A. Sellin (University of Tennessee) – appointed to three-year term on the Advisory Committee on Atomic and Molecular Physics, National Academy of Sciences
- G. G. Slaughter – reviewer for *Nuclear Science and Engineering* and *The Physical Review*
- P. H. Stelson – part-time faculty member with the Department of Physics, University of Tennessee; associate editor of *Nuclear Physics*; member of the executive committee of the Southeastern Section of the American Physical Society (1973); member of international committee for the International Conference on Nuclear Physics (Munich, Germany, August 27–September 1, 1973); chairman of International Conference on Reactions between Complex Nuclei (Nashville, Tennessee, June 10–14, 1974); member of Basic Science Subcommittee of the U.S. Nuclear Data Committee (1973–1975); member of the advisory committee for the ORNL Instrumentation and Controls Division; reviewer for *Nuclear Physics*, *Nuclear Science and Engineering*, and *The Physical Review*
- K. S. Toth – reviewer for *The Physical Review* and *Physical Review Letters*; Physics Division–UNISOR Liaison Officer; chairman, UNISOR Scheduling Committee; chairman, program arrangement, 1973 Fall Meeting of the Division of Nuclear Physics of the American Physical Society
- T. A. Welton – member, Council of Electron Microscopy Society of America; chairman, 31st Annual Meeting of Electron Microscopy Society of America (New Orleans, Louisiana, August 14–17, 1973); program chairman for the 1975 meeting of the Electron Microscopy Society of America; consultant on flow and separation theory for the gas centrifuge project at ORGDP; part-time faculty member with the Department of Physics, University of Tennessee

COLLOQUIA AND SEMINARS PRESENTED BY THE PHYSICS DIVISION STAFF AND ASSOCIATES

Members of the Physics Division receive numerous requests to present seminars and colloquia both in this country and abroad. Some of these are supported by the Traveling Lecture Program administered by Oak Ridge Associated Universities. In that program the cost of transportation for the lecture is provided by ORAU, and the local expenses are borne by the host institution. Following is a list of seminars and colloquia presented by Physics Division and associated staff during 1973.

- J. B. Ball – Institute for Nuclear Studies (K.V.I.), Groningen, Netherlands, May 8, 1973, “Transfer Reactions and Nuclear Structure in the $A = 90$ Region”; University Physics Laboratory, Utrecht, Netherlands, May 9, 1973, “Transfer Reactions and Nuclear Structure in the $A = 90$ Region”; Free University, Amsterdam, Netherlands, May 10, 1973, “Heavy-Ion Transfer Reactions on sd -Shell Nuclei – a Look at Small Angles”; Institute for Nuclear Physics (I.K.O.), Amsterdam, Netherlands, May 11, 1973, “Nuclear Structure in the $A = 90$ Region”; University of Bonn, Bonn, Germany, May 17, 1973, “Two-Neutron Transfer Reactions”; Institute for Nuclear Physics, Jülich, Germany, May 16, 1973, “Nuclear Reactions and Nuclear Structure in the $A = 90$ Region”
- R. L. Becker – Ohio State University, March 8, 1973, “The Renormalized Brueckner-Hartree-Fock Approximation”
- F. E. Bertrand – University of Rochester, March 19, 1973, “Bridging the Gap – Experimental Studies of Giant Resonances and Other Continuum Properties via Proton-Induced Reactions”; Kent State University, May 3, 1973, “Application of the Intranuclear Cascade Model to Continuum Spectra from 30–60 MeV Proton Bombardment of Nuclei”
- T. A. Carlson – University of Tennessee, May 29, 1973, “Electron Shake Up and Chemical Bonding”; University of Liege, Liege, Belgium, July 24, 1973, “Satellite Structure in X-Ray Photoelectron Spectroscopy”; Oak Ridge Associated Universities, August 21, 1973, “Electron Spectroscopy” as part of the course on Methods of Trace Analysis; Great Lakes Colleges Association Science Semester Program, Oak Ridge, Tennessee, October 16, 1973, “Electron Spectroscopy for Chemical Analysis”; Notre Dame University, October 25, 1973, “Use of Satellite Lines in X-Ray Photoelectron Spectroscopy for the Study of Chemical Bonding”
- J. W. T. Dabbs – University of Alabama, February 21, 1973, “Polarized Neutrons and Polarized Fissionable Targets”
- E. Eichler (Chemistry Division) – Michigan State University, May 11, 1973, “Coulomb Excitation by Actinide Nuclei with Argon Ions from ORIC”
- J. L. Fowler – Kernforschungszentrum Karlsruhe, Germany, September 3, 1973, “The Neutron as a Probe of Nuclear Structure near Closed Shells”; Harwell Atomic Energy Research Establishment, England, October 11, 1973, “The Neutron as a Probe of Nuclear Structure around Closed Shell Nuclei”
- C. B. Fulmer – University of Alabama, March 21, 1973, “Reactions Induced in Targets Bombarded with Electrons in the GeV Energy Region”; University of London, King’s College, June 13, 1973, “Large Angle Alpha Scattering Studies”; New Mexico State University, December 6, 1973, “Alpha and ^3He Scattering at Large Angles”; University of Texas – El Paso, December 7, 1973, “Alpha and ^3He Scattering at Large Angles”
- C. D. Goodman – University of Colorado, May 16, 1973, “The Electronic Logic Revolution: Do Fashions in Thinking Control Instrument Design?”
- Edith Halbert – University of Georgia, April 5, 1973, “Effective Interactions: A Hard Look at a Simple Case”
- M. L. Halbert – University of Georgia, March 29, 1973, “The Solar Neutrino Puzzle”; Virginia Polytechnic Institute, November 12, 1973, “The Solar Neutrino Puzzle”; Florida A & M University, November 14, 1973, “The Solar Neutrino Puzzle”
- J. A. Harvey – “Nuclear Physics with Intense Neutron Sources,” review talk presented at Workshop on Intense Neutron Sources, Brookhaven National Laboratory, May 30–June 1, 1973
- N. R. Johnson (Chemistry Division) – Vanderbilt University, November 15, 1973, “Lifetimes of Rotational States in Deformed Nuclei by the Doppler-Shift Recoil-Distance Technique”; Texas A & M University, November 28, 1973, “Lifetimes of Rotational States in Deformed Nuclei by the Doppler-Shift Recoil-Distance Technique”
- P. D. Miller – Institute Laue-Langevin, Grenoble, France, January 1973, “The Search for a Neutron Electric Dipole Moment – Past and Future”; Centre d’Etudes Nucléaire de Grenoble, Grenoble, France,

- March 1973, "Cherche pour le Moment Electrique Dipolaire du Neutron"; Institute Laue-Langevin, Grenoble, France, April 1973, "Progress on the Search for an EDM of the Neutron, and a Proposal for a Search for the Reaction $n + p \rightarrow d + 2\gamma$ "; Institute Laue-Langevin, Grenoble, France, April 3, 1973, "Possibilities for and Limitations of a Search for a Neutron EDM Using Ultracold Neutrons in a Storage Box"
- F. E. Obenshain – Georgia State University, April 13, 1973, "Mössbauer Effect Applied to Problems of Magnetism in Solids and Nuclei"
- S. Raman – Institute for Nuclear Study, University of Tokyo, Tokyo, Japan, May 15, 1973, "Log ft Values, Conversion Coefficients, Zero-Phonon Transitions and All That"; Osaka University, Osaka, Japan, June 1, 1973, "High Resolution Gamma-Ray Spectroscopy"
- M. J. Saltmarsh – University of Georgia, March 2, 1973, " $(^3\text{He}, n)$ Reactions at 25 MeV"; Florida State University, May 17, 1973, "Atomic Physics with Nuclear Beams"; University of Virginia, November 8, 1973, "Inner Shell Ionization"
- G. R. Satchler – Duke University, April 12, 1973, "New Giant Resonances in Nuclei"
- Alan Scott (University of Georgia) – Kernfysisch Versneller Instituut, University of Groningen, Netherlands, December 7, 1973, and Kernforschungsanlage Jülich, West Germany, December 12, 1973, "Our (p, p') Experiments with 61 MeV Protons from the Oak Ridge Isochronous Cyclotron"; University of Grenoble, Institut des Sciences Nucléaires, France, December 17, 1973, "Our Inelastic Scattering Experiments near $A = 90$ and $A = 208$ with 61 MeV Protons from the Oak Ridge Isochronous Cyclotron"
- W.-D. Schmidt-Ott (UNISOR) – University of Tennessee, February 6, 1973, "Interactions between Nucleus and Atomic Shell"; Virginia Polytechnic Institute, April 1973, "Investigation of Nuclei Far from Beta Stability Produced by Heavy Ion-Induced Reactions"
- P. H. Stelson – University of Michigan, June 28, 1973, "Heavy Ion x, n Reactions"
- C. Y. Wong – Texas Technological University, February 20, 1973, "Toroidal Nuclei, Bubble Nuclei, and Toroidal Stars"; North Texas State University, February 22, 1973, "Toroidal Nuclei, Bubble Nuclei, and Toroidal Stars"; University of Maryland, November 15, 1973, "Toroidal and Bubble Nuclei"

PHYSICS DIVISION SEMINARS

Divisional seminars are usually held weekly at 3:00 PM on Friday. Frequently, however, scheduling problems and the possibility of additional talks of special timeliness or interest require different times. Laboratory-wide advance notice is made of these seminars, which are open to employees and guests.

The seminar chairperson through August 1973 was Edith Halbert (theoretical physics); in September, G. Alton and J. B. McGrory jointly assumed those duties. The program for 1973 was as follows:

- January 4 – W. J. Roberts, ORNL, University of Tennessee, and Tennecomp Systems, "Isospin Conservation in the Reactions $^3\text{H}(^3\text{He}, ^4\text{He})^2\text{H}$ and $^3\text{He}(^3\text{He}, ^4\text{He})2p$ "
- January 11 – Ivo Zvara, Joint Institute for Nuclear Research, Dubna, U.S.S.R., and Chemistry Division, ORNL, "Research with Heavy Ions in Dubna"
- January 18 – P. H. Stelson, ORNL, "Coulomb Excitation of Niobium"
- January 23 – Gudrun Hagemann, Niels Bohr Institute, Copenhagen, Denmark, and Physics Division, ORNL, "Electromagnetic Properties of Rotational States in Dysprosium Nuclei"
- February 8 – Krishna Kumar, Vanderbilt University, "Some Surprises at High Spins"
- February 15 – K. T. R. Davies, ORNL, "Ten Years with Hartree-Fock and What Have We Got?"
- February 22 – Gareth Guest, ORNL, "Controlled Thermonuclear Research: A Status Report"
- March 1 – Eugene Guth, University of Tennessee, "What Is Interesting and Puzzling in Physics Today?"
- March 8 – H. T. Fortune, University of Pennsylvania, "Nuclear Structure Information from Heavy-Ion Reactions"
- March 22 – Ralph DeVries, University of Washington, "Heavy Ions, Recoil, DWBA, and All That Stuff"
- March 29 – G. R. Satchler, ORNL, "New Giant Resonances in Nuclei"
- April 5 – Edward L. Hart, University of Tennessee, "Expectations and Early Experimental Results from NAL-Energy-Range Accelerators"

- April 6 – A. M. Lane, Atomic Energy Research Establishment, Harwell, England, “Aspects of the Giant Dipole Resonance”
- April 17 – C. S. Wu, Columbia University, “The Dynamic Effects in Nuclear Probing by Muons”
- April 18 – G. C. Morrison, Argonne National Laboratory, “Nuclear Structure with Heavy Ion Transfer”
- April 19 – H. G. MacPherson, University of Tennessee, “How to Make Fast Reactors Safe”
- May 10 – M. Brack, State University of New York, Stony Brook, “Is the Strutinsky Method Still Appropriate?”
- May 17 – Alan Scott, University of Georgia, “Inelastic Scattering on a Shoestring”
- May 25 – David E. Fisher, University of Miami, “Dating the Spreading Sea Floor”
- June 1 – Larry Samick, Rutgers University, “The Density-Dependence and Spin-Dependence of Effective Interactions”
- June 7 – Dietmar Kolb, Duke University, “Realistic Single-Particle Model for Nuclear Fission”
- June 14 – Joyce J. Kaufman, Johns Hopkins University, “Spin and Symmetry Restrictions for the Understanding of Reactive Collisions and Molecular Decompositions, and Accurate Configuration Interaction Calculations Including Those for Electron Affinities”
- June 21 – F. E. Obenshain, ORNL, “Some Applications of the Mössbauer Effect in Nuclear and Solid State Physics”
- June 28 – John Philpott, Florida State University, “Microscopic Calculations for Nuclear Continuum Phenomena”
- July 12 – S. Raman, ORNL, “Land of the Rising Yen”
- July 26 – R. J. Griffiths, King’s College, London, England, “Optical Model – Quo Vadis?”
- August 9 – Rainer W. Hasse, University of Munich, Germany, “A Two-Nucleus Shell Model with Pairing, and Its Application to the Scission Region”
- August 23 – J. B. Ball, ORNL, “Heavy-Ion Transfer Reaction Studies at Copenhagen – a Forward Look”
- September 6 – B. C. Larson, ORNL, “X-Ray Diffuse Scattering Study of Crystal Defects”
- September 11 – Paul J. R. Soper, University of Surrey, Guildford, England, “Adiabatic Theory of Deuteron Stripping and Elastic Scattering”
- September 27 – X. Campi, McMaster University, Ontario, Canada, “Finite Nuclei in the Local Density Approximation”
- October 4 – J. S. Longworth, ORNL, “Electronic Energy Transfer in Proteins”
- October 11 – Alan Broad, University of Michigan, “Coupled-Channels Reaction and Form Factor Effects in Direct Reactions on Strongly Deformed Nuclei”
- October 11 – John S. Luce, Lawrence Livermore Laboratory, “Collective Ion Acceleration”
- October 18 – Hans Krappe, Lawrence Berkeley Laboratory, “Interaction Barriers for Heavy-Ion Scattering”
- October 25 – Günther Leibfreid, Technical University, Aachen, Germany, and Nuclear Research Center, Jülich, Germany, “Diffusive Reactions of Point Defects”
- October 30 – Dorian James, Atomic Energy Research Establishment, Harwell, England, “Sub-Threshold Fission Phenomena for U^{234} ”
- November 8 – W. C. Lineberger, Joint Institute for Laboratory Astrophysics, University of Colorado, “Laser Photodetachment of Negative Ions”
- November 15 – R. Ritchie, Health Physics, ORNL, “Plasma Effects in Condensed Matter”
- November 29 – D. Brayshaw, University of Maryland, “What Can One Learn from Three-Body Reactions?”
- December 6 – C. D. Goodman, ORNL, “A Scientific and Scenic View of Nuclear Physics at the University of Colorado”

Ph.D. THESIS RESEARCH

During 1973, 16 Physics Division staff members and associates served in either an advisory or supervisory capacity for research programs of 11 candidates for the Doctor of Philosophy degree. Doctoral degrees were conferred on four students during the year. Most of the research was conducted at Oak Ridge National Laboratory through fellowship appointments or guest assignment arrangements. A list of participants follows:

Ph.D. candidate	Advisor(s)	Field of research (thesis title listed if known)
W. J. Carter III University of Tennessee	T. A. Carlson	"Electron Spectroscopy Applied to Environmental Problems"
K. Dagenhart University of Tennessee	P. H. Stelson F. K. McGowan	Coulomb Excitation of ^{115}Sn , $^{111},^{113}\text{Cd}$
J. Gomez del Campo National University of Mexico	J. L. C. Ford, Jr. R. L. Robinson	Estudio de la Reaccion $^{10}\text{B}(^{16}\text{O},\alpha)^{22}\text{Na}$
M. Guidry University of Tennessee	N. R. Johnson E. Eichler G. D. O'Kelley	Coulomb excitation — lifetime measurements
J. P. Judish University of Tennessee	P. H. Stelson C. M. Jones	Superconducting rf cavities
Chan Mong-Hung University of Melbourne	R. D. Macklin	Neutron Capture Cross Sections of the Isotopes of Calcium
Muhammad Owais University of Georgia	A. Scott (University of Georgia)	"Experimental Study of Reaction Mechanisms in In-elastic Scattering of 61 MeV Protons"
F. Garcia Santibanez University of Mexico	T. A. Carlson	Studies in Electron Spectroscopy
D. P. Spears University of Oklahoma	T. A. Carlson	"Satellite Structure in the Photoelectron Spectra of Rare Gases, Some Simple Gaseous Molecules and Alkali Metal Halides"
W. K. Tuttle III University of Tennessee	P. H. Stelson	Coulomb Excitation of ^{113}In and ^{115}In
G. A. Vernon University of Illinois	T. A. Carlson	"Study of Satellite Structure in the Photoelectron Spectra of Transition Metal Compounds"

M.S. THESIS RESEARCH

During 1973, four students conducted thesis research leading to the Master of Science degree under the direction of Physics Division staff and associates. One student was awarded the M.S. degree during the year. Students, advisors, and topics are as follows:

Candidate	Advisor(s)	Field of research (thesis title given if known)
C. Guet University of Grenoble	W. B. Dress P. D. Miller	"Search for the Reaction $n + p \rightarrow d + 2\gamma$ "
Z. L. T. Lukuba University of Tennessee	C. B. Fulmer	"Cyclotron Yields of Radionuclides for Medical Applications"
R. S. Peterson University of Tennessee	I. A. Sellin University of Tennessee	Coherent Excitation of Foil-Transmitted Ions
R. A. Gallman University of Tennessee	I. A. Sellin University of Tennessee	"K-Shell X-Ray Production Cross Sections for Mn, Ni, Cu, Zn, Ge and Sn for Oxygen Ions from 80 to 30 MeV"

UNDERGRADUATE STUDENT GUESTS

M. T. Collins, ¹ Johns Hopkins University	Robert J. Schroeder, ¹ Gettysburg College
George B. Hudson, ¹ Oklahoma City University	James A. Smith, ¹ New College, Sarasota
Marian J. Kowalski, ² Ohio Wesleyan University	Joseph S. Smith, Furman University
Lawrence P. Lehman, ¹ University of Rochester	H. H. K. Tang, Kalamazoo College
Victor Odlikav, ² Earlham College	Ralph H. Tookey, ² DePauw University
Rafe H. Schindler, ¹ University of Rochester	
Pamela S. Scholl, ¹ Transylvania University	

1. ORAU undergraduate research trainee.
2. Great Lakes Colleges Association program.

COOPERATIVE EDUCATION PROGRAM

Undergraduate students in science and engineering may be selected to participate in the Cooperative Education Program of the Laboratory. Students alternate equal intervals of school attendance and work at the Laboratory. During 1973, four students participated in the program in the Physics Division. Following is a list of students, their institutions, and assignments.

S. D. Blazier, University of Tennessee – Theoretical Physics Program (completed assignments in June 1973)
P. B. Foster, Georgia Institute of Technology – Oak Ridge Electron Linear Accelerator (ORELA) Time-of-Flight Spectroscopy (completed assignments in August 1973)

GUEST ASSIGNEES – STUDENTS NOT ENGAGED IN THESIS RESEARCH AT ORNL

Christina C. Back, employee of the University of Tennessee – High Energy Physics Program (began indefinite assignment in July 1973)	Karen M. Smith, employee of the University of Tennessee – High Energy Physics Program (completed assignment January 4, 1974)
H. J. Hargis, graduate student at the University of Tennessee – High Energy Physics Program (continued indefinite assignment begun in October 1970)	

**CONSULTANTS UNDER SUBCONTRACT WITH UNION CARBIDE CORPORATION
NUCLEAR DIVISION – ORNL**

Faculty members of colleges and universities who have served as consultants under subcontract are listed below along with the programs with which they were associated. Numerous other consultants – those not faculty members or not under subcontract – have also been associated with the Division but are not included here.

- Michel Baranger, Massachusetts Institute of Technology – Theoretical Physics Program
- C. R. Bingham, University of Tennessee – Nuclear Physics Program
- H. G. Blosser, Michigan State University – Heavy Ion Laboratory Project
- D. A. Bromley, Yale University – Nuclear Physics Program
- W. M. Bugg, University of Tennessee – High Energy Physics Program
- J. W. Burton, Carson-Newman College – Mössbauer Experimental Program and Future Planning (Physics) Program
- R. W. Childers, University of Tennessee – High Energy Physics Program (contract closed September 1973)
- R. K. Cole, University of Southern California – ORIC Research Program (contract closed June 1973)
- G. T. Condo, University of Tennessee – High Energy Physics Program
- R. Y. Cusson, Duke University – Theoretical Physics Program and Physics of Fission Program
- R. M. Drisko, University of Pittsburgh – Theoretical Physics Program (contract closed June 1973)
- J. H. Goldstein, Emory University – Atomic and Molecular Spectroscopy Program (contract closed September 1973)
- L. B. Hubbard, Furman University – Theoretical Physics Program (contract closed August 1973)
- P. G. Huray, University of Tennessee – Mössbauer Experimental Program and Future Planning (Physics) Program
- S. J. Kreiger, University of Illinois, Chicago Circle – Theoretical Physics Program
- M. G. Mustafa, Vanderbilt University (presently at the University of Maryland) – Physics of Fission Program (contract closed August 1973)
- R. J. McCarthy, Carnegie-Mellon University – Theoretical Physics Program
- S. C. Pancholi, University of Delhi, India – Nuclear Data Project (contract closed October 1973)
- P. Z. Peebles, University of Tennessee – Van de Graaff Program
- D. J. Pegg, University of Tennessee – Van de Graaff Program
- L. L. Riedinger, University of Tennessee – Van de Graaff Program
- R. O. Sayer, Vanderbilt University (on leave from Furman University) – Van de Graaff Program and Oak Ridge Isochronous Cyclotron Program
- I. A. Sellin, University of Tennessee – Van de Graaff Program and Cyclotron Laboratory Program
- E. W. Thomas, Georgia Institute of Technology – Ion Source Physics Program (consultant with ORNL Thermonuclear Division)
- J. O. Thomson, University of Tennessee – Mössbauer Experimental Program and Future Planning (Physics) Program
- S. T. Thornton, University of Virginia – Van de Graaff Program
- Hendrik Verheul, Free University, Amsterdam, Netherlands – Nuclear Data Project
- Lawrence Wilets, University of Washington – Physics of Fission Program

**CONSULTANTS UNDER CONTRACT ARRANGEMENT WITH
OAK RIDGE ASSOCIATED UNIVERSITIES**

Under arrangements with Oak Ridge Associated Universities (“S” contracts and “U” contracts), 83 university or college faculty members visited the Physics Division for consultation and collaboration during 1973. These individuals and their affiliation are listed

below:

- F. T. Avignone, University of South Carolina
- S. Banharnsupavat, University of Missouri
- K. H. Baker, Georgia Institute of Technology

- L. Birdwell, Murray State University
 E. L. Bosworth, Vanderbilt University
 W. H. Brantley, Furman University
 D. D. Brayshaw, University of Maryland
 M. D. Brown, Kansas State University
 R. F. Carlton, Middle Tennessee State University
 R. P. Chaturvedi, State University of New York
 W. E. Collins, Fisk University
 F. L. Culp, Tennessee Technological University
 R. Y. Cusson, Duke University
 J. L. Duggan, North Texas State University
 R. D. Edge, University of South Carolina
 R. W. Fink, Georgia Institute of Technology
 C. C. Foster, University of Missouri
 J. D. Fox, Florida State University
 F. Gabbard, University of Kentucky
 R. M. Gaedke, Trinity University
 L. A. Galloway III, Centenary College of Louisiana
 G. J. Garcia-Bermudez, Vanderbilt University
 G. M. Gowdy, Georgia Institute of Technology
 T. J. Gray, North Texas State University
 M. Greenfield, Florida State University
 D. E. Gustafson, University of Virginia
 J. H. Hamilton, Vanderbilt University
 K. J. Hofstetter, University of Kentucky
 R. F. Holub, University of Kentucky
 L. B. Hubbard, Furman University
 D. L. Humphrey, Western Kentucky University
 M. A. Ijaz, Virginia Polytechnic Institute
 J. A. Jacobs, Virginia Polytechnic Institute
 R. L. Kauffman, Kansas State University
 G. J. KeKelis, Florida State University
 K. W. Kemper, Florida State University
 B. D. Kern, University of Kentucky
 Q. C. Kessel, University of Connecticut
 R. Lear, Montana State University
 R. S. Lee, Vanderbilt University
 Teck-Kah Lim, Drexel University
 G. L. Light, North Texas State University
 Jung Lin, Tennessee Technological University
 M. A. K. Lodhi, Texas Technological University
 J. C. Lovè, Florida Institute of Technology
 W. G. Love, University of Georgia
 J. R. MacDonald, Kansas State University
 D. A. McClure, Georgia Institute of Technology
 J. D. McCoy, University of Tulsa
 D. L. McShan, Florida State University
 R. J. de Meijer, Florida State University
 Nancy O'Fallon, St. Louis University
 J. M. Palms, Emory University
 T. F. Parkinson, University of Missouri
 H. S. Plendl, Florida State University
 B. P. Pullen, Southeastern Louisiana University
 A. V. Ramayya, Vanderbilt University
 P. V. Rao, Emory University
 P. Richard, Kansas State University
 P. J. Riley, University of Texas
 E. L. Robinson, University of Alabama
 R. M. Ronningen, Vanderbilt University
 P. G. Roos, University of Maryland
 K. S. R. Sastry, University of Massachusetts
 R. O. Sayer, Furman University
 Alan Scott, University of Georgia
 Enrique Silberman, Fisk University
 G. D. Stucky, University of Illinois
 S. T. Thornton, University of Virginia
 George Vourvopoulos, Florida A & M University
 R. F. Walker, Jr., Louisiana State University
 T. A. Walkiewicz, Edinboro State College
 B. Wehring, University of Illinois
 J. L. Weil, University of Kentucky
 J. C. Wells, Jr., Tennessee Technological University
 R. M. White, Baker University
 M. L. Whiten, Armstrong State College
 B. H. Wildenthal, Michigan State University
 R. R. Winters, Denison University
 J. L. Wood, Georgia Institute of Technology
 A. C. Xenoulis, Georgia Institute of Technology
 A. F. Zeller, Florida State University
 E. F. Zganjar, Louisiana State University

ANNUAL INFORMATION MEETING

Advisory Committees are appointed for the majority of the research divisions of the Laboratory to review the cogency and effectiveness of the research programs. The program review is conducted in conjunction with the Annual Information Meeting, at which the Division's research is summarized in brief reports. The 1973 meeting was held May 7 and 8. Members of the 1973 Advisory Committee were:

Professor John S. Blair, University of Washington

Dr. Richard M. Diamond, Lawrence Berkeley Laboratory

Professor Roy K. Middleton, University of Pennsylvania

Professor Ward Whaling, California Institute of Technology

RADIATION CONTROL AND SAFETY

The Divisional Radiation Control and Safety Officers, C. B. Fulmer for the Cyclotron Laboratory and Van de Graaff Laboratory and George Chapman (Neutron

Physics Division) for the Oak Ridge Electron Linear Accelerator (ORELA), report that there were no "unusual occurrences" during 1973.